THEORETICA CHIMICA ACTA

edenda curat

Hermann Hartmann

adiuvantibus

C. J. Ballhausen, København
R. D. Brown, Clayton
E. Heilbronner, Basel
J. Jortner, Tel-Aviv
M. Kotani, Tokyo
J. Koutecký, Praha
J. W. Linnett, Cambridge
E. E. Nikitin, Moskwa
R. G. Pearson, Evanston
B. Pullman, Paris
K. Ruedenberg, Ames
C. Sandorfy, Montreal
M. Simonetta, Milano
O. Sinanoğlu, New Haven

Vol. 26, 1972

Springer-Verlag · Berlin · Heidelberg · New York

The exclusive copyright for all languages and countries, including the right for photomechanical and any other reproductions, also in microform, is transferred to the publisher.

The use in this journal of registered or trade names, trademarks etc. without special acknowledgement does not imply that such names, as defined by the relevant protections laws, may be regarded as unprotected and thus free for general use.

Alle Rechte, einschließlich das der Übersetzung in fremde Sprachen und das der fotomechanischen Wiedergabe oder einer sonstigen Vervielfältigung, auch in Mikroform, vorbehalten. Jedoch wird gewerblichen Unternehmen für den innerbetrieblichen Gebrauch nach Maßgabe des zwischen dem Börsenverein des Deutschen Buchhandels e. V. und dem Bundesverband der Deutschen Industrie abgeschlossenen Rahmenabkommens die Anfertigung einer fotomechanischen Vervielfältigung gestattet. Wenn für diese Zeitschrift kein Pauschalabkommen mit dem Verlag vereinbart worden ist, ist eine Wertmarke im Betrage von DM 0,40 pro Seite zu verwenden. *Der Verlag läßt diese Beträge den Autorenverbänden zufließen.*

Die Wiedergabe von Gebrauchsnamen, Handelsnamen, Warenbezeichnungen usw. in dieser Zeitschrift berechtigt auch ohne besondere Kennzeichnung nicht zu der Annahme, daß solche Namen im Sinne der Warenzeichen- und Markenschutz-Gesetzgebung als frei betrachtet wären und daher von jedermann benutzt werden dürften.

Springer-Verlag Berlin Heidelberg New York
Printed in Germany by Brühlsche Universitätsdruckerei, Gießen
© by Springer-Verlag Berlin Heidelberg 1972

[illegible] /02
38964
24.4.82

Index

Commentationes et Relationes

Anderson, A.B., Parr, R.G.: A Poisson Equation for Vibrational Potentials of Diatomic Molecules . . . 301

Armstrong, D.R., Perkins, P.G., Scott, J.M., Stewart, J.J.P.: The Electronic Structures of Some Tetrazaborolines and Dimethyltetrazadieneirontricarbonyl . . . 237

Bacskay, G.B., Linnett, J.W.: Mixed Basis Functions in Molecular Quantum Mechanics. I. Computational Methods and Preliminary Study of the Helium Atom . . . 1

Bacskay, G.B., Linnett, J.W.: Mixed Basis Functions in Molecular Quantum Mechanics. II. A Study of the H_2 Molecule . . . 15

Bacskay, G.B., Linnett, J.W.: Mixed Basis Functions in Molecular Quantum Mechanics. III. The Linear Symmetric H_3 Molecule . . . 23

Bacskay, G.B.: Mixed Basis Functions in Molecular Quantum Mechanics. IV. The Linear, Equidistant System of Four Interacting Hydrogen Atoms . . . 33

Bailey, M.L.: Calculation of Oscillator Strengths for π-Electron Molecules . . . 87

Barber, M.S., see Palmer, M.H., et al. . . . 357
Berthier, G., Bonaccorsi, R., Scrocco, E., Tomasi, J.: The Electrostatic Molecular Potential for Imidazole, Pyrazole, Oxazole and Isoxazole . . . 101

Bonaccorsi, R., see Berthier, G., et al. . . . 101

Brogli, F., Heilbronner, E.: Correlation of Hückel Molecular Orbital Energies with π-Ionization Potentials . . . 289

Burrows, B.L.: Perturbation Theory for Excited States of Molecules. III . . . 267

Burrows, B.L.: Perturbation Theory for Excited States. IV . . . 273

Čársky, P., Zahradník, R.: A Remark on the Comparison between the Roothaan Open Shell and Half-Electron Method . . . 171

Cecchi, M.M.: Calculations of Molecular Wave Functions in Terms of Modulated Plane Waves . . . 351

Constanciel, R.: Introduction de la matrice densité de paire dans l'étude théorique du pK des états excités . . . 249

Czismadia, I.G., see Strausz, O.P., et al. . . . 367
Denes, A.S., see Strausz, O.P., et al. . . . 367

Duke, B.J., Stephens, D.G.: The Electronic Structure of the $B_2H_5^+$ Ion . . . 381

Ege, G., Vogler, H.: Zur Konjugation in makrocyclischen Bindungssystemen. XX. Charakterordnung, magnetische Suszeptibilitäten und chemische Verschiebungen von Corannulenen. Paramagnetischer Suszeptibilitätsanteil im Innern von Corannulenen 55

Eliezer, I., Reger, A.: Calculations on the Force Constants of Triatomic Group II Metal Halides . . . 283

Ellis, R.L., Kuehnlenz, G., Jaffé, H.H.: The Use of the CNDO Method in Spectroscopy. VI. Further $n - \pi^*$ Transitions . . . 131
Flurry, R.L., Jr., see Howland, J.C. . . . 157

Fueno, T., Nagase, S., Tatsumi, K., Yamaguchi, K.: An Intermolecular Perturbation Approach to the Cycloaddition of Carbenes toward Olefins. Reaction Path and Stereoselectivity . . . 43
Gaskell, A.J., see Palmer, M.H., et al. . . . 357

Goddard, W.A., III, Wilson, C.W., Jr.,: The Role of Kinetic Energy in Chemical Binding II. Contragradience . . . 211

Goddard, W. A., III, see Wilson, C. W., Jr. 195
Gosavi, R. K., see Strausz, O. P., et al. 367

Gouyet, J. F., Prat, M. T.: Correlation Effect on the Singlets $\pi\pi^*$ Transition Energies of Polyacenes 89

Graovac, A., Gutman, I., Trinajstić, N., Živković, T.: Graph Theory and Molecular Orbitals. Application of Sachs Theorem 67

Guidotti, C., Lamanna, U., Maestro, M.: Calculated Physical Properties of a Water Molecule in an Ice-Like Cluster 147
Gutman, I., see Graovac, A., et al. 67
Heilbronner, E., see Brogli, F. 289

Hirst, D. M., Linington, M. E.: The Method of Non-Paired Spatial Orbitals. II. The Benzyl Radical 179

Howland, J. C., Flurry, R. L., Jr.: Acceleration of Convergence by Density Matrix Extrapolation in CNDO/2 Calculations 157

Hush, N. S., Williams, M. L.: Finite Electric Field Valence Shell Calculations of Polarizability Gradients and Raman Depolarization Ratios for Diatomic Molecules 141
Inokuchi, H., see Ohno, K. 331
Jaffé, H. H., see Ellis, R. L., et al. 131

Johansson, A., Kollman, P., Rothenberg, S.: The Electronic Structure of the HCN Dimer and Trimer 97

Jug, K.: Operator Equations in Approximate Molecular Orbital Theories. II. Integral Approximations and Charge Distribution 231
Katriel, J.: An Interpretation of Hund's Rule 163
Kollman, P., see Johansson, A., et al. 97
König, E., Kremer, S.: Detailed Crossover Studies of Transition Metal Ions
I. The Octahedral and Tetrahedral d^4 and d^6 Electron Configurations 311
Kremer, S., see König, E. 311
Kuehnlenz, G., see Ellis, R. L., et al. 131
Labarre, J.-F., see Robinet, G., et al. 257
Laidlaw, W. G., Vasudevan, K.: The Stability of the Hartree Fock Solutions of Pentalene and Heptalene 387
Lamanna, V., see Guidotti, C., et al. 147
Leibovici, C., see Robinet, G., et al. 257
Linington, M. E., see Hirst, D. M. 179
Linnett, J. W., see Bacskay, G. B. 1, 15, 23
Loew, G. H., Steinberg, D. A.: Molecular Orbital Calculations of the Active Site Complex of Two Iron Ferredoxins.
II. Electron Distribution, Magnetic Moment, Field Gradients and Electronic Spectra of the Oxidized State 107
Maestro, M., see Guidotti, C., et al. 147
Nagase, S., see Fueno, T., et al. 43
Oberhammer, H.: CNDO/2 Rechnungen für einige Schwefelverbindungen 79
CNDO/2 *Calculations for Some Sulfur Compounds*
Ohno, K., Inokuchi, H.: A Self-Consistent Molecular Field Theory for Aggregates of Neutral Molecules. I 331

Palmer, M. H., Gaskell, A. J., Barber, M. S.: *Ab initio* Molecular Orbital Calculations
2. A comparison of Polarisation Function Addition to Minimal Bases, and Molecular Scaling. Computations on Furan, Pyrrole and 1,2,5-Oxadiazole 357
Parr, R. G., see Anderson, A. B. 301
Perkins, P. G., see Armstrong, D. R., et al. 237

Peterson, C., Pfeiffer, G. V.: *Ab initio* Valence-Bond Calculations of H_2O
I. Bond Dissociation Energies 321
Pfeiffer, G. V., see Peterson, C. 321

Pouzard, G., Pujol, L.: Energie des systèmes H_2, HHe^+ et LiH 187
Prat, M. T., see Gouyet, J. F. 89
Pujol, L., see Pouzard, G. 187

Reger, A., see Eliezer, I. 283
Reinsch, E.-A.: Das Kastenmodell als Grundlage für ein *ab initio* Verfahren IV. Bindungsbildung beim Wasserstoffmolekül 279
Robinet, G., Leibovici, C., Labarre, J.-F.: Analyse conformationnelle théorique du diméthylsulfoxyde $(CH_3)_2SO$ 257
Rothenberg, S., see Johansson, A., et al. 97
Salvetti, O., see Cecchi, M.M. 351
Scott, J.M., see Armstrong, D.R., et al. 237
Scrocco, E., see Berthier, G., et al. 101
Steinberg, D.A., see Loew, G.H. 107
Stephens, D.G., see Duke, B.J. 381
Stewart, J.J.P., see Armstrong, D.R., et al. 237
Strausz, O.P., Gosavi, R.K., Denes, A.S., Czismadia, I.G.: Molecular Orbital Calculations on the Ethylene Episulfide Molecule and Its Isomers 367
Tatsumi, K., see Fueno, T., et al. 43
Tomasi, J., see Berthier, G., et al. 101
Trinajstić, N., see Graovac, A., et al. 67
Vasudevan, K., see Laidlaw, W.G. 387
Vogler, H., see Ege, G. 55
Williams, M.L., see Hush, N.S. 141
Wilson, C.W., Jr., Goddard, W.A., III: The Role of Kinetic Energy in Chemical Binding I. The Nonclassical or Exchange Kinetic Energy 195
Wilson, C.W., Jr., see Goddard, W.A., III 211
Yamaguchi, K., see Fueno, T., et al. 43
Zahradník, R., see Čarsky, P. 171
Živković, T., see Graovac, A., et al.. 67

Annotatio

Grabenstetter, J.E., Whitehead, M.A.: Comment on a Paper by Stout and Politzer. . . 390
Whitehead, M.A., see Grabenstetter, J.E. 390

Recensiones

Englmann, R.: The Jahn-Teller Effect in Molecules and Crystals (Ref. C. J. Ballhausen) 391

Gutmann, V.: Chemische Funktionslehre. (Ref. F. Wasgestian) 194

Kutzelnigg, W., Re, G. del, Berthier, G.: σ and π Electrons in Organic Compounds (Ref. K. Jug) 392

Indexed in Current Contents

Theoret. chim. Acta (Berl.) 26, 1– 13 (1972)
© by Springer-Verlag 1972

Commentationes

Mixed Basis Functions in Molecular Quantum Mechanics

I. Computational Methods and a Preliminary Study of the Helium Atom

G. B. BACSKAY and J. W. LINNETT
Department of Physical Chemistry, Cambridge, England

Received February 3, 1972

Mixed sets of functions consisting of 1*s* Slater orbitals and floating spherical Gaussians are proposed as expansion functions for *ab initio* variational type calculations for small molecules. After the discussion of the basic computational methods the results of some trial calculations for the ground state of the helium atom are presented.

Für *ab initio* Rechnungen vom Variationstyp werden im Falle kleiner Moleküle gemischte Funktionssätze, die aus 1*s* Slater-Orbitalen bestehen, vorgeschlagen. Nach einer Diskussion der grundlegenden Rechenmethoden werden die Resultate von einigen Proberechnungen für den Grundzustand des Heliumatoms geschildert.

Introduction

The choice of basis functions is of fundamental importance in all *ab initio* variational type atomic and molecular calculations. From the purely theoretical viewpoint the basis functions should ideally form a complete set; from the computational viewpoint the functions should also possess good convergence properties, since in practice the expansions need to be as compact as possible. Furthermore, one must be able to evaluate all the basic integrals which arise in the course of the calculation with reasonable ease in order to make the computational work worth attempting.

The most widely used functions in atomic calculations have been the Slater type atomic orbitals (STO's), which have the advantage over other sets of functions in that they closely resemble atomic self-consistent orbitals [1–3]. STO's have found wide application in molecular calculations as well, although in the case of the more complex systems the problems associated with the evaluation of multicentre integrals often proves prohibitive, as most of these integrals cannot, in general, be evaluated in closed form. Gaussian type orbitals (GTO's) as expansion functions were first introduced by Boys [4], who showed that all the integrals which arise in a variational energy calculation could be calculated with reasonable ease. However, compared with STO's, Gaussians suffer from the disadvantage that, because they are not so closely related to self-consistent orbitals, their convergence properties are considerably poorer. This results in lengthy expansions. The basic 1*s*-type Gaussian function, defined as

$\psi = (2\alpha/\pi)^{3/4} \exp(-\alpha r^2)$ α being a constant, called the orbital exponent, differs most from a 1*s* Slater orbital at the origin, lacking a cusp there. A 1*s* STO takes the form

$$\psi = (\alpha^3/\pi)^{1/2} \exp(-\alpha r).$$

Consequently, a wavefunction constructed from Gaussians does not obey the nuclear cusp condition [5] and generally exhibits the worst behaviour at and near the nuclei. Hence, just to ensure a reasonably good description of the electron density in the regions near the nuclei, a relatively large number of Gaussians is needed as expansion functions.

The mixed basis sets advocated here arise naturally. Consider a wavefunction which is constructed from a small number of Slater functions, and which gives a reasonably good electron distribution, especially in the regions near the nuclei. To correct the electron density further, and to allow for electron correlation, Gaussians may be just as efficient as Slater functions, since there is no cusp requirement for the additional basis functions. The Gaussian functions could be placed at such points in space so as to be energetically the most effective. Furthermore, it is plausible to think that *p*- and *d*-type Slater functions, which are only used for correction purposes, may be successfully replaced by Gaussian functions of the same symmetry or even by Gaussian lobe functions. The latter are defined as normalized linear combinations of spherical Gaussians centred at different points in space, their transformation properties resembling those of *p*-, *d*- and possibly higher functions.

The use of such mixed basis sets was first proposed by Allen [6]. Calculations were first carried out by Riera and Linnett [7] for the linear, symmetric H_3 molecule. Because their results were encouraging, a more systematic and detailed study of mixed basis sets has been made.

In this paper we report a series of trial calculations on the helium atom, using various mixed basis sets consisting of just 1*s* Slater and floating spherical Gaussian orbitals. The first molecular calculation was carried out on H_2 and this was followed by calculations on the more complex systems of H_3 and H_4. The results are reported in some forthcoming papers. The calculations are *ab initio*, all the integrals having been evaluated to sufficient accuracy to make the resulting energy accurate to 1 part in 10^6. The method of configuration interaction (CI) was employed, i.e. a variational approach, minimizing the energy of a multiconfigurational wavefunction consisting of Slater determinants which were constructed from an orthonormalized set of symmetry orbitals. The final wavefunctions are generally expressed in terms of natural orbitals, obtained by the diagonalization of the spinless first order reduced density matrix.

Computational Methods

A typical CI calculation consisted of three main stages:

(a) Evaluation of the basic integrals;

(b) Construction of an orthonormal set of symmetry orbitals and th transformation of the integrals to this new basis;

(c) Construction of the required configurations and the Hamiltonian matrix followed by its diagonalization yielding the energy and the corresponding wavefunction. Calculation and diagonalization of the spinless first order reduced density matrix to give the natural orbitals and their occupation numbers.

In the larger calculations, e.g. in the case of H_3 and H_4, steps *a*, *b* and *c* were carried out separately, making use of the magnetic tape and disc facilities to store the integrals and other intermediate results. The He and H_2 calculations could easily be performed in a single run.

The computer used for our calculations has been the Cambridge University Computer Laboratory's Titan computer, with a maximum available fast store of 40000 words, requiring approximately 5 μsec for addition or subtraction and 8 and 25 μsec for multiplication and division respectively, in variable mode. All the calculations have been carried out in single precision, which is 11 significant figures in Titan.

The various computational steps will now be discussed in more detail.

a) Evaluation of the Basic Integrals

The integrals to be evaluated are the overlap, kinetic energy, nuclear attraction and electron repulsion integrals in a mixed set of 1s Slater and Gaussian type functions.

All the integrals involving only spherical Gaussians were readily calculated according to the expressions given by Boys [4]. The evaluation of the auxiliary functions $F_0(t)$ which occurs in the three-centre nuclear attraction and electron repulsion integrals is discussed in Appendix 1. The overlap, kinetic energy, one and two centre nuclear attraction, Coulomb and hybrid integrals involving only the Slater functions were calculated using the closed formulae of Roothaan *et al.* [8–10]. The remaining integrals, i.e. the three centre nuclear attraction, exchange, three and four centre electron repulsion integrals involving only Slater functions and all the mixed integrals, i.e. involving both types of functions, were evaluated by expanding the Slater functions in terms of Gaussians, followed by term-by-term integration and summation. Huzinaga's expansions were utilized for this purpose [11]. In order to achieve an accuracy of 1 in 10^6 in the total energy, all the one-electron integrals were evaluated using 10 Gaussians to expand the Slater functions. 8 Gaussians were generally used when evaluating two-electron integrals, although in some cases 4 Gaussians proved sufficient; for example, in the He calculations. Most integrals were accurate to within 1 in 10^6, although some multicentre 2-electron integrals were found to be less accurate (~ 1 in 10^4). The effect of this inaccuracy on the energy would, however, be very small. To illustrate the accuracy and convergence properties of the integrals calculated by the Gaussian expansion technique, the values of some exchange integrals are listed in Appendix 2.

The one electron integrals were stored as two-dimensional arrays in the computer, although only the upper (or lower) triangle needs to be evaluated as a result of the symmetric nature of these arrays. The two electron integrals were generated and stored as a one-dimensional array making use of the fact that a real orbital integral given as

$$[ij|kl] = \int \varphi_i(1)\,\varphi_j(1)\,\varphi_k(2)\,\varphi_l(2)\,r_{12}^{-1}\,d\tau_1\,d\tau_2$$

is unaffected by the interchanges of i and j, of k and l and of ij and kl.

In the calculation of the integrals full use was made of spatial symmetry.

In case of a large basis the integrals could be generated in several successive runs on the computer and then stored on magnetic tape or disc for future use.

b) Construction of Orthogonal Symmetry Orbitals

Whenever possible the basic orbitals were transformed so as to give an orthonormal symmetry orbital basis.

In the case of Gaussians which are not centred on the nuclei the symmetry orbitals usually transform according to the irreducible representation of some lower symmetry point group as, for example, in the case of He when 6 Gaussians are used to construct three p-type orbitals. The resulting orbitals, usually called Gaussian lobe functions, transform according to the O_h point group. When expanded about the origin the lobe functions are found to include contributions from higher spherical harmonics [12]. Consequently, a He wavefunction which is partly constructed from such lobe functions will have octahedral rather than spherical symmetry. However, this is not expected to introduce serious difficulties, since such functions are induced only to allow for correlation and would not affect the electron distribution, which ought to be symmetrical, to a significant extent.

Two methods of orthonormalization were used, the Schmidt method [13] and Löwdin's symmetric orthogonalization method [14]. Both were found to function satisfactorily, although the Schmidt method was preferred in the later work, when it was convenient to enlarge a given orbital basis by the addition of Schmidt orthogonalized orbitals to the existing orthonormal set.

c) Transformation of Integrals

Since the Slater determinants in the CI expansions are constructed from an orthonormal set of symmetry orbitals, the integrals need to be transformed to the new basis.

The method used is a standard one, explained in detail by Harris [15] for example, it makes use of intermediate arrays as much as possible to reduce comp. time requirements. In the case of two-electron integrals, for example, the number of computational steps is proportional to n^5, n being the number of basis functions used, as opposed to n^8 which would result if the elementary transformation method was used.

This part of the calculation is generally very time consuming, as well as having large store requirements. Hence, for a basis which contains more than 12 orbitals it was generally carried out separately, making use of tape and disc facilities as much as possible to store the integrals and parts of the intermediate working arrays.

d) *The* CI *Wavefunction and the Hamiltonian Matrix*

A CI wavefunction takes the form

$$\Psi = \sum_{i} C_i \Phi_i \tag{1}$$

where $\{\Phi_i\}$ is an orthonormal set of configurations, each with the correct spatial and spin symmetry properties; corresponding to the state under study, $\{C_i\}$ is a set of constants chosen so as to minimize the total energy.

For the singlet two-electron case there are two types of configurations,

$$\begin{aligned} \Phi^1 &= |\varphi_i \bar{\varphi}_i| \\ \Phi^2 &= 2^{-1/2}\{|\varphi_i \bar{\varphi}_j| + |\varphi_j \bar{\varphi}_i|\}, \quad i \neq j \end{aligned} \tag{2}$$

where $|\varphi_i \bar{\varphi}_j|$ is a normalized Slater determinant constructed from the spin orbitals φ_i and $\bar{\varphi}_j$ with α and β spins respectively.

The various matrix elements between such configurations are easily calculable, using the set of transformed integrals.

The 3 and 4 electron wavefunctions are discussed in the relevant later papers.

The lowest eigenvalue of the Hamiltonian matrix and the corresponding eigenvector, characterising the ground state of a given system, were calculated using Nesbet's method [16].

e) *The Natural Orbitals* [17–18]

The set of natural orbitals $\{\chi_i\}$ are defined by the transformation

$$\chi_i = \sum_{k} U_{ki} \psi_k \tag{3}$$

where $\{\psi_k\}$ is the set of basis functions and U is the unitary matrix which diagonalizes the spinless first order density matrix, given in the ψ_k representation.

The elements of the diagonalized density matrix are known as the occupation numbers of the natural orbitals, indicating the relative importance of each orbital in the CI expansion, their sum being equal to the number of electrons.

Natural expansions have the quickest convergence in any given basis and at any point in the expansion maximum overlap with the exact wavefunction is assured. Hence, the first term in a natural expansion closely resembles the Hartree-Fock wavefunction within the same basis. The total wavefunction to a good approximation is thus conveniently separated into SCF and correlation parts. Consequently, we introduce a quantity called *apparent correlation energy*, defined as the difference between the calculated total and the SCF energies, the latter estimated by the energy associated with the first term in the NO expansion. The magnitude of the apparent correlation energy can then serve as a guide as to the "amount" of correlation allowed for by a given CI wavefunction.

In the case of 2-electron systems the calculation of the natural orbitals is particularly simple. Since the singlet CI wavefunction can be written as

$$\Psi = 2^{-1/2}(\alpha\beta - \beta\alpha) \sum_{i,j} C_{ij} \varphi_i(1)\, \varphi_j(2) \tag{4}$$

the spinless first order reduced density matrix is simply

$$\gamma(1 \,|\, 1') = \sum_{i,j} (CC^+)_{ij} \varphi_i(1)\, \varphi_j^*(1') . \tag{5}$$

Since C and CC^+ are both diagonalizable by the same unitary transformation it suffices to diagonalize C to yield the natural orbitals. Expressed in terms of NO's the total wavefunction is also in diagonal form,

$$\Psi = 2^{-1/2}(\alpha\beta - \beta\alpha) \sum_{i} m_i \chi_i(1)\, \chi_i(2) . \tag{6}$$

The occupation numbers n_i of the NO's are just $2m_i^2$.

If the number of electrons is greater than two the calculation of the NO's is carried out by the diagonalization of the density matrix. This will be discussed in the forthcoming papers on H_3 and H_4.

Calculations for the Ground State of the He *Atom.*
Two and Three Orbital Calculations

Only radial functions were used in these calculations, orthonormalized by Löwdin's method, the total wavefunction in each case including all the possible configurations. All the orbital exponents were optimized by Powell's [21] method. Details of the various basis sets and the corresponding energies that were obtained are presented in Table 1. For the Gaussian functions the square root of the orbital exponents is also given so as to make the comparison with exponential functions simpler. (The "range" of a Gaussian is proportional to $\alpha^{-1/2}$, α being the exponent, as opposed to an exponential function whose range is proportional to α^{-1} [22]). The wavefunctions are given in Table 2, expressed in natural form, i.e. according to Eq. (6).

The energy results clearly indicate that the main shortcoming of a Gaussian basis lies in the poor description of the electron-nucleus interaction. This is due to the fact that a Gaussian is not a solution of the Schrödinger equation for the hydrogen-like problem, resulting in an electron distribution which is far from correct, consequently severely underestimating the magnitude of the nuclear attraction energy. The electron repulsion energy is much more independent of the basis used, whereas the kinetic energy also shows large fluctuations, paralleling those in the total energy, in accordance with the Virial Theorem [25].

The energy values of the NO expansions truncated to contain only the first, leading term display the same tendencies as the total energies, but the variations shown by the apparent correlation energy are much smaller. It is evident that wavefunctions constructed wholly or in part from Gaussians are poor as a result of unsatisfactory SCF parts and not because they describe correlation badly. Hence the need for a large basis when using Gaussians. It is

Table 1. **Basis functions for the 2 and 3 orbital He calculations and the resulting energy terms (in a.u.) together with some accurate results for comparison.** The square roots of the orbital exponents of the Gaussians are given in brackets (S = Slater function, G = Gaussian)

Calculation Ref.	Orbital types and exponents	Total energy	Kinetic energy	Nuclear attraction energy	Electron repulsion energy	Energy of truncated NO expansion	Apparent correlation energy
1	1: G: 0.5231 (0.7233) 2: G: 4.0063 (2.0016)	−2.75787	2.75787	−6.52205	1.00630	−2.74696	−0.01091
2	1: S: 1.579 2: G: 0.4810 (0.6935)	−2.86367	2.86408	−6.75075	1.00230	−2.85358	−0.01009
3	1: S: 1.325 2: S: 2.457	−2.87689	2.87686	−6.74418	0.99044	−2.86117	−0.01572
4	1: G: 0.3730 (0.6107) 2: G: 1.9629 (1.4010) 3: G: 13.1908 (3.6319)	−2.85121	2.85118	−6.69625	0.99387	−2.83554	−0.01567
5	1: S: 1.694 2: G: 0.972 (0.9859) 3: G: 4.574 (2.1387)	−2.87331	2.87329	−6.74780	1.00120	−2.86012	−0.01319
6	1: S: 1.389 2: S: 2.551 3: G: 1.388 (1.178)	−2.87852	2.87786	−6.74386	0.98748	−2.86149	−0.01703
7	1: S: 1.425 2: S: 2.495 3: S: 2.805	−2.87850	2.87708	−6.74282	0.98725	−2.86154	−0.01696
Schwartz [23]	Radial limit calculation	−2.879028					−0.01734
Roothaan *et al.* [24]	SCF calculation	−2.86168				−2.86168	

Table 2. The wavefunctions resulting from the 2 and 3 orbital He calculations expressed in natural form; the natural orbitals given in terms of the original basis

Calculation Ref.	Coefficient of configuration $\chi_i(1)\,\chi_i(2)$	Natural orbital χ_i	Coefficient of atomic orbital 1	2	3
1	0.999289	1	0.820139	0.290118	
	−0.037710	2	−0.825167	1.126659	
2	0.999146	1	1.187270	−0.19555	
	−0.041308	2	−3.59639	3.78225	
3	0.997749	1	0.692164	0.338112	
	−0.066644	2	−1.896261	1.990120	
4	0.998287	1	0.651603	0.414226	0.083418
	−0.058385	2	−0.058385	−1.064087	1.044166
	−0.003710	3	0.441146	−1.078287	1.218240
5	0.998805	1	1.203741	−0.014630	−0.200268
	−0.048251	2	−2.736116	1.263159	1.945947
	−0.007810	3	−3.293699	−0.565796	3.827433
6	0.997846	1	0.760462	0.284959	−0.020178
	−0.065279	2	−1.948360	1.533277	0.550329
	−0.006558	3	−0.253137	−4.005462	4.306479
7	0.997749	1	0.828095	−0.055060	0.254221
	−0.066644	2	−2.666421	5.914587	−3.205106
	−0.007489	3	3.996217	−25.11450	21.70878

noteworthy that the wavefunction built from two Slater functions and one Gaussian is energetically as good as the one from three Slater functions. Hence it ought to be possible to construct good wavefunctions using just a few Slater type orbitals and possibly a larger number of Gaussians as expansion functions, the latter used as correction functions to improve the SCF part of the wave-function further and to provide the extra flexibility to describe electron correlation.

The best energy, −2.87852 a.u., from calculation 6 compares favourably with the estimated radial or S limit of −2.879028 a.u. [23], despite the small basis. The energy of the truncated NO expansion from the same calculation, −2.86149 a.u., shows similar agreement with the exact SCF energy of −2.86168 a.u. [24]. The best calculated value for the apparent correlation energy is −0.01703 a.u., very close to the accurate radial correlation energy of −0.01734 a.u.[1]

The coefficients of the configurations from the various calculations show the strong convergence usually displayed by the occupation numbers of NO's. The magnitude of the first coefficient, being associated with the SCF part in the wave-function, shows an inverse type relationship with the apparent correlation energy. This behaviour is to be expected since higher configurations represent the correlation part in the wave-function, the coefficients indicating their relative importance, and as they become larger the first coefficient needs to decrease in order for the total wave-function to be normalized.

---

[1] The apparent correlation energy is not, in general, an upper bound to the true correlation energy, hence it needs to be used with caution.

Eight Orbital Calculations

In these calculations Gaussian lobe functions were introduced in order to test their effectiveness in the description of angular correlation. The complete orbital basis consists of two 1*s* Slater orbitals centred on the nucleus and six Gaussians positioned octahedrally around the nucleus as shown in Fig. 1.

The various linear combinations of the Gaussians defining the lobe functions are symmetry orbitals which transform according to the irreducible representations of the O_h point group; they are listed in Table 3. The symmetry properties of the orbitals are also tabulated together with the type of orbitals they are to represent.

The first CI wavefunction was constructed from the two 1*s* Slater orbitals and the p_x, p_y, p_z-type lobe functions, resulting in 6 configurations. (The number of configurations could be reduced to 4, since the configurations $p_x p_x$, $p_y p_y$, and $p_z p_z$ could be grouped together.) The exponent and position of the Gaussians, as specified by the distance *d* from the origin, were optimised, the exponents of the Slater orbitals having been kept at their optimum values as found in the relevant 2-orbital calculation. During the optimization procedure it became clear

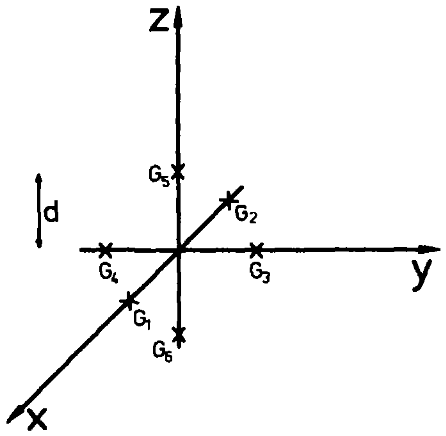

Fig. 1. Distribution of the Gaussians in the eight orbital He calculations

Table 3. The unnormalized symmetry orbitals formed from the octahedrally positioned Gaussians, $G_1 - G_6$

Symmetry orbitals	Symmetry type
$\varphi_1 = G_1 + G_2 + G_3 + G_4 + G_5 + G_6$	a_{1g} (s)
$\varphi_2 = G_1 - G_2$	t_{1u} (p_x)
$\varphi_3 = G_3 - G_4$	t_{1u} (p_y)
$\varphi_4 = G_5 - G_6$	t_{1u} (p_z)
$\varphi_5 = -G_1 - G_2 - G_3 - G_4 + 2G_5 + 2G_6$	e_g (d_{z^2})
$\varphi_6 = G_1 + G_2 - G_3 - G_4$	e_g $(d_{x^2-y^2})$

Table 4. Details of the 8 orbital basis and the calculated energies (a.u.) resulting from the CI calculations together with some literature values

Exponent of Slater functions	S_1 : 1.325	S_2 : 2.457
Exponent of Gaussians	1.287	
Values of the total energy from the 6 configuration calculation for various values of d (a.u.)	$d = 0.4$	$E = -2.89384$
	$d = 0.2$	$E = -2.89405$
	$d = 0.1613$	$E = -2.89407$
	$d = 0.0914$	$E = -2.89408$
	$d = 0.0143$	$E = -2.89408$
The total energy from the 11 configuration calculation with $d = 0.2$ a.u.	-2.89583	
Energy resulting from a CI calculation using a $1s$, $1s'$, $2p$ Slater basis [26]	-2.89518	
Exact energy [27]	-2.9037244	

Table 5. The 8 orbital 11 configuration wavefunction, yielding an energy of -2.89583 a.u. expressed in natural form (resulting in 8 configurations)

Coefficient of configuration $\chi_i(1)\,\chi_i(2)$	Natural orbital χ_i and its symmetry	Coefficient of atomic orbital S_1	S_2	G_1	G_2	G_3	G_4	G_5	G_6
0.996322	1 (s)	0.340104	0.694452	−0.000755	−0.000755	−0.000755	−0.000755	−0.000755	−0.000755
−0.055088	2 (s)	1.646348	−1.945622	0.068094	0.068094	0.068094	0.068094	0.068094	0.068094
−0.031573	3 (p_x)	0.0	0.0	2.260651	−2.260651	0.0	0.0	0.0	0.0
−0.031573	4 (p_y)	0.0	0.0	0.0	0.0	2.260651	−2.260651	0.0	0.0
−0.031573	5 (p_z)	0.0	0.0	0.0	0.0	0.0	0.0	2.260651	−2.260651
−0.007044	6 (s)	−3.755819	−0.044301	0.724852	0.724852	0.724852	0.724852	0.724852	0.724852
−0.005747	7 (d_{z^2})	0.0	0.0	−5.753096	−5.753096	−5.753096	−5.753096	11.50619	11.50619
−0.005747	8 ($d_{x^2y^2}$)	0.0	0.0	9.964656	9.964656	−9.964656	−9.964656	0.0	0.0

that numerical errors may arise as a result of two Gaussians coming too close together, introducing approximate linear dependency into the basis. The total energy is, however, quite insensitive to the separation of the Gaussians, hence to avoid the possibility of round-off errors it was decided to keep the Gaussians well separated in future calculations. A distance of 0.2 a.u. from the origin was settled on as a reasonable and safe value.

The second calculation made use of all the possible configurations, a total of 11, that could be constructed from the given 8 orbital basis. The orbital exponents were left unchanged from the previous calculation.

Details of the basis and the calculated energies from these calculations are given in Table 4.

The energy calculated using the 6 configuration function gives an improvement of 0.01719 a.u. over the function which contains just two Slater orbitals, this representing almost 70% of the total angular correlation energy. With a basis of two 1*s* and three 2*p* STO's Taylor and Parr [26] obtained an energy of -2.89518 a.u., only marginally better than our value.

The inclusion of the remaining three Gaussian lobe functions results in a significant decrease in the energy, bringing it within 4 kcal/mole of the Pekeris value of -2.9037244 a.u. [27]. The wavefunction from the 11 orbital calculation, given in terms of NO's, is presented in Table 5.

Conclusion

The results of the He calculations with mixed basis sets are very encouraging. Clearly, Gaussians are efficient when used to correct a wavefunction constructed from Slater orbitals, which is at least of SCF accuracy. In atomic calculations, of course, there is no need to use Gaussians since they offer no advantage over Slater functions. For molecules, however, mixed sets of the kind used in these calculations may provide a convenient and sufficiently accurate method to obtain energies and possibly other properties of interest as well. The success of Gaussian lobe functions in the description of angular correlation is especially gratifying since it is the *p* and higher Slater orbitals which prove most troublesome in molecular calculations.

Acknowledgements. G. B. Bacskay gratefully acknowledges the Research Scholarship from the Commonwealth Scientific and Industrial Research Organization (Australia).

Appendix 1

Evaluation of the Auxiliary Function $F_0(t)$

The auxiliary function $F_m(t)$ defined as

$$F_m(t) = \int_0^1 u^{2m} \exp(-t u^2)\, du \qquad (t > 0; m = 0, 1, 2, \ldots)$$

occurs in the nuclear attraction and electron repulsion integrals between Gaussian functions.

In case of 1*s* type Gaussians only $F_0(t)$ needs to be evaluated and the method used rests on the power series expansion [22]

$$F_0(t) = \exp(-t) \sum_{i=0}^{\infty} 2t^i/1 \times 3 \times 5 \ldots (2i+1) .$$

For $t \leqq 16$ the number of terms required in the summation is reasonably small ($\leqq 38$) to achieve the specified accuracy of one part per million, whereas for larger values of t it is possible to make use of the asymptotic expansion

$$\begin{aligned} F_0(t) &= \frac{\Gamma(1/2)}{2t^{1/2}} - \Phi_0(t) \\ &\approx \frac{\Gamma(1/2)}{2t^{1/2}} \quad \text{since} \quad \Phi_0(t) \leqq \frac{1}{2t} \exp(-t) . \end{aligned}$$

Hence $F_0(t) = \pi^{1/2}/2t^{1/2}$ which is accurate to more than six significant figures.

This method was found to be quite satisfactory, requiring, on the average, less than a millisecond comp. time.

Appendix 2

Exchange Integrals $[1S_A\,1S_B|1S_A\,1S_B]$, *Calculated by the Gaussian Expansion Technique, Compared with the Accurate Values* [28], *as a Funtion of the Internuclear Separation R. All Orbital Exponents are* 1.00

R (a.u.)	Number of Gaussians in expansion	Calculated value of integral	Accurate value of integral
1.0	4	0.436694	0.436651
	6	0.436653	
	8	0.436652	
	10	0.436652	
1.5	4	0.296836	0.296835
	6	0.296838	
	8	0.296836	
	10	0.296836	
3.0	4	0.058452	0.058508
	6	0.0585131	
	8	0.0585074	
	10	0.0585080	
5.0	4	0.00370653	0.00371704
	6	0.00371797	
	8	0.00371730	
	10	0.00371667	

The comp. times required to evaluate such integrals were 1.5, 7, 22 and 49 sec for the 4, 6, 8 and 10 Gaussian expansions respectively.

References

1. Zener, C.: Physic. Rev. **36**, 51 (1930).
2. Slater, J. C.: Physic. Rev. **36**, 57 (1930).
3. Duncanson, W. E., Coulson, C. A.: Proc. Roy. Soc. (Edinburgh) A **62**, 37 (1943).
4. Boys, S. F.: Proc. Roy. Soc. (London) A **200**, 542 (1950); A **201**, 125 (1950).
5. Kato, T.: Commun. Pure Appl. Math. **10**, 151 (1957).
6. Allen, L. C.: J. chem. Physics **31**, 736 (1958).
7. Riera, A., Linnett, J. W.: Theoret. chim. Acta (Berl.) **18**, 265 (1970).
8. Ruedenberg, K., Roothaan, C. C. J., Jaunzeins, W.: J. chem. Physics **24**, 201 (1955).
9. Roothaan, C. C. J.: J. chem. Physics **24**, 947 (1955).
10. — J. chem. Physics **19**, 1445 (1951).
11. O-ohata, K., Taketa, H., Huzinaga, S.: J. physic. Soc. Japan **21**, 2306 (1966).
12. Harrison, J. H. F.: J. chem. Physics **46**, 1115 (1967).
13. Courant, R., Hilbert, D.: Methods of mathematical physics, Vol. 1, p. 4. New York: Interscience Publishers Inc. 1970.
14. Löwdin, P. O.: J. chem. Physics **18**, 365 (1950); Adv. Physics **5**, 1 (1956).
15. Harris, F. E.: Computational methods of quantum chemistry, Quantum Chemistry Group, Uppsala University, Uppsala, Sweden, T 19 (1968).
16. Nesbet, R. K.: J. chem. Physics **43**, 311 (1965).
17. Löwdin, P. O.: Physic. Rev. **97**, 1474 (1955).
18. Coleman, A. J.: Rev. mod. Physics **35**, 668 (1963).
19. Schmidt, E.: Math. Ann. **63**, 433 (1907).
20. Löwdin, P. O.: Physic. Rev. **101**, 1730 (1955).
21. Powell, M. J. D.: The Computer Journal **7**, 155 (1964).
22. Shavitt, I.: Methods in computational physics, Alder, B., Fernbach, S., Rotenberg, M. (Ed.), Vol. 2, p. 16. New York: Academic Press 1963.
23. Schwartz, C.: Physic. Rev. **126**, 1015 (1962).
24. Roothaan, C. C. J., Sachs, L. M., Weiss, A. W.: Rev. mod. Physics **32**, 186 (1960).
25. Löwdin, P. O.: J. molecular Spectroscopy **3**, 46 (1959).
26. Taylor, G. R., Parr, R. G.: Proc. Natl. Acad. Sci., U.S. **38**, 154 (1952).
27. Pekeris, C. L.: Physic. Rev. **112**, 1649 (1958); **115**, 1216 (1959).
28. Hirschfelder, J. O., Linnett, J. W.: J. chem. Physics **18**, 130 (1950).

Prof. J. W. Linnett
University of Cambridge
Department of Physical Chemistry
Lensfield Road
Cambridge 56491, England

Theoret. chim. Acta (Berl.) 26, 15—21 (1972)
© by Springer-Verlag 1972

Mixed Basis Functions in Molecular Quantum Mechanics

II. A Study of the H_2 Molecule

G. B. BACSKAY and J. W. LINNETT
Department of Physical Chemistry, Cambridge, England

Received February 3, 1972

A series of calculations for the ground state of the H_2 molecule are reported, using full configuration interaction method and a mixed orbital basis of 1*s* Slater and floating spherical Gaussian functions. The results obtained compare favourably with the results of previous H_2 calculations using pure Slater type orbital bases.

Es wird über eine Reihe von Rechnungen für den Grundzustand des H_2-Moleküls berichtet, bei denen eine Methode mit vollständiger Konfigurationswechselwirkung und eine gemischte Orbitalbasis aus 1*s* Slater- und "floating" sphärischen Gauß-Orbitalen benutzt wird. Man erhält Resultate, die mit Ergebnissen von Rechnungen an H_2 mit Hilfe von Orbitalbasen reinen Slater-Typs vergleichbar sind.

Introduction

In the first paper of this series [1] the main ideas underlying the use of mixed basis sets were outlined as well as the basic computational methods. The results of some simple preliminary calculations on the He atom were also discussed.

In the present paper the results of a series of calculations on the H_2 molecule are summarized. This molecule is also treated in part as a test case. The basis sets consist of two 1*s*-type Slater orbitals on each nucleus and various combinations of spherical Gaussians positioned so as to be most effective as expansion functions. The calculations are of the full configuration interaction type within the framework of the Born-Oppenheimer approximation, for the ground state ($^1\Sigma_g$) of the H_2 molecule.

Calculations and Results

The details of the basis functions and the resulting energy terms are summarized in Tables 1 and 2, while in Figs. 1–4 the spatial arrangement of the Gaussian orbitals is shown. The first calculation, using a 1*s*, 1*s*′ STO-basis is identical to one reported by Shavitt *et al.* [2]. Since this basic set of four Slater functions was retained throughout all the other calculations the internuclear separation was kept constant at 1.4148 a.u. All the orbital exponents were optimized by Powell's method [3] in calculations Refs. [1] and [2], whereas in Refs. [3] and [4] the exponents of the STO's were kept constant at their previously determined optimum value. In calculations Refs. [6–9] only the exponents of

Table 1. The orbital bases used in the various H_2 calculations ($1S$ = 1s-type Slater orbital, G = spherical Gaussian function)

Calculation Ref.	Number of basis functions	Number of configurations	Orbital basis, exponents and position of orbitals
1	4	6	$1S_A = 1S_B = 1.122$, $1S_{A'} = 1S_B = 1.386$
2	5	9	$1S_A = 1S_B = 1.089$, $1S_{A'} = 1S_B = 1.616$, $G_1 = 1.073$
3	6	12	$1S_A = 1S_B = 1.089$, $1S_{A'} = 1S_{B'} = 1.616$, $G_2 = G_3 = 1.115$, $d = 0.698$
4	6	13	$1S_A = 1S_B = 1.089$, $1S_{A'} = 1S_{B'} = 1.616$, $G_1 = 1.277$, $G_2 = 0.344$, $d = 0.7074$
5	7	16	$1S_A = 1S_B = 1.089$, $1S_A = 1S_{B'} = 1.616$, $G_1 = 0.777$, $G_2 = G_3 = 0.655$, $d = 0.655$
6	9	16	$1S_A = 1S_B = 1.089$, $1S_{A'} = 1S_{B'} = 1.616$, $G_1 = 1.073$, $G_2 = G_3 = G_4 = G_5 = 0.570$
7	11	18	$1S_A = 1S_B = 1.089$, $1S_{A'} = 1S_B = 1.616$, $G_1 = 1.073$, $G_2 = G_3 = G_4 = G_5 = G_6 = G_7 = 0.600$
8	13	13	$1S_A = 1S_B = 1.089$, $1S_{A'} = 1S_{B'} = 1.616$, $G_1 = 1.073$, $G_2 = G_3 = G_4 = G_5 = G_6 = G_7 = G_8 = G_9 = 0.600$
9	13	22	as for calculation Ref. [8]

Table 2. Summary of the H_2 calculations together with some "exact" results for comparison purposes

Calculation Ref.	Number of basis functions	Number of configurations	Total energy	Kinetic energy	Nuclear attraction energy	Electron repulsion energy	Energy of truncated NO expansion	Apparent correlation energy
1	4	6	−1.15279	1.15287	−3.61624	0.60376	−1.12805	−0.02474
2	5	9	−1.15898	1.15881	−3.62954	0.60493	−1.13209	−0.02689
3	6	12	−1.15923	1.16025	−3.63101	0.60472	−1.13208	−0.02715
4	6	13	−1.15953	1.16061	−3.63345	0.60649	−1.13241	−0.02712
5	7	16	−1.16003	1.15692	−3.62702	0.60325	−1.13260	−0.02743
6	9	16	−1.16865	1.16240	−3.62912	0.58966	−1.13223	−0.03642
7	11	18	−1.16883	1.16465	−3.62981	0.58952	−1.13222	−0.03661
8	13	13	−1.16882	1.16420	−3.62764	0.58781	−1.13210	−0.03672
9	13	22	−1.16992	1.16535	−3.62981	0.58773	−1.13215	−0.03777
"Exact" [5]			−1.174474					−0.040845
SCF calculation [6]			−1.133630				−1.133630	

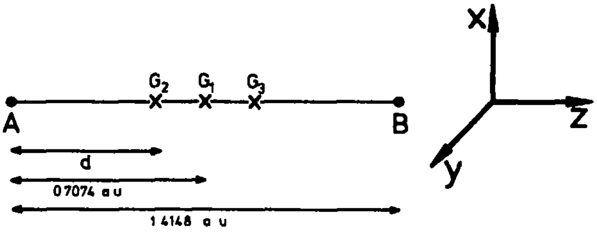

Fig. 1. Positions of the Gaussians in the 5, 6 and 7 orbital H_2 calculations [2-5]

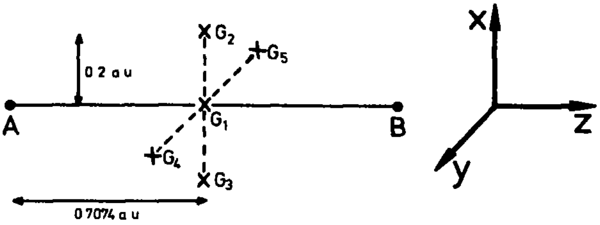

Fig. 2. Positions of the Gaussians in the 9 orbital H_2 calculation [6]

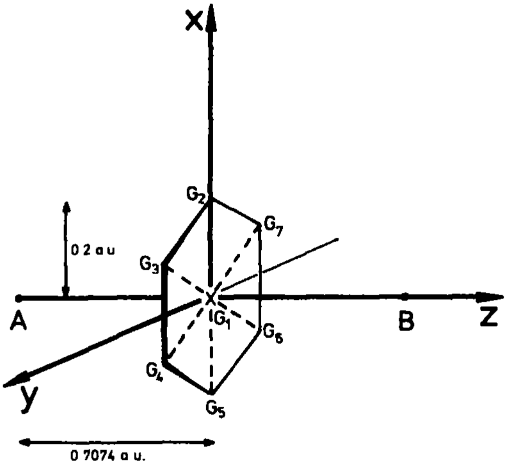

Fig. 3. Positions of the Gaussians in the 11 orbital H_2 calculation [7]

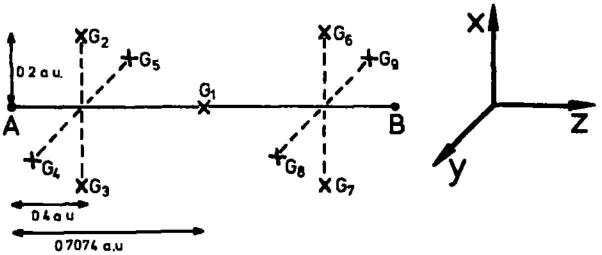

Fig. 4. Positions of the Gaussians in the 13 orbital H_2 calculations [8, 9]

able 3. The wavefunction expressed in natural form from the 13 orbital, 22 configuration H_2 calculation,
representations of the D_{4h} point group, giving

Coefficient of configuration $\chi_i(1)\chi_i(2)$	Natural orbital χ_i and its symmetry	Coefficient of atomic orbital				
		S_A	$S_{A'}$	S_B	$S_{B'}$	G_1
0.990962	1 a_{1g} (σ_g)	0.440248	0.076852	0.440248	0.076852	0.0494
0.105193	2 a_{2u} (σ_u)	0.845793	0.115353	−0.845793	−0.115353	0.0
0.056139	3 a_{1g} (σ_g)	−1.274842	0.852074	−1.274842	0.852074	0.6627
0.041081	4 e_{1u_x} (π_{u_x})	0.0	0.0	0.0	0.0	0.0
0.041081	5 e_{1u_y} (π_{u_y})	0.0	0.0	0.0	0.0	0.0
0.009842	6 a_{2u} (σ_u)	−4.237023	3.268382	4.237023	−3.268382	0.0
0.008768	7 e_{1g_x} (π_{g_x})	0.0	0.0	0.0	0.0	0.0
0.008768	8 e_{1g_y} (π_{g_y})	0.0	0.0	0.0	0.0	0.0
0.007305	9 a_{1g} (σ_g)	−1.722984	2.533367	−1.722984	2.533367	−2.8160
0.006635	10 b_{1g} (Δ_g)	0.0	0.0	0.0	0.0	0.0
0.006049	11 a_{1g} (σ_g)	−0.226189	−1.814420	−0.226189	−1.814420	−1.7868
0.003339	12 b_{1u} (Δ_u)	0.0	0.0	0.0	0.0	0.0
0.002578	13 a_{2u} (σ_u)	−1.844571	−2.184451	1.844571	2.189451	0.0

the off-axial Gaussians were optimized, while their distance from the molecular axis was kept constant at 0.2 a.u., this value having been found reasonable in our He calculations [1]. In calculation Ref. [8] the positions of the two sets of 4 Gaussians along the molecular axis were also determined so as to minimize the total energy. Full optimization of all non-linear parameters was not undertaken because of the limited computer time available for this work.

All the calculations were of the full configuration interaction type, the configurations constructed from a Löwdin orthonormalized set of symmetry orbitals, the point group of the molecule taken as $D_{\infty h}$ in all the calculations which use only σ-type orbitals. In calculations Refs. [6, 8, 9], i.e. when off-axial Gaussians were used as well, the point group of the molecule was taken to be D_{4h}, although the Gaussian lobe functions have close resemblance to the π- and Δ-type symmetry orbitals. Calculation Ref. [7] is more novel, since 6 Gaussians were placed around the molecular axis, forming a regular hexagon. The symmetry orbitals formed transform according to the irreducible representations of the D_{6h} point group. Calculations Refs. [8] and [9] differ inasmuch as the former makes use of only the π-type Gaussian lobe functions, whereas in calculation Ref. [9] the σ_g-, σ_u-, Δ_g- and Δ_u-type functions are included in the symmetry orbital basis. The wavefunctions were transformed to natural form, followed by the calculation of the energy corresponding to the dominant term in the expansion, furnishing an estimate of the SCF-energy as well as the apparent correlation energy, a concept introduced earlier [1].

The wavefunction, expressed in terms of natural orbitals, corresponding to the best H_2 energy, i.e. resulting from calculation Ref. [9], is presented in Table 3. The natural orbital expansion takes the form

$$\Psi = 2^{-1/2}(\alpha\beta - \beta\alpha) \sum_{i=1}^{13} C_i \chi_i(1) \chi_i(2), \qquad (1)$$

ral orbitals given in terms of the original basis. The orbitals are classified according to the irreducible :kets, the symmetry types they are to represent

fficient of atomic orbital							
	G_3	G_4	G_5	G_6	G_7	G_8	G_9
2508	0.002508	0.002508	0.002508	0.002508	0.002508	0.002508	0.002508
42161	0.142161	0.142161	0.142161	−0.142161	−0.142161	−0.142161	−0.142161
53444	0.053444	0.053444	0.053444	0.053444	0.053444	0.053444	0.053444
78757	−1.678757	0.0	0.0	1.678757	−1.678757	0.0	0.0
	0.0	1.678757	−1.678757	0.0	0.0	1.678757	−1.678757
26515	0.026515	0.026515	0.026515	−0.026515	−0.026515	−0.026515	−0.026515
54087	−7.054087	0.0	0.0	−7.054087	7.054087	0.0	0.0
	0.0	7.054087	−7.054087	0.0	0.0	−7.054087	7.054087
61080	0.161080	0.161080	0.161080	0.161080	0.161080	0.161080	0.161080
3659	10.83659	−10.83659	−10.83659	10.83659	10.83659	−10.83659	−10.83659
83154	0.683154	0.683154	0.683154	0.683154	0.683154	0.683154	0.683154
350	45.5350	−45.5350	−45.5350	−45.5350	−45.5350	45.5350	45.5350
60308	1.960308	1.960308	1.960308	−1.960308	−1.960308	−1.960308	−1.960308

where $\{\chi_i\}$ is the set of natural orbitals and $\{C_i\}$ is the set of coefficients, related to the occupation numbers of the NO's [1].

The wavefunctions from the other calculations are given elsewhere[1] [4].

Discussion

The addition of a single Gaussian to the four orbital basis results in a considerable lowering of the total energy, almost 4 kcal/mole, mostly as a result of the decrease in the nuclear attraction energy. Evidently the Gaussian has very successfully corrected the electron distribution in the molecule, which also shows up as an improvement in the energy of the dominant term of the natural orbital expansion. The decrease in the apparent correlation energy is less, indicating less improvement in the correlation part of the wavefunction than in the SCF part. The total energy −1.15898 a.u. compares favourably with the value −1.1591 a.u., calculated by Gianinetti *et al.*, who used a 1*s*, 2*s*, 2*p* STO-basis, 6 functions altogether [7]. Our six orbital calculations Refs. [3] and [4] are energetically superior to Gianinetti's calculation, although only marginally so. The result of the 7 orbital calculation [5], i.e. an energy of −1.16003 a.u., is to be compared with the estimated Σ limit of −1.160868 a.u. [8]. The discrepancy, ~1/2 kcal/mole, is small, considering the limited basis that was employed in this calculation. The SCF energy, as estimated by the energy of the truncated NO expansion, −1.13260 a.u., is in error by ~2/3 kcal/mole. The apparent correlation energy is, however, lower than the accurately calculated Σ correlation energy. As stated before [1], the apparent correlation energy, as defined, is not an upper bound to the true correlation energy, hence it needs to be used with some caution. It is interesting that all three Gaussians need to be in the internuclear region in order to minimize the total energy, indicating that the electron distribution needs most modification in that region and also that electron correlation is more important there. Originally two Gaussians were placed outside the internuclear region in an attempt to simulate the behaviour of two $2p_z$-type orbitals. This arrangement, however, proved inferior to the one described above. It would be interesting to investigate whether a 1*s*, 2*s*, 2*p* STO basis could be more successful if the *p* orbitals were allowed to float.

---

[1] The individual wavefunctions, expressed in terms of natural orbitals, are available from G. B. Bacskay, on request.

The introduction of π- and Δ-type Gaussian lobe functions bring about considerable improvement in the energy, mainly as a result of more electron correlation being allowed for. This is also manifested in the lowered electron repulsion energy. Our best energy, -1.16992 a.u., from calculation Ref. [9], is to be compared with the value -1.16959 a.u., calculated by Shavitt *et al.* [2], using a full 1*s*, 1*s*′, 2*p* STO-basis. The results of calculation Ref. [7], using 11 functions, with six Gaussians hexagonally around the molecular axis, are only as good as the results of the 13 orbital, 13 configuration calculation [8]. Consequently this approach of placing many Gaussians close together was not explored any further. Signs of approximate linear dependency also appeared in this calculation although no round-off errors are thought to be present in the results reported here. A comparison of the results from calculations Refs. [8] and [9] reveals that, although the π_u orbitals are the most important among the Gaussian lobe functions, the others also make a significant contribution to the wavefunction. The occupation numbers of the Δ_g and the extra σ_g orbitals, as inferred from the coefficients in Table 3, are fairly high, as expected.

Conclusion

The results of the various H_2 calculations have demonstrated that mixed basis sets containing both Slater and Gaussian type functions can provide just as satisfactory convergence as the more conventional STO bases.

The advantage of a mixed basis set is, however, the relative ease with which the basic integrals are evaluated. An increase in the size of the basis presents no problems other than the computer storage and manipulation of the large arrays that arise in the course of the calculations. With STO bases the introduction of atomic orbitals, higher than 2*p*, involves so much extra effort as to prevent their extensive use in molecular calculations. The largest single H_2 calculation reported here, i.e. the 13 orbital, 22 configuration one, required approximately 7 min comp. time, and a total store of 40K on the Cambridge University Computer Laboratory's Titan computer – this comp. time being equivalent to less than 1 min on the more modern third generation computers.

A further advantage of the Gaussians as correction functions is that they can be allowed to float, i.e. be spatially positioned so as to be most effective, without any added computational problems. Hence strong localization of these correction functions is easily achieved.

In order to improve the 13 orbital wavefunction for H_2 two or more Gaussians placed along the molecular axis should be added to the basis, so as to obtain a better Σ limit than that of the 5 orbital calculation [2]. To improve the angular correlation more π- and Δ-type Gaussian lobe functions are needed. It is probable that φ-type functions would be much less important, as Davidson and Jones [9] obtained an energy of −1.173044 a.u. with the use of 10 natural orbitals, none of them higher than Δ.

Acknowledgements. G. B. Bacskay gratefully acknowledges the Research Scholarship from the Commonwealth Scientific and Industrial Research Organization (Australia).

References

1. Bacskay, G. B., Linnett, J. W.: Theoret. chim. Acta (Berl.) **26**, 1 13 (1972).
2. Shavitt, I., Stevens, R. M., Minn, F. L., Karplus, M.: J. chem. Physics. **48**, 2700 (1968).
3. Powell, M. J. D.: The computer Journal 7, 155 (1964).
4. Bacskay, G. B.: Mixed basis functions in molecular quantum mechanics. Ph. D. Thesis, Cambridge 1971.
5. Kolos, W., Wolniewicz, L.: J. chem. Physics **49**, 404 (1968).
6. -- Roothaan, C. C. J.: Rev. mod. Physics **32**, 205 (1960).
7. Gianinetti, A., Majorino, G. F., Rusconi, E., Simonetta, M.: Int. J. quant. Chemistry **3**, 45 (1969).
8. Hagstrum, S., Shull, H.: Rev. mod. Physics **35**, 624 (1963).
9. Davidson, E. R., Jones, L. L.: J. chem. Physics **37**, 2966 (1962).

Prof. J. W. Linnett
University of Cambridge
Department of Physical Chemistry
Lensfield Road
Cambridge 56491, England

Theoret. chim. Acta (Berl.) 26, 23—32 (1972)
© by Springer-Verlag 1972

Mixed Basis Functions in Molecular Quantum Mechanics

III. The Linear Symmetric H_3 Molecule

G. B. BACSKAY and J. W. LINNETT
Department of Physical Chemistry, Cambridge, England

Received February 3, 1972

A series of calculations have been carried out for the linear symmetric H_3 molecule using configuration interaction wavefunctions constructed from a mixed set of 1*s* Slater and floating spherical Gaussian functions. The results, although they do not surpass the best CI results reported in the literature, are sufficiently good to encourage further work along these lines.

Es wurde eine Reihe von Rechnungen für das lineare, symmetrische H_3-Molekül durchgeführt, bei denen Wellenfunktionen mit Konfigurations-Wechselwirkung verwendet werden, die aus einem gemischten Satz von 1*s* Slater- und "floating" sphärischen Gauß-Funktionen konstruiert wurden. Obwohl die Resultate die besten CI Ergebnisse, über die in der Literatur berichtet wird, nicht übertreffen, sind sie so gut, daß sie zu weiterer Arbeit nach dieser Methode ermutigen.

Introduction

H_3 is a system of considerable interests to chemists since it is the activated complex of the exchange reaction

$$H + H_2 \rightleftarrows H_2 + H,$$

which is the simplest chemical reaction involving a transition state and as such it ought to be the easiest to investigate theoretically.

Experimental estimates of the activation energy, defined as the energy difference between H_3 and $H_2 + H$, range between 7 and 10 kcal/mole. The recent kinetic experiments of Le Roy and co-workers [1] point to an activation energy of 9.2 kcal/mole, whereas the more direct measurements of Kuppermann and White [2] yield a value of 7.6 ± 0.5 kcal/mole. One of the main difficulties associated with the experimental determination of the classical barrier height is the effect of quantum mechanical tunnelling, making the relationship of barrièr height to experimental activation energy very complex. In this paper the term activation energy will be used to mean the classical barrier height.

The first *ab initio* calculation for H_3 was carried out by Hirschfelder, Eyring and Rosen [3], using configuration interaction techniques with a basis of three 1*s* Slater orbitals with identical orbital exponents, one on each nucleus. The estimated activation energy was 25 kcal/mole, the H_2 energy being obtained by the use of a comparable wavefunction, i.e. constructed from two 1*s* STO's. Enlargement of the 1*s* Slater basis by three more 1*s* STO's resulted in an activation energy of 14.8 kcal/mole, this calculation carried out by Boys and Shavitt [4].

The inclusions of $2p$ orbitals in the basis yielded 11 kcal/mole for the activation energy [5], this being the best CI result so far. The lowest activation energy yet calculated was obtained by Contoy and Bruner [6], 7.7 kcal/mole, with error limits estimated to be ± 1.2 kcal/mole, using a correlated wavefunction. The calculated energy of H_3 was -1.6621 ± 0.002 a.u., which, however, is not an upper bound to the true energy. The calculated upper bound is -1.6551 a.u. which results in an upper bound of 12.1 kcal/mole for the activation energy. The best CI calculation using a Gaussian basis has been carried out by Edmiston and Krauss [7], who have obtained an activation energy of 13.5 kcal/mole.

The main obstacles encountered in variational calculations for a system as complex as H_3 are the problem of integral evaluation and the large number of configurations that need to be included in CI expressions, even in the case of moderately sized basis sets. In the work reported here the problem of integrals was made tractable by the use of mixed bases, containing a small number of $1s$ STO's, and floating spherical Gaussian functions. Mixed bases of this type have already been used for H_3 successfully by Riera and Linnett [8]. To avoid the lengthy CI expansions natural orbitals were used to construct the configurations, resulting in compact wavefunctions, quite easy to manage.

It has been established by other workers that the optimum geometry is the linear symmetric one, hence only this geometry was considered in the present work.

Calculations and Results

A series of configuration interaction calculations were carried out for the linear, equidistant system of three interacting hydrogen atoms, in an attempt to obtain a good upper bound to the ground state energy, in the Born-Oppenheimer approximation. The basic computational methods have been outlined elsewhere [9], so here only the construction of 3-electron configuration interaction wavefunctions and the calculation of the Hamiltonian matrix elements will be discussed.

The configurations included in a given wavefunction are constructed from an orthonormal set of symmetry orbitals, each configuration with the symmetry of the ground state of H_3, viz. $^2\Sigma_u^+$. The configurations are divided into three types:

$$\left.\begin{aligned} \Phi^1 &= (iij)^1 = |i\bar{i}j| \\ \Phi^2 &= (ijk)^2 = 6^{-1/2}\{-|i\bar{j}k| + |j\bar{i}k| - 2|i\bar{k}j|\} \\ \Phi^3 &= (ijk)^3 = 2^{-1/2}\{|i\bar{j}k| + |j\bar{i}k|\} \end{aligned}\right\}. \tag{1}$$

where $|i\bar{j}k|$ denotes a normalized Slater determinant constructed from the spin orbitals i, j, k; the bar denoting β spin associated with orbital j, opposed to α spin for orbitals i and k.

The total wavefunction is hence written as

$$\Psi = \sum_i C_i \Phi_i^k, \tag{2}$$

where $\{C_i\}$ is a set of coefficients which minimize the total electronic energy, the superscript k denoting the type of the configuration Φ_i.

The matrix elements of the Hamiltonian matrix,

$$H_{ij} = \langle \Phi_i^k | \mathscr{H} | \Phi_j^l \rangle, \tag{3}$$

where $\mathscr{H}$ is the Hamiltonian operator, were evaluated by a modified version of Kotani's method [10]. Let

$$\Phi_i^k = (i_1\, i_2\, i_3)^k$$

and

$$\Phi_j^l = (j_1\, j_2\, j_3)^l .$$

The matrix elements can then be calculated by the use of the equation

$$H_{ij} = \sum_P \langle i_1(1)\, i_2(2)\, i_3(3) | \mathscr{H}\mathscr{P} | j_1(1)\, j_2(2)\, j_3(3) \rangle\, U(P)_{kl}, \tag{4}$$

where $\mathscr{P}$ is the permutation operator acting on the electronic coordinates and $U(P)_{kl}$ is a coefficient which arises as a result of integration over the spin variables.

For each permutation $U(P)$ is a 3×3 matrix corresponding to the three types of configurations. The 2×2 matrix which results if the first column and the first row are omitted is the spin representation matrix, as given by Kotani [10], for the two linearly independent spin eigenfunctions obtained by the Geneological (or Branching Diagram) method. The $U(P)$ matrices are listed in the Appendix.

After the calculation of the energy and the wavefunction the spinless first order density matrix was calculated using the following method. The density matrix we want is given as

$$\gamma(1|1') = 3 \sum_{i,j} C_i C_j^* \int \Phi_i^k \Phi_j^{l*}\, d\tau_2\, d\tau_3\, d\sigma_1\, d\sigma_2\, d\sigma_3 , \tag{5}$$

where integration is to be carried out over all coordinates except the spatial coordinates of electron 1.

After integration the following equation is obtained:

$$\gamma(1|1') = \sum_{i,j} C_i C_j^* \sum_P U(P)_{kl} \sum_{m=1}^{3} i_m(1)\, j_m(1') \prod_{n \neq m}^{3} \delta_{i_n j_n} . \tag{6}$$

Hence the spinless first order reduced density matrix can be expressed in the form

$$\gamma(1|1') = \sum_{i,j} \gamma_{ij}\, \varphi_i(1)\, \varphi_j^*(1'), \tag{7}$$

where γ_{ij} is the sum of coefficients arising from the summations in Eq. (6).

The matrix γ is then diagonalized, yielding the natural orbitals and their occupation numbers.

Table 1. The orbital bases used in the various H_3 calculations ($1S$ = 1s-type Slater orbital. G = Spherical Gaussian function)

Calculation Ref.	Number of basis functions	Number of configurations	Orbital basis and exponents
1	6	34	$1S_A = 1S_C = 0.957$. $1S_B = 0.899$. $1S_A = 1S_C = 1.189$. $1S_B = 1.238$
2	8	83	STO basis as for calculation 1 + $G_1 = G_2 = 1.00$
3	8	28	as for calculation 2
4	8	75	as for calculation 2
5	12	32	STO basis as for calculation 1 + $G_1 = G_2 = 1.00$. $G_3 = G_4 = G_5 = G_6 = 0.45$
6	16	43	STO basis as for calculation 1 + $G_1 = G_2 = 1.00$. $G_3 = G_4 = \cdots = G_{10} = 0.45$
7	20	62	STO basis as for calculation 1 + $G_1 = G_2 = 1.00$. $G_3 = G_4 = \cdots = G_{14} = 0.45$
8	20	169	as for calculation 6

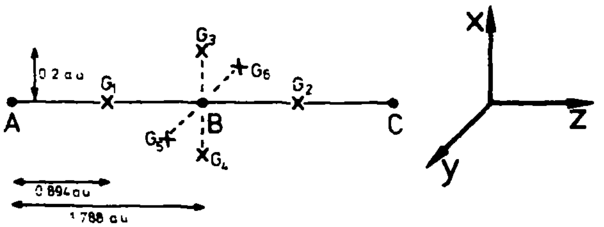

Fig. 1. Positions of the Gaussians in the 8 and 12 orbital H_3 calculations [2-5]

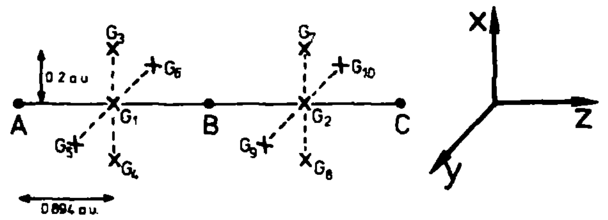

Fig. 2. Positions of the Gaussians in the 16 orbital H_3 calculation [6]

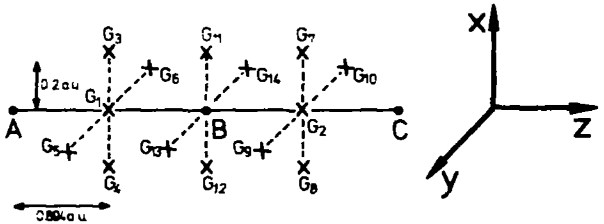

Fig. 3. Positions of the Gaussians in the 20 orbital H_3 calculations [7, 8]

The basis functions used in the various calculations are summarized in Table 1, the spatial arrangement of the Gaussians being shown in Figs. 1–3. The resulting energy terms are presented in Table 2.

Our first calculation is identical to one of Shavitt's [5] H_3 calculations, the STO basis containing six $1s$ type orbitals proved a very convenient starting point, just as in the H_2 calculations [11]. In the subsequent calculations this basis was enlarged by Gaussians only, keeping the internuclear separation constant at 1.788 a.u., this being the optimum distance in calculation Ref. [1].

Calculations Refs. [2, 3, and 4] employ the 6 orbital Slater basis enlarged by two Gaussians, both placed along the molecular axis, halfway between each pair of adjacent nuclei respectively (see Fig. 1). The exponent was chosen as 1.00 on the basis of an analogous H_2 calculation [11] and the results of Riera and Linnett [8]. The first 8 orbital wavefunction was of the full CI type, including all possible configurations, totalling 83, constructed from a Schmidt orthonormalized set of σ_g- and σ_u-type symmetry orbitals. Once the natural orbitals were available the calculation was repeated using the same number of configurations, now built from the NO set. The natural orbitals and their occupation numbers from this calculation are presented in Table 3. In the next calculation Ref. [3] the CI expansion was shortened to include only 28 configurations, those with the highest coefficients from the set of 83. The resultant energy is only 0.16 kcal/mole higher than the energy corresponding to the full CI wavefunction, a numerical illustration of the good convergence properties of natural orbitals. To put the 8 orbital calculations in perspective with similar calculations using STO bases a further calculation Ref. [4] was carried out. From the CI expansion all configurations of the form $(\sigma_u\sigma_u\sigma_u)$ were omitted, leaving 75 $(\sigma_g\sigma_g\sigma_u)$ types. The energy, -1.63415 a.u., is to be compared with the energy -1.6343 a.u., calculated by Gianinetti *et al.* [12], using a 9 orbital basis consisting of $1s$, $2s$ and $2p_\sigma$ type Slater functions. The two results show the same degree of agreement as the analogous H_2 results [11]. Consequently, significant improvement in the energy seemed unlikely, were the orbital exponents or the positions of the Gaussians allowed to vary. Thus no attempt was made to optimize any non-linear parameters at this stage.

Next the orbital basis was enlarged so as to include functions with angular dependence, i.e. linear combinations of off-axial Gaussians (calculations Refs. [5–8]). The symmetry orbitals formed from these additional Gaussians transform as the irreducible representations of the D_{4h} point group. After the Schmidt orthogonalization of these symmetry orbitals to the σ-type natural orbitals of calculation Ref. [2], CI wavefunctions of various lengths, which, however, always included the 28 basic $(\sigma\sigma\sigma)$ configurations, were constructed and used to calculate the energy. In calculation Ref. [5], 32 configurations were found to contribute significantly to the wavefunction; in calculations Refs. [6] and [7] this number became 43 and 62 respectively. The positions of the off-axial Gaussians were fixed as shown in Figs. 1–3, but their orbital exponents were optimized in calculations Refs. [5] and [6]. Although the orbital basis for calculations Refs. [7] and [8] consisted of 20 functions, the set of orthonormal molecular orbitals which were used for the construction of configurations contained only 16 orbitals, listed in Table 4. Tests showed that the omitted

Table 2. Summary of the results of the various H_3 calculations (all energies given in a.u.) for a constant internuclear separation of 1.788 a.u., together with the resulting activation energies; the energy of H_2 obtained from an "analogous" calculation [11]. Some literature values are also given for comparison purposes

Calculation Ref.	Number of basis functions	Number of configurations	Total energy	Kinetic energy	Nuclear attraction energy	Electron repulsion energy	Energy of dominant configuration	Apparent correlation energy	Activation energy (kcal mole)	"Analogous" H_2 calculation [11]
1	6	34	−1.63051	1.62994	−5.91530	1.25664	−1.58874	−0.04177	14.01	1
2	8	83	−1.63913	1.63786	−5.93409	1.25888	−1.59247	−0.04666	12.48	2
3	8	28	−1.63885	1.63976	−5.93639	1.25957	−1.59247	−0.04538		
4	8	75	−1.63415	1.63418	−5.93419	1.26765	−1.59247	−0.04168		
5	12	32	−1.64468	1.63901	−5.93216	1.25026	−1.59247	−0.05221		
6	16	43	−1.65075	−1.64120	−5.92818	1.23802	−1.59247	−0.05828	11.26	6
7	20	62	−1.65126	1.64077	−5.92685	1.23661	−1.59247	−0.05879	11.11	8
8	20	169	−1.65170	1.63933	−5.92547	1.23623	−1.59247	−0.05923	10.83	8
1s, 1s′, 2p STO basis, 176 configurations [5]			−1.65207						11.02	
Extensive Gaussian basis, limited CI calculation [7]			−1.6493						13.5	
Correlated wavefunction [6]			−1.6621 ± 0.0002						7.7 ± 1.2	

Table 3. Natural orbitals resulting from the 8 orbital, 83 configuration H_3 calculation, expressed in terms of the original basis, and their occupation numbers

Natural orbital and its symmetry	Occupation number	Coefficient of atomic orbital							
		$1S_A$	$1S_B$	$1S_C$	$1S_{A'}$	$1S_{B'}$	$1S_{C'}$	G_1	G_2
6 σ_g	1.95543	−0.071980	0.222910	−0.071980	0.388138	0.333717	0.388138	0.029482	0.029482
2 σ_u	0.999075	0.843834	0.0	−0.843834	−0.031866	0.0	0.031866	0.028977	−0.028977
4 σ_g	0.034023	0.951084	−1.719274	0.951084	0.200340	−0.019901	0.200340	−0.025052	−0.025052
5 σ_u	0.005327	−3.555260	0.0	3.555260	3.038208	0.0	−3.038208	0.512052	−0.512052
3 σ_g	0.005000	0.103535	3.429927	0.103535	−0.504551	−2.357188	0.504551	−0.419680	−0.419680
8 σ_u	0.000642	4.062570	0.0	−4.062570	−4.448283	0.0	4.448283	1.006045	−1.006045
1 σ_g	0.000433	7.020820	−9.900747	7.020820	−5.314858	7.694885	−5.314858	−0.440515	−0.440515
7 σ_g	0.000057	3.837769	0.444749	3.837769	−4.010764	−2.937294	−4.010764	1.723347	1.723347

Table 4. The orthonormal molecular orbital basis set $\{\varphi_i\}$ used in the 20 orbital H_3 calculations

$\varphi_1, \varphi_2, \ldots, \varphi_6$	are identical to the σ-type natural orbitals 1, 2…6 as listed in Table 3.	
φ_7	is identical to orbital 8 from Table 3.	
$\varphi_8 =$	$2.18046\,(G_3 - G_4 + G_7 - G_8)$	$e_{1u_x}\,(\pi_{u_x})$
$\varphi_9 =$	$2.18046\,(G_5 - G_6 + G_9 - G_{10})$	$e_{1u_y}\,(\pi_{u_y})$
$\varphi_{10} =$	$3.71273\,(G_3 - G_4 - G_7 + G_8)$	$e_{1g_x}\,(\pi_{g_x})$
$\varphi_{11} =$	$3.71273\,(G_5 - G_6 - G_9 + G_{10})$	$e_{1g_y}\,(\pi_{g_y})$
$\varphi_{12} =$	$16.2523\,(G_3 + G_4 - G_5 - G_6 + G_7 + G_8 - G_9 - G_{10})$	$b_{1g}\,(\Delta_g)$
$\varphi_{13} =$	$27.6738\,(G_3 + G_4 - G_5 - G_6 - G_7 - G_8 + G_9 + G_{10})$	$b_{1u}\,(\Delta_u)$
$\varphi_{14} =$	$-8.52780\,(G_3 - G_4 + G_7 - G_8) + 15.1800\,(G_{11} - G_{12})$	$e_{1u_x}\,(\pi_{u_x})$
$\varphi_{15} =$	$-8.52780\,(G_5 - G_6 + G_9 - G_{10}) + 15.1800\,(G_{13} - G_{14})$	$e_{1u_y}\,(\pi_{u_y})$
$\varphi_{16} =$	$3.83114\,(S_A + S_C) - 4.19685\,S_B - 2.79921\,(S_{A'} + S_{C'})$ $- 2.52582\,S_{B'} - 0.611406\,(G_1 + G_2)$ $+ 1.52691\,(G_{11} + G_{12} + G_{14})$	$a_{1g}\,(\sigma_g)$

Table 5. Occupation numbers of the natural orbitals from the 20 orbital, 62 configuration H_3 calculation

Natural orbital	Occupation number
6 σ_g	1.949173
2 σ_u	0.997099
4 σ_g	0.031928
5 σ_u	0.005044
3 σ_g	0.004892
8 π_{u_x}	0.003876
9 π_{u_y}	0.003876
10 π_{g_x}	0.001386
11 π_{g_y}	0.001386
7 σ_u	0.000544
1 σ_g	0.000339
14 π_{u_x}	0.000137
15 π_{u_y}	0.000137
12 Δ_g	0.000089
13 Δ_u	0.000050
16 σ_g	0.000039

orbitals would make an extremely small contribution to the wavefunction, their absence, however, reduced the computer time and store requirements for the transformation of integrals significantly. The final calculation Ref. [8] was a full CI treatment, using the 16 molecular orbitals of calculation Ref. [7]. The occupation numbers, resulting from the diagonalization of the spinless first order reduced density matrix calculated from the 62 configuration wavefunction, are given in Table 5. The configurations and their coefficients, also from calculation Ref. [7], are listed in Table 6. The wavefunctions resulting from any of the other calculations are given elsewhere [13][1].

The computational work was performed on the Cambridge University Computer Laboratory's Titan computer, details about which are given elsewhere

---

[1] The wavefunctions are available from G. B. Bacskay on request.

Table 6. Configurations and their coefficients, arranged in decreasing order, from the 20 orbital, 62 configuration H_3 calculation

Configuration		Coefficient	Configuration		Coefficient
Orbitals	Type		Orbitals	Type	
6 6 2	1	0.980958	8 10 6	2	0.011278
2 4 6	3	0.121686	9 11 6	2	0.011278
4 4 2	1	−0.073486	1 5 6	3	−0.010954
2 4 6	2	0.067037	2 3 6	2	−0.009617
2 2 5	1	0.040059	1 2 4	3	−0.009531
8 8 2	1	−0.038157	1 1 2	1	−0.008263
9 9 2	1	−0.038157	7 7 2	1	−0.008026
3 5 6	3	−0.034093	10 14 6	3	−0.007432
3 3 2	1	−0.031874	11 15 6	3	−0.007432
8 10 6	3	0.028271	4 5 6	3	0.007096
9 11 6	3	0.028271	2 5 7	2	−0.007028
2 3 6	3	−0.027147	2 2 7	1	−0.005982
5 5 2	1	−0.025171	12 12 2	1	−0.005434
4 5 6	2	−0.024091	14 14 2	1	−0.005234
2 3 4	2	−0.021463	15 15 2	1	−0.005234
2 3 4	3	0.014663	12 13 6	3	0.005232
10 10 2	1	−0.013307	8 10 4	3	0.005028
11 11 2	1	−0.013307	9 11 4	3	0.005028
4 6 7	2	0.012703	3 4 5	2	0.004925
3 5 6	2	−0.012543	10 14 6	2	−0.004377
4 6 7	3	0.012381	3 4 5	3	0.004345
11 15 6	2	−0.004377	8 14 2	3	−0.001552
16 16 2	1	−0.004231	9 15 2	3	−0.001552
1 6 7	3	−0.004189	6 16 2	3	−0.001534
13 13 2	1	−0.003135	8 10 3	3	−0.001504
6 6 5	1	−0.002594	9 11 3	3	−0.001504
8 14 2	2	0.002385	10 10 5	1	−0.001352
9 15 2	2	0.002385	11 11 5	1	−0.001352
4 16 2	3	0.002176	8 14 5	3	−0.001099
12 13 6	2	−0.001713	9 15 5	3	−0.001099
4 16 2	2	−0.001668	6 16 2	2	−0.000951

[9]. In a large calculation, the 16 orbital one for example, the integrals were calculated in several successive runs, the total comp. time required being 50 min. The number of Gaussians used to expand the Slater orbitals for the calculation of 1 and 2 electron integrals were 10 and 8 respectively. For the same calculation transformation of the integrals needed 6 min.; calculation of matrix elements between configurations for a 43 configuration wavefunction 15 sec.; evaluation of the lowest eigenvalue of the Hamilton matrix 6 sec.; calculation of the density matrix, natural orbitals and kinetic and nuclear attraction energies 9 sec.

Discussion

The energy, −1.63913 a.u., resulting from the 8 orbital calculation Ref. [2] is thought to be within 1–2 kcal/mole of the Σ limit for H_3. This belief is based on the results of the analogous H_2 calculation [11], i.e. the 5 orbital one, in which case the calculated energy was ~1.2 kcal/mole above the H_2 Σ limit.

Similarly the SCF energy for H_3, estimated by the energy of the leading term in the natural expansion, viz. – 1.59247 a.u., is believed to be accurate to within 1 kcal/mole. (Here, by SCF wavefunction, we mean the best single determinantal function with one doubly filled orbital.) The best SCF energy, corresponding to the same definition of SCF wavefunction, quoted in the literature is – 1.592965 a.u., calculated by Edmiston and Krauss [7], using an extensive Gaussian basis. By the addition of two or more Gaussians which could give rise to σ-type symmetry orbitals it should be possible to evaluate both the SCF energy and the Σ limit to an accuracy better than 1 kcal/mole.

The introduction of Gaussian lobe functions with angular dependence resulted in a gradual but considerable lowering of the total H_3 energy. These new functions have greatly improved the correlation part of the wavefunction as evidenced by the decrease in the electron repulsion energy and in the apparent correlation energy. (The latter quantity in calculations Refs. [5–8] was not calculated according to its strict definition, since the dominant configuration in the wavefunction was left unchanged from the 8 orbital calculations. However, the σ-type orbitals constructed from off-axial Gaussians are expected to have only marginal effects on the energy of the dominant configuration.) The close agreement between the two 20 orbital calculations Refs. [7] and [8] is very gratifying and encouraging, giving strong numerical support for the use of natural orbitals. The number of configurations could probably be further reduced if the π and Δ orbitals were transformed to natural basis as well.

The results of the 16 and 20 orbital calculations are to be compared with those of Shavitt *et al.* [5]. The differences are very small, in the case of our 20 orbital, 169 configuration wavefunction only ~ 1/4 kcal/mole. Hopefully, by the use of a larger number of Gaussian functions we will be able to find an improved variational upper bound to the H_3 energy that is of "chemical accuracy" (~ 1 kcal/mole). This should not be too difficult a task on the newer, third generation computers.

Unfortunately, we are unable to put forward a new, definitive upper bound for the classical activation energy for the H/H_2 exchange reaction. The values quoted in Table 2 are only meant as a guide since it is very debatable whether the H_2 energies used in the evaluation of activation energies were really resulting from an analogous calculation. Nevertheless, the results that were presented here are promising and the method of mixed basis functions may prove very useful in future work.

Acknowledgements. G. B. Bacskay gratefully acknowledges the Research Scholarship from the Commonwealth Scientific and Research Organisation (Australia).

Appendix

The Matrices U(P), Used in the Evaluation of Matrix Elements between the 3 Electron Configurations

3 Electrons, $S = 1/2$

The three types of configurations with $S = 1/2$ are defined according to Eq. (1). For computational reasons, in case of double occupancy the doubly occupied orbitals are written first, resulting in the following representation matrices $U(P)$

$$U(1)=\begin{pmatrix} 1 & 0 & \sqrt{2} \\ 0 & 1 & 0 \\ \sqrt{2} & 0 & 1 \end{pmatrix},$$

$$U(12)=\begin{pmatrix} 0 & 0 & 0 \\ 0 & -1 & 0 \\ 0 & 0 & 1 \end{pmatrix},$$

$$U(13)=\begin{pmatrix} -1 & \sqrt{3}/\sqrt{2} & -1/\sqrt{2} \\ \sqrt{3}/\sqrt{2} & 1/2 & \sqrt{3}/2 \\ -1/\sqrt{2} & \sqrt{3}/2 & -1/2 \end{pmatrix},$$

$$U(23)=\begin{pmatrix} 0 & -\sqrt{3}/\sqrt{2} & -1/\sqrt{2} \\ -\sqrt{3}/\sqrt{2} & 1/2 & -\sqrt{3}/2 \\ -1/\sqrt{2} & -\sqrt{3}/2 & -1/2 \end{pmatrix},$$

$$U(23.12)=\begin{pmatrix} 0 & 0 & 0 \\ 0 & -1/2 & -\sqrt{3}/2 \\ 0 & \sqrt{3}/2 & -1/2 \end{pmatrix},$$

$$U(23.13)=\begin{pmatrix} 0 & 0 & 0 \\ 0 & -1/2 & \sqrt{3}/2 \\ 0 & -\sqrt{3}/2 & -1/2 \end{pmatrix}.$$

References

1. Le Roy, D. J., Ridley, B. A., Quickert, K. A.: Discuss. Faraday Soc. **44**, 92 (1967).
2. Kuppermann, A., White, J. M.: J. chem. Physics **44**, 4352 (1966).
3. Hirschfelder, J. O., Eyring, H., Rosen, N.: J. chem. Physics **4**, 121 (1936).
4. Boys, S. F., Shavitt, I.: University of Wisconsin Naval Research Laboratory Tech. Rept. WIS-AF-13 (1959).
5. Shavitt, I., Stevens, R. M., Minn, F. L., Karplus, M.: J. chem. Physics **48**, 2700 (1968).
6. Conroy, H., Bruner, B. L.: J. chem. Physics **47**, 921 (1967).
7. Edmiston, C., Krauss, M.: J. chem. Physics **49**, 192 (1968).
8. Riera, A., Linnett, J. W.: Theoret. chim. Acta (Berl.) **18**, 265 (1970).
9. Bacskay, G. B., Linnett, J. W.: Theoret. chim. Acta (Berl.) **26**, 1–13 (1972).
10. Kotani, M., Amemiya, A., Ishiguro, E., Kimura, T.: Tables of molecular integrals Tokyo: Maruzen Co. 1963.
11. Bacskay, G. B., Linnett, J. W.: Theoret. chim. Acta (Berl.) **26**, 15–21 (1972).
12. Gianinetti, A., Majorino, G. F., Rusconi, E., Simonetta, M.: Int. J. quant. Chemistry **3**, 45 (1969).
13. Bacskay, G. B.: Mixed basis functions in molecular quantum mechanics. Ph. D. Thesis, Cambridge 1971.

Prof. J. W. Linnett
University of Cambridge
Department of Physical Chemistry
Lensfield Road
Cambridge 56491, England

Theoret. chim. Acta (Berl.) 26, 33—42 (1972)
© by Springer-Verlag 1972

Mixed Basis Functions in Molecular Quantum Mechanics
IV. The Linear, Equidistant System of Four Interacting Hydrogen Atoms

G. B. BACSKAY

Department of Physical Chemistry, Cambridge, England

Received February 3, 1972

A series of calculations have been carried out for the linear system of four equidistant hydrogen atoms for an internuclear separation of 1.7 a.u. The configuration interaction technique was used, the orbital basis consisting of a mixed set of 1*s* Slater and floating spherical Gaussian functions. The results obtained are encouraging although the effects of unoptimized non-linear parameters are noticeable.

Es wurde eine Reihe von Rechnungen für ein lineares System von vier äquidistanten Wasserstoffatomen (Kernabstand jeweils 1.7 a.u.) durchgeführt. Dabei benutzt man die Konfigurationswechselwirkungs-Technik, die Orbitalbasis bestand aus einem gemischten Satz von 1*s* Slater- und "floating" sphärischen Gauß-Orbitalen. Die Resultate sind ermutigend, obwohl die Effekte der nicht optimierten nichtlinearen Parameter merklich sind.

Introduction

In the previous papers a series of calculations were reported on 2 and 3 electrons systems, using mixed sets of functions as orbital bases [1–3]. The results were encouraging and as a further test of the method a series of calculations have been carried out on the linear, equidistant system of four hydrogen atoms. Extensive theoretical work on H_4 has been hindered by the difficulties involved in the calculation of the three- and four-centre integrals; so much so that the most sophisticated configuration interaction calculation to date has only made use of a 1*s*, 1*s*′ STO basis [4]. Another, less formidable problem is the large number of configurations which arise, even if only a moderately small basis were used. Linear H_4 has been used as a convenient model for a one-dimensional metallic crystal [5], although as yet it has not been experimentally observed.

The basis sets used in the current H_4 calculation consist of a 1*s*, 1*s*′ STO basis enlarged by Gaussians, much the same way as for H_2 and H_3, so as to improve both the SCF and correlation parts of the CI wavefunction [2, 3]. The calculation of the integrals does not present any fresh problems. The geometry is taken to be identical to the optimum one calculated by Rubinstein and Shavitt [4], i.e. linear, equidistant with an internuclear separation of 1.7 a.u.

Calculations and Results

A series of configuration interaction type calculations have been carried out for the ground state ($^1\Sigma_g^+$) of the linear, equidistant H_4 system, for a fixed internuclear distance of 1.7 a.u., in the Born-Oppenheimer approximation. The orbital bases used consist of a 1s, 1s′ type set of Slater orbitals, gradually enlarged by the addition of spherical Gaussian functions arranged spatially so as to allow for both axial and angular correlation, as well as to improve the SCF part of the wavefunction.

In order to keep the number of configurations at a reasonably low level an iterative procedure, very similar to the interative natural orbital method of Bender and Davidson [6], was introduced and found to function successfully. As a first approximation a CI wavefunction is constructed containing a limited number of configurations, the basis consisting of orthonormal symmetry orbitals. After the computation of the energy expectation value and corresponding eigenvector the spinless first order reduced density matrix is calculated and diagonalized resulting in a set of "approximate" natural orbitals; approximate because they were calculated using a limited CI wavefunction. In the next calculation the original symmetry orbital basis is replaced by the set of natural orbitals. The process is then repeated, gradually dropping those configurations which make too small a contribution to the wavefunction after a given iteration, until there is no change in the energy and in the natural orbitals. Hence a self-consistent set of orbitals are determined which are hopefully a good approximation to the exact natural orbitals. The process is essentially a multi-configurational SCF technique, although a great deal simpler to implement on the computer than the more conventional schemes hitherto proposed [7-9].

The Hamiltonian matrix elements between the configurations and the natural orbitals were calculated by the procedure already used in H_3 calculations [3]. There are two linearly independent spin eigenfunctions for the singlet state and four types of configurations, listed in the Appendix together with the representation matrices $U(P)$ which were used in these calculations.

The numerical and geometrical details of the various bases used in these calculations are given in Table 1 and in Figs. 1 and 2. The exponents of the orbitals were chosen on the basis of the H_3 results, since H_3 and H_4 have very similar geometries, as were the spatial distributions of Gaussians. No optimization of the non-linear parameters was undertaken at any stage of the calculations. The results are summarized in Table 2.

In calculation Ref. [1] from the 1s, 1s′ STO's eight symmetry orbitals were constructed and orthonormalized by the Schmidt method. The first CI wavefunction was taken to consist of a dominant single determinantal function

Table 1. The orbital bases used in the H_4 calculations
($1S$ = 1s-type Slater orbital, G = Spherical Gaussian function)

Calculation Ref.	Number of basis functions	Number of configurations	Orbital basis and exponents
1	8	48	$1S_A = 1S_D = 1.19$, $1S_B = 1S_C = 0.96$, $1S_{A'} = 1S_{D'} = 1.24$, $1S_{B'} = 1S_{C'} = 0.90$
2	11	55	STO basis as for calculation 1 $+ G_1 = G_2 = G_3 = 1.00$
3	15	69	As for calculation 2, $+ G_4 = G_5 = G_6 = G_7 = 0.40$
4	19	90	As for calculation 2, $+ G_4 = G_5 = \cdots = G_{11} = 0.40$

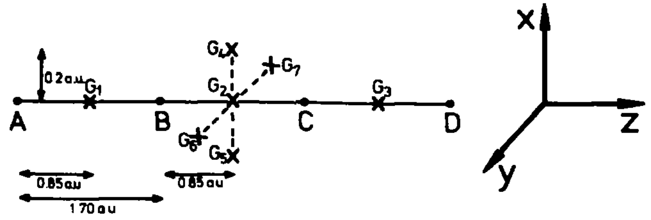

Fig. 1. Positions of the Gaussians in the 11 and 15 orbital H_4 calculations [2, 3]

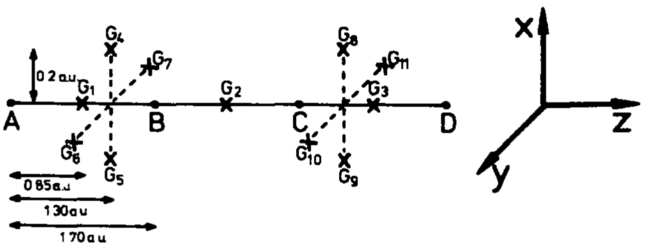

Fig. 2. Positions of the Gaussians in the 19 orbital H_4 calculation [4]

Table 2. Summary of the H_4 calculations (the energies, with the exception of those in the last column, given in atomic units); the H_2 energies required for the last entry were taken from calculations with comparable basis sets, namely the 4, 5 and 9 orbital calculations respectively [2]

Calculation Ref.	Number of basis functions	Number of configurations	Total energy	Kinetic energy	Nuclear attraction energy	Electron repulsion energy	Energy of dominant configuration	Apparent correlation energy	$E_{H_4} - 2E_{H_2}$ (kcal/mole^{-1})
1	8	48	−2.23723	2.23480	−9.33888	2.31783	−2.17833	−0.05890	43.08
2	11	55	−2.24302	2.22775	−9.34315	2.32336	−2.18282	−0.06020	44.30
3	15	69	−2.24720	2.22925	−9.34104	2.31557	−2.18282	−0.06438	
4	19	90	−2.25810	2.23210	−9.33559	2.29637	−2.18282	−0.07528	49.81
8 orbital calculation of Rubinstein and Shavitt [4]			−2.234						

Table 3. Natural orbitals expressed in terms of the original basis,

Natural orbital and its symmetry	Occupation number	Coefficient of atomic orbital $1S_A$	$1S_B$	$1S_C$	$1S_D$
1 σ_g	1.973563	0.304797	0.363791	0.363791	0.304797
2 σ_u	1.937014	0.269596	−0.007723	−0.007723	−0.269596
5 σ_g	0.063171	0.573758	−0.334194	−0.334194	0.573758
7 σ_u	0.017150	−0.078872	−0.166240	0.166240	0.078872
3 σ_g	0.00380	1.070388	1.952159	1.952159	1.070388
4 σ_u	0.003616	4.272493	0.277069	−0.277069	−4.272493
6 σ_u	0.000620	5.473303	−2.835818	−2.835818	5.473303
9 σ_g	0.000591	- 2.325916	−0.256812	−0.256812	−2.325916
10 σ_u	0.000274	−3.626281	−1.229978	1.229978	3.626281
8 σ_u	0.000196	4.672738	−9.311377	9.311377	−4.672738
11 σ_u	0.000006	0.300176	4.57332	4.575332	0.300176

$|1\bar{1}2\bar{2}|$, plus all the configurations which could be obtained by single and double substitutions in the above determinant, resulting in a total of 49 configurations. Orbitals 1 and 2 are simply given as

$$1 = a + b + c + d + a' + b' + c' + d'$$

$$2 = a + b - c - d + a' + b' - c' - d'$$

where a, b, c, d and a', b', c', d' are the $1s$ and $1s'$ STO's centred on nuclei a, b, c, d.

The resulting energy was −2.23416 a.u., the coefficient of the leading determinant being 0.945926, all the other coefficients an order of magnitude smaller. This seemed a clear indication that the determinant $|1\bar{1}2\bar{2}|$ was a fair approximation to the SCF wavefunction, hence the 49 term CI expansion was also expected to be a reasonable approximation to the full CI wavefunction. Next, the natural orbitals were used to construct the same set of configurations, the leading determinant constructed from the two NO's with the highest occupation numbers. After 3 iterations the change in the total energy was less than 10^{-5}, while the change in NO's was of the order of 10^{-4}, dropping to less than 10^{-8} after 6 iterations. In the final wavefunction the coefficient of the leading determinant was 0.977610, while the configurations obtained by single substitutions all had coefficients less than 10^{-6} and could be omitted from the expansion without a significant increase in the energy. Hence it appears that the iterative procedure used gives a set of Brueckner type orbitals such that all single excitations have vanishingly small coefficients [10, 11]. Next, the configuration wavefunction was extended to include triple and quadruple excitations as well, resulting in a total of 64 configurations. The iterations were then repeated, omitting those configurations which had sufficiently small ($\leq 10^{-3}$) coefficients, some of them double excitations, finally resulting in a 48 configuration wavefunction. This final wavefunction contains 4 triple and 4 quadruple excitations. Although these new configurations have zero matrix elements with the leading determinant, they make a small contribution to the energy (~0.38 kcal/mole) through second order effects. The energy terms calculated by this 48 configuration wavefunction are given in Table 2.

In calculation Ref. [2] three Gaussians, placed on the molecular axis, as shown in Fig. 1, were added to the 8 orbital basis. The symmetry orbitals formed from and their occupation numbers, from the 11 orbital H_4 calculation

Coefficient of atomic orbital						
$1S_{A'}$	$1S_{B'}$	$1S_{C'}$	$1S_{D'}$	G_1	G_2	G_3
−0.063644	0.042099	0.042099	−0.063644	0.022785	0.022593	0.022785
0.220148	0.489810	−0.489810	−0.220148	0.030459	0.0	−0.030459
0.302971	−0.268651	−0.268651	0.302971	−0.000002	0.0	−0.000002
1.087010	−1.747110	1.747110	−1.087010	−0.000164	0.0	0.000164
−0.758486	−2.023819	−2.023819	−0.758486	0.000478	0.000018	0.000478
−4.420480	−0.224360	0.224360	4.420480	−0.004076	0.0	0.004076
−6.470700	3.630527	3.630527	6.470700	−0.000004	0.0	−0.000004
1.777873	0.041838	0.041838	1.777873	1.108409	−0.524337	1.108409
3.443406	−0.780154	0.780154	−3.443406	1.648924	0.0	−1.648924
6.846303	14.24447	14.24447	6.846303	0.000078	0.0	−0.000078
0.165227	−2.970354	−2.970354	0.165227	−1.205726	−2.552824	−1.205726

these new orbitals were Schmidt orthogonalized to the set of natural orbitals from calculation Ref. [1] and used to construct 37 configurations which were added to the 48 of the previous calculation. Four iterations were performed, resulting in a 55 configuration wavefunction, all other configurations found to be negligible. The natural orbitals and their occupation numbers from this calculation are presented in Table 3.

In calculation Ref. [3] four off axial Gaussians were added to the orbital basis, as shown in Fig. 1. As in the analogous H_2 and H_3 calculations [2, 3], the point group of the molecule was taken to be D_{4h}, hence two e_{1u}, one b_{1g} and one a_{1g} symmetry orbitals could be formed from these new Gaussians. The a_{1g} orbital was Schmidt orthogonalized to the NO basis from calculation Ref. [2], the other three already orthogonal by virtue of their symmetry properties. 69 configurations were found significant enough to be included in the expansion.

The final H_4 calculation [4] employed two sets of four off-axial Gaussians, as shown in Fig. 2, in addition to the 11 orbitals from calculation Ref. [2]. The orthonormal basis, however, contained only 16 molecular orbitals, since orbital 11 from the 11 orbital NO set and the a_{1g} and a_{2u} Gaussian lobe functions were discarded from the set. The omission of these orbitals was not expected to increase the energy by more than 0.0002 a.u., this belief based on similar results for H_3. The molecular orbitals, constructed from the off-axial Gaussians, are listed in Table 4. The final wavefunction contains 90 configurations, these were selected after a few trial runs testing which new configurations would be important enough to be used. The occupation numbers of the natural orbitals resulting from this calculation are listed in Table 5, while in Table 6 the 90 configurations and their coefficients are presented.

The wavefunctions from the other H_4 calculations are given elsewhere [12][1].

Discussion

The results of calculation Ref. [1] represent a slight improvement (~2 kcal/mole in the total energy) over the results of Rubinstein and Shavitt [4], despite the small number of configurations in the wavefunction. Clearly, the orbital

---

[1] Also available from G. B. Bacskay on request.

Table 4. Additional molecular orbitals, expressed in terms of the original basis, for the 19 orbital H_4 calculation (the first 10 orbitals are orbitals 1–10, as listed in Table 3)

Molecular orbital	Coefficient of atomic orbital							
and its symmetry	G_4	G_5	G_6	G_7	G_8	G_9	G_{10}	G_{11}
11 e_{1u_x} (π_{u_x})	2.404816	−2.404816			2.404816	−2.404816		
12 e_{1u_y} (π_{u_y})	0.0	0.0	2.404816	−2.404816	0.0	0.0	2.404816	−2.404816
13 e_{1g_x} (π_{g_x})	3.335528	−3.335528	0.0	0.0	−3.335528	3.335528	0.0	0.0
14 e_{1g_y} (π_{g_y})	0.0	0.0	3.335528	−3.335528	0.0	0.0	−3.335528	3.335528
15 b_{1g} (Δ_g)	19.63822	19.63822	−19.63822	−19.63822	19.63822	19.63822	−19.63822	−19.63822
16 b_{1u} (Δ_u)	26.3699	26.3699	−26.3699	−26.3699	−26.3699	−26.3699	26.3699	26.3699

Table 5. The occupation numbers of the natural orbitals from the 19 orbital H_4 calculation

Natural orbital and its symmetry	Occupation number
1 σ_g	1.966401
2 σ_u	1.933892
5 σ_g	0.060481
7 σ_u	0.016261
11 π_{u_x}	0.004195
12 π_{u_y}	0.004195
3 σ_g	0.003638
4 σ_u	0.003501
13 π_{g_x}	0.002857
14 π_{g_y}	0.002857
6 σ_g	0.000602
9 σ_g	0.000550
10 σ_u	0.000262
8 σ_u	0.000176
15 Δ_g	0.000082
16 Δ_u	0.000066

Table 6. Configurations and their coefficients from the 19 orbital H_4 calculation

Configuration		Coefficient
Orbitals	Type	
Dominant configuration		
1 1 2 2	1	0.974926
Double substitutions		
1 1 3 3	1	−0.013578
1 1 4 4	1	−0.024375
1 1 5 5	1	−0.144772
1 1 3 5	2	−0.0182899
1 1 6 6	1	−0.007985
1 1 3 6	2	−0.008532
1 1 5 6	2	0.007147
1 1 7 7	1	−0.033975
1 1 4 7	2	0.004494
1 1 8 8	1	−0.003537
1 1 4 8	2	−0.001029
1 1 7 8	2	0.004358
2 2 3 3	1	−0.019727
2 2 4 4	1	−0.009980
2 2 4 8	2	0.001990
2 2 5 5	1	−0.056799
2 2 3 5	2	0.021110
2 2 6 6	1	−0.004344
2 2 3 6	2	0.003026
2 2 5 6	1	−0.011914
2 2 7 7	2	−0.039707
1 1 12 12	1	−0.014631
2 2 12 12	1	−0.031911
1 2 12 14	3	0.038480
1 2 12 14	4	0.012622
1 1 13 13	1	−0.020239
2 2 13 13	1	−0.013440
1 1 14 14	1	−0.020240
2 2 14 14	1	−0.013443
1 1 15 15	1	−0.001788
2 2 15 15	1	−0.004499
1 1 16 16	1	−0.003188
2 2 16 16	1	−0.002294
1 2 15 16	3	0.005738
1 2 15 16	4	0.001621
2 2 4 7	2	0.007694
2 2 8 8	1	−0.004610
2 2 7 8	2	−0.007631
1 3 2 4	3	−0.019882
1 3 2 4	4	−0.020626
1 3 2 7	3	0.016904
1 3 2 7	4	0.021685
1 5 2 4	4	−0.032073
1 5 2 7	3	−0.084147
1 5 2 7	4	−0.048863
1 6 2 4	3	−0.005128
1 6 2 4	4	−0.009776
1 6 2 7	3	−0.001704
1 6 2 7	4	−0.002517
1 6 2 8	3	−0.004026
1 1 9 9	1	−0.009064
1 1 10 10	1	−0.005558
2 2 9 9	1	−0.010441
2 2 10 10	1	−0.004503
1 9 2 10	3	−0.007572
1 9 2 10	4	−0.010026
1 1 11 11	1	−0.014683
2 2 11 11	1	−0.031975
1 2 11 13	3	0.038503
1 2 11 13	4	0.012605
Triple substitutions		
7 7 1 3	2	0.002077
1 6 2 8	4	−0.003923
7 7 1 5	2	−0.001513
7 4 1 5	3	−0.003339
7 4 1 5	4	0.003554
1 5 11 11	2	0.001457
1 7 11 13	3	0.001140
2 5 11 13	4	−0.001465
1 5 12 12	2	0.001464
2 7 12 12	2	−0.000729
1 7 12 14	3	0.001133
2 5 12 14	4	−0.001459
1 5 13 13	2	−0.001912
2 7 13 13	2	0.000909
1 5 14 14	2	−0.001912
2 7 14 14	2	0.000933
Quadruple substitutions		
5 5 7 7	1	0.013058
5 5 4 4	1	0.003677
7 4 5 3	4	0.002806
5 5 3 3	1	0.004505
9 9 5 5	1	0.002191
10 10 5 5	1	0.000986
5 5 11 11	1	0.005652
7 7 11 11	1	0.001697
5 5 12 12	1	0.005765
5 5 13 13	1	0.003126
7 7 13 13	1	0.001253
5 5 14 14	1	0.003120
7 7 14 14	1	0.001298

exponents used in our calculation are closer to the optimum values. Rubinstein and Shavitt used the exponents 1.230 and 0.615 for the 1*s* and 1*s*′ orbitals respectively, their ratio kept fixed as 2:1 during the optimization procedure, judged too large by the authors themselves. Furthermore, it appears that the 48 configuration wavefunction may be very close to a good multiconfigurational SCF wavefunction. Hence, no significant improvement in the energy would be expected, were the wavefunction of the full CI type, i.e. containing 176 configurations.

The introduction of Gaussians with σ symmetry resulted in a relatively small decrease in the total energy (0.00579 a.u.), most of it appearing as an improved energy for the leading configuration, i.e. the "SCF part" of the wavefunction. Compared to the H_3 results [3] where the analogous energy decrease was ~ 0.009 a.u., the above change seems too small. Optimization of the exponents in this case is probably desirable to improve the above results.

The effect of the first set of functions with angular dependence is disappointingly little (calculation Ref. [3]). Obviously the π_u functions are unable to bring about sufficient angular correlation between electrons delocalized over a molecule which is far too long to be efficiently covered by the simple π_u functions. A smaller orbital exponent should have been used for the off-axial Gaussians, or more functions with angular dependence. In the final calculation Ref. [4] we chose the second alternative by the addition of another set of four off-axial Gaussians. The effects are quite marked, obviously the new π_u orbitals especially are much more successful in allowing for angular correlation than the earlier ones, which consisted of only two Gaussians.

The H_4 wavefunctions in these calculations were developed in terms of a dominant configuration (that is expected to approximate to the SCF wavefunction in the given basis) and double, triple and quadruple substitutions in the above single determinant. As pointed out earlier, the absence of single excitations implies Brueckner self-consistency, since in the case of Hartree-Fock self-consistency single excitations could still appear, even though Brillouin's theorem was satisfied, due to second order effects. Quadruple excitations seem an order of magnitude more important than triple excitations, this is not unexpected, since the latter are thought to correspond to unlinked clusters of electrons, or "simultaneous binary collisions" between electrons in different regions of space [13].

Unfortunately, no definite new value has been produced for the upper bound of the energy difference of H_4 and two H_2 molecules, apart from the very first entry in Table 2, i.e. 43.08 kcal/mole, resulting from the simplest calculation in this series. As the basis for the H_4 calculations was increased the above energy difference increased also, indicating that the H_4 basis was becoming progressively poorer than the comparable H_2 basis. As pointed out earlier, optimization of the nonlinear parameters should definitely be carried out to improve these results.

Conclusion

It has been demonstrated again that mixed basis sets could be very useful for future work on multicentre systems of this kind. The iterative scheme used in this work has proved very useful too; all the CI expansions were successfully kept reasonably short. It would be very interesting and profitable to do some calculations for H_4, using the set of basic integrals computed for the present work, but employing SCF and multi-configurational SCF techniques. A full CI calculation would also be worth attempting. Such calculations will be undertaken shortly.

Acknowledgements. G. B. Bacskay gratefully acknowledges the Research Scholarship from the Commonwealth Scientific and Industrial Research Organisation (Australia).

Appendix

The Representation Matrices U(P), Used in the Evaluation of Matrix Elements between the 4 Electron Configurations

The four types of configurations with $S = 0$ are defined as

$$\Phi^1 = (i\,i\,j\,j)^1 = |i\bar{i}j\bar{j}|\,,$$

$$\Phi^2 = (i\,i\,j\,k)^2 = 1/\sqrt{2}\,\{|i\bar{i}j\bar{k}| + |i\bar{i}k\bar{j}|\}\,,$$

$$\Phi^3 = (i\,j\,k\,l)^3 = 1/2\,\{|i\bar{j}k\bar{l}| + |j\bar{i}k\bar{l}| + |i\bar{j}l\bar{k}| + |j\bar{i}l\bar{k}|\}\,,$$

$$\Phi^4 = (i\,j\,k\,l)^4 = 1/\sqrt{12}\,\{|i\bar{j}k\bar{l}| + |j\bar{i}k\bar{l}| + |i\bar{j}l\bar{k}| + |j\bar{i}k\bar{l}| - 2|i\bar{k}j\bar{l}| - 2|j\bar{l}i\bar{k}|\}\,.$$

Φ^2 could also be written as $(j\,k\,i\,i)^2$.

The $U(P)$ matrices are:

$$U(1) = U(23.14) = \begin{pmatrix} 1 & \sqrt{2} & 2 & 0 \\ \sqrt{2} & 1 & \sqrt{2} & 0 \\ 2 & \sqrt{2} & 1 & 0 \\ 0 & 0 & 0 & 1 \end{pmatrix},$$

$$U(12.34) = U(13.24) = \begin{pmatrix} 0 & 0 & 0 & 0 \\ 0 & 1 & \sqrt{2} & 0 \\ 0 & \sqrt{2} & 1 & 0 \\ 0 & 0 & 0 & 1 \end{pmatrix},$$

$$U(12) = U(34) = U(14.12.13) = U(13.12.14) = \begin{pmatrix} 0 & 0 & 0 & 0 \\ 0 & 0 & 0 & 0 \\ 0 & 0 & 1 & 0 \\ 0 & 0 & 0 & -1 \end{pmatrix},$$

$$U(13) = \begin{pmatrix} -2 & -1/\sqrt{2} & -1 & \sqrt{3} \\ -1/\sqrt{2} & -1/2 & -1/\sqrt{2} & \sqrt{3}/\sqrt{2} \\ -1 & -1/\sqrt{2} & -1/2 & \sqrt{3}/2 \\ \sqrt{3} & \sqrt{3}/\sqrt{2} & \sqrt{3}/2 & 1/2 \end{pmatrix},$$

$$U(24) = \begin{pmatrix} 0 & -1/\sqrt{2} & -1 & \sqrt{3} \\ -1/\sqrt{2} & -1/2 & -1/\sqrt{2} & \sqrt{3}/\sqrt{2} \\ -1 & -1/\sqrt{2} & -1/2 & \sqrt{3}/2 \\ \sqrt{3} & \sqrt{3}/\sqrt{2} & \sqrt{3}/2 & 1/2 \end{pmatrix},$$

38964
Date 24.4.80

$$U(14.13.12) = U(12.13.14) \begin{pmatrix} 0 & 0 & 0 & 0 \\ 0 & -1/2 & -1/\sqrt{2} & \sqrt{3}/\sqrt{2} \\ 0 & -1/\sqrt{2} & -1/2 & \sqrt{3}/2 \\ 0 & \sqrt{3}/\sqrt{2} & \sqrt{3}/2 & 1/2 \end{pmatrix}$$

$$U(13.12) = U(34.14) = U(24.34) = U(24.12) = \begin{pmatrix} 0 & 0 & 0 & 0 \\ 0 & 0 & 0 & 0 \\ 0 & 0 & -1/2 & -\sqrt{3}/2 \\ 0 & 0 & \sqrt{3}/2 & -1/2 \end{pmatrix},$$

$$U(13.14) = U(23.34) = U(23.12) = U(14.12) = \begin{pmatrix} 0 & 0 & 0 & 0 \\ 0 & 0 & 0 & 0 \\ 0 & 0 & -1/2 & \sqrt{3}/2 \\ 0 & 0 & -\sqrt{3}/2 & -1/2 \end{pmatrix},$$

$$U(14) = U(23) = \begin{pmatrix} 0 & -\sqrt{2} & -1 & -\sqrt{3} \\ -\sqrt{2} & -1/2 & -1/\sqrt{2} & -\sqrt{3}/\sqrt{2} \\ -1 & -1/\sqrt{2} & -1/2 & -\sqrt{3}/2 \\ -\sqrt{3} & -\sqrt{3}/\sqrt{2} & -\sqrt{3}/2 & 1/2 \end{pmatrix},$$

$$U(13.14.12) = U(12.14.13) = \begin{pmatrix} 0 & 0 & 0 & 0 \\ 0 & -1/2 & -1/\sqrt{2} & -\sqrt{3}/\sqrt{2} \\ 0 & -1/\sqrt{2} & -1/2 & -\sqrt{3}/2 \\ 0 & -\sqrt{3}/\sqrt{2} & -\sqrt{3}/2 & 1/2 \end{pmatrix},$$

References

1. Bacskay, G. B., Linnett, J. W.: Theoret. chim. Acta (Berl.) **26**, 1—13 (1972).
2. — Theoret. chim. Acta (Berl.) **26**, 15—21 (1972).
3. — — Theoret. chim. Acta (Berl.) **26**, 23—32 (1972).
4. Rubinstein, M., Shavitt, I.: J. chem. Physics **51**, 2014 (1969).
5. Taylor, R.: Proc. physic. Soc. (London) **64** A, 249 (1951).
6. Bender, C. F., Davidson, E. R.: J. physic. Chem. **70**, 2675 (1966).
7. Mukherjee, N. G., McWeeny, R.: Int. quantum Chem. **4**, 97 (1970).
8. Das, G., Wahl, A. C.: J. chem. Physics **44**, 87 (1966); **47**, 2934 (1967).
9. Veillard, A., Clementi, E.: Theoret. chim. Acta (Berl.) **7**, 133 (1967).
10. Nesbet, R. K.: Physic. Rev. **109**, 1632 (1958).
11. Löwdin, P. O.: J. math. Physics **2**, 1171 (1962).
12. Bacskay, G. B.: Mixed Basis Functions in Molecular Quantum Mechanics. Ph. D. Thesis, Cambridge 1971.
13. Sinanoğlu, O.: J. chem. Physics **33**, 1212 (1960); **36**, 706 (1962).

Dr. G. B. Bacskay
Department of Theoretical Chemistry
University of Sydney
Sydney, N.S.W. 2006
Australia

Theoret. chim. Acta (Berl.) 26, 43—54 (1972)
© by Springer-Verlag 1972

An Intermolecular Perturbation Approach to the Cycloaddition of Carbenes toward Olefins. Reaction Path and Stereoselectivity

T. FUENO, S. NAGASE, K. TATSUMI, and K. YAMAGUCHI

Department of Chemistry, Faculty of Engineering Science, Osaka University, Toyonaka, Osaka, Japan

Received February 25, 1972

The perturbation theory of Murrell, Randić and Williams for intermolecular interaction has been combined with the assumption of local zero-differential overlaps. The theory has been applied to the cycloadditions of singlet methylene and halocarbenes toward olefins. The results, obtained by use of the CNDO/2 energies and wave functions for isolated molecules, quantitatively assess the roles of various types of energies influencing the stereochemical courses of reaction. The syn/anti stereoselectivities of halocarbenes in their cycloadditions toward *cis*-butene-2 are found to be governed by the Coulombic, dispersion, charge-transfer and exchange-repulsion energies altogether. Participation of the *d* orbitals of the chlorine atom in charge transfer is emphasized.

Die Störungsrechnung von Murrell, Randić und Williams für intermolekulare Wechselwirkung wurde in Verbindung mit der Annahme von lokalen ZDO zur Berechnung der Cycloaddition von Singulett-Methylen oder -Halogencarbenen an Olefine angewendet. Die Resultate, die über die CNDO/2-Ergebnisse für die isolierten Moleküle erhalten wurden, lassen die Rolle der einzelnen Energieanteile erkennen, die die Stereochemie der Reaktion beeinflussen. Die syn/anti-Stereoselektivität der Halogencarbene gegenüber *cis*-2-Buten wird durch die Coulomb-, Dispersions-, Chargetransfer- und Austausch-Wechselwirkung gemeinsam bestimmt. Auch die D-Orbitale von Chlor sind für den Charge transfer von Bedeutung.

Introduction

The cycloaddition of singlet carbenes toward olefins has been the subject of intensive investigation in organic chemistry for the past ten years [1]. Studies on the stereochemical details of the reaction have yielded valuable informations concerning the chemical properties of singlet carbene intermediates. It is generally accepted that at the incipient stage of reaction they interact with both the olefin carbons in a concerted manner, to give cyclopropanes with the initial olefin configuration (*cis* or *trans*) retained perfectly.

It is also well recognized that unsymmetrically substituted carbenes show, in addition to the above-mentioned stereospecificity, a definite pattern of stereoselection as to the placement of their substituent(s) in the products. Thus, bulkier substituents of carbene tend to be imbedded at a position *cis* to the larger number of olefin substituents [1–3]. The formations of presumably thermodynamically less stable syn isomers in prevalence over the anti isomers clearly reflect the operation of electronic attractive forces outweighing steric repulsion between the carbene and olefin substituents in the transition state. Nonetheless, the precise nature of these intermolecular forces is still a moot point; apparently, little effort has been expended on theoretical studies of this problem.

The primary purpose of this paper is to attempt an intermolecular-interaction approach to the syn/anti stereoselectivity of halocarbenes. To this end, the intermolecular perturbation theory of Murrell *et al.* [4] was used, in combination with the CNDO wave functions and energies [5–7] of the reacting partners. For assumed geometries of the reacting systems, various types of interaction energies, i.e., the Coulomb, exchange-repulsion, induction, dispersion and charge-transfer energies, were evaluated separately, and their relative importances to stereoselectivity were assessed. The results were found to be of value to the understanding of the stereochemistry of the carbene intermediates.

Theory and Calculation Method

It is presumed that for the interaction systems of our present interest the effect of the orbital overlaps between the components is significant. For treatments of such systems, the intermolecular perturbation theory presented by Murrell *et al.* [4] is a particularly suited starting point.

Let us denote the component closed-shell molecules by A and B. The theory of Murrell *et al.* is essentially the configuration interaction treatment, in which the locally excited (A^*B and AB^*), doubly excited (A^*B^*) and charge-transfer (A^+B^- and A^-B^+) configurations of the aggregate are allowed to mix with the ground-state configuration (AB). The wave function of each configuration was antisymmetrized with respect to electron exchange between the components. Under this requirement, they calculated the stabilization energy of the ground state due to the configuration interaction, by a double perturbation expansion with respect to the intermolecular potential U and overlap S up to the order of U^2S^2. General expressions for the Coulombic (U^1S^0), exchange-repulsion (U^1S^2), induction-dispersion (U^2S^0) and charge-transfer (U^2S^2) energies were thus derived.

We further expand each of these general expressions into terms associated with atomic orbitals, χ. For the sake of computational economy, we decided to adopt the assumption of zero-differential overlaps [5] within molecules but retain the overlaps between the interacting molecules. The intermolecular atomic-orbital integrals required to consider are the electron-core attraction, interelectronic repulsion, and atomic overlap integrals of the form:

$$V_{a,rs} = -\int \chi_r(1) \frac{Z_a e^2}{r_{1a}} \chi_s(1)\, d\tau_1 , \tag{1}$$

$$(rs|tu) = \int \chi_r(1)\, \chi_s(1) \frac{e^2}{r_{12}} \chi_t(2)\, \chi_u(2)\, d\tau_1\, d\tau_2 , \tag{2}$$

and

$$S_{rs} = \int \chi_r(1)\, \chi_s(1)\, d\tau_1 \tag{3}$$

respectively, where the suffix a signifies atomic core while r, s, t and u, valence-shell atomic orbitals.

Expansions were somewhat tedious but straightforward. The final forms obtained for the Coulombic (E_Q), exchange-repulsion (E_K), induction (E_I), dispersion (E_D) and charge-transfer (E_{CT}) energies were as follows:

$$\begin{aligned} E_Q = {} & \sum_{r}^{\mathrm{A}}\sum_{b}^{\mathrm{B}} P_{rr}V_{b,rr} + \sum_{s}^{\mathrm{B}}\sum_{a}^{\mathrm{A}} P_{ss}V_{a,ss} \\ & + \sum_{r}^{\mathrm{A}}\sum_{s}^{\mathrm{B}} P_{rr}P_{ss}(rr|ss) + \sum_{a}^{\mathrm{A}}\sum_{b}^{\mathrm{B}} Z_aZ_be^2/R_{ab}, \end{aligned} \tag{4}$$

$$\begin{aligned} E_K = {} & -\frac{1}{2}\sum_{r}^{\mathrm{A}}\sum_{s}^{\mathrm{B}}\sum_{t}^{\mathrm{A}}\sum_{u}^{\mathrm{B}} P_{rt}P_{su}(rs|tu) \\ & -2\sum_{i}^{\mathrm{A}}\sum_{j}^{\mathrm{B}}\sum_{r}^{\mathrm{A}}\sum_{s}^{\mathrm{B}}\sum_{a}^{\mathrm{A}}\sum_{b}^{\mathrm{B}} S_{ij}C_{ir}C_{js}(V_{a,rs}+V_{b,rs}) \\ & -2\sum_{i}^{\mathrm{A}}\sum_{j}^{\mathrm{B}}\sum_{r}^{\mathrm{A}}\sum_{s}^{\mathrm{B}} S_{ij}C_{ir}C_{js}\left\{\sum_{t}^{\mathrm{A}}(P_{tt}-C_{it}^2)(rs|tt) + \sum_{u}^{\mathrm{B}}(P_{uu}-C_{ju}^2)(rs|uu)\right\} \\ & +2\sum_{i}^{\mathrm{A}}\sum_{j}^{\mathrm{B}} S_{ij}^2\left\{\sum_{r}^{\mathrm{A}}\sum_{b}^{\mathrm{B}} C_{ir}^2V_{b,rr} + \sum_{s}^{\mathrm{B}}\sum_{a}^{\mathrm{A}} C_{js}^2V_{a,ss}\right\} \\ & +2\sum_{i}^{\mathrm{A}}\sum_{j}^{\mathrm{B}}\sum_{r}^{\mathrm{A}}\sum_{s}^{\mathrm{B}} S_{ij}^2(P_{rr}C_{js}^2+P_{ss}C_{ir}^2-C_{ir}^2C_{js}^2)\,(rr|ss), \end{aligned} \tag{5}$$

$$\begin{aligned} E_I = {} & 2\sum_{i}^{\mathrm{A}}\sum_{k}^{\mathrm{A}}\left\{\sum_{r}^{\mathrm{A}} C_{ir}C_{kr}\left[\sum_{b}^{\mathrm{B}} V_{b,rr} + \sum_{s}^{\mathrm{B}} P_{ss}(rr|ss)\right]\right\}^2 \Big/ (E_0-E_{i\to k}) \\ & +2\sum_{j}^{\mathrm{B}}\sum_{l}^{\mathrm{B}}\left\{\sum_{s}^{\mathrm{B}} C_{js}C_{ls}\left[\sum_{a}^{\mathrm{A}} V_{a,ss} + \sum_{r}^{\mathrm{A}} P_{rr}(rr|ss)\right]\right\}^2 \Big/ (E_0-E_{j\to l}), \end{aligned} \tag{6}$$

$$E_D = 4\sum_{i}^{\mathrm{A}}\sum_{k}^{\mathrm{A}}\sum_{j}^{\mathrm{B}}\sum_{l}^{\mathrm{B}}\left\{\sum_{r}^{\mathrm{A}}\sum_{s}^{\mathrm{B}} C_{ir}C_{kr}C_{js}C_{ls}(rr|ss)\right\}^2 \Big/ (E_0-E_{i\to k,j\to l}), \tag{7}$$

$$\begin{aligned} E_{CT} = {} & 2\sum_{i}^{\mathrm{A}}\sum_{l}^{\mathrm{B}}\Bigg\{\sum_{r}^{\mathrm{A}}\sum_{s}^{\mathrm{B}} C_{ir}C_{ls}\left[\sum_{b}^{\mathrm{B}} V_{b,rs} + \sum_{u}^{\mathrm{B}} P_{uu}(rs|uu)\right] \\ & -S_{ij}\sum_{r}^{\mathrm{A}} C_{ir}^2\left[\sum_{b}^{\mathrm{B}} V_{b,rr} + \sum_{s}^{\mathrm{B}} P_{ss}(rr|ss)\right]\Bigg\}^2 \Big/ (E_0-E_{i\to l}) \\ & +2\sum_{k}^{\mathrm{A}}\sum_{j}^{\mathrm{B}}\Bigg\{\sum_{r}^{\mathrm{A}}\sum_{s}^{\mathrm{B}} C_{kr}C_{js}\left[\sum_{a}^{\mathrm{A}} V_{a,rs} + \sum_{t}^{\mathrm{A}} P_{tt}(rs|tt)\right] \\ & -S_{ij}\sum_{s}^{\mathrm{B}} C_{js}^2\left[\sum_{a}^{\mathrm{A}} V_{a,ss} + \sum_{r}^{\mathrm{A}} P_{rr}(rr|ss)\right]\Bigg\}^2 \Big/ (E_0-E_{j\to k}). \end{aligned} \tag{8}$$

In Eqs. (4) through (8), we have used the following notations for molecule A (and B in parentheses): i (and j), the occupied molecular orbital; k (and l), the unoccupied virtual molecular orbital; r, t (and s, u), the atomic orbitals involved; and a (and b), the atomic core present. In addition, C_{ir} etc. and P_{rr} etc. respectively denote the LCAO coefficients and atomic-orbital populations for the isolated molecule, and S_{ij} signifies the intermolecular orbital overlap.

$$S_{ij} = \sum_{r}^{\mathrm{A}}\sum_{s}^{\mathrm{B}} C_{ir}C_{js}S_{rs}. \tag{9}$$

E_0 is the electronic energy of the ground configuration AB while $E_{i\to k}$ etc. are t energies of the configurations resulting from the electron transitions indicate R_{ab} is the distance between atomic cores a and b.

In evaluating the various energies (4)–(8) numerically, we made use of the CNDO/2 wave functions and orbital energies [6, 7] for the interacting components. For chlorocarbenes, both of those obtained with and without inclusion of the chlorine 3d orbitals were used. The one- and two-electron integrals involving intermolecular differential overlaps were approximated by Mulliken's formula [8], viz.,

$$V_{a,rs} = (V_{a,rr} + V_{a,ss})\, S_{rs}/2 \qquad (10)$$

and

$$(rs|tu) = \{(rr|tt) + (rr|uu) + (ss|tt) + (ss|uu)\}\, S_{rs}S_{tu}/4\,. \qquad (11)$$

The integrals, $V_{a,rr}$, $(rr|rr)$ and $(rr|ss)$, were evaluated for the Slater valence-shell s atomic orbitals [9]. The overlap integrals S_{rs} were also evaluated for Slater orbitals, using the formula given by Mulliken *et al.* [10].

Molecular geometries of ethylene [11], *cis*-butene [12], methylene [13], fluorocarbene [14] were obtained from the literature. The geometries for fluorochlorocarbene ($\sphericalangle$FCCl = 103°) and methylchlorocarbene ($\sphericalangle$CCCl = 106°) were estimated by reference to those reported for chlorocarbene [15]. The interaction energies were computed for several assumed spatial geometries of the aggregates AB. All computations were programed in FORTRAN and performed on the FACOM 230-60 at the Kyoto University Computation Center. The CNDO/2 wave functions were required to be precise to within 0.0001 for the charge densities obtained.

Additions of Methylene

Before dealing with stereoselectivity, we consider in this section the additions of singlet methylene $CH_2(^1A_1)$ toward ethylene and *cis*-butene-2. Examination of the geometry of the transition states is the main purpose.

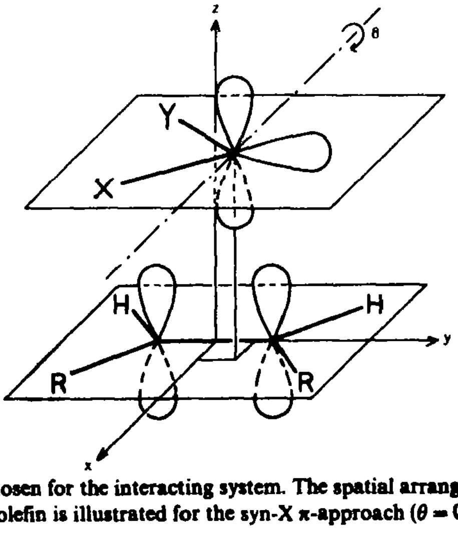

Fig. 1. Coordinate axes chosen for the interacting system. The spatial arrangement of carbene relative to olefin is illustrated for the syn-X π-approach ($\theta = 0°$)

We consider various spatial geometries of CH_2 relative to olefin, each component retaining its initial planar structure. Fig. 1 illustrates such geometries. The middle of the olefin double bond is taken as the origin of the Cartesian coordinates, x, y and z. The methylene plane was allowed to rotate around the auxiliary axis which passes through the carbon atom and is parallel to the x axis. The nodal axis of the methylene lone pair orbital was fixed to be parallel to the yz plane, and its declination downward was defined as the rotation angle θ of methylene. Thus, the geometry of the entire system is characterized by the notation (x, y, z, θ) in units of Å and degree.

1. Addition to Ethylene

In the first place, methylene was assumed to approach ethylene along the z-axis. Two extreme geometries were considered: $\theta = 0$ and 90°, which may be referred to as the π- and σ-approach models, respectively. The various types of energies, given by Eqs. (4)–(8), were calculated for the varying intermolecular distance z. The results are summarized in Table 1.

Table 1 shows that, as the intermolecular distance decreases, the π-approach tends to be stabilized increasingly whereas the σ-approach suffers increasing destabilization. The main contribution to the stability of the former model is E_{CT}, while in the latter the stabilization due to E_{CT} is overshadowed by the destabilization arising from exchange repulsion E_K. These results are compatible with Hoffmann's demonstration [16] based on the total energy calculations by the extended Hückel method, and are well consistent with the Woodward-Hoffmann selection rule for thermal cycloadditions [17].

Next, we calculated the interaction energies for two π-approach models: $B(0, -0.3, 3.2, 0)$ and $C(0, 0.3, 3.2, 0)$. The displacements $y = \pm 0.3$ Å correspond to about one-fourth the length of the double bond, while the separation $z = 3.2$ Å is approximately twice the van der Waals radius of the carbon $p\pi$ orbital [18].

Table 1. Energies of interaction between CH_2 and ethylene[a]

z (Å)	E_Q	E_K	E_I	E_D	E_{CT}	E_{total}
σ-approach ($\theta = 90°$)						
2.8	−0.985	3.440	−0.000	−0.112	−0.723	1.619
3.2	−0.171	0.822	−0.000	−0.056	−0.166	0.430
3.6	−0.027	0.177	−0.000	−0.030	−0.035	0.086
4.0	−0.004	0.035	−0.000	−0.017	−0.007	0.008
5.0	−0.000	0.000	−0.000	−0.005	−0.000	−0.005
π-approach ($\theta = 0°$)						
2.8	−1.205	2.449	−0.001	−0.292	−6.844	−5.892
3.2	−0.217	0.582	−0.000	−0.151	−1.627	−1.413
3.6	−0.037	0.128	−0.000	−0.083	−0.348	−0.340
4.0	−0.006	0.027	−0.000	−0.048	−0.069	−0.096
5.0	−0.000	0.000	−0.000	−0.014	−0.001	−0.015

[a] Energies given in units of kcal/mole. Geometry: $x = y = 0$ Å.

Table 2. Interaction energies for π-approaches of CH_2 toward ethylene and *cis*-butene-1[a]

Geometry (x, y)[b]	E_Q	E_K	E_I	E_D	E_{CT}	E_{total}
Ethylene						
$A(0, 0)$	−0.217	0.582	−0.000	−0.151	−1.627	−1.413
$B(0, -0.3)$	−0.210	0.543	−0.000	−0.134	−1.577	−1.377
$C(0, 0.3)$	−0.218	0.596	−0.000	−0.161	−1.571	−1.353
cis-Butene-2						
$A(0, 0)$	−0.284	0.816	−0.000	−0.260	−1.553	−1.281
$B(0, -0.3)$	−0.308	0.860	−0.000	−0.252	−1.547	−1.246
$C(0, 0.3)$	−0.276	0.773	−0.000	−0.265	−1.530	−1.299
$D(-0.3, 0)$	−0.253	0.716	−0.000	−0.242	−1.485	−1.264
$E(0.3, 0)$	−0.296	0.860	−0.000	−0.269	−1.504	−1.209

[a] Energies given in units of kcal/mole.

[b] $z = 3.2$ Å and $\theta = 0°$.

The results of calculation are given in Table 2, together with those for Model $A(0, 0, 3.2, 0)$. The total stability is found to decrease in the order of $A > B > C$. From his extended Hückel calculations, Hoffmann [16] pointed out that a π-approach which is slightly off-centered toward the position C would be favorable as a result of steric interactions between hydrogens. Our results conflict with his view. The repulsions between the lone pair electrons of methylene and the π-electrons of ethylene appears to be greater than those between the hydrogens.

2. *Addition to cis-Butene-2*

The various types of interaction energies were calculated as the functions of θ for fixed coordinates $x = y = 0$ and $z = 3.2$ Å. The results obtained are shown in Fig. 2.

As can be seen in Fig. 2, the total interaction energy E_{total} is determined almost exclusively from two opposing contributions, E_{CT} and E_K. E_{CT} is a sensitive function of θ and attains a minimum (the largest negative value) at $\theta = 0°$, as is easily anticipated. By contrast, E_K takes on a minimal value at $\theta = 30°$, an angle which probably permits the best compromise between the steric crowdings associated with the hydrogen atoms of methylene on one hand and its lone pair electrons on the other. As a consequence, E_{total} first decreases with the increase in θ, giving a shallow minimum at $\theta = 10°$, beyond which it sharply increases. The π-approach model ($\theta = 0°$) can thus be regarded as a useful approximation to the present interaction system.

With the above indications in mind, we next looked into differential responses of the system to slight changes in x and y. For fixed values of $z = 3.2$ Å and $\theta = 0°$, we considered the following five geometries: $A(0, 0, 3.2, 0)$, $B(0, -0.3, 3.2, 0)$, $C(0, 0.3, 3.2, 0)$, $D(-0.3, 0, 3.2, 0)$ and $E(0.3, 0, 3.2, 0)$. Fig. 3 is the top view of the whole system, illustrating the locations of the carbene carbon in the geometries A to E.

The interaction energies calculated for the five geometries are given in Table 2. The most important stabilizing factor is E_{CT}. The relative stability of the system

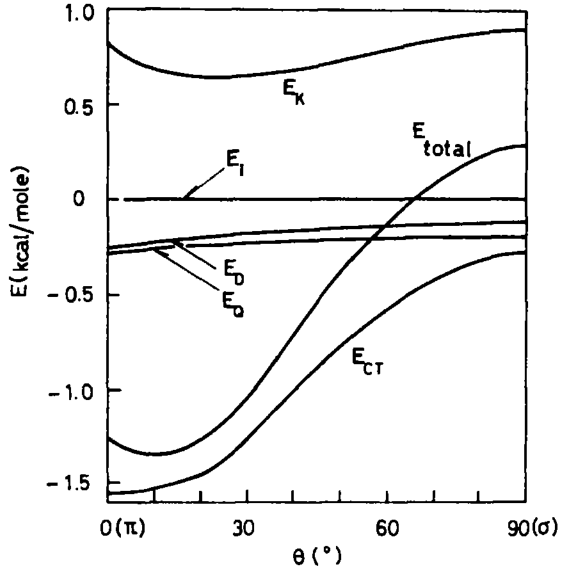

Fig. 2. Angular dependences of various types of interaction energies for the CH_2-*cis*-butene system

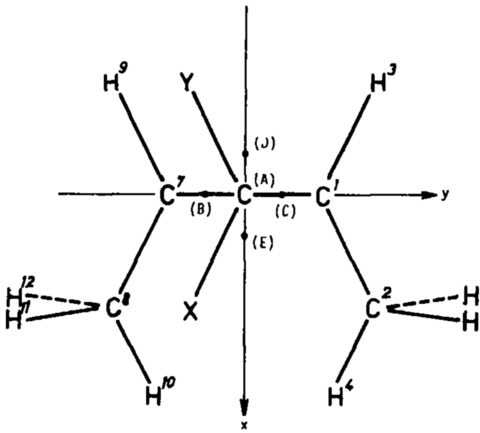

Fig. 3. Projection of CXY on the *cis*-butene-2 plane. The symbols (*A*), (*B*), (*C*), (*D*) and (*E*) indicate the projected positions of the carbene carbon atom. The numbers 1-12 are the atom numberings for *cis*-butene-2

decreases in the order of $C > A > D > B > E$. The relative instabilities of B and E are primarily due to the repulsion term E_K, which is large because of the close proximity of a methylene hydrogen atom to the methyl group of butene. It is of interest to note that, unlike the case of ethylene, C is more stable than A, indicative of the large repulsive forces associated with the methyl group.

As a summary for this section, one may state that the stabilities of the incipient methylene-olefin aggregates are determined primarily by the balancings between the two opposing contributions, E_{CT} and E_K. The π-approach along the z-axis would not be a very unlikely reaction path. E_Q is unimportant, as it should be for systems comprising non-polar molecules. Neither is E_D relatively important, except for large intermolecular separations. E_I is extremely small and thus can be neglected.

Stereoselectivity of Halocarbenes

Calculations analogous to those described in the preceding section have been carried out for the additions of some halocarbenes toward *cis*-butene-2. The halocarbenes treated are fluorocarbene (CHF), fluorochlorocarbene (CFCl) and methylchlorocarbene (CH_3CCl). The specific purpose is to compare the relative eases of the two stereo-courses leading to the formations of syn and anti cycloadducts (Fig. 1).

1. CHF

Free fluorocarbene generated by the thermolysis of fluorodiazomethane is known to be least stereoselective, giving an approximately 1 : 1 mixture of syn and anti addition products with *cis*-butene-2 [19]. Nonetheless, it will be theoretically of interest to diagnose its intrinsic character in the interaction.

The energies of interaction between CHF and *cis*-butene-2 were calculated for the syn-F and anti-F π-approach models at the interplanar distances $z = 2.8$, 3.2 and 3.7 Å. Table 3 summarizes the results obtained for the cases in which both x and y were assumed to be 0.

It can be seen in Table 3 that at every distance studied the total stabilization energy ($-E_{\text{total}}$) is slightly greater for the syn-F orientation. At the greatest distance studied (3.7 Å), E_D and E_{CT} are of dominant importance to the stability of the system. However, the factors which tend to lead the F atom to the syn orientation are E_Q, E_K and E_D. As the distance diminishes, E_K and E_{CT} increase in magnitude far more rapidly than do the remaining energies. This is because E_K and E_{CT} involve a greater overlap dependence (S^2) as compared with the rest. To the selection of the syn-F orientation, however, E_Q and E_D would also make some contribution. At $z = 2.8$ Å, contributions of the four types of energies are almost equally important.

Small changes in x, y and θ did not alter the results materially. The overall situations were much the same as those delineated for the methylene-*cis*-butene system. In what follows, we will treat problems with the carbon atom of carbenes fixed at a point where $x = y = 0$ and $z = 3.2$ Å.

Table 3. Stereoselectivity of CHF in the addition toward *cis*-butene-2[a]

z(Å)	Configuration[b]	E_Q	E_K	E_I	E_D	E_{CT}	E_{total}
2.8	syn	−1.539	3.203	−0.021	−0.646	−5.479	−4.482
	anti	−1.365	3.179	−0.015	−0.566	−5.227	−3.994
3.2	syn	−0.311	0.744	−0.012	−0.352	−1.336	−1.266
	anti	−0.255	0.774	−0.008	−0.312	−1.303	−1.104
3.7	syn	−0.055	0.110	−0.006	−0.175	−0.200	−0.327
	anti	−0.022	0.122	−0.004	−0.158	−0.202	−0.265

[a] Energies given in units of kcal/mole. Geometry: $x = y = 0$ Å and $\theta = 0°$.

[b] With respect to the F atom.

2. CFCl

Fluorochlorocarbene produced by the action of potassium *t*-butoxide on sym-tetrachlorodifluoroacetone is reported to add to *cis*-butene-2 in the syn-Cl/anti-Cl ratio of 2.40 [20]. The greater syn selectivity of the chlorine atom as compared with the fluorine atom has been interpreted as being due to the greater electrostatic attraction of the more polarizable chlorine atom [20]. It is implicit that this stabilizing effect overcomes the differential in the adverse steric effects of the halogens.

Results of our calculation are interesting in connection with the above-mentioned qualitative view. As will be described below, the sum of the attractive interaction energies is certainly greater in magnitude for the syn-Cl orientation but that it cannot offset the disadvantage arising from the repulsion energy unless the 3*d* vacant orbitals of the chlorine atom is taken into consideration.

Because of the bulkiness of the chlorine atom, the π-approach can hardly be satisfactory approximation. Thus, the rotation angle which minimizes E_{total} for the syn-Cl orientation was searched. It was found to be ca. 20°. Table 4 lists the results of calculation for three cases: (1) $\theta = 0°$ without the *d* orbitals; (2) $\theta = 20°$ without the *d* orbitals; and (3) $\theta = 20°$ with the *d* orbitals included.

For both Cases 1 and 2, the syn-Cl orientation is calculated to be the less stable. In Case 1, the relative instability of the syn orientation is due to its outstandingly large value of E_K. In Case 2, this repulsion is reduced considerably at a slight sacrifice of E_{CT}. In the meanwhile, the anti-Cl orientation gains extra stability through E_Q. The net result is that the anti-Cl form is still the more stable. In Case 3, uniquely among the three cases studied, the syn-Cl orientation is predicted to be more stable than the anti-Cl, in agreement with observation. Clearly, this is due to a significant decrease in E_{CT} for the syn-Cl form. Both forms are more stabilized than in Case 2, primarily as a consequence of the decrease in

Table 4. Stereoselectivities of CFCl and CH_3CCl in the addition toward cis-butene-2[a]

Basis set	θ(°)	Configuration[b]	E_Q	E_K	E_I	E_D	E_{CT}	E_{total}
CFCl								
sp	0	syn	−2.014	2.242	−0.028	−0.607	−1.403	−1.809
		anti	−1.237	1.056	−0.028	−0.496	−1.183	−1.888
sp	20	syn	−1.978	1.040	−0.019	−0.423	−1.239	−2.618
		anti	−1.947	0.719	−0.020	−0.365	−1.214	−2.827
spd	20	syn	−2.403	1.048	−0.015	−0.480	−1.916	−3.766
		anti	−2.567	0.736	−0.013	−0.395	−1.316	−3.555
CH_3CCl								
sp	20	syn	−1.464	1.312	−0.011	−0.622	−1.125	−1.910
		anti	0.396	2.288	−0.018	−0.876	−1.441	0.349
spd	20	syn	−1.468	1.322	−0.013	−0.704	−1.760	−2.623
		anti	0.404	2.312	−0.024	−0.926	−1.556	0.211

[a] Energies given in units of kcal/mole. Geometry: $x = y = 0$ Å and $z = 3.2$ Å.

[b] With respect to the Cl atom.

E_Q. The E_Q term appears to favor the anti-Cl orientation, which is, however, immaterial to the overall stereoselectivity.

The possibility that a *d*-orbital of second-row elements importantly participates in charge transfer was first pointed out by Schöllkopf *et al.* [21] in order to account for the syn selectivity of phenylthiocarbene (or, more strictly, its carbenoid). However, the type of such interactions still remains to be characterized. Thus, by analyzing the E_{CT} term for the CFCl-*cis*-butene system, we were able to verify that the interaction between the lowest vacant molecular orbital ϕ_{lv} of CFCl and the highest occupied orbital ψ_{ho} of the butene constitutes the most dominant contribution. Both these oribtals are predominantly of the π-type. Importantly, the inclusion of the chlorine *d* orbitals in the basis set greatly lowers the lowest vacant level of CFCl, thus facilitating the inter-orbital interaction mentioned above. The energies ε and wave functions of these orbitals were as follows (for the coordinate axes and atom numberings, see Fig. 3 with X=Cl and Y=F):

CFCl(*sp*):

$$\begin{aligned} \phi_{lv} &= 0.9204\,\chi(\mathrm{C}, p_z) - 0.2936\,\chi(\mathrm{F}, p_z) - 0.2582\,\chi(\mathrm{Cl}, p_z) \\ \varepsilon_{lv} &= 2.0711\ \mathrm{eV}\,. \end{aligned} \tag{12}$$

CFCl(*spd*):

$$\begin{aligned} \phi_{lv} &= 0.7960\,\chi(\mathrm{C}, p_z) - 0.2810\,\chi(\mathrm{F}, p_z) - 0.3019\,\chi(\mathrm{Cl}, p_z) \\ &\quad - 0.3403\,\chi(\mathrm{Cl}, d_{xz}) + 0.2837\,\chi(\mathrm{Cl}, d_{yz}) \\ \varepsilon_{lv} &= 0.6702\ \mathrm{eV}\,. \end{aligned} \tag{13}$$

cis-Butene-2:

$$\begin{aligned} \psi_{ho} &= 0.5709\,[\chi(\mathrm{C}_1, p_z) + \chi(\mathrm{C}_7, p_z)] - 0.2228\,[\chi(\mathrm{C}_2, p_z) + \chi(\mathrm{C}_8, p_z)] \\ &\quad - 0.2494\,[\chi(\mathrm{H}_5, s) - \chi(\mathrm{H}_6, s) + \chi(\mathrm{H}_{11}, s) - \chi(\mathrm{H}_{12}, s)] \\ \varepsilon_{ho} &= -12.9075\ \mathrm{eV}\,. \end{aligned} \tag{14}$$

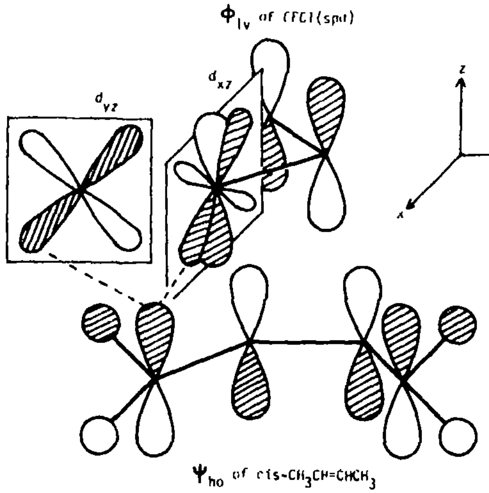

Fig. 4. Schematic representation of the ϕ_{lv} for CFCl and the ψ_{ho} for *cis*-butene-2, illustrating favorable overlappings of the Cl $d\pi$ orbitals with the $\mathrm{CH_3}$ $p\pi$ orbital. The hatched lobes are minus in sign in the molecular orbitals in question. For CFCl, Eq. (13) was multiplied by -1

The functional forms of ϕ_{l_v} and ψ_{k_o} also match for such an interaction, as is illustrated in Fig. 4. The greater stability of the syn-Cl orientation as compared with the anti-Cl is thus ascribable to its greater $\phi_{l_v} - \psi_{k_o}$ interaction as a result of the spatially more favorable $p\pi - d\pi$ overlapping.

3. CH_3CCl

Moss and Mamantov [22] have recently reported that methylchlorocarbene generated by photolysis of methylchlorodiazirine adds to *cis*-butene-2 in the syn-Cl/anti-Cl ratio of 2.84. The product isomer ratio, which is relatively large, has been interpreted to be a consequence of the greater polarizability plus the lesser steric hindrance of Cl as compared with CH_3.

The interaction energies for the CH_3CCl-*cis*-butene system were calculated at $\theta = 20°$, with and without the 3*d* orbitals of Cl included. The two sets of calculations correspond to Cases 2 and 3 defined for the CFCl-*cis*-butene system. The results obtained are listed in Table 4.

A glance at the CH_3CCl data of Table 4 readily shows that, for both cases studied, the syn-Cl orientation should be significantly more stable than the anti-Cl. The large differences in E_{total} between the two orientations are ascribable to the E_Q and E_K terms, both of which greatly favor the syn-Cl orientation. This is readily understandable if one considers the electronic character and bulkiness of the methyl group relative to the chlorine atom. In both respects, the anti-Cl orientation should be disadvantageous as the methyl group of CH_3CCl lies in a closer proximity to one of the methyl groups of *cis*-butene-2.

One thing that we would like to comment on here is the relative magnitude of E_{CT} for the two orientations. When the *d* orbitals of Cl were not included, the E_{CT} was calculated to be greater in magnitude for the anti-Cl orientation. This implies that the methyl group can somehow enter into intermolecular overlap interactions at least to the same extent as the $p\pi$ orbital of the chlorine atom. By the inclusion of the Cl 3*d* orbitals into calculations, only the E_{CT} for the syn-Cl orientation is increased considerably in magnitude, just as in the case of CFCl.

Discussion

Using a ZDO version of the intermolecular-interaction theory of Murrell *et al.*, we have been able to elucidate favorable stereo courses for the addition reactions of singlet carbenes toward olefins. The syn/anti stereoselectivity of halocarbenes has been found to be influenced by various types of interaction energies altogether, no single energy term being of exclusive importance in this respect. Roughly, however, it often hinges on the balancings between charge-transfer attraction and exchange repulsion. Participation of the vacant *d* orbitals of the chlorine atom in charge transfer would also have to be stressed in this connection.

Several points might be raised, however, against the theoretical procedure adopted in this work. First, we have precluded the effect of molecular structure deformations, which should develop as the reaction proceeds. The results that the intermolecular interactions lead to net stabilization of the aggregates ($E_{\text{total}} < 0$), are at least partly ascribable to the neglect of this effect. Second, no attention has been paid to self-consistency of the molecular orbitals for components present *in* molecular aggregates. Presumably, this aspect will be of particular importance in describing intermolecular interactions associated with molecules bearing polar substituents. Third and finally, we have combined the intramolecular ZDO assumption with the intermolecular-interaction theory which was formulated in special consideration of intermolecular orbital overlaps. In a sense, the overall formalism is internally inconsistent.

Despite these inaccuracies, we believe that our present formalism is still useful as a working tool for unraveling the nature of a reaction at its early stage. The first point mentioned above is apparently beside the primary purpose of the present work. The second and third approximations would probably be tolerable in consideration of the need for a compromise between theoretical rigorousness and computational economy.

Assessments of the roles of various types of energies involved in the courses of chemical reactions are of general interest. Applications of the present method to other types of reactions (including those of carbenoids) and extensions to open-shell cases are under way and will be reported elsewhere.

References

1. For a recent review, see: Moss, R. A.: Chem. Eng. News. June 16, 60 (1969); June 30, 50 (1969).
2. Closs, G. L., Moss, R. A.: J. Amer. chem. Soc. **86**, 4042 (1964).
3. Moss, R. A.: J. org. Chem. **30**, 3261 (1965).
4. Murrell, J. N., Randić, M., Williams, D. R.: Proc. Roy. Soc. (London) A **284**, 566 (1965).
5. Pople, J. A., Santry, D. P., Segal, G. A.: J. chem. Physics **43**, S 129 (1965).
6. Segal, G. A.: J. chem. Physics **44**, 3289 (1966).
7. Santry, D. P., Segal, G. A.: J. chem. Physics **47**, 158 (1967).
8. Mulliken, R. S.: J. Chim. physique **46**, 497 (1949).
9. Roothaan, C. C. J.: J. chem. Physics **19**, 1445 (1951).
10. Mulliken, R. S., Rieke, C. A., Orloff, D., Orloff, M.: J. chem. Physics **17**, 1248 (1949).
11. Mitchell, A. D., ed.: Table of interatomic distances and configuration in molecules and ions. London: The Chemical Society 1958.
12. Kondo, S., Sakurai, Y., Hirota, E., Morino, Y.: J. molecular Spectroscopy **34**, 231 (1970).
13. Herzberg, G.: Proc. Roy. Soc. (London) A **262**, 291 (1961).
14. Merer, A. J., Travis, D. N.: Canad. J. Physics **44**, 1541 (1966).
15. — — Canad. J. Physics **44**, 525 (1966).
16. Hoffmann, R.: J. Amer. chem. Soc. **90**, 1475 (1968).
17. — Woodward, R. B.: J. Amer. chem. Soc. **87**, 2047 (1965).
18. Pauling, L.: The nature of the chemical bond, 3rd. ed, p. 263. Ithaca, N. Y.: Cornell University Press 1960.
19. Tang, Y.-N., Rowland, F. S.: J. Amer. chem. Soc. **89**, 6420 (1967).
20. Moss, R. A., Gerstl, R.: J. org. Chem. **32**, 2268 (1967); Tetrahedron **23**, 2549 (1967).
21. Schöllkopf, U., Lehmann, G. J., Paust, J., Härtl, H.-D.: Chem. Ber. **97**, 1527 (1964).
22. Moss, R. A., Mamantov, A.: J. Amer. chem. Soc. **92**, 6951 (1970).

Professor T. Fueno
Department of Chemistry
Faculty of Engineering Science
Osaka University
Toyonaka, Osaka, Japan

Theoret. chim. Acta (Berl.) 26, 55—65 (1972)
© by Springer-Verlag 1972

Zur Konjugation in makrocyclischen Bindungssystemen [1]

XX. Charakterordnung, magnetische Suszeptibilitäten und chemische Verschiebungen von Corannulenen*

Paramagnetischer Suszeptibilitätsanteil im Innern von Corannulenen

G. Ege und H. Vogler

Organisch-Chemisches Institut der Universität Heidelberg

Eingegangen am 30. September 1971

Conjugation in Macrocyclic Bonding Systems

XX. Order of Character, Magnetic Susceptibility and Chemical Shifts of Corannulenes

By means of calculations of the Polansky character order, ring current contributions to the magnetic susceptibilities and to the chemical shift in the Hückel approximation, it is shown, that corannulenes cannot be treated as macrocyclic annulenes.

Mit Hilfe von Berechnungen der Polansky-Charakterordnungen, der magnetischen Suszeptibilitäten und der chemischen Verschiebungen (^{1}H–NMR) im Rahmen der HMO-Theorie wird gezeigt, daß Corannulene nicht als makrocyclische Annulensysteme aufgefaßt werden können.

Des calculs des caractères annulènoides, des contributions du courant cyclique à la susceptibilité magnétique et aux déplacements chimiques dans la méthode de HMO montrent, que les corannulènes ne peuvent pas considérer comme des annulènes macrocycliques.

Einleitung

Corannulene sind Moleküle, die aus zwei Perimetern bestehen, die durch sog. Radialenbindungen verknüpft sind. Bisher sind nur wenige Corannulene bekannt: Pyren I, Coronen II und das eigentliche „Corannulen“ [2]. Ein weiteres Corannulen konnte nur massenspektrometrisch nachgewiesen werden [3]. Über Versuche zur Synthese makrocyclischer Corannulene wurde berichtet [4, 5]. Bei diesen Verbindungen interessiert die Frage, ob derartige Kohlenwasserstoffe als makrocyclisch konjugierte Annulene aufgefaßt werden können. Diese Frage soll im Rahmen der HMO-Theorie beantwortet werden.

Wir beschränken uns auf alternierende Corannulene, die nur aus Benzoleinheiten aufgebaut sind, da bei ihnen die Anwendung der HMO-Theorie gerechtfertigt ist. Unsere Untersuchungen wurden auch auf die strukturell ähnlichen Polyacene ausgedehnt, um die Verläßlichkeit der Theorie zu prüfen.

Erste Hinweise darauf, daß die Kopplung zwischen beiden Perimetern sehr stark ist, ergaben frühere Berechnungen der Bindungsordnungen einiger Corannulene [6]. Ebenso ergaben die Berechnungen der Radialen-HMO-Bindungsordnungen von den Corannulenen I bis VII Werte zwischen 0,65 und 0,47, was einem Bindungsabstand von 1,40–1,43 Å entspricht [7]. Früher [6] wurde schon festgestellt, daß bei derartigen makrocyclischen Bindungssystemen die mit der HMO-Methode berechneten Bindungslängen ungefähr mit denen nach der SCF-Methode übereinstimmen.

---

* Teilweise vorgetragen auf dem VII. Symposium für Theoretische Chemie vom 29. 3. bis 2. 4. 1971 in Göttingen.

Wir untersuchten u. a.[1] folgende Corannulene:

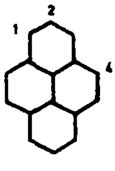

I
(2, 14)

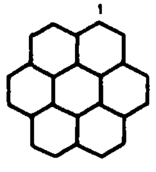

II
(6, 18)

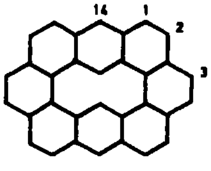

III
(10, 22)

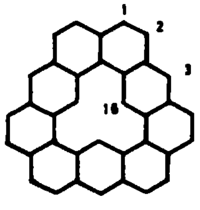

IV
(12, 24)

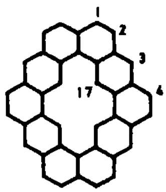

V
(14, 26)

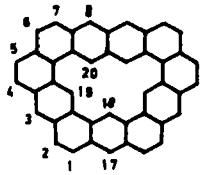

VI
(16, 28)

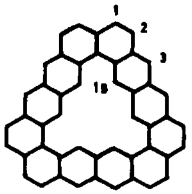

VIIa
(18, 30)

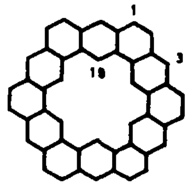

VIIb
(18, 30)

In Klammern wird die Zentrenzahl (n_i, n_a) des inneren und äußeren Perimeters angegeben. Dabei gilt immer $n = n_i + n_a$ und $n_a = n_i + 12$. Alle Corannulene (außer IV und VI) haben zwei $(4q+2)$-Perimeter. Wir nennen diese Corannulene einfach $(4q+2)$-Corannulene im Gegensatz zu IV und VI, die entsprechend $(4q)$-Corannulene genannt werden.

Annulenoide Charakterordnungen von Polyacenen und Corannulenen

Polansky u. Derflinger [8] entwickelten eine Methode, die es erlaubt, den benzoiden, butadienoiden usw. Charakter der entsprechenden Teilstruktur einer konjugierten Verbindung zu berechnen. Sie definierten eine Maßzahl r_L, die sog. Charakterordnung der Teilstruktur L, die in dem Gesamtmolekül enthalten ist

$$r_L = \frac{1}{2n_L} \sum_{\mu=1}^{n} \sum_{\nu=1}^{n} P^L_{\mu\nu} P_{\mu\nu} \qquad 0 \leqq r_L \leqq 1 .$$

$P_{\mu\nu}$: π-Bindungsordnungen im Gesamtsystem,
$P^L_{\mu\nu}$: π-Bindungsordnungen in der isolierten Teilstruktur L,
n: Gesamt-π-Zentrenzahl,
n_L: π-Zentrenzahl der Teilstruktur L, $n_L \leqq n$.

---

[1] Weitere untersuchte Corannulene s. [7].

Es bedeutet

$$r_L = \begin{cases} 1 & \text{vollständige Beteiligung der bindenden MO's der isolierten Teilstruktur am Gesamtmolekül,} \\ 0 & \text{entsprechende vollständige Beteiligung der antibindenden MO's.} \end{cases}$$

Tabelle 1. Annulenoide Charaktere einiger Polyacene und Corannulene

Verbindung	n	n_a	n_i	$r_a \cdot 10^3$	$r_i \cdot 10^3$
Benzol	6	6		1000	
Naphthalin	10	10		988	
Anthracen	14	14		981	
Tetracen	18	18		975	
Pentacen	22	22		971	
Hexacen	26	26		967	
Heptacen	30	30		964	
I	16	14	2	962	768
II	24	18	6	955	877
III	32	22	10	946	890
IV	36	24	12	924	859
V	40	26	14	940	896
VI	44	28	16	926	878
VIIa	48	30	18	937	900
VIIb	48	30	18	936	900

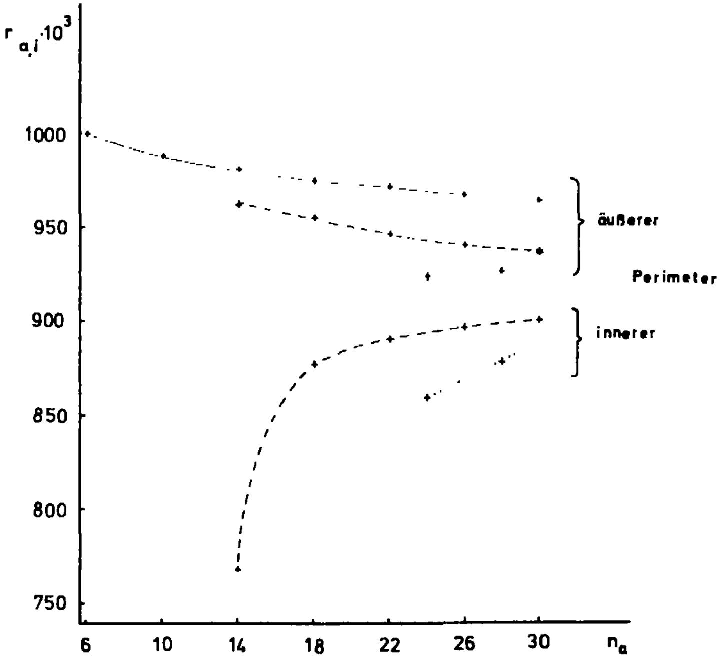

Fig. 1. Annulenoide Charaktere von linearen Polyacenen (— · -), $(4q+2)$-Corannulenen (----) und $(4q)$-Corannulenen (······)

Wir haben diese Methode zur Berechnung des annulenoiden Charakters $r_{a(i)}$ des äußeren (inneren) Perimeters verwendet. Je schwächer die Kopplung zwischen beiden Perimetern ist, desto näher sollte $r_{a(i)}$ bei 1 liegen. Tab. 1 und Fig. 1 geben die berechneten $r_{a(i)}$-Werte wieder. In Fig. 1 wurde als Abszisse n_a gewählt, und zwar sowohl für r_a als auch für r_i, da sich n_a und n_i nur um den konstanten Summanden 12 unterscheiden.

Bei Polyacenen entfällt n_i und r_i.

Diskussion der annulenoiden Charakterordnungen bei Polyacenen und Corannulenen

Bei diesen Substanzklassen ergibt sich das folgende Bild:

1. Der annulenoide Charakter der Corannulene ist kleiner als der von linearen Polyacenen gleicher Zentrenzahl.

2. Der annulenoide Charakter von $(4q)$-Corannulenen ist kleiner als der von $(4q+2)$-Corannulenen.

3. r_a nimmt mit wachsendem n_a ab, r_i nimmt jedoch zu. r_a ist stets größer als r_i, d. h. der äußere Perimeter ist weniger gestört als der innere Perimeter und somit das „bessere“ Annulen.

4. Für Corannulene mit großer Zentrenzahl ändern sich die Werte für $r_{a(i)}$ kaum noch.

Suszeptibilitäten und chemische Verschiebungen bei Polyacenen und Corannulenen

Die magnetische Suszeptibilität und die chemische Verschiebung (^{1}H–NMR) ermöglicht, die Charakterordnungen mit meßbaren Werten zu korrelieren. Wir berechneten die von der Delokalisierung der π-Elektronen herrührende magnetische Suszeptibilität χ^R und die Störungsenergie 2. Ordnung E_{20}, die mit χ^R in folgender Weise verknüpft ist

$$\chi^R = -2E_{20}$$

sowie die chemischen Verschiebungen δ' von äußeren und inneren Protonen[2]. Für diese Berechnungen wählten wir die Methode von Amos und Roberts [9–11] im Rahmen der HMO-Theorie. Diese Methode basiert auf dem Ansatz von London [12] und ist numerisch bequemer durchzuführen als die Methoden von Pople [13] und McWeeny [14]. Für E_{20} bzw. δ' ergeben sich aus der störungstheoretischen Behandlung des Problems die folgenden Gleichungen [9–11]

$$E_{20} = 2f_1 \sum_{i} \sum_{s,t} [c_{is}^0 c_{it}^0 F_{st}(20) + c_{is}^0 c_{it}(10) F_{st}(10)], \qquad (1)$$

$$\delta' = -\frac{\beta}{3} f_2 \sum_{i} \sum_{s,t} [2c_{is}^0 c_{it}(10)\, F_{st}(01) + c_{is}^0 c_{it}^0 F_{st}(11)]. \qquad (2)$$

---

[2] $\delta' := 0$ für ein nicht cyclisch konjugiertes olefinisches Proton und $\delta' < 0$ für Verschiebungen nach tiefem Feld.

Darin bedeuten
β HMO-Resonanzintegral, wir verwendeten den Wert $\beta = -4{,}15$ eV nach [11],
c_{is}^{0} Hückelkoeffizienten des i-ten MO's,
F_{st}^{0} Matrixelemente des Hückeloperators in β-Einheiten,
$F_{st}(10) = i\alpha S_{st} F_{st}^{0}$,
$F_{st}(01) = i\alpha S_{st} K_{st} F_{st}^{0}$,
$F_{st}(20) = -\alpha^2 S_{st}^{0} F_{st}^{0}$,
$F_{st}(11) = -\alpha^2 S_{st}^{0} K_{st} F_{st}^{0}$,
$\alpha = \dfrac{e}{\hbar c}$,
$S_{st} = \frac{1}{2}(x_s y_t - y_s x_t)$,
$K_{st} = \dfrac{1}{R_s^3} + \dfrac{1}{R_t^3}$,

f_1 und f_2 sind Skalenfaktoren. Mißt man Koordinaten in Å-Einheiten, F_{st}^{0} in β-Einheiten und bezieht man auf 1 Mol, so erhält man für f_1 und f_2 die folgenden Werte

$$f_1 = 2{,}22760 \qquad f_2 = 3{,}698491\,.$$

E_{20} hat dann die Dimension $[10^{-6}\,\mathrm{cm}^3\,\mathrm{Mol}^{-1}]$ und δ' wird in Einheiten von 10^{-6}, d. h. ppm gemessen.

Die $c_{it}(10)$ erhält man durch Lösen des folgenden Gleichungssystems [9]

$$\sum_t (F_{st}^{0} - \varepsilon_i^{0}\,\delta_{st})\,c_{it}(10) = -\sum_t F_{st}(10)\,c_{it}^{0}\,,$$

ε_i^{0} HMO-Eigenwert des i-ten MO's in β-Einheiten.

Da in den Summanden der Gl. (1) und (2) jeweils die ungestörten Hückelmatrixelemente auftreten, für die gilt $F_{st}^{0} = 0$, falls die Zentren s und t nicht gebunden sind, läßt sich E_{20} (bzw. χ^R) in Beiträge einzelner Teilstrukturen aufteilen. Insbesondere gilt

$$E_{20} = E_{20}^{P_a} + E_{20}^{P_i} + E_{20}^{R_a}\,.$$

Dabei beziehen sich P_a bzw. P_i auf Beiträge des äußeren bzw. inneren Perimeters und R_a auf die Beiträge aller Radialenbindungen. Diese Aufteilung ist deshalb möglich, da es sich gezeigt hat [7], daß die Perimeterterme $E_{20}^{P_a(i)}$ von der Wahl des Koordinatenursprungs weitgehend unabhängig sind und für den Term $E_{20}^{R_a}$, der stark von dieser Wahl abhängig ist, gilt

$$E_{20}^{R_a} \ll E_{20}^{P_a(i)}\,.$$

Wie man Gl. (1) entnimmt, ist die magnetische Suszeptibilität proportional dem Quadrat der umschlossenen Fläche. Um Verbindungen verschiedener Fläche vergleichen zu können, wurden die E_{20}-Werte auf die gleiche Fläche bezogen, indem durch das Quadrat des Vielfachen der Benzolfläche dividiert wurde. Dabei wurde die Benzolfläche gleich 1 gesetzt. Wir nennen diese Werte $E_{20}^{P_a(i)}$(red). Bei schwacher Kopplung erwarten wir eine Suszeptibilität der beiden Perimeter, die der der isolierten Annulene nahekommt. Bekanntlich zeigen $(4q+2)$-Annulene starken Diamagnetismus, $(4q)$-Annulene jedoch Paramagnetismus [15–18]. Die

Tabelle 2. Magnetische Suszeptibilitäten von Polyacenen und Corannulenen

Verbindung[a]	n_a	χ^{R} [b]	$E_{20}^{P_a}$ [c]	$E_{20}^{P_i}$ [c]	$E_{20}^{R_a}$ [c]	$E_{20}^{P_a}$(red)	$E_{20}^{P_i}$(red)
Benzol	6	− 52,815	− 6,363		0,0	−6,363	
Naphthalin	10	−115	− 13,9		0,0	−3,48	
Anthracen	14	−182	− 21,5		−0,41	−2,39	
Tetracen	18	−250	− 29,2		−1,00	−1,83	
Pentacen	22	−320	− 36,9		−1,66	−1,47	
Hexacen	26	−390	− 44,7		−2,32	−1,24	
I	14	−242	− 29,9	+ 0,0	+0,8	−1,87	[d]
II	18	−517	− 64,9	+ 2,7	+0,0	−1,33	+2,69
III	22	−625	− 84,2	+ 9,8	−0,9	−0,84	+2,45
IV	24	−403	− 73,7	+27,1	−1,9	−0,51	+3,00
V	26	−735	−110	+23,6	−2,3	−0,51	+1,48
VI	28	−530	−101	+40,5	−3,5	−0,39	+1,62
VIIa	30	−807	−135	+42,1	−4,1	−0,42	+1,17
VIIb	30	−808	−138	+45,3	−4,6	−0,38	+0,92

[a] Bei allen Bindungen wurde die Benzolbindungslänge von 1,397 Å zu Grunde gelegt. Die Berücksichtigung der experimentellen Bindungslänge ändert die Ergebnisse nur unwesentlich (s. [7]).

[b] In Einheiten von $10^{-6}\,\mathrm{cm}^3\,\mathrm{Mol}^{-1}$. Zur Berechnung von mittleren Suszeptibilitäten aus den χ^R-Werten vergleiche [7, 9]. Die Übereinstimmung mit bekannten experimentellen Werten ist gut.

[c] In Einheiten von $10^{-6}\,\mathrm{cm}^3\,\mathrm{Mol}^{-1}\,\beta'^{-1}$. β' ist der Wert des Resonanzintegrals in eV.

[d] Dieser Wert ist nicht definiert, da die Fläche des „inneren Perimeters" Null ist.

berechneten annulenoiden Charaktere (Tab. 1) deuten darauf hin, daß der Diamagnetismus bei den $(4q+2)$-Corannulenen I, II, III, V, VIIa und VIIb vor allem im inneren Perimeter stark verkleinert ist im Vergleich zum freien Annulen. Bei den $(4q)$-Corannulenen IV und VI sollte gemäß der $r_{a(i)}$-Werte der Paramagnetismus der $(4q)$-Perimeteranteile ebenfalls kleiner sein als in den jeweils ungestörten Perimetern. Die Verkleinerung des Paramagnetismus ist möglicherweise im äußeren Perimeter größer als im inneren (obwohl $r_a > r_i$ ist), da bei größerem $(4q)$-Perimeter die Abnahme des Paramagnetismus infolge Bindungsalternanz mehr ins Gewicht fällt als bei kleinerem $(4q)$-Perimeter [15]. Die berechneten Suszeptibilitäten zeigen Tab. 2 und Fig. 2.

Es ergibt sich ein qualitativ ähnlicher Verlauf der Abhängigkeit von $E_{20}^{P_{a(i)}}$(red) bzw. $r_{a(i)}$ von n_a, wie der Vergleich der Figs. 2 und 1 zeigt. Die Korrelation von $E_{20}^{P_{a(i)}}$(red) und $r_{a(i)}$ zeigt die Fig. 3.

Bemerkenswert ist vor allem, daß sowohl bei $(4q)$- als auch bei $(4q+2)$-Corannulenen der äußere Perimeter einen diamagnetischen Beitrag (negatives Vorzeichen von $E_{20}^{P_a}$), der innere jedoch einen paramagnetischen Beitrag (positives Vorzeichen von $E_{20}^{P_i}$) zur Gesamtsuszeptibilität liefert. Letzterer ist bei $(4q)$-Corannulenen besonders groß. Daraus folgt, daß die Kopplung zwischen beiden Perimetern stark ist, denn sonst müßte bei $(4q+2)$-Corannulenen der auf den inneren Perimeter entfallende Anteil der Suszeptibilität diamagnetisch sein. Entsprechend müßte bei schwacher Kopplung bei $(4q)$-Corannulenen der auf den äußeren Perimeter entfallende Anteil der Suszeptibilität paramagnetisch sein (vgl. Fig. 4).

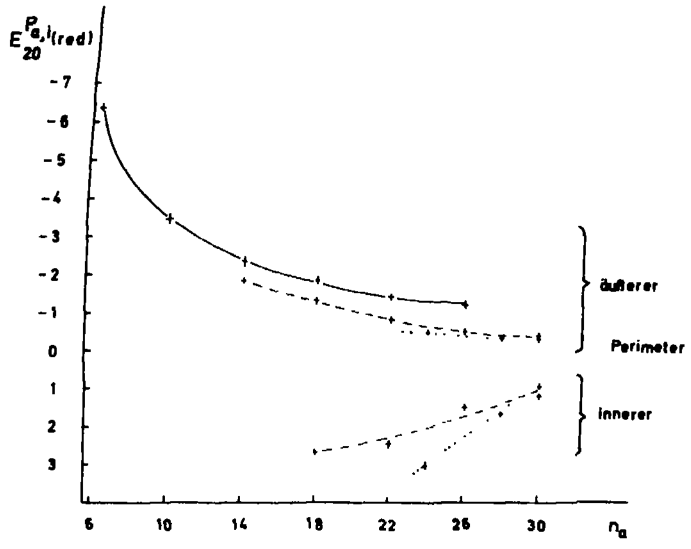

Fig. 2. Störungsenergien $E_{20}^{P_a,i}$(red) von linearen Polyacenen (———), (4q + 2)-Corannulenen (- - - -) und (4q)-Corannulenen (······)

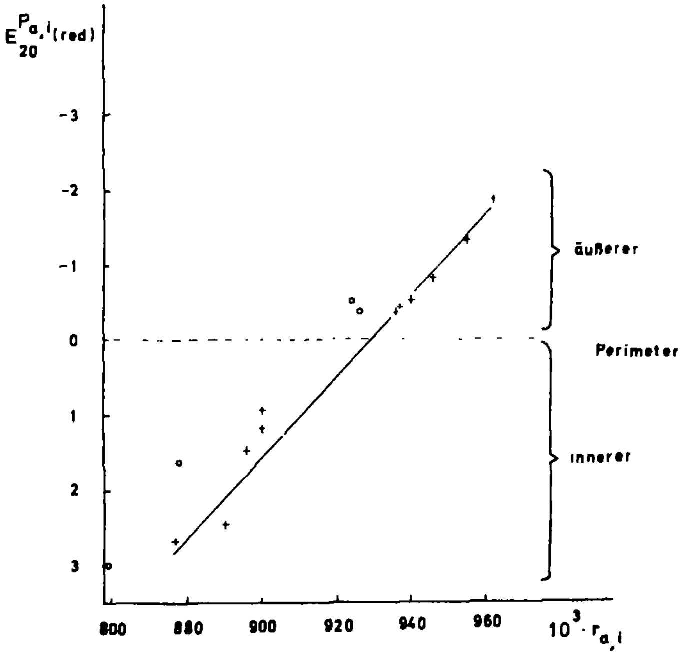

Fig. 3. Korrelationen zwischen annulenoiden Charakteren und Störungsenergien $E_{20}^{P_a,i}$(red) für (4q + 2)-Corannulene (+) und (4q)-Corannulene (O)

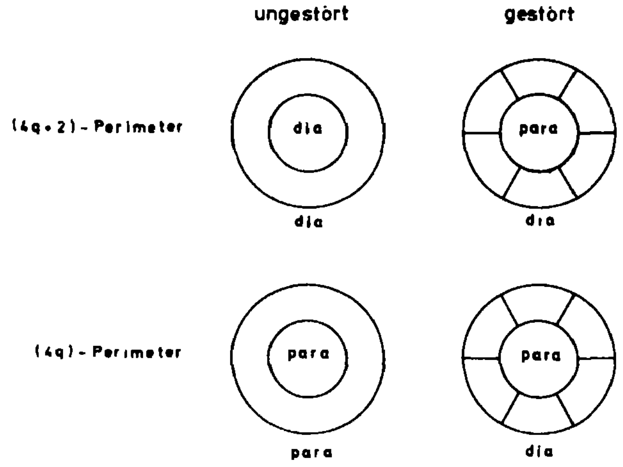

Fig. 4 Suszeptibilitätsbeiträge von $(4q+2)$- bzw. $(4q)$-Perimetern in Corannulenen ohne und mit Kopplung zwischen beiden Perimetern

Die Perimeterbeiträge zur Gesamtsuszeptibilität sind experimentell durch eine Suszeptibilitätsmessung nicht zugänglich. Jedoch erhalten wir indirekt Hinweise auf den diamagnetischen Beitrag des äußeren Perimeters durch die zu erwartende chemische Verschiebung der äußeren Protonen nach tiefem Feld und bei paramagnetischem Anteil der Suszeptibilität des inneren Perimeters durch eine chemische Verschiebung der inneren Protonen ebenfalls nach tiefem Feld. Wir berechneten deshalb die chemischen Verschiebungen nach Gl. (2). Da die berechneten Verschiebungen durchweg zu groß sind (δ'_{Benzol} experimentell $-1{,}55$ ppm nach [11, 19], berechnet $-2{,}17$ ppm), wird zum Vergleich mit gemessenen Größen das Verhältnis

$$\varrho = \frac{\delta'}{\delta'_{\text{Benzol}}}$$

gebildet. In der Tab. 3 sind die so berechneten chemischen Verschiebungen für einige Polyacene und die Verbindungen I bis VII wiedergegeben. Bekannte experimentelle Werte sind zum Vergleich mit aufgeführt. Die Übereinstimmung zwischen beiden ist gut, wenn man von angulären Protonen absieht, bei denen van der Waals'sche Wechselwirkung eine Rolle spielt [20].

Bildet man aus den chemischen Verschiebungen ϱ Mittelwerte ($\bar{\varrho}_a$ über alle Außenprotonen, anguläre Protonen ausgenommen, $\bar{\varrho}_i$ über alle Innenprotonen), so erhält man folgendes Bild (Fig. 5).

1. Die berechneten mittleren chemischen Verschiebungen nehmen bei linearen Polyacenen mit zunehmender Zentrenzahl langsam zu (d. h. sie gehen nach tiefem Feld) und nähern sich bald einem Maximalwert.

2. Bei $(4q+2)$-Corannulenen nimmt mit zunehmender Zentrenzahl $\bar{\varrho}_a$ ab, $\bar{\varrho}_i$ jedoch geringfügig zu. Dies ist in Übereinstimmung mit dem Verlauf der annulenoiden Charaktere und der Störungsenergien $E_{20}^{P,s(1)}$(red).

Tabelle 3. Chemische Verschiebungen

Verbindung[a]	Proton	Berechnete Werte			Experimentelle Werte[d]	
		$-\delta'$[b]	ϱ	$-\delta$[b,c]	$-\delta'$[b]	ϱ
Benzol	1[e]	2,17	1,00	7,34	1,55	1,00
Naphthalin	1	2,55	1,17	7,60	1,74	1,12
	2	2,84	1,31	7,82	2,09	1,35
Anthracen	1	3,01	1,39	7,94	2,19	1,41
	2	2,60	1,20	7,65	1,67	1,08
	9	3,70	1,71	8,44	2,59	1,67
I	1	3,55	1,64	8,33	2,44	1,57
	2	3,25	1,50	8,11	2,27	1,46
	4	3,01	1,39	7,94	2,34	1,51
II	1	4,42	2,04	8,95	3,12	2,01
III	1	4,00	1,85	8,66		
	2	3,89	1,79	8,56		
	3	4,09	1,89	8,72		
	14	4,91	2,26	9,29		
IV	1	2,60	1,19	7,63		
	2	2,70	1,24	7,71		
	3	3,45	1,59	8,25		
	16	10,8	4,98	13,5		
V	1	3,71	1,71	8,44		
	2	3,82	1,76	8,52		
	3	4,55	2,10	9,04		
	4	3,48	1,60	8,27		
	17	3,95	1,82	8,61		
VI	8	3,81	1,76	8,52		
	6/7	2,80	1,29	7,79		
	5	2,83	1,30	7,80		
	4	2,93	1,36	7,90		
	3	3,55	1,63	8,32		
	2	2,55	1,18	7,62		
	1	2,54	1,17	7,60		
	17	3,40	1,57	8,22		
	18	7,15	3,30	10,9		
	19	8,51	3,92	11,9		
	20	8,12	3,74	11,6		
VIIa	1	3,25	1,49	8,10		
	2	3,40	1,56	8,21		
	3	4,40	2,05	8,97		
	19	5,60	2,58	9,79		
VIIb	1	3,11	1,43	8,01		
	3	4,19	1,93	8,78		
	19	4,04	1,86	8,67		

---

[a] Alle C–H-Bindungslängen wurden bei 1,08 Å fixiert.

[b] In ppm.

[c] Die Umrechnung der ϱ-Werte auf δ(TMS)-Werte erfolgt nach der Gleichung:

$$\delta = -1{,}55 \cdot (\varrho - 1) + \delta_{\text{Benzol}} \, .$$

δ Benzol beträgt bezüglich TMS $-7{,}34$ ppm in $CDCl_3$.

[d] Die experimentellen Werte wurden für Benzol [19] und für Naphthalin, Anthracen, Pyren I und Coronen II [20] entnommen.

[e] Protonenbezeichnung:

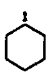

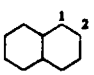

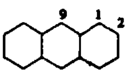

Theoret. chim. Acta (Berl.) 26, 67—78 (1972)
© by Springer-Verlag 1972

Graph Theory and Molecular Orbitals

Application of Sachs Theorem

A. GRAOVAC, I. GUTMAN, N. TRINAJSTIĆ, and T. ŽIVKOVIĆ
Institute "Rudjer Bošković", P.O.B. 1016, 41001 Zagreb, Croatia, Yugoslavia

Received March 1, 1972

The Sachs theorem [1] is discussed, and Kekulé and Sachs graphs are defined. The simple consequences of Sachs theorem which are of interest in chemistry are presented. Thus, it is shown that the pairing theorem, Hückel ($4m+2$) rule, and Longuet-Higgins and Dewar rule [2] can be obtained easily with the use of Sachs theorem. The dependence of the number of Kekulé structures on the molecular topology is also shown.

Das Theorem von Sachs [1] wird diskutiert und Kekulé- und Sachs-Graphen werden definiert. Die einfachen Folgerungen aus dem Theorem von Sachs, die in der Chemie von Interesse sind, werden abgeleitet. So wird gezeigt, daß die Paarregel von Coulson und Rushbrooke, die Hückelsche ($4m+2$)-Regel und die Regel von Longuet-Higgins und Dewar [2] leicht mit dem Sachsschen Theorem erhalten werden können. Die Abhängigkeit der Zahl der Kekulé-Strukturen von der molekularen Topologie wird ebenfalls gezeigt.

Introduction

In this work our intention is to investigate the applicability of the mathematical apparatus of Graph theory (GT) to the simple molecular orbital theory. Without insisting on rigid mathematical formalism (which can be found elsewhere [3 5]), we define a graph as an ordered pair

$$(\mathscr{N}, \mathscr{A}) \tag{1}$$

where $\mathscr{N}$ is a set of some elements ("nodes") and $\mathscr{A}$ is a relation defined on the set $\mathscr{N}$, which is symmetrical and antireflexive, i.e.:

$$(X, Y) \in \mathscr{A} \Rightarrow (Y, X) \in \mathscr{A}\,, \tag{2a}$$

$$(X, Y) \in \mathscr{A} \Rightarrow X \neq Y. \tag{2b}$$

So, two nodes can either belong to the relation $\mathscr{A}$ (than we say that this nodes are adjacent), or not (then this nodes are not adjacent). A usual sketch representation of a graph is obtained when the nodes (elements of the set $\mathscr{N}$) are drawn as small circles and if two nodes belong to the relation $\mathscr{A}$ they are connected by a line (so called "edge"). The analogy between the nodes and edges of a graph and the atoms and bonds in a structural formula of a molecule is obvious.

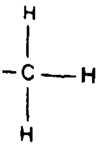

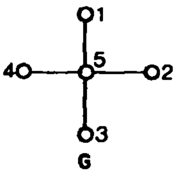

G

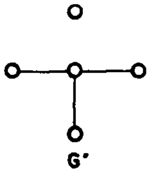
G'

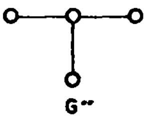
G''

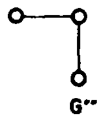
G'''

For example, the graph G which is a representation of the structural formula of methane has five nodes. The relation $\mathscr{A}$ is then the following set of pairs:

$$\{(1,5), (5,1), (2,5), (5,2), (3,5), (5,3), (4,5), (5,4)\}\,.$$

If some edges of a graph are removed a ***subgraph*** of the graph is obtained. If some nodes together with all adjacent edges are removed a ***partial graph*** is obtained. A subgraph of a partial graph is called a ***partial subgraph*** of the graph. G' is a subgraph, G'' is a partial graph and G''' is a partial subgraph of the graph G.

The graph with two nodes and one edge:

will be denoted as Γ.

Using GT, different combinatorial problems of the Organic chemistry can be solved: The number of structural isomers [6], the number of conformations [7], the number of Kekulé structures [8]. However, using a graph theory representation of a molecule, all geometric properties (bond lengths, angles) are neglected. The only molecular property considered is the existence or non-existence, respectively, of the chemical bond between two atoms. This molecular property is usually called "topology" [9] and, although the expression is not the most precise one, it is in common use.

Relation between the Graph Theory and Hückel Theory

There is some scepticism towards the attempts to obtain any useful conclusion about chemical and physical properties of compounds only from the knowledge of their topology [10]. However, in the last few years, various modifications of the HMO method enabled to predict chemical behaviour of conjugated molecules as well as by using more complicated SCF calculations [11]. Similarly, the Hückel formalism using additional elements of GT was successfully applied to different classes of inorganic compounds [12].

The relation between GT and HMO theory can be presented in the following manner.

After a numeration of the nodes is performed, there is one to one correspondence between a graph and so called "adjacency matrix" A, defined as:

$$A_{pq} = \begin{cases} 1 \text{ if the nodes } p \text{ and } q \text{ are adjacent} \\ 0 \text{ if they are not.} \end{cases} \tag{3}$$

The Hamiltonian matrix in the Hückel approximation can be now written as:

$$\boldsymbol{H} = \alpha \boldsymbol{I} + \beta \boldsymbol{A} \tag{4}$$

where $\boldsymbol{I}$ is a unit matrix; α and β are the Coulomb and the resonance integrals.

When conjugated hydrocarbons are examined in the HMO approach, the related graphs correspond to the carbon-carbon σ-bond skeleton, while the

π-bonds and the C–H σ-bonds are neglected:

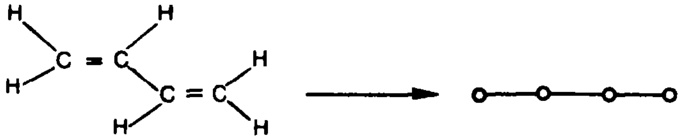

In this work all graphs are assumed to be of the above type.

The secular equation:

$$\det|H - \varepsilon S| = 0 \tag{5}$$

can be written, after adopting the zero-overlap approximation [13], as:

$$\det|xI - A| = 0 \tag{6}$$

where:

$$x = \frac{\varepsilon - \alpha}{\beta}. \tag{7}$$

In other words, the problem of the Hückel orbital energies can be completely reduced to the adjacency matrix eigenvalue problem. Albeit this fact should have been known, at least implicitly, to everyone who once solved a Hückel problem, its fundamental meaning was discovered relatively recent [4, 5, 12c, 14].

Eq. (6) was exhaustively studied within GT [1, 15, 16]. Many useful results were obtained. Some of them we shall comment here.

In the GT the following nomenclature is used. $\det|xI - A| \equiv P_G(x)$ is the "characteristic polynomial". The set of its roots:

$$\{x_1, x_2, \dots, x_N\}$$

being called the "spectrum" of the corresponding graph.

So, let

$$P_G(x) = \sum_{n=0}^{N} a_n x^{N-n} \tag{8}$$

where N is the number of nodes in the graph. Since the characteristic polynomial $P_G(x)$ is uniquely defined by the graph G, the coefficients a_n can be found without going through the procedure of solving the determinant, but solely knowing the topological structure of the graph.

If we define a Sachs graph as such graph which has no other components but graphs Γ and rings, a following formula, originally given by Sachs [1], determins those coefficients:

$$\begin{aligned} a_n &= \sum_{s \in S_n} (-)^{c(s)} 2^{r(s)} \quad \text{for} \quad 0 < n \leqq N \\ a_0 &= 1 . \end{aligned} \tag{9}$$

Here s is a Sachs graph and S_n is the set of all Sachs graphs with n nodes. $c(s)$ and $r(s)$ denote respectively the number of components and the number of ring components in s. The summation in (9) is over all elements of the set S_n. If there is $S_n = \emptyset$, where $\emptyset$ is an empty set, then $a_n = 0$. We notice although that for odd n every $s \in S_n$ must contain at least one ring with odd number of nodes.

Let us illustrate Eq. (9) by two examples:

I

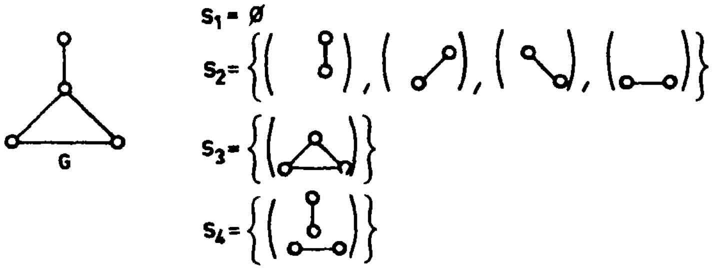

s are drawn in small brackets. Now it can be seen that:

$$a_1 = 0$$
$$a_2 = (-)^1 2^0 + (-)^1 2^0 + (-)^1 2^0 + (-)^1 2^0 = -4$$
$$a_3 = (-)^1 2^1 = -2$$
$$a_4 = (-)^2 2^0 = +1$$

and hence:

$$P_G(x) = x^4 - 4x^2 - 2x + 1 \, .$$

The use of Eq. (9) often requires a same amount of work as a direct solving of the determinant. But, some coefficients, which prove to be important for different reasons (see discussion later on), can be obtained in a rather simple way:

II

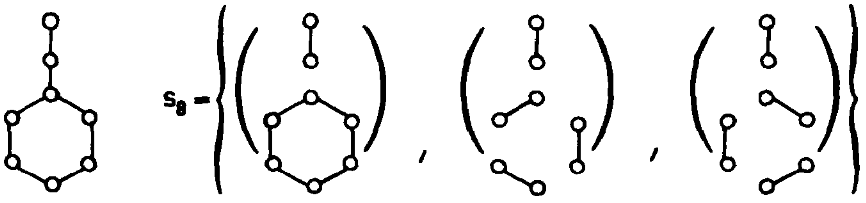

$$a_8 = (-)^2 2^1 + (-)^4 2^0 + (-)^4 2^0 = 4 \, .$$

Application of Sachs Formula to Conjugated Hydrocarbons

We will give now a survey of some simple consequences of Sachs formula which are of particular interest in chemistry.

A) According to the definition of S_n there is always:

$$S_1 = \emptyset \, , \qquad (10a)$$

i.e.

$$a_1 = 0 \, . \qquad (10b)$$

Since

$$a_1 = \sum_{j=1}^{N} x_j$$

it follows that:

$$\sum_{j=1}^{N} x_j = 0 . \tag{11}$$

The total π-electron energy of the molecule in the singlet ground state is:

$$E_\pi = 2\beta \sum_{j=1}^{N/2} x_j \tag{12}$$

where x_j are the roots given in decreasing order.

B) It is simple to see that:

$$-a_2 = \text{number of edges.} \tag{13}$$

As a consequence of the Eq. (11), the following relation holds:

$$a_2 = -\frac{1}{2} \sum_{j=1}^{N} x_j^2 . \tag{14}$$

This can be proved in a simple manner:

$$a_2 = \sum_{i<j} x_i x_j = \frac{1}{2}\left(\sum_{i=1}^{N} \sum_{j=1}^{N} x_i x_j - \sum_{j=1}^{N} x_j^2\right)$$

$$= -\frac{1}{2} \sum_{j=1}^{N} x_j^2 + \frac{1}{2} \sum_{i=1}^{N} x_i \sum_{j=1}^{N} x_j = -\frac{1}{2} \sum_{j=1}^{N} x_j^2 ,$$

the first step being known from algebra.

Eqs. (10), (11), (13) and (14) are already obtained by Günthard and Primas [5] using the theorem of Collatz and Sinogowitz [15], which is equivalent to Sachs theorem.

Since a_2 can be obtained from the graph it would be very useful if some correlation between E_π and a_2 could be established. Fortunately, such a correlation exists [17]. Almost in all cases when the number of edges is increased (the number of nodes being the same) the total π-electron energy increases too. In chemistry it corresponds to ring closure [18].

Example:

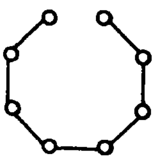

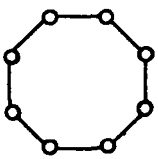

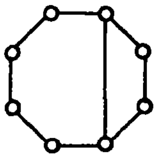

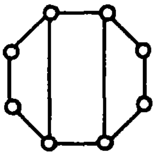

a_2	7	8	9	10
E_π	9.52	9.66	10.38	10.47

C) We will now consider the important class of alternant hydrocarbons. The graphs which correspond to these molecules have the property that their nodes can be painted with two colors in such a manner that two adjacent nodes always have different color. Hence, they are called "bichromatic graphs". It can be proved [3] that a graph is bichromatic if and only if it does not have any odd membered ring as its partial subgraph. Hence

$$S_n = \emptyset \tag{15a}$$

and

$$a_n = 0 \tag{15b}$$

for all odd n. So, the characteristic polynomial of the graph is of the form:

$$P_G(x) = x^N + a_2 x^{N-2} + a_4 x^{N-4} + \cdots \tag{16}$$

and the spectre of the graph is symmetrically arranged with respect to $x = 0$.

It is interesting to note that this fact (the pairing theorem) was first proved by Coulson and Rushbrooke [19] long before and independent of the GT [20].

D) The even alternant hydrocarbons[1], as a consequence of the pairing theorem, have triplet ground state if there is at least one zero in the spectre of the corresponding graph [2a]. In other words, such molecules are expected to be unstable within the framework of the HMO theory. This important chemical implication of the HMO theory has therefore a topological background.

Since

$$a_N = x_1 x_2 \ldots x_N \equiv \prod_{j=1}^{N} x_j \tag{17a}$$

and, hence, for alternant hydrocarbons

$$a_N = (-)^{N/2} \prod_{j=1}^{N/2} x_j \tag{17b}$$

it is sufficient to investigate if

$$a_N = 0\,. \tag{18}$$

If Eq. (18) holds, there is at least one zero in the spectrum of $P_G(x)$ and, thus low chemical stability is to be expected. Further discussion about this problem will be reported in the subsequent publication [21].

a) One can show that Eq. (18) holds if there is no Kekulé structure for the given hydrocarbon.

First, if there is at least one Sachs graph $s \in S_N$ corresponding to the given molecule, it implies the existence of Sachs graphs without rings (see below).

The Sachs graphs without rings and with N nodes are in an obviously manner analogous to Kekulé structures of the molecule. We will call them "Kekulé graphs", and denote by

$$k_1, k_2, \ldots, k_K\,.$$

The set of all K Kekulé graphs will be denoted as $\mathcal{K}$. It is clear that $\mathcal{K} \subseteq S_N$.

---

[1] We restrict our considerations only to the case of even number of π centers and electrons.

Therefore, the nonexistence of Kekulé graphs implicates the nonexistence of any Sachs graph with N nodes, and, hence, according to (9) there is

$$S_N = \emptyset .$$

b) Conversely, if there exists only one Kekulé structure (i.e. only one Kekulé graph and, hence, only one $s \in S_N$ as, for example, in the case of noncyclic molecules), then

$$a_N = (-)^{N/2} \tag{19}$$

and, of course, there is no zero in the spectre.

E) For rings (annulenes) the Hückel $(4m+2)$rule can be proved by considering:

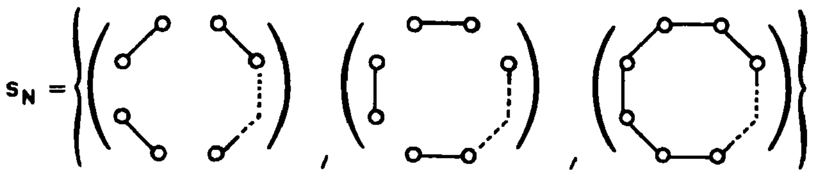

$$a_N = (-)^{N/2}2^0 + (-)^{N/2}2^0 + (-)^1 2^1 = \begin{cases} 0 \text{ for } N = 4m \\ -4 \text{ for } N = 4m+2 . \end{cases}$$

It means that only the $(4m+2)$-annulenes have a singlet ground state (in HMO theory).

Recently, Goldstein and Hoffmann [22] presented an other approach to Hückel $(4m+2)$rule.

F) For polycyclic alternant hydrocarbons the rule of determining the value of a_N (and thus molecular stability) is given by Longuet-Higgins and Dewar [2]. This rule is interesting because it express a relationship between MO and VB theory (see also Ref. [23]).

Before the proof of this rule is given, we will point out an important special case.

a) Let the graph G possess an edge $\underset{\sim}{e}$ such that by removing this edge the graph separates into two components G_1 and G_2, and let the number of nodes in these graphs: N, N_1 and N_2 be even. Than it is valid:

$$a_N(G) = a_{N_1}(G_1)\, a_{N_2}(G_2) . \tag{20}$$

This is the consequence of the fact that no Sachs graph with N nodes possess the edge $\underset{\sim}{e}$.

The meaning of Eq. (20) is that by joining of two stable molecules (by one bond) we always obtain a stable molecule, and if, at least, one of the joined molecules is unstable (but have even number of atoms) the resulting is unstable too.

Example:

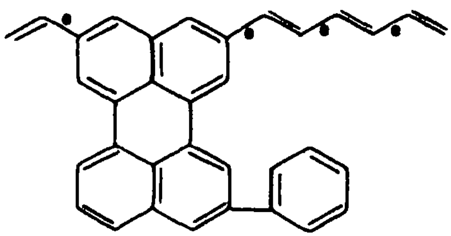

stable
(singlet ground state)

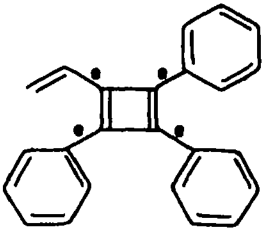

unstable
(triplet ground state)

It is of special chemical importance that the introduction of vinyl-, phenyl- and similar groups at arbitrary positions of molecule cannot cause the essential stabilisation of unstable molecules and the destabilisation of stable molecules.

b) Let the conjugated hydrocarbon have K Kekulé structures. A definite permutation can be assigned to every Kekulé structure (for details see [2]). The formula derived by Longuet-Higgins and Dewar is:

$$a_N = (-)^{N/2}\left(\sum_{j=1}^{K} p_j\right)^2 \tag{21}$$

where

$$p_j = \begin{cases} +1 \text{ if the permutation is even,} \\ -1 \text{ if the permutation is odd.} \end{cases} \tag{22}$$

Specially, if the parity of all permutations is the same (it occurs to molecules without $(4m)$-membered rings), then it is:

$$a_N = (-)^{N/2} K^2 . \tag{23}$$

In order to derive Eq. (21) from the Sachs formula (9) we will define the "summation" of two graphs with the same set of nodes as:

$$(\mathcal{N}, \mathcal{A}_1) \oplus (\mathcal{N}, \mathcal{A}_2) = (\mathcal{N}, \mathcal{A}_1 \cup \mathcal{A}_2) . \tag{24}$$

It can be easily seen that:

$$G_1 \oplus G_1 = G_1 , \tag{25}$$

$$G_1 \oplus G_2 = G_2 \oplus G_1 . \tag{26}$$

Then, the following theorem about the summation of Kekulé graphs is valid:

$$\mathcal{K} \oplus \mathcal{K} = S_N \tag{27}$$

where $\mathcal{K} \oplus \mathcal{K}$ is the set of all $k_A \oplus k_B$.

First notice that every even membered ring (only such rings can occur in Sachs graphs of bichromatic graphs) can be obtained as:

$$\gamma_1 \oplus \gamma_2 \quad \text{and} \quad \gamma_2 \oplus \gamma_1$$

where γ_1 and γ_2 are the Kekulé graphs of the ring. Naturally these are the only two possibilities for obtaining this ring by summation of Kekulé garphs. Hence, for every Sachs graph $s \in S_N$ there exist at least one pair of Kekulé graphs k_A, k_B such that

$$k_A \oplus k_B = s\,.$$

Thus

$$S_N \subseteq \mathscr{K} \oplus \mathscr{K}\,. \tag{28}$$

Let us suppose that the summation of k_A and k_B gives a graph σ such that $\sigma \notin S_N$. For example, such a graph may be:

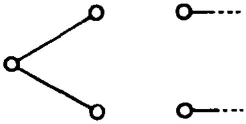

σ

The only way to obtain σ from Kekulé graphs is to sum:

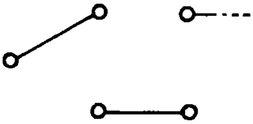

k_A

and

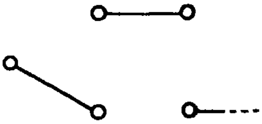

k_B

However, $k_A \oplus k_B$ gives not σ but σ':

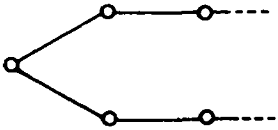

σ'

If $\sigma' \notin S_N$, we can repeat our considerations again.

It can be shown by a completely analogous argumentation that graphs:

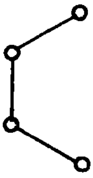

and

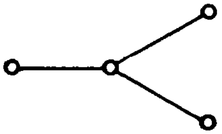

cannot be obtained by summation of Kekulé graphs.

The above mentioned three cases cover all possible non-Sachs graphs. So we have shown that it is always

$$k_A \oplus k_B \in S_N, \quad \text{i.e.}$$

$$\mathscr{K} \oplus \mathscr{K} \subseteq S_N \tag{29}$$

which completes the proof of Eq. (27).

An important corollary of the theorem (27) is that if a Sachs graph $s \in S_N$ contains r ring components, then there exist exactly 2^r different ordered pairs (k_A, k_B) with the property:

$$k_A \oplus k_B = s .$$

Since the set $\mathscr{K} \oplus \mathscr{K}$ contains K^2 elements it is therefore valid:

$$\sum_{s \in S_N} 2^{r(s)} = K^2 . \tag{30}$$

This equation shows explicitly the dependence of the number of Kekulé structures on the molecular topology (see also Ref. [8]).

For bichromatic graphs Sachs formula (9) can be written in the form:

$$a_N = (-)^{N/2} \sum_{s \in S_N} (-)^{r'(s)} 2^{r(s)} \tag{31}$$

where $r'(s)$ is the number of $(4m)$-membered rings in the Sachs graph s, because the generating of a $(4m+2)$-membered ring from Γ graphs does not alter the parity of the number of components, while a $(4m)$-membered ring does.

By comparison of Eqs. (30) and (31) it can be seen that

$$a_N = (-)^{N/2} \sum_{A=1}^{K} \sum_{B=1}^{K} (-)^{r'(k_A \oplus k_B)} , \tag{32}$$

because $k_A \oplus k_B$ is an element of S_N, and there are exactly 2^r pairs which give by summation the same Sachs graph.

Now, it is not difficult to see that:

$$(-)^{r'(k_A \oplus k_B)} = p_A p_B \tag{33}$$

what leads straightforwardly to the Longuet-Higgins-Dewar formula (21).

If the permutations of two Kekulé structures have opposite parity, then the sum of the corresponding two Kekulé graphs contains odd number of $(4m)$-membered rings. This enables us to estimate the parity of Longuet-Higgins-Dewar's permutations in a proper and simple manner.

We will use as illustration the same two examples which were considered by Wilcox [2b].

I

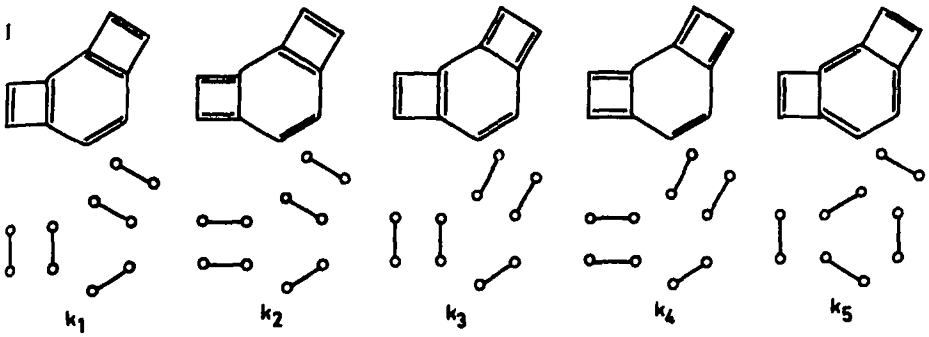

$p_1 \overset{\text{def}}{=} +1$

$k_1 \bullet k_2 =$ 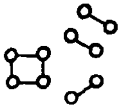 $\Longrightarrow p_2 = -1$

$k_1 \bullet k_3 =$ 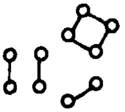 $\Longrightarrow p_3 = -1$

$k_1 \bullet k_4 =$ 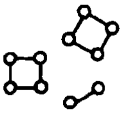 $\Longrightarrow p_4 = +1$

$k_1 \bullet k_5 =$ 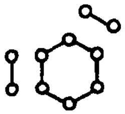 $\Longrightarrow p_5 = +1$

II

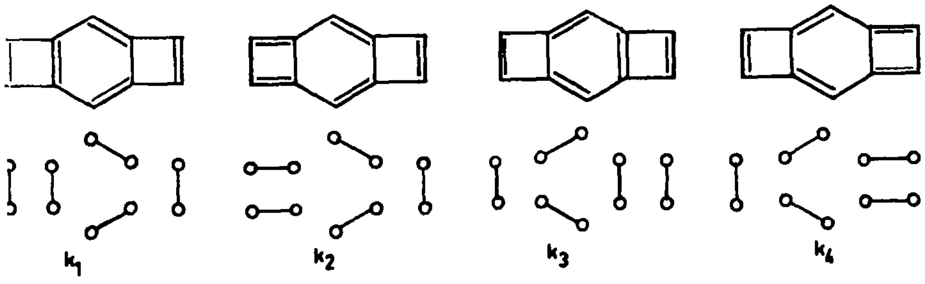

${}_1 \overset{\text{def}}{=} +1$

${}_1 \bullet k_2 =$ 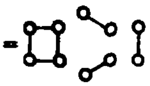 $\Longrightarrow p_2 = -1$

${}_1 \bullet k_3 =$ 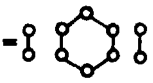 $\Longrightarrow p_3 = +1$

${}_1 \bullet k_4 =$ 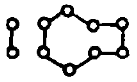 $\Longrightarrow p_4 = -1$

So, $a_{10}=(-)^5(1-1-1+1+1)^2=-1\neq 0$, and singlet ground state is to be expected.

So, $a_{10}=(-)^5(1-1+1-1)^2=0$ and triplet ground state, i.e. very low chemical stability or even nonexistence is to be expected.

References

1. Sachs, H.: Publ. Math. (Debrecen) **9**, 270 (1962).
2a. Longuet-Higgins, H. C.: J. chem. Physics **18**, 265 (1950); Dewar, M. J. S., Longuet-Higgins, H. C.: Proc. Royal Soc. (London) A **214**, 482 (1952).
2b. Wilcox, C. F.: Tetrahedron Letters 795 (1968).
3. Berge, C.: Théorie des graphes et ses applications. Paris: Dunod 1958.
4. Schmidtke, H. H.: J. chem. Physics **45**, 3920 (1966).
5. Günthard, H. H., Primas, H.: Helv. chim. Acta **39**, 1645 (1956).
6. Polya, G.: Acta Math. **68**, 145 (1937). — Harary, F.: Uspekhi mat. Nauk (USSR) **24**, 179 (1969). — Ruch, E., Hässelbarth, W., Richter, B.: Theoret. chim. Acta (Berl.) **19**, 288 (1970).
7. Balaban, A. T.: Tetrahedron **27**, 6115 (1971) and references therein.
8. Gordon, M., Davison, W. H. T.: J. chem. Physics **20**, 428 (1952). — Teh Fu Yen: Theoret. chim. Acta (Berl.) **20**, 399 (1971).
9. Ruedenberg, K.: J. chem. Physics **34**, 1861 (1961).
10. Polansky, O. E.: Private communication.
11. Figeys, H. P.: Tetrahedron **26**, 4615, 5225 (1970). — Kruszewski, J., Krygowski, T. M.: Tetrahedron Letters 319 (1970). — Hess, B. A., Jr., Schaad, L. J.: J. Amer. chem. Soc. **93**, 305, 2413 (1971); J. org. Chem. **36**, 3418 (1971). — Milun, M., Sobotka, Ž., Trinajstić, N.: J. org. Chem. **37**, 139 (1972).
12a. Kettle, S. F. A.: Theoret. chim. Acta (Berl.) **3**, 211 (1965); **4**, 150 (1966). — Kettle, S. F. A., Tomlinson, V.: Theoret. chim. Acta (Berl.) **14**, 175 (1969).
12b. Schmidtke, H. H.: Coord. chem. Rev. **2**, 3 (1967); Int. J. quant. Chemistry **2s**, 101 (1968); J. chem. Physics **48**, 970 (1968).
12c. Schmidtke, H. H.: Theoret. chim. Acta (Berl.) **9**, 199 (1968).
13. *e.g.* Jug, K.: Theoret. chim. Acta (Berl.) **14**, 91 (1969).
14. Ruedenberg, K.: J. chem. Physics **34**, 1884 (1961).
15. Collatz, L., Sinogowitz, U.: Abh. math. Sem. Univ. Hamburg **21**, 63 (1957).
16. Cvetković, D.: Thesis, Beograd 1971.
17. McClelland, B. J.: J. chem. Physics **54**, 640 (1971). — Hakala, R. W.: Int. J. quant. Chemistry **1s**, 187 (1967).
18. Dewar, M. J. S.: Tetrahedron Suppl. **8**, 75 (1966). — Dewar, M. J. S., Pettit, R.: J. chem. Soc. 1617 (1954). - Peters, J.: J. chem. Soc. 1023, 1028 (1958). — Gutman, I., Milun, M., Trinajstić, N.: Croat. chem. Acta **44** (1972) in press. — Gutman, I., Trinajstić, N., Živković, T.: Chem. Physics Letters (in press).
19. Coulson, C. A., Rushbrooke, G. S.: Proc. Cambridge philos. Soc. **36**, 196 (1940).
20. Cvetković, D.: Matematička Biblioteka (Beograd) **41**, 193 (1969).
21. Cvetković, D., Gutman, I., Trinajstić, N.: Croat. chem. Acta submitted for publication.
22. Goldstein, M. J., Hoffmann, R.: J. Amer. chem. Soc. **93**, 6193 (1971).
23. Ham, N. S.: J. chem. Physics **29**, 1229 (1958). — Heilbronner, E.: Helv. chim. Acta **45**, 1722 (1962).

Dr. N. Trinajstić
Institute "Rudjer Bošković"
P.O.B. 1016
41001 Zagreb
Croatia, Yugoslavia

Theoret. chim. Acta (Berl.) 26, 79—86 (1972)
© by Springer-Verlag 1972

CNDO/2 Rechnungen für einige Schwefelverbindungen

HEINZ OBERHAMMER

Zentrum Chemie-Physik-Mathematik der Universität Ulm, 7500 Karlsruhe, Hertzstraße 16, Bau 35

Eingegangen am 30. September 1971

CNDO/2 Calculations for Some Sulfur Compounds

CNDO/2 calculations were performed for some sulfur compounds in order to investigate the influence of different substituents on bondlengths and bondangles. It was shown that geometric parameters depend very strongly on the radial distribution of the sulfur 3*d*-orbitals. This radial distribution depends on the kind and number of substituents. Quantitatively the results of the CNDO/2 calculations in some cases agree badly with the experimental values for geometric parameters but qualitatively these calculations give a correct description of the influence of different substituents on bond lengths and bond angles in all cases.

Das CNDO/2-Verfahren wurde auf einige Schwefelverbindungen angewandt, um den Einfluß verschiedener Substituenten auf Bindungslängen und Bindungswinkel zu untersuchen. Es zeigt sich dabei, daß geometrische Parameter sehr stark von der radialen Verteilung der 3*d*-Orbitale am Schwefel abhängen, die wiederum von der Art und Zahl der Liganden bestimmt wird. Die Ergebnisse der CNDO/2-Rechnungen stimmen quantitativ teilweise schlecht mit den experimentell bestimmten Werten überein, geben aber rein qualitativ den Einfluß verschiedener Substituenten auf geometrische Parameter richtig wieder.

Seit einigen Jahren sind eine Reihe von self-consistent field Verfahren, bei denen sämtliche Valenzelektronen berücksichtigt werden, entwickelt worden, um Moleküleigenschaften zu berechnen [1]. Je nach der speziellen Moleküleigenschaft, die bestimmt werden soll, erwiesen sich bestimmte Verfahren als besonders geeignet. Von den derzeit bekannten Varianten ist das CNDO/2-Verfahren [2] (Complete Neglect of Differential Overlap) zur Berechnung von Molekülgeometrien am erfolgreichsten. Dieses Verfahren wurde zuerst für Moleküle konzipiert, die aus Atomen der ersten Reihe des periodischen Systems bestehen. Die Erweiterung auf Moleküle, die auch Atome der zweiten Reihe enthalten, und somit die Hinzunahme von *d*-Orbitalen war eine natürliche Folge [3].

Es sollte hier untersucht werden, wie gut mit dieser semiempirischen MO-Methode geometrische Parameter für Moleküle, die ein Schwefelatom enthalten, vorausgesagt werden können. Dazu wurden einige Schwefelverbindungen untersucht, deren Struktur vorher von uns bestimmt worden war. Dabei ging es nicht so sehr darum, Absolutwerte von Bindungslängen und Bindungswinkeln zu berechnen, sondern es sollte untersucht werden, ob Unterschiede in bestimmten Parametern, die durch Substitution hervorgerufen werden, durch das CNDO/2-Verfahren richtig beschrieben werden.

Verfahren

Für die MO-Rechnungen wurde die von Santry und Segal angegebene Methode [3] verwendet. Da untersucht werden sollte, welchen Einfluß die Wahl des Orbital-Exponenten Z_{3d} für die *d*-Orbitale am Schwefel auf die geometrischen Parameter des Moleküls hat, wurden diese in weitem Bereich variiert. Durch Einführung verschiedener Coulomb-Integrale für *s*-, *p*- und *d*-Orbitale wird die Invarianz gegenüber Verwendung von Hybrid-Orbitalen als Basisfunktionen zerstört [3]. Levison und Perkins [4] zeigten mit Hilfe von Testrechnungen, daß der Einfluß von Ähnlichkeitstransformationen der Basisfunktionen auf die Gesamtenergie in diesem Falle sehr gering ist.

Hinsichtlich der radialen Verteilung der *d*-Orbitale am Schwefel bestehen große Unsicherheiten. Sicherlich ist der von Santry und Segal [3] gegebene Orbital-Exponent (effektive Kernladungszahl $Z_{3d} = 2{,}52$) zu klein, d. h. die radiale Verteilung zu diffus. Nach den verfeinerten Regeln von Burns [5] müßte die effektive Kernladungszahl für die 3*d*-Orbitale am Schwefel $Z_{3d} = 3{,}00$ betragen. Cruickshank *et al.* [6] berechneten die Hartree-Fock-SCF-Wellenfunktion für den ^7F-Term von $S\ (sp^3d^2)$. Nach den Hundschen Regeln sollte dieser Term der energetisch niedrigste Term für diese Elektronenkonfiguration sein. Hierbei ergibt sich eine gegenüber dem Slater-Orbital stark kontrahierte Funktion für die radiale Verteilung. Eine Slater-Funktion mit dem Maximum in derselben Entfernung vom Kern müßte einen Exponenten $Z_{3d} = 4{,}02$ haben.

Craig und Zauli [7] hingegen vertreten die Ansicht, daß die Kontraktion der *d*-Orbitale erst im Felde der Liganden vor sicht geht, wobei natürlich diese Kontraktion von der Art und von der Zahl der Liganden abhängig ist. So finden sie für den Fall SF_6 eine optimale effektive Kernladungszahl von $Z_{3d} = 3{,}6$ für die *d*-Orbitale am Schwefel.

Ohne Kontraktion der *d*-Orbitale gegenüber der von Santry und Segal gegebenen radialen Verteilung können diese nicht effektiv zu einer Bindung beitragen. Das Maximum von $D(r)$ liegt für $Z_{3d} = 2{,}52$ bei 1,89 Å, also außerhalb der hier betrachteten Bindungslängen. Bei dem von Cruickskank angegebenen Wert von $Z_{3d} = 4{,}02$ liegt das Maximum von $D(r)$ bei 1,18 Å, also innerhalb der Entfernung vom Kern, in der sich die Liganden befinden. Als maximal mögliche Kontraktion wurde der Fall angesehen, bei dem die radiale Verteilung der *d*-Orbitale gleich der für die *s*- und *p*-Orbitale ist. Auf Grund der Slater-Regeln ergibt sich hierfür ein Wert von $Z_{3d} = 5{,}45$, das entsprechende Maximum von $D(r)$ liegt bei 0,87 Å.

HNSO und CLNSO

Die geometrischen Parameter beider Moleküle wurden mit Hilfe von mikrowellenspektroskopischen Messungen [8] bzw. Elektronenbeugung an Gasen [9] bestimmt. Bei Vergleich beider Molekülstrukturen fällt der starke Einfluß des Substituenten am Stickstoff auf den N—S-Bindungsabstand auf. Für Sulfinimid wurde ein Wert von 1,511 ± 0,009 Å bestimmt, für N-Chlor-Sulfinylamin fanden wir eine N—S-Bindungslänge von 1,559 ± 0,004 Å. Dieser große Unterschied in den Bindungslängen (ca. 0,05 Å) spiegelt sich auch in den entsprechenden Kraftkonstanten wieder [10]. Auch der NSO-Bindungswinkel unterscheidet sich in diesen beiden Molekülen erheblich: 120,3 ± 0,7° für HNSO bzw. 116,0 ± 0,6° für ClNSO. Im N-Chlor-Sulfinylamin fanden wir innerhalb der Fehlergrenzen der Elektronenbeugungsergebnisse ausschließlich eine *cis*-Stellung des Chloratoms. Ein geringer Anteil an *trans*-Konfiguration kann nicht ausgeschlossen werden, jedoch müßte dieser $\leq 2\%$ sein. Auch im Falle des Sulfinimids wurde die Struktur der *cis*-Konfiguration bestimmt. Kirchhoff *et al.* fanden jedoch im Mikrowellenspektrum auch Übergänge, die einer *trans*-Konfiguration zugeordnet werden könnten. Über das relative Verhältnis von *cis*- zu *trans*-Konfiguration läßt sich keine Aussage machen. Während bei der Berechnung der geometrischen Parameter des Sulfinimids aus den Rotationskonstanten auf Grund des kleinen Trägheitsdefektes eine ebene Struktur vorausgesetzt werden konnte, fanden wir für das N-Chlor-Sulfinylamin eine nicht ebene Molekülstruktur. Der Diederwinkel beträgt 35,5 ± 3,6°. Es unterscheiden sich auch die S—O-Bindungslängen dieser beiden Moleküle, jedoch ist die Differenz hier nicht so auffallend wie bei den S—N-Bindungslängen, und sie liegt innerhalb der Fehlergrenzen beider Methoden (1,456 ± 0,011 Å für HNSO bzw. 1,445 ± 0,004 Å für ClNSO).

Es sollte hier untersucht werden, ob semiempirische MO-Rechnungen nach dem CNDO/2-Verfahren die oben angegebenen experimentellen Befunde qualitativ wiederzugeben im Stande sind. Dabei wurden nur diejenigen geometrischen Parameter untersucht, für die sich ein eindeutiger Unterschied zwischen den beiden Molekülen ergab, und zwar der S—N-Bindungsabstand und der NSO-Bindungswinkel. Außerdem sollte die Frage untersucht werden, ob das energetische Verhältnis zwischen *trans*- und *cis*-Konfiguration richtig wiedergegeben wird und ob sich für den Fall des N-Chlor-Sulfinylamins die Verdrehung des Chloratoms aus der NSO-Ebene mit diesem Verfahren voraussagen läßt.

Das SCF-Verfahren wurde mit verschiedenen Werten für den S—N-Abstand durchgeführt und der Wert, bei dem das Energieminimum erreicht wird, durch Parabelausgleich ermittelt. Fig. 1 zeigt die so bestimmten Werte für den S—N-Abstand für beide Moleküle in Abhängigkeit von der effektiven Kernladungszahl für die 3*d*-Orbitale am Schwefel. Daraus ist ersichtlich, daß die 3*d*-Orbitale, jedenfalls in diesem Falle, wo ein freies Elektronenpaar am Stickstoff zur Verfügung steht, einen sehr starken Einfluß auf den Bindungsabstand haben und nicht vernachlässigt werden dürfen.

Bestimmt man in beiden Molekülen den Orbitalexponenten, bei dem die Energie ein Minimum wird, so ergibt sich $Z_{3d} = 3{,}69$ für HNSO bzw. $Z_{3d} = 3{,}48$ für ClNSO. Diesen effektiven Kernladungszahlen entsprechen S—N-Abstände von 1,55 Å bzw. 1,60 Å. Die Absolutwerte sind zwar um ca. 0,04 Å zu lang, aber für die Differenz beider Werte erhält man ein mit dem experimentellen Befund übereinstimmendes Ergebnis. Ein Grund für das Abweichen der theoretischen Absolutwerte von den experimentellen Ergebnissen kann neben anderen darin liegen, daß die Slater-Regeln die Orbitalexponenten für 3*s*- und 3*p*-Orbitale des Schwefels schlecht bestimmen.

Als Maß für die Stärke einer Bindung wurden die kovalenten Bindungsordnungen aus den Überlappungsbesetzungszahlen (overlap population) nach

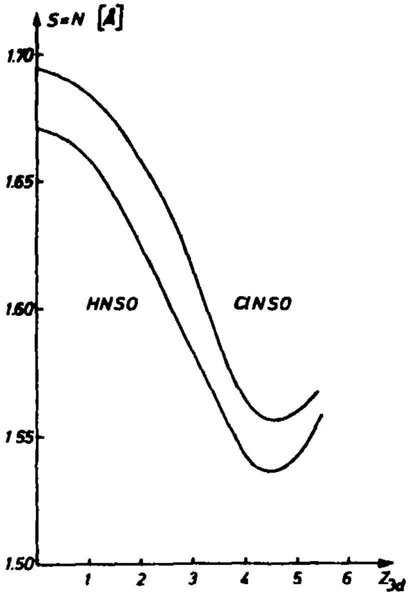

Fig. 1. S=N-Bindungsabstand in HNSO und ClNSO in Abhängigkeit von Z_{3d}

Mulliken [11] berechnet, und zwar für die oben angegebenen optimalen Werte für Z_{3d}. Für Sulfinimid erhält man dabei eine Bindungsordnung von 1,34, für N-Chlor-Sulfinylamin 1,25. Der Anteil an der Bindungsordnung, der durch Beteiligung der 3*d*-Orbitale des Schwefels beigetragen wird, ist nur zu einem geringeren Teil für den Unterschied in den Bindungsordnungen verantwortlich (0,62 verglichen zu 0,59). Der Unterschied in den Bindungsordnungen rührt hauptsächlich von dem Anteil her, den die *s*- und *p*-Orbitale beitragen (0,72 verglichen zu 0,66).

Tabelle 1. Ladungsverteilung für Sulfinimid und N-Chlor-Sulfinylamin nach CNDO/2-Verfahren

Molekül	X	N	S	O
HNSO	+0.22	−0.20	+0.02	−0.04
ClNSO	+0.11	−0.02	+0.02	−0.11

Die Ladungsverteilung für beide Moleküle ist in Tab. 1 angegeben. Der Hybridisierungszustand des Schwefels ist in beiden Molekülen annähernd gleich. Für HNSO erhält man:

$$3s^{1.77}\,3p^{2.86}\,3d^{1.35}$$

und für ClNSO:

$$3s^{1.77}\,3p^{2.89}\,3d^{1.32}\,.$$

Die Untersuchung der Abhängigkeit des NSO-Bindungswinkels von der radialen Verteilung für die 3*d*-Orbitale am Schwefel ergab für den in Frage kommenden Bereich von Z_{3d} einen linearen Zusammenhang (Fig. 2). Die Abhängigkeit des Bindungswinkels von Z_{3d} ist dabei im Sulfinimid bedeutend stärker als im N-Chlor-Sulfinylamin. Für die oben angegebenen optimalen Orbitalexponenten erhält man für HNSO einen NSO-Winkel von 130,0° (experimenteller Wert 120,3°), für ClNSO 118,8° (experimenteller Wert 116,0°). Rein qualitativ wird das experimentelle Ergebnis richtig wiedergegeben (Bindungswinkel im HNSO größer als im ClNSO), die quantitative Übereinstimmung ist jedoch besonders im Falle des HNSO sehr schlecht.

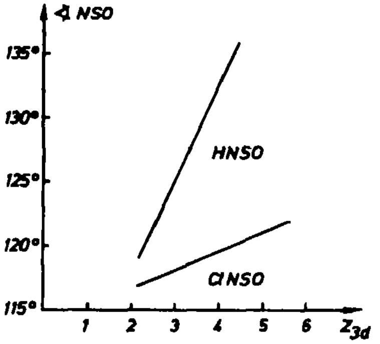

Fig. 2. NSO-Bindungswinkel in HNSO und ClNSO in Abhängigkeit von Z_{3d}

Auch bei der Frage nach der Konfiguration der beiden Moleküle sind die CNDO/2-Ergebnisse nicht befriedigend. Im Falle des ClNSO stellt zwar die *cis*-Konfiguration den energetisch günstigeren Zustand dar, jedoch beträgt die Energiedifferenz zwischen *cis*- und *trans*-Stellung des Chloratoms nur 0,34 kcal/Mol. Aufgrund der experimentellen Ergebnisse, die einen Anteil an *trans*-Konfiguration von maximal 2% zulassen, müßte diese Energiedifferenz einige kcal/mol betragen. Für Sulfinimid findet man, daß die *trans*-Konfiguration um ca. 3,0 kcal/mol energetisch tiefer liegt als die *cis*-Konfiguration. Im Mikrowellenspektrum waren die der *cis*-Konfiguration zugeordneten Übergänge stärker als andere Übergänge, die der *trans*-Konfiguration zugeschrieben wurden. Daraus läßt sich jedoch keine Aussage über das tatsächliche Verhältnis beider Konfigurationen machen, da das Dipolmoment der *trans*-Konfiguration nicht bekannt ist. Diese Energiedifferenzen zwischen *cis*- und *trans*-Konfiguration müssen jedoch mit Vorsicht betrachtet werden, da für den Fall der *trans*-Konfiguration bei den Rechnungen die für die *cis*-Stellung gefundenen optimalen geometrischen Parameter übernommen wurden. Sicherlich sind der HNS- bzw. ClNS-Winkel in beiden Konfigurationen leicht verschieden. Die Variation des Diederwinkels in N-Chlor-Sulfinylamin ergab das Energieminimum bei 0°, d. h. bei ebener Struktur, während im Experiment eine Verdrehung des Chloratoms aus der NSO-Ebene festgestellt wurde.

$(CH_3)_2SO_2$, $(CH_3)_2SONH$ und $(CH_3)_2S(NH)_2$

Die Strukturen dieser drei isoelektronischen Verbindungen wurde mit Hilfe der Elektronenbeugung an Gasen bestimmt [12–14]. Dabei ergab sich eine sehr starke Abhängigkeit des Winkels zwischen den Doppelbindungen von den jeweiligen Liganden (Tab. 2). Es sollte hier untersucht werden, ob dieser Tatbestand auch durch semiempirische MO-Rechnungen beschrieben wird. Dabei ergibt sich auch hier ein starker Einfluß des Orbitalexponenten für die 3*d*-Orbitale am Schwefel auf diesen Winkel (Fig. 3). Die optimale effektive Kernladungszahl, also der Wert für Z_{3d}, für den die Energie minimal wird, ist abhängig von der Art der Liganden, und zwar erhält man in diesen drei Molekülen dafür die Werte $Z_{3d} = 3{,}45$, 3,30 bzw. 3,15. Die diesen Orbitalexponenten entsprechenden Winkel zwischen den Doppelbindungen sind in Tab. 2 angegeben. Die übrigen geometrischen Parameter dieser drei Moleküle wurden nicht variiert, es wurden dafür die experimentell ermittelten Werte eingesetzt.

Tab. 2 zeigt, daß die CNDO/2-Rechnungen den Gang der Bindungswinkel am Schwefel richtig wiedergeben, d. h. Vergrößerung des Winkels bei schrittweisem Ersetzen des Sauerstoffatoms durch NH-Gruppen, daß aber die ent-

Tabelle 2. Experimentelle und theoretische Bindungswinkel zwischen den Doppelbindungen, optimale effektive Kernladungszahl, Ladungsverteilung und Hybridisierungszustand für die isoelektronische Verbindungsreihe $(CH_3)_2SXY$ (X, Y=O, NH)

Molekül	Winkel $\sphericalangle$ =S= expt.	Winkel $\sphericalangle$ =S= CNDO/2	Z_{3d}	Ladungsverteilung	Hybridisierungszustand
$(CH_3)_2SO_2$	127,1 ± 2,4°	113,8°	3,45	$S^{0,35}O^{-0,13}$	$3s^{1,32}3p^{3,08}3d^{1,95}$
$(CH_3)_2SONH$	132,6 ± 0,9°	116,7°	3,30	$S^{-0,55}O^{-0,10}(NH)^{+0,03}$	$3s^{1,34}3p^{3,21}3d^{2,00}$
$(CH_3)_2S(NH)_2$	135,0 ± 1,2°	120,7°	3,15	$S^{-0,71}(NH)^{+0,03}$	$3s^{1,35}3p^{3,32}3d^{2,04}$

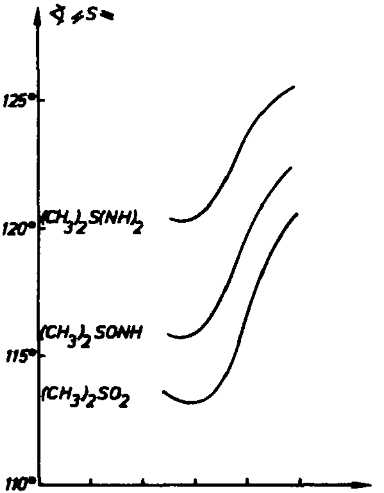

Fig. 3. Winkel zwischen den Doppelbindungen in den Molekülen $(CH_3)_2SXY$ (X, Y=O, NH) in Abhängigkeit von Z_{3d}

sprechenden Werte quantitativ schlecht mit den experimentellen Eregebnissen übereinstimmen. Die aus den MO-Rechnungen bestimmten Ladungsverteilungen für diese drei Moleküle (Tab. 2) zeigt, daß die negative Ladung am Schwefelatom mit wachsender Zahl der NH-Gruppen zunimmt. Die positive Ladung in diesen Molekülen verteilt sich zum größten Teil auf die Methylwasserstoffatome. Die negative Ladung am Schwefelatom kann durch starke Donatorwirkung der Methylgruppen erklärt werden, die in diesem Verfahren wahrscheinlich überschätzt wird. Die ebenfalls in Tab. 2 angegebenen Besetzungszahlen der Valenzorbitale des Schwefels zeigen, daß sich die Besetzung der 3*s*- und 3*d*-Orbitale innerhalb dieser Molekülreihe kaum ändert, daß aber stärkere Unterschiede in den Besetzungszahlen der 3*p*-Orbitale bestehen. Eine stärkere Besetzung dieser 3*p*-Orbitale führt dabei zu einer Vergrößerung des hier untersuchten Winkels.

Schlußbemerkungen

Dewar und Haselbach [15] haben gezeigt, daß man für Kohlenwasserstoffe mit semiempirischen Verfahren gute Ergebnisse für Molekülgeometrien erhalten kann, wenn man die empirischen Parameter geeignet wählt. Um auch bei Molekülen, die ein Element der zweiten Reihe des periodischen Systems enthalten, mit dem CNDO/2-Verfahren quantitativ richtige Aussagen über die Molekülgeometrie machen zu können, müßten die von Santry und Segal [3] angegebenen empirischen Parameter entsprechend angepaßt werden.

Trotz unbefriedigender quantitativer Ergebnisse liefert das CNDO/2-Verfahren in den hier untersuchten Fällen qualitativ richtige Ergebnisse, d. h. experimentell beobachtete Trends in geometrischen Parametern werden richtig wiedergegeben. Außerdem kann aus den hier durchgeführten Rechnungen geschlossen werden, daß bei MO-Rechnungen für Moleküle, die Atome der zweiten Reihe des periodischen Systems enthalten, zumindest in bestimmten Fällen die *d*-Orbitale unbedingt berücksichtigt werden müssen, da sie die Voraussagen hinsichtlich der Molekülgeometrie sehr stark beeinflussen. Die radiale Verteilung der *d*-Orbitale kann dabei für ein bestimmtes Atom nicht als konstant angenommen werden, sondern muß für jedes Molekül optimiert werden, da sie stark von der Art und Zahl der Liganden bzw. auch von der weiteren Umgebung des betreffenden Atoms abhängig ist. Die Slater-Regeln und auch die von Burns angegebenen verfeinerten Regeln zur Bestimmung der effektiven Kernladungszahlen liefern in allen hier betrachteten Fällen eine zu diffuse radiale Verteilung für die *d*-Orbitale.

Literatur

1. Klopmann, G., O'Leary, B.: Fortschritte der Chem. Forschung **15**, 447 (1970).
2. Pople, J. A., Segal, G. A.: J. chem. Physics **44**, 3289 (1966).
3. Santry, D. P., Segal, G. A.: J. chem. Physics **47**, 158 (1967).
4. Levison, K. A., Perkins, P. G.: Theoret. chim. Acta (Berl.) **17**, 1 (1970).
5. Burns, G.: J. chem. Physics **11**, 1521 (1964).
6. Cruickshank, D. W. J., Webster, B. C., Mayers, D. F.: J. chem. Physics **40**, 3733 (1964).
7. Craig, D. P., Zauli, C.: J. chem. Physics **37**, 601 (1962).
8. Kirchhoff, W. H.: Dissertation, Harvard University 1964.

9. Oberhammer, H.: Z. Naturforsch. **25 a**, 1497 (1970).
10. Eysel, H. H.: J. molecular Structure **5**, 275 (1970).
11. Mulliken, R. S.: J. chem. Physics **23**, 1833 (1955).
12. Oberhammer, H., Zeil, W.: J. molecular Structure **6**, 399 (1970).
13. – – Z. Naturforsch. **25a**, 845 (1970).
14. – – Z. Naturforsch. **24a**, 1612 (1969).
15. Dewar, M. J. S., Haselbach, E.: J. Amer. chem. Soc. **92**, 590 (1970).

Dr. H. Oberhammer
Zentrum Chemie-Physik-Mathematik
Universität Ulm
Hertzstraße 16, Bau 35 II
D-7500 Karlsruhe 21
Deutschland

Theoret. chim. Acta (Berl.) 26, 87—88 (1972)
© by Springer-Verlag 1972

Relationes

Calculation of Oscillator Strengths for π-Electron Molecules

MARGARET L. BAILEY
Chemistry Department, Victoria University of Wellington, Wellington, New Zealand

Received November 15, 1971

A comparison of oscillator strengths calculated by the Mulliken and Rieke approximation and by the Hansen expression involving the geometric mean of the dipole-length and dipole-velocity formulae shows that the former method gives values twice as large as those from the latter method.

The choice of formula to be used in the calculation of oscillator strengths for π-electron molecules has been the subject of much discussion. In most calculations performed using the Pariser-Parr-Pople method, the Mulliken and Rieke approximation [1] is employed. This method does not require the calculation of any integrals, as only the diagonal elements of the dipole-length operator are included. However, the oscillator strengths obtained are usually larger than experimental values.

In recent calculations of the absorption spectra of a series of small aromatic molecules [2] and a number of purines and pyrimidines [3], the oscillator strengths were obtained from the geometric mean formula of Hansen [4] in which both dipole-length and dipole-velocity operators were used. This mean value has an advantage over its two component values in that the geometric mean formula contains no energy term; its disadvantage is in the need to calculate two sets of integrals. However, the oscillator strengths obtained are in reasonable agreement with experimental values [2, 3].

A comparison of oscillator strengths calculated by the Mulliken and Rieke method and by the Hansen method for the molecules previously studied [2, 3] showed that the values from the former method were twice as large as those from the latter method. All oscillator strengths calculated by the Mulliken and Rieke method were therefore multiplied by 0.5, and compared again with those from the Hansen method. For the twenty-one small aromatic molecules – azines, aminopyridines, aminopyrimidines, phenylenediamines and dihydroxybenzenes – the largest difference between the two sets of values was 0.03, this being calculated for eight transitions with energies between 6.5 eV and 8.0 eV and with oscillator strengths greater than 0.30. The remaining eighty-seven transitions gave values which differed by up to 0.02 for oscillator strengths in the range of 0.0–0.60, the average difference being less than 0.01. Similarly, for the four bases of RNA – adenine, guanine, cytosine and uracil – the largest difference between the two sets of values was 0.04, this being calculated for three transitions with energies between 5.9 eV and 6.6 eV and with oscillator strengths greater than 0.30. The remaining twenty-three transitions gave values which differed by less than 0.01 on average. Therefore the two sets of values were remarkedly constant.

It is therefore proposed that the simpler Mulliken and Rieke method can be used to obtain oscillator strengths which are in close agreement with those obtained from the Hansen method, provided a factor of 0.5 is included in the expression.

References

1. Mulliken, R. S., Rieke, C. A.: Rep. Progr. Physics **8**, 231 (1941).
2. Bailey, M. L.: Theoret. chim. Acta (Berl.) **13**, 56 (1969).
3. Theoret. chim. Acta (Berl.) **16**, 309 (1970).
4. Hansen, A. E.: Molecular Physics **13**, 425 (1967).

Dr. Margaret L. Bailey
Consumers' Institute
Private Bag
Te Aro P.O.
Wellington 1, New Zealand

Theoret. chim. Acta (Berl.) 26, 89 - 96 (1972)
© by Springer-Verlag 1972

Correlation Effect on the Singlets $\pi\pi^*$ Transition Energies of Polyacenes

J. F. GOUYET and M. T. PRAT

Groupe de Physique Moléculaire, Laboratoire OPM, Ecole Polytechnique, Paris, France

Received January 8, 1972

The π correlation effect of the first singlet states of polyacenes has been studied for naphthalene, anthracene, tetracene using a perturbation expansion up to second order. The influence of the extent of configurations has been analysed.

1. Introduction

The π-π^* transition energies of polyacenes are examined from the point of view of the effect of π orbitals in complete configuration interaction by a Rayleigh-Schrödinger perturbation expansion up to second order. A minimal basis set has been used and the π molecular orbitals obey self consistent conditions for the ground state. The study is concerned firstly with troncature effect of the configuration interaction expansion on transition energies, secondly with the variation in term of the cycles number of the transition energies for naphthalene, anthracene, tetracene.

2. The Theoretical Method

The zero order hamiltonian matrix is built with the ground state self-consistent π orbitals. These are given as the result of a Pariser-Parr-Pople calculation [1] using the program written by Bessis-Chalvet [2]. The model hamiltonian is given by:

$$H = \sum_{pq} H_{pq}^{N} a_p^+ a_q + \tfrac{1}{2} \sum_{pq} \gamma_{pq} a_p^+ a_q^+ a_q a_p$$

where a_p^+ and a_p are respectively creation and annihilation operators for one electron on the orbital $2pz$. The parameters have been taken to be:

$$Z = 3.25; \quad E = 0.69; \quad W = 11.22; \quad \beta = -2.39 .$$

The Hartree Fock hamiltonian is:

$$H^0 = \sum_{p} \varepsilon_p b_p^+ b_p$$

b_p^+ being the operator of creation of a self consistent orbital φ_p and the total hamiltonian according to the Moller-Plesset partition is merely given by:

$$H = H^0 + V .$$

The second order approximation on the energy of the ground singlet state S_0 is:

$$e_0^{(2)} = \sum_{I \neq 0} \frac{|\langle 0|V|I\rangle|^2}{E_0^0 - E_I^0}$$

whereas the second order energy of the S_α excited singlet state is given by:

$$e_\alpha^{(2)} = \sum_{J \neq \alpha} \frac{|\langle \alpha|V|J\rangle|^2}{E_\alpha^0 - E_J^0}$$

S_α is assumed to be non degenerate.

In the following expressions for the transition energy:

$$E_{S_\alpha \leftarrow S_0} = E_\alpha^{\text{SCF}} - E_0^{\text{SCF}} + e_\alpha^{(2)} - e_0^{(2)}$$

an important cancellation [3] appears. Let:

$$|\alpha\rangle = S^+ |0\rangle ,$$
$$|I\rangle = T^+ |0\rangle ,$$
$$|J\rangle = T^+ |\alpha\rangle .$$

All the configurations $|I\rangle$ and $|J\rangle$ coming from the same excitation T^+ applied to $|0\rangle$ and $|\alpha\rangle$ respectively, and so that this excitation T^+ has no orbital common with S^+, disappear.

The Epstein-Nesbet *partition* [4, 5]

In practice, the Möller-Plesset perturbation expansion converges rather slowly. A new partition of H can be obtained by inserting certain groups of terms in the zeroth order hamiltonian:

$$H = H'^0 + V'$$
$$H'^0 = H^0 + \sum_I \langle I|V|I\rangle \, |I\rangle \langle I| .$$

With this choice the diagonal elements of V' are zero. This partition (Epstein-Nesbet) has been used in our calculation.

The second order energy is now:

$$e_0^{(2)} = \sum_{I \neq 0} \frac{|\langle 0|V|I\rangle|^2}{E_0^{\text{SCF}} - E_I^{\text{SCF}}} .$$

The exact cancellation previously described does not occur because the denominators now differ by coulombian exchange integrals. It can be shown however that these terms contribute only to the third and higher order energy[1].

---

[1] This means that, when one neglects the diagrams which previously cancel in Möller-Plesset, then the effect is of third and higher order on the Rayleigh-Schrödinger perturbation using the Epstein-Nesbet partition of the hamiltonian.

In the degenerate case, we have to evaluate non-diagonal elements such as:

$$e^{(2)}_{\alpha\beta} = \sum_{J \neq D} \frac{\langle\alpha|V|J\rangle\langle J|V|\beta\rangle}{E_D^{\mathrm{SCF}} - E_J^{\mathrm{SCF}}}$$

where $|\alpha\rangle$ and $|\beta\rangle$ belong to the degenerate sub space D.

The different perturbation subroutines were written by Levy and Malrieu [6, 7]. One calculates the oscillator strengths $S_0 \to S_i$ by a double perturbation technique to first order both in V' and $\boldsymbol{d}$, the electric dipole moment. The program has been adapted to PPP approximation and completely automatized.

We expect from such a perturbation expansion the benefit of the inclusion of all interacting configurations; for instance, highly excited states are seen to be described as accurately as lowest ones. In the highly excited states however, frequently occurring quasi degeneracies necessitate a special treatment. Of course, the inconveniences linked to the choice of the basis and to the PPP approximation do not disappear. The third order correction has been completely neglected. The computing time grows roughly as $n^{2.5}$ where n is the number of π electrons.

3. Study of Some Polyacenes

a) *The Influence of the* CI *Extent*

Two calculations were carried out, the first concerning the α and β naphthalene bands, the second, the p band of antracene. Let

$$\psi_0 = a_0|0\rangle + a_1|1\rangle + a_2|2\rangle + \cdots$$
$$\psi_\alpha = b_0|\alpha\rangle + b_1|1\alpha\rangle + b_2|2\alpha\rangle + \cdots$$

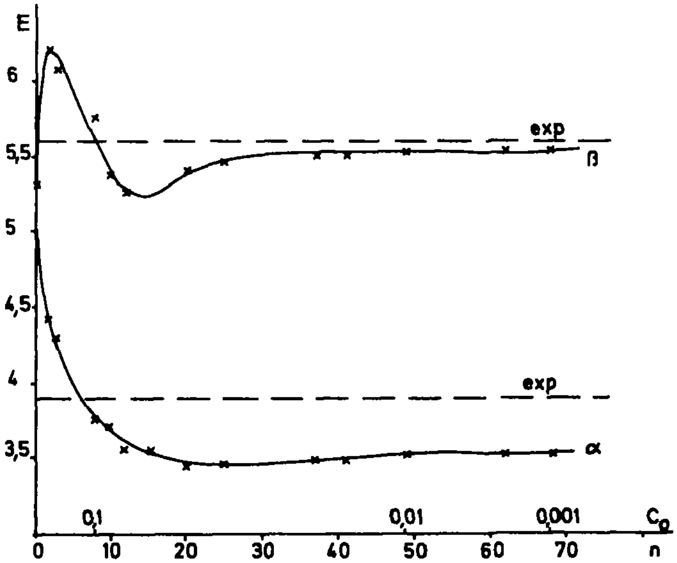

Fig. 1. Naphthalene – α and β bands. Energy in eV in function of n, number of configurations and of C_0, upper limit for the absolute value of the weight of the configuration

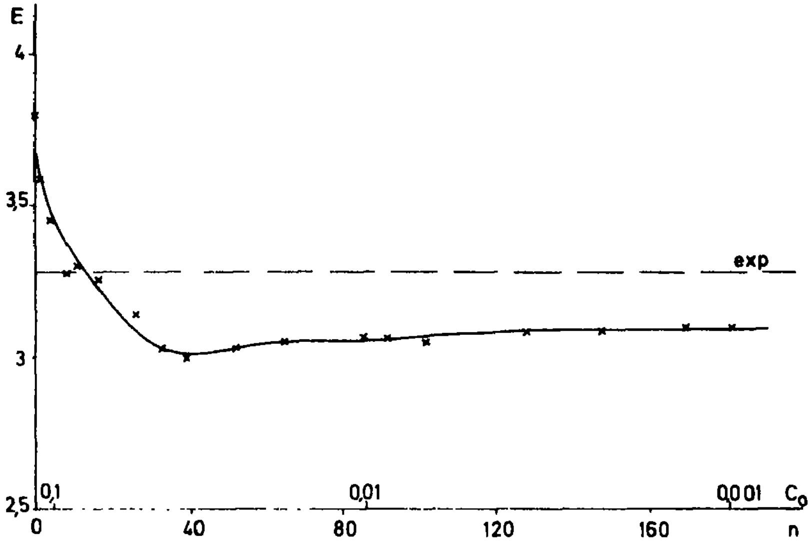

Fig. 2 Anthracene p band. Energy in eV in function of n number of configurations and of C_0 weight of the configuration

with

$$a_I = -\frac{\langle 0|V|I\rangle}{E_0^{\mathrm{SCF}} - E_I^{\mathrm{SCF}}}; \quad b_J = -\frac{\langle \alpha|V|J\rangle}{E_\alpha^{\mathrm{SCF}} - E_J^{\mathrm{SCF}}}.$$

In the first step, only the configurations which have a weight greater than a given C_0 have been taken into account

$$|a_I|, \quad |b_J| \geqq C_0$$

then C_0 is varied from 0 (all configurations) to 0.3 or 0.5 (1 configuration). The results are reproduced in Figs. 1 and 2. Oscillations are important when the number of configurations occurring is small because their amplitude is about $\frac{|\langle V\rangle|^2}{\Delta E}$.

Table 1. Most active configurations in the value of the transition energy in anthracene p-band

Excitation with respect to ground state		$C_0 = 0.06$
		7-7→8-8 6-7→9-8
with respect to 7-8	mono exc.	4→8 7→11 5→9 6→10
	doubly exc.	7-8→10-9 6-5→7-8 3-8→12-7 6-8→9-7

The curves show that stabilization is obtained at about 40 configurations in the case of α and β naphthalene bands, 90 in the case of the antracene p-band; in both cases, the value of C_0 can then be estimated around 0.01.

For instance in Fig. 2 the 90 configurations comprise 10 monoexcited B_{2u}, 40 doubly excited B_{2u} with respect to 7–8 and 40 doubly excited with respect to the ground state A_g; no monoexcited configuration with respect to the ground state can intervene due to Brillouin's theorem. *Furthermore, all configurations giving equal contribution in both S_0 and S_α have disappeared.* By these methods, the configurations which most influence the value of the transition energy are selected; for instance Table 1 reproduces the 10 configurations having the highest weight in the case of the anthracene p-band.

b) Calculation of the Singlet-Singlet Transition Strengths and Transition Energies of Naphthalene, Anthracene, Tetracene

Many theoretical studies were undertaken since Pariser [8] published his important and exhaustive "theory of electronic spectra and structure of the polyacenes", which includes a configuration interaction very limited, on a LCAO MO basis. Nishimoto [9] calculates these transition energies with a variable β-modification of the Pariser-Parr-Pople method.

Table 2. Naphthalene

Etat	Perturbation				Pariser [8]		Exper.	
	Principal excitation	Trans.^{b} energ.	Oscil. strength	Pol.	Trans.^{b} energ.	Oscil. strength	Trans.^{b} energ.	Oscil. strength
$^1B_{2u}^+$	5–6 (p)	4.27	0.049	y	4.49	0.256	4.29^a	0.18?
	4–7	5.48	0.608	y	6.31	0.699	6.51?^{a}	0.21
	3 8	7.07	0.618	y	8.18	0.851	7.40^a	0.6??
	4–10, 1–7	9.47	0.023	y	8.77			
$^1B_{2u}$	4 → 10, 1 → 7	8.09	0		9.20	0		0
$^1B_{1u}^+$	5–7, 4–6 (β)	5.54	1.37	x	5.94	2.115	5.62^a	1.70
	5 10, 1–6	8.05	0.769	x	7.96	0.043		
$^1B_{3u}^-$	5 7, 4–6 (α)	3.52	0		4.02	0	3.97^a	0.002
	5-10, 1-6	7.37	0		8.01	0		
$^1A_g^+$	4–8, 3–7	6.61	0		7.09			
	5–9, 2 6	6.69	0		7.42			
	3–10, 1–8	9.47	0		10.21			
$^1A_g^-$	4–8, 3-7	5.29	0		5.72			
	5–9, 2-6	6.09	0		7.36			
	3-10, 1-8	9.43	0		10.74			
$^1B_{1g}^+$	3–6, 5–8	5.47	0		5.50			
	4–9, 2–7	7.73	0		7.56			
$^1B_{1g}^-$	3–6, 5–8	5.07	0		5.98			
	4–9, 2–7	7.39	0		8.22			

[a] Platt [11].

[b] Energy in eV.

Mestechkin [10] who performs a semi-empirical variant of a random-phase approximation, gives a review of all these works to which the reader is brought back.

The experimental data concerning the absorption spectra of aromatic hydrocarbons studied here are mainly those of Klevens and Platt [11, 12] and we refer to their assignments except for a few ones, according to the indications, relating the polarisation given by Zimmermann and Joop [13].

The singlet-singlet transition energies (in eV) and the corresponding oscillator strengths for the *u*-bands of the naphthalene, anthracene and tetracene molecules are reproduced in Tables 2–4. In the first column the symmetry labels of various energy levels are indicated; in columns 2 to 5, our results are grouped under the heading "perturbation". We have named principal excitation this monoexcited configuration which represent at zero order the singlet state S_α. Fig. 3 shows values calculated and observed for the energies of the p, α and β bands.

The experimental and theoretical results are seen to agree very well for the β band and to be slightly too small for the α band. Generally, our result are smaller than experimental values, on the contrary of Pariser's one which were greater.

Table 3. Anthracene

Etat	Perturbation				Pariser [8]		Exper.	
	Principal excitation	Trans. energ.	Oscil. strength	Pol.	Trans. energ.	Oscil. strength	Trans. energ.	Oscil. strength
${}^1B_{2u}^+$	7 8 (p)	3.08	0.099	y	3.65	0.386	3.27[a]	0.10
	7 12, 3-8	5.35	0.324	y	5.25	0.091	5.61[b]	0.28
	6 9	5.63	0.139	y	6.58	0.644		
	5 10	5.80	1.16	y	7.84		6.66[a]	0.65
${}^1B_{2u}$	7 12, 3 8	4.86	0		5.69	0		
${}^1B_{3u}^+$	7 9, 6-8 (β)	4.89	2.016	x	5.50	3.23	4.83[a]	2.28
	4–10, 5-11	7.15	0.10	x	7.22	0.091		
${}^1B_{3u}^-$	7 9, 6-8 (α)	3.09	0		3.71	0	3.47[c]	
	4 10, 5 11	6.47	0		6.24	0		
${}^1A_g^+$	4 8, 7 11	5.86			6.74	0		
	6-10, 5 9	6.49			7.03	0		
	1 8, 7 14	7.59			7.68	0		
	2 10, 5-13	8.49			9.51	0		
${}^1A_g$	4 8, 7–11	5.04			5.00	0		
	6-10, 5 9	5.06			6.81	0		
	1-8, 7–14	7.15			7.75	0		
	2-10, 5-13	7.82			9.17	0		
${}^1B_{1g}^+$	5–8, 7 10	4.42			4.61	0		
	4 9, 6-11	7.32			7.19	0		
${}^1B_{1g}$	5–8, 7–10	3.73			4.94	0		
	4–9, 6–11	6.70			8.68	0		

[a] Platt [11].

[b] Platt [11], however this band is given as an A_g^+ band by Platt and a B_{2u}^+ band by Mestechkin [10].

[c] Zimmermann and Joop.

Table 4. Tetracene

Etat	Perturbation				Pariser [8]		Exper.	
	Principal excitation	Trans. energ.	Oscil. strength	Pol.	Trans. energ.	Oscil. strength	Trans. energ.	Oscil. strength
B_{2u}^+	9–10 (*p*)	2.56	0.11	*y*	3.11	0.44	2.62[a]	0.08
	8–11	4.83	0.141	*y*	4.68	0.16	4.23[b]	
	6–10, 9–13	4.87	0.998	*y*	6.54	0.001	5.40[a]	0.28
	7–12	5.81	3.29	*y*	6.94	1.20	5.87[a]	0.45
B_{2u}^-	6–10, 9–13	4.16	0		5.14	0		
B_{3u}^+	9–12, 7–10 (*β*)	4.45	2.71	*x*	5.09	3.78	4.55[a]	1.85
	7–13, 6–12	6.96		*x*	7.19	0.086	6.89[a]	0.68
							6.62[a]	0.27
B_{3u}	9–12, 7–10 (*α*)	2.85	0		3.56	0	3.22[c]	
	7–13, 6–12	5.42	0		5.78	0		
A_g^+	7–11, 8–12	5.84	0		4.51	0		
A_g^-	7–11, 8–12	4.38	0		6.33	0		
B_{1g}'	8–10, 9–11	3.66	0		3.90	0		
	8–13, 6–11	6.04	0		5.09	0		
	5–12, 7–14	7.27	0		7.02	0		
B_{1g}	8–10, 9–11	2.98	0		4.26	0		
	8–13, 6–11	5.95	0		5.56	0		
	5–12, 7–14	6.33	0		8.12	0		

[a] Platt [11].
[b] Meyer [14].
[c] Zimmermann and Joop [13].

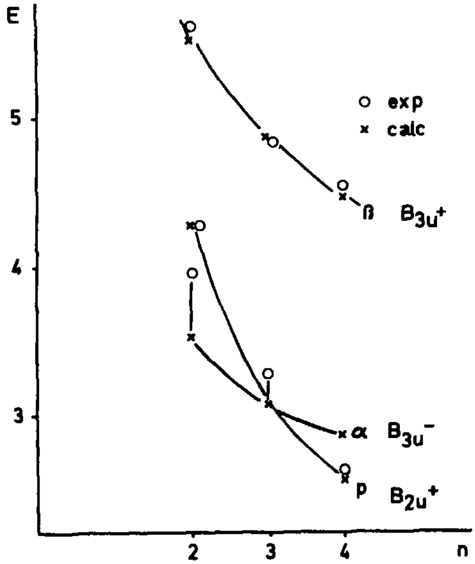

Fig. 3. *α*, *β*, *p* bands of naphthalene, anthracene and tetracene. Energy in eV in function of *n*, number of cycles

The parametrization should eventually be better adapted for this perturbation type of calculation which includes all configurations.

In conclusion, this work firstly gives energy values which are independent of any artificial truncature of the configurations and depends only of the order of the perturbation and the numerical results show that the second order agree well with experiment; secondly shows that the evolution of the energy is stabilized around $C_0 = 0.01$ and that the number of most interacting configurations is in general greater than usually considered in classical interactions of configurations (the difference being partly implicitely included in the semi-empirical parameters).

Acknowledgments. We should like to thank Dr. F. Guerin for her contribution in the adaptation of the computer program, and Dr. Y. Meyer for many discussions and comparisons with experimental results.

References

1. Parr, R. G.: Quantum theory of molecular electronic structure. New York: W. A. Benjamin Inc. 1963.
2. Bessis, G., Chalvet, O.: Faculté des Sciences de Lyon et Centre de mécanique ondulatoire appliquée. Paris.
3. Diner, S., Claverie, P., Malrieu, J. P.: Theoret. chim. Acta (Berl.) **8**, 390 (1967).
4. Epstein, P. S.: Physic. Rev. **28**, 695 (1926).
5. Nesbet, R. K.: Proc. Royal Soc. (London) A **230**, 312, 922 (1955).
6. Denis, A., Malrieu, J. P.: J. chem. Physics **52**, 9, 4762 (1970)
7. – J. chem. Physics **52**, 12, 6076 (1970).
8. Pariser, R.: J. chem. Physics **24**, 250 (1956).
9. Nishimoto, K., Forster, L. S.: Theoret. chim. Acta (Berl.) **3**, 407 (1965).
10. Mestechkin, M., Gutyria, L., Poltavets, V.: Optics and Spectro. **28**, (3), 244 (1970).
11. Platt, J. R.: Systematics of the electronic spectra of conjugated molecules. J. Wiley and Sons Inc 1964.
12. Klevens, H. B., Platt, J. R.: J. chem. Physics **17**, 470 (1949).
13. Zimmermann, H., Joop, N.: Z. Elektrochem. **64**, 1215 (1960).
14. Meyer, Y.: Thèse. Paris 1970.
15. Clar, E.: Aromatische Kohlenwasserstoffe, second edition. Berlin: Springer 1952.

Dr. J. F. Gouyet
Groupe de Physique Moléculaire
Laboratoire OPM
Ecole Polytechnique
F-75 Paris, France

Theoret. chim. Acta (Berl.) 26, 97 - 100 (1972)
© by Springer-Verlag 1972

The Electronic Structure of the HCN Dimer and Trimer

ALLAN JOHANSSON
Department of Inorganic Chemistry, Helsinki University of Technology, Helsinki, Finland

PETER KOLLMAN
Department of Pharmaceutical Chemistry, University of California, School of Pharmacy,
San Francisco, California 94122, USA

STEVE ROTHENBERG
Information Systems Design, 7817 Oakport Avenue, Oakland, California 94621, USA

Received January 5, 1972

The electronic structure and energy of dimerization and trimerization of HCN are computed with an STO-3G basis and the results found to be in good agreement with the experimental ΔE. Unlike CNDO/2, this small *ab initio* basis predicts the correct geometry for the dimer of hydrogen cyanide. The charge redistribution effects found in this H-bond involving a C–H proton donor and *sp* hybridized acceptor are similar to those found in previous H-bonded studies.

Hydrogen cyanide, unlike water [1] and hydrogen fluoride [2] [1], forms a well-characterized dimer in the gas phase. As early as in 1939, definitive thermodynamic measurements [3] on the gas phase association of HCN gave an enthalpy of dimerization of − 3.3 kcal/mole and an enthalpy of trimerization of − 8.7 kcal/mole.

There have been two previous attempts to calculate the energy of dimerization of HCN. One, by Hoyland and Kier [4] used the CNDO/2 semi-empirical molecular orbital method [5] and found cyclic $(HCN)_2$ far more stable than the linear structure found experimentally [6]. This failure of CNDO/2 was in contrast to the success it enjoyed in predicting properties of other H-bonded systems [5, 7] and indicated that this system would be a very interesting one to study with a minimum *ab initio* basis set.

Rae has computed [8] the dimerization energy and minimum energy geometry for the HCN linear dimer and found a dimerization energy of 4.7 kcal/mole and $R(\mathrm{N} \ldots \mathrm{C}) = 3.3$ Å. He used a very good SCF wave function for the HCN monomer and separately computed the electrostatic, polarization, exchange repulsion and dispersion contribution to the intermolecular energy.

We have computed the energy for both the linear (HCN... HCN) and cyclic $\begin{pmatrix} \mathrm{H{-}C{\equiv}N} \\ \mathrm{N{\equiv}C{-}H} \end{pmatrix}$ structures of $(HCN)_2$ as well as the energy for the linear trimer (HCN...HCN...HCN) at $R_1(\mathrm{N} \ldots \mathrm{C}) = R_2(\mathrm{N} \ldots \mathrm{C}) = 3.2$ Å using an STO-3G basis set and the results of the calculations are listed in Table 1.

The monomer geometry was assumed fixed at the experimental value [10], this approximation has been found to be excellent in previous studies of weak hydrogen bonds [11]. Unlike the CNDO/2 results, we found the cyclic dimer very

---

[1] HF forms mainly a hexamer but IR studies indicate that under appropriate conditions, the dimer could be characterized.

Table 1

HCN monomer

$E = -91.67527$ a. u.

$r(\mathrm{C-H}) = 1.07$ Å

$r(\mathrm{C{\equiv}N}) = 1.15$ Å

Linear dimer HCN $\overset{R}{\ldots}$ HCN

R(N...C) (Å)	E (a. u.)
2.7	−183.31595
3.0	−183.35563
3.2	−183.35640
3.3	−183.35634
3.6	−183.35522

Cyclic dimer $\begin{array}{c} \mathrm{H-C\equiv N} \\ \mathrm{N\equiv C-H} \end{array} \Big| \, R$

R (between monomers) (Å)	E (a. u.)
2.0	−183.25790
2.6	−183.34160
2.9	−183.34942
3.2	−183.35164
3.5	−183.35207
3.8	−183.35210

Linear trimer HCN $\overset{R_1}{\ldots}$ HCN $\overset{R_2}{\ldots}$ HCN

$R_1(\mathrm{N}\ldots\mathrm{C}) = R_2(\mathrm{N}\ldots\mathrm{C}) = 3.2$ Å

$E = -275.03854$ a. u.

little stabilized relative to the HCN monomers and the linear dimer was found to have a stabilization energy of 3.7 kcal/mole at $R(\mathrm{C}\ldots\mathrm{N}) = 3.2$ Å, the same length as found in the crystal [12] where the HCN molecules form infinite linear chains. The neglect of three and four center repulsions in CNDO/2 clearly is the cause why a cyclic structure, with the 2C's and N's close together, is computed to be especially stable in a CNDO/2, calculation. Our ΔE is in better agreement with the experimental value than Rae's, mainly because a molecular orbital calculation does not include the attraction due to dispersion forces, which Rae finds to be 1.3 kcal/mole at the minimum energy geometry. The ΔE calculated by us is too large probably because charge transfer and polarization effects are exaggerated in this minimal basis calculation. Our calculated $R(\mathrm{C}\ldots\mathrm{N})$ length is probably a bit too short, since one would expect the dimer length to be longer than that found in the crystal.

The stabilization energy for the linear trimer at $R_1(\mathrm{C}\ldots\mathrm{N}) = R_2(\mathrm{C}\ldots\mathrm{N}) = 3.2$ Å was calculated to be 8.1 kcal/mole which is in good agreement with the experimentally found value.

The charge distribution changes found for the linear dimer and trimer are given in Table 2. The calculated dipole moments for the monomer and dimer are

Table 2

Monomer population

H	0.8502
C	5.9896
N	7.1602

Linear dimer $R = 3.2$ Å

	Population	Δ population[a]
H	0.8407	0.0095
C	5.9688	0.0208
N	7.1748	−0.0146
H	0.8231	0.0271
C	6.0098	−0.0202
N	7.1828	−0.0226

Linear trimer $R_1 = R_2 = 3.2$ Å

	Population	Δ population
H	0.8391	0.0111
C	5.9664	0.0232
N	7.1783	−0.0181
H	0.8140	0.0362
C	5.9890	0.0006
N	7.1974	0.0372
H	0.8208	0.0294
C	6.0107	−0.0211
N	7.1843	−0.0241

[a] Δ population = (monomer population)–(polymer population). Negative sign denotes increase of electronic charge on atom.

Table 3. Dipole moments

Configuration	Dipole moment (D)
Monomer	2.48
Linear dimer ($R = 3.2$ Å)	5.58

presented in Table 3. The enhancement of the dipole moment due to H-bonding is of the same magnitude as found for the water dimer [13].

As has been found in previous studies on H-bonding, the proton donor hydrogen loses charge on hydrogen bond formation, and the C≡N of the proton donor fragment gains. On the proton acceptor, nitrogen actually gains electrons at the expense of the less electronegative C and H atoms, who are big losers of charge. It is very interesting to note that in the linear trimer, the central HCN stays nearly neutral (−0.0004) and acts as a charge transmitter from one end fragment (+0.0162) to the other (−0.0158). This phenomenon has been previously observed in CNDO/2 calculations on HF and water polymers containing as many as 12 monomers [15]. In the cyclic dimer, as the fragments approach each other the charge shifts from H → N in each fragment.

The field gradient at the proton is 0.362 a. u. in the monomer, 0.335 a. u. at the H-bonded proton in the linear dimer. This field gradient for the monomer is 20% smaller than the experimental value [16]; but the interesting fact is that the percent decrease of the field gradient going from monomer → dimer (8%) is similar to that found in the water dimer (9%) [15].

These calculations add additional support for the adequacy of a small contracted *ab initio* basis to represent the energies and geometries of hydrogen bonding found experimentally and encourages the use of this basis on larger systems where an extensive basis set calculation would be prohibitive. This basis set tends to underestimate the distance between monomers by 0.1–0.3 Å and to overestimate the dimerization energy by 20–40% [14].

References

1. Eisenberg, D., Kauzmann, W.: The structure and properties of water. Oxford: University Press 1970
2. Janzen, J., Burtell, L. S.: J. chem. Physics **50**, 3611 (1969); Couzi, M., Huong, P. V.: J. Chim. physique **66**, 1309 (1969).
3. Giaque, W. F., Ruehrwein, R. A.: J. Amer. chem. Soc. **61**, 2626 (1939).
4. Hoyland, J. R., Kier, L. B.: Theoret. chim. Acta (Berl.) **15**, 1 (1969).
5. Pople, J. A., Santry, D. P., Segal, G. A.: J. chem. Physics **43**, S129, S136 (1965).
6. King, C. M., Nixon, E. R.: J. chem. Physics **48**, 1685 (1968).
7. Kollman, P. A., Allen, L. C.: J. Amer. chem. Soc. **91**, 753 (1970).
8. Rae, A. I. M.: Molecular Physics **16**, 257 (1969).
9. Hehre, W. I., Steward, R. F., Pople, J. A.: J. chem. Physics **51**, 2657 (1968); standard exponents were used in this calculation.
10. Douglas, A. E., Sharma, D.: J. chem. Physics **21**, 448 (1953).
11. Kollman, P. A., Allen, L. C.: J. chem. Physics **52**, 5085 (1970).
12. Dulmage, W. J., Lipscomb, W. N.: Acta crystallogr. **4**, 330 (1951).
13. Kollman, P. A., Allen, L. C.: J. chem. Physics **51**, 3286 (1969).
14. Del Bene, J., Pople, J. A.: J. chem. Physics **52**, 4858 (1970).
15. Kollman, P. A., Allen, L. C.: Theory of the hydrogen bond. Chem. Reviews (in press), 1972.
16. Kern, C. W., Karplus, M.: J. chem. Physics **42**, 1065 (1965).

Dr. P. Kollman
University of California
School of Pharmacy
Department of Pharmaceutical Chemistry
San Francisco, California 94122, USA

Theoret. chim. Acta (Berl.) 26, 101–105 (1972)
© by Springer-Verlag 1972

The Electrostatic Molecular Potential for Imidazole, Pyrazole, Oxazole and Isoxazole

G. Berthier
Laboratoire de Biochimie Théorique associé au CNRS, Institut de Biologie physico-chimique,
13 Rue Pierre et Marie Curie, Paris V, France

R. Bonaccorsi
Laboratorio di Chimica Quantistica ed Energetica Molecolare del C.N.R.,
Via Risorgimento 35, 56100 Pisa, Italy

E. Scrocco and J. Tomasi
Istituto di Chimica Fisica dell'Università, Via Risorgimento 35, 56100 Pisa, Italy

Received February 11, 1972 / April 6, 1972

The electrostatic molecular potentials arising from *ab initio* MO LCAO GTO SCF wavefunctions for some five membered heterocycles are used to make evident differences in reactivity of some sites (tertiary nitrogen, carbon atoms) towards electrophilic reagents. Results are in general accordance with experiment.

Introduction

The electrostatic potential arising from the charge distribution of a molecule calculated in the SCF approximation may be used to obtain an estimate of the chemical reactivity of specific positions of the molecule[1].

The definition of the electrostatic molecular potential $V(\boldsymbol{r})$ and some tentative applications may be found in Refs. [1–7]. In this paper we shall concern ourselves with the following five-membered heterocycles: imidazole, pyrazole, oxazole and isoxazole (see Table 1). The SCF wavefunctions here employed were calculated by one of the authors [8] via a gaussian basis set [9] roughly equivalent to a minimal STO. Some information on the influence of the basis on the $V(\boldsymbol{r})$ value may be found in Ref. [5]; such influence may be considered inessential to a qualitative discussion and the results here presented may be regarded as sufficiently representative of the exact molecular potentials.

Results and Discussion

The physical observable $V(\boldsymbol{r})$ is a function of the point in space and its interpretation depends on the value as well as on the neighbouring shape of the function itself. The most direct presentation is obtained by three-dimensional iso-potential graphs or by maps in selected planes[2]. To save space, however, we present here the essential information as numerical indexes pertaining to the relevant atoms, although we are aware of the fact that such a description neglects a considerable portion of the information from the complete $V(\boldsymbol{r})$ function.

---

[1] In particular, such an approach can be of some use in characterizing the approach channels of the two partners.

The discussion of the results is here partitioned in two sections, the first concerning the molecular plane and the second the regions above (and below) the ring.

Molecular Plane

In the molecular plane, regions of positive $V(\boldsymbol{r})$ values (repulsive for positively charged reagents) surround the entire molecule, except the areas near the O and N— atoms. Each of these regions exhibits a minimum clearly related to each —N or —O atoms, even in isoxazole, where a unique negative region encloses both adjacent heteroatoms. The values of such minima are reported in Table 1.

In any case the N heteroatoms result clearly more reactive, with respect to positively charged reagents, than O atoms, in accordance with chemical evidence.

The relative depths of the minima found near the =N— atoms are in qualitative accordance with the general chemical behaviour of the present set of molecules.

Several types of reactions involving the =N— atoms in the neutral molecules can, in principle, be related to this first-order picture of the interaction energy with respect to an approaching positively charged reagent[3]. Among them, the most important are: the quaternization reactions, formation of coordination compounds and hydrogen-bridged associates, and electrophilic substitutions (in imidazole and pyrazole). For the last type of reaction a connection with the electrostatic potential around =N — is of course possible only in the cases where an electrophilic attack at the tertiary nitrogen is followed by a loss of the proton from the imino-group (S_E2' mechanism).

Unfortunately, only very few quantitative data concerning the chemical behaviour of these compounds are available. For the simplest reaction, protonation, quantitative thermodynamics data exist, but they are not supplemented by analogous kinetic information. Moreover, such data are given as acidic ionization constants (pK_a's). In order to compare the free energies of protonation in solution obtained from the pK values with the electrostatic interaction energy values, it is necessary to assume that the entropy variations and changes in solvation energy following the protonation are fairly constant along the series considered. Such assumptions do not seem to be completely unrealistic and consequently we may consider the order of pK_a values as reproducing the ordering of the related proton affinities (gas phase enthalpies). The correlation between the $V(\boldsymbol{r})$ minima and pK_a values is gratifying (pK_a values: I, 6.95 [10]; II, 2.48 [11]; III, 0.8 [12]; IV, −2.03 [12][4]).

---

[2] Some of the maps are available upon request to the authors.

[3] Some of these reactions do not necessarily involve charged reagents: *mutatis mutandis* the picture is still valid at least for reagents exhibiting permanent dipole moments. As an example, see Ref. [6].

[4] A discussion about the reliability of these values is beyond the scope of this paper. We note, however, that an older value for isoxazole; +1.3 [13] is commonly quoted. The value given in Ref. [12] is, at least from an operative point of view, more comparable with the oxazole pK_a in the same reference.

Table 1. Values of the electrostatic molecular potential $V(r)$ in some characteristic regions

Molecule	Position	$V(r)$[a]
Imidazole 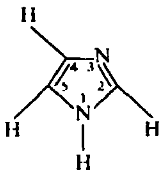	C_2–H	− 5.0
	C_4–H	−15.1
	C_5–H	− 7.5
	N_1–H	0
	N_3	*−82.0*
Pyrazole 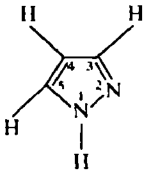	C_3–H	−13.6
	C_4–H	−16.7
	C_5 H	− 7.5
	N_1 H	− 2.0
	N_2	*− 74.0*
Oxazole 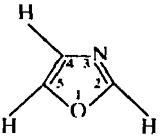	C_2–H	+ 5.0
	C_4–H	− 3.6
	C_5 H	+ 2.0
	O_1	*−31.2*
	N_3	*− 68.4*
Isoxazole 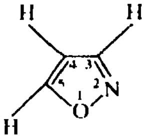	C_3 H	− 1.8
	C_4 H	− 2.8
	C_5 H	+ 2.0
	O_1	*37.0*
	N_2	*66.8*

[a] All $V(r)$ values are expressed in kcal/mole. The values in italic refer to ring plane points; the other to points 2 Å above the ring plane.

Quantitative comparisons for other reactions are not possible on account of the lack of pertinent experimental data. From a qualitative perusal on the whole set of experimental results (see, e. g. Refs. [14–18]), the reactivity of tertiary nitrogens in these molecules does not seem to be in conflict with the electrostatic potential indications.

Regions Outside the Ring Plane

It is convenient to point out that the path of the electrophilic reagent approaching the —N= atoms (as well as the O atoms) is not limited to the ring plane because the negative region spreads out above (and below) such a plane giving rise to a relatively large solid angle where the approach is electrostatically favoured. There is clear evidence that in these aromatic compounds only one minimum near the O atom (on the ring plane) occurs: note the difference from paraffinic heterocycles (e. g. oxirane and oxaziridine [2, 3]) where two minima near each O atom, corresponding to the two lone pair regions, have been found. The situation found in the present set of molecules is akin to that already found in Ref. [4] for the DNA bases (incidentally, we point out the strictly similar behaviour of $V(r)$ in imidazole and in the imidazole moiety of adenine). More interesting is the behaviour of $V(r)$ in the regions above the C—H groups. The electrostatic potential, repulsive in the proximity of the ring, becomes attractive at larger distances. Such a finding is in agreement with the fact that electrophilic reaction channels may reach the hydrocarbon portion of the molecule through its π region[5].

In order to underline differences in such a behaviour related to single C—H positions, we have chosen the value of $V(r)$ at about 2 Å above the C atoms (values reported in Table 1).

Such a presentation is not sufficient to give hints on the classical reaction paths available for charged reagents, but it is however sufficient for our comparative purposes.

It is convenient to consider separately, in first instance, the two imidazole oxazole and pyrazole – isoxazole pairs, differing in the relative positions of the two heteroatoms. In the first couple attacks by electrophilic reagents are favoured in position 4. Positions 2 and 5 are nearly equivalent in oxazole but they show a little asymmetry (with position 5 favoured) in imidazole. The reaction channels in imidazole are deeper than in oxazole and a higher reactivity of the former with respect to the latter could be anticipated. In the second couple, position 4 is again favoured and some differences between positions 3 and 5 are evident (especially in pyrazole)[6]. Differences between homologous positions in pyrazole and isoxazole are manifest, and agree with chemical experience [16].

The comparisons between the two pairs of molecules are more difficult to substantiate with experimental data. The Friedel-Craft acylation however offers a hint: for this series of compounds one finds experimentally that such a reaction is possible only in position 4 of pyrazole in accordance with the greater depth of the minimum found above and beneath the C_4—H_4 bond in that molecule.

In conclusion, for neutral molecules the predictions from electrostatic potentials are in accordance with the experimentally known properties (ordering of pK_a values, higher reactivity of position 4) and they also indicate the two-nitrogen ring molecules (I and II) to be more reactive than the N—O heteroatomatics (III and IV). More general statements about reactivity should be made only after an analysis of the corresponding conjugate acids, BH^+, because many of the characteristic reactions in acidic media with electrophilic reagents seem to involve the protonated species directly. Moreover it is evident that the molecule polarization induced by the approaching reagent plays an important role in determining reactivity properties. Such a polarization is not accounted for by the electrostatic picture which is a valuable one only in the first phases of the partners approach. We hope however that this type of information, although rather limited, may be of some use for interpreting chamical reactivity.

---

[5] The occurence of the negative regions and the differences among different sites might be considered as mainly due to π electrons; it is to be pointed out, however, that the best agreement with our $V(r)$ findings is obtained by using total net charges instead of π charges only. (For the population analysis of the wavefunctions here employed see Ref. [8].)

[6] It may be noted that the experimental reactivity properties, as estimated on the basis of reaction products, may sometimes be misleading in the case of both pyrazole and imidazole, because the rapid exchange of the iminic hydrogen between the two N's makes the molecule more symmetrical in a time-average basis.

References

1. Bonaccorsi, R., Scrocco, E., Tomasi, J.: Theoret. Section Progress Report, p. 35. Laboratorio di Chimica Quantistica del CNR e Istituto di Chimica Fiscia dell' Università, Pisa, 1969 1970.
2. — — — J. chem. Physics **52**, 5270 (1970).
3. — — — Theoret. chim. Acta (Berl.) **21**, 17 (1971).
4. — Pullman, A., Scrocco, E., Tomasi, J.: Theoret. chim. Acta (Berl.) **24**, 51 (1972).
5. — — — - Chem. Physics Letters, **12**, 622 (1972).
6. -- Petrongolo, C., Scrocco, E., Tomasi, J.: Theoret. chim. Acta (Berl.) **20**, 331 (1971).
7. Alagona, G., Cimiraglia, R., Scrocco, E., Tomasi, J.: Theoret. chim. Acta (Berl.) **25**, 103 (1972).
8. Berthier, G., Praud, L., Serre, J.: In Quantum aspects of heterocyclic compounds in chemistry and biochemistry (E. D. Bergmann and B. Pullmann Eds.). Jerusalem Symposia, **2**, 40. New York: Academic Press 1970.
9. Clementi, E.: J. chem. Physics **46**, 4725 (1967).
10. Kirby, A. H. M., Neuberger, A.: Biochem. J. **32**, 1146 (1938).
11. Dedichen, G.: Ber. dtsch. chem. Ges. B. **39**, 1831 (1906).
12. Brown, D. G., Gosh, P. B.: J. chem. Soc. (London) (B) **1969**, 270.
13. Speroni, G., Pino, P.: Gazz. Chim. ital. **80**, 549 (1950).
14. Grimmett, M. R.: Advances in Heterocyclic Chemistry **12**, 104 (1970).
15. Kost, A. N., Grandberg, I. I.: Advances in Heterocyclic Chemistry **6**, 347 (1966).
16. Kochetko, N. K., Sokolov, S. D.: Advances in Heterocyclic Chemistry **2**, 365 (1963).
17. Albert, A.: Heterocyclic chemistry. London: Athlone Press 1968.
18. Duffin, G. F.: Advances in Heterocyclic Chemistry **3**, 2 (1964).

Prof. Dr. E. Scrocco
Istituto di Chimica Fisica dell'Università
Via Risorgimento 35
I-56100 Pisa, Italy

The 6th Jerusalem Symposium

An International Symposium on:

Chemical and Biochemical Reactivity

sponsored jointly by the Hebrew University, Jerusalem and the Institut de Biologie Physico-Chimique (Fondation Edmond de Rothschild), Paris will be hold, under the auspices of the Israël Academy of Sciences and Humanities, in Jerusalem, Israël, from April 9th to April 13th 1973.

The aim of this meeting will be the confrontation of the present status of our knowledge about the theoretical and experimental aspects of the problem. A particular emphasis will be laid on theoretical computations using refined allvalence electrons or all electrons methods in relation to experimental data obtained with modern techniques. The collaboration of both theoreticians and experimentalists is therefore wellcome at this symposium. The biochemical section implies also studies in the field of pharmacology.

Correspondance and applications should be send to Prof. E. D. Bergmann, Dept. of Organic Chemistry, the Hebrew University, Jerusalem, Israël and Prof. B. Pullman, Fondation Edmond de Rothschild, 13, rue Pierre et Marie Curie, Paris 5è, France.

Theoret. chim. Acta (Berl.) 26, 107—130 (1972)
© by Springer-Verlag 1972

Molecular Orbital Calculations of the Active Site Complex of Two Iron Ferredoxins

II. Electron Distribution, Magnetic Moment, Field Gradients and Electronic Spectra of the Oxidized State

GILDA H. LOEW and DAVID A. STEINBERG
Department of Genetics, Stanford University Medical Center, Stanford, California 94305, USA

Received August 11, 1971/February 14, 1972

In this report we present further results of molecular orbital calculations for a model of the active site complex of two iron ferredoxins, using the Iterative Extended Hückel Method for our calculations. In the first paper of this series we dealt mainly with energy-conformation calculations which helped establish the salient chemical and conformational features of the lowest energy forms for such a complex. Presented here are the nature and energy ordering of the 70 molecular orbitals in the active site model, a calculation of room temperature magnetic moment, of the electric field gradient at the Fe nucleus and an assignment of the optical absorption spectra in the one electron approximation for the lowest energy conformer of the oxidized state of these proteins. For each property, we compare our calculated results with experiment whenever possible, and with the results of previous correlations. In addition, we indicate the sensitivity of these properties to variations in conformation about the Fe atoms.

In der vorliegenden Arbeit werden weitere Resultate der Untersuchung eines Modells des an der aktiven Stelle gebildeten Komplexes von zwei Eisen-ferredoxinen mitgeteilt, die mit Hilfe der iterativen erweiterten Hückel-Methode gewonnen wurden. In der ersten Veröffentlichung dieser Reihe wurden hauptsächlich die Ergebnisse der Berechnungen von Konformationsenergien angegeben, die dazu beitrugen, die wichtigsten chemischen Eigenschaften sowie die Konformationen solcher Komplexe mit der niedrigsten Energie zu ermitteln. Hier werden nun die Eigenschaften der 70 niedrigsten Molekülorbitale des Modells, eine Berechnung des magnetischen Moments bei Raumtemperatur und des elektrischen Feldgradienten am Fe-Kern sowie die Zuordnung des optischen Absorptionsspektrums in der Einelektronennäherung für die Konformation niedrigster Energie des oxydierten Zustandes dieser Proteine veröffentlicht. Die Ergebnisse werden soweit möglich mit dem Experiment und früheren Interpretationen verglichen. Zusätzlich wird auf die Empfindlichkeit dieser Eigenschaften bezüglich einer Variation der Konformation in der Nähe des Fe-Atoms hingewiesen.

1. Introduction and Background

The iron-sulfur proteins, now called "plant-type" ferredoxins, participate primarily as one-electron transfer agents in a wide variety of biological processes. Diverse biochemical and physical observations indicate that these proteins share a characteristic active site for electron transfer composed of two Fe atoms, two acid-labile S atoms of unknown origin, and four S atoms from nearby cysteine residues all in close proximity, as shown in Fig. 1 [1]. However, detailed chemical and conformational information about the active site is not known, nor are the variations from protein to protein in this class.

Presuming the biological activity to be centered on the two Fe atoms in the protein, a crystal field model of the active site as two Fe atoms perturbed by an

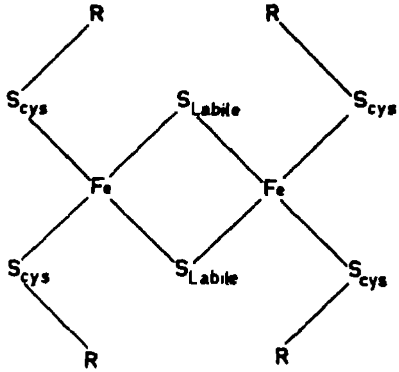

Fig. 1. General model of the active site of two-iron ferredoxins

electric field created by neighboring atoms [2–4], has been used in the past to try to understand some of its properties. In this crystal field approach the other atoms need not be specified and no interatomic interactions can be explicitly considered. Moreover even with these assumptions, no bona fide crystal field calculations characterizing these perturbed Fe ions have been made. Rather specific observations have been used to estimate further characteristics of the crystal field. Also for this reason and since there are important properties of these systems indicating interatomic interactions, we have undertaken a molecular orbital study of the active site which expands explicit consideration from two perturbed Fe ions to a molecular complex involving the core of atoms shown in Fig. 1.

The first step in our molecular orbital study was to select a reasonable model for the active site based on bona fide criteria. To this end, we have recently reported [5] the results of energy-conformation studies for a series of fifteen plausible active site models using the so-called Iterative Extended Hückel Theory (IEHT) for the molecular orbital calculations [6–12].

Previous applications of this method, including our own [9, 13, 14] indicate that such calculations yield total configuration energies whose variation with molecular geometry parallels that of the total energy and hence allows the prediction of a lowest energy conformation. The results of our calculations [5] showed persistent stability of a tetrahedral arrangement over a square planar one for all chemical variations studied of the oxidized state. In the lowest energy chemical-conformer, with RS^- in Fig. 1 $= SCH_3^-$ each Fe has a distorted tetrahedral environment, the Fe–Fe distance is a maximum and the S_b–S_b distance is a minimum, typical of that of disulfide bonds in proteins. In the present study we use this most stable conformer to calculate the electric field gradient at the Fe nucleus, the room temperature paramagnetic susceptibility and to assign the optical spectra in the one-electron approximation of our calculations.

For each property discussed, our calculated results are compared with experimental results whenever possible and to previous explanations offered in the crystal field format. Since the conformer chosen is based on energy considerations only, agreement with observed properties is further independent verification of the validity of the general nature of the active site complex which emerges from the molecular orbital description. In general, the satisfying result is obtained, that the lowest energy conformer is also the one which explains the observed properties most accurately and most consistently.

We proceed now to a general discussion of the nature of the molecular orbitals and energies which result from our calculations and then to a discussion of the three specific properties of the oxidized state mentioned above.

2. MO Results: Energy Ordering and Nature of the Molecular Orbitals

In our model for the oxidized state of the active site of the two-iron ferredoxins with RS = SCH_3^- and no other added ligands, we have considered the four geometric variations shown in Fig. 2, and described in the table accompanying this figure, all of which have D_{2h} symmetry. As shown by the relative energies given in this table, the most stable conformer is IA_4. In these active site models there are 20 atoms, 70 valence atomic orbitals and 80 valence electrons which are all included in our IEHT calculation of the molecular orbital energies and eigen-

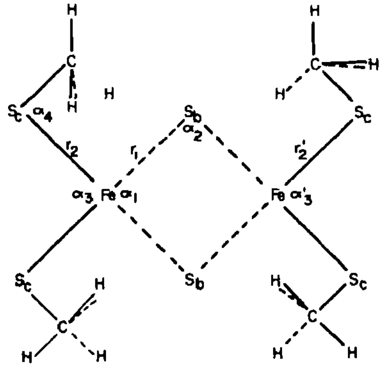

	A_1	A_2	A_4	A_5
α_1	109°	90°	45°	90°
α_2	71°	90°	135°	90°
α_3	109°	90°	109°	109°
α_4	90°	90°	90°	90°
r_1	2.32	2.32	2.42	2.32
r_2	2.32	2.32	2.32	2.32
r_2'	2.32	2.32	2.32	2.32
r(Fe-Fe)	2.66	3.26	4.20	3.26
r(S_b-S_b)	3.76	3.26	2.08	3.26
Energy	1151.7	1122.3	1163.7	1159.9

Fig. 2. Specific conformers of the active site: input geometries and calculated energies in eV

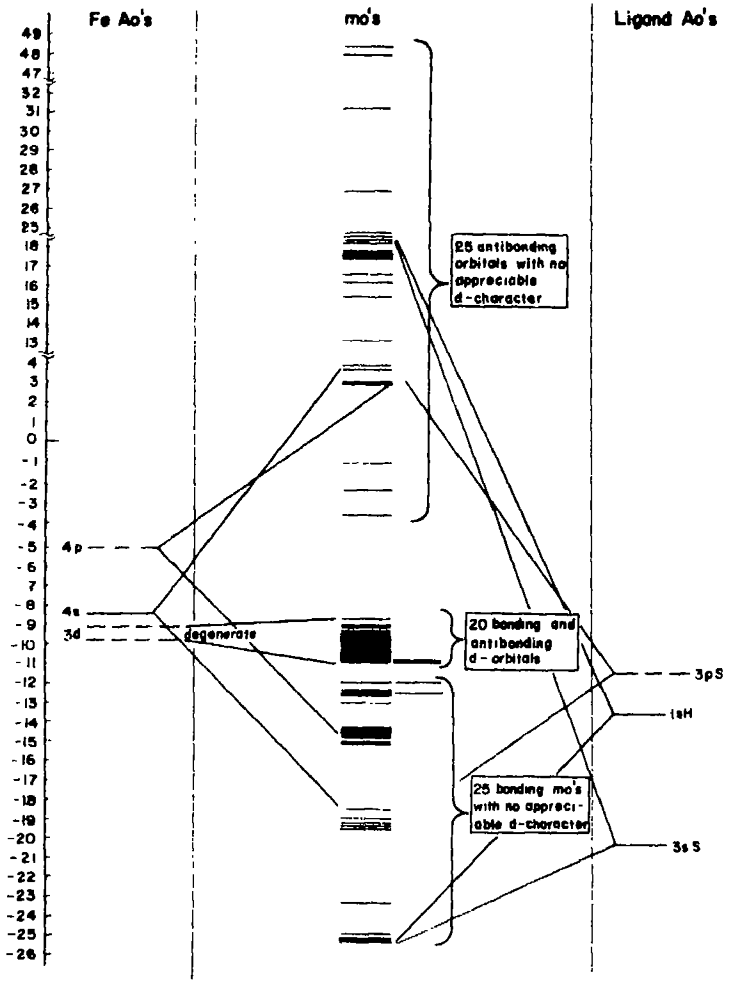

Fig. 3. Molecular orbital energy pattern for lowest energy conformer of the active site complex of two iron ferredoxins

functions. The resulting molecular orbital energy pattern is shown in Fig. 3 for the lowest energy conformer, together with the energy of the atomic orbitals and some indication of the nature of the molecular orbitals. While the details of this pattern depend on the molecular active site model chosen, the general features indicated are shared by all. In general then, there are a series of low lying bonding orbitals which involve no appreciable Fe 3*d* atomic orbitals. These result primarily from interactions among the ligand atoms themselves with some participation of the Fe 4*s* and 4*p* orbitals. In this model, the first 25 molecular orbitals are of this "perturbed ligand" type. These bonding orbitals have 25 anti-bonding partners of much higher energy (orbitals 46–70), also with no appreciable 3*d* orbital character. The energy difference between the highest filled bonding orbital and lowest empty non-bonding orbital of this type i.e.

$L \rightarrow L^*$ is 8.15 eV and is much too high an energy to be observed in UV or visible optical absorptions.

Between the 25 bonding and antibonding perturbed ligands and orbitals there are 20 very closely spaced energy levels. These are the energies of all the molecular orbitals which have appreciable $3d$ character. The first ten orbitals (26–35) have primarily sulfur ($3p$) ligand character, while the remaining ten (36–45) have primarily Fe $3d$ character, i.e. greater than 50% d orbital participation. These 20 orbitals correspond to the bonding and antibonding d-orbitals of the ligand field. However there is no large energy gap between these types of MO and the total energy separation among these 20 orbitals is only 1.85 eV or 15000 cm^{-1}. This value is much lower than that estimated from the crystal field formulation [2] and indicates weak-to-intermediate interaction of the $3d$ orbitals of Fe with the S ligands. The small perturbation of d orbitals by molecule formation can also be seen in Fig. 3 by noting the small energy difference between the $3d$ atomic and molecular orbitals. Perhaps this result of weak interaction which is the first attempt to characterize the bonding of Fe with S ligands, explains why the active site complex cannot be removed as an intact entity from these proteins in contrast to the heme group for which calculated metal-ligand interactions are much stronger [17, 18].

While the energies of the 20 molecular orbitals involving d-orbitals are closely spaced they are not pairwise degenerate and do not correspond to two separate Fe complexes. Moreover, the combination of AO's in these 20 orbitals is quite different from those in the two sets of ten orbitals that would be obtained from a ligand field description of two separated Fe atoms in tetrahedral symmetry. Each molecular orbital can be written as

$$\Psi_i(\Gamma_i) = \sum_{J=1}^{s} \alpha_{iJ} A_{iJ}(\Gamma_i) \,,$$

where $\Psi_i = i^{\text{th}}$ MO belonging to irreducible representation Γ_i of D_{2h} symmetry group $A_J = J^{\text{th}}$ symmetry orbital of equivalent atoms A belonging to same irreducible representation

$$\mathrm{A} = \mathrm{Fe}, \mathrm{S}_b, \mathrm{S}_c, \mathrm{C}_m, \mathrm{H}_m, \mathrm{H}'_m \,.$$

Table 1. Symmetry of binuclear d orbitals in D_{2h} symmetry

i	$d_{x^2-y^2}$	d_{z^2}	d_{xy}	d_{xz}	d_{yz}
$d_i + d_{i'}$	a_{1g}	a_{1g}	b_{1g}	b_{2g}	b_{3g}
$d_i - d_{i'}$	b_{3u}	b_{3u}	b_{2u}	b_{1u}	a_{1u}
T_D	e	e	t_2	t_2	t_2

In our active site complex there are six sets of symmetry equivalent atoms: The two Fe atoms, the two bridge S atoms (Sb), the four systeine S atoms (Sc), and four methyl carbon atoms (Cm), four of the methyl hydrogens which are in the plane of the major part of the molecule (Hm) and the 8 remaining methyl hydrogens which make up the tetrahedrally bonded carbon atoms (H'm). The ten $3d$ atomic orbitals participate in both the bonding and antibonding molecular orbitals as 10 binuclear pairs in the form: $(d_J \pm d'_J)$. Table 1 gives the irreducible

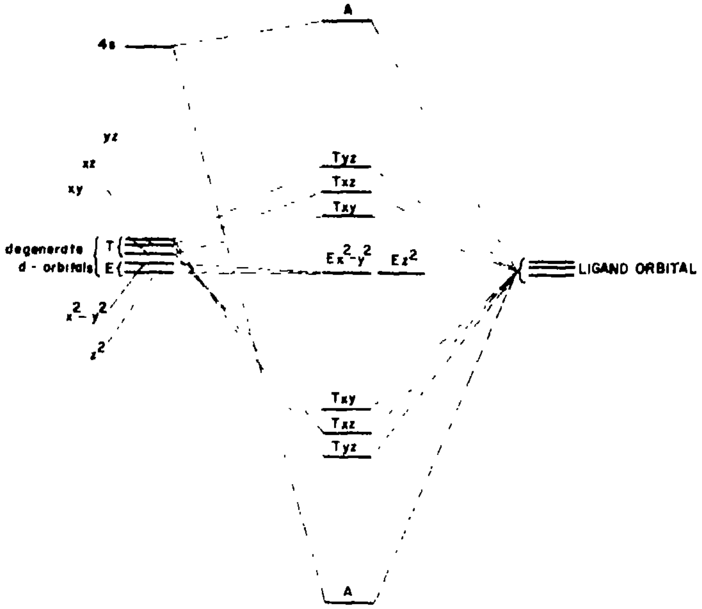

Fig. 4. Schematic ligand field bonding pattern for transition ion in T_d symmetry

representations to which the 10 combinations of *d* orbitals belong in the D_{2h} molecular symmetry. Also given for comparison in this table is the representations to which the individual d_j orbitals belong in the single centered Fe complexes of regular T_d symmetry.

We see that in the binuclear D_{2h} complex *d* orbitals can participate in MO's with both *g* and *u* symmetry.

A more detailed picture of the 10 antibonding, primarily *d*-orbitals so important in determining the observed properties is given in Fig. 5a for the lowest-energy active-site conformer. The symmetry labeling and % participation of the *d* orbitals in each molecular orbital is also given. These 10 states are shown separated into their *g* and *u* subsets. Each MO involves the participation of both Fe atoms. If the two parts of the binuclear complex were to separate and provided we supplied each Fe with its own bridge S atoms, which would involve an energy renormalization, this orbital diagram would approach two identical sets of 5 non-interacting, single 3*d* Fe molecular orbitals each with five electrons. The *g* or *u* subset alone of 5 antibonding primarily 3*d* orbitals correspond then to the five e^* and t_2^* orbitals shown in the Ballhausen type single metal ion in T_d symmetry diagram of Fig. 4 [16]. Contrary to the ligand field analysis of T_d symmetry, in which *E* orbitals are non-bonding, however, both the e^* and t_2^* orbitals contain some ligand character and both are separated in energy from their bonding partners.

The degree of interaction of the two Fe atoms can then be measured as the extent to which the *g* and *u* partners of the same *d* orbitals have different energies and different % covalences. We see from Fig. 5a that even with our lowest energy

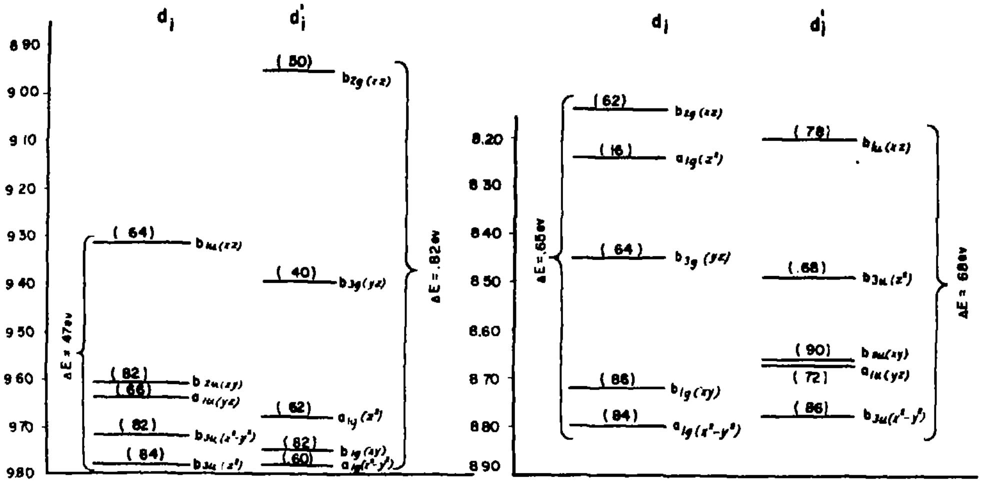

Fig. 5. Nature and energy ordering of the 10 antibonding *d* orbitals in active site complex of two iron ferredoxins. a tetrahedral conformation, b planar conformation of sulfur atoms about each Fe atom

conformer which involves a maximum Fe–Fe energy separation, this interaction is non-negligible on both criteria.

In the *u*-subset of molecular orbitals the two "e^*" ($d_{x^2-y^2}$ and d_{z^2}) orbitals are lower in energy than the three "t_2^*" orbitals and the partners of each type have non-degerate energies. For this series then the traditional energy interval called $10D_q = Et_2^* - E_e^* = 0.47\,\text{eV}\,(3800\,\text{cm}^{-1})$ analogous to the definition in single centered Fe complexes of regular T_d symmetry. For the *g*-subset we analogously define a second value of $10D_q$, as shown in Fig. 5, which is equal to 0.82 eV ($\sim 6500\,\text{cm}^{-1}$). These small values are similar to those empirically associated with four coordinated Fe T_d complexes [27b] and much less than values of 18000–36000 cm^{-1} previously proposed but not calculated for these ferredoxins [2, 3].

In Fig. 5b we give results obtained for a planar arrangement of all S atoms about each Fe atom. We see from this figure, that even though the Fe–Fe distance is smaller in this form, the effect of Fe–Fe interaction is somewhat less, and that the % of covalency and energy ordering of the various *d* orbitals is different in each case. The bonding MO's are also similarly rearranged.

In the ground state configuration, all of the 10 bonding orbitals and five of the ten antibonding orbitals shown in Fig. 5a involving 3*d* orbital character are completely filled. There are thus 5 primarily *d* electrons/Fe atom. In this respect then they resemble two formal Fe^{+3} ions. However, the MO occupancy is the result of our calculations and does not involve the preselection of the charge or the net spin on the Fe atoms or the specification of the number of 3*d* electrons. In fact, the total number of *d* electrons/Fe atom and the net charge on each which we calculate is quite different from the Fe^{+++} ion and resembles more closely a neutral Fe atom. This general result is shown in Table 2 and is true for all the chemical conformations studied independent of the formal charge on the Fe and ligand atoms.

Table 2. Net atomic charge and Fe valence electron density as a function of conformation

	q_{Fe}[a]	q_{sb}	q_{sc}	Z_{4s}[b]	Z_{4p_x}	Z_{4p_y}	Z_{4p_z}	$Z_{d_{x^2-y^2}}$	$Z_{d_{xy}}$	$Z_{d_{yz}}$	$Z_{d_{xz}}$	$Z_{d_{z^2}}$	$Z_t(d)$[c]	$Z_t(p)$	$Z_t(s)$
A_4	+0.10	−0.006	−0.102	0.44	0.23	0.16	0.18	1.97 (1.83)	1.18 (0.818)	0.85 (0)	0.88 (0)	1.99 (1.85)	6.87	0.57	0.44
A_5	0.14	−0.11	−0.08	0.52	0.21	0.34	0.24	1.82 (1.60)	1.01 (0.28)	1.40 (0.54)	1.40 (0.56)	0.92 (0.26)	6.65	0.79	0.52
A_1	+0.12	−0.13	−0.08	0.49	0.19	0.33	0.24	1.65 (1.36)	1.41 (0.46)	0.90 (0)	1.47 (0.98)	1.18 (0.46)	6.61	0.76	0.49
A_2	+0.02	+0.02	−0.20	0.40	0.22	0.18	0.14	1.86 (1.71)	2.00 (1.76)	1.35 (0.74)	0.57 (0)	1.15 (0.18)	7.03	0.54	0.40
Fe atm.[d]	0			2	0	0	0	1.2	1.2	1.2	1.2	1.2	6	0	2

[a] q_i = net charge on atom i.

[b] Z_i = electron density in Fe atomic orbital i.

[c] $Z_t(i)$ = total electron density in all Fe atomic orbitals of type i.

[d] Fe atom is the electron distribution in a neutral Fe atom.

Table 2 also gives the distribution of Fe valence electrons in the active site molecules for the four conformers studied. For comparison, the free atom configuration $(4s)^2(3d)^6(4p)^0$ is given with the six $3d$ electrons shown evenly distributed in the 5 degenerate d orbitals. For the lowest energy conformer A_4 each Fe has a total of 6.87($3d$) electrons, 0.57($4p$) electrons and 0.44($4s$) electrons. Thus in their bonding the Fe atoms have donated a total of 1.56($4s$) electrons to the ligands and in turn have received back 0.87($3d$) and 0.57($4p$) electrons resulting in a net forward donation of $+0.12e$ and the corresponding small positive charge on the Fe. In Table 2 is also indicated the total number of valence electrons in each Fe atomic orbital, and in parenthesis, the number of electrons in each atomic orbital involved in non-bonding orbitals. As seen, all of the $4s$ and $4p$ electron density is in bonding orbitals, since the corresponding antibonding orbitals are empty. However, the d electrons are involved in bonding to differing degrees. The strongest bonding orbitals are the d_{xz} and d_{yz} orbitals pointing more or less directly at the S ligands. These are 100% bonding. However only 7% of the $d_{x^2-y^2}$ and d_{z^2} and 31% of the d_{xy} electrons are involved. For the other conformers, we see that the net charge on each atom and in particular the distribution of the d electrons and the extent to which they are used in bonding varies even within a given symmetry type, i.e. different distorted T_D, and depends on the nature of the distortion. It is precisely the valence electron distribution together with the nature and energy of the molecular orbitals given in Figs. 3 and 5 which determine many properties of the complex such as the electric field gradient at the Fe nucleus as measured by the quadrupole splitting in Mössbauer resonance spectra of Fe^{57}. In the remainder of the paper then, we use the results just presented to calculate and discuss the magnetic moment, electric field gradient and electronic spectra of the oxidized active site for these two iron ferredoxins.

3. Magnetic Moment

It may be seen from Fig. 5 how we can explain the observed low temperature diamagnetism of the oxidized state of the two-iron ferredoxins directly from our molecular orbital results. It is simply that in the ground state configurations, the 5 lowest antibonding orbitals depicted are filled pairwise to give a diamagnetic state. As we indicated in our initial report [5], we have further confirmed this to be the lowest energy configuration by redoing the entire molecular orbital calculation for a number of biradical excited configurations in which an empty orbital is half filled by promotion of an electron from a totally paired orbital. On the other hand, for the two separate Fe^{+3} complexes which are used as the basis for the crystal field or ligand field models, there is no such natural way to obtain a totally diamagnetic state. Thus in the past [2–4] an antiferromagnetic exchange interaction has been invoked between the separated Fe^{+3} ions. However, no actual calculations of this interaction have been reported. Also, the temperature of > 100° K at which appreciable paramagnetic susceptibility has been reported [19, 20] would correspond to an abnormally large exchange energy for such coupling.

Having obtained a diamagnetic ground state configuration we wished to make further use of our molecular orbital results by calculating a value for the room temperature magnetic moment. The calculation of μ_{eff}^2 was carried out for all field independent terms, i.e. to second order. Since μ_{eff}^2 is a defined quantity given by:

$$\chi = \frac{N\beta^2}{3kT}\,\mu_{\mathrm{eff}}^2\,, \tag{1}$$

where χ is the magnetic susceptibility, the calculation must proceed through χ. Now χ is the magnetization per unit field strength, i.e.

$$\chi = M/H \tag{2}$$

and

$$\chi = \frac{M}{H} = \frac{N}{H}\cdot\frac{\sum\limits_N \mu_N e^{-E_N/kT}}{\sum\limits_N e^{-E_N/kT}}\,, \tag{3}$$

where μ_N = magnetic moment of state (N)

$$\mu_N = -\partial E/\partial H \tag{4}$$

E_N = magnetic field energy of state (N).

To second order, the field independent value of χ is:

$$\chi = \frac{N\beta^2}{3kT}\,\Sigma N\,\frac{\left|\langle N/L+2S/N\rangle^2 + 2kT\sum\limits_M \dfrac{\langle N/L+2s/M\rangle\langle M/L+2S/N\rangle}{E_M - E_N}\right| e^{-\Delta E_N/kT}}{\sum\limits_N e^{\Delta E_N/kT}}\,. \tag{5}$$

By comparing Eq. (1) and (5) we obtain a working definition of the effective magnetic moment to second order

$$\mu_{\mathrm{eff}}^2 = \mu_x^2 + \mu_y^2 + \mu_z^2 = \mu_{\mathrm{eff}}^2(1) + \mu_{\mathrm{eff}}^2(2)\,, \tag{6}$$

$$\mu_{\mathrm{eff}}^2(1) = \frac{\sum\limits_N \langle N/L+S/N\rangle^2 e^{-\Delta E_N/kT}}{\sum\limits_N e^{-\Delta E_N/kT}}\,, \tag{7}$$

$$\mu_{\mathrm{eff}}^2(2) = 2kT\sum_N\sum_M \frac{\langle N/L+2S/M\rangle\langle M/L+2S/N\rangle}{E_M^0 - E_N^0}\, e^{-\Delta E_N/kT}/\Sigma e^{-\Delta E_N/kT}\,. \tag{8}$$

$\mu_{\mathrm{eff}}^2(1)$ is the first order contribution of N electronic states to the effective magnetic moment. The sum over N is terminated when

$$\exp(-\Delta E_N^0/kT)$$

becomes negligible, i.e. $\leqq 0.01$. $\mu^2_{eff}(2)$ is the second order contribution of all states N due to their interactions with a series of states M. The sum over M is terminated when $(E^0_M - E^0_N)$ becomes large compared to the momentum interactions of the two states. χ will obey the Curie Law i.e., vary as $1/T$ only insofar as the ground state alone contributes to the magnetic moment, which is then T independent. Deviations from Curie Law behavior are then a sign that low lying excited states are contributing to the paramagnetic susceptibility. Since the angular momentum operator is a one-electron operator it can only connect configurations differing by one molecular orbital i.e. singly excited biradical states: $40 \rightarrow j$. Our calculations for the lowest energy conformer of the active site (A_4) indicate two such excited configurations might make a significant contribution to the room temperature susceptibility

$$\text{state (1)} \quad 40 \rightarrow 41 \quad \exp(-\Delta E_1/kT) = 0.23$$

$$\text{state (2)} \quad 40 \rightarrow 42 \quad \exp(-\Delta E_2/kT) = 0.05 \ ,$$

where ΔE_N in each case is the orbital promotion energy. Thus we include 3 product functions $\overline{\psi}_0, \overline{\psi}_1$, and ψ_2 in our calculations:

$$\begin{aligned} \overline{\psi}_0 &= \prod_L^{\text{val}} \cdots \phi_{40} \phi_{\bar{40}} = \cdots \phi_r \phi_s \ , \\ \overline{\psi}_1 &= \prod_L^{\text{val}} \cdots \phi_{40} \phi_{40} = \cdots \phi_r \phi_{s'} \ , \\ \psi &= \prod_L^{\text{val}} \cdots \phi_{40} \phi_{42} = \cdots \phi_r \phi_{s''} \ . \end{aligned} \tag{9}$$

Each molecular orbital is a linear combination of real atomic orbitals χ_i:

$$\phi_r = \sum_i C_{ri} \chi_i \tag{10}$$

and the molecular orbitals are ortho-normal.

Using such function for ψ_N, ϕ_r, and χ_l the first order orbital contribution to μ^2_{eff} is zero for each total state. The reason for this is as follows. For each state:

$$\langle N | L_i | N \rangle = \sum_i \sum_j C_{ri} C_{rj} \langle \chi_i | L | \chi_j \rangle + \sum_l \sum_m C_{sl} C'_{sm} \langle \chi_l | L | \chi_m \rangle \ . \tag{11}$$

Since the χ_i are real functions, they are not eigenfunctions of any component of L. Thus there will be a first order orbital contribution only if the orbital momentum operator transforms one atomic orbital into another in the same orbital. This condition is not met for any molecular orbital then

$$\langle \phi_s | L | \phi_{s'} \rangle = \langle \phi_r | L | \phi_r \rangle = 0$$

Table 3. Matrix elements of spin operators for triplet state components

$S_i M_s$ \ $S' M_s$	$\lvert 2S_z\rvert^2$				$(2S_x)^2$				$(2S_y)^2$			
	0,0	1,1	1,0	1,−1	0,0	1,1	1,0	1,−1	0,0	1,1	1,0	1,−1
0,0	0											
1,1		4					2				2	
1,0			0			2		2		2		2
1,−1				4			2				2	

and orbital angular momentum contribution is "quenched". To first order then there is only a spin contribution to μ^2_{eff} and that only from the excited biradical states, since the ground state is totally spin paired.

Each excited configuration has the same orbital function but four possible spin states; three states with $S=1$, $M_s=1,0,-1$ and a single state with $S=0$, $M_s=0$. Assuming equal weighting of the four states in the Boltzman averaging, the first order spin contribution of each configuration is a sum over four degenerate spin states q for each component of spin angular momentum S_i:

i.e. $$\langle N|2S_i|^2 N\rangle = \sum_{q',q}^{4} \langle N^q_{Sm_s}|2S_i|^2 N^{q'}_{S'm_s'}\rangle \quad i = x,y,z\,.$$

For the $4|SM_s\rangle$ states possible from a biradical configuration, the non-zero matrix elements are given in Table 3. We see from this table that the 1st order spin contribution from both excited configurations are equal:

$$\sum_i \langle\psi_1|2S_i|^2\psi_1\rangle = \sum_i \langle\psi_2|2S_i|^2\psi_2\rangle = 3(8)\,.$$

The 2nd order contributions are of the form:

$$\langle N_{SM_s}|L+2S/M_{S'M_s'}\rangle\langle M_{S'M_s'}|L+2s|N_{Sm_s'}\rangle\,, \tag{12}$$

where states N and M differ by 1 orbital function. The spin operator does not alter the orbital function and all spin operator matrix elements are of the form:

$$\langle N|2S_i|M\rangle\, S_{rr'}\, S_{ss'}\,.$$

Since the molecular orbitals are orthogonal, $S'_{ii}=0$ and the second order spin contributions vanish.

For the orbital contribution; again because of orthogonality the only non-zero terms are of the form:

$$\langle\phi_s|L_i|\phi_s'\rangle = \sum_{j,k} c_{sj}c_{s'k}\langle\chi_j|L_i|\chi_k\rangle\,. \tag{13}$$

Table 4. Contributions[a] to $\mu_{eff}^2(300)$ in oxidized state of two-iron ferredoxins

$\vert M\rangle$ $\langle N\vert$	$\langle N\vert\mu_{eff}^2\vert M\rangle$		
	0^b	1^b	2^b
0	0	0.62	0.82
1	0	5.52	0.04
2	0	−0.01	1.20

[a] Diagonal elements are 1st order contributions off-diagonal elements are 2nd order contributions.

[b] 0 = ground state contribution; 1, 2 = first and second excited state contribution.

To calculate these non-zero contributions, we make the approximation that the only significant contributions to L_t are from 3*d* atomic orbitals. Since the molecular orbitals ϕ_s which enter the calculation of magnetic moment are antibonding, nearly-pure *d* orbitals this is a reasonable simplification.

With these approximations then we have calculated the 1st and 2nd order contributions to $\mu_{eff}^2(300)$ from the ground and the first two excited state configurations. The individual terms in the numerators of Eqs. (7) and (8) are given in Table 4. To obtain μ_{eff}^2 these must be divided by

$$\sum_N \exp(-\Delta E_N^0/kT) = 1 + 4(0.23) + 4(0.05) = 2.16\,. \tag{14}$$

Then

$$\mu_{eff}^2 = [(1.44) + (5.56) + (1.19)]/2.16\,,$$

$$\mu_{eff}^2 = 8.19/2.16 = 3.78\,,$$

$$\mu_{eff} = 1.9\,BM/\mathrm{Fe}\,.$$

This result compares very favorably with Ehrenberg's measured room temperature value of 2.2 *BM*/Fe [21] and with the range of 1.3 − 2.2 *BM* which have been reported elsewhere [19–21].

Thus both the low temperature diamagnetism and the room temperature paramagnetism can be quantitatively accounted for from our calculations. It is apparent that there is no need to invoke an exchange interaction between the two irons since the interaction is a natural product of electron delocalization in the molecule. Furthermore, the calculated value of the effective magnetic moment is in impressive agreement with experiments thus additionally eliminating the necessity of considering an anomalously energetic exchange interaction.

Field Gradient Calculation

Mössbauer Resonance studies of Fe^{57} substituted plant-type ferredoxins [15, 22] have made considerable contributions to the understanding of the nature of the electron distribution about the two iron atoms. For example, recently it has been convincingly demonstrated [15] that two quadrupole doublets are present in the Mössbauer resonance spectra of the reduced ferredoxins indicating quite strongly the existence of two inequivalent iron sites in the reduced state. On the other hand, the oxidized state of seven different two-iron ferredoxins appear to have only one quadrupole split doublet and hence to have equivalent iron sites. From these experimentally derived results various explanations have been presented all within the crystal field framework. The concensus of opinion [2–4, 15] seems to favor a reduction scheme where one iron remains in the same oxidation state, ferric, while the other is reduced from ferric to ferrous. This model is proposed primarily on the basis that one of the quadrupole splittings in the reduced state has the same value as the oxidized state, a value of $\Delta E_Q \simeq +0.66$ mm/sec, while the second has a value of -2.63 mm/sec. In the crystal field format the smaller value is associated with a ferric ion and the larger value with a ferrous ion. Of course, in the molecular active site complex, it is naive to assume that any electron added will remain completely localized at one site of the molecule. Our preliminary results for one reduced site model [5], clearly show that both the added charge density and the spin density are distributed on all Fe and S atoms at the active site in agreement with observed hyperfine splitting of ESR spectra [29]. Because of the sensitivity of the electric field gradient (*efg*) to environment, as we shall indicate below, much smaller differences than gross spin or charge changes can account for large differences in electric field gradient and hence measured quadrupole splittings. It is unfortunate then that the physical data appears to corroborate in a superficial way the crystal field phenomenology which in turn is forced by the necessity of treating each iron atom separately. In any case, there has not been a calculation of the *efg* at the Fe^{57} nucleus in two-iron plant type ferredoxins. It was for these reasons then, that we chose to examine the problem from a molecular orbital viewpoint. The quadrupole Hamiltonian representing the interaction of the quadrupole moment with the electric field gradient can be written as follows:

$$\mathscr{H} = \frac{eQ}{4I(2I-1)}\{V_{zz}[3I_z^2 - I(I+1)] + (V_{xx} - V_{yy})(I_x^2 - I_y^2)\}\,, \tag{15}$$

where I is the nuclear spin vector, V_{xx}, V_{yy}, and V_{zz} are the principal axis components of the electric field gradient tensor, and Q is the quadrupole moment of the nucleus. By evaluating the matrix elements for the $I = 3/2$ state of the iron, the energy separation of the split states, ΔE_Q can be represented as

$$\Delta E_Q = \tfrac{1}{2}e^2qQ[1 + \tfrac{1}{3}n^2]^{\frac{1}{2}}\,. \tag{16}$$

Where $q = V_{zz}/e$, $nq = (V_{xx} - V_{yy}/e)$ and = Quadrupole moment of $I = 3/2$ state, and the sign convention is such that for V_{zz} positive the $M_I = \pm 1/2$ state lies lowest.

It is this splitting ΔE_Q which is directly observed in Mössbauer Resonance spectra. Neither q, nq nor Q can be measured separately. Estimates of the quadrupole moment for the excited $I = 3/2$ nuclear state of Fe^{57} are available from Mössbauer resonance of other Fe containing complexes. Our object then was to calculate values of q and nq for various conformations of the ferredoxin active site including the lowest energy conformer to determine the sensitivity of electric field gradients to conformation about the Fe and also to determine if the calculated values of q and nq from our model of the active site were consistent with the measured values of ΔE_Q from Mössbauer resonance.

Since the electric field gradient operators are both one-electron operators and hence should yield reasonable expectation values with the product form for a total state function:

Since each MO is in turn a linear combination of atomic orbitals, the expectation value of the *efg* for each state is:

$$\langle\psi_N|eqg|\psi_N\rangle = \sum_{l}^{\text{a.o.}}\left[\sum_{j,l} C_{ij}C_{il}\langle\chi_l|eqf_{\text{Fe}}|\chi_j\rangle\right] , \tag{17}$$

where we use the term *efg* to mean either the q or nq operator. The coefficients C_{ij} of each atomic orbital in each molecular orbital are known as the result of our approximate solution of the Schroedinger equation. The matrix elements with the electric field gradient at the Fe nucleus are one, two and three-centered, one-electron integrals depending on the atoms to which the X_j and X_L orbitals belong. The 2 and 3 centered integrals, the "Lattice contributions" are attenuated in two ways from the one centered integrals or valence contributions. They are multiplied by a factor of $1/R^3$ where R is the distance from the ligand atom to the Fe nucleus and also by the overlap S_{jl} of the two atomic orbitals. Thus we consider them to be negligible compared to the valence contribution.

The total values of q and nq are then assumed to be the sum of the first order valence contribution of all electronic states of the molecule within thermal range of the ground state.

$$q_{\text{total}} = \frac{\sum\limits_{N}\langle\psi_N|q|\psi_N\rangle\, e^{-\Delta E/kT}}{\sum e^{-\Delta E_N/kT}} , \tag{18}$$

$$(nq)_{\text{total}} = \frac{\sum\limits_{N}\langle\psi_N|nq|\psi_N\rangle\, e^{-\Delta E_N/kT}}{\sum\limits_{N} e^{-\Delta E_N/kT}} . \tag{19}$$

In the temperature range of 2.4–77° K for which the Mössbauer resonance spectra of the oxidized state of eight of the two-iron ferredoxins were obtained, no temperature dependence of the quadrupole splitting was observed [15]. In our lowest energy conformer, the first excited state is 0.04 eV above the ground state and $(\exp(-\Delta E/n \simeq 0.008))$. Hence, in agreement with observation, it would make a negligible contribution to the electric field gradient in the experimental temperature range. Thus we need only calculate the ground state contribution to the electric field gradients, i.e.

$$\langle\psi_0|q|\psi_0^0\rangle + \langle\psi_0|nq|\psi_0\rangle \cdot$$

Table 5. Angular part of $\langle d_J|efg|d_l\rangle$ for $efg = q, \eta q$

χ_J	χ_l	q_{Jl}	$(\eta q)_{Jl}$
d_{xy}	d_{xy}	4/7	+3/7
d_{xz}	d_{xz}	−2/7	−3/7
d_{yz}	d_{yz}	−2/7	
$d_{x^2-y^2}$	$d_{x^2-y^2}$	−4/7	
d_{z^2}	d_{z^2}	+4/7	
p_z	p_z	+4/7	
p_x	p_x	+2/5	$-3\sqrt{10}/25$
p_y	p_y	+2/5	$+3\sqrt{10}/25$
$d_{x^2-y^2}$	d_{z^2}		$2\sqrt{3}/7$

The electric field gradient is a one electron operator centered on a specific atom and can be expressed as the product of a radial and an angular function which is a spherical harmonic $Y_l^m(\theta, \phi)$

$$\langle q\rangle = \langle V_{zz}/e\rangle = -\langle 3z^2 - r^2/r^5\rangle = \langle 4\sqrt{\pi/5}\, Y_2^0(\theta,\phi)\, r^{-3}\rangle = Kq r^{-3} Y_2^0\,, \tag{20}$$

$$\begin{aligned}\langle nq\rangle &= \left\langle \frac{V_{xx}-V_{yy}}{e}\right\rangle = -\left\langle \frac{3(x^2-y^2)}{r^5}\right\rangle = -\langle 2\sqrt{6\pi/5}(Y_2^2 + Y_2^{-2})\, r^{-3}\rangle \\ &= Knq\, r^{-3}(Y_2^2 + Y_2^{-2})\,.\end{aligned} \tag{21}$$

Each atomic orbital is also the product of a radial and spherical harmonic function:

$$\chi = N_J R_J Y_J(\theta, \phi)\,. \tag{22}$$

Where N_J is a normalization constant.

Substituting expression (20), (21) and (22) into Eq. (17) for q and nq we have:

$$\begin{aligned}\langle \chi_J|q|\chi_L\rangle &= \langle R_J|r^{-3}|R_L\rangle \langle Y_J|Y_2^0|Y_L\rangle N_J N_L K_q \\ &= \langle R_J|r^{-3}|R_J\rangle q_{JL}\end{aligned} \tag{23a}$$

$$\begin{aligned}&= \langle R_J|r^{-3}|R_L\rangle \langle Y_L|Y_2^2 + Y_2^{-2}|Y_L\rangle N_J N_L K_{nq} \\ &= \langle R_J|r^{-3}|R_L\rangle (nq)_{JL}\,.\end{aligned} \tag{23b}$$

Using these expressions then we have evaluated the angular portions of the one-electron, one-centered matrix elements of both the q and nq operators with the five ($3d$) and the three ($4p$) orbitals of the Fe atom. These matrix elements q_{JL} and $(nq)_{JL}$ are given in Table 5. It is interesting to note from this table that only diagonal elements in the atomic orbital basis set q_{JJ} contribute to the value of q while for nq there is one off-diagonal element $(nq)_{JL}$ between $d_{x^2-y^2}$ and d_{z^2}. There are then two "rhombic" corrections to the electric field gradient q; inequivalent diagonal contributions $(nq)_{JJ}$ from the two pairs of atomic orbitals d_{xz} and d_{yz} and p_x and p_y which cancel in axial symmetry and the cross term contribution between $d_{x^2-y^2}$ and d_{z^2} which is zero in axial symmetry.

Substitution the angular portions q_{Jl} and nq_{Jl} of the atomic Matrix elements into Eq. (17) we obtain for the angular part of the total ground state contribution:

$$q^{\text{val}} = \langle\psi_0|q|\psi_0\rangle = \sum_J^{\text{a.o.}} Z_J q_J \tag{24}$$

Table 6. Electric field gradient as a function of geometry in oxidized two-iron ferredoxins

	A_1	A_5	A_4	A_2
q^{val}	-0.119	-0.25	$+0.151$	$+0.204$
ηq^{val}	$+0.30$	$+0.50$	$+0.064$	$+0.311$
q_r^{val}	-0.204	-0.38	$+0.151$	$+0.271$

and for nq:

$$(nq)^{\mathrm{val}} = \langle \psi_0 (nq) \psi_0 \rangle = \sum_J^{\mathrm{a.o.}} Z_J (nq)_J + 4 \sum_i C_{iJ} C_{il} (nq)_{Jl} \,, \tag{25}$$

where Z_J = total electron density in atomic orbital,
C_{ij} = coefficient of the $d_{x^2-y^2}$ orbital in molecular orbital i,
C_{il} = coefficient of d_{z^2} orbital in molecular orbital i.

Assuming r^{-3} is the same for all atomic orbitals of Fe and using the antishielding factor $(1-R)$ to correct for polarization of core electrons the total contribution can be written in the form

$$q = (1-R) \langle r^{-3} \rangle q^{\mathrm{val}} \,, \tag{26a}$$

$$nq = (1-R) \langle r^{-3} \rangle (nq)^{\mathrm{val}} \,. \tag{26b}$$

Combining (26a) and (26b) we may further define the final rhombic-corrected "electric field gradient" as:

$$q_R^{\mathrm{val}} = q^{\mathrm{val}} \left(1 + \left[\frac{(nq)^{\mathrm{val}}}{3(q)^{\mathrm{val}}} \right]^{\frac{1}{2}} \right) . \tag{27}$$

Then Eq. (16) becomes:

$$\Delta Eq (\mathrm{mm/sec}) = 9.18\, Q (\mathrm{barns}) \, (1-R) \, \langle r^{-3} \rangle \ \mathrm{a.u.}\ q_R^{\mathrm{val}} \left(\frac{esu}{cm^3} \right) \,, \tag{28}$$

where the sign of q_R^{val} is determined by the sign of q^{val} and q^{val} is positive if the $M_I = \pm 1/2$ state lies lowest. From Eqs. (24) and (25) we see that the sensitivity of the electric field gradient and hence the observed quadrupole splitting to changes in the molecular environment about the Fe nuclei will be manifest primarily as changes in the electron density Z_J in the $4p$ and $3d$ orbitals of the Fe atoms. Substituting the values of Z_J listed in Table 2, the values of q_{JJ} and $(nq)_{JL}$ listed in Table 5, and the calculated values of C_{ij}, C_{il}, into Eq. (24), (25), and (27) we have calculated the values of q^{val}, $(nq)^{\mathrm{val}}$ and q_R^{val} for the four conformers of the active site. These are given in Table 6. We see from this table that both the magnitude and sign of q^{val} and the magnitude of the $(nq)^{\mathrm{val}}$ term are quite sensitive to the systematic small changes in geometry. Hence different values of electric field gradient are not necessarily an indication of gross difference in the nature of the Fe such as change in oxidation state or spin state or even of large conformation changes. It is interesting to note that the variation in q_R^{val} is greater within the 3 tetrahedral conformers than it is between tetrahedral and square planar conformation.

We obtain a minimum value of q_R^{val} for our lowest energy conformer. For this active site geometry moreover, q^{val} is positive and the value of η itself

$$\eta = \frac{(nq)^{\mathrm{val}}}{q^{\mathrm{val}}} = \frac{V_{xx} - V_{yy}}{V_{zz}} = 0.236 .$$

In the most recent Mössbauer resonance experiments reported [15] for seven ferredoxins all values of q were found to be positive and a value of η was reported which varied among the seven proteins from (0.05 ± 0.2) to (0.5 ± 0.2). Our calculated value of $\eta = 0.236$ then is not only well within the experimental range, it is a value which fits all of the observed values for the seven compounds. To compare our value of q_R^{val} with the quantity measured experimentally ΔE_Q we can use Eq. (28). Indirect experimental estimates of Q have yielded estimates varying from 0.187–0.47 Barns [23], with the lower end of this range favored. For the value of $(1 - R) \cdot r^{-3}$ we have used 3.3 a.u. the results of the Freeman and Watson SCF calculation for Fe atom [24]. Using these values of $Q(I - R)(r^{-3})$ and our calculated value of q_R^{val} in Eq. (28) we obtain

$$\Delta E_Q = +0.91 \text{ mm/sec} .$$

This value while high is in remarkably good agreement with the experimental values of +0.61 to +0.73 (mm/sec) for the seven oxidized ferredoxins measured [15]. Hence the results of our molecular orbital calculations for a minimum energy conformer with equivalent Fe sites, gives the correct sign for ΔE_Q, corroborates its temperature independent magnitude in the range 4.2–77°, gives a value of η that agrees with all of the observed estimates, and finally gives reasonable numerical agreement with all of the measured values of ΔE_Q.

4. Optical Absorption Spectra

The optical absorption spectra of a number of two-iron ferredoxins, in particular spinach, putidaredoxin and adrenodoxin, have been obtained at low temperatures both in the oxidized and reduced state in the region of 2000–10000 Å by a number of investigators [25, 26]. More recent investigations have extended this region from 10000–25000 Å [27]. The spectra of different proteins are extremely similar and in general exhibit several poorly defined maxima even at low temperatures superimposed on a long-absorption tail. A composite spectra of the oxidized form of two of these proteins, putidaredoxin and spinach ferredoxin, from several experimental results is schematically presented in Fig. 6 in the well-studied region of 2000–10000 Å. Table 7 presents the assigned wave lengths of the absorption maxima including shoulders, with transition energies in eV and the molar extinction coefficient per Fe when experimentally available. We see from this table that the intensity of the absorption decreases gradually towards longer wave lengths from an ε of about 22000 at 2760 Å to 440 at 7000 Å. Recent work has also indicated the presence of a very weak transition at 6000 cm^{-1} [23].

Experimentally, the identification and assignment of these spectra has been quite difficult. Further insight into the nature of the electronic transitions comes

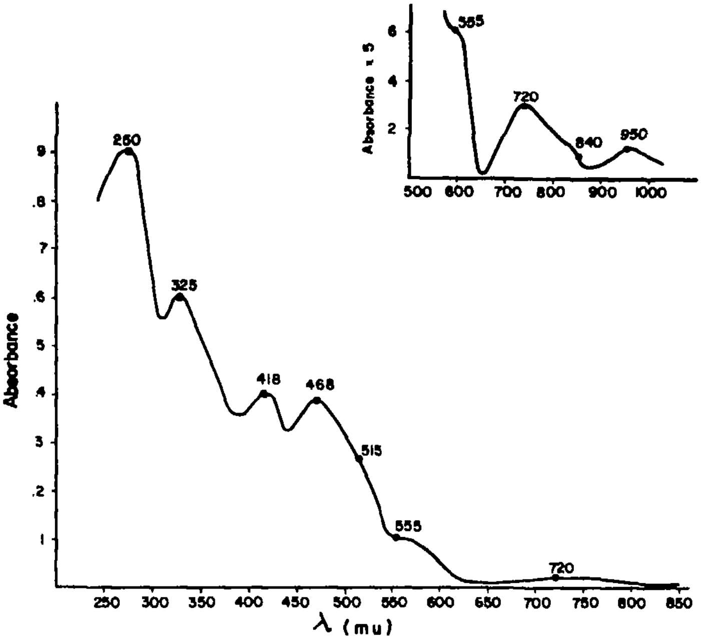

Fig. 6. Composite experimental spectra of two-iron ferredoxins in oxidized state

Table 7. Absorption maxima and shoulders of composite spectrum

λ(Å)	2760[a]	3250	4200	4680	(5150)[b]	7200	(8400)	9500
ΔE(cm^{-1})	35200	307000	25000	213000	19400	14300	12000	10800
ΔE(eV)	4.4	3.8	2.9	2.63	2.4	1.8	1.5	1.3
E mmolar/Fe	10500	7000	5160	4650	3000	440	110	120

[a] From putidaredoxin spectrum.
[b] ( ) means shoulder.

from the circular dichroism spectra of oxidized spinach and adrenodoxin [28]. The CD spectra in the region of 3000–7000 Å indicate that all the observed transitions are electric dipole allowed. Given the one-electron nature of our energy levels, i.e. the use of configuration rather than total state energies and the neglect of configuration interaction, we cannot hope for a quantitative one-to-one assignment of the spectra at this point. We reserve this task for a later study in which total state energies will be estimated. However it is possible to gain significant insight into three areas of much general interest. These are; (1) the nature of the transitions in the UV, visible, and IR; (2) a tentative identification of some observed transitions; (3) a theoretical rationale for continuous absorption of decreasing intensity from the UV to near IR. The general nature of the transitions can be seen by reference to Fig. 3. For example our results indicate that no observed transition is of the $L-L^*$ type, from a bonding to an antibonding perturbed-ligand orbital with no d character. The lowest of such transitions is 8.24 eV

(1500 Å) a higher energy than the limit of the observed UV region. Further reference to Fig. 3 shows that the entire observed spectra must be due to transitions between the closely spaced molecular orbitals 19–46, most of which contain some *d* orbital character. These are of three types in order of decreasing energy: $L \rightarrow d^*$, $d \rightarrow d^*$ and $d_i^* \rightarrow d_j^*$. The first two can be called charge transfer since they are from filled ligand bonding orbitals to empty-antibonding orbitals. Only the last type from filled to empty antibonding orbitals can be called $d \rightarrow d$ transitions where i = MO 36–40 and j = MO 41–45. Our results predict that these transitions would occur in the IR. At this point it is important to note that some $d \rightarrow d$ transitions can be electric dipole allowed since, as we have shown above, *d* orbitals participate in both *g* and *u* molecular orbitals in these binuclear D_{2h} complexes.

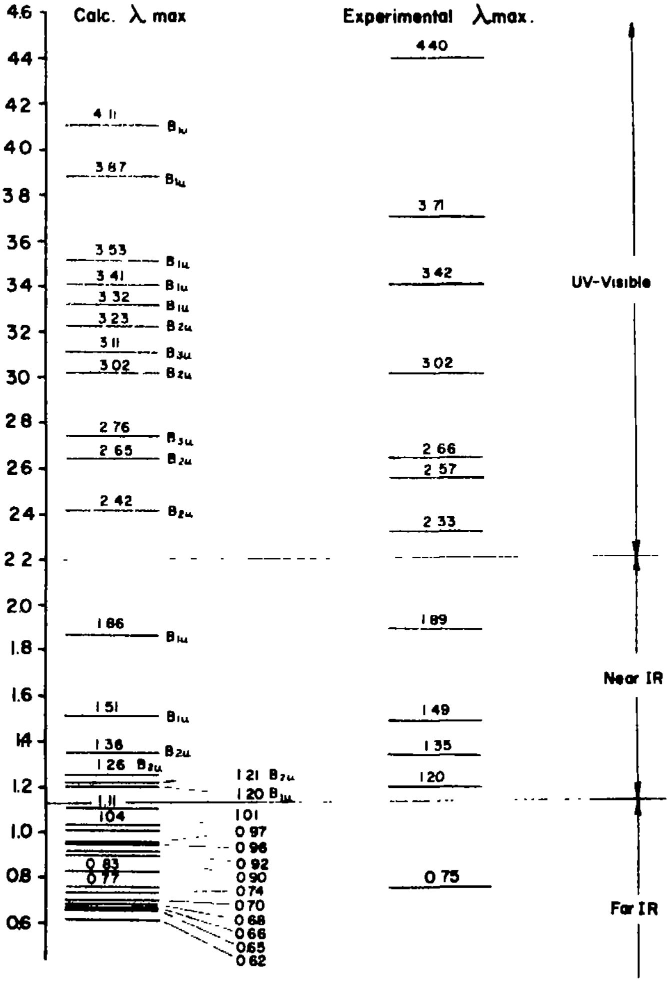

Fig. 7. Comparison of experimental and calculated values of absorption maxima for oxidized two-iron ferredoxin spectra

To further categorize and possibly assign the spectra, the symmetry-allowed electric dipole transitions were determined. The energy and symmetry of each of these are given in Fig. 7 together with the experimentally observed maxima. In Table 8a, b and c more detailed information is given for these transitions. They are divided into a) the well studied UV and visible region, b) the near IR region from 7000–10000 cm^{-1} and c) the newly explored far IR region below 10000 Å. In these tables are given along with the transition energy, the two orbitals involved in the transitions, the total symmetry of the excited state, the type of transition and the % *d*-character of the promoting orbital.

We see from Table 8a that all of the transition in the UV and visible are of the charge transfer type $L-d^*$, with about the same % *d*-character in each promoting orbital. From Fig. 7, we see that for each of the 7 observed peaks or shoulders in this region of the spectra there is a corresponding calculated value of transition energy. However there are four more symmetry allowed transitions calculated than peaks observed. These are bunched in the visible region between 3500 and 5500 Å. This density of states then can perhaps explain the almost continuous absorption and the lack of resolution of the individual transitions in this region.

Table 8a. UV-visible transitions

$(b\rightarrow d)$[a]	b[a]	ΔE	TSS[b]	Type	$f_d(L)$[c]
$(m\rightarrow 45)$	19	4.11	B_{1u}	$L\rightarrow d^*$	$0.14(x^2-y^2, z^2)$
$(m\rightarrow 45)$	21	3.87	B_{1u}	$L\rightarrow d^*$	$0.10(x^2-y^2, z^2)$
$(l\rightarrow 44)$	20	3.53	B_{1u}	$L\rightarrow d^*$	$0.12(x^2-y^2, z^2)$
$(k\rightarrow 43)$	22	3.41	B_{1u}	$L\rightarrow d^*$	$0.11(xy)$
$(l\rightarrow 44)$	23	3.32	B_{1u}	$L\rightarrow d^*$	$0.09(x^2-y^2, z^2)$
$(j\rightarrow 42)$	20	3.23	B_{2u}	$L\rightarrow d^*$	$0.12(x^2-y^2, z^2)$
$(m\rightarrow 45)$	24	3.11	B_{3u}	$L\rightarrow d^*$	$0.09(xz)$
$(j\rightarrow 42)$	23	3.02	B_{2u}	$L\rightarrow d^*$	$0.09(x^2-y^2, z^2)$
$(l\rightarrow 44)$	25	2.76	B_{3u}	$L\rightarrow d^*$	$0.07(xz)$
$(k\rightarrow 43)$	24	2.65	B_{2u}	$L\rightarrow d^*$	$0.09(xz)$
$(i\rightarrow 41)$	25	2.42	B_{2u}	$L\rightarrow d^*$	$0.07(xz)$

[a] b = promoting orbital, d = excited orbital.

[b] TSS = Total state symmetry.

[c] $f_d(L)$ = d electron density in the lower energy orbital.

Table 8b. Near IR transitions

$(b\rightarrow d)$	b	ΔE	TSS[a]	Type	$f_d(L)$
$(m\rightarrow 45)$	27	1.86	B_{1u}	$d\rightarrow d^*$	$0.29(x^2-y^2, z^2)$
$(l\rightarrow 44)$	26	1.51	B_{1u}	$d\rightarrow d^*$	$0.31(x^2-y^2, z^2)$
$(m\rightarrow 45)$	32	1.36	B_{2u}	$d_i^*\rightarrow d_j^*$	$0.41(yz)$
$(l\rightarrow 44)$	30	1.26	B_{3u}	$d_i^*\rightarrow d_j^*$	$0.45(xz)$
$(j\rightarrow 42)$	26	1.21	B_{2u}	$d\rightarrow d^*$	$0.31(x^2-y^2, z^2)$
$(k\rightarrow 43)$	29	1.20	B_{1u}	$d\rightarrow d^*$	$0.26(xy)$

[a] TSS = Total state symmetry.

Table 8c. Far IR

$(b \rightarrow d)$[a]	b	ΔE	TSS[b]	Type	$f_d(L)$[c]
$(m \rightarrow 45)$	34	1.11	B_{3u}	$d_i^* \rightarrow d_j^*$	$0.40(xz)$
$(l \rightarrow 44)$	31	1.04	B_{2u}	$d_i^* \rightarrow d_j^*$	$0.47(yz)$
$(j \rightarrow 42)$	28	1.01	B_{3u}	$d \rightarrow d^*$	$0.29(xy)$
$(i \rightarrow 41)$	28	0.97	B_{1u}	$d \rightarrow d^*$	$0.29(xy)$
$(l \rightarrow 44)$	33	0.96	B_{2u}	$d \rightarrow d^*$	$0.10(yz)$
$(i \rightarrow 41)$	30	0.92	B_{2u}	$d_i^* \rightarrow d_j^*$	$0.44(xz)$
$(k \rightarrow 43)$	32	0.90	B_{3u}	$d_i^* \rightarrow d_j^*$	$0.41(yz)$
$(m \rightarrow 45)$	36	0.83	B_{1u}	$d_i^* \rightarrow d_j^*$	$0.86(x^2-y^2, z^2)$
$(m \rightarrow 45)$	39	0.77	B_{1u}	$d_i^* \rightarrow d_j^*$	$0.89(x^2-y^2, z^2)$
$(j \rightarrow 44)$	31	0.74	B_{1u}	$d_i^* \rightarrow d_j^*$	$0.47(yz)$
$(i \rightarrow 41)$	31	0.70	B_{3u}	$d_i^* \rightarrow d_j^*$	$0.47(yz)$

[a] b = promoting orbital, d = excited orbital.

[b] State TSS = Total state symmetry.

[c] f_d = Coefficient of d atomic orbital in molecular orbital b.

From Table 8b we see that the assignment in the near IR region below 7000 Å are characterized in our calculation by a significant increase in d character of the promoting orbital so that we can label most of the transitions in the near IR region $d \rightarrow d^*$ charge transfer transitions. In this region from 1.86–1.20 there is an almost 1 for 1 assignment of observed and calculated absorption maxima and shoulders possible. Three different excited states are almost superimposed at 10000 Å, and three other calculated transitions correspond almost exactly to the other three higher energy transitions.

Below 10000 Å we see from Table 8c and from Fig. 7 that there are a large number of closely spaced, symmetry-permitted transitions. All but 3 of these 11 states are $d_i^* \rightarrow d_j^*$ transitions from filled to empty antibonding d orbitals. There is then another marked increase in the % d character in the promoting orbital in going from the near to far IR. While the experimental results are not yet definitive it appears that there is only one observed transition in this region at about 0.75 eV. Having indicated the nature of the UV, visible, and the transitions, and examined some of the specific maxima involved, we turn to a discussion of the relative absorption intensities observed in the different wave length regions.

Transition moments, are often assumed to be proportional to the overlap of the atomic orbitals in the two molecular orbitals involved in the transition. Since the two Fe atoms are fairly far apart in this model, the overlap of the two centered d orbitals is very small i.e. $\langle d_i | d_j' \rangle = 0.04$ while the one-centered 3d overlaps are exactly zero. Thus while $d_i^* \rightarrow d_j^*$ transitions are not strictly symmetry forbidden, they are likely to be very weak. With this reasoning then, since then overlap of orbitals between the Fe and S ligands is much greater than on the two Fe atoms, and since all the excited orbitals are antibonding primarily d orbitals, the more ligand character in the promoting orbitals i.e. the greater the intensity would be, i.e. $I(L \rightarrow d_i^*)\, I(d \rightarrow d^*)\, I(d_i^* \rightarrow d_j^*)$. The elimination of the $L \rightarrow L^*$ transition by energy consideration explains the lower observed intensity of the UV spectra for ferredoxins than for one iron complexes such as hemes, and at the same time explains why the UV and visible transitions which are all of the $L \rightarrow d^*$

type with very little d character in the bonding orbitals are the most intense in this protein. We would also predict a sharp decrease in intensity between the transition at 2.42 eV (about 5100 Å) and the one at 1.86 eV (7200 Å) and in general between the invisible and IR spectra which are mainly $d \rightarrow d^*$. This result is in agreement with the observed order of magnitude decrease in intensity indicated in Table 7. If the intensity is decreased another order of magnitude or more by the increase in d character in the antibonding over the bonding d orbitals i.e. in $d_i^* \rightarrow d_j^*$ over $d_i \rightarrow d^*$ it is then understandable why no measurable for IR absorption is obtained. The exception would be the $L \rightarrow d^*$ transition at 0.96 eV. This then may correspond to the one observed transition maximum at 6000 cm^{-1} seen in this region [23].

To summarize then, our one-electron approximation to the assignment of the optical spectra of the oxidized ferredoxins, we have tentatively identified the type of absorptions involved in the UV, visible, near IR and far IR regions, accounted for their diminishing intensity and for the regions of continuous absorption. We have also made some actual numerical correspondence between calculated and observed transition maxima. Further elucidation of these spectra await our two-electron and configuration-interaction corrections and a more quantitative estimate of relative oscillator strengths of the different allowed transitions.

Acknowledgement. The authors wish to gratefully acknowledge sponsorship of NSF Grant GB 17980.

Bibliography

1. Tsibris, J. C. M., Woody, R. W.: Coordin. chem. Rev. **5**, 417 (1970).
2. Brintzinger, H., Palmer, C., Sands, R. H.: Biochem. **55**, 397 (1966).
3. Gibson, J. F., Hall, D. O., Thornley, T. H. M., Whatley, F. R.: Proc. nat. Acad. Sci. USA **56**, 987 (1966).
4. Thornley, J. H. M., Gibson, J. F., Whatley, F. R., Hall, D. O.: Biochem. biophysic. Res. Commun. **24**, 877 (1966).
5. Loew, G., Steinberg, D.: Theoret. chim. Acta (Berl.) **23**, 239 (1971).
6. Rein, R., Fukuda, N., Win, H., Clarke, G. A., Harris, F. E.: J. chem. Physics **45**, 4743 (1966).
7. Zerner, M., Gouterman, M.: Theoret. chim. Acta (Berl.) **4**, 44 (1966).

8a. Hoffman, R.: J. chem. Physics **39**, 1397 (1963).

8b. -- J. chem. Physics **40**, 2480 (1964).

9. Hoyland, J. R.: Semiemperical MO theories: A critique and a review of progress.
10. Zerner, M., Gouterman, M., Kobayashi, H.: Theoret. chim. Acta (Berl.) **6**, 363 (1966).
11. Pullman, A., Pullman, B.: Progress in Nucleic Acid Research and Molecular Biology **9**, 327 (1969).
12. Wolfberg, M., Helmholtz, L.: J. chem. Physics **20**, 837 (1952).

13a. Pan, D. C., Allen, L. C.: J. chem. Physics **46**, 1797 (1967).

13b. Allen, L. C., Russell, J. D.: J. chem. Physics **46**, 1029 (1967).

14. Loew, Gilda: Theoret. chim. Acta (Berl.) **20**, 203 (1971).
15. Bearden, A. J., Dunham, W. R.: Structure and Bonding **8**, 1 (1970).
16. Ballhausen, C. J.: Introduction to ligand field theory. San Francisco: McGraw-Hill 1970.

17a. Harris, G.: Theoret. chim. Acta (Berl.) **10**, 119 (1968).

17b. Harris-Loew, G.: Theoret. chim. Acta (Berl.) **17**, 18 (1970).

18. Gouterman, M.: J. molecular Spectroscopy **6**, 138 (1961).
19. Palmer, G.: Private communication, Sept. 1970.
20. Moss, T. H., Petering, D., Palmer, G.: J. biol. Chemistry **244**, 2275 (1969).
21. Ehrenberg, A.: Private communication, Aug. 1966.
22. Johnson, B. D., Bray, R. C., Commeda, R., Hall, D. O.: Proc. nat. Acad. Sci. USA **63**, 1234 (1969).
23. Harris, G. M., Weissbluth, M.: Physic. Rev. **149**, 198 (1966).
24. Freeman, A. J., Watson, R. E.: Physic. Rev. **131**, 2566 (1963).
25. Woody, R. W., Tsibris, J. C. M., Gunsalus, I. C.: Private communication.

26. Wilson, D. F.: Arch. Biochem. Biophysics **122**, 254 (1967).
27a. Palmer, G.: Private communication, Jan. 1971.
27b. Eaton, W.: Private communication, June 1971.
28. Palmer, G., Brintzinger, H., Estabrook, R. W.: Biochem. **6**, 1658 (1967).
29. Orme-Johnson, W. H., Beinert, H.: Ann. New York Acad. Sci. **158**, 336 (1968).

Dr. G. H. Loew
Departments of Genetics
Stanford University Medical Center
Stanford, California 94304, USA

Theoret. chim. Acta (Berl.) 26, 131–140 (1972)
© by Springer-Verlag 1972

The Use of the CNDO Method in Spectroscopy

VI. Further $n-\pi^*$ Transitions*

R. L. Ellis**, G. Kuehnlenz, and H. H. Jaffé
Department of Chemistry, University of Cincinnati, Cincinnati, Ohio 45221, USA

Received November 11, 1971 / February 21, 1972

The Pariser approximation for the two center Coulomb repulsion integrals Γ_{rs} has been replaced by the Nishimoto-Mataga approximation in the original CNDO/S method. This modification has significantly improved the calculated position of the benzene ${}^1B_{1u} \leftarrow {}^1A_{1g}({}^1L_a)$ electronic transition in benzenoid compounds. The calculation of transition moments of $n-\pi^*$ transitions is also considered. These moments vanish formally in any theory employing the ZDO approximation since integrals of the form $\langle 2s|er|2p\rangle$ vanish even when the $2s$ and $2p$ atomic orbitals are on the same center. In this work the ZDO approximation is abandoned in the evaluation of the electronic transition moment resulting in calculated intensities for $n-\pi^*$, ${}^1W \leftarrow {}^1A$, transitions which are in good agreement with experiment.

Die Näherung für die Zweizentrencoulombintegrale nach Pariser in der ursprünglichen Form des CNDO/S-Verfahrens wurde durch die von Nishimoto-Mataga ersetzt, wodurch sich der ${}^1B_{1u} \leftarrow {}^1A_{1g}({}^1L_a)$-Übergang in benzoiden Verbindungen besser ergibt. Die $n-\pi^*$-Übergangsmomente, die bei ZDO-Annahme immer verschwinden, weil dann $\langle 2s|er|2p\rangle$ auch für an gleichen Zentren liegende Orbitale Null ist, werden hier berechnet, und zwar für den ${}^1W \leftarrow {}^1A$-Übergang, wobei die Übereinstimmung mit dem Experiment befriedigend ausfällt.

Introduction

In previous papers [1], a modified CNDO method (CNDO/S) has been developed and used to calculate the electronic spectra of a large number of unsaturated hydrocarbons and heterocycles. It was observed, however, that the ${}^1L_a$ (analogous to the benzene ${}^1B_{1u} \leftarrow {}^1A_{1g}$ transition) bands in benzenoid compounds were regularly calculated at an energy 0.8–1.0 eV too low. We have reinvestigated this problem and have found that this discrepancy is largely eliminated by the introduction of the Nishimoto-Mataga approximation [2] to the Coulomb repulsion integrals.

In the original calculations [1], the oscillator strengths [3] for $\pi-\pi^*$ transitions were in good agreement with experiment. However, use of the ZDO approximation makes the electronic transition moments for $n-\pi^*$ transitions formally zero. In the present work, we relax the ZDO approximation by retaining one center integral of the form $\langle 2s|er|2p\rangle$ in the transition moment calculation. These integrals are analogous to those retained by Pople in the calculation of ground state dipole moments [4].

---

* Supported in part by NSF Grant No. GP 15944.

** Procter and Gamble Research 1969–70; Ethyl Corporation Research Fellow 1970–71.

Parameterization

In the original CNDO/S method, the Coulomb repulsion integrals Γ_{rs} between two centers r and s were approximated according to the original suggestions of Pariser [5]. This approximation has been replaced by the one proposed by Nishimoto and Mataga [2]. If R_{rs} (in atomic units) is the distance between atoms r and s, Γ_{rs} (in atomic units) is given by

$$\Gamma_{rs} = [R_{rs} + 2/(\Gamma_{rr} + \Gamma_{ss})]^{-1} ,$$

where Γ_{rr} are the one-center repulsion integrals obtained from the ionization potentials and electron affinities, as used in our earlier work [1].

The basis set used in these calculations is a set of 2*s* and 2*p* Slater atomic orbitals centered on each second row atom and a 1*s* Slater orbital on each hydrogen atom. The Slater exponents, core integrals, and repulsion integrals used in this calculation are given in Table 1. The ionization potentials and electron affinities used to calculate the core integrals and electron repulsion integrals are those given by Hinze and Jaffé [6]. In the original work [1], the valence states of the various atoms were chosen such that they would be one electron π donors in the molecule. Since this choice is rather restrictive, we have, in the present work, chosen the valence state of carbon as $2s^1\,2p^3$, of nitrogen as $2s^2\,2p^3$ and oxygen as $2s^2\,2p^4$. Such a choice of valence states is much more general than a choice which should be restricted to molecules with π electronic systems. The actual differences between the core integrals and repulsion integrals used in this work and in the original work are quite small and do not significantly affect the calculated spectral properties. Also included in Table 1 are the values of β_r^0 which are the same as previously used, except that β_c^0 has been changed from -17.0 eV to -17.5 eV; the latter value gives, in general, slightly better results. The parameter κ, introduced in previous work, has been retained unchanged. Since some misunderstanding about its significance and its use appears to have arisen in the literature, it is worthwhile to reiterate the nature of the approximation made. The core matrix element $H_{\mu\nu}$ between orbitals μ and ν on centers r and s respectively, is taken proportional to the total overlap between them. However, the overlap between two orbitals μ and ν is evaluated as a sum of two components. One component arises from projection of orbitals μ and ν onto the bond axis, and hence is a σ component, $S_{\mu\nu}^{\sigma}$. The other part arises from the projections of μ and ν normal to the bond axis, and is a π component of overlap, $S_{\mu\nu}^{\pi}$. The element $H_{\mu\nu}$ is then obtained by

$$H_{\mu\nu} = (1/2)\,(\beta_r^0 + \beta_s^0)\,(S_{\mu\nu} + \kappa S_{\mu\nu}^{\pi}) .$$

Table 1. Parameters used in CNDO/S method[a]

Atom		H	C	N	O
Slater exponents		1.2	1.625	1.95	2.275
Core integral	s	14.35	29.92	40.97	54.51
	p	—	11.61	16.96	21.93
Repulsion integral, Γ_{rr}		12.85	10.93	11.88	15.13
β_r^0		-12.0	-17.5	-26.0	-45.0

[a] The core integrals, repulsion integral, and β_r^0 are given in units of eV.

As a consequence of this formulation, $H_{\mu\nu}$ is truly invariant to rotation of the coordinate system.

Calculation of Electronic Transition Moments

The oscillator strength (f) of a transition between two, non-degenerate, electronic states of a molecule is given by

$$f(k, 1) = (8\pi^2 mc\nu(k, 1)/3he^2)\,[\boldsymbol{M}^*(k, 1) \cdot \boldsymbol{M}(k, 1)]\ , \tag{1}$$

where $\boldsymbol{M}$ is the transition dipole moment, m and e are the mass and charge of an electron, and ν is the frequency of the transition. The transition moment of an electronic transition in the dipole approximation, expressed in terms of the wavefunction of the initial and final states is

$$\boldsymbol{M}(k, 1) = \int \Psi_k^* \sum_p e\boldsymbol{r}_p \Psi_1\, d\boldsymbol{r} \equiv \left\langle \Psi_k \middle| \sum_p e\boldsymbol{r}_p \middle| \Psi_1 \right\rangle\ , \tag{2}$$

where Ψ_1 and Ψ_k are, respectively, the wavefunctions of the initial and final state, $\boldsymbol{r}_p$ is the position vector of the p'th electron and the summation extends over all electrons. In principle, if the wavefunctions of the two states involved in the transition are known, $\boldsymbol{M}$ may be obtained by direct evaluation of Eq. (2).

Within the framework of the CNDO/S method the wavefunction of the ground state is given by a single Slater determinant, and the excited state wavefunction is a linear combination of spin configurations [1]. The transition moment, $\boldsymbol{M}(k, 0)$, can be written, in a general LCAO approximation, as:

$$\begin{aligned}\boldsymbol{M}(k, 0) = \sqrt{2} \sum_S \sum_\mu^{(S)} C_{ak}^* c_{\mu i} \Big\{ & c_{\mu j'}^* \langle \varphi_\mu | e\boldsymbol{r} | \varphi_\mu \rangle + \sum_{\nu \neq \mu}^{(S)} c_{\nu j'}^* \langle \varphi_\nu | e\boldsymbol{r} | \varphi_\mu \rangle \\ & + \sum_{T \neq S} \sum_\lambda^{(T)} c_{\lambda j'}^* \langle \varphi_\lambda | e\boldsymbol{r} | \varphi_\mu \rangle \Big\}\ ,\end{aligned} \tag{3}$$

where the C_{ak}^* are the coefficients of the various spin configurations in the excited state, μ and ν are atomic orbitals on center S and the λ are atomic orbitals on center T.

The strict application of the ZDO approximation to Eq. (3) requires that the integrals in the second and third terms vanish. This leaves only the first term to contribute to $\boldsymbol{M}(k, 0)$. At this level of approximation the transition moment for both $\sigma - \pi^*$ and $n - \pi^*$ transitions is identically zero since the product $c_{\mu i} c_{\mu j}$ is always zero for such transitions.

In the present work we shall abandon the ZDO approximation, and retain the first two integrals on the rhs of Eq. (3) in the calculation of the transition moment.

We shall evaluate the first integral on the rhs of Eq. (3) in the manner first suggested by Mulliken and used by us in previous work [1]. The second integral on the rhs of Eq. (3) may be evaluated analytically using Slater orbitals. This integral vanishes except in the case when one of the atomic orbitals is an s orbital and the other is a p orbital. In terms of $2s$ and $2p$ Slater orbitals, this integral is

$$\langle \varphi_s | e r_x | \varphi_{p_x} \rangle = \langle \varphi_s | e r_y | \varphi_{p_y} \rangle = \langle \varphi_s | e r_z | \varphi_{p_z} \rangle = 5ea_0/2\zeta\sqrt{3}\ , \tag{4}$$

where ζ is the orbital exponent of the $2s$ and $2p$ electrons on center S. In Eq. (5) r_x, r_y and r_z are the three cartesian components of the position vector, $\boldsymbol{r}$, of the electron. All other integrals similar to those given in Eq. (8), such as $\langle \varphi_s | er_x | \varphi_{p_y} \rangle$ vanish.

The x component of the transition moment M of Eq. (7) may now in general be written as

$$M^x(k,0) = \sqrt{2} \sum_{aS} \sum_{\mu}^{(S)} C_{ak} c_{\mu i} \left\{ c^*_{\mu j'} X_S e + \sum_{\nu \neq \mu}^{(S)} \Lambda_{sp_x} c^*_{\mu j'} (5ea_0/2\zeta_S \sqrt{3}) \right\} , \qquad (5)$$

where X_s is the x coordinate of atom S, and

$$\Lambda_{sp_x} = \begin{cases} 1 & \mu = \varphi_s, \quad \nu = \varphi_{p_x} \quad \text{or} \quad \mu = \varphi_{p_x}, \quad \nu = \varphi_s \\ 0 & \text{all other} \quad \mu, \nu . \end{cases}$$

The expression for the y and z components of the transition moment are analogous to the expression for the x component, X_S being replaced by Y_S or Z_S and Δ_{sp_x} being replaced by Δ_{sp_y} or Δ_{sp_z} depending on the component being computed. Once the three components of the transition moment vector have been calculated, the entire vector M needed in the evaluation of Eq. (1) is obviously

$$M(k,0) = M^x i + M^y j + M^z k .$$

As has been stated above the first term of Eq. (5) vanishes for all transitions of $n - \pi^*$ and $\sigma - \pi^*$ type. The second term vanishes if the transition is forbidden by molecular symmetry. However, this term also vanishes in the case where the state, ${}^1\Psi_k$, is composed entirely of configurations in which the molecular orbital ψ_l is made up of only p atomic orbitals. Platt considers a transition of this type to be forbidden by local symmetry and gives it the notation ${}^1U \leftarrow {}^1A$. The $n - \pi^*$ transitions allowed by local symmetry are symbolized as ${}^1W \leftarrow {}^1A$.

Results and Discussion

Benzene

The ultraviolet spectrum of benzene shows three distinct transitions:

$${}^1B_{2u} \leftarrow {}^1A_{1g}, \ {}^1B_{1u} \leftarrow {}^1A_{1g}, \ {}^1E_{2u} \leftarrow {}^1A_{1g} .$$

In Platt notation [9], these transitions are termed ${}^1L_b$, ${}^1L_a$, ${}^1B$, respectively, and we shall use both the symmetry and Platt notations in this work. Although the original CNDO/S calculations for the first and third transitions were in good agreement with experiment, the ${}^1L_a$ transition was calculated to be at 5.2 eV, compared to an observed value of 6.1 eV.

The inability to properly calculate the energy of this transition has also been observed in PPP calculations whenever the Pariser approximation to Γ_{rs} is used. As we have pointed out [3], the PPP method is a special case of the more general CNDO method; and it is not unexpected that problems arising in one method should also arise in the other. As in the case of PPP calculations, the replacement of the Pariser Γ_{rs} with the Mataga approximation in the CNDO/S significantly improves the calculated position of the ${}^1L_a$ transition, which now is calculated at 6.0 eV. The three benzene transitions given are the lowest three singlet-singlet transitions calculated by the CNDO/S method; i.e., there are no transitions involving $\sigma - \pi^*$ or $\pi - \sigma^*$ states in the region below 6.6 eV.

According to a recent report by Hirota and Nagakura [8], the extension of the configuration interaction calculation to doubly excited configurations in the framework of the PPP method, using the Pariser Γ_{rs} has greatly impoved the energies predicted of ^1L_a transition in benzoid compounds. On the basis of their results, we should expect that the proper inclusion of doubly excited configurations into our original CNDO/S program should lead to similar results.

Pyridine and the Picolines

The electronic spectra of pyridine [9] and the picolines [10, 11] have been the subject of much experimental work over the past two decades. The most logical approach to discussing the spectra of these compounds is first to treat the $\pi-\pi^*$ transition with respect to their relation to benzene, and then discuss the two types of $n-\pi^*$ transitions which appear in the spectra.

The calculated and experimental transition energies and oscillator strength are given in Table 2. In each of the spectra there are four calculated transitions of $\pi-\pi^*$ types in the spectral region above 150 nm. The two lowest energy transitions correspond to the ^1L_b and ^1L_a benzene transitions. Whereas these two

Table 2. The calculated and experimental transition, $\Psi_n \leftarrow \Psi_0$, of pyridine and the picolines[g]

Compound	Type	Symmetry[a]		Energy above ground state (eV)[b]		f[c]	
				cal.	obs.	cal.	obs.
Pyridine[d]	$n-\pi^*$	$^1B_1$	(^1W)	4.2	4.3	0.00	0.003
	$\pi-\pi^*$	$^1B_2$	(^1L_b)	4.9	4.7	0.06	0.030
	$n-\pi^*$	$^1A_2$	(^1W)	5.6	NR	0.0	
	$\pi-\pi^*$	$^1A_1$	(^1L_a)	6.0	6.2	0.22	0.200
	$\pi-\pi^*$	$^1A_1$; $^1B_2$	(^1B)	6.8 (2)	7.0	0.76	1.30
α-Picoline[e,f]	$n-\pi^*$	$^1A''$	(^1W)	4.4	4.3	0.003	0.0019
	$\pi-\pi^*$	$^1A'$	(^1L_b)	4.9	4.6	0.09	0.047
	$n-\pi^*$	$^1A''$	(^1W)	5.4	NR	0.0	
	$\pi-\pi^*$	$^1A'$	(^1L_a)	5.9	NR	0.25	
	$\pi-\pi^*$	$^1A'$; $^1A'$	(^1B)	6.9 (2)	NR	0.79	
β-Picoline[e,f]	$n-\pi^*$	$^1A''$	(^1W)	4.0	4.3	0.003	0.0029
	$\pi-\pi^*$	$^1A'$	(^1L_b)	4.8	4.6	0.080	0.045
	$n-\pi^*$	$^1A''$	(^1W)	5.4	4.4	0.0	W
	$\pi-\pi^*$	$^1A'$	(^1L_a)	5.8	NR	0.204	
	$\pi-\pi^*$	$^1A'$	(^1B)	6.7	NR	0.560	
		$^1A'$		6.9	NR	0.668	
γ-Picoline[e,f]	$n-\pi^*$	$^1A''$	(^1W)	4.3	4.3	0.003	0.0023
	$\pi-\pi^*$	$^1A'$	(^1L_b)	5.0	4.7	0.040	0.032
	$n-\pi^*$	$^1A''$	(^1W)	5.3	NR	0.0	
	$\pi-\pi^*$	$^1A'$	(^1L_a)	6.0	NR	0.108	
	$\pi-\pi^*$	$^1A'$; $^1A'$	(^1B)	6.5 (2)	NR	0.762	

[a] Two symmetries appearing on the same line refer to accidentally degenerate states.

[b] NR, not reported.

[c] W, weak; m, medium; s, strong.

[d] Ref. [9].

[e] Ref. [10].

[f] Ref. [11].

[g] The coordinate system used for the symmetry designations is the same as in Ref. [12].

transitions are symmetry forbidden in benzene, the reduction of molecular symmetry in pyridine and the picolines make these transitions allowed. The calculated values for the transition energies and oscillator strength for ^1L_b band in all four compounds is in good agreement with experiment. Unfortunately, experimental information for the ^1L_a band is available for only pyridine. In this case, the calculated and experimental results are in good agreement.

The highest energy pair of transitions correspond to the two components of the degenerate benzene ^1B transition. In pyridine, α-picoline, and β-picoline, the two components remain degenerate to within the limit to the calculated transition energies. In γ-picoline, the calculations indicate the two components are split by an energy of about 0.2 eV. Experimental transition energies and oscillator strengths are again available for these transitions only in pyridine, and the calculated and experimental results are in good agreement.

The $n-\pi^*$ transitions in pyridine and the three isomeric picolines, all ^1W, can be divided into two groups, in Platt orbital notation [9] $n \rightarrow g$ and $n \rightarrow h$. In order to classify these transitions by symmetry, we consider the methyl group, which probably rotates freely as a pseudoatom; then the $n \rightarrow g$ transitions become $^1B_1 \leftarrow {}^1A_1$ in pyridine and α-picoline, $^1A'' \leftarrow {}^1A'$ in α- and β-picoline, all allowed by molecular symmetry. These, as expected, are the lowest wavelength transitions and are calculated in good agreement with experiment (cf. Table 2). The calculated oscillator strengths, which arise from the non-zero nature of the second term in Eq. (7), are also in good agreement with experiment.

In addition, $n \rightarrow h$ transitions are calculated in all four compounds. They have $^1A_2 \leftarrow {}^1A_1$ symmetry in pyridine and α-picoline, but $^1A'' \leftarrow {}^1A'$ in the α- and β-isomers; consequently, they are forbidden in the first two molecules by molecular symmetry, but allowed in the latter two. These transitions are predicted to occur near 5.5 eV in all four compounds (cf. Table 2). The only suggestion of an observation of this type of transition is due to Sponer and Rush [10] who suggest that they have seen such a transition and have tentatively assigned the 0–0 band to be at 4.4 eV. Since their work, no further work on this band seems to have been reported.

The Diazines: Pyrazine, Pyrimidine, and Pyridazine

The spectra of the three isomeric diazines in the region above 150 nm have received considerable attention. Much of the experimental work has recently been reviewed by Innes [12]. The results of the present calculations along with the experimental result are summarized in Table 3.

Theory suggests that there are two electronic transitions of an $n-\pi^*$ type lying to the long wavelength side of the ^1L_b band in the diazines. Both transitions are $^1W \leftarrow {}^1A$, but one is symmetry allowed while the other is symmetry forbidden in all three compounds. There exists some question in the experimental literature regarding the positions of the 0–0 band for these two transitions. Innes [13] has shown that the two bands chosen by Ito and co-workers [14] in pyrazine were in fact due to the same electronic transition. El-Sayed and Robinson [15], in a low temperature study of the long wavelength region of the diazine spectra, report the observation of both types of $n-\pi^*$ transitions in all three diazines. These authors

Table 3. The calculated and experimental ${}^1\Psi_n \leftarrow {}^1\Psi_0$ transition in pyrazine, pyrimidine, and pyridazine[d]

Compound	Type	Symmetry	Energy above ground state (eV)[a]		f[c]	
			cal.	obs.	cal.	obs.
Pyrazine[b]	$n-\pi^*$	${}^1B_{3u}$ $({}^1W)$	3.2	3.8	0.006	0.010
	$n-\pi^*$	${}^1B_{2g}$ $({}^1W)$	4.5	3.7	0.0	W
	$\pi-\pi^*$	${}^1B_{2u}$ $({}^1L_b)$	4.8	4.8	0.16	0.100
	$n-\pi^*$	${}^1A_u$ $({}^1W)$	5.2	NR	0.0	
	$\pi-\pi^*$	${}^1B_{1u}$ $({}^1L_a)$	6.3	6.3 6.9	0.12	0.145
	$\pi-\pi^*$	${}^1B_{1u}$ $({}^1B)$	7.2	7.5	0.48	1.000
	$n-\pi^*$	${}^1A_u$ $({}^1W)$	7.2	NR	0.0	
	$\pi-\pi^*$	${}^1B_{2u}$ $({}^1B)$	7.5	7.5	0.97	1.000
Pyrimidine[b]	$n-\pi^*$	${}^1B_1$ $({}^1W)$	4.2	3.9	0.012	0.0069
	$n-\pi^*$	${}^1A_2$ $({}^1W)$	4.6	3.8	0.0	W
	$\pi-\pi^*$	${}^1B_2$ $({}^1L_b)$	5.1	5.0	0.07	0.020
	$n-\pi^*$	${}^1A_2$ $({}^1W)$	5.6	NR	0.0	
	$\pi-\pi^*$	${}^1A_1$ $({}^1L_a)$	6.1	6.5	0.11	0.100
	$n-\pi^*$	${}^1B_1$ $({}^1W)$	6.4	6.4	0.005	0.005
	$n-\pi^*$	${}^1A_2$ $({}^1W)$	7.0	NR	0.0	
	π-Rydberg			7.0		
	$\pi-\pi^*$	${}^1B_2$ ${}^1A_1$ $({}^1B)$	7.1 7.1	7.3 7.2	0.62 0.63	1.000
Pyridazine[b]	$n-\pi^*$	${}^1B_1$ $({}^1W)$	3.3	3.3	0.008	0.0058
	$n-\pi^*$	${}^1A_2$ $({}^1W)$	4.4	2.3	0.0	W
	$\pi-\pi^*$	${}^1B_2$ $({}^1L_b)$	5.1	4.9	0.05	0.030
	$n-\pi^*$	${}^1A_2$ $({}^1W)$	5.6	NR	0.0	
	$\pi-\pi^*$	${}^1A_1$ $({}^1L_a)$	6.1	6.2	0.11	0.200
	$n-\pi^*$	${}^1B_1$ $({}^1W)$	6.2	6.4	0.005	W
	$\pi-\pi^*$	${}^1B_2$ ${}^1A_1$ $({}^1B)$	6.9	7.1	0.69 0.61	1.300

[a] NR, not reported.
[b] Ref. [12].
[c] W, weak.
[d] The coordinate system used for the symmetry designations is the same as in Ref. [12].

have also calculated the expected separation between the two excited singlet states, assuming that the nitrogen lone-pair could be represented in terms of a localized orbital. The results of a recent semi-empirical calculations reported by Kato *et al.* [16], and of an *ab initio* calculation on pyrazine reported by Hackmeyer and Whitten [17] agree with our calculations in predicting that the symmetry forbidden transition should be expected to lie at higher energies than the symmetry allowed transition in all three compounds. The calculated splitting and the experimental results of El-Sayed indicate just the opposite order. We have been unable to find any other experimental results which might help clarify this situation. More experimental work on the nature of the spectral bands in the diazines is certainly indicated.

The three sets of calculation on pyrazine all show a rather large energy gap between the upper states of the symmetry allowed and forbidden transitions. This gap can be ultimately traced to the very large splitting between the two molecular orbitals containing the positive and negative combination of nitrogen "lone-pair" atomic orbitals. A better understanding of this result is facilitated by a more detailed examination of the "lone-pair" molecular orbitals.

We can visualize these MO's as formed by linear combination of hybrid AO's n_1 and n_2, of the two nitrogen atoms, but we must recognize that other AO's may also enter into the MO, as determined by the SCF procedure. The two MO's will be called n_+ and n_-, the former containing the combination n_1+n_2, the latter, n_1-n_2. In pyrazine, with D_{2h} symmetry, n_+ belongs to a_g, n_- to b_{1u}; in the other two diazines, with C_{2v} symmetry, n_+ still belongs to the totally symmetric representation a_1, and n_- belongs to b_2. In the SCF procedure, the symmetry adapted

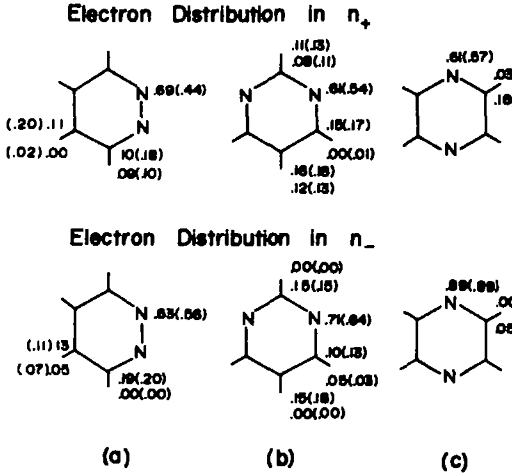
Electron Distribution in n_+
Electron Distribution in n_-
N
(a)
(b)
(c)

Fig. 1. The electron delocalization in the n_+ and n_- molecular orbitals of (a) pyridazine, (b) pyrimidine and (c) pyrazine

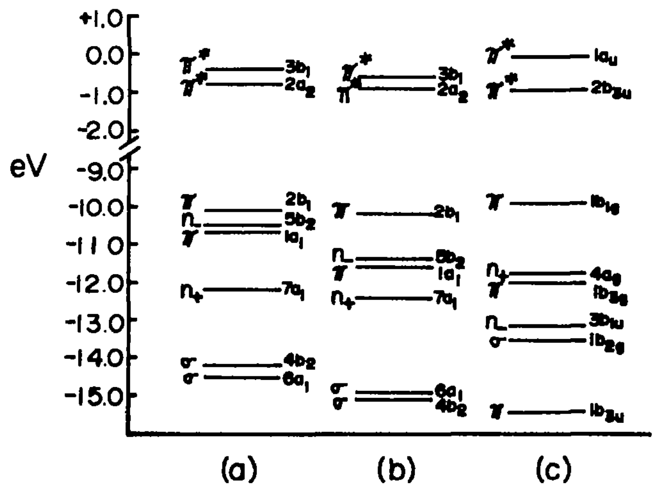

Fig. 2. Molecular orbitals of (a) pyridazine, (b) pyrimidine and (c) pyrazine

combinations $n_1 + n_2$ and $n_1 - n_2$ combine with any other symmetry adapted combination of the carbon and hydrogen orbitals. This causes the "lone-pair" electrons to be delocalized to a greater extent than is the case when n_+ and n_- are pure "lone-pairs". A comparison of the delocalization in the present work and the original work of Del Bene and Jaffé [1] is made in Fig. 1. As can be seen, the delocalization of the lone-pair electrons is somewhat greater where the Mataga approximation is used.

Another interesting feature of the diazene MO's is revealed when we inspect Fig. 2. This figure shows schematically the position of the six highest energy occupied molecular orbitals along with the two lowest energy virtual orbitals. If we compare the position of n_+ and n_- in the three compounds, we immediately see that in pyrimidine and pyridazine n_- is the highest energy of the two, while in pyrazine n_+ is the highest. The order of n_+ and n_- in pyrazine as predicted by the CNDO/S calculation is in agreement with the order predicted by recent *ab initio* calculation of Whitten [17] and of Clementi [18]. There are no *ab initio* calculations available for pyrimidine and pyridazine with which to compare the CNDO/S results[1].

Table 4. The calculated and observed $^1\Psi_n \leftarrow {}^1\Psi_0$ transitions in *s*-triazine and *s*-tetrazine[b]

Compound	Type	Symmetry	Energy above ground state (eV)		f	
			cal.	obs.	cal.	obs.
s-Triazine[a]	$n-\pi^*$	$^1E''$ (^1W)	4.5	4.0		
	$n-\pi^*$	$^1E''$ (^1W)	4.5	4.0	0.0	
	$n-\pi^*$	$^1A_2''$ (^1W)	4.6	3.9	0.027	0.018, 0.024
	$n-\pi^*$	$^1A_2''$ (^1W)	5.1		0.0	
	$\pi-\pi^*$	$^1A_1'$ (^1L_b)	5.6	5.5	0.0	0.002
	$\pi-\pi^*$	$^1A_2''$ (^1L_a)	6.6		0.0	
	$\pi-\pi^*$	$^1E^1$ (^1B)	7.2		0.62	
					0.62	
s-Tetrazine[a]	$n-\pi^*$	$^1B_{3u}$ (^1W)	2.6	2.3	0.018	0.004
	$n-\pi^*$	^1A_u (^1W)	4.3	3.9	0.0	0.001
	$n-\pi^*$	$^1B_{1g}$ (^1W)	4.3			
	$\pi-\pi^*$	$^1B_{2u}$ (^1L_b)	4.9	4.3	0.15	
	$n-\pi^*$	B_{2g} (^1W)	5.1			
	$n-\pi^*$	A_u (^1W)	5.4			
	$\pi-\pi^*$	B_{1u} (^1L_b)	6.6		0.02	
	$n-\pi^*$	B_{3u} (^1W)	6.7		0.01	
	$\pi-\pi^*$	B_{1u} (^1B)	7.3		0.89	
	$\pi-\pi^*$	B_{2u}	7.8		0.52	

[a] Ref. [12].

[b] The coordinate system used for the symmetry designations is the same as in Ref. [12].

---

[1] We wish to thank the referee for pointing out that the order of the MO's given in Fig. 2 is not in agreement with the order determined by R. Gleiter, E. Heilbroner, and V. Horminey using photoelectron spectroscopy [Angew. Chem. 82, 878 (1970)]. Since the CNDO/S method is parameterized to yield information about excited states, disagreement on the position of individual MO's is not too surprising. However, before commenting we wish to look at this problem in greater detail.

s-Triazine, s-Tetrazine

The spectra of *s*-triazine and *s*-tetrazine have been less intensively studied than the diazines, but we include the calculated and experimental results for the sake of completeness. The calculated and experimental spectra of these molecules are given in Table 4.

The ^1L_b transition is the only benzenoid transition reported in the two compounds. Inspection of Table 4 shows that the calculations are in good agreement with experiment. In the case of *s*-triazine, the ^1L_b transition is forbidden by molecular symmetry. As a consequence, the calculated oscillator strength is zero. In accordance with the symmetry forbiddenness of this transition, the experimental oscillator strength is small, being about the same size as in benzene itself. In the case of *s*-tetrazine, the singlet ^1L_b transition is symmetry allowed. The calculated oscillator strength ($f = 0.15$) has about the same magnitude as the value for the corresponding quantity in the diazines.

The number of lone-pair electrons in these two compounds implies that we should expect a considerable number of transitions corresponding to the promotion of lone-pair electrons. Of the many possible transitions, only the lowest energy transition in each of the two compounds have been observed. The calculated value in *s*-triazine is in fair agreement with experiment, and in *s*-tetrazine, the calculations are in good agreement with experiment.

Acknowledgements. We wish to thank the University of Cincinnati Computer Center for providing computer time for this project. One of us, RLE, would like to thank both The Procter and Gamble Co. and The Ethyl Corporation for their support.

References

1. Del Bene, J., Jaffé, H. H.: J. chem. Physics **48**, 1807 (1968); **48**, 4050 (1968); **49**, 1221 (1968).
2. Nishimoto, K., Mataga, N.: Z. physik. Chem. (Frankfurt) **12**, 335 (1957); **13**, 140 (1957).
3. The oscillator strengths reported in Ref. [1] are a factor of two to low.
4. Pople, J. A., Segal, G. A.: J. chem. Physics **44**, 3289 (1966).
5. Pariser, R., Parr, R. G.: J. chem. Physics **21**, 767 (1953).
6. Hinze, J., Jaffé, H. H.: J. Amer. chem. Soc. **84**, 540 (1962).
7. Platt, J. R.: J. chem. Physics **17**, 484 (1949).
8. Hirota, F., Nagakura, S.: Bull. chem. Soc. Japan **43**, 1010 (1970).
9. Sponer, H., Stücklen, H.: J. chem. Physics **14**, 101 (1946).
10. Rush, J. H., Sponer, H.: J. chem. Physics **20**, 1847 (1952).
11. Stephenson, H. P.: J. chem. Physics **22**, 1077 (1954).
12. Innes, K. K., Byrne, J. P., Ross, I. G.: J. molecular Spectroscopy **22**, 125 (1967).
13. — Simmons, J. D., Tilford, S. G.: J. molecular Spectroscopy **11**, 257 (1963).
14. Ito, M., Shimada, R., Kusuishi, T., Meyushima, W.: J. chem. Physics **26**, 1508 (1956).
15. El-Sayed, M. A., Robinson, G. W.: Molecular Physics **4**, 273 (1961).
16. Yonezawa, T., Kato, H., Kato, H.: Theoret. chim. Acta (Berl.) **13**, 125 (1969).
17. Hackmeyer, M., Whitten, J. L.: J. chem. Physics **54**, 3739 (1971).
18. Clementi, E.: J. chem. Physics **46**, 4731 (1967).

Prof. Dr. H. Jaffé
Centre de Méchanique Ondulaire Appliquée
23, Rue du Maroc
F-75 Paris XIX, France

Theoret. chim. Acta (Berl.) 26, 141–146 (1972)
© by Springer-Verlag 1972

Finite Electric Field Valence Shell Calculations of Polarizability Gradients and Raman Depolarization Ratios for Diatomic Molecules

N. S. HUSH* and M. L. WILLIAMS

Department of Inorganic Chemistry, The University of Bristol, U. K.

Received June 29, 1971

Calculation of polarizability gradients have been made for a number of diatomic molecules using the Finite Field CNDO/II approximate SCF method. Comparison with experimental results suggests that the method will be generally useful for the prediction and interpretation of Raman intensities.

Es wurden die Polarisierbarkeitsgradienten einer Anzahl zweiatomiger Moleküle mit Hilfe der CNDO/II-SCF Näherungsmethode mit endlichem Feld durchgeführt. Der Vergleich der Ergebnisse mit experimentellen Werten zeigt, daß diese Methode allgemein zur Vorhersage und zur Interpretation von Raman-Intensitäten geeignet ist.

Introduction

Measurement of the absolute intensities and depolarization ratios of vibrational Raman lines leads, in principle, to a determination of the derivative with respect to the appropriate normal co-ordinate of the mean value of the polarizability tensor. The following relation holds for unpolarized incident light:

$$I_p = A\,[45\,(\bar{\alpha}')^2 + 13\,(\gamma')^2]\ , \tag{1}$$

where I_p is the intensity of the scattered light and A is a factor depending on the temperature, the frequency and intensity of the incident light, the frequency of the Raman shift, the degeneracy of the normal mode and the molar concentration. The quantities $\bar{\alpha}'$ and γ' are respectively the mean value and anisotropy of the polarizability gradient. This relation, combined with the equation defining the depolarization ratio for unpolarized incident light ϱ_n:

$$\varrho_n = \frac{6\gamma'^2}{45\,(\bar{\alpha}')^2 + 7\gamma'^2} \tag{2}$$

then yields a value for $\bar{\alpha}'$. A fuller discussion of the experimental determination of polarizability derivatives is given in Ref. [1].

Experimental work on Raman intensities has been quite extensive [2, 3] but few theoretical calculations have been reported. The advent of the laser source has provided the stimulus for further experimental measurements of these quantities and it therefore seems appropriate to present here the results of our calculations of polarizability derivatives and to compare them with existing experimental values.

---

* Present address: Department of Theoretical Chemistry, University of Sydney, Sydney, N.S.W. 2006, Australia.

Apart from the delta-function model used by Long and Plane [4] and a consideration of dispersion forces by Oksengorn [5], the only molecular calculations of polarizability derivatives appear to have been concerned with the simple diatomics H_2^+ and H_2 [6–10]. In this communication we present calculations of polarizability derivatives for the stretching vibration of some diatomic molecules using a valence-orbital semi-empirical SCF-MO method.

Method of Calculation

In calculating polarizabilities and their derivatives we have used the Finite-Field CNDO/2 method described elsewhere [11]. The polarizability of each molecule was calculated at intervals of 0.005 Å up to 0.01 Å either side of the calculated field-free equilibrium bond length R_e. The polarizability derivatives were then obtained as the slope, at R_e, of the variation in α with change in bond length R. The relation between α and R was found in all cases to be linear in the range of R values examined. By performing the calculations with the electric field along (‖) and perpendicular to (⊥) the bond axis, the derivative of the mean value of the electronic polarizability is then obtained as

$$\bar{\alpha}' = \frac{\partial\bar{\alpha}}{\partial R} = \frac{1}{3}\left(\frac{\partial\alpha_{\parallel}}{\partial R} + 2\frac{\partial\alpha_{\perp}}{\partial R}\right), \tag{3}$$

where the normal co-ordinate in this simple case is R.

For linear molecules the square of the anisotropy of the derived polarizability tensor reduces to

$$\gamma'^2 = (\alpha'_{\parallel} - \alpha'_{\perp})^2 \tag{4}$$

and the depolarization ratio for unpolarized light ϱ_n is then

$$\varrho_n = \frac{6\,(\alpha'_{\parallel} - \alpha'_{\perp})^2}{45\,(\bar{\alpha}')^2 + 7\,(\alpha'_{\parallel} - \alpha'_{\perp})^2}\,. \tag{5}$$

Table 1 H_2

	$\alpha'_{\parallel}$	$\alpha'_{\perp}$	$\bar{\alpha}'$	ϱ_n
This work	1.280	0.000	0.427	0.500
Bell and Long	1.86	1.31	1.49	0.018
Tang and Albrecht	2.351	1.009	1.456	0.100
	2.506	0.931	1.837	0.088
	5.537	2.762	1.909	0.212
Hirschfelder	1.02	0.89	0.93	0.012
	1.08	0.80	0.89	0.003
	1.02	0.98	0.99	0.003
	1.10	0.95	1.00	0.002
Ishiguro *et al.*	1.9695	1.1319	1.4111	0.045
Kolos and Wolniewicz	1.776	0.831	1.146	0.082
Expt.[a]	1.69	0.85	1.13	0.07
Expt.[b]	1.98	0.96	1.30	0.073

[a] Ref. [14].

[b] Ref. [15].

Table 2

	This work						Expt.[a]	This work	Expt.[b]
Molecule	Bond order	$\alpha'_Q(\parallel)$	$\alpha'_{sp}(\parallel)$	$\alpha'(\parallel)$	$\alpha'_\perp$	$\bar{\alpha}'$	$\bar{\alpha}'$	ϱ_n	ϱ_n
N_2	3.000	2.096	0.488	2.584	0.600	1.261	1.73	0.139	0.18
							1.75		0.19
O_2	2.000	2.540	0.702	3.242	0.055	1.117	1.48	0.479	0.33
							1.46		0.26
CO	2.770	0.610	1.190	1.800	1.164	1.376	1.44	0.0275	0.31
							1.50		0.29
F_2	1.000	1.256	0.161	1.417	−0.095	0.409	0.110[c]	0.583	0.110
HF	1.275	1.260	0.057	1.317	−0.427	0.756	–	0.388	–
O_2^-	1.500	4.058	1.247	5.305	0.545	2.132	–	0.374	≃0.06[d]

[a] Values from Refs. [19, 2] respectively unless otherwise stated.

[b] The value obtained in Ref. [2] is quoted followed by the literature value given in Ref. [2].

[c] Ref. [16].

[d] Ref. [18].

Our calculated values of $\alpha'_{\parallel}$, $\alpha'_{\perp}$, $\bar{\alpha}'$ and ϱ_n are shown in Tables 1 and 2. We shall discuss the results obtained for the hydrogen molecule separately from those obtained for the remaining diatomic molecules.

The Hydrogen Molecule

In the Finite Field CNDO/2 approximation the solution of the problem of the hydrogen molecule in a static uniform electric field directed along the molecular axis may be obtained analytically. The expression for the parallel polarizability component so obtained is [11]

$$\alpha_{\parallel} = \frac{R^2}{\gamma_{AA} - \gamma_{AB} - 2\beta}, \tag{6}$$

where R is the internuclear separation and $\beta = \beta^0_{AB} S_{AB}$ in the notation of Pople and Segal [12]. The electron repulsion integrals γ_{AA} and γ_{AB} are calculated as the two-centre Coulomb integrals involving valence orbitals using formulae given by Roothaan [13]. Thus, differentiating the expression for $\alpha_{\parallel}$ with respect to R we have

$$\alpha'_{\parallel} = 2\left(\frac{\alpha_{\parallel}}{R}\right) - \left(\frac{\alpha_{\parallel}}{R}\right)^2 \left[\frac{\partial \gamma_{AA}}{\partial R} - \frac{\partial \gamma_{AB}}{\partial R} - 2\beta^0_{AB}\frac{\partial S_{AB}}{\partial R}\right]. \tag{7}$$

Using the value of $\alpha_{\parallel}$ given earlier [11] ($\alpha_{\parallel} = 0.457\,\text{Å}^3$ at $R = 0.741114\,\text{Å}$) together with the original values of β^0_{AB} and the hydrogen 1s orbital exponent of Pople and Segal we obtain $A' = 1.2798\,\text{Å}^2$ in agreement with the value found by calculating the polarizability near the equilibrium distance where the relation between $\alpha_{\parallel}$ and R was found to be linear.

Since the method used here considers only 1*s* orbitals on the hydrogen atoms $\alpha_\perp$ is always zero and so, therefore, is $\alpha'_\perp$. Consequently our calculated value of $\bar{\alpha}'$ is just $\frac{1}{3}\alpha'_{||} = 0.4266\,\text{Å}^2$ compared with the experimental figures 1.13 Å^2 and 1.30 Å^2 [14, 15]. Our value for $\alpha'_{||}$ of 1.2798 Å^2 compares very well with both experiment and previous calculations; it is closer to the experimental value than any of the different values quoted by Tang and Albrecht [10] and Hirschfelder [6]. The restriction of the basis set to 1*s* orbitals is clearly quite a severe one as our low value for $\bar{\alpha}'$ indicates. This is not an inherent restriction in the method and the result obtained for $\alpha'_{||}$ suggests that inclusion of higher orbitals may also yield a reasonable value for α'.

Diatomic Molecules

In Table 2 we present the results of calculations of $\bar{\alpha}'$ and ϱ_n for some First Row diatomic molecules.[1] Comparison of $\bar{\alpha}'$ and ϱ_n with experiment is possible only for N_2, O_2 and CO, while a value for ϱ_n for F_2 can be obtained from the value of ϱ_s (for polarized incident light) given in Ref. [16] from the relation [17]

$$\varrho_s = \frac{\varrho_n}{2 - \varrho_n}. \tag{8}$$

A value for ϱ_n has also been estimated for O_2^- [18]. The agreement between our calculated values of $\bar{\alpha}'$ and the experimental ones of both Yoshino and Bernstein [14] and Spiro and Fontal [19] is good. The agreement is best for CO for which we calculate $\bar{\alpha}' = 1.376\,\text{Å}^2$, compared with the experimental value of 1.44 Å^2 and 1.50 Å^2. The values of $\bar{\alpha}'$ for N_2 and O_2 are also in good agreement with experiment.

Our calculated values of the depolarization ratios ϱ_n for N_2 and O_2 are in good agreement with the experimental results of Yoshino and Bernstein and with the literature values quoted by these authors. For the CO molecule our value of 0.0275 is an order of magnitude smaller than the experimental results. This arises from the relatively large $\alpha'_\perp$ calculated for this molecule, implying that the field-induced mixing of 2*s* and 2*p* orbitals on the carbon and oxygen atoms is quite sensitive to variation in bond length.

An approximate value of 0.06 for the depolarization ratios of the Raman band of O_2^- in a host lattice has been obtained by Holzer *et al.* [18]; our value of 0.374 suggests that the calculated contribution of $\alpha_\perp$ is underestimated, provided that the experimental value can be assumed to be close to that for the free ion. For the F_2 molecule our value of ϱ_n is slightly higher than that deduced from the experimental measurements of Claasen, Selig and Shamir [16] but is of the correct order of magnitude.

---

[1] Correlations between bond order and bond polarizability derivatives have frequently been suggested. Bond orders are also listed in Table 2, and it can be seen that for the neutral molecules studied here the very simple relationship

$$\bar{\alpha}' \simeq 0.5P\,\text{Å}^2$$

reproduces the calculated average polarizability gradients with an accuracy of about ±0.2 Å^2.

The negatively charged O_2^- ion, which is calculated to have a much higher value of $\bar{\alpha}'$ than for any of the neutral molecules, does not conform to this trend.

It is interesting to note that for the fluorine containing molecules HF and F_2 we calculate a negative sign for $\alpha'_{\perp}$. In the CNDO/2 valence shell approximation, $\alpha_{\perp}$ arises purely from the one-centre mixing of $2s$ and $2p$ orbitals and in the case of HF from this effect on the fluorine atom alone. Therefore a negative sign for $\alpha'_{\perp}$ means that the field induced dipole moment due to $2s$ and $2p$ mixing decreases as the bond length increases.

In order to obtain more insight into the factors contributing to $\bar{\alpha}'$ we have calculated the charge displacement and $2s$–$2p$ hybridisation polarizability derivatives and these are listed in Table 2. They are defined in the following way. To first order in the electric field F, we can write

$$\mu_i^F = \mu_i^0 + \alpha_{ij} F_j \tag{9}$$

in conventional notation.

In the CNDO/2 method, the total dipole moment can be expressed as the sum of a charge displacement term and a term arising from $2s$–$2p$ mixing [11, 12]

$$\mu_i^F = \sum_{\mathrm{A}} (Z_{\mathrm{A}} - P_{\mathrm{AA}}^F)\, i_{\mathrm{A}} - \frac{5}{\sqrt{3}} \sum_{\mathrm{A}} \frac{1}{Z'_{\mathrm{A}}} P^{F\cdots}_{2s,2p_i(\mathrm{A})}\,, \tag{10}$$

where $i = x, y$ or z. Assuming that the bond density matrix is a differentiable function of the normal co-ordinate we have:

$$\frac{\partial}{\partial Q}(\mu_i^F) = \frac{\partial}{\partial Q}\left|\sum_{\mathrm{A}} (Z_{\mathrm{A}} - P_{\mathrm{AA}}^F)\, i_{\mathrm{A}}\right| - \frac{5}{\sqrt{3}} \sum_{\mathrm{A}} \frac{1}{Z'_{\mathrm{A}}} \frac{\partial}{\partial Q}(P^F_{2s,2p_i(\mathrm{A})}) \tag{11}$$

or, to first order in F,:

$$(\alpha)'_{ij} = (\alpha_Q)'_{ij} + (\alpha_{sp})'_{ij}\,. \tag{12}$$

Since $(\alpha_Q)'_{ij}$ is a function of the cartesian co-ordinates of the atoms it might be expected that this term will be the dominant one. For all the molecules studied, except CO, this is found to be the case. For CO the situation is reversed, α'_{sp} being approximately twice α'_Q for this molecule. The contribution of $2s - 2p$ mixing to the zero-field dipole moment of CO is roughly three times the charge displacement term and clearly for this molecule the hybridization term is the more sensitive to perturbation.

Conclusion

There is a generally good correlation between our calculated polarizability derivatives and the experimental values. The agreement for corresponding depolarization ratios is reasonable, bearing in mind the fact that these are proportional to the *square* of the calculated polarizability gradient anisotropies. For the series of molecules studied, the factors determining the Raman transition probabilities can thus be fairly well interpreted within a valence orbital scheme. Further work on diatomic and larger molecules is in progress.

Acknowledgement. This work was performed during the tenure of a Science Research Council grant to one of us (M.L.W.).

References

1. Hester, R. E.: In: Raman spectroscopy, Ed. H. A. Szymanski. New York: Plenum Press 1967.
2. Murphy, W. F., Holzer, W., Bernstein, H. J.: Appl. Spectroscopy **23**, 211 (1969).
3. Hester, R. E.: Anal. Chem. Ann. Revs. **42**, 231 R (1970).
4. Long II, T. V., Plane, R. A.: J. chem. Physics **43**, 457 (1965).
5. Oksengorn, B.: Spectrochim. Acta **20**, 99 (1964).
6. Hirschfelder, J. O.: J. chem. Physics **3**, 555 (1935).
7. Bell, R. P., Long, D. A.: Proc. Roy. Soc. (London) **A203**, 364 (1950).
8. Ishiguro, E., Arai, T., Mizushima, M., Kotani, M.: Proc. physic. Soc. (London) **A65**, 178 (1952).
9. Kolos, W., Wolniewicz, L.: J. chem. Physics **46**, 1426 (1967).
10. Tang, J., Albrecht, A. C.: J. chem. Physics **49**, 1144 (1968).
11. Hush, N. S., Williams, M. L.: Chem. Physics Letters **5**, 507 (1970).
12. Pople, J. A., Segal, G. A.: J. chem. Physics **44**, 3289 (1966).
13. Roothaan, C. C. J.: J. chem. Physics **19**, 1445 (1951).
14. Yoshino, T., Bernstein, H. J.: J. molecular Spectroscopy **2**, 213 (1958).
15. Golden, D. M., Crawford, B.: J. chem. Physics **36**, 1654 (1952).
16. Claassen, H. H., Selig, H., Shamir, J.: Appl. Spectroscopy **23**, 8 (1969).
17. Herzberg, G.: Infrared and Raman spectra, p. 247. New York: D. Van Nostrand Inc. 1945.
18. Holzer, W., Murphy, W. F., Bernstein, H. J., Rolfe, J.: J. molecular Spectroscopy **26**, 543 (1968).
19. Spiro, T. G., Fontal, B.: Private communication.

Prof. Dr. N. S. Hush
The University of Sydney
Department of Theoretical Chemistry
Sydney, N.S.W. 2006, Australia

Theoret. chim. Acta (Berl.) 26, 147—156 (1972)
© by Springer-Verlag 1972

Calculated Physical Properties of a Water Molecule in an Ice-Like Cluster

C. GUIDOTTI*
Laboratorio di Chimica Quantistica ed Energetica Molecolare del C.N.R.,
Via del Risorgimento 35, Pisa, Italy

U. LAMANNA*
Istituto di Chimica Analitica dell'Università di Bari, Via Amendola 173, Bari, Italy

M. MAESTRO*
Istituto di Chimica Fisica dell'Università di Pisa, Via del Risorgimento 35, Pisa, Italy

Received January 18, 1972

Some properties of a H_2O molecule surrounded by the four nearest neighbours arranged as in the ice I geometry have been calculated within a SCF scheme in terms of an extended STO's basis. The effect of the outer molecules is treated as a coulombic perturbation. The different possible geometric configurations of the perturbators have been taken into account. Comparisons are made with the experimental changes of some physical properties of water in passing from vapor to condensed phase.

Es werden einige Eigenschaften des Wassermoleküls, das von seinen vier nächsten Nachbarn in Eis-I-Geometrie umgeben ist, mit Hilfe eines SCF-Schemas mit erweiterter STO-Basis berechnet. Dabei wird der Effekt der äußeren Moleküle als Coulombstörung behandelt. Die verschiedenen möglichen geometrischen Konfigurationen der Störmoleküle sind in Betracht gezogen worden. Die Rechenergebnisse werden mit den experimentellen Änderungen einiger physikalischer Eigenschaften des Wassers beim Übergang von der Gasphase zur kondensierten Phase verglichen.

Introduction

In spite of noticeable progresses in the last years the study of water in its condensed phases, presents some still open problems. At any rate, the persistence in the liquid phase of a more or less extended and stable ice-like tetrahedral structure seems to be largely accepted, and it may be supposed that the differences known to exist between the physical properties of a water molecule in the gas and in the condensed phases can be ascribed to this type of structure.

The most recent "ab initio" calculations on this subject have been mainly devoted to clarify the essence of the hydrogen bond and to attain a quantitative estimate of the related energy. At this regard the papers issued in the last years [1–5] seem to indicate that a complete SCF calculation based on a small cluster of water molecules is sufficient to obtain a correct prediction of this experimental datum. This paper is instead mainly focused to a different objective: the attempt of establishing if a relatively crude model for the effect of the neigbouring molecules is sufficient to explain the changes in physical properties which occur when the water molecule is embedded in a condensed phase.

---

* Work performed with the C.N.R. financial aid.

The suggested model and the calculation scheme are discussed in the second section, while the third one is devoted to the discussion of the results.

Model and Calculation Scheme

The adopted model presents the following peculiarities:

1) The changes in the physical properties of water, in passing from gas to condensed phase, are supposed to be related to two different effects:

a) The distortion of the internal geometry, with small lengthening of the OH bond and widening of the HOH angle;

b) the change of the charge distribution caused by the neighbouring molecules.

The first effect is taken into account by the proper choice of the geometry of the molecule and no attempt is made to deduce from the model the new equilibrium positions of the atoms, while the second effect will be treated as due to a perturbation.

Only the first (and, partially, the second) shell of neighbours has been taken into account.

2) Consequently, a water molecule, with a rigid geometry corresponding to that of ice I, is supposed to be surrounded by four other similar molecules, the over-all structure corresponding to a tetrahedral five-member cluster. The distance between the oxygen nuclei is that of normal ice (2.76 Å) and the O and H nuclei, that form the hydrogen bond, are supposed to be collinear.

3) Both the central molecule and the external ones are described by SCF LCAO MO wave functions.

It is known that such an approximation allows to obtain satisfactory results for most of the gas phase observables [6–8].

Since the interaction between the central molecule and the outer ones is treated as a perturbation, a rather extended basis set of STO's has been employed for the description of the former, while a minimal basis set has been considered to be adequate for each of the surrounding molecules.

4) The charge distribution of the perturbing molecules has been adjusted to render it as far as possible suited to the description of the mean situation of a water molecule in the condensed phase. Therefore an iterative process has been carried out starting from an SCF calculation of a water molecule on a minimal basis set of STO's.

The SCF wave function of the isolated central molecule was perturbed by the interaction with its four surrounding ones, neglecting the exchange terms. The iterative process has been then accomplished, by attributing the SCF charge distribution so obtained for the central molecule to the surrounding ones, and so on, up to convergence of the energy. The final wave function has been used in the subsequent calculation stage, where as already stated, the central molecule is described in terms of an extended basis set.

5) Also in this case, the interaction is supposed to be purely coulombic so that exchange and dispersion contributions are neglected. This approximation, that simplifies noticeably the calculation at the actual distances of atoms in the hydro-

gen bond, is a rather drastic one as for as the energy of the bond is concerned, but, hopefully it is not so heavy in considering other physical properties. At this stage, all mutual interactions of the four outer molecules are neglected and their charge distribution is supposed completely rigid.

The hamiltonian of the perturbed central molecule is therefore written as follows:

$$H = H^0 + H', \tag{1}$$

H^0 being the Hartree-Fock hamiltonian of the unperturbed system and

$$\begin{aligned} H' &= \sum_{j=1}^{N_{\text{elect.}}} V'(j); \quad V'(j) = \sum_{\alpha=1}^{4} V'_\alpha(j) \\ &= \sum_{\alpha=1}^{4} \left\{ \sum_{i_\alpha=1}^{3} \frac{Z_{i_\alpha}}{r_{i_\alpha j}} - 2 \sum_{l_\alpha=1}^{5} \int \frac{\varphi^*_{l_\alpha}(k)\, \varphi_{l_\alpha}(k)}{r_{l_\alpha k}} d\tau_k \right\}. \end{aligned} \tag{2}$$

φ_{l_α} denotes the occupied molecular orbitals of the perturbing systems, the meaning of the other symbols in (2) being obvious.

6) The SCF solution corresponding to the hamiltonian (1) is employed to evaluate some first and second-order observables to be compared with the corresponding ones evaluated for an isolated water molecule with a geometry characteristic of the gas phase. The last system has been already treated by one of us [8], and the STO's set for the central molecule of the present paper is the same. Since the aim of the calculation is the comparison of the results with the data one can obtain from experiment, one must take into account the fact that particularly in a condensed phase, the perturbation that one can suppose to act on a single molecule, has to be averaged with respect to the different configurations of its surrounding partners. In accordance with the Pauling picture [9], these may be deduced by allowing all the protons to jump from the proximity of an Oxygen atom to another. In our case, since the central molecule is considered fixed in his geometry and position, the different configurations are simply obtained by allowing the four perturbators to rotate around O—O axes (see Fig. 1). Moreover,

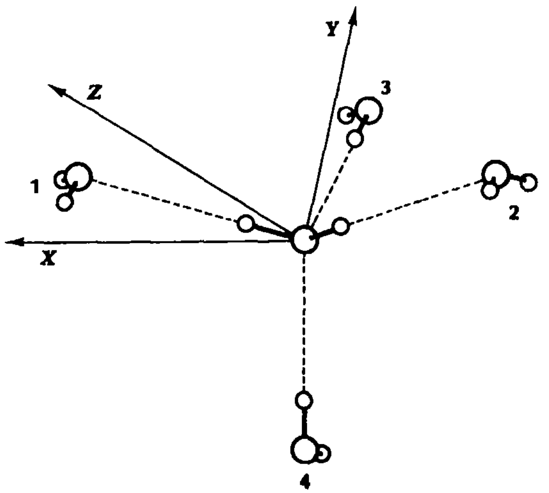

Fig. 1. Geometry of the cluster

if one retains the ice-like geometry, these rotations must be limited only to 120° and 240°, with respect to the original configuration, so that one obtains 3^4 different geometrical configurations. In an infinite crystal, these configurations are all equivalent; in the case of a cluster of limited dimensions the energy and properties of the central perturbed molecule will be generally different for the different configurations of the surrounding ones (although in some cases they coincide, for symmetry reasons). Therefore, the perturbative calculation has been repeated for all the required configurations, and the values of the observables so obtained have been linearly averaged. A similar process has been used in the first stage of the calculation, all minimal set, when the perturbing SCF wave function has been produced.

A Boltzmann average process would mean that the condensed phase has been represented as an infinite replication of non interacting clusters, such as that here considered. Obviously if this cannot be a useful picture of an ice crystal, it is certainly an extremely reductive picture of the liquid phase.

7) The perturbed wave function of the central molecule does not present, in principle, the C_{2v} symmetry characteristic of the isolated molecule. This fact would lead to some unphysical features of the calculated observables. We have therefore imposed an additional constraint to all the SCF perturbing procedures, in order to preserve the symmetry of the wave function identical with that of the unperturbed case. This same constraint has been retained in the first stage of the calculation. As a control of the errors introduced with this last approximation we have performed a complete calculation on the minimal set and for a configuration on the extended set by relaxing the symmetry constraint. In both cases the spurious contributions to the electric dipole moment were not greater than 0.01 *D* while the *z* component was varied on the 3^{th} decimal place. The variation of the total energy values was of an unit on the 4^{th} decimal place.

8) In order to have an estimate of the error introduced, by neglecting all outer shells but the first one, an additional calculation involving also the twelve second nearest-neighbours has been carried out. In this case, only one configuration of the molecules has been taken into account.

Results and Discussion

In Table 1 the geometrical parameters for the molecule either isolated or embedded in the cluster are reported. For the first case we have employed the same data as in Ref. [8] which are very close to the experimental equilibrium ones while in the second case the data of Eisemberg and Kauzmann [10] have been utilized. In the same table are reported the coordinates of all the molecules of the cluster in one of the considered configurations, specifically that represented in Fig. 1.

In Table 2 the minimal set orbitals and energies are reported for the central molecule of the cluster. The coefficients are those obtained from the preliminary symmetry constrained SCF process described at point 4 of the previous section, after linear averaging of all the considered configurations. These coefficients are therefore employed in describing the wave functions of the perturbing molecules

Table 1. Geometrical parameters and coordinates for isolated molecule (I) and for the cluster (II)

I	II
HOH = 105°	HOH = 109° 28′
R_{OH} = 1.8103[a]	R_{OH} = 1.90854

Coordinates of the atoms in the configuration shown in Fig. 1

		x	y	z
Central molecule	O	0.0	0.0	0.0
	H_1	1.558266	0.0	1.101950
	H_2	−1.558266	0.0	1.101950

		x	y	z			x	y	z
Mol. 1	O	−4.258235	0.0	3.011280	Mol. 3	O	0.0	4.258235	−3.011280
	H_1	−4.258235	−1.558266	4.113232		H_1	1.558266	4.258235	−4.113232
	H_2	−5.816501	0.0	1.909328		H_2	0.0	2.699969	−1.909328
Mol. 2	O	4.258235	0.0	3.011280	Mol. 4	O	0.0	−4.258235	−3.011280
	H_1	5.816501	0.0	1.909328		H_1	0.0	−2.699969	−1.909326
	H_2	4.258235	−1.558266	4.113232		H_2	0.0	−3.738578	−4.847715

[a] All data are in atomic units.

Table 2. Minimal set STO's, MO's and energies of H_2O molecule in a cluster

Orbital	ζ	Φ_1	Φ_2	Φ_3	Φ_4	Φ_5
$1s_H$	1.27	−0.00328	0.14238	0.26628	0.41176	0.0
$1s$	7.66	0.99685	−0.22593	0.08123	0.0	0.0
$2s$	2.25	0.01466	0.87159	−0.45169	0.0	0.0
$2p_z$	2.21	0.00264	0.09531	0.80756	0.0	0.0
$2p_x$	2.21	0.0	0.0	0.0	0.63230	0.0
$2p_y$	2.21	0.0	0.0	0.0	0.0	1.0
$1s_H$	1.27	−0.00328	0.14238	0.26628	0.41174	0.0
ε (a.u.)		−20.52788	−1.24607	−0.44890	−0.58927	−0.39709

$E^{P.M.} = -75.7541$ $\mu^{P.M.} = 2.026$

$E^{I.M.} = -75.7034$ $\mu^{I.M.} = 1.920$

in the main calculation. In the same table, the total energy and the electric dipole moment corresponding to this charge distribution are compared with the corresponding values for an isolated molecule with the geometry in the gas case.

From the reported data one can see that the average energy for the hydrogen bond results to be:

$$E_{H.B.} = 5/16\,(E^{P.M.} - E^{I.M.}) = 9.9\ \text{kcal/mole}.$$

The ratio 5/16 can be understood by considering that in order to separate five molecules (which are assumed to be equivalent to each other) one must break sixteen bonds.

Table 3. Extended basis STO's. MO's and energies for isolated molecule (I.M.) and for a perturbed case (Cluster)

Atomic basis set			Molecular orbitals									
			Simm. A_1							Simm. B_1		
				Φ_1		Φ_2		Φ_3			Φ_4	
Order number	Orbital	ζ	O.N.	I.M.	Clust.	I.M.	Clust.	I.M.	Clust.	O.N.	I.M.	Clust.
1	$1s$	13.00	1	0.04813	0.04811	0.02295	0.02268	−0.00530	−0.00525	7	0.22344	0.22263
2	$1s'$	7.45	2	0.95048	0.95058	−0.27020	−0.27142	0.07646	0.06415	9	0.38010	0.38668
3	$2s$	3.50	3	0.01992	0.01953	0.08886	0.09224	−0.05783	−0.05651	11	0.15828	0.20356
4	$2s'$	2.17	4	−0.01011	−0.00984	0.73840	0.77011	−0.36478	−0.26340	13	0.07001	0.07089
5	$3s$	1.50	5	0.00726	0.00671	−0.22486	−0.18243	−0.22117	−0.18014	20	0.17337	0.09929
6, 7, 15	$2p_z, 2p_x, 2p_y$	3.50	6	0.00420	0.00350	0.01626	0.00746	0.25263	0.25926	21	0.18408	0.19878
8, 9, 16	$2p'_z, 2p'_x, 2p'_y$	2.15	8	−0.00428	−0.00361	0.10743	0.09442	0.40615	0.40010	22	−0.05598	−0.04597
			10	0.00356	0.00304	−0.08234	−0.08153	0.24486	0.30521	23, 28	−0.04969	−0.04004
10,11,17	$3p_z, 3p_x, 3p_y$	1.50	12	0.00032	0.00024	−0.00073	−0.00297	0.05155	0.03962	25	−0.17337	−0.09929
12,13,14	$3d_{z^2}, 3d_{xz}, 3d_{x^2-y^2}$	1.50	14	0.00017	0.00018	−0.00132	−0.00374	−0.00091	0.01691	26	−0.18408	−0.19878
			20, 25	−0.00561	−0.00503	0.20987	0.18186	0.19935	0.13062	27	0.05598	0.04597
18,19	$3d_{yz}, 3d_{xy}$	1.50	21, 26	0.00353	0.00317	0.05704	0.05032	0.07377	0.09269	ε (a.u.)	−0.72618	−0.70822
			22, 27	−0.00016	−0.00012	−0.02944	0.02475	−0.02350	0.02025			
20,25	$1s_H$	1.00	23	0.00030	0.00031	−0.04932	−0.04839	−0.03989	−0.02894			
			28	−0.00030	−0.00031	0.04932	0.04839	0.03989	0.02894			
21,26	$1s'_H$	1.50	ε (a.u.)	−20.58241	−20.60226	−1.36011	−1.34049	−0.58856	−0.58792			
22,27	$2p_{zH}$	1.10										
23,28	$2p_{xH}$	1.10										
24,29	$2p_{yH}$	1.10										

$E_{HF}^{I.M.} = -76.0384$

$E_{HF}^{Clust.} = -76.1000$

Simm. B_2		
	Φ_5	
O.N.	I.M.	Clust.
15	0.28220	0.29112
16	0.47240	0.44113
17	0.33373	0.38384
18	0.03916	0.01292
24, 29	0.03390	0.01931
ε (a.u.)	−0.51232	−0.52459

The electric dipole moment displays a very small variation, in accordance with the rigidity of the charge distribution in the minimal basis set case. In Table 3 are reported the extended basis set and the corresponding orbitals for the particular configuration of the perturbing molecules described in Fig. 1 and in Table 1.

The orbitals of the isolated molecule on the same basis set, and with the gas geometry, are also reported from [8] for comparison. It can be seen that the most relevant variations involve the most external molecular orbitals, and, particularly, the charge distribution on the hydrogen atoms. Also the coefficients of the oxygen *d*-type STO's result to be remarkably changed.

In Table 4 some comparison is made between the calculated results and those that one may deduce from experiment. At this stage, one is faced by the known difficulty of deducing unambiguously the physical data referring to a molecule embedded in the condensed phase. When possible we have reported the data derived from measurement on ice I but in some cases (e.g. the chemical shift), only the liquid phase data are known. As far as the hydrogen bond energy is concerned, the calculation must now be carried out in a way slightly different from that employed in the minimal set case. Due to the fact that now the perturbing molecules are retained rigid while they are taken away to an infinite distance from the central one, the average energy of the hydrogen bond can be assumed to be one fourth of the difference between the energy of the central molecule perturbed into the cluster and that of the unperturbed molecule with its original gas phase geometry.

Table 4. Calculated and experimental physical properties

	Calc.[a] I.M.	Exp. (gas)	Calc. (mean cluster value)	Max. var.	Exp. condensed phase	ΔCalc.	ΔExp.
Total energy (a.u.)	−76.0384	−76.481[b]	−76.0971	0.00539		9.2[h]	5.6–7.7[h, i]
$\mu(D)$	1.926	1.85 ± 0.02[b]	2.537	0.2823	2.71[f]	0.61	0.86
$\langle r^2 \rangle$ (10^{-16} cm^2)	5.510	5.10 ± 0.7[b]	5.727	0.024	12.65[g]		
χ(c.g.s. p.p.m/mole)	−14.373	−13.1 ± 1.8[l]	−14.718	0.034		−0.355	+0.45
σ_H(g.H) (p.p.m.)	48.4		42.57	0.56		−5.83	
σ_H(g.O) (p.p.m.)	28.41	30.03 ± 0.6[c]	24.601	0.4		−3.81	−4.58[j]
σ_O(g.O) (p.p.m.)	346.39		333.05	0.905		−13.34	−36[k]
$\bar{\alpha}$ (Å^3)	1.170	1.444[d]	1.258[e]			0.088	

[a] Arrighini, G. P., Guidotti, C., Salvetti, O.: J. chem. Physics **52**, 1037 (1970).

[b] See Refs. [7] and [8].

[c] For a discussion of this date see: Arrighini, G. P., Maestro, M., Moccia, R.: J. chem. Physics **52**, 6411 (1970), Table 3.

[d] Moelwyn-Hughes, E. A.: Physical chemistry, 2nd edn. New York: Macmillan 1964.

[e] This result is referred to the configuration of Fig. 1.

[f] Hollins, G. T.: Proc. physic. Soc. **84**, 1001 (1964).

[g] Landolt-Börnstein: Zahlenwerte und Funktionen, 6th edn. Vol. 10, II, pag. 21. Heidelberg: Springer 1967.

[h] kcal/mole for an hydrogen bond.

[i] See Ref. [10].

[j] Schneider, W. G., Bernstein, H. J., Pople, J. A.: J. chem. Physics **28**, 601 (1958).

[k] Florin, A. E., Alei, M.: J. chem. Physics **47**, 4268 (1967).

[l] Taft, H., Dailey, B. P.: J. chem. Physics **51**, 1002 (1969).

Therefore one has:

$$E_{\mathrm{H.B.}} = 1/4\,(E^{\mathrm{Cl}} - E^{\mathrm{I.M.}}) = 9.2\ \mathrm{kcal/mole}\,.$$

The hydrogen bond energy data reported in the last column of the Table 4 present a large spectrum of values due to possibility of different definitions of this quantity [10]. Also in this case, to neglect the exchanged interactions causes an overestimate of the quantity.

As far as the electric dipole moment is concerned, static dielectric constant measurements do not lead immediately to a value of this quantity for a molecule in the ice crystal. The values of Hollins [11] reported in the table, or that (2.60) calculated by Coulson and Eisenberg [12] seem to be the most reliable ones and the agreement with our calculated result may be considered satisfactory. For the quadrupole moment variation, we have not found experimental data for comparison.

The deduction of the molecular electric polarizability, in the condensed phase presents some problems analogous to those concerning the dipole moment. In the classical formulae (see for instance [13]) these two quantities appears tied together and, in principle, one could deduce both of them from measurements of dielectric constant and its temperature coefficient. Unfortunately, this type of procedure gives, in the case of highly polar substances, completely unreliable results. Therefore, as far as this quantity is concerned we limit the calculations only to the case of the configuration shown in Fig. 1. Among the reported magnetic properties only the nuclear magnetic shielding constant allows for a rather direct evaluation of the difference between the gas and condensed phase on the basis of the experimental measurements. The reported value for the proton is referred to the association shift introduced in Ref. [14] and it is a datum largely accepted [15]. One can see that the result of the calculation is of the right order of magnitude, although highly dependent from the choice of the gauge of the external field.

Previous calculations [16] have shown that the best results are obtained with the choice that minimizes the total magnetic susceptibility, and, practically, of the oxygen nucleus. As far as the O^{17}shielding value is concerned the agreement with the only experimental result we have found, is decisely unsatisfactory. For the magnetic susceptibility we have reported in the table a very recent result for the gas phase, that seems to confirm the assumption of Eisenberg and Kauzmann that the variation should not be greater than 15%. In contrast with these data, our result shows an increment in passing to the condensed phase.

All the data reported in Table 4 are obtained as averages among configurations that have been considered equivalent. The corresponding values (in the same units) for a Boltzmann average at 0° C (i.e. the temperature to which the experimental values are referred), are the following:

$$E = -76.0993$$

$$\mu = 2.629$$

$$\langle r^2 \rangle = 5.719$$

$$\chi = -14.709$$

$$\sigma_{\mathrm{H}}(g.\mathrm{O}) = 24.495$$

$$\sigma_{\mathrm{O}} = 333.32.$$

Table 5. Observables[a] in presence of the second shell[b]

E	-76.09683	-76.10431
μ	2.5132	2.66419
$\langle r^2 \rangle$	5.7287	5.717
α	8.492	8.495
χ	-14.722	-14.720
σ_H (g.H)	42.674	42.230
σ_H (g.O)	24.628	24.309
σ_O	333.03	335.007

[a] The units are the same as in the Table 4.

[b] The configuration of the perturbing molecules is different from that in Fig. 1.

One can see that no result (with the partial exception of the electric dipole moment) presents sensible variations.

In the fourth column of Table 4 are reported the maximum splittings between two different configurations of the perturbing molecules for each observables. One can see that the result for the dipole moment is the only one for which this splitting has some importance.

As an appendix to the main calculation, the observables of the central molecule have been calculated, by adding the second shell of molecules, in one of their possible configurations to a particular configuration of the first shell which has been chosen with an energy value very close to the linear average.

The calculation has been carried out within the already explained approximations. The results are reported in Table 5; for comparison, in the same table in the first column are reported the results relative to the case of the central molecule perturbed only by the four nearest neighbours to which the second shell has been added.

One can observe that the addition of the second shell brings a not negligible contribution, showing that (particularly in the case of the dipole moment) an addition of at least another shell would probably be needed in order to attain a convergence in the limits of the experience. It is confortable that the obtained result for this last observable comes to be very near to the value deduced from experiment by Hollins. Also the result for proton association shift (-4.1) shows an improvement.

As a conclusion, it seems that the following points can be stated:

1) A coulombic perturbation (classical electrostatic + polarization effects) is sufficient to explain a large part of the variation of the physical properties of a water molecule in passing from an isolated state to a condensed one. As it was already known, this approximation is not suited to attain a quantitative agreement with the experimental energy of the hydrogen bond, and even less, to justifie the equilibrium geometry of the nuclei.

2) At least in the above approximations and with the exception of the dipole moment, the effect of the rapidly fluctuation of the configuration of the nearest neighbours on the considered molecular observables has not a decisive importance.

3) The second shell brings a modification which is not greater (and often largely less) of the 20% of that of the first; unfortunately this fact is not sufficient

to establish the quickness of the convergence of the observables with the growth of the cluster.

All the calculations have been achieved by the IBM 360/65 of C.S.A.T.A. at Bari.

Acknowledgements. The authors wish to thank Prof. E. Scrocco for useful discussion on the subject.

References

1. Morokuma, K., Pedersen, L.: J. chem. Physics **48**, 3275 (1968).
2. Kollman, P. A., Allen, L. C.: J. chem. Physics **51**, 3286 (1969).
3. Morokuma, K., Winick, J. R.: J. chem. Physics **52**, 1301 (1970).
4. Del Bene, J., Pople, J. A.: Chem. Physics Letters **4**, 426 (1969).
5. Hankins, D., Moskowitz, J. W., Stillinger, F. H.: J. chem. Physics **53**, 4544 (1970).
6. Aung, A., Pitzer, R. M., Chan, S. I.: J. chem. Physics **49**, 2071 (1968).
7. Neumann, D., Moskowitz, J. W.: J. chem. Physics **49**, 2056 (1968).
8. Arrighini, G. P., Guidotti, C., Salvetti, O.: J. chem. Physics **52**, 1037 (1970).
9. Pauling, L.: The nature of the chemical bond. Itaha, N. Y.: Cornell 1940.
10. Eisenberg, D., Kauzmann, W.: The structure and properties of water. Oxford: Clarendon Press 1966.
11. Hollins, G. T., Proc. physic. Soc. **84**, 1001 (1964).
12. Coulson, C. A., Eisenberg, D.: Proc. Royal. Soc. (London) A **291**, 445 (1966).
13. Böttcher, C. J. F.: Theory of electric polarization. Amsterdam: Elsevier 1952.
14. Schneider, W. G., Bernstein, H. J., Pople, J. A.: J. chem. Physics **28**, 601 (1958).
15. Hindman, J. C.: J. chem. Physics **44**, 4582 (1966).
16. Arrighini, G. P., Maestro, M., Moccia, R.: J. chem. Physics **52**, 6411 (1970).

Dr M. Maestro
Istituto di Chimica Fisica
dell' Università di Pisa
Via del Risorgimento 35
I-56100 Pisa, Italy

Theoret. chim. Acta (Berl.) 26, 157—161 (1972)
© by Springer-Verlag 1972

Acceleration of Convergence by Density Matrix Extrapolation in CNDO/2 Calculations

J. C. HOWLAND and R. L. FLURRY, JR.
Department of Chemistry, Louisiana State University in New Orleans,
New Orleans, Louisiana 70122, USA

Received February 16, 1972

A five-point extrapolation procedure has been applied to the first-order density matrix in CNDO/2 calculations. A number of deviations from the usual procedures are employed which protect the overall extrapolation from failure when the points used in the extrapolation of a given element form a linear or divergent series. Overall the method saves about 20–50% on the number of iterations required to attain self-consistency.

Eine Extrapolation mittels fünf Punkten wurde für die Dichtematrix 1. Ordnung bei CNDO/2-Rechnungen vorgenommen. Dabei muß man in einigen Punkten vom normalen Verfahren abweichen, um Divergenzen zu vermeiden. Man spart dann 20–50% der Iterationsschritte.

Introduction

We have been correlating the electronic structure of pharmacalogically active compounds with their biological activity. This involves calculating various electronic indices within the CNDO/2 approximation [1]. In early studies we were unable to duplicate the calculated frontier electron densities and dipole moments to more than three significant figures after we had made some minor changes in the program to increase its speed and accuracy. Careful examination of the data for formaldehyde revealed that elements of the first-order density matrix were self-consistent only to within two significant figures when the electronic energy had converged to seven significant figures (Table 1). Decreasing the energy convergence criterion by a factor of ten did not significantly improve the self-consistency of the density matrix.

Since we were primarily interested in properties related to atomic charges, it was decided to converge directly on the first-order density matrix rather than on electronic energy as is done in most CNDO/2 programs. It was found that saturated molecules converged satisfactorily, but non-hydrocarbon compounds with π bonding systems took much longer to converge. In fact, 3-methylxanthane, which converged on electronic energy to a relative tolerance of 1×10^{-7} after 17 iterations failed to converge on the charge-density bond-order matrix to a absolute tolerance of 1×10^{-4} within 30 iterations. By studying the density matrix after each iteration we observed that some elements were oscillating about a value rather than converging. Therefore, if the SCF calculations were to converge within a reasonable number of iterations, some extrapolation procedure was required. Extrapolating to a "final" density matrix was chosen over extrapolating to a "final" coefficients matrix, due to the fact that the coefficients of degenerate orbitals can vary widely from iteration to iteration and still be valid solutions

Table 1. Atomic orbital charges in formaldehyde at energy convergence

Atom	Orbital	Cycle 7[a]	Cycle 8[a]	Diff.
H_1	1s	1.01344	1.01344	0.00000
H_2	1s	1.01344	1.01344	0.00000
C	2s	1.07827	1.07841	0.00014
O	2s	1.73230	1.73204	0.00026
C	$2p_x$	0.92842	0.92883	0.00041
O	$2p_x$	1.36556	1.36510	0.00046
C	$2p_y$	0.94167	0.94184	0.00017
O	$2p_y$	1.92690	1.92688	0.00002
C	$2p_z$	0.83472	0.83822	0.00350
O	$2p_z$	1.16529	1.16178	0.00351

[a] At cycle 7 the electronic energy was 1.2141777×10^3 eV and at cycle 8 1.2141778×10^3 eV. The relative error was 8.23×10^{-8}.

to the Hartree-Fock equations unless symmetry is explicitely included. Elements of the density matrix do not show such variation. Small errors, representing electron loss or gain, introduced into the density matrix by the extrapolation are corrected in the next cycle of the SCF procedure. Our procedure differs from the usual procedures in three important points: a) It extrapolates on the density matrix rather than the eigenvectors. b) Extrapolation on a given elements is not carried out if that element has met the convergence criterion. c) A trap is provided to prevent extrapolation failures due to linear convergence of some elements.

Method and Application

The extrapolation procedure employed was a modification of Aitken's generalized δ^2 process as described by Winter and Dunning [2]. This procedure is a five point extrapolation which requires saving density matrices from five successive iterations.

Using the notation of Winter and Dunning, the process is described as follows: $P_0^0\ P_0^1\ P_0^2\ P_0^3\ P_0^4$ are specific elements of the density matrix from five successive iterations. (Actually, our program uses the charge density, bond order matrix, i.e. twice the first order density matrix.) An extrapolation triangle is constructed in which successive columns of the triangle are generated by the expression

$$P_{i+1}^m = P_{i-1}^{m+1} + \frac{1}{P_i^{m+1} - P_i^m}. \tag{1}$$

When $i = 0$, P_{i-1}^{m+1} is set to zero. The resulting triangle is

$$\begin{array}{ccccc}
P_0^0 & & & & \\
 & P_1^0 & & & \\
P_0^1 & & P_2^0 & & \\
 & P_1^1 & & P_3^0 & \\
P_0^2 & & P_2^1 & & P_4^0 \\
 & P_1^2 & & P_3^1 & \\
P_0^3 & & P_2^2 & & \\
 & P_1^3 & & & \\
P_0^4 & & & &
\end{array} \tag{2}$$

in which P_4^0 is the final extrapolated value.

This method extrapolates successfully when the points converge asymptotically or oscillate. However, if the extrapolation is attempted on elements which have already converged, random roundoff errors frequently force extrapolation to a value outside of the convergence range. This problem was overcome by testing each element of the density matrix for convergence before extrapolating and extrapolating on only those that had not met the convergence criterion. The method also fails if the points, P_0^i, approach linearity because the denominator in Eq. (1) approaches zero at the third stage in the extrapolation. In an actual calculation, elements of the triangle are tested at different stages of the extrapolation to avoid a failure due to near linearity of the points. At the end of the second stage of the extrapolation the difference between P_2^0 and P_2^1 as well as the difference between P_2^1 and P_2^2 is compared with the convergence criterion. If either of these two differences are less than the criterion the extrapolation is stopped at this point and P_2^1 is used as the final extrapolated value. Usually when one of the differences is very small and the other difference much larger, the correction to P_2^1 to form P_4^0, the final value, is negligible.

At the end of the third stage, P_3^0 and P_3^1 are tested to determine whether or not they are nearly equal. If the original points used in the extrapolation are nearly linear, then the difference between P_3^0 and P_3^1 will be close to zero and the extrapolation will fail. To protect against such a failure, the extrapolation is abandoned if the difference between P_3^0 and P_3^1 would yield a correction to P_2^1 that would be greater than 2 times the maximum difference between P_2^0, P_2^1 and P_2^1, P_2^2, found at the end of the second stage of the extrapolation. When the extrapolation failed

Table 2. Maximum difference between elements of the current and previous density matrices and the number of elements that failed the convergence test

Formaldehyde

Cycle	Unextrapolated		Extrapolated	
	No. failures	Maximum diff.[a]	No. failures	Maximum diff.[a]
2	31	0.13016	31	0.13066
3	31	0.04955	31	0.04955
4	29	0.03931	29	0.03931
5	31	0.01130	31	0.01130
6	24	0.01147	24	0.01147
7	28	0.00313	28	0.00313
8[b]	*11*	*0.00350*	*11*	*0.00350*
9	18	0.00111	(not tested)	
10	3	0.00115	6	0.00035
11	11	0.00041	2	0.00013
12	2	0.00040	0	0.00009
13	4	0.00015		
14	2	0.00015		
15	0	0.00006		

[a] These numbers are actually for the charge-density bond-order matrix, i.e. twice the density matrix.

[b] Energy converged to eight significant figures.

Table 3. Maximum difference between elements of the current and previous density matrices and the number of elements that failed to meet the convergence test

Cytosine

Cycle	Unextrapolated		Extrapolated	
	No. failures	Maximum diff.[a]	No. failures	Maximum diff.[a]
2	467	0.47835	467	0.47835
4	463	0.23970	463	0.23970
6	453	0.12335	453	0.12335
8	438	0.06025	438	0.06025
9	437	0.04238	(not tested)	
10	416	0.02929	215	0.00250
14	282	0.00690	*41*[b]	*0.00064*
16	179	0.00340	18	0.00031
17	131	0.00236	(not tested)	
18	87	0.00165	0	0.00006
23	*16*[b]	*0.00027*		
24	5	0.00019		
25	2	0.00013		
26	0	0.00009		

[a] These numbers are actually for the charge-density, bond-order matrix, i.e. twice the density matrix.
[b] Energy converged to eight significant figures.

at this stage, the original points were fit to a linear least squares equation (of P_0^i as a function of i) and extrapolated to one iteration past the latest iteration. Without this linearity trap, no significant improvement in convergence was obtained by use of the extrapolation. The procedure was tested with both the actual elements of five successive iterations as well as the successive averages of density matrices from six successive iterations. Averaging did not appear to improve the extrapolation. In fact, the damping due to the averaging made many of the extrapolations near enough to the linear case to yield a poor extrapolation.

Table 2 lists, for formaldehyde, the maximum difference in the element of the density matrices that was observed at each cycle and the number of elements that failed the convergence test. Since the extrapolation was done at cycle 8, no testing for convergence was done at cycle 9. Note that with the extrapolation, the problem converged in 12 iterations as opposed to 15 iterations without extrapolation. Table 3 presents similar information for cytosine.

Our subsequent experience has shown that one cycle beyond the extrapolation is sufficient for the density matrix to stabilize. Thus, the extrapolation can be carried out every six cycles. This has been chosen as our standard procedure in our CNDO/2 program. We have performed numerous calculations on systems with up to 146 basis functions. These routinely converge to 5×10^{-5} in all elements of the first-order density matrix in 20 iterations or less. For example, 3-methylxanthine converged to only 5×10^{-4} in 27 unextrapolated iterations, but to 5×10^{-5} in 20 iterations with extrapolation. Overall, the procedure saves from approximately 20 to 50% on the number of iterations required for a given convergence limit.

This extrapolation method can accelerate convergence when criteria other than electronic energy or elements of the density matrix are used. For example, calculations of water with one O–H bond two times the normal length required 34 iterations for the orbital energies to converge to an absolute error less than 1×10^{-4}. The total electronic energy converged to a relative error of less than 1×10^{-8} in 20 iterations and the elements of the density matrix converged to an absolute error less than 1×10^{-4} in 28 iterations. Extrapolating every six cycles, only 24 iterations were required for the orbital energies to converge, 14 for the total electronic energy to converge and 17 for the density matrix to converge.

This example with the water molecule also illustrates how this extrapolation procedure can accelerate convergence when the geometry is less than optimal. This procedure could prove very useful in studies designed to determine preferred conformations and structures of reaction intermediates. However, this extrapolation procedure does not help when the geometry is such that the CNDO/2 calculations would normally diverge, as, for example, in water with an O–H bond length three times normal [3]. In this instance, some diagonal elements of the density matrix maintain nearly the same absolute value, but change sign. In this case, the resulting extrapolated element would be near zero.

In the course of this study we also examined a three point procedure [4]. It was found that the three point procedure was about as good as the five point in most cases. In some instances, however, the five point procedure was clearly superior.

In order for the three-point extrapolation to be successful, the points used must be tested for linearity or divergence and suitable action taken. In our case, we fit the points to a linear least squares line and extrapolated to the next value. In the three point procedure, it was helpful to use the averages of four successive density matrices to define the three points used for the extrapolations.

Acknowledgements. The calculations were done on the Digital Equipment Corp. PDP-10 system at L.S.U.N.O. supported in part by NSF grant no. GJ-131. Partial financial support for the work came from NSF grants no. GY-2632 and GP-10418.

References

1. Pople, J. A., Beveridge, D. L.: Approximate molecular orbital theory. New York: McGraw-Hill Book Company 1970.
2. Winter, N. W., Dunning, T. H., Jr.: Chem. Physics Letters **8**, 169 (1971).
3. Jakubetz, W., Lischka, H., Rosmus, P., Schuster, P.: Chem Physics Letters **11**, 38 (1971).
4. Roothan, C. C. J., Bagus, P. S.: Methods in computational physics, Vol. 2, p. 47. Ed. by B. Alder, S. Fernbach and M. Rotenberg. New York: Academic Press 1963.

Prof. Dr. R. L. Flurry
Department of Chemistry
Louisiana State University in New Orleans
New Orleans, Louisiana 70122, USA

Theoret. chim. Acta (Berl.) 26, 163–170 (1972)
© by Springer-Verlag 1972

An Interpretation of Hund's Rule*

J. KATRIEL

Department of Chemistry, Nuclear Research Centre – Negev, P.O.B. 9001, Beer Sheva, Israel

Received January 28, 1972

An interpretation of Hund's rule is presented. The Pauli principle, the variational principle and the virial theorem are shown to be essentially sufficient to account for the roles of the various energetic components in establishing the inter-multiplet separation.

Es wird eine Interpretation der Hundschen Regel gegeben. Das Pauliprinzip, das Variationsprinzip und das Virialtheorem sind im wesentlichen ausreichend, um die Rollen der verschiedenen energetischen Komponenten beim Zustandekommen der Inter-Multiplett-Separation zu erklären wie hier gezeigt wird.

1. Introduction

It has been obvious since the early days of quantum mechanics that Hund's rule is closely related to the Pauli principle and should be interpreted in terms of it. The conventional interpretation consists of invoking the Pauli principle to argue that electrons with parallel spins tend to stay further away and therefore repel each other to a lesser extent than electrons with antiparallel spins. The observation made by Davidson [1], Lemberger and Pauncz [2] and Messmer and Birss [3] that in some atomic systems the interelectronic repulsion is higher in the higher multiplicity terms corresponding to a given configuration than in the lower multiplicity terms, has disproved this interpretation. A further analysis [4] resulted in the following conjectures, which are more rigorously established in what follows:

1) The nuclear attraction is always higher in absolute value in the higher multiplicity term. For highly positive atomic ions the interelectronic repulsion is lower in the higher multiplicity term. It may, and usually will, become higher in the higher multiplicity term of the isoelectronic neutral atom.

2) The energy difference between different multiplicity terms is always mainly due to differences in the nuclear attractions and not in the interelectronic repulsions.

A preliminary study of the electronic pair distribution [5] exhibited a dramatic reversal of the commonly expected behaviour. The statement that electrons with parallel spins stay mostly further away than electrons with anti-parallel spins was shown not to apply to light neutral atoms.

A quantum mechanical interpretation of Hund's rule is presented in the concluding section of the present contribution. The energetic ordering of different multiplicity terms is rigorously derived within the Hartree-Fock approximation.

---

* Based on a section of a thesis to be submitted to the senate of the Technion – Israel Institute of Technology, in partial fulfilment of the requirements for the D. Sc. degree.

The disturbing observations concerning the roles of the nuclear attraction and of the interelectronic repulsion are accounted for. A study of the electronic pair distribution and of the role of inner shell electrons precedes the final interpretation and constitutes an essential part of the motivation towards it.

2. The Electronic Pair Distribution

The $(1s, 2p)^{1,3}P$ terms of the He isoelectronic sequence have been studied within the independent particle model with the orbitals represented by linear combinations of Gaussian functions.

$$\phi_{1s} = \sum_{i=1}^{N} C_i e^{-\alpha_i r^2}; \qquad \alpha_i = \alpha \varepsilon^{i-1},$$

$$\phi_{2p} = x \cdot \sum_{i=1}^{N} D_i e^{-\beta_i r^2}; \qquad \beta_i = \beta \delta^{i-1}.$$

The four nonlinear parameters $\alpha, \beta, \varepsilon, \delta$ have been independently optimized for each term, as well as the $2N$ linear coefficients. The results for He are presented in Table 1. An analysis of the high Z behaviour of the parameters is carried out in Fig. 1 for the Gaussian approximation ($N=1$). Each one of the parameters satisfies the asymptotic relation $\eta = Z^2(\eta_0 + \eta_1/Z)$ such that η_0 is the same for both the triplet and the singlet and the difference arises because of η_1. The asymptotic values of α and β are just the values obtained by Reeves [16] for the $1s$ and $2p$ orbitals of the hydrogen atom. This is in agreement with the perturbation theoretic results which are constructed so that the zero order wavefunctions are the appropriate combinations of the products of unscreened hydrogenic orbitals. The $2p$ orbital is noted to possess a larger parameter in the triplet than in the singlet. It is thus spatially more contracted towards the nucleus. The reverse situation is observed for the inner $1s$ orbital. This observation is in agreement with Eckart's hydrogenic orbital calculations [7] as well as with analogous results in other atoms [2, 4]. The origin of this behaviour and its fundamental significance will be discussed in the concluding section.

A closer observation is enabled by evaluating the pair distribution function $\varrho(r'_{12}) = \langle \Psi | \delta(r_{12} - r'_{12}) | \Psi \rangle$ or rather the pair distribution difference $\Delta(r_{12}) = {}^3\varrho(r_{12}) - {}^1\varrho(r_{12})$. The latter function is plotted in Fig. 2 for $N = 2, 3, 4, 5$.

Table 1. Independent particle model results for ${}^{1,3}P$ He

N	Energy		Nuclear attraction		Electronic repulsion	
	Triplet	Singlet	Triplet	Singlet	Triplet	Singlet
2	−2.06991	−2.06491	−4.39798	−4.37138	0.25817	0.24156
3	−2.11317	−2.10577	−4.49061	−4.45446	0.26428	0.24293
4	−2.12591	−2.11750	−4.51737	−4.47843	0.26554	0.24343
5	−2.12947	−2.12074	−4.52492	−4.48502	0.26598	0.24355
∞[a]	−2.13143	−2.12246			0.2661	0.2436

[a] Ref. [1].

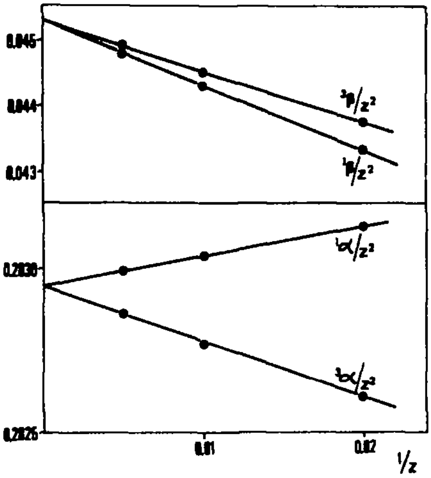

Fig. 1. Asymptotic behaviour of the parameters in the Gaussian approximation

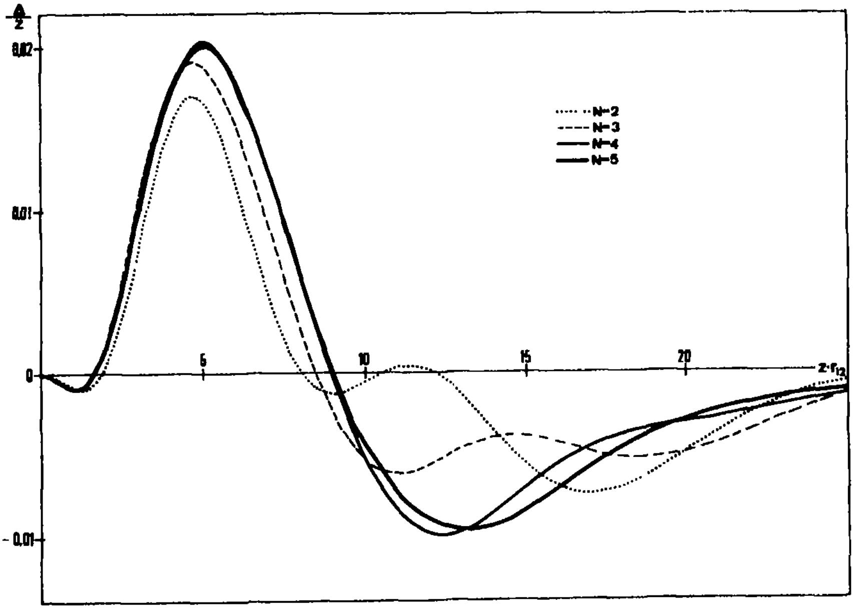

Fig. 2. The pair distribution difference for the $^3P - {}^1P$ terms of He

Preliminary results for $N = 1$ have recently been reported [5]. The results are noted to have practically converged for $N = 5$, which therefore essentially represents the Hartree-Fock limit. They indicate that the conventional assertion according to which parallel spin electrons keep further apart than antiparallel spin electrons does not properly describe the situation studied. It still is true that parallel spin electrons, as a consequence of the Pauli principle, do not come close

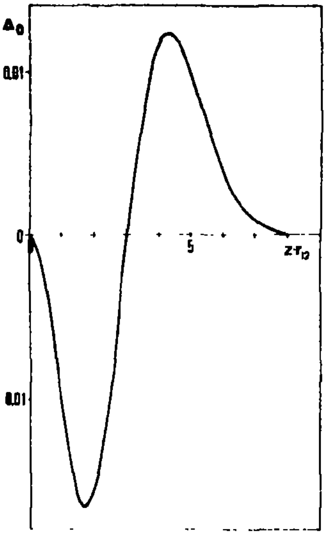

Fig. 3

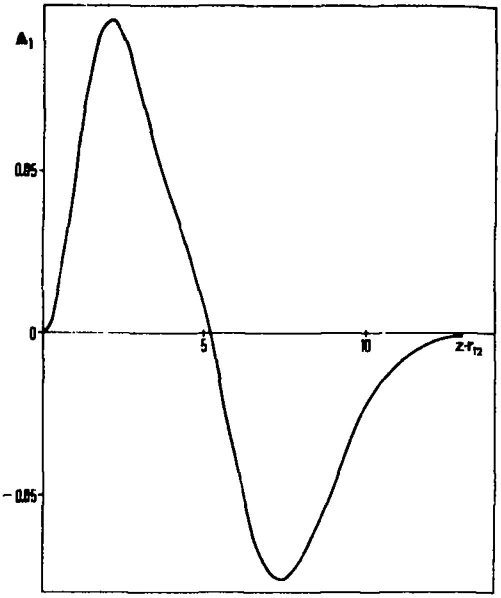

Fig. 4

Fig. 3. The zero order component of the pair distribution difference for the $^3P - {}^1P$ terms of the He isoelectronic sequence, in the Gaussian approximation

Fig. 4. The first order component of the pair distribution difference for the $^3P - {}^1P$ terms of the He isoelectronic sequence, in the Gaussian approximation

together, but the extrapolation from the local behaviour at $r_{12} \simeq 0$ to the whole of space is totally misleading. It has already been observed [5] that for the highly positive isoelectronic ions the pair distribution difference obtains the shape conventionally deduced from the Pauli principle. The asymptotic behaviour of the variational wavefunction as well as the perturbation theoretic expansion suggest that the asymptotic form of the pair distribution difference is

$$\Delta(r_{12})/Z = \Delta_0(\mathbf{r}_{12}) + (1/Z)\cdot\Delta_1(\mathbf{r}_{12})$$

where $\mathbf{r}_{12} = Z\cdot r_{12}$.

$\Delta_0(r_{12})$ represents the pair distribution difference obtained with equal unscreened orbitals for the singlet and the triplet whereas Δ_1 represents the first order correction. Comparing the relation

$$\Delta C = \int_0^\infty \Delta(r_{12})\,dr_{12}/r_{12} = Z\cdot\int_0^\infty \Delta_0(r_{12})\,dr_{12}/r_{12} + \int_0^\infty \Delta_1(r_{12})\,dr_{12}/r_{12}$$

with the perturbation theoretic expression $\Delta C = \alpha(Z - 2Z_0)$ one obtains

$$\int_0^\infty \Delta_0(r_{12})\,dr_{12}/r_{12} = \alpha < 0 \quad\text{and}\quad \int_0^\infty \Delta_1(r_{12})\,dr_{12}/r_{12} = -2\alpha Z_0 > 0\,.$$

From the normalization of the pair distributions it follows that $\int_0^\infty \Delta_0(r_{12})\,dr_{12} = 0$ and similarly for $\Delta_1(r_{12})$. $\Delta_0(r_{12})$ is therefore necessarily negative at low r_{12} and positive at higher separation, in accordance with the Pauli principle. This is just the behaviour expected for a pair distribution difference constructed with equal orbitals for both terms. $\Delta_1(r_{12})$ is just reversed, being positive at low interelectronic separations and negative at high ones. The results of a numerical analysis of high Z values of the pair distribution difference in the Gaussian approximation are plotted in Figs. 3 and 4. The qualitative agreement with the discussion just made is entirely satisfactory. The reversal in the interelectronic repulsion as well as in the values of $\langle r_{12}\rangle$ and $\langle r_{12}^2\rangle$ [5] is therefore accounted for by the first order term in the pair distribution difference. The conventional argument is correct only to zero'th order and therefore fails as the first order correction becomes important, namely at sufficiently high values of the perturbation parameter $1/Z$ (sufficiently low Z).

3. The Role of the Inner Shells

In all the systems hitherto considered in connection with the interpretation of Hund's rule there are at least two occupied major shells. A different situation occurs in autoionizing configurations such as $(2s, 2p)$ and $2p^2$. It has been shown [4] that independent scaling of the wavefunction is sufficient to associate most of the energetic difference between the different multiplicity terms with nuclear attraction rather than with interelectronic repulsion differences. Scaling has further been shown to be incapable of reversing the order of interelectronic repulsions. Independent optimization of the parameters, even with a minimal basis set of Slater or Gaussian functions, is sufficient to give rise to this reversal in those cases in which it is observed in more accurate computations. The discussion in the previous section indicated that the reversal of interelectronic repulsions is due to the first order correction to the wavefunction, in a perturbation theoretic approach. This correction is asymptotically similar to that obtained by variationally optimizing a wavefunction constructed of Slater orbitals which in the limit $Z \to \infty$ becomes identical with the zero order wavefunction in perturbation theory. The fact that optimized Slater orbital computations lead to the correct qualitative conclusions concerning the relative magnitudes of interelectronic repulsions is thus fairly established. For configurations with only one shell occupied, such as $2p^2$ and essentially also $(2s, 2p)$ there is only one variational parameter in the minimal basis set, and therefore complete optimization is equivalent to simple scaling. For such configurations no reversal of the order of interelectronic repulsions can be effected by the independent optimization of the parameter within the minimal basis set scheme. In view of the comments just made this is sufficient to exclude such reversal even in accurate computations.

Approximate perturbation expansions of the Hartree-Fock solutions for the terms derived from the $2p^2$ configuration of the He isoelectronic sequence are available [8]. The interelectronic repulsion contribution can be obtained by application of the Hellmann-Feynman theorem. The reversal is easily noted not to occur for $Z > 1$. It therefore seems that the reversal of interelectronic respulsions is closely related to the interrelationship between an inner and an outer shell.

4. An Interpretation of Hund's Rule

A theoretical interpretation of Hund's rule should account for the energetic order of terms corresponding to a given configuration. It should also, desirably, account for the roles of the various energetic components and for the characteristic qualitative features of the wavefunctions corresponding to the different terms.

The energetic aspect of Hund's rule is accounted for as follows. Consider two terms belonging to a certain configuration. For the lower multiplicity term we obtain the best wavefunction within the independent particle model. We shall use the one electron orbitals thus obtained to construct an approximate wavefunction for the higher multiplicity term. The energy corresponding to this wavefunction differs from that of the lower multiplicity term only in the interelectronic repulsion. Due to the Pauli principle, the interelectronic repulsion is lower for the higher multiplicity term if the same one electron orbitals are used. The orbitals are already optimized for the lower multiplicity term, but they may be further improved for the higher multiplicity term. Due to the variational principle this improvement of the orbitals can only lower the energy and thus increase the intermultiplet separation. It is thus shown that within the independent particle model (Hartree-Fock approximation) the higher multiplicity terms is lower in energy, in accordance with Hund's rule. The energetic order is therefore a straightforward consequence of the Pauli principle. The conventional reasoning is an essential part of the argumentation just made. It is incorporated in the particular sequence of arguments in such a way as to provide, in conjunction with the variational principle, a generally valid prediction of the ordering of terms, within the Hartree-Fock approximation. This would have constituted an improvement even if no difficulties had been noted with respect to the conventional interpretation, as the Hartree-Fock approximation is considerably more sophisticated than the approximation conventionally employed in connection with Hund's rule, namely the one in which the same one electron orbitals are used for both terms. It is obvious that the relaxation of the shape of the orbitals in the higher multiplicity term towards their Hartree-Fock shape may result in an extreme change in the roles of the various energetic components, but as far as the total energy is to be accounted for this is of no relevance. Our energetic argument is essentially that a wavefunction can be formed with the lower multiplicity orbitals but with the higher multiplicity symmetry, whose energy is lower than the Hartree-Fock energy of the lower multiplicity term, due to the Pauli principle, but higher than the energy of the higher multiplicity term, due to the variational principle. The philosophy behind this argument is similar to that discussed by Feinberg and Ruedenberg [9] in a different context. The only difficulty which still remains, as far as the energy is concerned, is associated with effect of correlation. Due to the fact that the correlation energy is higher in the lower multiplicity term [10] it is obvious that correlation tends to decrease the energetic difference between the different multiplicity terms. A satisfactory and general ab initio argument which would guarantee that correlation could never reverse the order of terms predicted within the Hartree-Fock approximation is not yet available. One should, however, note that from the point of view of $1/Z$ perturbation theory the intermultiplet separation is a first order effect because even the zero order wavefunction, though not the zero order energy, is different for the different terms. Correlation is a second order effect because both in the Hartree-Fock and in the exact schemes the zero order wavefunction is the same antisymmetrized product of hydrogenic functions. It is therefore highly plausible, though not rigorously guaranteed, that correlation effects are of minor significance as far as the qualitative features of the ordering of the multiplets are considered.

To account for the roles of the various energetic components we note that in the first step we have constructed the higher multiplicity wavefunction using the lower multiplicity Hartree-Fock orbitals. As a consequence of this construction the one electron energy (kinetic and nuclear attraction) is not changed whereas the interelectronic repulsion decreases. The virial theorem, which is satisfied for the lower multiplicity wavefunction, is not satisfied for the one thus obtained for the higher multiplicity term. The most naive improvement, simple scaling, would result in a uniform contraction of the whole wavefunction. This is in only partial agreement with more accurate treatments. If there are two different major shells then the inner orbitals remain essentially hydrogenic, whereas the outer electrons are rather strongly screened by the inner ones. It is therefore obvious that the relaxation necessary for the satisfaction of the virial theorem will mainly affect the outer orbitals. As the kinetic energy has to increase these orbitals ought to contract. As a consequence of the fact that they account for only a small fraction of the total energy the contraction of these orbitals is considerably more significant than the contraction expected assuming uniform scaling. Along with the contraction of the outer orbitals we observe a slight expansion of the inner orbitals which is probably due to the slight screening due to the penetrating part of the contracted outer orbitals. The balance, which occurs so as to satisfy the virial theorem, results in an increase in both the kinetic energy and the nuclear attraction, due to the contraction of the outer orbitals and their approach towards the nucleus. The approach towards the inner electrons results in an increase of the interelectronic repulsion which is more significant than under the assumption of uniform scaling. It is therefore rather plausible that inversion of the order of interelectronic repulsions may occur. The total energy increases quadratically with the nuclear charge whereas the interelectronic repulsion increases only linearly. Thus, upon increasing the nuclear charge, the amount of contraction of the outer orbitals decreases so that the change in the interelectronic repulsion is less significant. It is, however, obvious that the change predicted by the scaling model [4], in which both orbitals contract, is a lower bound to the change observed in the Hartree-Fock approximation in which the much higher contraction of the outer orbitals and the concomitant expansion of the inner orbitals are much more effective in increasing the interelectronic repulsion. It is therefore shown, within the Hartree-Fock approximation, that nuclear attraction differences are always the dominant ones, as this has been shown to be true for the scaling approximation [4].

The fact that for configurations with only one major shell there is no reversal of interelectronic repulsions fits in rather logically at this stage. The only source of increase of the interelectronic repulsion is the contraction of the single shell which is necessary for the kinetic energy to increase so as to satisfy the virial theorem. It is clear that this contraction causes an increase in both the kinetic energy and the nuclear attraction which is more rapid than the increase in the interelectronic repulsion. The whole change essentially necessary in the kinetic energy is of the order of magnitude of the interelectronic repulsion difference before the orbital relaxation was introduced. This change is effected with only a minor change in the interelectronic repulsion. A measure of the relative sensitivity of the interelectronic repulsion and the nuclear attraction to a contraction of the orbitals is the ratio of the screening due to the other electrons and the total nuclear charge. Hence, no reversal of the interelectronic repulsion can be expected without the expansion of an inner shell towards the contracting outer shell.

It seems appropriate at this stage to characterize the difficulties encountered with respect to the interpretation of Hund's rule. It is obvious that the term in the Hamiltonian which is the origin of the energy difference between the different multiplets of a given configuration is the interelectronic repulsion. It is nevertheless observed that the introduction of interelectronic repulsion in the Hamiltonian modifies the wavefunction so as to associate the energetic effect with the one electron part of the Hamiltonian. This is a consequence of the non-commutativity of the interelectronic repulsion with the one electron Hamiltonian. The quantum mechanical origin of Hund's rule is thus more strictly emphasized than in the conventional electrostatic interpretation [11] which takes into account the quantum mechanical nature of the problem by evoking the Pauli principle but disregards the rather surprising dynamic consequences.

Acknowledgements. Most helpful discussions with Prof. R. Pauncz are gratefully acknowledged. It is a pleasure to thank Prof. J. W. Linnett for his interest and encouragement.

References

1. Davidson, E. R.: J. chem. Physics **42**, 4199 (1965).
2. Lemberger, A., Pauncz, R.: Acta physica hung **27**, 169 (1969).
3. Messmer, R. P., Birss, F. W.: J. physic. Chem. **73**, 2085 (1969).
4. Katriel, J.: Theoret. chim. Acta (Berl.) **23**, 309 (1972).
5. -- Physic. Rev. A (in press).
6. Reeves, C. M.: J. chem. Physics **39**, 1 (1963).
7. Eckart, C.: Physic. Rev. **36**, 878 (1930).
8. Eliezer, I., Moualem, A.: Theoret. chim. Acta (Berl.) **23**, 39 (1971).
9. Feinberg, M. J., Ruedenberg, K.: J. chem. Physics **54**, 1495 (1971).
10. Clementi, E.: J. chem. Physics **38**, 2248 (1963).
11. Condon, E. U., Shortley, G. H.: The theory of atomic spectra. Cambridge: University Press 1935; Koster, G. F.: Physic. Rev. **98**, 514 (1955).

J. Katriel
Nuclear Research Centre-Negev
P.O.B. 9001
Beer Sheva, Israel

Theoret. chim. Acta (Berl.) 26, 171—178 (1972)
© by Springer-Verlag 1972

A Remark on the Comparison between the Roothaan Open Shell and Half-Electron Method

P. Čársky and R. Zahradník
Institute of Physical Chemistry, Czechoslovak Academy of Sciences, Prague, Czechoslovakia

Received March 15, 1972

Using Pople π-electron and CNDO/2 approaches for various open-shell ground states, a comparison is made for total SCF energies calculated by the half-electron and Roothaan methods. Types of electronic configurations are ascertained for which the two methods yield identical total energies.

Unter Anwendung der π-Elektronen- und der CNDO/2-Näherung werden die totalen SCF-Energien für verschiedene "open shell"-Grundzustände im "half electron"-Verfahren und im Roothaanschen Verfahren verglichen. Es werden Typen von elektronischen Konfigurationen ermittelt, für die beide Verfahren zu der gleichen Gesamtenergie führen.

En utilisant les méthodes π-électroniques de Pople et CNDO/2 pour des états fondamentaux avec couche incomplète différente, on fait la comparaison pour les énergies totales de champs autocohérent calculées par la méthode «sémiélectronique» et celle de Roothaan. On a determiné les types des configurations électroniques pour lesquels ces deux méthodes livrent les énergie totales identiques.

Introduction

The open shell SCF procedure of Longuet-Higgins and Pople [1] has proved very useful for the study of electronic spectra and ground state properties of radicals [2] having a singly occupied nondegenerate orbital. Dewar and co-workers [3] derived this procedure in a different way, extended it to treatments of triplet states [4] and called it "the half-electron method". Recently a general extension of this method was reported [5] which makes it possible to treat any electronic configuration regardless of symmetry and spin multiplicity.

The half-electron procedure is an approximate open shell method because some singly excited configurations interact with the ground state configuration [2]. Some authors argue that its deficiencies are negligible, inasmuch as its results for heat of formation of radicals are reasonable [2, 3, 6–8], and for many other characteristics are very close [9] to values given by the Roothaan open shell method [10]. Others (e.g. [11]) prefer the Roothaan method, which can be anticipated to give more accurate heats of formation. Nevertheless this method is inferior to the half-electron method in two respects:

1. Open shell calculations require an entirely new computer program, whereas the half-electron method affords open shell SCF results by means of a closed shell program with only slight modifications (cf. the next section).

2. In general the Roothaan SCF procedure is slower to converge, sometimes even diverging [12].

In the present paper we compare the two methods and examine the possibility of performing routine semiempirical calculations on systems with degenerate open shells.

Calculations

We employed the standard SCF π-electron method of Pople and the standard CNDO/2 method, combining them with the half-electron or Roothaan open shell procedures. In the π-electron calculations we used the following parameters: $I_C = 11.22$ eV; $\gamma_{CC} = 10.53$ eV; two-centre repulsion integrals were evaluated by means of the formula of Mataga and Nishimoto. If the half-electron method is adopted, the F matrix elements in the frame of both computational schemes remain unchanged, except for the new definition of the electron-density and bond-order matrix

$$P_{\mu\nu} = \sum_k 2c_{k\mu}c_{k\nu} + \sum_m 2fc_{m\mu}c_{m\nu}, \qquad (1)$$

where k and m run over closed shell and open shell MO's respectively, and f is the fractional occupation [10] of the open shell (cf. Table 1). Both in the π-electron and CNDO/2 treatments, the half-electron total energies of open shell ground states were calculated by means of the following formulas [5]

$E = E_R - \frac{1}{4}J_{mm}$ Doublet, nondegenerate φ_m singly occupied (2)

$E = E_R - \frac{1}{4}(J_{mm} + J_{nn} + 2K_{mn})$ Triplet (3)

$E = E_R - \frac{1}{16}(J_{mm} + J_{nn} + 4J_{mn} - 2K_{mn})$ Doublet $\varphi_m \pm \varphi_n$ and $\varphi_m^2\varphi_n \pm \varphi_m\varphi_n^2$ states (4)

where φ_m and φ_n are degenerate, J and K have usual meaning of coulomb and exchange integrals, and

$$E_R = \sum_k \varepsilon_k + \sum_m f\varepsilon_m + \frac{1}{2}\sum_\mu \sum_\nu H_{\mu\nu}P_{\mu\nu}, \qquad (5)$$

where ε_k and ε_m are orbital energies of closed and open shells.

The use of the Roothaan open shell method in the PPP and CNDO/2 treatments has been described elsewhere [2, 13, 14]. Here we repeat only the formulas for the total energy

$$E = E_R - \sum_\mu \sum_\nu Q_{\mu\nu}(D_{C,\mu\nu} + fD_{O,\mu\nu}), \qquad (6)$$

Table 1. Numerical constants for open shell states (φ_m and φ_n are degenerate) [10]

Configuration	Spin	f	α	β
φ_m	Doublet	$\frac{1}{2}$	0	-2
$\varphi_m\varphi_n$	Triplet	$\frac{1}{2}$	0	-2
$\varphi_m \pm \varphi_n$	Doublet	$\frac{1}{4}$	$\frac{4}{3}$	$\frac{4}{3}$
$\varphi_m^2\varphi_n \pm \varphi_m\varphi_n^2$	Doublet	$\frac{3}{4}$	$\frac{4}{9}$	$\frac{4}{9}$

where E_R is given by (5) and

$$Q_{\mu\nu}=\delta_{\mu\nu}2\alpha\sum_{\sigma}D_{O,\sigma\sigma}\gamma_{\mu\sigma}-\beta\gamma_{\mu\nu}D_{O,\mu\nu}\,. \tag{7}$$

$$D_{C,\mu\nu}=\sum_{k}c_{k\mu}c_{k\nu}\,;\quad D_{O,\mu\nu}=f\sum_{m}c_{m\mu}c_{m\nu}\,. \tag{8}$$

Total density matrix elements used in (5) are given by

$$P_{\mu\nu}=2(D_{C,\mu\nu}+D_{O,\mu\nu})\,. \tag{9}$$

Numerical constants f, α, β depending on the specific case, are summarized in Table 1. Formula (6) can be rewritten as

$$E=E_R-f^3\sum_{m}\sum_{n}(2\alpha J_{mn}-\beta K_{mn})-f\sum_{k}\sum_{m}(2\alpha J_{km}-\beta K_{km})\,. \tag{10}$$

In π-electron calculations, idealized molecular geometries were assumed, i.e. $r_{CC}=1.4$ Å and $\sphericalangle CCC=120°$. In nonalternant hydrocarbons, regular five and seven-membered rings were considered. For BH_2, NH_2, HCO, NO_2, NF_2, CNC, N_2O^+, N_3, BO_2 [15], O_2, O_2^+ [16] radicals, experimental geometries were employed. The CNC anion was calculated for the same geometry as the CNC radical. In the cyclopropenyl anion and radical, and in the cyclopentadienyl cation the idealized geometry ($r_{CH}=1.1$ Å, $r_{CC}=1.4$ Å) was considered. For the remaining systems, the following geometries were assumed (the order is the same as in Tables 3–6):

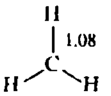

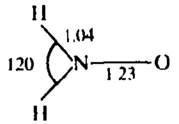

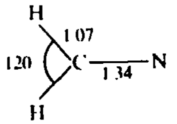

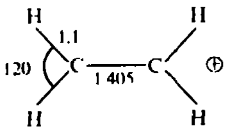

[2]

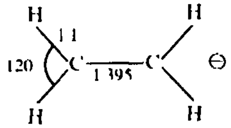

[2]

$\mathrm{H}\overset{1.1}{\;}\mathrm{C}\cdot \quad \mathrm{H}\;\;\mathrm{C}\overset{1.28}{\;}\mathrm{C}\overset{1.24}{\;}\mathrm{N}$ (both triplet and radical)

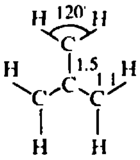

$\mathrm{N}\overset{1.15}{-\!-}\mathrm{O} \qquad \mathrm{N}\overset{1.20}{-\!-}\mathrm{C}\overset{1.20}{-\!-}\mathrm{O}$

$\mathrm{O}\overset{1.17}{-\!-}\mathrm{C}-\!-\!-\mathrm{O}^{\oplus} \qquad \mathrm{H}\overset{1.06}{-\!-}\mathrm{C}\overset{1.20}{-\!-}\mathrm{C}\overset{1.38}{-\!-}\mathrm{C}-\;-\mathrm{C}-\!-\!-\mathrm{H}^{\oplus}$

Results and Discussion

The results of π electron calculations for unsaturated radicals having a singly occupied nondegenerate orbital are summarized in Table 2. Here both methods yield very similar results; except for the fulvene anion, the differences are negligible from the practical point of view. In light of these results, one can understand why heats of atomization of conjugated radicals are so well interpreted by the half-electron method [2, 3]. The radicals listed in Table 3 have formally the same electronic configuration – the nondegenerate frontier orbital is occupied by one electron. A somewhat more complicated picture of CNDO/2 results in Table 3 can be explained in part by examination of the formula for the open shell Roothaan total energy. On putting $f=\frac{1}{2}$, $\alpha=0$, and $\beta=-2$, (10) reduces to

Table 2. Total SCF energies obtained by the open shell calculation in the π electron approximation for conjugated systems having a nondegenerate singly occupied molecular orbital. (All entries are in eV)

Radical	LHP[a]	R[b]	Difference
Butadiene$^+$	− 40.074	− 40.077	0.003
Butadiene	− 51.984	− 51.987	0.003
Hexatriene$^-$	− 78.001	− 78.004	0.003
Octatetraene$^-$	−103.799	−103.806	0.007
Decapentaene$^-$	−129.480	−129.491	0.011
Dodecahexaene$^-$	−155.091	−155.106	0.015
Allyl	− 36.711	− 36.711	0.0
Pentadienyl	− 62.153	− 62.175	0.022
Naphthalene$^-$	−132.436	−132.441	0.005
Anthracene	−185.310	−185.331	0.021
Tetracene	−237.885	−237.910	0.025
Pentacene	−290.300	−290.330	0.030
Phenanthrene	−185.167	−185.188	0.021
Benz-[a]-anthracene$^-$	−237.923	−237.960	0.037
Chrysene$^-$	−237.995	−238.011	0.016
Pyrene	−212.274	−212.274	0.0
Phenalenyl	−169.022	−169.022	0.0
Fulvene$^+$	− 66.785	− 66.797	0.012
Fulvene$^-$	− 79.661	− 79.859	0.198
Azulene$^+$	−120.092	−120.159	0.067
Azulene$^-$	−132.176	−132.198	0.022
Acenaphthylene	−159.681	−159.685	0.004

[a] The method of Longuet-Higgins and Pople, i.e. the half-electron method.
[b] The Roothaan method.

$$E=E_R-\tfrac{1}{4}J_{mm}-\sum_k K_{km}\,. \tag{11}$$

If all exchange K_{km} integrals vanish, (11) becomes equivalent to (2) and the Roothaan SCF procedure becomes equivalent to that of the half-electron method, the corresponding SCF eigen-values and eigen-vectors being identical. This is the case with CH_3 and NH_2 where an unpaired electron occupies a $2p_z$ atomic orbital of carbon and nitrogen, respectively, and with the ethylene cation where an unpaired electron occupies a bonding π molecular orbital. The same situation

Table 3. Total CNDO/2 energies for systems having a non-degenerate singly occupied molecular orbital. (All entries are in eV)

Radical	LHP[a]	R[a]	Difference
BH_2	− 133.856	− 134.493	0.637
NH_2	− 352.391	− 352.391	0.0
HCO	− 704.143	− 704.178	0.035
NO_2	−1317.506	−1317.632	0.126
NF_2	−1824.938	−1825.070	0.132
CH_3	− 248.021	− 248.021	0.0
H_2CN	− 541.969	− 542.220	0.251
H_2NO	− 858.385	− 858.521	0.136
Ethylene$^+$	− 449.570	− 449.570	0.0
Ethylene$^-$	− 460.189	− 460.189	0.0

[a] See footnotes in Table 2.

occurs, if *one* from the K_{km} integrals, say K_{im}, is non-zero and the singly occupied orbital, φ_m, is *unambiguously* determined by molecular symmetry. By considering the forms of the $\hat{F}$ operators [5, 10]

$$\hat{F}_{\text{half-electron}} = \hat{H}_c + \sum_k (2\hat{J}_k - \hat{K}_k) + f \sum_m (2\hat{J}_m - \hat{K}_m), \tag{12}$$

$$\begin{aligned}\hat{F}_{\text{Roothaan}} = \hat{H}_c + \sum_k (2\hat{J}_k - \hat{K}_k) + f \sum_m (2\hat{J}_m - \hat{K}_m) \\ + 2\alpha(\hat{L}_T - \hat{J}_0) - \beta(\hat{M}_T - \hat{K}_0)\end{aligned} \tag{13}$$

and by comparing the respective expanded $\langle\varphi|\hat{F}|\varphi\rangle$ terms, we obtain for orbital energies

$$\varepsilon_k^{\text{Roothaan}} = \varepsilon_k^{\text{half-electron}} + K_{km}, \tag{14}$$

$$\varepsilon_m^{\text{Roothaan}} = \varepsilon_m^{\text{half-electron}}. \tag{15}$$

Thus the effect of both $\hat{F}$ operators on closed shell and open shell orbitals is the same with exception of φ_i. Moreover, φ_m being unambiguously determined by molecular symmetry, all corresponding eigen-vectors (including φ_i) yielded by the two methods are identical. Also orbital energies of all closed and open shells are identical, except φ_i for which (14) holds. By introducing (14) and (15) into (5) and (11), K_{im} cancels and the total energy in both computational schemes becomes identical. This is the case of the ethylene anion, φ_i and φ_m being the bonding and antibonding π MO's and of the allyl radical (cf. Table 2), where φ_i and φ_m are bonding and nonbonding π MO's. For the remaining six radicals in Table 3, the average difference between the total energies given by the two methods amounts to 0.22 eV, i.e. to about 5 kcal/mole. In actual calculations on the heats of formation of radicals, as e.g. in the MINDO/2 treatment, this difference will probably be smaller. From (11) and (14) it can be inferred that the total energy differences are proportional to the K_{km} terms. As a consequence, replacement of theoretically calculated repulsion integrals by the smaller semiempirical values in the computation should give a smaller total energy difference. If the energy difference were still greater than the range of experimental errors, a small scaling factor could be employed as the half-electron values are always higher (or equal) to Roothaan values. Another way how to arrive at more accurate total energies is to mix the half-electron SCF ground state with several A-type and B-type singly excited configurations (for a description of the CI treatment see [2]).

Table 4 Total CNDO/2 energies for triplet state configurations having a doubly degenerate frontier orbitals. (All entries are in eV)

System	Half-electron method	Roothaan method	Difference
CNC	677.587	− 677.587	0
CCN	− 681.278*	no convergence	
O_2	− 1000.588	− 1000.588	0
CH_2	− 219.921	− 219.921	0
Trimethylenemethane	− 884.967	− 884.967	0
Cyclopropenyl	− 627.996	627.996	0
Cyclopentadienyl$^+$	− 1052.505	− 1052.505	0

* No convergence unless the damping [17] with the factor 0.5 is employed.

Table 4 comprises data for several triplet state configurations having frontier φ_m and φ_n degenerate. Here analogous expressions to (11), (14) and (15) hold:

$$E = E_R \quad \tfrac{1}{4}(J_{mm} + J_{nn} + 2K_{mn}) - \sum_k K_{km} - \sum_k K_{kn}, \tag{16}$$

$$\varepsilon_k^{\text{Roothaan}} = \varepsilon_k^{\text{half-electron}} + K_{km} + K_{kn}, \tag{17}$$

$$\varepsilon_m^{\text{Roothaan}} = \varepsilon_m^{\text{half-electron}} \tag{18}$$

For all systems considered in Table 4 except CCN^- the open shell φ_m and φ_n orbitals are unambiguously determined by molecular symmetry and all exchange integrals K_{km} and K_{kn} vanish except one K_{im} and one K_{in} integral. In CH_2 all these exchange integrals vanish. By comparing (3) and (16) and by making use of arguments given above in the discussion of doublet states, one can understand why both open shell treatments give the same total energies here also. In less symmetrical molecules such as CCN^-, where a total energy difference is to be expected, the divergence of the Roothaan SCF procedure precludes any comparison.

Divergence of the Roothaan procedure was also found with all $\varphi_m \pm \varphi_n$ and $\varphi_m^2\varphi_n \pm \varphi_m\varphi_n^2$ doublet systems listed in Tables 5 and 6. Either the oscillation of orbital levels reported by Sleeman [12] occured (as in the case of O_2^+), or the electronic configuration changed in the first iteration, the frontier open shell becoming nondegenerate. Neither damping [17] nor continuation in the SCF procedure with changed f, α, and β values lead to convergence. Unfortunately, no simple comparison of (4) and (10) serves to show where the Roothaan method can safely be replaced by the half-electron method. Therefore it seems the total energies obtained by the half-electron calculations for such systems as those in Tables 5 and 6 must be tested by means of the observed heats of formation.

Table 5. Total CNDO/2 energies calculated by the half-electron method for doublet state $\phi_m \pm \phi_n$ configurations having a doubly degenerate frontier orbital occupied by one electron (in eV)

System	Half-electron method
CNC	−678.666
CCN	−680.763
O_2^+	−986.723
NO	−813.424
Cyclopropenyl	−631.014

Table 6. Total CNDO/2 energies calculated by the half-electron method for doublet $\phi_m^2\phi_n \pm \phi_m\phi_n^2$ configurations having a doubly degenerate frontier orbital occupied by three electrons (in eV)

System	Half-electron method
NCO	no convergence
NNO^+	no convergence
NNN	− 941.576
OCO^+	−1171.165
OBO	−1090.641
$Diacetylene^+$	− 783.753

References

1. Longuet-Higgins, H. C., Pople, J. A.: Proc. physic. Soc. **68** A, 591 (1955).
2. Zahradník, R., Čársky, P.: Progr. physic. org. Chem., submitted for publication.
3. Dewar, M. J. S., Hashmall, J. A., Venier, C. G.: J. Amer. chem. Soc. **90**, 1953 (1968).
4. Trinajstić, N.: Chem. Comm. **1970**, 646.
5. Ellison, F. O., Matheu, F. M.: Chem. Physics Letters **10**, 322 (1971).
6. Baird, N. C., Dewar, M. J. S.: J. chem. Physics **50**, 1262 (1969).
7. Dewar, M. J. S., Haselbach, E.: J. Amer. chem. Soc. **92**, 590 (1970).
8. Kollmar, H.: Chem. Physics Letters **8**, 533 (1971).
9. Čársky, P., Zahradník, R.: Collect. czechoslov. chem. Commun. **36**, 961 (1971).
10. Roothaan, C. C. J.: Rev. mod. Physics **32**, 179 (1960).
11. Hoyland, J. R.: Theoret. chim. Acta (Berl.) **22**, 229 (1971).
12. Sleeman, D. H.: Theoret. chim. Acta (Berl.) **11**, 135 (1968).

13. Adams, O. W., Lykos, P. G.: J. chem. Physics **34**, 1444 (1961).
14. Zahradník, R., Čársky, P.: J. physic. Chem. **74**, 1235 (1970).
15. Herzberg, G.: Molecular spectra and molecular structure, Part III. New York: Van Nostrand Reinhold Comp. 1966.
16. Sutton, L. E. (Editor): Tables of interatomic distances and configurations in molecules and ions, Special Publ No. 11 London: The Chemical Society 1958.
17. Ehrenson, S.: Theoret. chim. Acta (Berl.) **14**, 136 (1969).

Dr. P. Čársky
Dr. R. Zahradník
Institute of Physical Chemistry
Czechoslovak Academy of Sciences
7 Máchova
Prague 2, Vinohrady
Czechoslovakia

Theoret. chim. Acta (Berl.) 26, 179–186 (1972)
© by Springer-Verlag 1972

Relationes

The Method of Non-Paired Spatial Orbitals

II. The Benzyl Radical

D. M. Hirst and Mary E. Linington

Department of Molecular Sciences, The University of Warwick, Coventry CV4 7AL, England

Received February 28, 1972

The calculation of non-paired spatial orbitals and alternant molecular orbital wavefunctions for the benzyl radical is described. The NPSO and AMO methods give comparable energy lowerings which indicate that they make substantial allowance for electron correlation. The calculated spin densities are not in very good accord with experiment and it is thought that this reflects inadequacies in the integral approximations used.

1. Introduction

In a recent paper [1] we have described the extension of the method of non-paired spatial orbitals (NPSO) to the ten electron π-systems of naphthalene and azulene and compared the NPSO method with the alternant molecular orbital (AMO) calculations of Pauncz and his coworkers [2, 3]. Applications of the NPSO method to open shell systems have so far been restricted to three electron systems [4, 5]. We describe in this paper the application of the method to the seven electron π-system of the benzyl radical.

The benzyl radical continues to be of great interest to theoretical chemists (e.g. [6–8]) on account of the discrepancy between the calculated spin densities and the experimental proton hyperfine coupling constants. Suggestions for resolving this discrepancy have recently been put forward [7, 8].

The AMO method has had limited application to open shell systems and spin density calculations. Apart from calculations on the allyl radical [9, 10] and trimethylene methyl [11] in which the energies were optimised, the only other AMO calculations on such systems seem to be spin density calculations [12, 13] in which the AMO parameters were determined by criteria other than minimum energy. We therefore performed AMO calculations on the benzyl radical both for comparison with the NPSO results and for their intrinsic interest.

Molecular orbital calculations were also made in order to assess the lowering in energy resulting from the use of correlated wavefunctions.

2. Methods

a) Molecular Orbital Calculations

We performed three types of MO calculations. The crudest method used was to calculate the eigenvectors of the overlap matrix. This procedure yields the Hückel-Wheland orbitals [16] and is considerably inferior to self-consistent field

(SCF) methods. For open shell SCF calculations, one has the choice between the restricted Hartree-Fock (RHF) method [14] and the unrestricted Hartree-Fock (UHF) method [15] which makes allowance for electron correlation by using different orbitals for the α and β electrons. The UHF method has the disadvantage that the wavefunction is not a spin eigenfunction. Both methods were used in this work.

A regular geometry was assumed with bond lengths of 1.40 Å. Two sets of calculations were made using the Ruedenberg method [16] and the Goeppert-Mayer Sklar (GMS) [17] method for the calculation of one electron integrals. All overlap integrals were included and the two electron integrals were calculated from accurate Coulomb integrals by the Mulliken approximation. The integrals used are tabulated in the Appendix.

b) Alternant Molecular Orbital Method

Calculations were made by the methods described by Paunez [18] using the eigenvectors of the overlap matrix as starting orbitals. If the molecular orbitals are denoted φ_i $(i = 1, 2 \ldots 7)$ in order of ascending energy, the alternant molecular orbitals ψ_j and $\bar{\psi}_j$ $(j = 1, 2, 3)$ are given by

$$\psi_j = \cos\theta \varphi_j + \sin\theta \varphi_{8-j}\,, \tag{1}$$

$$\bar{\psi}_j = \cos\theta \varphi_j - \sin\theta \varphi_{8-j}\,, \tag{2}$$

where θ is a parameter which is varied to minimise the energy. It is usual to report the optimum value of θ in terms of a parameter λ which is, in fact, $\cos 2\theta$. ψ_4 is simply the non-bonding orbital φ_4. The wavefunction is then given by

$$\Psi = O_D A [\psi_1 \psi_2 \psi_3 \psi_4 \bar{\psi}_1 \bar{\psi}_2 \bar{\psi}_3]\,, \tag{3}$$

where O_D is a doublet projection operator and A is the antisymmetrizer. Spin densities were calculated using the methods of Paunez [18] and Harris [19]. It should be noted that there are typographical errors in Eq. (6.72) of Ref. [18]. The correct formula is

$$\begin{aligned} \langle \Psi | F_z | \Psi \rangle = \frac{1}{2}\,\frac{S}{S+1} \Bigg\{ \sum_{i=1}^{\nu} \Bigg[\sum_{r=0}^{\nu-1} (-1)^r C_r{}^i S_r [\,|a_1(0)|^2 \\ - |\bar{a}_1(0)^2] - \sum_{r=0}^{\nu-1} (-1)^{r+1} C_{r+1}{}^i S_r [-2|a_1(0)|^2 + a_1^*(0)\,\bar{a}_1(0)\,\lambda_i \\ + \bar{a}_1^*(0)\,a_1(0)\,\lambda_i] \Bigg] + \sum_{i=\nu+1}^{\mu} |\psi_i(0)|^2 \sum_{r=0}^{\nu} (-1)^r (C_r - 2C_{r+1}) S_r \Bigg\}. \end{aligned} \tag{4}$$

c) Method of Non-Paired Spatial Orbitals

Wavefunctions in the NPSO method are constructed by the application of symmetry and spin projection operators to a single determinantal wavefunction formed by assigning electrons as far as possible to semi-localized bonding orbitals. This is done in such a way as to span the bonding regions of the molecule and as far as possible so that electrons in adjacent semi-localized bonding orbitals have opposite spins.

The wavefunctions for the benzyl radical are constructed from the $2p\pi$ orbitals χ_i located on the carbon atoms. The numbering scheme is shown in the figure

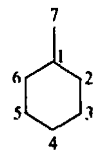

Two choices are possible for the initial single determinantal NPSO wavefunctions for this species, namely:

Function A

$$\Psi_{\mathrm{I}(A)} = A[(\chi_1 + k\chi_2)\,\alpha(\chi_3 + k\chi_4)\,\alpha(\chi_5 + k\chi_6)\,\alpha \\ (\chi_1 + k\chi_7)\,\alpha(\chi_2 + k\chi_3)\,\beta(\chi_4 + k\chi_5)\,\beta(\chi_6 + k\chi_1)\,\beta] \tag{5}$$

and Function B

$$\Psi_{\mathrm{I}(B)} = A[(\chi_1 + k\chi_2)\,\alpha(\chi_3 + k\chi_4)\,\alpha(\chi_5 + k\chi_6)\,\alpha \\ (k\chi_1 + \chi_7)\,\alpha(\chi_2 + k\chi_3)\,\beta(\chi_4 + k\chi_5)\,\beta(\chi_6 + k\chi_1)\,\beta]\,. \tag{6}$$

In these functions k is a parameter to be varied to minimise the energy.

As discussed in Paper I, a wavefunction transforming as one of the irreducible representations of the point group of the molecule may be generated by the application of a symmetry projection operator. Applying the operator for the B_2 representation gives, for function A, the wavefunction

$$\Psi_{(A)} = [\Psi_{\mathrm{I}(A)} + \Psi_{\mathrm{II}(A)}]\,, \tag{7}$$

where

$$\Psi_{\mathrm{II}(A)} = A[(k\chi_2 + \chi_3)\,\alpha(k\chi_4 + \chi_5)\,\alpha(k\chi_6 + \chi_1)\,\alpha \\ (\chi_1 + k\chi_7)\,\alpha(k\chi_1 + \chi_2)\,\beta(k\chi_3 + \chi_4)\,\beta(k\chi_5 + \chi_6)\,\beta]\,. \tag{8}$$

The wavefunction for function B is derived similarly.

A doublet wavefunction is generated by applying a doublet projection operator O_D to wavefunction (7)

$${}^2\Psi_{(A)} = O_D[\Psi_{\mathrm{I}(A)} + \Psi_{\mathrm{II}(A)}]\,. \tag{9}$$

The difficulties of including full spin projection in the calculation were discussed in Paper I. With full spin projection the energy would be given by

$$E = \frac{\langle(\Psi_\mathrm{I} + \Psi_\mathrm{II})|H|O_D(\Psi_\mathrm{I} + \Psi_\mathrm{II})\rangle}{\langle(\Psi_\mathrm{I} + \Psi_\mathrm{II})|O_D(\Psi_\mathrm{I} + \Psi_\mathrm{II})\rangle} \tag{10}$$

because the spin projection operator is idempotent and commutes with the Hamiltonian operator H. The difficulty lies in the calculation of $\langle\Psi_\mathrm{I}|H|O_D\Psi_\mathrm{II}\rangle$. We performed four sets of calculations with varying degrees of spin annihilation.

1. *No Spin Projection*

These calculations were made with wavefunction (7). The transformation of King *et al.* [20] was used for the calculation of integrals between individual Slater determinants.

2. *Spin Annihilation*

The quartet component was annihilated from the wavefunction $(\Psi_{\rm I}+\Psi_{\rm II})$ using the modification of the method of Amos and Hall [21] discussed in Paper I. In this approximation

$$E=\frac{\langle\Psi_{\rm I}|H|A'_Q\Psi_{\rm I}\rangle+\langle\Psi_{\rm I}|H|A'_Q\Psi_{\rm II}\rangle}{\langle\Psi_{\rm I}|A'_Q\Psi_{\rm I}\rangle+\langle\Psi_{\rm I}|A'_Q\Psi_{\rm II}\rangle}, \qquad (11)$$

where A'_Q represents annihilation of the quartet component.

3. *Partial Spin Projection*

An improvement on method 2 is to use the energy expression

$$E=\frac{\langle\Psi_{\rm I}|H|O_D\Psi_{\rm I}\rangle+\langle\Psi_{\rm I}|H|A'_Q\Psi_{\rm II}\rangle}{\langle\Psi_{\rm I}|O_D\Psi_{\rm I}\rangle+\langle\Psi_{\rm I}|A'_Q\Psi_{\rm II}\rangle}. \qquad (12)$$

4. *Spin Projection in Diagonal Term of Energy Expression*

In view of the fact that methods 2 and 3 involve considerable computation, we suggested in Paper I that a reasonable way of doing the calculation would be to use the energy expression

$$E=\frac{\langle\Psi_{\rm I}|H|O_D\Psi_{\rm I}\rangle+\langle\Psi_{\rm I}|H|\Psi_{\rm II}\rangle}{\langle\Psi_{\rm I}|O_D\Psi_{\rm I}\rangle+\langle\Psi_{\rm I}|\Psi_{\rm II}\rangle}. \qquad (13)$$

We included this method in order to see whether our assertion was true in the case of the benzyl radical. In the calculation of the integrals $\langle\Psi_{\rm I}|H|O_D\Psi_{\rm I}\rangle$ and $\langle\Psi_{\rm I}|H|A'_Q\Psi_{\rm I}\rangle$ the orbitals were first transformed to "corresponding" [21] or "paired" orbitals [22] and the formulae of Harris [19] were then used. In the integrals $\langle\Psi_{\rm I}|H|A'_Q\Psi_{\rm II}\rangle$, $A'_Q\Psi_{\rm II}$ was expressed as a sum of Slater determinants and the method of King *et al.* [20] was used for each individual integral in the expression.

3. Results

The results of the energy calculations using both sets of integral approximations are given in Table 1. The pattern of the results is roughly the same for both methods of calculating the one electron integrals. We examined two different integral approximations because in our initial UHF calculations using the Ruedenberg method, we obtained unreasonable orbitals although the energy was of the correct order. The same behaviour was observed with the GMS integrals. The UHF results must therefore be regarded with suspicion. Several possible explanations for the anomalous orbitals were considered but did not resolve the matter. The SCF program behaved perfectly normally for closed shell calculations on naphthalene and azulene [1].

The results in Table 1 indicate that NPSO functions of type A are more successful in lowering the energy than those of type B. The performance of the NPSO method is comparable with that of the AMO method for this system. Both methods give substantially lower energies than the RHF method, showing that they are effective in allowing for electron correlation.

Table 1. Energies for wavefunctions for the benzyl radical

Method	Ruedenberg one electron integrals		Goeppert-Mayer Sklar one electron integrals	
	Energy (eV)	k	Energy (eV)	k
Molecular orbital				
Eigenvectors of overlap matrix	−303.9154		−218.8816	
RHF	−305.6740		−219.8315	
UHF	−308.8357		−223.1363	
Alternant molecular orbital method	−308.6701	0.5866[a]	−223.5855	0.5898[a]
NPSO (function A)				
1	−308.6047	4.2	−223.0043	4.99
2	−309.4675	4.83	−223.8714	5.78
	(−309.4167	4.0)	(−223.7067	4.0)
3	−309.5968	4.85	−223.9927	5.75
	(−309.5413	4.0)	(−223.8199	4.0)
4	−309.1104	4.87	−223.5265	5.8
	(−309.0564	4.0)	(−223.3551	4.0)
NPSO (function B)				
1	−307.5750	0.236	−222.2996	0.227
2	−308.3498	0.208	−223.0785	0.2005
	(−308.3075	0.25)	(−223.0169	0.25)
3	−308.4520	0.209	−223.1799	0.20
	(−308.4090	0.25)	(−223.1173	0.25)
4	−307.9956	0.205	−222.7274	0.197
	(−307.9477	0.25)	(−222.6590	0.25)

[a] This value is $\lambda = \cos 2\theta$.

The results for the NPSO functions using methods 2, 3, 4 (energy expressions (11–13)) follow the pattern we observed for naphthalene and azulene and support our suggestion that calculations using energy expression (13) are a reasonable approximation. The use of methods 2 and 3 (i.e. with more complete annihilation of the quartet component) produces only a slight improvement in the energy and the value of k changes very little. The optimum values for k are also in the region of 4 (or 0.25) and the results for these values show that no serious errors would be introduced by the assumption of $k = 4$ (or 0.25). Thus, the results of our present calculations are in accord with the suggestion of Empedocles and Linnett [23]. We feel that we can now write down reasonable NPSO functions for larger systems such as polycyclic aromatic hydrocarbons on the basis of the calculations for smaller systems [1, 23].

The diagonal elements of the calculated spin density matrices are given in Table 2 for the NPSO function A obtained by methods 3 and 4. Function B gave spin densities which were not in accord with experiment and must therefore be rejected. The pattern of the spin densities calculated by the NPSO method is in poor accord with the observed hyperfine coupling constants [24]. The method

Table 2. Calculated spin densities for the benzyl radical

Method	ϱ_1	ϱ_2	ϱ_3	ϱ_4	ϱ_7
	a) Ruedenberg one electron integrals				
RHF	0.006	0.065	0.000	0.030	0.850
AMO	−0.264	0.451	−0.270	0.455	0.537
NPSO (function A)					
3	−0.589	0.696	−0.594	0.687	0.709
4	−0.483	0.616	−0.501	0.604	0.658
	b) Goeppert-Mayer Sklar one electron integrals				
RHF	0.002	0.031	0.000	0.014	0.960
AMO	−0.263	0.450	−0.269	0.454	0.538
NPSO (function A)					
3	−0.619	0.718	−0.618	0.711	0.722
4	0.516	0.641	−0.530	0.631	0.673
Experimental[a] hyperfine coupling constants (gauss)		5.14	1.75	6.14	16.35

[a] Ref. [24].

grossly overestimates the spin densities on the ring atoms. The RHF and AMO spin densities are also not in very good agreement with experiment.

There are several possible explanations for the poor results for the spin density calculations. The assumption of a regular geometry appears to be an invalid assumption [7, 8] but would not be expected to distort seriously the results. The present calculations are the only published calculations on the benzyl radical which have used the Ruedenberg or the GMS one electron integrals and included all the two electron integrals. It would appear that these approximations do not yield good results for spin density calculations. The omission of full spin projection may be a reason for the poor performance of the NPSO method. This neglect seems to have only a small effect on the energy but may have a more profound effect on the spin density distribution.

4. Conclusion

The calculations presented in this paper indicate that the use of NPSO wavefunctions for the benzyl radical leads to considerably lower energies than those given by molecular orbital methods which do not allow for electron correlation. Using one adjustable parameter, the NPSO and AMO methods give comparable lowerings. Although on the energy criterion the NPSO method seems to be successful in allowing for electron correlation, the calculated spin densities are in poor accord with experiment. On the basis of our calculations it seems that the use of the Ruedenberg and GMS methods for one electron integrals and the use of theoretical values for Coulomb integrals is much less successful than the use of semi-empirical methods [6].

Appendix

Table 3 contains the integral values used in these calculations. The orbital exponents for the carbon atom were those quoted by Ruedenberg [16].

Table 3

	Overlap integral	Coulomb integral (eV)	One electron integral (eV)	
			Ruedenberg approximation	GMS approximation
11	1.0	17.227026	−70.476281	−56.533172
22	1.0	17.227026	−64.635252	−52.514399
33	1.0	17.227026	−62.783655	−50.654663
44	1.0	17.227026	−62.351705	−50.220483
77	1.0	17.227026	−53.508749	−43.192025
12	0.246821	9.028474	−18.248177	−15.286945
13	0.034704	5.651135	− 2.011101	− 2.011578
14	0.015452	4.949867	− 0.892108	− 0.892315
37	0.001934	3.799537	− 0.100433	− 0.100458
47	0.000585	3.367587	− 0.030258	− 0.030260
17			−17.179095	−14.217767
23			−17.602871	−14.641567
24			− 1.945002	− 1.945453
25			− 0.869352	− 0.869559
26			− 1.984626	− 1.985087
27			− 1.834309	− 1.834756
34			−17.321058	−14.359686
35			− 1.920368	− 1.920836
36			− 0.869352	− 0.869559

Acknowledgements. We wish to thank Dr. P. H. Martin for providing some integral values. One of us (M.E.L.) wishes to thank the Science Research Council for a Research Studentship.

References

1. Hirst, D. M., Linington, M. E.: Theoret. chim. Acta (Berl.) **22**, 315 (1971).
2. Silberman, Z., Paunez, R.: Theoret. chim. Acta (Berl.) **10**, 254 (1968).
3. - Gershgorn, Z., Paunez, R.: Int. J. quant. Chemistry **2**, 453 (1968).
4. Hirst, D. M., Linnett, J. W.: J. chem. Physics **43**, S74 (1965) and references therein.
5. Chong, D. P., Linnett, J. W.: J. chem. Soc. (London) **1965**, 1798.
6. Amos, A. T., Burrows, B. L.: J. chem. Physics **52**, 3072 (1970).
7. Benson, H. G., Hudson, A.: Molecular Physics **20**, 185 (1971).
8. Beveridge, D. L., Guth, E.: J. chem. Physics **55**, 458 (1971).
9. Dearman, H. H., Lefebvre, R.: J. chem. Physics **34**, 72 (1961).
10. Chong, D. P., Linnett, J. W.: Molecular Physics **8**, 151 (1964).
11. — — Molecular Physics **8**, 541 (1964).
12. Vincow, G., Johnson, P. M.: J. chem. Physics **39**, 1143 (1963).
13. Lefebvre, R., Dearman, H. H., McConnell, H. M.: J. chem. Physics **32**, 176 (1960).
14. Roothaan, C. C. J.: Rev. mod. Physics **32**, 179 (1960).

15. Pople, J. A., Nesbet, R. K.: J. chem. Physics **22**, 571 (1954).
16. Ruedenberg, K.: J. chem. Physics **34**, 1861 (1961).
17. Goeppert-Mayer, M., Sklar, A. L.: J. chem. Physics **6**, 645 (1938).
18. Pauncz, R.: *Alternant molecular orbital method. Philadelphia: W. B. Saunders Company 1967.*
19. Harris, F. E.: Advances in quant. Chemistry **3**, 61 (1967).
20. King, H. F., Stanton, R. E., Kim, H., Wyatt, R. E., Parr, R. G.: J. chem. Physics **47**, 1936 (1967).
21. Amos, A. T., Hall, G. G.: Proc. Royal Soc. (London) A **263**, 483 (1961).
22. Löwdin, P. O.: J. Appl. Phys. Suppl. **33**, 251 (1962).
23. Empedocles, P. B., Linnett, J. W.: Theoret. chim. Acta (Berl.) **4**, 377 (1966).
24. Carrington, A., Smith, I. C. P.: Molecular Physics **9**, 137 (1965).

Dr. D. M. Hirst
Department of Molecular Sciences
The University of Warwick
Coventry CV4 7AL, England

Theoret. chim. Acta (Berl.) 26, 187—193 (1972)
© by Springer-Verlag 1972

Energie des systèmes H_2, HHe^+ et LiH*

GUY POUZARD et LOUIS PUJOL
Laboratoires de Chimie Organique Structurale et de Chimie Structurale Théorique
(Associés CNRS n° 109)
Université de Provence – Centre de Saint-Jérôme – 13 Marseille (13°), France

Reçu le 17 février 1972

Energy of the Systems H_2, HHe^+ *and* LiH

The ground state and first electronic transitions energies are calculated by the OMSCF method for H_2, HHe^+ and LiH. The basis consists in a Slater type orbitals of atoms and in a product of these. First transition energies are improved in comparison with minimal basis.

1. Introduction

Les molécules H_2, HHe^+ et LiH sont des systèmes électroniques simples qui ont servi de base à de très nombreux calculs. En général, on s'efforce de trouver des fonctions conduisant à la meilleure énergie calculée possible.

Notre propos est de présenter une base de description qui conduise à une meilleure énergie de l'état fondamental que celle obtenue par la méthode des orbitales moléculaires en base minimale de Slater, sans qu'elle représente une extension trop importante. Nous montrerons de plus, que l'utilisation de cette base améliore l'énergie des premières transitions électroniques qui est toujours surestimée dans la méthode des orbitales moléculaires sans interaction de configuration.

La méthode que nous avons utilisée est celle des orbitales moléculaires du champ auto-cohérent (OMCAC ou OMSCF). L'hamiltonien du système est l'hamiltonien électronique non relativiste, dans l'approximation des noyaux fixes de Born Oppenheimer. La fonction qui décrit l'état fondamental est un déterminant de Slater construit sur un jeu d'orbitales moléculaires ψ_i, elles-mêmes combinaisons linéaires d'orbitales de base.

2. Orbitales de base

Chaque OM est de la forme $\psi_i = \sum_{\mu=1}^{N} C_{i\mu}\phi_\mu$, où ϕ_μ est une des N orbitales de base et $C_{i\mu}$ un coefficient réel. Le tableau suivant résume le choix des orbitales de base dans les différents cas:

---

* Ce mémoire constitue une partie du Doctorat ès Sciences Physiques que doit soutenir G. Pouzard devant l'Université de Provence (n° CNRS AO 6610).

Molécule		Base	Utilisée
H_2	$\phi_1 = N_1 e^{-\alpha r_H}$	$\phi_2 = N_2 e^{-\alpha r_H}$	$\phi_3 = N_3 \phi_1 \phi_2$
HHe^+	$\phi_1 = N_1 e^{-\alpha r_H}$	$\phi_2 = N_2 e^{-\beta r_{He}}$	$\phi_3 = N_3 \phi_1 \phi_2$
LiH	$\phi_1 = N_1 e^{-\alpha r_H}$	$\phi_2 = N_2 e^{-\gamma r_{Li}}$	$\phi_3 = N_3 r_{Li} e^{-\beta r_{Li}}$
		$\phi_4 = N_4 \phi_1 \phi_3$	

Nous utilisons les orbitales de type Slater des atomes A et B et un produit de ces orbitales que nous normons. A notre connaissance, l'utilisation conjointe de la base de Slater minimale et de la fonction produit n'a été faite de façon explicite que dans le cas de la molécule H_2^+ [1, 2], où il n'y a qu'un seul électron. Le calcul de l'énergie de l'état fondamental est fait en minimisant celle-ci par rapport aux coefficients $C_{i\mu}$ et par rapport aux exposants α, β et γ, pour une distance égale à la distance d'équilibre de la molécule. A partir des orbitales moléculaires du fondamental, nous avons également évalué l'énergie des premiers états excités monoélectroniques (singulet et triplet) pour comparer les résultats obtenus avec ceux donnés par la description en base de Slater minimale.

Les intégrales intervenant dans le calcul sont pour la majeure partie évaluées par le programme de Corbato et Switendick [3]. Certaines intégrales cinétiques ne pouvant être évaluées à partir de ce programme sont calculées séparément en coordonnées elliptiques.

3. Résultats

Les valeurs calculées de l'énergie de l'état fondamental pour les molécules H_2, HHe^+ et LiH se trouvent dans les Tableaux 1, 2 et 3. Nous y avons adjoint, pour comparison, les valeurs trouvées par d'autres auteurs utilisant la méthode OMCAC sans interaction de configuration. Nous donnons également le diagramme des orbitales moléculaires correspondant, ainsi que la valeur optimisée des exposants.

Tableau 1. Energie de la molécule H_2. Méthode OMCAC avec optimisation des exposants

Base utilisée	Energie totale (en u.a.)	R (u.a.)	Références
$1S_{H_A}$, $1S_{H_B}$, $1S_{H_A} \cdot 1S_{H_B}$	$-1{,}13291^a$	1,44	Ce travail
Orbitales de bases monocentriques	$-1{,}03447$	1,4	Joy *et al.* [7]
Orbitales monocentriques, série d'harmoniques sphériques	$-1{,}12817$	1,4	Keefer *et al.* [8]
Base de Slater minimale	$-1{,}12891$	1,383	Coulson [4]
Base de Slater étendue	$-1{,}13363$	1,44	Kolos *et al.* [9]
Expérience	$-1{,}1744$	1,44	Herzberg *et al.* [10]

[a] La valeur absolue du Viriel (rapport de l'énergie cinétique à l'énergie potentielle) est trouvée égale à 0,497.

Diagramme des orbitales moléculaires

$$
\begin{aligned}
e_3 &= 1{,}27398 & \psi_3 &= -0{,}9521\,\phi_1 - 0{,}9521\,\phi_2 + 1{,}9818\,\phi_3 \\
e_2 &= 0{,}52514 & \psi_2 &= 1{,}2287\,\phi_1 - 1{,}2287\,\phi_2 \\
e_1 &= -0{,}58866 & \psi_1 &= 0{,}4902\,\phi_1 + 0{,}4902\,\phi_2 + 0{,}1098\,\phi_3 \qquad \alpha = 1{,}106\,.
\end{aligned}
$$

L'énergie calculée par Kolos et Roothaan [9] représente pratiquement la limite de Hartree-Fock. L'introduction de la seule fonction ϕ_3 permet d'arriver à $7 \cdot 10^{-4}$ u.a. de cette limite alors que la base minimale de Slater donne une valeur située à $5 \cdot 10^{-3}$ u.a.

Tableau 2. Energie de l'ion moléculaire HHe^+. Méthode OMCAC, optimisation des exposants

Base utilisée	Energie totale (u.a.)	R (u.a.)	Références
$1S_{H}, 1S_{H_e}, 1S_{H} \cdot 1S_{H_e}$	$-2{,}92717^{a}$	1,44	Ce travail
Base de Slater *minimale*	$-2{,}91281$	1,482	Coulson [5]
Orbitales monocentriques développées en série d'harmoniques sphériques	$-2{,}91742$	1,4	Keefer *et al.* [8]
Cinq orbitales de Slater	$-2{,}93213$	1,4	Anex [11]
Douze orbitales de Slater	$-2{,}93259$	1,44	Peyerimhoff [12]

[a] La valeur absolue du Viriel est de 0,5001.

Diagramme des orbitales moléculaires pour HHe^+ *à* $R = 1{,}44$ u.a.

$$
\begin{aligned}
e_3 &= 1{,}93468 & \psi_3 &= -0{,}6740\,\phi_1 - 1{,}3876\,\phi_2 + 2{,}0328\,\phi_3 \\
e_2 &= -0{,}03449 & \psi_2 &= 1{,}1370\,\phi_1 - 0{,}7285\,\phi_2 - 0{,}0472\,\phi_3 \\
e_1 &= -1{,}63991 & \psi_1 &= 0{,}2090\,\phi_1 + 0{,}7396\,\phi_2 + 0{,}0979\,\phi_3\,.
\end{aligned}
$$

La valeur des exposants optimisés est: $\alpha = 1{,}412$, $\beta = 1{,}845$.

Tableau 3. Energie de LiH. Méthode OMCAC, optimisation des exposants

Base utilisée	Energie calculee (u.a.)	R (u.a.)	Références
$1S_{H}, 1S_{Li}, 2S_{Li}, 1S_{H} \cdot 2S_{Li}$	$-7{,}96940^{a}$	3,015	Ce travail
Orbitales monocentriques développées en série d'harmonies sphériques	$-7{,}9357$	3,015	Keefer *et al.* [8]
Orbitales monocentriques	$-7{,}59411^{b}$	3,6971	Bishop *et al.* [14]
Base de Slater minimale incluant $2p_\sigma$	$-7{,}9699$	3,015	Ransil [6]
Base Gaussienne avec 14 OG sur Li et 7 OG sur H	$-7{,}98421$	3,02	Czizmadia [15]
24 orbitals de Slater	$-7{,}98731$	3,015	Cade *et al.* [16]
Expérience	$-8{,}075$	3,015	Cade *et al.* [17]

[a] La valeur absolue du Viriel est de 0,5005 et le moment dipolaire vaut $-5{,}79$ *D*, dans le sens Li^+H^-.

[b] Cette valeur est calculée pour une distance différente de la distance d'équilibre, ce qui explique la grande variation par rapport aux autres valeurs du tableau.

Pour cette molécule, la limite de Hartree-Fock semble être la valeur obtenue par Peyerimhoff [12]. La fonction que nous avons utilisée conduit à une énergie ne différent de cette limite que de $5 \cdot 10^{-3}$ u.a. alors qu'elle donne une amélioration de $1{,}5 \cdot 10^{-2}$ u.a. par rapport à la base minimale.

Diagramme des orbitales moléculaires de LiH *pour* $R = 3{,}015$ u.a.

$$\begin{aligned} e_4 &= 0{,}4471 & \psi_4 &= -0{,}3867\,\phi_1 - 0{,}0365\,\phi_2 - 0{,}2436\,\phi_3 - 3{,}5859\,\phi_4 \\ e_3 &= 0{,}0216 & \psi_3 &= -1{,}8372\,\phi_1 - 0{,}0889\,\phi_2 + 1{,}1609\,\phi_3 + 1{,}0197\,\phi_4 \\ e_2 &= -0{,}3052 & \psi_2 &= -0{,}3712\,\phi_1 - 0{,}1549\,\phi_2 + 0{,}2469\,\phi_3 + 0{,}4910\,\phi_4 \\ e_1 &= -2{,}4196 & \psi_1 &= -0{,}0460\,\phi_1 + 0{,}9965\,\phi_2 + 0{,}0156\,\phi_3 + 0{,}0510\,\phi_4 . \end{aligned}$$

La valeur optimisée des exposants est: $\alpha = 0{,}8133$; $\beta = 0{,}5843$; $\gamma = 2{,}692$.

L'orbitale moléculaire interne ψ_1 est essentiellement constituée par l'orbitale atomique $1S_{Li}$, avec un exposant pratiquement égal à celui obtenu par application des règles de Slater. Cesi est en accord avec la localisation des deux électrons $1S$ du lithium au voisinage de ce noyau.

Pour cette molécule, nous avons à $4 \cdot 10^{-4}$ u.a. près, la même valeur que celle donnée par Ransil [6]. Elle se situe à $1{,}8 \cdot 10^{-2}$ u.a. de la limite de Hartree-Fock donnée par les calculs de Cade et Huo [16]. Cependant, Ransil tient compte de l'hybridation, en introduisant une orbitale $2p_\sigma$ sur l'atome de lithium. Nous n'utilisons que des orbitales de type s, ce qui représente un avantage certain pour les calculs numériques.

4. Discussion

Par rapport à une base d'orbitales atomiques minimale, notre fonction, sans étendre la base d'une façon importante améliore d'une manière satisfaisante l'énergie de l'état fondamental de ces systèmes, aussi bien pour un système non polaire comme H_2 que pour un système fortement polaire comme HHe^+. Il nous a paru intéressant de voir si l'introduction de la fonction produit dans la base de description permettait d'abaisser les énergies des premières transitions électroniques qui, en base minimale sont toujours surestimées.

Bien que, pour les systèmes étudiés, la géométrie des états excités soit très différente de celle du fondamental [21], nous avons calculé les énergies de transition à partir de la géométrie de l'état fondamental et en utilisant la valeur des exposants déterminés dans ce cas. Nous pensons en effet étendre la méthode à des molécules plus importantes, pour lesquelles en général, la géométrie des états excités est beaucoup plus voisine de celle de l'état fondamental. Les résultats obtenus pour les énergies de transition sont résumés dans le tableau [5].

Tableau 4. Energie des premières transitions électroniques calculés en eV

Molécule	$E_{\text{triplet}} - E_{\text{fond.}}$		$E_{\text{singulet}} - E_{\text{fond}}$		ΔE	
	Base mini	Ce travail	Base mini	Ce travail	Trip.	Sing.
H_2	14,4	13,1	23,7	21,8	1,3	1,9
HHe^+	24,9	23,5	34.4	32,8	1,4	1,6

ΔE représente l'abaissement apporté par notre base par rapport à la base minimale.

Dans tous les cas, l'énergie des transitions est abaissée de 1,3 à 1,9 eV. Qualitativement cette amélioration peut se prévoir par l'examen de la structure des fonctions décrivant les différents états de la molécule H_2 par exemple:

Etat $^1\Sigma_u^+$.

En base minimale, les OM utilisées pour décrire le singulet $^1\Sigma_u^+$ sont:

$$\psi_1 = 1/(2(1+S))^{1/2} \cdot (s_a + s_b) \quad \text{et} \quad \psi_2 = 1/(2(1-S))^{1/2} \cdot (s_a - s_b) .$$

La fonction d'espace est alors:

$$\psi(^1\Sigma_u^+) = 2/(1-S^2)^{1/2} \cdot [s_a(1) s_a(2) - s_b(1) s_b(2)] .$$

Cette fonction possède un caractère essentiellement ionique qui la rend impropre à une bonne description de l'état excité. Avec notre base, les OM utilisées sont les suivantes:

$$\psi_1 = c_1(s_a + s_b) + c_2 s_a s_b \quad \text{et} \quad \psi_2 = 1/(2(1-S))^{1/2} \cdot (s_a - s_b) .$$

En effet par raison de symétrie, le produit n'apparaît pas dans l'OM ψ_2 pour la molécule H_2.

Dans ces conditions la fonction d'espace s'écrit:

$$\psi(^1\Sigma_u^+) = 2/(2(1-S))^{1/2} \cdot [c_1\{s_a(1)\, s_a(2) - s_b(1)\, s_b(2)\} + c_2\{s_a(1)\, s_a(2)\, s_b(1) + s_a(2)\, s_a(1)\, s_b(2) - s_b(1)\, s_b(2)\, s_a(1) - s_b(2)\, s_b(1)\, s_a(2)\}] .$$

Le caractère purement ionique est atténué par le caractère covalent des produits de la forme $s_a(2)\, s_b(1)$ qui sont introduits dans la deuxième partie de la fonction, grâce à la fonction de base bicentrique. L'introduction de ce caractère covalent se traduit par une amélioration de la description de l'énergie de l'état singulet. Une discussion plus approfondie de ce cas est donnée par Hansen et Kampp [18], également par Kolos et Wolniewicz [19].

Etat $^3\Sigma_u^+$.

En base minimale, la fonction de l'état triplet s'écrit:

$$\psi(^3\Sigma_u^+) = 2/(1-S^2)^{1/2}\{s_a(1)\, s_b(2) - s_a(2)\, s_b(1)\} .$$

Elle a donc un caractère essentiellement covalent, à inverse de la fonction du singulet. Elle n'est donc pas correcte pour décrire l'état triplet. Avec notre base, la fonction de l'état $^3\Sigma_u^+$ s'écrit:

$$\psi(^3\Sigma_u^+) = 2c_1\{2(1-S)\}^{1/2}\{s_a(1)\, s_b(2) - s_a(2)\, s_b(1)\} + 2c_2\{2(1-S)\}^{1/2} \cdot \{s_a(1)\, s_a(2)\, s_b(1) - s_a(1)\, s_a(2)\, s_b(2) + s_b(1)\, s_b(2)\, s_a(2) - s_b(1)\, s_b(2)\, s_a(1)\} .$$

Dans ce cas, c'est le caractère purement covalent de la fonction qui est atténué par le caractère ionique des produits de type $s_a(1)\, s_a(2)$ qui apparaissent dans la deuxième partie de la fonction.

Dans les deux cas, la fonction produit permet donc d'atténuer le caractère limite des fonctions écrites en base minimale. Cesi se traduit par une amélioration de l'énergie des états excités[1]. Si l'on désire améliorer les énergies de transitions, il est nécessaire que l'état fondamental soit moins stabilisé que les états excités. Pour cela, nous devons examiner la structure de la fonction qui décrit l'état fondamental $^1\Sigma_g^+$ en base minimale:

$$\psi(^1\Sigma_g^+) = 1/(1+S)\,\{s_a(1)\,s_a(2) + s_b(1)\,s_a(2) + s_a(1)\,s_b(2) + s_b(2)\,s_b(1)\}\,.$$

Elle contient donc un double caractère ionique et covalent. Aussi, l'introduction de la fonction produit en atténuant le caractère limite des fonctions écrites en base minimale pour les états excités améliore davantage l'énergie de ces états que celle du fondamental. L'énergie des transitions électroniques est de ce fait mieux décrite.

Ce résultat peut également s'interpréter en comparant l'énergie des états fondamentaux de l'ion H_2^+ et de la molécule H_2. Pour cette dernière, une fonction de type $s_a + s_b$ donne de meilleurs résultats que la fonction $s_a \cdot s_b$, alors que c'est le contraire pour H_2^+ [20, 21]. Or, schématiquement, on peut dire que dans l'état excité, l'un des électrons est en «moyenne» plus proche des noyaux que l'autre. Il s'apparente plus à électron de H_2^+ et de ce fait il doit être mieux décrit par une orbitale moléculaire contenant le produit $s_a \cdot s_b$. L'autre électron en «moyenne» plus loin des noyaux doit être mieux décrit par une orbitale moléculaire qui ne contient pas le produit. Ceci est rigoureux dans le cas de la molécule H_2 où par raison de symétrie, la fonction $s_a \cdot s_b$ n'apparaît pas dans l'orbitale moléculaire ψ_2. L'état excité, qui représente une situation intermédiaire entre le fondamental et l'état ionisé, mais plus voisin de ce dernier [21], est donc mieux décrit que le fondamental lorsque l'on introduit la fonction produit dans la base.

Les mêmes résultats se retrouvent pour la molécule HHe^+, bien que la symétrie moins élevée de la molécule se prête moins bien à une interprétation aussi simple. On peut cependant remarquer que le poids de la fonction produit est moins élevé dans la fonction ψ_2 que dans la fonction ψ_1, ce qui est en accord avec ce modèle simplifié.

En conclusion, l'introduction de la fonction produit dans la base de description des systèmes simples H_2, HHe^+ et LiH, améliore la description de l'énergie de l'état fondamental par rapport à la base minimale. D'autre part, l'énergie des premières transitions électroniques est abaissée de 5 à 10% suivant les cas.

Les calculs relatifs à ce travail ont été réalisés sur L'IBM 360-44 du centre de calcul de la faculté des Sciences de Luminy, à Marseille.

Références

1. Dalgarno, A., Poots, G.: Proc. Roy. Soc. (London) **67** A, 343 (1953).
2. Radel, S. R., Gorman, R., Cutler, C., Kahn, L.: J. chem. Physics **50**, 3642 (1969).
3. Switendick, A. C., Corbato, F. J.: Diatomic Molecular Integral Program, Q.C.P.E. n° 29.
4. Coulson, C. A.: Trans. Faraday Soc. **33**, 1479 (1937).
5. - Duncanson, W. E.: Proc. Roy. Soc. (London) A **165**, 90 (1938).
6. Ransil, B. J.: Rev. mod. Physics **32**, 245 (1960).

---

[1] L'importance de la fonction produit serait accrue si l'on effectuait une minimisation directe de l'énergie des états excités par rapport aux différents paramètres.

7. Joy, H. W., Parr, R. G.: J. chem. Physics **28**, 448 (1958).
8. Keefer, J. A., Su-Fu, J. K., Belford, R. L.: J. chem. Physics **50**, 160 (1969).
9. Kolos, W., Roothaan, C. C. J.: Rev. mod. Physics **32**, 219 (1960).
10. Herzberg, G., Monfils, A.: J. molecular Spectroscopy **5**, 482 (1960).
11. Anex, B. G.: J. chem. Physics **38**, 1651 (1963).
12. Peyerimhoff, S.: J. chem. Physics **43**, 998 (1965).
13. Wolniewicz, L.: J. chem. Physics **43**, 1087 (1965).
14. Bishop, D. M., Hoyland, J. R.: Molecular Physics **7**, 161 (1963).
15. Czizmadia, I. G.: J. chem. Physics **44**, 1849 (1966).
16. Cade, P. E., Huo, W. M.: J. chem. Physics **47**, 614 (1967).
17. — — J. chem. Physics **45**, 1063 (1966).
18. Hansen, A. E., Kampp, K.: Theoret. chim. Acta (Berl.) **13**, 109 (1969).
19. Kolos, W., Wolniewicz, L.: J. chem. Physics **45**, 509 (1966).
20. Lyon, W. D., Matcha, R. L., Sanders, W. D., Meath, W. J., Hirschfelder, J. O.: J. chem. Physics **43**, 1095 (1965).
21. Kauzmann, W.: Quantum chemistry, p. 396. New York: Academic Press Inc. 1957.

Dr. G. Pouzard
Laboratoires de Chimie Organique Structurale
et de Chimie Structurale Théorique
(Associés au C.N.R.S. n° 109)
Université de Provence
Centre de Saint-Jérôme
F-13013 Marseille, France

Theoret. chim. Acta (Berl.) 26, 194 (1972)
© by Springer-Verlag 1972

Recensio

V. Gutmann: Chemische Funktionslehre. Wien-New York: Springer 1971. 159 Seiten. Preis: DM 47, -.

Die „Chemische Funktionslehre" ist ein Versuch, das chemische Reaktionsgeschehen aufgrund einfacher Prinzipien zu verstehen. Die zentralen Begriffe dieser Lehre sind die Elektronendonor- und -acceptorfunktionen einerseits und die Elektronen*paar*donor- und -acceptorfunktionen andererseits. Die ersten beschreiben die Redoxvorgänge, die zweiten die Komplexbildungsreaktionen. Das Verdienst dieser Monographie besteht darin, daß sie die beiden Reaktionstypen in einen Zusammenhang bringt. Dieser Zusammenhang ist durch das Prinzip der chemischen Reaktionsfolge bestimmt. Damit können so verschiedene Aspekte chemischen Reaktionsgeschehens verstanden werden wie: Redoxpotentiale (Kap. II, III), Stabilisierung von Oxidationszahlen (Kap. IV), Ionensolvatation (Kap. V), Ionisation (Kap. VI, VII), Komplexbildung (Kap. VIII, IX), Kinetik (Kap. X), Charge-Transfer-Komplexe (Kap. XI), Reaktionsmechanismen in der organischen Chemie (Kap. XII), die Dynamik der Errichtung chemischer Bindungen (Kap. XIII), Katalyse (Kap. XIV) und die Thermochemie der chemischen Bindung. Die Vielseitigkeit dieses einfachen Modells ist überraschend.

Das Buch wird sich vor allem für den anorganischen Anfangsunterricht als äußerst nützlich erweisen. Dem experimentellen Anorganiker eröffnet es neue Wege, und der Theoretiker fragt sich, warum dieses einfache Modell so verblüffend gut ist.

F. Wasgestian

Eingegangen am 8. Mai 1972

Theoret. chim. Acta (Berl.) 26, 195—210 (1972)
© by Springer-Verlag 1972

Commentationes

The Role of Kinetic Energy in Chemical Binding

I. The Nonclassical or Exchange Kinetic Energy*

C. WOODROW WILSON, JR.** and WILLIAM A. GODDARD III***
Arthur Amos Noyes Laboratory of Chemical Physics†,
California Institute of Technology, Pasadena, California 91109, USA

Received February 10, 1972

The wavefunctions and various partitions of the energy are examined for a variety of small molecules (H_2, H_3, H_4, HeH, HeH_2, He_2, LiH, and BH) in order to isolate the factors crucial for bond formation. We find that a natural partition of the energy leads to the conclusion that the crucial factor is the exchange, or nonclassical, part of the kinetic energy, T^x. The change in T^x upon pushing the atoms towards one another is the dominant term in the binding energy; it is negative when the resulting molecule is stable and positive when it is unstable. We show that T^x is related to the interference kinetic energy considered by Ruedenberg.

Die Wellenfunktionen und verschiedene Zerlegungen der Energie werden für eine Reihe kleiner Moleküle untersucht (H_2, H_3, H_4, HeH, HeH_2, He_2, LiH und BH), um die Faktoren zu finden, die für die Bindungsbildung ausschlaggebend sind. Die natürliche Zerlegung der Energie läßt die Folgerung zu, daß der bestimmende Faktor der Austauschanteil T^x (oder nichtklassische Anteil) der kinetischen Energie ist. Die Änderung von T^x beim Zusammenführen der Atome ist der dominierende Term für die Bindungsenergie; er ist negativ, wenn das resultierende Molekül stabil ist, und positiv, falls es instabil ist. Es wird gezeigt, daß T^x im Zusammenhang zum Wechselwirkungsanteil der kinetischen Energie nach Ruedenberg steht.

1. Introduction

A number of molecules, such as H_2, BH, and HF are strongly bound, with binding energies on the order of several electron volts and bond distances of less than three bohr[1]. This type of bond is often referred to as a chemical bond and is often viewed as involving sharing of electrons between the bonding atoms [1]. On the other hand many other systems, such as He_2 are only very weakly bound, with energies of less than 0.1 eV and bond distances of more than five bohr. This type of bond is often referred to as a van der Waal's bond is viewed as involving instantaneous correlation between the motions of the electrons of the two atoms [1]. The chemical forces dominate at short distances and the van der Waal's forces dominate at large distances. Compressing molecules such as He_2 to distances

---

* Partially supported by a grant (GP-15423) from the National Science Foundation. This paper is based on a portion of the PhD thesis (California Institute of Technology, 1970) by CWW.

** National Science Foundation Predoctoral Trainee. Present address: Department of Chemistry, Argonne National Laboratory, Argonne, Illinois 60439, U.S.A.

*** Alfred P. Sloan Foundation Research Fellow.

† Contribution No. 3917.

[1] Atomic units are used throughout; in these units $e = \hbar = m_e = 1$, 1 hartree = 27.211 eV = 627.51 kcal mole^{-1} is the unit of energy, and 1 bohr = 0.52917 Å is the unit of length. (Cohen, E. R., Du Mond, J. W. M.: Rev. mod. Physics 37, 537 (1965).)

characteristic of chemical binding generally leads to large repulsive or antibonding forces; that is, the chemical forces are antibonding but short range and the van der Waal's forces are bonding but long range. Thus the binding energy and equilibrium geometry involve a balance between those two effects. On the other hand for molecules such as BH, both forces are attractive and the stronger chemical forces determine the equilibrium geometry. This distinction between chemical and van der Waal's forces is especially meaningful since we can actually construct wave functions which include the first but not the second effect (see below).

In this paper our objective is to study the chemical forces and determine why they lead to bonding in some systems (e. g., H_2) and antibonding in others (e. g., He_2). We will start from rigorous self-consistent field wave functions and attempt to effect a partition of the energy in such a way that the parts responsible for chemical bonding are separated out from the other terms. The resulting partition leads to the conclusion that the dominant term for bonding is the change in the exchange or nonclassical part (T^x) of the kinetic energy (T). This term is negative for systems such as H_2 and LiH and positive for systems such as He_2 and H_3, and the sign of this term can be predicted from general considerations of the states of the separated molecules.

The conclusion that it is a decrease in the kinetic energy which is responsible for chemical bonding is in agreement with the earlier ideas of Hellmann [2] and Ruedenberg [3]. In addition the general philosophy of our approach is very much the same as Ruedenberg's and some of our concepts are similar to his. However the details of our approach are distinctly different and the final definition of the nonclassical part of T is not at all the same, as will be discussed later.

Although the total energy and its partitions are very important to us here, we wish to extract other information out of the wave function. In particular we want to be able to make a quantitative comparison of, say, the orbitals of the H_2 molecule and the H_2 part of H_2H, in order to determine just why H_2H is not stable and why the energy is lower for linear H_2H than for the bent case. Unfortunately, it is not possible, in general, to discuss the exact wave functions in terms of orbitals in such a way. However there is a class of very accurate wave functions which does allow a somewhat rigorous discussion of the many-electron wave function in terms of orbitals. Since use will be made of such wave functions, we summarize next some of their important features.

2. Independent Particle Wave Functions

In some approximations the wave function, Ψ, of a system of N identical particles may be discussed in terms of a set of N one-particle functions, called orbitals, each of which may be interpreted as the eigenstate of an individual particle moving in the average field due to the other $N-1$ particles. In this section, we will discuss several approximations which lead to such interpretations.

In the Hartree method the N-electron wave function, Ψ^{H}, is taken as a simple product of orbitals and spin functions,

$$\Psi^{H}=\Phi^{H}\chi, \tag{1}$$

where

$$\Phi^{H}(1,2,\ldots,N)=\varphi_1^{H}(1)\,\varphi_2^{H}(2)\cdots\varphi_N^{H}(N) \tag{2}$$

and χ is a suitable product of one-electron spin functions. In this case the total energy is given by

$$E^{\mathrm{H}} = \sum_{i}^{N} \langle \phi_i | h | \phi_i \rangle + \sum_{i>j}^{N} J_{ij}, \tag{3}$$

where $h = -\frac{1}{2}\nabla^2 + v^{\mathrm{N}}$, v^{N} is the nuclear attraction operator, and J_{ij} is the usual Coulomb integral

$$J_{ij} = \left\langle \phi_i \phi_j \left| \frac{1}{r_{12}} \right| \phi_i \phi_j \right\rangle . \tag{4}$$

The orbitals in (2) should be optimized so as to minimize the total energy (3). The resulting equations for the optimum orbitals can be written

$$H_k^{\mathrm{H}} \phi_k = \varepsilon_k \phi_k , \quad k = 1, \ldots, N \tag{5}$$

where

$$H_k^{\mathrm{H}} = h + U_k^{\mathrm{H}} , \tag{6}$$

$$U_k^{\mathrm{H}} = \sum_{j \neq k}^{N} J_j , \tag{7}$$

and J_j is the Coulomb operator

$$J_j(1) = \left\langle \phi_j(2) \left| \frac{1}{r_{12}} \right| \phi_j(2) \right\rangle . \tag{8}$$

(In (8) the integration is over the coordinates of electron 2.)

Unfortunately the wavefunction of (1) is in general not appropriate for Fermions (or Bosons) since it is not an eigenfunction of the transposition operators. Note that the spin function χ in (1) could be taken as an eigenfunction of $\hat{S}^2$ (rather than a simple product) and the Eqs. (3)–(8) would still apply. Thus the primary fault of the Hartree wavefunction is that it violates the Pauli Principle, not that it has the wrong spin symmetry.

For (1) the probability distribution (i.e., electron density) is

$$\varrho^{\mathrm{H}}(1) = \sum_{i}^{N} |\phi_i(1)|^2 \tag{9}$$

and the total energy (3) and potential (7) are just those expected classically from such a charge distribution (omitting self-repulsion terms).

In the Hartree-Fock method the wave function is taken as a Slater determinant

$$\psi^{\mathrm{HF}} = \mathscr{A}(\Phi^{\mathrm{HF}} \chi) , \tag{10}$$

where $\mathscr{A}$ is the N-particle antisymmetrizer and Φ^{HF} and χ are products of one-electron spatial and spin functions, respectively. In this case the energy expression is the same as (3) except for additional terms, called exchange integrals, which result from the permutation of orbitals of the same spin in (10). The orbitals in Φ^{HF} are required to be optimized (so as to make the total energy stationary), resulting in the following equations

$$H_k^{\mathrm{HF}} \phi_k = \varepsilon_k \phi_k , \quad k = 1, \ldots, N \tag{11}$$

where

$$H_k^{\mathrm{HF}} = h + U_k^{\mathrm{HF}} \tag{12}$$

and U_k^{HF} is the same as U_k^{H} except for the presence of exchange terms. However, the electron density still has the form of (9) and all one-electron spatial properties can be expressed in the same form as in the Hartree case,

$$\langle F\rangle=\sum_{i}^{N}\langle\phi_i|f|\phi_i\rangle,$$

where f is a one-electron spatial operator, and F is the corresponding many-electron operator. The wave function (10) satisfies the Pauli principle for any Φ^{HF} but *is not necessarily an eigenfunction of* $\hat{S}^2$. In order to obtain the correct spin symmetry, we generally force the orbitals to be doubly occupied (once with each spin). However this double-occupation restriction then leads to difficulties due to improper dissociation of the wave function[2]. We can obtain the correct dissociation by dropping the double occupation restriction (to obtain the unrestricted Hartree-Fock (UHF) wave function); however the resulting wave function does not have the correct spin symmetry.

This leads us to consider the wave functions [4]

$$\psi^{G1}=G_1^{\gamma}(\Phi^{G1}\chi) \tag{13}$$

analogous to (10) but in which the group operator, G_1^{γ}, takes care of both the Pauli and spin symmetry [5] so that (13) satisfies Pauli's Principle and is an eigenfunction of $\hat{S}^2$ for *all* spatial functions Φ^{G1}. We restrict Φ^{G1} and χ to be products of spatial and spin functions, respectively, but require that the orbitals be optimized (with respect to the total energy). The resulting variational equations have the form

$$H_k^{G1}\phi_k^{G1}=\varepsilon_k\phi_k^{G1}, \quad k=1,\dots,N \tag{14}$$

where the one-particle operator H_k^{G1} has the form

$$H_k^{G1}=h+U_k^{G1} \tag{15a}$$

with the effective potential U_k^{G1} similar to U_k^{H} except for the occurrence of many exchange terms (involving both h and $1/r_{ij}$). Here U_k^{G1} can be expressed as

$$U_k^{G1}=U_k^{Cl}+U_k^{x}, \tag{15b}$$

where U_k^{Cl} is given by (7) and is just the average classical electrostatic potential and U_k^x contains *all* of the exchange terms (arising from the Pauli principle and spin symmetry requirements). Similarly, the total energy may be expressed as

$$E^{G1}=E^{Cl}+E^{x}, \tag{16}$$

where E^{Cl} is the energy we would obtain if the wave function were a simple product of orbitals, as given in (3). Note that E^x involves exchange contributions not only from the electron-electron interactions but also from the one-electron terms, i. e., kinetic energy and nuclear attraction. The orbitals in Φ^{G1} cannot be taken as orthogonal and thus the one-electron properties are given by[3]

$$\langle F\rangle=\sum_{ij}^{N}\langle\phi_i|f|\phi_j\rangle D_{ij},$$

---

[2] By improper dissociation we mean those cases in which the energy of the molecular system with $R=\infty$ is higher than the sum of the atomic energies (using the same method of calculation), e.g., this is true for H_2. For further discussion, see Ref. [4].

[3] The normalization constant is included in the D_{ij}'s. For a further discussion of these orbital density matrices see Ref. [4] (where they are denoted as D_j^i).

where D_{ij}, the orbital density matrix, is no longer the unit matrix ($D_{ij} = \delta_{ij}$) as it was in the Hartree and HF cases [4]. Here we can write the value for a one-electron property as

$$\langle F \rangle = F^{Cl} + F^{x}, \tag{17a}$$

where

$$F^{Cl} = \sum_{i=1}^{N} \langle i | f | i \rangle \tag{17b}$$

is the classical part (arising from an orbital product wave function) and[4]

$$F^{x} = \sum_{i>j=1}^{N} D_{ij}[2\langle i | f | j \rangle - \langle i | j \rangle (\langle i | f | i \rangle + \langle j | f | j \rangle)] \tag{17c}$$

is the quantum mechanical or *exchange part* of the property. Thus the electron density is no longer given by (9) but becomes

$$\varrho^{G1}_{(1)} = \sum_{i,j} D_{ij} \phi_i^*(1)\, \phi_j(1)\,,$$

which can be written as

$$\varrho^{G1}_{(1)} = \varrho^{Cl}_{(1)} + \varrho^{x}_{(1)}\,. \tag{18}$$

In this case

$$\int d^3 x_1 \varrho^{Cl}(1) = N$$

$$\int d^3 x_1 \varrho^{x}(1) = 0,$$

so that ϱ^{x} might be described as an interference density (a somewhat related term, ϱ^{I}, has been defined by Ruedenberg [3] in terms of an expansion of the density in terms of atomic basis functions).

3. Analysis of Energies of the Wave Functions

Next we consider the G^1 wave functions for several molecules and examine various partitions of the classical and nonclassical energies and the variation of these energies with internuclear distance, R. We consider the starting point as systems A and B infinitely far apart, with the wave functions as optimum for the separated A and B systems (note here that A and B may be atoms or molecules). Then we will consider A and B at a distance $R = R_{\text{large}}$, such that chemical forces may already be operating, but for which the wave function is still well approximated by the product of the wave functions of the separated systems A and B. At R_{large} we will consider wave functions in which the orbitals are forced to be those appropriate for $R = \infty$ (but displaced to the new nuclear positions), and we will also consider the wave functions with the orbitals reoptimized for $R = R_{\text{large}}$. These two types of wave functions will be referred to as the *frozen* and SCF wavefunctions, respectively. Note here that at all finite R we take the many-electron wave function to be the $G1$ wave function[5]; that is, even at large R, we correctly include the exchange of electrons of A with those on B. In some cases we will examine the energies over a large range of R, but our primary concern is to establish how the various types of energy change from $R = \infty$ to $R = R_{\text{large}}$ and especially which energy changes are different for bonding systems such as H_2 as compared to nonbonding systems such as He_2.

---

[4] Here, for convenience, we assume the orbitals are real.

[5] For the molecules with three or more electrons, we should optimize the spin coupling to obtain the spin-coupling optimized GI or SOGI wave function. (Ladner, R. C., Goddard III, W. A.: J. chem. Physics 51, 1073 (1969).) However for these systems and the larger distances considered here, the differences between $G1$ and SOGI are negligible for our present analysis.

First we will consider the H_2 molecule for various internuclear distances from $R = R_e$ to $R = \infty$.

A. *The* H_2 *Molecule*

One typical partition of the energy is to separate it into the kinetic energy, T, and the total potential energy V,

$$E = T + V.$$

However as shown[6] in Fig. 1 for H_2, neither T nor V is monotonic as R decreases from $R = \infty$ to $R = R_e$. Since the binding energy *is* monotonic in this region, it is clear that the T, V partition does not effect a partition of the bonding effects from those unrelated to bonding. One might also consider partitioning V into electron-electron repulsion (V^{en}), electron-nuclear attraction (V^{en}), and nuclear-nuclear repulsion (V^{nn}) parts. These qunatities are monotonic but vary far more rapidly

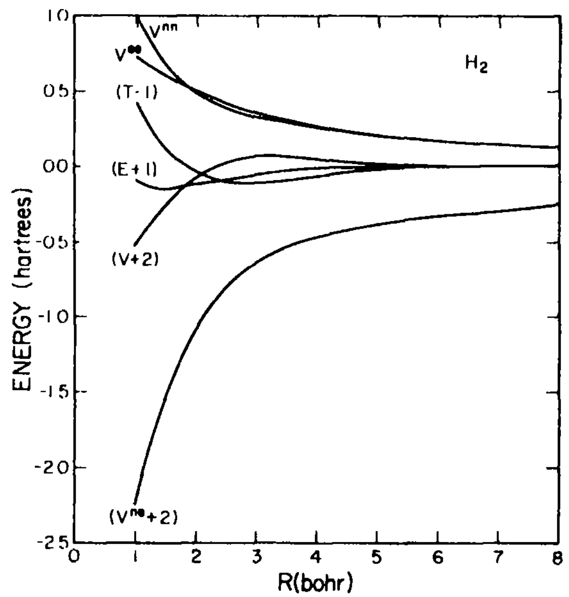

Fig. 1. The total binding energy (E), kinetic energy (T) and potential energy (V) for H_2 molecule (obtained for GI wavefunctions, see Footnote 6). The potential energy has also been partitioned into the electron-electron (V^{ee}), electron-nuclear (V^{en}), and nuclear-nuclear (V^{nn}) parts. All quantities have been referenced with respect to the value for $R = \infty$

---

[6] The GI wavefunctions discussed here are all for optimized minimum basis set wavefunctions. In Appendix A we consider the effect of the basis set upon the partitions considered here and find it to be minimal.

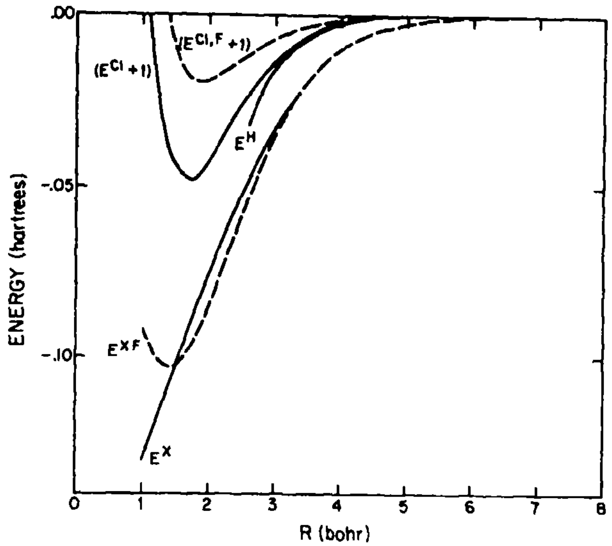

Fig. 2. The classical (E^{Cl}) and exchange (E^x) parts of the total energy of H_2. The broken lines indicate the quantities obtained from the frozen wavefunctions

with R than does E or V (see Fig. 1). That is, there are various parts of these quantities that cancel each other out.

An alternative partition of E into the classical and exchange parts (16), leads to quantities which vary monotonically with R (see Fig. 2) [6]. In this case E^x is larger than E^{Cl}, accounting for about two-thirds of the binding at R_e. However it would appear that some binding effects are contained in both E^{Cl} and E^x.

We considered partitioning E^x into its kinetic energy (T^x), nuclear-electron attraction (V^{nx}), and electron-electron repulsion (V^{ex}) parts

$$E^x = T^x + V^{nx} + V^{ex}$$

and found that E^x is dominated by T^x, with the other contributions both repulsive [6]. In addition, T^x follows the binding energy rather well suggesting a partition of the energy into T^x plus everything else (ω),

$$E = T^x + \omega\,. \tag{19}$$

In Fig. 3 we see that T^x and the total energy behave similarly and that the change in ω is relatively small and smooth.

Below we will examine partitions (16) and (19) for a number of other molecules, both stable and unstable ones, to test the generality of the above results. First, however, there is an additional point to consider concerning the above partitions. All energies were calculated for the optimum orbitals at the specific R being considered[6]. However at large enough distances the self-consistent orbitals should be essentially the same as the orbitals for $R = \infty$. If our partitions are meaningful, they should not be overly sensitive to whether the frozen or SCF orbitals are used. The E^{Cl} and E^x for the frozen orbitals of H_2 are also shown in Fig. 2 where we see that $E^{xF} \approx E^x$ for $R > 2.5\,a_0$, whereas for $R > 3a_0$ we had $\Delta E^{Cl,F} \approx \frac{1}{2}\Delta E^{Cl}$

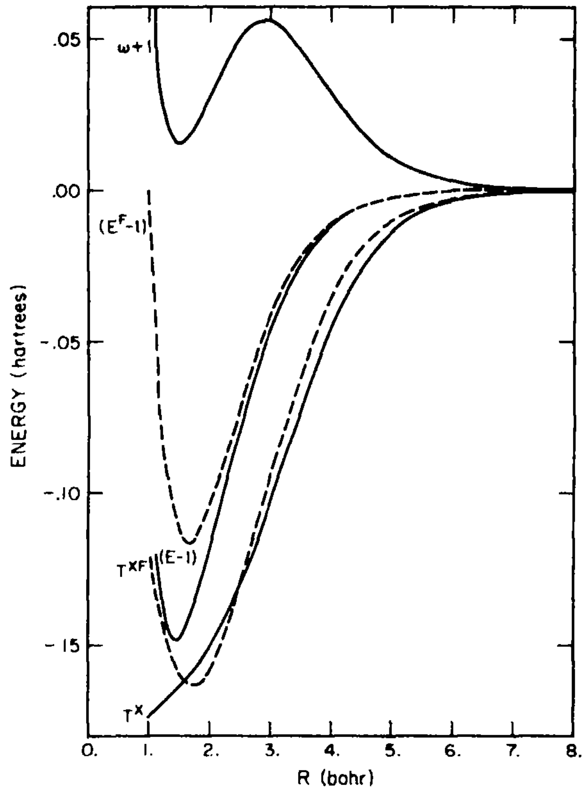

Fig. 3. The energy E and exchange kinetic energy T^x for H_2. The broken lines indicate the quantities obtained from the frozen wavefunctions. For the SCF case $\omega = E - T^x$ is also shown

(where ΔE is the difference between the value at R and the value at $R = \infty$). Thus it is the classical energy which seems primarily affected by self-consistency. In addition, the T^x for the frozen case is shown in Fig. 3, where we find that $T^{xF} \approx T^x$. Thus not only does T^x seem to include the terms responsible for bond formation but it is not very sensitive to the optimization of the orbitals[7].

B. Other Systems

In order to test the generality of the results for H_2, we considered a number of small systems of varying degrees of stability and instability. For each one we have considered two distances, $R = \infty$ and $R = R_{\text{large}}$, where R_{large} is chosen so that the chemical forces would be small but significant. The basis sets and other details of these calculations are given in Appendix A. For each system we have considered both the frozen and SCF orbitals at R_{large} and calculated E^{Cl}, E^x, T^x, and ω. In Table 1, we show how these change from $R = \infty$ to $R = R_{\text{large}}$ (here ΔT^x denotes the change in T^x, etc.).

---

[7] The Weinbaum wave function (Weinbaum, S.: J. chem. Physics 1, 593 (1933)) is equivalent to the minimum basis set $G1$ wave function for H_2, and the Heitler-London wave function (Heitler, W., London, F.: Z. Physik 44, 455 (1927)) is equivalent to the frozen $G1$ wave function for H_2.

Table 1. Partitions of the *G*1 energy for several systems. The energies are in Hartree atomic units[a]. Here Δ refers to the value at finite R minus the value at $R = \infty$

System	Self-consistent orbitals[b]				Frozen orbitals[c]			
	ΔE^{Cl}[d]	ΔE^{x}[d]	ΔT^{x}[e]	$\Delta \omega$[e]	ΔE^{ClF}[d]	ΔE^{xF}[d]	ΔT^{xF}[e]	$\Delta \omega^{F}$[e]
H_2[f]	−0.00188	−0.00766	−0.03598	0.02644	−0.00118	−0.00729	−0.02851	0.02005
HeH[g]	−0.00004	0.00103	0.00451	−0.00353	−0.00031	0.00142	0.00649	−0.00637
H_2H[h]	0.00023	0.00126	0.00730	−0.00581	−0.00060	0.00229	0.00974	−0.00805
H_2H[i]	0.00002	0.00147	0.00806	−0.00657	−0.00062	0.00244	0.01034	−0.00852
He_2[j]	0.00009	0.00005	0.00063	−0.00050	−0.00005	0.00020	0.00122	−0.00107
HeH_2[k]	0.00072	−0.00031	0.00062	−0.00021	−0.00013	0.00059	0.00312	−0.00266
$(H_2)_2$[l]	0.00071	0.00017	0.00300	−0.00212	−0.00029	0.00130	0.00580	−0.00479
LiH[m]	0.00188	−0.01195	−0.02877	0.01870	−0.00132	−0.00706	−0.02107	0.01269
BH[j]	−0.00633	−0.01073	−0.04220	0.02514	0.01221	−0.02456	−0.03248	0.02013

[a] See Footnote 1.

[b] By self-consistent orbitals we mean that the optimum *G*1 orbitals are used.

[c] By frozen orbitals we mean that the orbitals are optimum for $R = \infty$, but that the wavefunction is a *G*1-like wavefunction for the finite R.

[d] E^{Cl} and E^{x} are the classical and exchange parts of the energy, $E = E^{Cl} + E^{x}$.

[e] T^{x} is the exchange part of the kinetic energy and ω contains the remaining parts of the energy, $\omega = E - T^{x}$.

[f] $R \;= 4.2\, a_0$.

[g] $R \;= 4.643\, a_0$.

[h] $R_{12} = 1.4304242\, a_0$, $R_{23} = 4.285\, a_0$, linear.

[i] $R_{12} = 1.4304242\, a_0$, $R_{23} = 4.285\, a_0$, $\theta = 30°$.

[j] $R \;= 5.0\, a_0$.

[k] $R_{12} = 4.643\, a_0$, $R_{23} = 1.4304242\, a_0$, linear.

[l] $R_{12} = R_{34} = 1.4304242\, a_0$, $R_{23} = 4.285\, a_0$, linear.

[m] $R \;= 6.0\, a_0$.

For the frozen orbitals we find (see Table 1) that T^x decreases with R for the bound systems H_2, LiH, and BH and increases for the unbound systems. The remaining energy term, ω, behaves in the opposite direction; however T^x dominates in every case. Upon adjusting the orbitals self-consistently, we find that ΔT^x is still negative for bound systems and positive for unbound systems, and all cases ΔT^x still dominates $\Delta \omega$. Thus it would seem that the terms responsible for binding or antibinding are isolated into T^x for all of these systems.

For each of these systems we have also listed in Table 1 the ΔE^x and ΔE^{Cl} for the frozen and self-consistent cases. For the frozen orbitals we find that $E^{Cl,F}$ decreases with R in every case, except BH, whether the system is bound or unbound. Correspondingly E^{xF} decreases for the bound systems, increases for the unbound systems, and dominates ΔE^{Cl}. However when the orbitals are adjusted for self-consistency the above trends change. Here we find that except for H_2 and HeH, E^{Cl} increases as R decreases and that except for H_2, HeH_2, LiH, and BH, ΔE^x also increases. Thus it would appear that the terms responsible for binding are not well isolated by the $\{E^x, E^{Cl}\}$ partition.

From the calculations discussed above it appears that the factors responsible for the chemical bond are isolated into the exchange kinetic energy.

Next we will consider the H_2^+ ion. Since H_2^+ has only one electron, it would appear that $T^x = 0$ at all R; yet H_2^+ is more than half as stable as H_2 [7].

C. The H_2^+ Molecule

Consider first two H atoms separated by a large distance, R; let one be in the $1s$ state, ϕ_{1s}, and the other in the ns state, ϕ_{ns}. There are two possible states of the system the excitation could be on the left proton or on the right one. We will denote the wave functions for these states as

$$\Phi^{L}(1,2)=\phi^{L}_{ns}(1)\,\phi^{R}_{1s}(2) \tag{20}$$

and

$$\Phi^{R}(1,2)=\phi^{L}_{1s}(1)\,\phi^{R}_{ns}(2) \tag{21}$$

respectively. Classically we could specify which atom is excited, and the wave function would be (20) or (21), but quantum mechanically the total wavefunction for the adiabatic states of the system must be the symmetric (or antisymmetric) combination of the above states,

$$\Phi^{\text{total}}=\Phi^{L}+\Phi^{R}\,. \tag{22}$$

In addition we have to take into account Pauli's Principle, and for a singlet state the spatial part of the total wave function becomes

$$\Psi^{\text{total}}=[e+(12)]\,(\Phi^{L}+\Phi^{R})\,, \tag{23}$$

where e is the identity permutation and (12) interchanges particles 1 and 2. Thus in the total wave function we not only obtain exchange terms arising from the $[e+(12)]$ operator (which we also found for the ground state), but in addition we get exchange terms [8] from the degeneracy of the states (20) and (21).

Now consider the limit in which ϕ_{ns} is in the continuum, that is, the H_2^+ molecule. In this case at large R we have

$$\Phi^{L}=\phi^{R}_{1s}\,, \tag{24}$$

$$\Phi^{R}=\phi^{L}_{1s} \tag{25}$$

and the total wave function is

$$\Psi^{\text{total}}=\phi^{R}_{1s}+\phi^{L}_{1s}\,. \tag{26}$$

Here the classical wave function is either (24) or (25) and the quantum mechanical wave function is (26). Thus here we do not find the type of exchange term due to $[e+(12)]$, but we still have the other type of exchange term due to the degeneracy of the states (24) and (25). Thus for H_2^+ we define E^{Cl} as

$$E^{Cl}=\langle\phi^{L}_{1s}|h|\phi^{L}_{1s}\rangle=\langle\Phi^{R}|h|\Phi^{R}\rangle\,,$$

where h is the total one-electron Hamiltonian. In this case we define the exchange energy as[8]

$$\bar{E}^{x}=E-E^{Cl}\,,$$

---

[8] Feinberg, M. J., Ruedenberg, K., Mehler, E. L. (Advances quant. Chem. 5, 28 (1970)) have started with a quasi-classical density function ϱ^{QC} and defined an interference density function ϱ^{I} as the remainder of the total density. Because of the symmetry of the system, the energies they associate with ϱ^{QC} are equivalent to our classical energies and their interference energies are exactly our exchange energies. Thus their conclusions on the H_2^+ system are in agreement with our own. We thank Dr. Ruedenberg for a copy of this paper prior to publication. Feinberg and Ruedenberg (Feinberg, M. J.: Theoret. chim. Acta (Berl.) 19, 109 (1970); Feinberg, M. J., Ruedenberg, K.: J. chem. Physics 54, 1495 (1971); 55, 5804 (1971)) have also found their analysis to be valid for other one-electron diatomics.

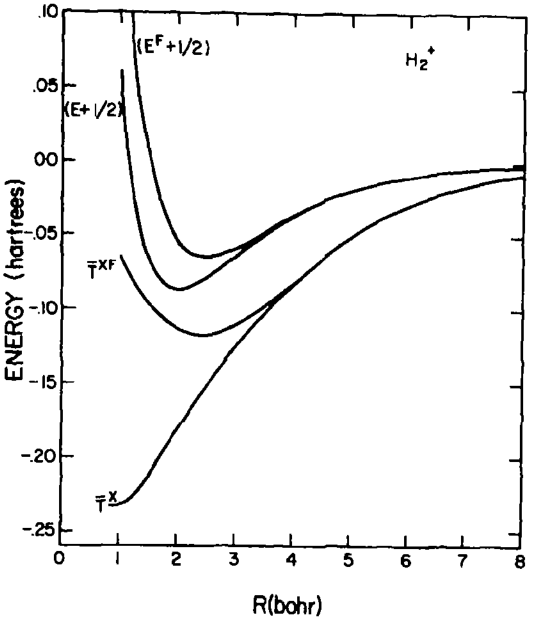

Fig. 4. Comparison of the total energy E and exchange kinetic energy $\bar{T}^x$ for the frozen and exponent optimized wave function of H_2^+. (A minimum basis set was used)

where the bar over $\bar{E}^x$ indicates that the second kind of exchange is involved, and similarly for the exchange kinetic energy, $\bar{T}^x = T - T^{Cl}$. Fig. 4 shows $\bar{T}^x$ and E for H_2^+ in the case where the orbitals are frozen (i. e., H atom orbitals). We see that E^F is negative for all R and is dominated by $\bar{T}^{xF}$. Thus again it seems that the exchange kinetic energy is the crucial term in forming the chemical bond.

We also carried out self-consistent calculations as a function of R (these were minimum basis set calculations, thus only the orbital exponents were really free to vary). The resulting total energy is shown in Fig. 4, where we see that down to about 3 a_0, the results were only slightly lower than for the frozen orbitals.

Given a $\phi^{\rm L}$ or a $\phi^{\rm R}$ it is simple to solve for $\phi^{\rm total}$ as in (22); however there does not appear to be a nonarbitrary, unique way of solving for $\phi^{\rm L}$ or $\phi^{\rm R}$ when $\Phi^{\rm total}$ is given[9]. In the case of H_2^+, $\Phi^{\rm total}$ is a symmetric function and there are an infinite number of $\phi^{\rm L}$ and $\phi^{\rm R}$ which add up to yield $\phi^{\rm total}$. For this reason we have arbitrarily defined the SCF $\phi^{\rm L}$ as just the part of $\phi^{\rm total}$ which uses basis functions centered on the left proton. This is consistent with $\phi^{\rm L}$ for the frozen case and yields reasonable results as shown in Fig. 4. We see that just as in H_2, $\bar{T}^x$ continues to drop as R decreases through R_e (the equilibrium value). In any case $\bar{T}^{xF}$ and $\bar{T}^x$ are nearly the same for $R > 3a_0$, and we still find that the exchange kinetic energy dominates.

In general for degeneracies such as in H_2^+, a definition of the classical energy as the energy for a single one of the degenerate states leads to a reasonable and satisfactory partition of the energy into classical and exchange parts. This applies not only to ions such as Li_2^+, but also to excited states of molecules, which often lead to such additional degeneracies. Such cases will be deferred to a later paper.

---

[9] The total energy is invariant under transformations symmetrically mixing $\phi^{\rm R}_1$ and $\phi^{\rm L}_1$ of (26), and hence a subsidiary condition such as maximum localization of the orbitals would have to be applied.

D. Summary

In summary we see that the partition of the $G1$ energy into T^x and ω appears to isolate into T^x the major effects characterizing chemical forces.

4. Comparison with Other Analyses of Bonding

In a lucid and erudite discussion of chemical binding Ruedenberg [3] suggested partitioning the pair density kernel into classical and exchange parts. He then proceeded to partition the kinetic, nuclear attraction, and electron repulsion energies into various types of quasi-classical, promotion, interference, and self-pairing terms. These partitions were based on an analysis of the wave function in terms of atomic-like basis functions and hence were independent of the type of wave function being considered (e. g., configuration interaction or Hartree-Fock). In this approach the classical density, ϱ^{Cl}, is defined in terms of the *atomic basis functions* (not the molecular orbitals) used in the expansion of the wave function, so that ϱ^{Cl} has the form

$$\varrho^{Cl}(1,1') = \sum_{A} \varrho_A^{Cl}(1,1'),$$

where the summation is over atomic centers (A), ϱ_A^{Cl} involves only basis functions on center A and the trace of ϱ^{Cl} is just the number of electrons. The remainder of $\varrho(1,1')$ is defined as the interference density, ϱ^I. The classical and interference parts of the kinetic energy are then defined in terms of these densities. Ruedenberg found [3, 9] that bound molecules exhibit a large negative interference kinetic energy, T^I.

Since Ruedenberg's ϱ^{Cl} is defined in terms of the atomic basis functions and our ϱ^{Cl} [see (18)] is defined in terms of the $G1$ molecular orbitals, there clearly is no direct correspondence between them. For the Weinbaum wavefunction (equivalent to the minimum basis set $G1$ wave-function) of H_2, Ruedenberg obtains $T^{Cl} = 1.0 + T^P = 1.423$ and $T^I = -0.275$, whereas we obtain $T^{Cl} = 1.312$ and $T^x = -0.164$ for the SCF $G1$ orbitals, and $T^{Cl,F} = 1.0$ and $T^x = -0.156$ for the frozen $G1$ orbitals (the calculated binding energy is 0.148).

We should make it clear here that despite the differences between T^x and T^I, Ruedenberg was the first person to recognize and quantify the importance of the nonclassical kinetic energy to chemical binding, one of the more significant developments in the theory of chemical bonding since Pauling's classic papers [10]. Ruedenberg and co-workers performed analyses on the Hartree-Fock wavefunctions of several systems including H_2O and several diatomics [9], and found the bond to be due largely to a large drop in the interference kinetic energy, T^I. This approach can be applied to any wavefunction involving basis functions, including GI wavefunctions. As we saw above for H_2 the resulting T^I is different from T^x; however we have not applied Ruedenberg's approach to GI wavefunctions for other molecules. Since the Ruedenberg partition is basis set dependent, it is not obvious how close the correspondence between T^x and T^I will be for larger basis sets and for systems with more electrons. For example, for a numerical wavefunction, the Ruedenberg partition is not well defined, but since T^x is defined in terms of GI orbitals and not basis functions, there is no difficulty in obtaining T^x.

Hellmann [2] used a model of the atom and the molecule to study bond formation and found that an initial drop in the kinetic energy was responsible for bonding. This model corresponds to a frozen calculation, and therefore, contrary to some arguments against his conclusions, need not satisfy the virial theorem [3]. (Only wave functions optimized with respect to a scaling need satisfy the virial theorem.) Pauling [10] and London [11] suggested that "resonance" was responsible for bonding. The "resonance" energy is, of course, quite similar to E^x. Pauling also noticed the density contraction effect.

The above studies of Ruedenberg, Hellmann, London, and Pauling examined how the molecule is formed. There is a second type of study [12] that examines only electron density from the final SCF wavefunction for the molecule. Since such treatments can treat only the final density contraction, these studies necessarily miss T^x. Thus if T^x is the significant quantity important for binding, any attempt to analyze bonding in terms of electron density would be futile since the information needed to construct T^x would be absent. (The first-order density matrix, however, can be used to construct T^x and hence could be used in analyzing bonding.)

Recently the charge density interpretation of binding has been extended by by Bader and Preston [13]. They partition the total kinetic energy density $K(x)$ as

$$K(x) = L(x) + G(x),$$

where $L(x) = -\frac{1}{4}\nabla^2 \varrho(x)$ is the Laplacian of the density and $G(x)$ is the remainder (involving gradients of $\varrho(x)$). Although the integral of $L(x)$ is zero,

$$\int L(x)\, dx = 0,$$

they note that a small negative curvature in $\varrho(x)$ leads to small positive contributions to $L(x)$ and thus (they suggest) a smaller local contribution to the kinetic energy than would otherwise be expected. They conclude that bound molecules are systems for which it is favorable to decrease the curvature in the bonding region. Of course, any change in the charge distribution would lead to $\Delta \int L(x)\, dx = 0$ and hence no net change in the contribution of $L(x)$ to the kinetic energy.

The integral of $G(x)$, is the total kinetic energy and includes both T^{Cl} and T^x. Thus for a stable molecule the integral of $G(x)$ dominates the potential terms and aids bonding at large distances but opposes binding and is dominated by the potential terms at short distances. That is, this partition into kinetic and potential terms would seem to lead to bonding effects in either term depending on the distance. As discussed in Section 3 the partition of the kinetic energy into T^{Cl} and T^x leads to the quantity T^x which dominates the bonding in molecules such as H_2 from R_e to ∞.

5. Discussion

Our whole discussion here has been based on GI-type wavefunctions which involve an orbital product modified by an operator which takes care of the necessary symmetries of the molecular system[10]. For such a wavefunction it is quite natural to partition the energy and other quantities into the classical part involving just the orbital product and the remainder involving orbital exchanges. The orbitals involved in such wavefunctions lead to a qualitative description of molecular systems similar to the valence bond description and compatable with common intuitive ideas about such systems. Since other types of wavefunctions such as obtained from configuration interaction (CI) also lead to a proper description of bonding, we might wonder how our interpretation would apply to such wavefunctions. The orbitals in a CI wavefunction do not generally correspond directly chemically interpretable quantities and so one problem will be to transform the wavefunction to obtain more interpretable orbitals. Since the GI and CI wavefunctions both lead to very good descriptions of the total wavefunction, the overlap of these wavefunctions should be very large. Thus we might start with the CI wavefunction and obtain from it a set of GI-like orbitals by maximizing the overlap [14]

$$\frac{|\langle\Phi_{GI}|\Phi_{CI}\rangle|^2}{\langle\Phi_{GI}|\Phi_{GI}\rangle\langle\Phi_{CI}|\Phi_{CI}\rangle}.$$

That is, we find a GI-like wavefunction with largest projection on the CI wavefunction. Using these new GI-like orbitals, we can interpret the CI wavefunction just as if it were a GI wavefunction. Such an approach might also be used to obtain approximate GI-like orbitals from Hartree-Fock wavefunctions [15]. Thus although the GI orbitals form a natural framework for interpreting bonding, one can probably obtain similar orbitals from other types of wavefunctions without actually carrying out GI calculations.

6. Summary

We find from an analysis of various partitions of the total energy that the nonclassical or exchange kinetic energy appears to dominate chemical bonding. This has been tested by examining the results for several stable and unstable molecular systems.

Appendix A: Basis Sets

We will now describe the basis sets used in the calculations reported herein.

Most of the calculations of H_2 used a minimum basis set. The reason is that this basis yields partitions of the energy quite comparable to those of larger basis sets, as is shown in Table 2, and in addition calculations can be simply and efficiently carried out for a number of internuclear distances. It is apparent from Table 2 that our conclusions are not greatly altered by the use of a larger basis set. Note in particular, how insensitive the total contragradience is with respect to the basis set.

---

[10] As indicated in the H_2^+ discussion, this type of analysis applies also to cases in which the usual group operator, G_i^γ (used to ensure spin and Pauli symmetry), is supplemented by spatial symmetry operators to ensure the proper spatial symmetry.

Table 2. Basis set dependence of the energy partitions for self-consistent $G1$ wavefunctions of H_2 (all calculations for $R = 1.4\,a_0$)

Number of basis functions	E^a	T^{xa}	V^{nxa}	ω^a	$-DC^b$
2^c	−1.147777	−0.164937	0.031475	−0.982840	−0.142663
4^d	−1.151345	−0.152065	0.022477	−0.999280	−0.146613
6^e	−1.151526	−0.159958	0.029630	−0.991568	−0.148577
8^f	−1.151887	−0.157300	0.026950	−0.994587	−0.148252

[a] E is the total energy, T^x is the exchange kinetic energy, V^{nx} is the exchange nuclear attraction, and ω is $E - T^x$.
[b] $-DC$ is the contragradience energy, see Ref. [6].
[c] $\zeta_{1s} = 1.2005$.
[d] $\zeta_{1s} = 1.1909$, $\zeta_{2p} = 2.0928$.
[e] $\zeta_{1s} = 1.3129$, $\zeta_{2s} = 1.1566$, $\zeta_{2p} = 1.9549$.
[f] $\zeta_{1s} = 1.3092$, $\zeta_{2s} = 1.1273$, $\zeta_{2p} = 1.700$, $\zeta_{3d} = 2.35$.

In polyatomic systems involving H_2, we have used the optimum[11] minimum basis set and distance calculated for H_2, $R_e = 1.4304242$ and $\zeta_{1s} = 1.1937847$ (not all of these figures are significant).

The He atom basis set for the HeH and HeH_2 calculations consists of four Slater functions [16] with ζ_{1s}, $\zeta_{2s} = 3.30$ and $\zeta_{1s'}$, $\zeta_{2s'} = 1.433$, whereas the He_2 calculations[12] used an added optimized $2p\sigma$ orbital (orbital exponent 0.4). The intermolecular distances used here were chosen to be approximately comparable, based on he van der Waals radii of the molecules involved. From the resulting $\Delta E'$ it appears that the He_2 distance is somewhat too large in comparison to the $(H_2)_2$ distance.

The Li atom basis set for LiH consists of seven Slater functions [16] with one $1s(\zeta = 3.0)$, four $3s's(\zeta = 5.4, 2.999, 1.347, 0.841)$, and two $4s's(\zeta = 5.33, 7.32)$, all optimized for a Li atom.

The basis set for BH consists of an $(11s, 5p/4s)$ primitive set of Gaussian-type orbitals contracted to a $(5s, 3p/2s)$ set [17].

References

1. Pauling, L.: The nature of the chemical bond, 3rd. ed., New York: Cornell University Press 1960; or Sienko, M. J., Plane, R. A.: Chemistry, 2nd. ed., New York: McGraw-Hill Publishing Co. 1961.
2. Hellmann, H.: Z. Physik **85**, 180 (1933).
3. Ruedenberg, K.: Rev. mod. Physics **34**, 326 (1962).
4. Goddard III, W. A.: Physic. Rev. **157**, 81 (1967).
5. — Physic. Rev. **157**, 73 (1967).
6. Wilson, Jr., C. W., Goddard III, W. A.: Chem. Physics Letters **5**, 45 (1970).
7. Herzberg, G.: Spectra of diatomic molecules, p. 546. Princeton, New Jersey: D. Van Nostrand Co. 1950.
8. Pauling, L.: J. Amer. chem. Soc. **53**, 3225 (1931).

---

[11] The optimum R we calculated is somewhat different from the Weinbaum value[7] $R = 1.4166$, but is in good agreement with the value obtained by Adamov and Bulychev (Adamov, M. N., Bulychev, V. P.: Zh. Teor. Eksp. Khim. **2**, 685 (1966); English Translation: J. theoret. Exp. Chem. **2**, 502 (1966)).

[12] We wish to thank Dr. W. E. Palke for his unpublished He_2 results.

9. Edmiston, C., Ruedenberg, K.: J. physic. Chem. **68**, 1628 (1964); Layton, E., Ruedenberg, K.: J. physic. Chem. **68**, 1654 (1964); Rue, R. R., Ruedenberg, K.: J. physic. Chem. **68**, 1676 (1964).
10. Pauling, L.: Proc. nat. Acad. Sci. USA **14**, 359 (1928); J. Amer. chem. Soc. **53**, 1367, 3225 (4131).
11. London, F.: Z. Physik **46**, 455 (1928).
12. Bader, R. F., Henneker, W. H., Cade, P. E.: J. chem. Physics **46**, 3341 (1967); Bader, R. F., Bandrauk, A. D.: J. chem. Physics **49**, 1653 (1968); Smith, P. R., Richardson, J. W.: J. physic. Chem. **71**, 924 (1967); Bader, R. F., Keaveny, I., Cade, P. E.: J. chem. Physics **47**, 3381 (1967); Bader, R. F., Bandrauk, A. D.: J. chem. Physics **49**, 1666 (1968).
13. Bader, R. F. W., Preston, H. J. T.: Int. J. quant. Chemistry **3**, 327 (1969).
14. Hunt, W. J., Blint, R. J., Kahn, L. R.: Private communications.
15. Kapral, R.: Ph. D. Thesis, Princeton University, 1967.
16. Goddard III, W. A.: J. chem. Physics **48**, 1008 (1968).
17. Blint, R. J., Goddard III, W. A.: J. chem. Physics **56** (1972)

Dr. C. W. Wilson
Arthur Amos Noyes Laboratory
of Chemical Physics
California Institute of Technology
Pasadena, California 91109, USA

Theoret. chim. Acta (Berl.) 26, 211—230 (1972)
© by Springer-Verlag 1972

The Role of Kinetic Energy in Chemical Binding

II. Contragradience*

William A. Goddard III** and C. Woodrow Wilson, Jr.***

Arthur Amos Noyes Laboratory of Chemical Physics[†],
California Institute of Technology, Pasadena, California 91109

Received February 16, 1972

In a preceding paper, we examined the GI wavefunctions of small molecules and found that the nonclassical or exchange kinetic energy, T^x, dominates the changes in energy involved in chemical binding. Here we examine more closely the changes in T^x with internuclear separation and find that ΔT^x is large for valence orbitals centered on different atoms because of the large region in which the orbitals are contragradient (i.e., have gradients in obtuse directions). In fact for H_2 this contragradience accounts for 93% of the calculated binding energy. In addition, the behavior of T^x and ΔT^x can usually be predicted from consideration of the permutational symmetry (Young tableau) involved in the wavefunction. The concepts developed here provide an alternative interpretation of the nature of the chemical bond.

Die in einer vorhergehenden Arbeit durchgeführten Untersuchungen der GI-Wellenfunktionen kleiner Moleküle führten zu dem Ergebnis, daß der nichtklassische oder Austauschanteil der kinetischen Energie T^x bei Änderungen der Energie chemischer Bindungen überwiegt. In dieser Arbeit werden die Änderungen von T^x mit dem Kernabstand näher untersucht. Wir finden ein großes ΔT^x für an verschiedenen Atomen zentrierte Valenzorbitale wegen der großen Region, in der die Orbitale „kontragradient" (d. h. sie haben Gradienten in Richtungen, die einen stumpfen Winkel miteinander bilden) sind. Für H_2 sind 93% der berechneten Bindungsenergie auf diese „Kontragradienz" zurückzuführen. Ferner kann das Verhalten von T^x und ΔT^x normalerweise aus der Permutationssymmetrie (Young Tafeln) der Wellenfunktionen vorausgesagt werden. Die hier entwickelten Methoden erlauben eine alternative Interpretation der chemischen Bindung.

1. Introduction

In a preceding paper [1] we examined the GI wavefunctions [2, 3] of a number of small systems (both bound and unbound) and found in every case that chemical binding is dominated by the change in one term in the energy expression: the *exchange kinetic energy*, T^x. Here we investigate why T^x is so important and find that T^x is dominated by a term (the contragradience) that is uniquely large for multicentered systems, i.e., molecules. Further examination of this term leads to concepts in terms of which general aspects of binding can be predicted using simple considerations of the spatial permutation symmetry forced on the elec-

---

* Partially supported by a grant (GP-15423) from the National Science Foundation. This paper is based on a portion of the PhD thesis (California Institute of Technology, 1970) by CWW.

** Alfred P. Sloan Foundation Research Fellow.

*** National Science Foundation Predoctoral Trainee. Present address: Department of Chemistry, Argonne National Laboratory, Argonne, Illinois 60439, U.S.A.

[†] Contribution No. 4251.

tronic wavefunction by the spin symmetry coupled with the Pauli Principle. This leads to an alternative simple model of the chemical bond.

The GI wavefunction involves a number of orbitals (equal to the number of electrons), each of which is solved for self-consistently in the field due to the other electrons. As the nuclear configuration changes, the fields change, and hence the orbitals change. However, in some cases it is useful to consider to treat a molecular complex AB using the orbitals appropriate for the separated systems A and B. Such wavefunctions will be referred to as the *frozen wavefunctions* of AB or sometimes more simply as the frozen AB case.

2. The Magnitude of the Exchange Terms

In Fig. 1 we see that for the H_2 molecule the magnitude of T^x is much larger than the exchange part of the electron-nuclear attraction energy (V^{nx}) or the exchange part of the electron repulsion energy (V^{ex}). In Table 1 of I, we saw that ΔT^x (the change in T^x from the value at $R = \infty$) dominates the binding energy for all molecules considered, determining its sign in every case. Consequently, it is of interest to understand why the magnitude of ΔT^x is much larger than the other terms in the binding energy. First we will consider the ground state of H_2.

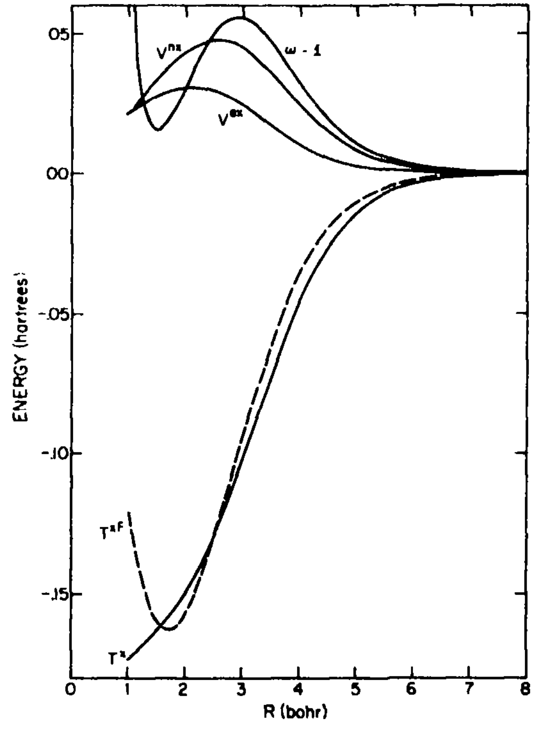

Fig. 1. The exchange kinetic energy (T^x), exchange nuclear attraction energy (V^{nx}) and exchange electron repulsion energy (V^{ex}) for the ground state of H_2. T^{xF} refers to the T^x for the frozen wavefunction, and $\omega = E - T^x$

A. *The* H_2 *Singlet State*

In Fig. 1 we see that T^{xF} (T^x for the frozen wavefunction of H_2) behaves very much like the T^x from $R = \infty$ to $R = R_e$. In addition, in Table 1 of I we saw that ΔT^x and ΔT^{xF} are comparable (and of the same sign) for a number of bound and unbound systems (all systems considered). Since ΔT^{xF} is also much easier to study (requiring only the wavefunctions for $R = \infty$), we will concentrate in this section on T^{xF}.

The spatial part of the frozen G1 wavefunctions is

$$\Phi^{sp} = O_{11}ab = \tfrac{1}{2}[ab+ba], \tag{1}$$

where a and b are just H 1s functions on the two protons. Thus, from Eq. (A-8) of Appendix A, the exchange kinetic energy is given by [4]

$$T^x = -SD\left\{\langle a|t|a\rangle + \langle b|t|b\rangle - \frac{2}{S}\langle a|t|b\rangle\right\}, \tag{2a}$$

where $S = \langle a|b\rangle$ is the orbital overlap, and $D = S/(1+S^2)$ is the off-diagonal element of the orbital density matrix. Integrating by parts in (2a), we obtain

$$T^x = -\tfrac{1}{2}SD\left\{\langle \nabla a\cdot\nabla a\rangle + \langle \nabla b\cdot\nabla b\rangle - \frac{2}{S}\langle \nabla a\cdot\nabla b\rangle\right\}, \tag{2b}$$

where

$$\langle \nabla a\cdot\nabla b\rangle = \int d^3x_1[\nabla\phi_a(1)]\cdot[\nabla\phi_b(1)].$$

All other one-electron properties can also be divided into classical and exchange parts with the exchange part of the form in (2a); however, Eq. (2b) is specific to the case of kinetic energy.

Now we will compare the changes upon molecule formation of the exchange parts of various properties in order to determine why the magnitude of ΔT^x is so large. Replacing the t operator in (2a) by the simple scalar operators 1 and v^n, we obtain

$$N^x \equiv -SD\left[\langle a|a\rangle + \langle b|b\rangle - \frac{2}{S}\langle a|b\rangle\right], \tag{3a}$$

$$V^{nx} = -SD\left[\langle a|v^n|a\rangle + \langle b|v^n|b\rangle - \frac{2}{S}\langle a|v^n|b\rangle\right], \tag{3b}$$

for the exchange parts of the total change and of the nuclear attraction energy, respectively. Eqs. (3a) and (3b) can be rewritten as

$$N^x = \int dx_1^3\varrho^x(1) \tag{4}$$

and

$$V^{nx} = \int dx_1^3 v^n(1)\varrho^x(1), \tag{5}$$

where

$$\varrho^x(1) \equiv (-SD)\left[\phi_a(1)\phi_a(1) + \phi_b(1)\phi_b(1) - \frac{2}{S}\phi_a(1)\phi_b(1)\right] \tag{6}$$

is the *exchange electron density* [see (18) of I]. We cannot write T^x in this way because of the ∇^2 operator; however, from (2b) the quantity

$$t^x(1) = -\tfrac{1}{2}SD\left[|\nabla\phi_a(1)|^2 + |\nabla\phi_b(1)|^2 - \frac{2}{S}\nabla\phi_a(1)\cdot\nabla\phi_b(1)\right] \tag{7}$$

can be defined so that

$$T^x = \int d^3x_1 t^x(1) . \tag{8}$$

Even though the form (8) is similar to that of (4) and (5), there is still an essential difference due to the difference in the form of the *interchange term* (the third term) of t^x as compared to the interchange term of ϱ^x. If ϕ_a and ϕ_b are positive everywhere (as for frozen H_2), then $-(2/S)\,\phi_a(1)\,\phi_b(1)$ is negative everywhere and the interchange term may cancel a large part of the noninterchange terms (the first two terms in fact, for N^x the cancellation is sufficient to lead to $N^x = 0$ for all R. However, the interchange term in t^x involves a dot product and thus is positive wherever $\nabla\phi_a\cdot\nabla\phi_b$ is negative, that is, in the region in which the orbitals are *contragradient*. In this region the interchange term of T^x adds to the other terms and enhances binding. In order to isolate the effect of this contragradience on t^x, we will define a new function,

$$t^{nc} \equiv \tfrac{1}{2}SD\left[|\nabla\phi_a|^2 + |\nabla\phi_b|^2 - \frac{2}{S}\,|\nabla\phi_a|\,|\nabla\phi_b|\right], \tag{9}$$

called the *noncontragradient* part of t^x. The total noncontragradient part of T^x is then

$$T^{nc} = \int dr^3 t^{nc}(r) .$$

We also define

$$c(r) \equiv [|\nabla\phi_a|\,|\nabla\phi_b| - \nabla\phi_a\cdot\nabla\phi_b] \tag{10}$$

to be the *contragradience function* and

$$C = \int d^3r c(r)$$

to be the *total contragradience*. Thus the contribution of the contragradience to T^x is given by $-DC$ and we obtain

$$T^x = T^{nc} - DC . \tag{11}$$

Since $c(r)$ is always positive, C is always positive; thus, since D is always positive for a singlet state, the contragradience contribution to T^x is always negative (or zero). However, just as for ϱ^x, the interchange term of t^{nc} opposes the noninterchange terms and thus leads to a reduced value for T^{nc}. In fact for the frozen wavefunction of H_2, the resulting T^{nc} is zero for all R. That is, in this case *all of the bonding* effect of T^x is due to the contragradience, C. The essential reason for this difference between N^x, V^{nx}, and T^x can be seen in Fig. 2, where the integrands of the interchange terms are plotted along the internuclear axis. We see that for N^x, V^{nx}, and T^{nc} the plots are comparable. But $-c(r)$ is zero outside the bonding region and quite negative in the bonding region, leading to a $t^x(r)$ term which is positive outside and negative inside the bonding region. In fact, the interchange term of T^x is negative only in a sphere of diameter R passing through both nuclei.

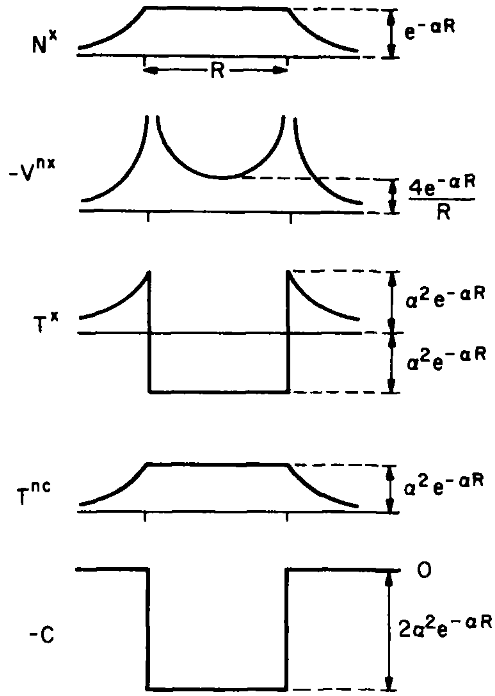

Fig. 2. The interchange part of the integrand of various operators using the frozen G 1 wavefunctions of H_2

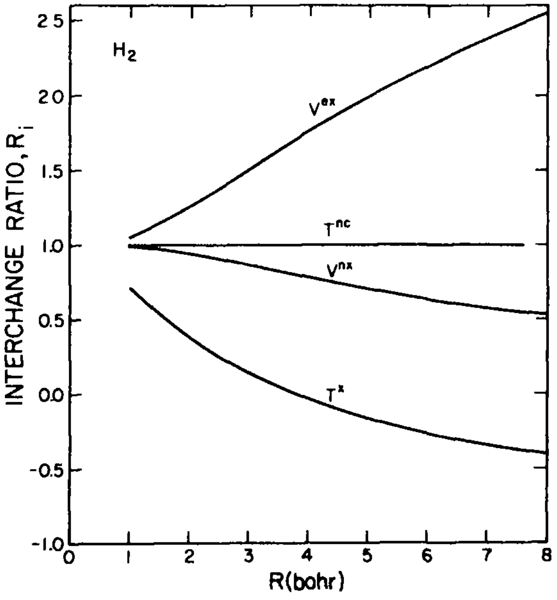

Fig. 3. Ratio of the interchange term to the noninterchange term in the expressions for T^x, V^{nx}, V^{ex}, and T^{nc} as a function of R using the frozen wavefunction of H_2. A ratio of 1.0 corresponds to exact cancellation, a negative ratio corresponds to enhancement of the quantity

As will be discussed below, a consideration of the contragradience function $c(\boldsymbol{r})$ leads to a reasonable indication of which region of space contributes most to the bond.

In Fig. 3 we show the ratio, R_i, of the interchange term to the non-interchange terms as a function of internuclear distance (frozen H_2) for T^x, V^{nx}, and the exchange electron-electron interaction energy

$$V^{ex} = -SD\left\{[aa|bb] - \frac{1}{S}[ab|ab]\right\}, \tag{12}$$

where $[aa|bb]$ and $[ab|ab]$ are the Coulomb and exchange integrals. For V^{nx} and V^{ex} we have $R_i \leqq 1$, and thus $V^{nx} \geqq 0$ at all distances. Only for T^x is $R_i \leqq 1$, and consequently $T^x \leqq 0$ at all distances. As a result of these effects, T^x is inordinately large in molecules.

In summary, for H_2 T^x *is large and negative because of the contragradient nature of the orbitals on different centers and the concomitant effect on the interchange term in* T^x.

So far we have examined the energy changes for frozen orbitals. For each fixed R we should now allow the orbitals to readjust self-consistently. Since C dominates the ΔE we would expect the self-consistency readjustments of the orbitals to also modify C. In fact for H_2 the change in C in proceeding from the frozen wavefunction to the SCF wavefunction is small for larger R, and even at $R_e = 1.4a_0$ the change in proceeding from the minimum basis SCF result to the large basis (optimized basis with s, p, and d functions) SCF result is only 1% (see Table 2 of I).

B. Comparison with Other Descriptions

The lowering of the kinetic energy associated with chemical bonding has been observed by a number of workers starting with Hellmann [5] who viewed molecule formation as an expansion of the effective confines of the valence electrons, thereby decreasing their kinetic energy. A more quantitative description was provided by Feinberg and Ruedenberg [6] who partitioned the kinetic energy of H_2^+ into contributions parallel and perpendicular to the bond axis. In confirmation of Hellmann's original suggestion, they found a large decrease in the parallel contribution, $T_{||}$, while the perpendicular components $T_{\perp}$ maintained essentially unchanged (from the value for the separated atoms). They traced this effect to the small magnitude of $\partial\phi/\partial z$ in the region between the nuclei (ϕ is the wavefunction and z is parallel to the internuclear axis); in fact, the decrease occurs predominately in the portion, $T_{||}^b$, of $T_{||}$ arising from the bond region.

Our previous analysis [1] of the frozen wavefunction of H_2^+ differs from our above treatment of frozen H_2 only in the form of the density matrix D; hence the effects described by Fig. 2 carry over to the H_2^+ case. Clearly then for H_2^+, C contains the same kinetic energy annihilating effect as does $T_{||}^b$. The shape of $C(\boldsymbol{r})$ shown in Fig. 2 has about the same shape for all σ bonds. Consequently, we expect the conclusions of Feinberg and Ruedenberg about $T_{||}^b$ to be correct also for σ bonds of many-electron systems even though the corresponding $\{\partial\varphi_i/\partial z\}$ need not decrease drastically between the nuclei. It should also apply to polyatomic systems where the bond region may not be readily definable.

C. Other Two-Electron States

So far in this section only the singlet state of H_2 has been considered. For a two-electron triplet state the G1 spatial wavefunction is

$$\Phi^{sp} = O_{11}ab = \tfrac{1}{2}[e-(12)]ab = \tfrac{1}{2}(ab-ba), \tag{13a}$$

[cf. Eq. (1)] and thus the off-diagonal element of the orbital density matrix becomes [2]

$$D = -\frac{S}{(1-S^2)} \tag{13b}$$

rather than as in (2a). All the quantities (1)–(12) will have the same form, but now D is negative. Hence the contragradience is still dominant but now *opposes* bond formation.

For a given pair of frozen orbitals the contragradient part of the energy is

$$-\frac{SC}{1+S^2} \tag{14a}$$

for the singlet state and

$$+\frac{SC}{1-S^2} \tag{14b}$$

for the triplet state. For a typical bond distance ($1.4a_0$) and pair of bonding valence orbitals, $S \sim 0.7$ so that the magnitude of (14b) is about three times that of (14a). Thus antisymmetric coupling of orbitals as in (13a) is three times as antibonding as symmetric coupling (1) would be bonding.

Since C opposes bonding for the triplet state, we may expect that the changes in ϕ_a and ϕ_b upon going from frozen to SCF will now be such as to minimize the magnitude of C. In fact this is the case and for many-electron systems, similar arguments can be used in understanding the changes that occur as orbitals readjust self-consistently.

D. Atoms and Ions

We have considered pairs of orbitals centered at different points and found that if each orbital decreases monotonically, then the orbitals are contragradient in the bonding region and lead to a positive value of

$$\left[\langle a|t|a\rangle + \langle b|t|b\rangle - \frac{2}{S}\langle a|t|b\rangle\right].$$

However, if both orbitals are centered on the same center this need not occur. Consider a two-electron singlet state as in He or H^-. Here each orbital is spherically symmetric and monotonically decreasing. Thus

$$\nabla\phi_a \cdot \nabla\phi_b = |\nabla\phi_a|\,|\nabla\phi_b|$$

everwhere and C is identically zero; that is, there is no contragradience. Since it is C that makes T^x so important for molecules, it may be that completely different parts of the energy are important for the stability of atoms and ions.

E. Larger Systems

For systems with more electrons, the projection operator O_{11} involved in the wavefunction is more complicated and involves many permutations. However, as shown in Appendix A, T^x can still be discussed in terms of pair contributions, each of which has the form of (2b). Just in the above comparison of the singlet and triplet states of two electrons, the sign of T^x is generally determined by the corresponding permutation numbers, $U_{11\tau}$, in the projection operator and thus by the tableau, as will be discussed in the next section.

3. The Effect of the Pauli Principle on Bond Formation

The Pauli Principle (PP) states that the total wavefunction of a collection of identical particles must be either *symmetric* (in which case, the particles are called Bosons) or *antisymmetric* (where they are called Fermions) under transposition of the particle coordinates (spatial and spin). Which way the wavefunction behaves is determined by the spin of the particles-integral spin leads only to symmetric wavefunctions; half-integral spin leads only to antisymmetric wavefunctions [7]. We will be interested here in electronic systems and hence with Fermion wavefunctions.

To a good approximation in small molecules, the Hamiltonian may be taken to be independent of spin, so that the energy will depend only on the spatial part of the wavefunction. However, for a given spin symmetry, the PP fixes the permutational symmetry of the spatial part of the wavefunction and thereby determines the form of the energy [3]. For example, for two electrons a singlet spin function is antisymmetric, and thus for Fermions the spatial part of the wavefunction must be symmetric (Fig. 4a) in order that the total spatial-spin wave-

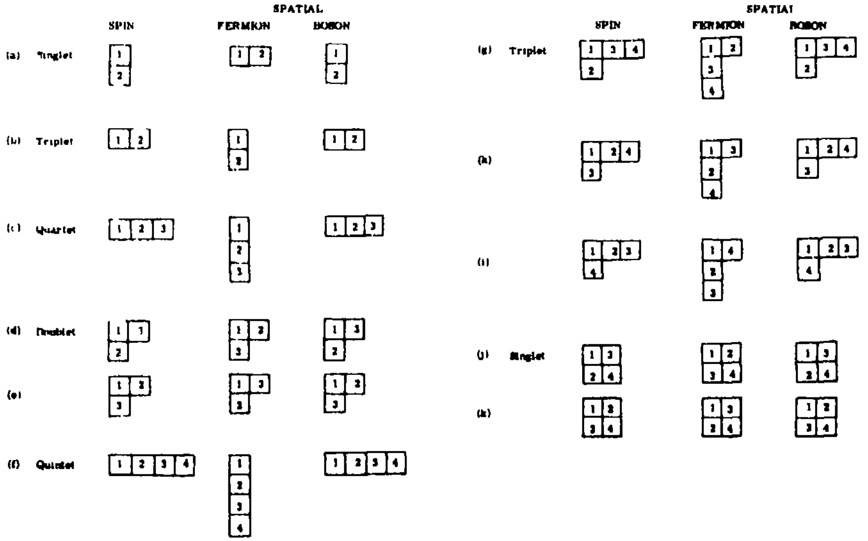

Fig. 4. The spin and spatial tableaux for two, three, and four particle wavefunctions for both Fermion and Boson systems

function be antisymmetric. On the other hand, if electrons were spin-$\frac{1}{2}$ Bosons [7], the spatial wavefunction would have to be antisymmetric (Fig. 4a). Similarly, a two-electron triplet spin function is symmetric; therefore, the Fermion spatial function must be antisymmetric and the Boson spatial function must be symmetric (Fig. 4b).

For more than two particles, discussions of this type are most simply carried out in terms of the Young Tableaux (see Fig. 4), which graphically indicate the permutational symmetry [2, 3]. Here, successive numbers in the same column of a tableau indicate antisymmetrization, and successive numbers in the same row indicate symmetrization (see Ref. [3] for further discussion of the tableaux). For Bosons the spatial and spin tableaux must be the same in order for the total wavefunction to be symmetric, whereas for Fermions these tableaux must be conjugates (that is, related by the interchange of the rows and columns) in order for the total wavefunction to be antisymmetric. The spin tableaux have at most two rows since the spin transformation space is two-dimensional. As a result, the spatial tableaux for Boson wavefunctions can have no more than two rows and those for Fermion wavefunctions can have no more than two columns.

It is well known [8] that for a spin-free Hamiltonian with no nonlocal interactions, the spatial part of the ground state wavefunction is symmetric unless it is forbidden to be so by the PP. Thus we should expect the ground state of a two-Fermion system (spin-$\frac{1}{2}$) to be a singlet state and that of two spin-$\frac{1}{2}$ Bosons to be a triplet state (see Fig. 4ab). The restriction that the spin tableaux have at most two rows for spin-$\frac{1}{2}$ particles implies that for Fermions the spatial tableaux have no more than two columns. Thus for more than two Fermions, the spatial state *cannot* be totally symmetric. For Bosons no such restriction arises, and we would expect the ground state to be a quartet for three particles, a quintet for four particles, *etc.* (see Fig. 4).

A. The Partition of T^x

As shown in Appendix A the exchange part of the kinetic energy can be written as

$$T^x = \sum_{j>k} T^x_{jk} \tag{15}$$

for GI type wavefunctions, where the pair term T^x_{jk} has the form

$$T^x_{jk} = -\sigma_{jk}\tau_{jk}, \tag{16}$$

the factor τ_{jk} has the form

$$\tau_{jk} = \left[\langle j|t|j\rangle + \langle k|t|k\rangle - \frac{2}{S_{jk}}\langle j|t|k\rangle\right] \tag{17}$$

[identical with the bracketed factor of (2a)], and σ_{jk} has the form

$$\sigma_{jk} = -D_{jk}S_{jk} \tag{18}$$

Table 1. The diagonal matrix elements $U_{ii(jk)}$ for the various transpositions (jk)

Partition	$[1^2]$	$[2]$	$[1^3]$	$[2,1]$		$[1^4]$	$[2,1^2]$				$[2^2]$	
Spin	0	1	$\frac{3}{2}$	$\frac{1}{2}$		2	1				0	
Tableau	1 2	1 2	1 2 3	1 2 3	1 3 2	1 2 3 4	1 2 3 4	1 3 2 4	1 4 2 3	1 2 3 4	1 3 2 4
Transposition											
(12)	+1	−1	−1	+1	−1	−1	+1	−1	−1	+1	−1
(13)			−1	$-\frac{1}{2}$	$+\frac{1}{2}$	−1	$-\frac{1}{2}$	$+\frac{1}{2}$	−1	$-\frac{1}{2}$	$+\frac{1}{2}$
(23)			−1	$-\frac{1}{2}$	$+\frac{1}{2}$	−1	$-\frac{1}{2}$	$+\frac{1}{2}$	−1	$-\frac{1}{2}$	$+\frac{1}{2}$
(14)						−1	$-\frac{1}{2}$	$-\frac{5}{6}$	$+\frac{1}{3}$	$-\frac{1}{2}$	$+\frac{1}{2}$
(24)						−1	$-\frac{1}{2}$	$-\frac{5}{6}$	$+\frac{1}{3}$	$-\frac{1}{2}$	$+\frac{1}{2}$
(34)						−1	−1	$-\frac{1}{3}$	$+\frac{1}{3}$	+1	−1

[cf., Eq. (2a)]. Usually σ_{jk} of (18) is dominated by the term [9]

$$\sigma_{jk} \sim -U_{ii(jk)} S_{jk}^2 , \qquad (19)$$

where $U_{ii(jk)}$ is the number specifying the coefficient of the (jk) exchange term in the many-electron wavefunction; the coefficients for various two, three, and four electron systems are given in Table 1 and are easily obtained from a consideration of the tableaux [3].

We will be interested in the intermolecular potentials and hence in the change in the energy, ΔE, as atoms are brought together. Assuming that ΔE is dominated by ΔT^x, we will want to examine the contributions to ΔT^x. Since

$$T_{jk}^x \sim -U_{ii(jk)} S_{jk}^2 \tau_{jk} \qquad (20)$$

we expect (especially for the frozen wavefunctions) that the largest changes with internuclear distance will occur for terms for which orbitals ϕ_j and ϕ_k are on different atoms. Of these interatomic T_{jk}^x terms, we expect binding contributions from pairs for which $U_{ii(jk)} > 0$ and antibonding contributions from pairs for wich $U_{ii(jk)} < 0$.

B. The HeH *and* H_2H *Systems*

Consider, for example, the HeH system at large separations. At infinite separation the He and H atoms are independent, with the spatial symmetry of the He atom described by the tableau

$$\begin{array}{|c|c|}\hline 1 & 2 \\ \hline \end{array} \qquad (21)$$

(since He is in the singlet state). The third electron of HeH ($R = \infty$) can be coupled to the He function in two ways,

$$\begin{array}{|c|c|c|}\hline 1 & 2 & 3 \\ \hline \end{array} \tag{22}$$

and

$$\begin{array}{|c|c|}\hline 1 & 2 \\ \hline 3 & \multicolumn{1}{c}{} \\ \cline{1-1} \end{array} \tag{23}$$

The interatomic exchange terms $U_{11(13)}$ and $U_{11(23)}$ are positive (+1) for (22) and negative ($-\frac{1}{2}$) for (23) (see Table 1); hence we expect

$$\Delta T^x_{13} < 0, \quad \Delta T^x_{23} < 0$$

for (22) and

$$\Delta T^x_{13} > 0, \quad \Delta T^x_{23} > 0$$

for (23). Thus the wavefunction for (22) should be bound and the wavefunction for (23) should be unbound.

As shown in Table 2, the ΔT^x and ΔE have the signs expected. In addition we note that ΔT^x for (23) is $-\frac{1}{2}$ times the ΔT^x for (22) as expected from the magnitudes of the interatomic $U_{ii(jk)}$. Consistent with this we see that (22) is more stable than (23) is unstable.

Indeed, we would have expected the wavefunction of symmetry (22) to have the lowest energy since it is totally symmetric. However for Fermions (22) is forbidden by the PP. Thus the ground state Fermion wavefunction must be described

Table 2. Comparison of the Energies for HeH, H_2H, H_2H_2, HeH_2, and HeHe with Boson and Fermion spin-one-half electrons. In all cases the orbitals were frozen as the solutions for infinite separation. Here Δ refers to the energy at finite R minus the energy for $R = \infty$

System	Fermions		Bosons	
	ΔE[a]	ΔT^x[a]	ΔE[a]	ΔT^x[a]
HeH[b]	+0.001114	0.006488	−0.003018	−0.012844
H_2H linear[c]	+0.001693	0.009738	−0.004879	−0.01903
H_2H nonlinear[d]	+0.001823	0.010344	−0.005235	−0.020191
H_2H_2 linear[e]	+0.001009	0.005796	−0.002436	−0.011472
HeH_2 linear[f]	+0.000460	0.003119	−0.001212	−0.006214
HeHe[g]	+0.000148	0.001221	−0.000382	−0.002439

[a] E is the total energy and T^x is the exchange part of the kinetic energy. Atomic units are used throughout, $e = \hbar = m_e = 1$; in these units 1 hartree = 27.211 eV = 627.51 kcal · mole^{-1} is the unit of energy, and 1 bohr = 0.52917 Å is the unit of length. Cohen, E. R., DuMond, J. W. M.: Rev. mod. Physics 37, 537 (1965).

[b] $R = 4.643$.

[c] H_2 bond length = 1.4304242, the distance from the free H to the closest H of H_2 is 4.285.

[d] Same as c with the angle between the H_2 axis and the vector from middle to third $H = 30°$.

[e] H_2 bond length = 1.4304242, IMD = 4.285 (IMD is the distance between midpoints of the H_2 molecules) [10].

[f] H_2 bond length = 1.4304242, IMD = 4.643.

[g] He_2 bond length = 5.0.

by (23) while the ground state spin $-\frac{1}{2}$ Boson wavefunction is described by (22). In the following, we will refer to (22) as the Boson wavefunction and (23) as the Fermion wavefunction.

For the system H_2 and D at infinite separation the H_2 part of the wavefunction is described by the tableau (21) and the possible tableaux for H_2D are (22) and (23). Thus at large separations the above discussion of HeH applies also to H_2D. As expected the results in Table 2 show that for the frozen wavefunctions of H_2D the Boson wavefunction leads to a bound state while the Fermion wavefunction leads to repulsion between the H_2 and D.

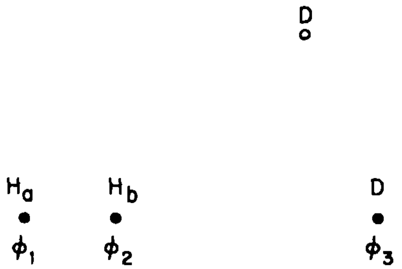

Fig. 5 Geometries for H_2D. The location of each orbital is indicated

For H_2 and D we also can vary the angle between the D and H_2. Consider the geometries indicated in Fig. 5, where D is moved from the linear configuration while maintaining a fixed H_b-D distance. In this case for the frozen wavefunction ΔT^x_{23} is nearly unchanged since ϕ_2 and ϕ_3 are the same distance apart (some changes occur due to the presence of a term in D_{23} involving the overlap of ϕ_1 and ϕ_3). However large changes should occur in ΔT^x_{13} since ϕ_1 and ϕ_3 move closer together, leading to an increased overlap, S_{13} (since τ_{jk} is dominated by the diagonal terms of (17), we expect only small changes in τ_{13}). From (20) we expect for such nonlinear distortions, that ΔT^x_{13} will become more negative in the Boson case and more positive in the Fermion case. Thus for Fermions the most favorable geometry should be linear, and for Bosons the bent geometry should be favored. As shown in Table 2 this is the case. (On the basis of such arguments with frozen wavefunctions one would expect the optimum geometry for Boson H_3 to be an equilateral triangle.) Thus even fine structural details are reflected by T^x!

C. The He_2, H_2He, *and* H_2H_2 *Systems*

Now consider He_2 at large separations. At infinite separation we have two independent He atoms described by the tableaux

$$\begin{array}{|c|c|}\hline 1 & 2 \\ \hline \end{array} \text{ and } \begin{array}{|c|c|}\hline 3 & 4 \\ \hline \end{array} \tag{24}$$

respectively. Two ways of coupling these tableaux are

$$\begin{array}{|c|c|c|c|}\hline 1 & 2 & 3 & 4 \\ \hline \end{array} \tag{25}$$

and

$$\begin{array}{|c|c|}\hline 1 & 2 \\ \hline 3 & 4 \\ \hline \end{array}\,. \qquad (26)$$

Here (25) should have the lowest energy and should lead to binding, but is allowed only for Bosons. For Fermions the lowest allowed state is (26).

The intermolecular terms now involve the pairs

13, 14, 23, and 24

each of which leads to $U_{11x} = +1$ for (25) and $U_{11x} = -\frac{1}{2}$ for (26) (see Table 1). Thus we expect

$$\Delta T^x < 0 \quad \text{and} \quad \Delta E < 0$$

for (25) and

$$\Delta T^x > 0 \quad \text{and} \quad \Delta E > 0$$

for (26). These expectations are verified by Table 2.

For H_2 and He or H_2 and H_2 the tableaux at infinite internuclear separation are also as in (24) so that the relevant four-electron tableaux are again (25) and (26). Thus for Bosons we obtain binding and for Fermions we obtain repulsion. Fixing the shorter H-He distance and moving the He off axis we see that (just as for H_2D) the Boson wavefunction favors nonlinear geometries for H_2He while the Fermion wavefunction favors linear geometries. Similarly for H_2 and D_2 if the closest H-D distance is fixed and the positions of the other H and D are varied, we see that the Boson wavefunction favors nonlinear geometries while the Fermion wavefunction favors the linear geometry [10].

D. *The* LiH *Molecule*

The Li^+ ion is a singlet state and is described by the tableau (21). Since the core orbitals ϕ_1 and ϕ_2 of Li^+ should be essentially the same in Li atom, we expect (correctly [11]) the tableau for Li atom to be

$$\begin{array}{|c|c|}\hline 1 & 2 \\ \hline \multicolumn{1}{|c|}{3} \\ \cline{1-1} \end{array}\,, \qquad (27)$$

where ϕ_3 refers to the valence orbital. For Li and H at infinite separation the allowed tableaux for Fermions are then

$$\underset{(28)}{\begin{array}{|c|c|}\hline 1 & 2 \\ \hline 3 & 4 \\ \hline \end{array}} \quad \text{and} \quad \underset{(29)}{\begin{array}{|c|c|}\hline 1 & 2 \\ \hline \multicolumn{1}{|c|}{3} \\ \cline{1-1} \multicolumn{1}{|c|}{4} \\ \cline{1-1} \end{array}}\,,$$

where ϕ_4 refers to the H_{1s} orbital. Here (28) describes a singlet state while (29) describes a triplet state. The intermolecular terms involve the pairs

$$14,\ 24,\ \text{and}\ 34;$$

however ϕ_1 and ϕ_2 being Li core orbitals are much more concentrated near the Li nucleus than is the valence orbital ϕ_3. Thus we expect

$$S_{34} \gg S_{14}, S_{24}$$

and for sufficiently large distances

$$|\Delta T^x_{34}| \gg |\Delta T^x_{14}|,\ |\Delta T^x_{24}|.$$

For (28)

$$U_{11(34)} = +1$$

while for (29)

$$U_{11(34)} = -1.$$

Thus from (20) we expect the singlet state of LiH to be bound while the triplet state should be unbound, in agreement with calculations [12] and experiment.

For very short distances we would also have to consider ΔT^x_{14} and ΔT^x_{24} (note that $\tau_{14}, \tau_{24} \gg \tau_{34}$) both of which are positive for (28) and (29). Thus when the H orbital starts penetrating the Li core we expect new large repulsive terms and consequently a steeply repulsive energy curve. At larger distances the non-involvement of ΔT^x_{14} and ΔT^x_{24} is consistent with the usual assumption that the core orbitals are not involved in the binding.

E. Interaction between Triplet State Molecules

So far we have examined interactions between systems A and B where A and B are both singlet states or both doublet states or one of each. Now we consider separated systems both of which are triplet states. We will consider A and B to each have two electrons so that the tableaux at infinity will correspond to

$$\begin{array}{|c|}\hline 1\\ \hline 2\\ \hline\end{array} \quad \text{and} \quad \begin{array}{|c|}\hline 3\\ \hline 4\\ \hline\end{array}$$

[e.g., He(^3S) plus He(^3S)] although a more interesting example would be two ground state methylenes, $CH_2(^3B_1)$, combining to form ethylene. At infinite separation the possible tableaux are

$$\underset{(30)}{\begin{array}{|c|}\hline 1\\ \hline 2\\ \hline 3\\ \hline 4\\ \hline\end{array}} \qquad \underset{(31)}{\begin{array}{|c|c|}\hline 1 & 3\\ \hline 2 & 4\\ \hline\end{array}}$$

and the combination

$$\sqrt{\frac{2}{3}}\;\begin{array}{|c|c|}\hline 1 & 3 \\ \hline 2 \\ \cline{1-1} 4 \\ \cline{1-1}\end{array} \;-\; \frac{1}{\sqrt{3}}\;\begin{array}{|c|c|}\hline 1 & 4 \\ \hline 2 \\ \cline{1-1} 3 \\ \cline{1-1}\end{array} \qquad (32)$$

such that $U_{ii(34)} = -1$. The intermolecular terms involve the pairs

13, 14, 23, and 24

for which

$$U_{11\pi} = -1 \quad \text{for (30)}$$

$$U_{11\pi} = +\tfrac{1}{2} \quad \text{for (31)} \qquad (33)$$

and

$$U_{11\pi} = 0 \quad \text{for (32)}.$$

Thus the quintet state should be quite repulsive, the singlet state should be quite attractive, and the triplet state binding should be determined by higher order terms [13] and self-consistency effects (to become attractive). These conclusions are in agreement with the results of Klein [14] on He(^3S) plus He(^3S). For the interactions of two triplet methylenes we would expect from these considerations that the singlet potential curve should be attractive with no hump at large R.

F. Summary

Considering the above results for Fermion and Boson systems, we see that interacting species A and B are expected to lead to attractive terms when the combined tableau contains electrons in the same row originating on different species, as in (25), (28), and (31). Repulsive terms result when electrons in *different* rows originate on different species, as in (26), (29), and (30). Analyzing these interactions in terms of ΔT_{jk}^{π} for the frozen wavefunctions allows one to predict stabilities and geometries of molecules without detailed computations.

4. Contragradience and the Bond Region

Since the structure and properties of large molecules can generally be rationalized in terms of bonds each localized near a pair of atoms, one would expect that the part of the wavefunction important for a particular bond would be just the part in between (or near) the pair of nuclei. However despite the intuitively clear idea of where the bond region is, it has not been easy to obtain a useful quantitative definition of the bond region. For example, one definition used for diatomic molecules is the region enclosed by the parabolas $-\eta_0 \leqq (r_a - r_b)/R \leqq \eta_0$, where η_0 is an adjustable parameter [6, 14, 15]. By this definition, the bond region includes points infinitely far from either nucleus, contrary to the usual chemical concept. Such a definition leads to obvious problems for polyatomics (for example, empirically established rules such as bond additivity clearly require a finite bond region).

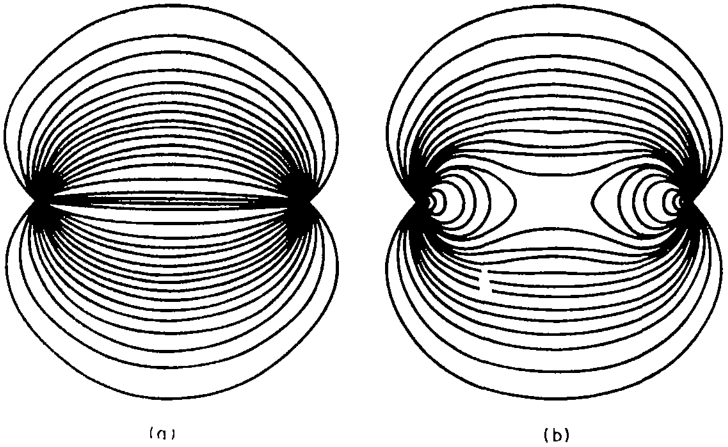

Fig. 6a and b The contragradience function for the G1 wavefunction of H_2 at $R = 1.4$. (The contours are equally spaced starting at 0.0045 a.u. for the outer contour with increments of 0.0045 a.u.). a Frozen wavefunction. b SCF wavefunction (eight basis functions)

On the other hand, an examination of T^x and the contragradience yields a useful criterion for the bond region. In Section 2, we found that the main contribution to ΔT^x arises from the contragradient nature of the orbitals in the region between the nuclei. We also saw that it is the large drop in the contragradience part of T^x which is reponsible for bond formation. Indeed we might almost say that it is this contragradient nature of the orbitals which is responsible for bonding. Thus it would seem appropriate to consider the regions of largest contragradience to be the regions most important to bonding. This would lead to a natural definition of the bond region as that part of space containing, say, 80% of the contragradience. In Fig. 6 we show the plots of the contragradience for the frozen and SCF (eight basis function) wavefunctions of H_2 for $R = 1.4$. (The regions shown here include about 80% of the total contragradience.) We see that despite the large changes in the wavefunctions due to self-consistency, the contragradience is relatively unchanged except in the heart of the bond region. More importantly the resulting picture of the bond is rather close to the intuitive idea of what a bond is.

Similarly for a pair of orbitals exhibiting antibonding, the plot corresponding to Fig. 6 would display the region important in the antibonding interactions. (The SCF contragradience would be greatly reduced and would differ greatly from Fig. 6b.)

5. Discussion

First we will summarize some of the conclusions from the previous sections.

It is the change in the exchange kinetic energy, ΔT^x, which determines whether a molecular system will be stable, and it is the contragradient part of ΔT^x, which is primarily responsible for this. The contragradience function, $c(\boldsymbol{r})$, for a pair of orbitals is just the product of the magnitudes of the gradients of the two orbitals minus the dot product of the gradients. Thus for a bonding pair such as H_2, $c(\boldsymbol{r})$ favors binding in the region in which the orbitals are contragradient, namely the region between the nuclei and close to the axis. Thus by defining the bond as the region where $c(\boldsymbol{r})$ is large, we arrive at something rather close to the intuitive idea of where the bond is.

As Ruedenberg [17] (also see Ref. [1]) has discussed elsewhere, the bond does not result from electrostatic considerations (such as putting the electron where it can attract both nuclei) [18]. Rather we find that the strength of a bond is determined by the existence of a region in which the orbitals on the two atoms have large slopes in oblique directions, i.e., where the contragradience is large. In general, we find that the sign of ΔT^x is determined by consideration of the tableau appropriate for the spin symmetry of the system being considered. In particular the ΔT^x can be partitioned into terms arising from various pairs, and for the case of frozen orbitals, the sign of each intermolecular component can be predicted from the tableau. When the combined tableau is GI [e.g. (26)] this sign is positive for a pair in the same row of the tableau and negative for a pair from different rows. Thus closed-shell systems repel each other because the intermolecular pair terms, T^x_{jk}, involve orbitals in different rows.

From these considerations we would view the aspects important for bond formation in terms of the following steps: (1) freeze the orbitals of the separated atoms; (2) bring the atoms together to their positions in the molecule (this leads to T^{xF} and to about the correct binding energy); and (3) allow the orbitals to relax to their SCF forms. In step (3) the orbitals rehybridize somewhat and contract more about each nucleus but also spreading onto the other centers, readjusting the various nuclear attraction, electron repulsion, the kinetic energy terms until self-consistency is achieved (after which the virial theorem, Hellmann-Feynman theorem, etc., would hold). However *the crucial step is* (2). In order for a strong bond to form, this must lead to a large negative ΔT^{xF}, through a decrease in the contragradience contribution to the energy.

Appendix A: The Partition of T^x

The spatial part of the GI wavefunctions has the form

$$O_{ii}\Phi \tag{A-1}$$

where Φ is a product of orbitals and O_{ii} is the permutational operator [2, 3]

$$O_{ii} = \frac{1}{\theta^\gamma} \sum_{\pi \in \mathscr{S}_N} U_{ii\pi}\pi\,. \tag{A-2}$$

Here the $U_{ii\pi}$ is the ii matrix element of the representation matrix for the permutation π (see Table 1 for the values of some $U_{ii\pi}$).

The kinetic energy, T, of the wavefunction (A-1) is given by

$$T = \left\langle \Phi \left| \sum_{j=1}^{N} t_j \right| O_{ii}\Phi \right\rangle \Big/ \langle \Phi | O_{ii}\Phi \rangle\,, \tag{A-3}$$

where t_j is the one-electron kinetic energy operator, $-\frac{1}{2}\nabla^2$, for electron j. Eq. (A-3) is expanded as

$$T = \sum_{j,k=1}^{N} D_{jk} \langle \phi_j | t | \phi_k \rangle \tag{A-4}$$

in terms of the *orbital density matrix*, [19] D_{jk}, which depends upon the representation matrices $U_{ii\pi}$ and upon the overlaps of the various orbitals. For most cases of interest to us here [see, for example (A-13) to (A-16)] D_{jk} is dominated by the term

$$D_{jk} \sim U_{ii(j,k)} S_{jk} \tag{A-5}$$

where S_{jk} is the overlap of orbitals ϕ_j and ϕ_k.

Next we consider the partition of the exchange kinetic energy (T^x) into pair terms, T^x_{jk}. The classical part of T is defined as

$$T^{Cl} = \sum_{j=1}^{N} \langle j | t | j \rangle . \tag{A-6}$$

Thus since the total kinetic energy is given by (A-4), we obtain [20]

$$T^x \equiv T - T^{Cl} = \sum_{j>k}^{N} 2 D_{jk} \langle j | t | k \rangle - \sum_{i}^{N} (1 - D_{jj}) \langle j | t | j \rangle$$

But by the definition of D_{jk} (see Ref. [2]),

$$\sum_{j} D_{jk} S_{jk} = 1$$

for any k. Thus we obtain

$$T^x = \sum_{j>k}^{N} T^x_{jk} , \tag{A-7}$$

where

$$T^x_{jk} \equiv D_{jk} \{ 2 \langle i | t | k \rangle - S_{jk} [\langle j | t | j \rangle + \langle k | t | k \rangle] \} . \tag{A-8}$$

When $S_{jk} \neq 0$, it is more convenient to define

$$\tau_{jk} = \left| \langle j | t | j \rangle + \langle k | t | k \rangle - \frac{2}{S_{jk}} \langle j | t | k \rangle \right| \tag{A-9}$$

and

$$\sigma_{jk} = D_{jk} S_{jk} \tag{A-10}$$

so that

$$T^x_{jk} = -\sigma_{jk} \tau_{jk} . \tag{A-11}$$

In this case if orbitals j and k are on different centers, τ_{jk} is relatively insensitive to the internuclear separation and only σ_{jk} varies rapidly with distance. From (A-5) the leading term of σ_{jk} is

$$\sigma_{jk} \sim U_{ii(j,k)} S^2_{jk} . \tag{A-12}$$

So that the sign of T^x_{jk} is determined by the sign of $U_{ii(j,k)}$.

For convenience in the discussions in this paper we list below the σ_{jk} for several tableaux. For a two-electron singlet state. (see Fig. 4a)

$$\sigma_{12} = S^2_{12} / (1 + S^2_{12}) . \tag{A-13}$$

For a two-electron triplet state (see Fig. 4b)

$$\sigma_{12} = -S_{12}^2/(1 - S_{12}^2)\,. \tag{A-14}$$

For a three-electron doublet state (see Fig. 4d)

$$\left.\begin{aligned} \sigma_{12} &= S_{12}^2(1 - \tfrac{1}{2}S_{13}S_{23})/N_3 \\ \sigma_{13} &= -\tfrac{1}{2}S_{13}^2(1 + S_{12}S_{23})/N_3 \\ \sigma_{23} &= -\tfrac{1}{2}S_{23}^2(1 + S_{12}S_{13})/N_3 \\ N_3 &= 1 + S_{12}^2 - \tfrac{1}{2}S_{13}^2 - \tfrac{1}{2}S_{23}^2 - S_{12}S_{13}S_{23}\,. \end{aligned}\right\} \tag{A-15}$$

where

For a four-electron singlet state (see Fig. 4*j* and 4*k*)

$$\begin{aligned} \sigma_{ij} = S_{ij}(&S_{ij} - \tfrac{1}{2}S_{ik}S_{kj} - \tfrac{1}{2}S_{il}S_{lj} - \tfrac{1}{2}S_{il}S_{lk}S_{kj} \\ &- \tfrac{1}{2}S_{ik}S_{kl}S_{lj} + S_{ij}S_{kl}^2)/N_4 \end{aligned} \tag{A-16a}$$

and

$$\begin{aligned} \sigma_{ik} = -\tfrac{1}{2}S_{ik}(&S_{ik} + S_{ij}S_{jk} + S_{il}S_{lk} + S_{ij}S_{jl}S_{lk} \\ &- 2S_{ik}S_{jl}^2 - 2S_{il}S_{lj}S_{jk})/N_4 \end{aligned} \tag{A-16b}$$

where *i* and *j* are in one row and *k* and *l* are in the other. Here

$$N_4 = \sum_{m=1}^{4} \sigma'_{nm}$$

for any *n*, where $\sigma'_{nm} = \sigma_{nm}N_4$ [that is, σ'_{nm} is the numerator in (A-16)]. Thus

$$N_4 = N_3 + \sigma'_{14} + \sigma'_{24} + \sigma'_{34}\,,$$

which is useful in considering LiH at large *R*. For a system where both S_{12} and S_{34} are large and the S_{ik} are small, then

$$N_4 \sim (1 + S_{12}^2)(1 + S_{34}^2)\,.$$

References

1. Wilson, C. W., Jr., Goddard III, W. A.: Theoret. chim. Acta (Berl.), **26**, 195 (1972) (Hereafter we will refer to this as paper I.)
2. Goddard III, W. A.: Physic. Rev. **157**, 82 (1967).
3. — Physic. Rev. **157**, 73 (1967).
4. Wilson, C. W., Jr., Goddard III, W. A.: Chem. Physics Letters **5**, 45 (1970).
5. Hellmann, H.: Z. Physik **85**, 180 (1933).
6. Feinberg, M. J., Ruedenberg, K.: J. chem. Physics **54**, 1495 (1971).
7. As shown by Pauli [Physics Rev. **58**, 716 (1940)], Bosons must have integral spins and Fermions half-integral spin; however, here we consider spin-½ Bosons in order to demonstrate the effects of the Pauli principle on bonding.
8. Lieb, E., Mattis, D.: Physic. Rev. **125**, 164 (1962); Courant, R., Hilbert, D.: Methods of mathematical physics, p. 451. New York: Interscience 1953.
9. A better approximation would be obtained by including a proportionality constant d_{jk} in (19) where d_{jk} is typically in the range 0.2 to 0.8.
10. Wilson, C. W., Jr., Goddard III, W. A.: J. chem. Physics **51**, 716 (1969).
11. Ladner, R. C., Goddard III, W. A.: J. chem. Physics **51**, 1073 (1969).
12. Bender, C. F., Davidson, E. R.: J. chem. Physics **49**, 4222 (1968).

13. Using (33) and (20), we find that the energy separations between the states described by (30)–(32) are consistent with the interatomic potential terms being proportional to $S(S+1)$ (where S is the total spin). That is, at this level of approximation the interaction energies could be described by a Heisenberg Hamiltonian using an atomic spin of one on each atom.
14. Klein, D. J.: J. chem. Physics **50**, 5152 (1969).
15. Feinberg, M. J., Ruedenberg, K., Mehler, E. L.: Advances in quant. Chemistry **5**, 28 (1970). (We thank Dr. Ruedenberg for a copy of this paper prior to publication.)
16. Bader, R. F., Henneker, W. H., Cade, P. E.: J. chem. Physics **46**, 3341 (1967); Bader, R. F., Baudraut, A. D.: J. chem. Physics **49**, 1653 (1968).
17. Ruedenberg, K.: Rev. mod. Physics **34**, 326 (1962).
18. See, for example, Van Vleck, J. H., Sherman, A.: Rev. mod. Physics **7**, 167 (1935); Moore, W. J.: Physical chemistry (Prentice-Hall, Inc., Englewood Cliff, N. J., 1962), pp. 517ff.
19. We denote the orbital density matrices as D_{jk} rather than D_k^j as in Ref. [2]. In addition, the normalization terms are now included in D_{jk}.
20. Taking the orbitals to be real.

Dr. W. A. Goddard
Arthur Noyes Laboratory of Chemical Physics
California Institute of Technology
Pasadena, California 91109, USA

Theoret. chim. Acta (Berl.) 26, 231—236 (1972)
© by Springer-Verlag 1972

Operator Equations in Approximate Molecular Orbital Theories

II. Integral Approximations and Charge Distributions

KARL JUG

Department of Chemistry, Saint Louis University, Saint Louis, Missouri 63156, USA
and Institut für Theoretische Chemie der Universität Stuttgart*

Received March 27, 1972

The general concept of integral approximations based on the Heisenberg equation of motion $[r, h] = p$ is developed for one- and two-electron operators in polyatomic molecules. The formalism leads to a new definition of atomic charge distributions in molecules. Mulliken's integral approximation and population analysis are included as special cases.

Das allgemeine Konzept von Integralapproximationen, die auf der Heisenbergschen Bewegungsgleichung $[r, h] = p$ basieren, wird für Ein- und Zweielektronenoperatoren in mehratomigen Molekülen entwickelt. Der Formalismus führt zu einer neuen Definition von Atomladungen in Molekülen. Mullikens Integralapproximation und Verteilungsanalyse sind als Spezialfälle enthalten.

1. Introduction

In a previous paper [1], we tested the suitability of commutator relations $[t, x] = u$ with hermitian and antihermitian operators t, x and u as a basis for approximations in semiempirical molecular orbital methods. In particular, we were interested in integral approximations based on the Heisenberg uncertainty principle $[r, p] = -1$ and the Heisenberg equation of motion $[r, h] = p$. The approximate integral relations resulted from truncated expansions of the commutator integrals. We derived formulas for $\bar{\beta}$'s over non-orthogonal atomic orbitals and β's over orthogonalized atomic orbitals [2]. The accuracy of the relations was tested for $2s$-, $2p\sigma$- and $2p\pi$-orbitals in homonuclear diatomics. A way to generalize the concept to polyatomics was briefly described. In the present paper, we want to develop the general formalism for polyatomic molecules both for one- and two-electron operators. This leads also to a new definition of atomic charge distributions in molecules.

2. One-Electron Integrals

From the commutator equation

$$u = [t, x] \tag{2.1}$$

---

* Present address.

we obtain an infinite expansion

$$u_{\mu\nu} = \sum_{\lambda} t_{\mu\lambda} x_{\lambda\nu} - x_{\mu\lambda} t_{\lambda\nu} \tag{2.2}$$

for integrals $u_{\mu\nu} = \langle \mu | u | \nu \rangle$ etc. over hermitian or antihermitian operators u, t, x and atomic orbitals μ, ν. λ is taken over a complete, orthogonal set of orbitals. In case that a truncated expansion consisting of two orthogonalized orbitals [2] corresponding to μ and ν is used, the following approximations result for integrals over one-electron operators [1].

$$\begin{aligned} \bar{x}_{ab} = \tfrac{1}{2} S_{ab}(\bar{x}_{aa} + \bar{x}_{bb}) + \frac{\bar{t}_{ab} - \frac{1}{2} S_{ab}(\bar{t}_{aa} + \bar{t}_{bb})}{\bar{t}_{aa} - \bar{t}_{bb}} (\bar{x}_{aa} - \bar{x}_{bb}) \\ + \frac{(1 - S_{ab}^2)}{\bar{t}_{aa} - \bar{t}_{bb}} \bar{u}_{ab} \,, \end{aligned} \tag{2.3}$$

$$x_{ab} = \frac{t_{ab}}{t_{aa} - t_{bb}} (x_{aa} - x_{bb}) + \frac{1}{t_{aa} - t_{bb}} u_{ab} \,. \tag{2.4}$$

Quantities with bar refer to non-orthogonal AO's $\bar{a}$, $\bar{b}$, without bar to symmetrically orthogonalized AO's a, b. These approximations have been investigated for cases where $\bar{a}$ and $\bar{b}$ are orbitals of the same type on different centers A and B, e.g. $2s_a - 2s_b$, $2p\sigma_a - 2p\sigma_b$, $2p\pi_a - 2p\pi_b$. Approximation (2.3) was previously [1] denoted by (B), (2.4) by (B').

In case that we use $t = \boldsymbol{r}$, $x = T$, $u = \boldsymbol{p}$, we obtain for the kinetic energy

$$\bar{T}_{ab} = \tfrac{1}{2} S_{ab} \left| (\bar{T}_{aa} + \bar{T}_{bb}) + \frac{\Delta R}{R} (\bar{T}_{aa} - \bar{T}_{bb}) \right| + \frac{1 - S_{ab}^2}{R} \frac{dS_{ab}}{dR} \,, \tag{2.5}$$

$$\begin{aligned} T_{ab} &= \frac{\frac{1}{2} S_{ab}}{(1 - S_{ab}^2)^{\frac{1}{2}}} \frac{\Delta R}{R} (T_{aa} - T_{bb}) + \frac{1}{R} \frac{dS_{ab}}{dR} \\ \Delta R &= R - 2R_0 \,. \end{aligned} \tag{2.6}$$

In case that $\bar{a}$ and $\bar{b}$ are orbitals of the same type, $\Delta R = R - 2R_0$ is twice the shift of the center of charge from the midpoint between atoms A and B toward either A or B. R_0 is the distance between the center of charge and atom A. ΔR is positive if the center of charge is moved toward A and negative otherwise.

For Coulombic potential energy operators V, we obtain $t = \boldsymbol{r}$, $x = V$, $\boldsymbol{u} = \boldsymbol{0}$, so that

$$\bar{V}_{ab} = \tfrac{1}{2} S_{ab} \left[(\bar{V}_{aa} + \bar{V}_{bb}) + \frac{\Delta R}{R} (\bar{V}_{aa} - \bar{V}_{bb}) \right] , \tag{2.7}$$

$$V_{ab} = \frac{\frac{1}{2} S_{ab}}{(1 - S_{ab}^2)^{\frac{1}{2}}} \frac{\Delta R}{R} (V_{aa} - V_{bb}) \,. \tag{2.8}$$

For a single-electron Hamiltonian

$$h = T + V$$

with

$$V = \sum_{i}^{\text{nuclei}} V_i \,,$$

(2.5) and (2.7) resp. (2.6) and (2.8) yield the general formulas for polyatomics

$$\bar{\beta}_{ab} = \tfrac{1}{2} S_{ab} \left[(\bar{\alpha}_a + \bar{\alpha}_b) + \frac{\Delta R}{R} (\bar{\alpha}_a - \bar{\alpha}_b) \right] + \frac{1 - S_{ab}^2}{R} \frac{dS_{ab}}{dR}, \tag{2.9}$$

$$\beta_{ab} = \frac{\tfrac{1}{2} S_{ab}}{(1 - S_{ab}^2)^{\frac{1}{2}}} \frac{\Delta R}{R} (\alpha_a - \alpha_b) + \frac{1}{R} \frac{dS_{ab}}{dR}. \tag{2.10}$$

These formulas were derived previously[1] for diatomics, here we have shown in a simple breakdown that they are the same in polyatomics.

3. Two-Electron Integrals

A generalization to two-electron integrals is straightforward and was hinted at in an earlier paper [3]. We generalize Eqs. (2.1) and (2.2) to the suitable many-electron form

$$u = [t, x] \tag{3.1}$$

with

$$\begin{gathered} u = \sum_i u_i, t = \sum_i t_i, x = \sum_l x_l + \sum_{l<j} x_{ij} \\ u_{ab,cd} = \sum_{\lambda,\mu} t_{a\lambda,c\mu} x_{\lambda b,\mu d} - x_{a\lambda,c\mu} t_{\lambda b,\mu d} \end{gathered} \tag{3.2}$$

with

$$u_{ab,cd} = \langle ac | u | bd \rangle \text{ etc.}$$

Since the case of two electrons is representative, we shall pursue it for the Heisenberg equation of motion. From

$$p_1 + p_2 = \left[r_1 + r_2, T_1 + T_2 + V_1 + V_2 + \frac{1}{r_{12}} \right] \tag{3.3}$$

the one-electron part can be separated so that

$$0 = \left[r_1 + r_2, \frac{1}{r_{12}} \right]. \tag{3.4}$$

Eq. (3.4) is all we need for the general two-electron problem. If we use the two pairs of orthogonalized orbitals *a*, *b* and *c*, *d* in the double expansion of

$$\left\langle \overline{ac} \left\| \left[r_1 + r_2, \frac{1}{r_{12}} \right] \right\| \bar{b}\bar{c} \right\rangle = 0, \tag{3.5}$$

where $\bar{a}$, $\bar{b}$, $\bar{c}$, $\bar{d}$ are non-orthogonal orbitals on various centers, we obtain the simplest approximation for a multi-center electron repulsion integral

$$(\bar{a}\bar{b} | \bar{c}\bar{c}) = \tfrac{1}{2} S_{ab} \left\{ [(\bar{a}\bar{a} | \bar{c}\bar{c}) + (\bar{b}\bar{b} | \bar{c}\bar{c}) + \frac{\Delta R_{ab}}{R_{ab}} [(\bar{a}\bar{a} | \bar{c}\bar{c}) - (\bar{b}\bar{b} | \bar{c}\bar{c})] \right\}. \tag{3.6}$$

The general approximation for a multi-center integral is obtained by the same expansion of

$$\left\langle \bar{a}\bar{c} \left\| \left[r_1 + r_2, \frac{1}{r_{12}} \right] \right\| \bar{b}\bar{d} \right\rangle = 0 \tag{3.7}$$

---

[1] In [1], several quantities were lumped together in the definition of $\Delta\varrho$; the relation of $\Delta\varrho$ and ΔR here is $\Delta\varrho = \tfrac{1}{2} S \zeta \Delta R$. The above definition of ΔR is possible for all cases where S is different from zero, otherwise the definition of $\Delta\varrho$ is preferable.

with subsequent elimination of the hybrid integrals by means of (3.6). The result is

$$
\begin{aligned}
(\bar{a}\bar{b}|\bar{c}\bar{d}) = \tfrac{1}{4} S_{ab} S_{cd} \Big\{ & [(\bar{a}\bar{a}|\bar{c}\bar{c}) + (\bar{b}\bar{b}|\bar{c}\bar{c}) + (\bar{a}\bar{a}|\bar{d}\bar{d}) + (\bar{b}\bar{b}|\bar{d}\bar{d})] \\
& + \frac{\Delta R_{ab}}{R_{ab}} [(\bar{a}\bar{a}|\bar{c}\bar{c}) - (\bar{b}\bar{b}|\bar{c}\bar{c}) + (\bar{a}\bar{a}|\bar{d}\bar{d}) - (\bar{b}\bar{b}|\bar{d}\bar{d})] \\
& + \frac{\Delta R_{cd}}{R_{cd}} [(\bar{a}\bar{a}|\bar{c}\bar{c}) + (\bar{b}\bar{b}|\bar{c}\bar{c}) - (\bar{a}\bar{a}|\bar{d}\bar{d}) - (\bar{b}\bar{b}|\bar{d}\bar{d})] \\
& + \frac{\Delta R_{ab} \Delta R_{cd}}{R_{ab} R_{cd}} [(\bar{a}\bar{a}|\bar{c}\bar{c}) - (\bar{b}\bar{b}|\bar{c}\bar{c}) - (\bar{a}\bar{a}|\bar{d}\bar{d}) + (\bar{b}\bar{b}|\bar{d}\bar{d})] \Big\} .
\end{aligned} \tag{3.8}
$$

It is obvious that (3.8) includes (3.6) as a special case. It also contains many other special cases as $c = a$ and $d = b$ etc. The formula (3.8) reduces any kind of multicenter hybrid and exchange integral to a combination of Coulomb integrals. It represents the simplest generalization of the Mulliken approximation [4]. Cases where charge distributions $\bar{a}\bar{b}$ or $\bar{c}\bar{d}$ are composed of different orbitals on the same center are excluded.

If we base our approximations on (3.4) but use orthogonalized orbitals a, b, c, d in the expansion, our results are

$$
(ab|cc) = \frac{\tfrac{1}{2} S_{ab}}{(1 - S_{ab}^2)^{\frac{1}{2}}} \, \frac{\Delta R_{ab}}{R_{ab}} [(aa|cc) - (bb|cc)] \tag{3.9}
$$

$$
\begin{aligned}
(ab|cd) = {} & \frac{\tfrac{1}{4} S_{ab} S_{cd}}{(1 - S_{ab}^2)^{\frac{1}{2}} (1 - S_{cd}^2)^{\frac{1}{2}}} \, \frac{\Delta R_{ab} \Delta R_{cd}}{R_{ab} R_{cd}} \\
& \cdot [(aa|cc) - (aa|dd) - (bb|cc) + (bb|dd)] .
\end{aligned} \tag{3.10}
$$

The integrals $(ab|cc)$ and $(ab|cd)$ vanish, if equivalent orbitals, i.e. of same type and equal exponents, on different centers are involved. This special case of equivalence between (3.9) or (3.10) and the Mulliken approximation for the non-orthogonal counterpart of the orbitals was discussed by Löwdin [5]. The approximations (3.9) and (3.10) are not as good as (3.6) and (3.8). For example, they imply that the exchange integrals are generally smaller than the hybrid integrals. A counter example can be found in a paper by Fischer-Hjalmars [6]. The above conclusion about the relative accuracy of electron repulsion integral formulas on non-orthogonal and orthogonalized basis sets parallels our findings for $\bar{\beta}$'s and β's [1].

4. Charge Distributions

A careful investigation of (3.6) and (3.8) shows the underlying pattern: the charge distribution $\bar{a}\bar{b}$ (or $\bar{c}\bar{d}$) of each electron is expanded in the following way

$$
\bar{a}\bar{b} = \tfrac{1}{2} S_{ab} \left[(\bar{a}\bar{a} + \bar{b}\bar{b}) + \frac{\Delta R_{ab}}{R_{ab}} (\bar{a}\bar{a} - \bar{b}\bar{b}) \right] . \tag{4.1}
$$

It is not difficult to show that the underlying operator equation is

$$
[\boldsymbol{r}, 1] = 0 . \tag{4.2}
$$

This opens the way to a new definition of atomic charges in molecules. Mulliken's population analysis [7] distributes overlap distributions $c_a c_b S_{ab}$ equally over atoms A and B. Instead, we obtain from (4.1) by regrouping of the terms and integration

$$S_{ab} = \tfrac{1}{2}\kappa_a S_{ab} + \tfrac{1}{2}\kappa_b S_{ab} \tag{4.3}$$

with

$$\kappa_a = 1 + \frac{\Delta R_{ab}}{R_{ab}}$$

$$\kappa_b = 1 - \frac{\Delta R_{ab}}{R_{ab}}\,.$$

κ_a is the weighting factor for the part of the distribution belonging to atom A, κ_b the corresponding factor for atom B. They are equal only if the center of charge of the distribution $\bar{a}\bar{b}$ is in the middle between atoms A and B. In this case $\Delta R_{ab} = 0$ holds.

5. Discussion and Conclusion

The derivation of approximate formulas in Sect. 2 and 4 was based on a two-orbital expansion. This seems to be a reasonable approach if $\bar{a}$ and $\bar{b}$ are orbitals of the same type. In this case the movement of the center of charge from the midpoint toward one of the atoms is a useful consideration[2]. However, in molecular orbital methods, integrals $S_{ab'}(\bar{a}\bar{b}|\bar{c}\bar{c})$ etc. occur where $\bar{a}$ and $\bar{b}$ are not of the same type. We have investigated this case also and found that the form of the relations remains unchanged, if we generalize our definition of ΔR. Let us start with the non-orthogonal expansion corresponding to (2.2)

$$\bar{u}_{ab} = \sum_{\chi,\chi'} \bar{t}_{a\chi}(S^{-1})_{\chi\chi'}\,\bar{x}_{\chi'b} - \bar{x}_{a\chi}(S^{-1})_{\chi\chi'}\,\bar{t}_{\chi'b}\,. \tag{5.1}$$

In case that a and b are not orbitals of the same type on atoms A and B, we include also the corresponding orbitals of the same type on both atoms in the expansion. Let us denote $\bar{a}'$ corresponding to $\bar{b}$ and $\bar{b}'$ corresponding to $\bar{a}$. The shielding exponents of the corresponding orbitals are allowed to be different. χ, χ' are taken as $\bar{a}$, $\bar{b}$, $\bar{a}'$, $\bar{b}'$. If we rearrange the terms according to their magnitude and keep only the dominant ones, the following definition of ΔR would be the simplest, more general than (2.6).

$$-S_{ab}\Delta R = 2\bar{z}_{ab} - (S_{a'b}\bar{z}_{aa'} + S_{ab'}z_{bb'}) - S_{ab}(\bar{z}_{au} + \bar{z}_{bb})\,. \tag{5.2}$$

z is an axis through atoms A and B. The second term in (5.2) is the one which did not occur previously. It refers to atomic dipole moments of distribution $\bar{a}\bar{b}$. So ΔR is defined as twice the distance between the midpoint of atoms A and B and that point on the internuclear axis for which the higher averaged dipole moments in the expansion of $\bar{z}_{ab}$ can be neglected. This means that we define R_0

---

[2] The case of $2p\sigma_a 2p\sigma_b$ is more sophisticated for different exponents, because the centers of negative and positive part of the distribution will be separated. Here $\Delta\varrho \sim S\Delta R$ is relevant. It will be non-vanishing and non-singular for $S = 0$, when ΔR itself is not finite.

so that $z_a = z_0 + R_0$ with

$$2\langle \bar{a} | z_0 | \bar{b} \rangle = S_{a'b} \bar{z}_{aa'} + S_{ab'} \bar{z}_{bb'} . \tag{5.3}$$

It is obvious that (5.2) contains (2.6) as a special case if the right side of (5.3) vanishes. This is approximately correct for $\bar{a}, \bar{b}$ of same type because the two terms on the right side of (5.3) try to cancel each other.

We have qualitatively investigated the consequences of (5.2) for the case $\bar{a} = 2s_a$, $\bar{b} = 2p\sigma_b$ and found the formula without singularities[3]. It is worthwile to note that in the case of an asymmetrical $2s_a 2p\sigma_b$ charge distribution, the partitioning cannot be equal among atom A and B, even if the exponents are the same. In a superficial conclusion, one might consider this as a shortcoming. However, one has also to consider that in a homonuclear bond, there should exist also a $2p\sigma_a 2s_b$ charge distribution the partitioning of which counterbalances the one of $2s_a 2p\sigma_b$. This allows for an equal gross atomic population on two atoms despite intermediate asymmetrical partitioning.

The formalism developed in this paper is sufficient for use in approximate molecular orbital theories. However, one word of caution may be appropriate. The Heisenberg equation of motion $p = [r, h]$ is valid for the exact Hamiltonian and certain model Hamiltonians, but not for an SCF Hamiltonian. The reason is that the exchange operator does in general not commute with the position operator. This means that approximations for β's which refer to an SCF Hamiltonian cannot be valid in the same way as those derived for effective single-electron Hamiltonians.

The formulas developed so far seem to offer a greater insight into integral approximations. To complement the qualitative aspects of this work, we plan to investigate applications in the future. In particular, effects of these formulas for gross atomic populations in hetero molecules is one of our aims.

Acknowledgement I thank Prof H Preuß for the hospitality in his institute.

References

1. Jug, K : Theoret chim. Acta (Berl.) **23**, 183 (1971).
2. Löwdin, P.O : J. chem Physics **18**, 365 (1950).
3. Jug, K.: Theoret. chim. Acta (Berl.) **16**, 95 (1970).
4. Mulliken, R.S.: J. Chim. physique **46**, 497, 675 (1949).
5. Löwdin, P.O.: J. chem. Physics **21**, 374 (1953).
6. Fischer-Hjalmars, I.: J. chem. Physics **42**, 1962 (1965).
7. Mulliken, R.S : J. chem. Physics **23**, 1833 (1955).

Prof. Dr. K. Jug
Institut für Theoretische Chemie
Universität Stuttgart
D-7000 Stuttgart 1, Relenbergstr. 32
Germany

---

[3] For some cases, *e.g.* $1s_a 2p\sigma_b$ and $2s_a 2p\sigma_b$, the value of $S_{ab} \Delta R/R$ may go to infinity as R approaches zero. This is, however, of no practical importance, because it involves a single-center charge redistribution.

Theoret. chim. Acta (Berl.) 26, 237–248 (1972)
© by Springer-Verlag 1972

The Electronic Structures of Some Tetrazaborolines and Dimethyltetrazadieneirontricarbonyl

D. R. Armstrong, P. G. Perkins, J. M. Scott, and J. J. P. Stewart
Department of Pure and Applied Chemistry, University of Strathclyde, Glasgow, C. 1, Scotland

Received January 31, 1972

Self-consistent field calculations have been performed on some Δ^2 tetrazaborolines using both an *ab initio* and a semi-empirical (CNDO) approach. The first method was employed in order to examine completely the ground-state and the properties of the π-electrons in the parent molecule. The excited states of several boron-substituted derivatives of tetrazaboroline have also been calculated semi-empirically, including configuration interaction, and good agreement with the observed electronic absorption spectra was obtained. The results of the calculations were also invoked to distinguish between isomeric boron-substituted derivatives of tetrazaborolines. The electronic structures of two of the possible geometries of dimethyltetrazadieneirontricarbonyl, in which the N_4 moiety is attached in a 'σ' or a 'π' fashion were examined by CNDO calculations and it was found that the more stable form involves σ bonding between the nitrogens and the iron atom.

Für einige Δ^2-tetrazaborwasserstoff-Derivate wurden SCF-Rechnungen nach einem *ab initio*- und nach einem semiempirischen (CNDO)-Verfahren durchgeführt. Die erste Methode wurde angewandt, um den Grundzustand und die Eigenschaften der π-Elektronen im Ausgangsmolekül zu untersuchen. Die angeregten Zustände einiger am Boratom substituierter Derivate wurden semiempirisch unter Einschluß von Konfigurationenwechselwirkung berechnet, wobei gute Übereinstimmung mit den experimentellen Elektronenspektren erzielt wurde. Die Resultate wurden ebenfalls zur Unterscheidung verschiedener isomerer Derivate benutzt. Die Elektronenstruktur von zwei möglichen Geometrien des Dimethyltetrazadieneisentricarbonyl, in denen der N_4-Rest mit einer σ- oder π-Bindung gebunden ist, wurde mit CNDO-Rechnungen untersucht. Es wurde gefunden, daß die stabilere Form σ-Bindungen zwischen den Stickstoffatomen und dem Eisenatom enthält.

Introduction

An interesting series of compounds which have been synthesised in the last decade are the stable Δ^2 tetrazaborolines [7, 11]. The geometry of the parent compound H_2N_4BH (Fig. 1a) is a planar five-membered ring [5]. An intriguing feature of these compounds is the presence of four nitrogens bonded together as a stable N_4 unit: such a system would normally be expected to decompose rapidly, yielding molecular nitrogen.

A compound which is formally related to tetrazaboroline is dimethyltetrazadieneirontricarbonyl [10] and this is of particular interest on account of the two plausible possible configurations which it could have. The first configuration (Fig. 2a) is the "π complex" in which the tetrazadiene moiety lies above the pyramidal $Fe(CO)_3$ group, the nitrogen atoms being non-coplanar with the iron atom. This structure is similar to the isoelectronic compound butadieneirontricarbonyl [13] in which the bonding involves the π system of the butadiene molecule [16].

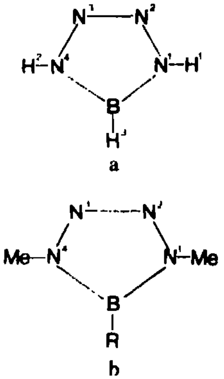

Fig 1 Tetrazaboroline and substituted tetrazaborolines

In the second possible structure (Fig. 2b), the four nitrogen atoms are coplanar with the iron atom, the $Fe(CO)_3$ entity retaining its pyramidal configuration. The latter configuration is structurally related to the tetrazaboroline ring system and X-ray diffraction studies have shown that the compound does, indeed, have this geometry [6]. It seemed important, therefore, to try to rationalise (a) why the preferred configuration of the iron complex is the coplanar form, (b) how the bonding in this complex is related to that of the more conventional tetrazaboroline, and (c) the origin of the electronic absorption bands of the tetrazaborolines, and to correlate these with their detailed geometry.

Previous calculations carried out on various tetrazaborolines employed a simple iterative Hückel approach [14a] and concentrated attention on the six π electron system. The observed electronic absorption spectra were, therefore, interpreted solely in terms of $\pi \rightarrow \pi^*$ transitions. These previous calculations showed that, in all cases, there is a small drift of π electrons towards the boron atom, together with a large π bond order between nitrogen atoms 2 and 3. Weaker

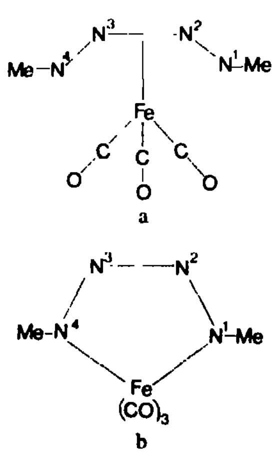

Fig 2 Possible geometries of dimethyltetrazadieneirontricarbonyl

π bonds between nitrogens 1 and 2 and between nitrogens 1, 4 and boron were also revealed. As there seems to be only limited delocalisation of the π electrons in the system, then the reason for its stability could well be connected with the σ electrons. Hence, in order to try and establish these points with some degree of finality, we have carried through *ab initio* calculations on the ground-state of the parent compound H_2N_4BH together with CNDO-type all-valence electron calculations on selected compounds of the type Me_2N_4BR (Fig. 1b) so as to recalculate the excited states and, if necessary, to reassign the allowed bands.

The iron tricarbonyl complex contains too many atoms for an *ab initio* calculation to be feasible, and so here again we resorted to an all-valence electron CNDO method [1, 16, 17] to investigate the electronic structures of both configurations shown in Fig. 2. The geometrical parameters for the tetrazaboroline ring were taken from Ref. [5].

Results and Discussion

1. *Ab initio Calculations on Tetrazaboroline*

The calculational procedure assumed the LCAO MO SCF framework, the atomic orbital bases being linear combinations of gaussian-type orbitals [4]. The basis set comprised seven *s* and three *p* primitive gaussian orbitals contracted to three *s* and one *p* orbitals for the boron and nitrogen atoms and three *s* primitive gaussians [19] contracted to one atomic orbital for the hydrogen atom. The choice of this basis set was determined so as to be consistent and allow comparison with earlier calculations on borazine [2].

The results of a Mulliken population analysis [15] on tetrazaboroline are presented in Table 1. The figures indicate that the boron is positively charged (+0.475) and that this stems from a σ electron flow (0.950) to nitrogens 1 and 4, offset by a much smaller π-electrons drift (0.494) from these nitrogens to the boron. Nitrogen atoms 1 and 4 are highly negatively charged, due to electron movement from both the hydrogens and the boron atom. By contrast, nitrogen atoms 2 and 3 are virtually electrically neutral. The bond populations imply that the N_2—N_3 bond is almost 50% stronger than the N_1—N_2 bond. This difference in strength is due entirely to a large π-electron contribution to the former bond, whereas this facet of the bonding is weak in the latter. The π-electron system consists, therefore, of a partially delocalised six-electron arrangement in which the electrons are largely concentrated in the N_2—N_3 and the two N—B bonds. These results correspond largely with those of the previous "π only" calculations [14].

It is of interest to compare these results with those for borazine [2]. The gross atomic populations on the boron and the hydrogen atoms are very similar in both molecules but, as might be expected, differences arise in the charge which resides on the nitrogen atoms: those in borazine are more negatively charged than those in tetrazaboroline. The bond overlap populations found for borazine are B—H 0.446; N—H 0.364; and B—N 0.425; of which 0.327 is σ and 0.098 is of π type. These are all strikingly close to the corresponding quantities calculated in the present work for tetrazaboroline, especially those appertaining to the B—N bond.

Table 1. Mulliken population analysis of tetrazaboroline

Atom populations		Overlap populations		
Boron				
S	2.673	B—H		0.493
P_x	0.529	N—H		0.399
P_y	0.829			
P_z	0.494	B $N_{1,4}$	σ	0.310
Total	4.525		π	0.117
			Total	0.427
Nitrogens 1, 4				
S	3.477	N_1 N_2	σ	0.271
P_x	1.339		π	0.041
P_y	1.120		Total	0.312
P_z	1.645			
Total	7.581	N_2 N_3	σ	0.294
			π	0.177
			Total	0.471
Nitrogens 2, 3				
S	3.628	N_1 N_4	σ	−0.109
P_x	1.087		π	0.007
P_y	1.214		Total	−0.116
P_z	1.108			
Total	7.037			
Hydrogen 3				
	1.021			
Hydrogen 1, 2				
	0.609			

The B—H overlap populations in the two molecules can usefully be correlated with the observed B—H stretching frequencies, i.e., $\nu_{B-H} = 2627\ \text{cm}^{-1}$ and $2530\ \text{cm}^{-1}$ for dimethyltetrazaboroline [11b] and borazine respectively [18]. It seems, then, that the stability of the tetrazaboroline system can be, in part, attributed to the B—N bonds therein, since these are of similar strength to those in the stable molecule borazine.

The total and orbital energies of tetrazaboroline are given in Table 2. The highest filled orbital is of π-type and is equally distributed over the atoms. Its energy predicts an ionisation potential of 11.9 eV which can be compared with the experimental value of 10.4 eV for Me_2N_4BH [14b]. The first virtual orbital is also of π-symmetry but, surprisingly, contains no contribution from the boron π-orbital. In fact, it is the second virtual orbital (also of π type) which is largely concentrated on boron. This is the first example of a planar compound containing boron whose first π-type virtual orbital is *not* concentrated on the boron atom, and the implications of this are deeply significant. This finding explains why the boron atom in tetrazaboroline exhibits no acceptor properties and it also leads to the revolutionary suggestion that the compound could perhaps form complexes

Table 2. The total and orbital energies of tetrazaboroline (a.u.)

(a) Delocalised model	(b) Localised model
Electronic energy	
-407.0372	-406.9384
Nuclear energy	
163.5349	163.5349
Total energy	
-243.5023	-243.4035
0.155 $(b_2)\pi$	
0.132 $(a_2)\pi$	
-0.439 $(b_2)\pi$	
-0.491 (b_1)	
-0.529 $(a_2)\pi$	
-0.551 (a_1)	
-0.618 (a_1)	
-0.697 $(b_2)\pi$	
-0.708 (b_1)	
-0.782 (a_1)	
-0.892 (a_1)	
-0.911 (b_1)	
-1.188 (a_1)	
-1.292 (b_1)	
-1.518 (a_1)	
-7.818 (a_1)	
-15.699 (b_1)	
-15.699 (a_1)	
-15.744 (a_1)	
-15.745 (b_1)	

with electron donors in which the nitrogen atoms 2 and 3 would function as *acceptor* sites. This somewhat startling conclusion may also afford an explanation of why these cyclic compounds behave so curiously with known electron acceptors: thus with BCl_3 a simple 1 : 1 complex is formed but, with electron acceptors containing atoms which can act as electron donors, e. g., the chlorine atoms in Al_2Cl_6, $GaCl_3$, and $TiCl_4$, then ill-defined compounds or adducts with unusual stoicheiometry are produced [8]. It is clear that a completely new approach to the structural chemistry of the complexes formed by this "ligand" must be adopted.

In order to estimate the π-delocalisation energy of the N—B—N section of the molecule, the *ab initio* calculation was repeated with the π orbital of the boron atom excluded. Some of the results of this calculation are also given in Table 2. From the total energies, the π-delocalisation energy of the molecule is calculated to 61.9 kJ mol^{-1}. By comparison, the π-delocalisation energy of borazine is 119.1 kJ mol^{-1}. In the latter case this amounts to some 80 kJ per bond, whereas for the tetrazaboroline the corresponding quantity is ~ 130 kJ per bond. Although it is recognised that the molecules are not strictly comparable, these figures do indicate that the π-stabilisation energy is substantial for tetrazaboroline.

2. *All-Valence Electron Calculations on the Excited States of* $Me_2N_4B—X$ *Derivatives*

In this section of the work, a series of compounds of the type Me_2N_4BR (Fig. 1b) was examined theoretically in order to discover details of the nature o the excited states of the systems and the effects of the substituents R on the ring states and electronic spectra. Of these, the derivatives formed in the following way are particularly interesting: when the B-halogeno compounds are treated with silver cyanide or silver thiocyanate, as might be expected, the pseudohalogen replaces the halogen atom. However, infra-red and Raman spectroscopy hav been unable to establish whether the products contain the normal or *iso* pseudohalogen groups [12].

In this series of calculations, a common geometry was assumed for the tetrazaboroline moiety. The bond lengths and angles were abstracted from the recent work of Bauer [5]. The geometries assumed for the B—R group are detailed in Table 3 and for the vinyl derivative two isomers were studied, in which the vinyl group was positioned parallel or perpendicular to the N_4B ring plane. The excited states were obtained by considering one-electron excitations forming a specified set of σ- and π-based configurations. Interaction between all the excited configurations was included in the usual way. The result of this treatment, together with the observed absorption bands of the compounds, are presented in Table 4. The experimental data are taken mainly from the work of Leach and Morris [11, 12].

Table 3. Bond lengths (n m.) for substituents in boron substituted tetrazaborolines

Substituent	Bond lengths		
R			
$-CH_3$, C_2H_3	B—C, 0.154;	C—C, 0.135^a	
$-CN$	B—C, 0.154;	C—N, 0.1157^a	
NC	B—N, 0.142;	N—C, 0.1167^a	
SCN	B—S, 0.161,	S—C, 0.161;	C—N, 0.121^a
NCS	B—N, 0.142;	N—C, 0.122;	C—S, 0.156^a

^{a} Ref. [9]

Of the two vinyl compounds, the "perpendicular" isomer has the lowest total energy: we shall, therefore, restrict discussion to this derivative and only results appertaining to it are given in Table 4.

When (a) chlorine, (b) vinyl, and (c) hydrogen are the substituents on boron, the agreement between the observed and calculated electronic transition energies is good. In general, the low-energy non-allowed transitions are all of $\sigma-\pi^*$ type and these states resemble those calculated for the vinyl boranes [3].

As a more detailed illustration, we will consider the calculated spectrum of the chloro derivative: the spectra of the other compounds are closely related to this case.

Table 4. Electronic state energies (eV) of some boron-substituted tetrazaborolines

		E_{calc}	f_{calc}	$E_{expt.}$		$E_{calc.}$	f_{calc}	E_{expt}
(a) R = Cl	$^1\Psi_1$	4.25	0.00		(b) R = H	3.81	0.00	
	$^1\Psi_2$	4.39	0.00			4.28	0.00	
	$^1\Psi_3$	5.07	0.00			5.62	0.02	
	$^1\Psi_4$	5.68	0.09	5.79		6.25	0.05	6.26
	$^1\Psi_5$	6.62	0.00			6.41	0.00	
(c) R = —CH═CH$_2$	$^1\Psi_1$	3.43	0.00					
	$^1\Psi_2$	3.97	0.00					
	$^1\Psi_3$	4.21	0.00					
	$^1\Psi_4$	4.72	0.00					
	$^1\Psi_5$	5.41	0.99	5.77				
	$^1\Psi_6$	6.11	0.03					
(d) R = —SCN	$^1\Psi_1$	4.23	0.00		(e) R = —NCS	4.13	0.00	
	$^1\Psi_2$	4.30	0.00			4.29	0.00	
	$^1\Psi_3$	5.09	0.00			4.53	0.00	
	$^1\Psi_4$	5.57	0.10			4.57	0.04	4.84(sh.)
	$^1\Psi_5$	5.84	0.00			4.79	0.00	
	$^1\Psi_6$	6.10	0.00			5.52	0.00	
	$^1\Psi_7$	6.12	0.05			6.01	0.28	6.11
	$^1\Psi_8$	6.56	0.00			6.26	0.00	
(f) R = —CN	$^1\Psi_1$	4.12	0.00		(g) R = —NC	4.27	0.00	
	$^1\Psi_2$	4.13	0.00			4.31	0.00	
	$^1\Psi_3$	4.76	0.00			4.59	0.00	
	$^1\Psi_4$	5.06	0.00			4.77	0.00	
	$^1\Psi_5$	5.34	0.00			5.28	0.00	
	$^1\Psi_6$	5.44	0.07			5.83	0.07	
	$^1\Psi_7$	6.48	0.04	6.20		6.70	0.02	

The first calculated band stems from a $\sigma - \pi^*$ transition, of which the main contributing configuration is an excitation from a $p_\sigma - p_\sigma$ bond between the inner nitrogens to a π^* orbital situated mainly on the two inner nitrogen atoms. The second and third bands are also of $\sigma - \pi^*$ character. The first $\pi - \pi^*$ transition gives rise to the observed spectrum and occurs from a π-orbital which is evenly distributed about the boron and nitrogen atoms. The excited π^* orbital here is that appertaining to the B—Cl bond.

From the calculated excited states of the thiocyanate and isothiocyanate derivatives, it can be seen that better agreement with the observed spectra is obtained from the isothiocyanate. The allowed transitions are $\pi - \pi^*$ in nature and they are lower in energy than the corresponding states in compounds (a–c). The total valence energies obtained from the calculations are not *absolutely* meaningful but do indicate that the isothiocyanate is to be energetically preferred over the thiocyanate derivative.

Charge Distribution in Tetrazaborolines

The data relating to the distribution of charge over the series of molecules are given in Table 5. The atoms may be identified by the generic numbering scheme in Fig. 3. The whole series reveals itself as one of remarkably non-polar compounds, particularly around the central ring.

The bonding in the "normal" and *iso* thiocyanate groups in these compounds proves to be very interesting. The classical formulation of the bonds is —S—C≡N and —N=C=S, whereas the data in Table 6 reveal that there is, in each case, a strong bonding component between the sulphur and nitrogen atoms which is mainly of π type. This is a most uncommon feature and arises because the "bonding power" of the sulphur atom is markedly increased by 3*d* orbital participation in the π system of the group.

Table 5 Charge distribution in substituted tetrazaborolines, Me_4N_4BR

Substituent R	C_2H_5	Cl	H	—CN	—NC	CH_3	—NCS	—SCN
B	+0.11	+0.17	−0.10	+0.02	+0.13	+0.15	+0.15	+0.11
N_1	−0.06	−0.04	−0.00	−0.02	−0.05	−0.08	−0.06	−0.07
N_2	−0.05	−0.04	−0.05	−0.05	−0.04	−0.06	−0.04	−0.04
C_1	−0.18	−0.16	−0.17	−0.17	−0.17	−0.18	−0.17	−0.18
H_1	+0.09	+0.10	+0.09	+0.09	+0.09	+0.08	+0.09	+0.09
H_2	+0.08	+0.10	+0.09	+0.09	+0.09	+0.08	+0.09	+0.09
H_3	+0.09	+0.10	+0.09	+0.09	+0.09	+0.08	+0.09	+0.09
X_1	0.14	−0.28	+0.01	−0.02	−0.03	−0.38	−0.15	+0.01
X_2	−0.15			−0.08	−0.13	-	+0.25	+0.08
X_3					-		−0.25	−0.16
H_4	+0.09				-	+0.11	-	-
H_5, H_6	+0.07					-		

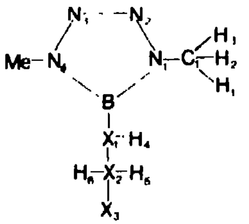

Fig 3. Key to numbering for charge distribution in substituted tetrazaborolines

Table 6. Bond orders in the —N—C—S and —S—C—N groups

π	N—C	1.048	π	C—N	1.575
	C—S	0.795		S—C	0.406
	N—S	0.407		S—N	0.307
$\sigma+\pi$	N—C	2.017	$\sigma+\pi$	C—N	2.548
	C—S	1.820		S—C	1.404
	N—S	0.444		S—N	0.350

3. *All-Valence Electron Calculations on* $Me_2N_4Fe(CO)_3$

The same calculational procedures with the same parametrisation as in previous calculations [16] on butadieneirontricarbonyl were employed to examine dimethyltetrazadiene and its complex with iron tricarbonyl. The geometry of the σ complex was taken from recent crystallographic work [6]. That of the π-complex was assumed to be broadly similar to that of butadieneirontricarbonyl [13] (see Fig. 2). The dimethyltetrazadiene moiety was positioned in a plane above and perpendicular to a pyramidal $Fe(CO)_3$ group. The bond lengths and angles within the separate dimethyltetrazadiene and iron tricarbonyl units were the same as in the σ complex. The $Fe—N_1,N_4$ and $Fe—N_2,N_3$ bond distances were taken to be equal to that of the $Fe—N_1$ distance in the known complex: the tetrazadiene plane was hence situated at a distance 0.161 nm from the iron atom.

In this problem we are concerned with determining the minimum energy configuration and, hence, the total valence electronic energy, and the charge distribution for the two structures shown in Fig. 2 are presented in Table 7. It can immediately be seen that the order of total energies for the structures confirms the crystallographic result [6] that the σ-bonded structure (Fig. 2b) is the more stable of the two.

The electron population distribution shows that, in the σ-complex, there is, overall, a limited movement of electrons to the iron tricarbonyl unit: this comprises a π-electron drift (0.50) towards the iron tricarbonyl unit, coupled with a σ-electron (0.46) polarisation towards the complexed dienoid moiety. Examina-

Table 7. Electronic energies (eV) and charge distributions for the "σ"- and "π"-structures of dimethyltetrazadieneirontricarbonyl

	σ-complex		π-complex	
Electronic energy	−15693.9		−15804.9	
Nuclear energy	12114.9		12239.2	
Total energy	− 3579.0		− 3565.7	
Electronic density				
Iron				
4*s*	0.44		0.44	
4*p*	0.87		0.88	
3*d*	7.21		7.25	
Total	8.52		8.57	
Nitrogen (N_1) σ	3.38		3.86	
π	1.61		1.17	
Total	4.99		5.03	
Nitrogen (N_2) σ	3.91		3.92	
π	1.14		1.03	
Total	5.05		4.95	
Carbon (methyl)	4.29		4.19	
Carbon (carbonyl)	3.77*	3.85	3.85*	3.82
Oxygen	6.07*	5.99	5.97*	6.07
Hydrogen	0.92*	0.89	0.92*	0.90

* Unique carbonyl group and hydrogen atom.

tion of the electron densities of the Me_2N_4 unit before and after complexing reveals that π-electrons are evenly supplied from both the inner (0.10) and outer (0.15) nitrogens. The σ-electron distribution is interesting as the "extra" electron density from the $Fe(CO)_3$ unit is distributed throughout the σ-electron system of Me_2N_4, with a bias towards the inner nitrogens. One overall result of this two-way electron flow is to reduce the electron density on the outer nitrogens and to increase the electron density on the inner nitrogens, i. e., complex formation tends therefore to equalise the electron density over the nitrogen atoms. The iron is negatively charged (0.51) and most of this (0.48) originates from the tricarbonyl moiety. The iron charge stems from σ donation of electrons which originate from the s and p_σ orbitals of the carbonyl carbon. A modicum of π-back donation from iron to the CO moieties is also evident. The result of the latter charge movement is to alter the electron distribution on both C and O as compared with free carbon monoxide calculated by the same method. Thus, the charge on carbon is altered from 0.15 to +0.23 and that on oxygen changes from +0.15 to −0.17. The σ-donation thus reduces the carbon density and the π-back donation increases the oxygen population. A comparison of the bond order data shows that there is a small decrease in all the nitrogen-nitrogen bond orders on complexing but that the σ bonds formed between the iron and the outer nitrogens are strong (bond order, 0.41). Furthermore, in the tetrazadiene moiety, the "π" (i. e., those antisymmetric to the N_4H_2 plane) contain 5.50 electrons and so, together with the "π" orbitals on the iron, form a six-π-electron ring system similar in nature to that of the tetrazaborolines. The stability of the complex results from this factor and the strong bonding between Fe and N_1, N_4.

The electron distribution in the π complexed structure is, overall, rather similar to that of the σ complex. The most significant difference occurs in the π electron population of the nitrogen atoms, being 4.40, and 5.50 for the π and σ complexes respectively. The bond orders in the π complex show that the iron atom forms bonds to both the inner (0.20) and the outer (0.26) nitrogen atoms. This electron-withdrawing process reduces the π electron population of all the nitrogens but leaves the σ orbitals of the outer pair essentially unchanged, and the iron has appreciable bond orders only with the outer nitrogens (0.41).

4. *The Electronic Structures of Tetrazadiene and Butadiene*

Although tetrazadiene (N_4H_2) and butadiene are isoelectronic systems, they form different types of complex with the iron tricarbonyl group. It is not surprising that the latter does not yield an adduct which is σ bonded from the terminal carbons, since this would (a) require prior rotation of the two end —CH_2 groups out of the plane of the molecule, and (b) cause disruption of the stable totally-symmeric all-spin-paired σ bonding situation in the molecule. However, it is interesting to enquire why the latter does not apply equally to tetrazadiene (the former reason is clearly not relevant) and hence we also carried through Gaussian calculations with limited basis sets on the two ligands.

The orbital energy levels are presented in Table 8 and show several interesting features. Firstly, in both cases there are only two filled π orbitals. Secondly, in

Table 8. The energy levels of butadiene and tetrazadiene

Butadiene	Tetrazadiene
0.372 (a_1)	0.412 (a_1)
0.227 (a_2) π	0.177 (a_2) π
0.055 (b_2) π	0.010 (b_2) π
− 0.403 (a_2) π	− 0.407 (b_1)
− 0.529 (b_2) π	− 0.426 (a_2) π
− 0.571 (a_1)	− 0.486 (a_1)
− 0.575 (b_1)	− 0.554 (b_1)
− 0.636 (b_1)	− 0.622 (b_2) π
− 0.671 (a_1)	− 0.665 (a_1)
− 0.743 (a_1)	− 0.770 (a_1)
− 0.781 (b_1)	− 0.871 (b_1)
− 0.905 (a_1)	− 1.115 (a_1)
− 1.062 (b_1)	− 1.262 (b_1)
− 1.176 (a_1)	− 1.480 (a_1)
− 11.406 (a_1)	− 15.675 (a_1)
− 11.406 (b_1)	− 15.675 (b_1)
− 11.428 (a_1)	− 15.744 (a_1)
− 11.428 (b_1)	− 15.745 (b_1)

tetrazadiene there is a low-lying vacant π-orbital which becomes occupied on σ bonding with the $Fe(CO)_3$ groups. This is an interesting feature and its occupancy represents a diversion of electron density from σ-type orbitals to those of π type in the final complex. This orbital thus brings about the stable six-π-electron ring. The highest filled orbital of tetrazadiene is of σ type (b_1 symmetry) and it is built from a linear combination of orbitals situated on the outer nitrogens. This orbital helps bring about the important Fe—N_1 σ bonds.

Acknowledgement. One of us (J.J.P.S.) thanks the S.R.C. for the award of a Maintenance Grant.

References

1. Armstrong, D.R., Perkins, P.G., Stewart, J.J.P.: J. chem. Soc. (London) A **1971**, 3674.
2. – Clark, D.T.: J. chem. Soc. (London) D **1970**, 99.
3. – Perkins, P.G.: Theoret. chim. Acta (Berl.) **9**, 412 (1968)
4. Boys, S.F.: Proc. Royal Soc. (London) **200** A, 542 (1950).
5. Chang, C.V., Porter, R.F., Bauer, S.H.: Inorg. Chemistry **8**, 1677 (1969).
6. Doedens, R.J.: Chem. Comm. **1968**, 1271.
7. Greenwood, N.N., Morris, J.H.: J. chem. Soc. (London) **1965**, 6205.
8. Hessett, B., Morris, J.H., Perkins, P.G.: J. chem. Soc. (London) A **1971**, 2466.
9. Interatomic distances in molecules and ions, No. 11. London: Chem. Soc. Special Publ. 1958.
10. Knox, G.R., Dekker, M.: Chem. Comm. **1967**, 1243.

11a. Leach, J.B., Morris, J.H.: J. Organomet. Chem. **13**, 313 (1968).
11b. — — J. chem. Soc. (London) **1967**, 1590.
12. — — Private communication.
13. Mills, O.S., Robinson, G.: Proc. chem. Soc. (London) **1960**, 421.
14a. Morris, J.H., Perkins, P.G.: J. chem. Soc. (London) A **1966**, 576.
14b. — — J. chem. Soc. (London) A **1966**, 580.

15. Mulliken, R. S.: J. chem. Physics **23**, 1933 (1955).
16. Perkins, P. G., Robertson, I. C., Scott, J. M.: Theoret. chim. Acta (Berl.) **22**, 299 (1971).
17. Pople, J. A., Santry, D. P., Segal, G. A.: J. chem. Physics **43**, S 129 (1965).
18. Price, W. C., Fraser, R. D. B., Robinson, T. S., Longuet-Higgins, H. C.: Discuss. Faraday Soc. **9**, 131 (1950)
19. Whitman, D R., Hornback, C. J.: J. chem. Physics **51**, 398 (1969).

Dr. D. R. Armstrong
Department of Pure and Applied Chemistry
University of Strathclyde
Glasgow, C. 1, Scotland

Theoret. chim. Acta (Berl.) 26, 249—256 (1972)
© by Springer-Verlag 1972

Introduction de la matrice densité de paire dans l'étude théorique du *pK* des états excités

R. Constanciel

Centre de Mécanique Ondulatoire Appliquée, 23, rue du Maroc, Paris et Université de Paris VI

Reçu le 3 janvier 1972

Introduction of the Pair Density Matrix in the Theoretical Study of the pK-Value of Excited States

We have shown, by applying the perturbation theory to the excited states, the influence of the pair polarizability on the first order variation of the energy. The introduction of this new term allows us to account for the *pK* difference between the first excited states, singlet and triplet, of the conjugated molecules.

On a mis en évidence, en appliquant la théorie des perturbations aux états excités, l'influence de la polarisabilité de paire dans la variation de l'énergie au premier ordre. L'introduction de ce nouveau terme permet de rendre compte de la différence de *pK* entre les premiers états excités, singulet et triplet, des molécules conjuguées.

Mit Hilfe einer Anwendung der Störungstheorie erster Ordnung wird der Einfluß der Paarpolarisierbarkeit auf die Energie gezeigt. Die Einführung dieses neuen Terms erlaubt eine Berücksichtigung der Differenz des *pK*-Wertes zwischen dem ersten angeregten Singulett- und Triplettzustand eines konjugierten Moleküls.

Introduction

Förster [1], Weller [2], puis Jackson et Porter [3] ont étudié les réactions d'équilibre acido-basique des molécules dans leur état fondamental et dans leurs premiers états excités. Ils ont montré que les valeurs du *pK* sont susceptibles de subir des variations lorsque le système en équilibre est soumis à l'action d'un rayonnement ultraviolet.

La méthode du cycle de Förster [1] permet de calculer la variation de *pK* avec l'excitation, en fonction de grandeurs obtenues au moyen des méthodes de la chimie quantique. Ainsi,

$$\Delta pK = pK^{*} - pK^{F} \# \frac{\Delta E_{A^-} - \Delta E_{AH}}{kT} \log e$$

où ΔE_{AH} et ΔE_{A^-} représentent les énergies des premières transitions, singulet ou triplet, pour l'acide ou la base conjuguée respectivement.

Coulson et Jacobs [4] ont pu établir, dans l'approximation de Hückel, que les différences de *pK* entre l'état fondamental et le premier état excité singulet sont liées qualitativement à la variation de charge, lors de l'excitation, de l'atome qui subit la protonation ou la déprotonation. Plus généralement, il existe une relation entre les différences de *pK* et la variation de tous les éléments de la matrice de densité monoélectronique *P* pouvant se traduire, par exemple, par une modification du moment polaire [5]. De même, après avoir introduit explicitement les termes de répulsion électronique, de nombreux auteurs ont tenté de rendre compte de la différence de comportement des états excités singulet et triplet par l'emploi des charges [6–7], mais la valeur explicative de ces grandeurs est dans ce cas plus discutable. En effet, on constate que, pour une configuration donnée, les matrices de densité $\boldsymbol{P}^S$ de l'état singulet et $\boldsymbol{P}^T$ de l'état triplet sont égales. On peut, il est vrai, faire apparaitre des différences entre $\boldsymbol{P}^S$ et $\boldsymbol{P}^T$ en effectuant un calcul d'interaction de configuration: malheureusement les éléments de ces matrices sont très sensibles au choix de la base de configurations [8], l'ordre de grandeur relatif des charges pouvant même être inversé lorsqu'on étend la base [9]. Il semble donc très dangereux de vouloir interpréter l'expérience à l'aide des charges calculées dans les états excités si on ne peut développer les fonctions d'onde sur une base complète de configurations. Dans les cas favorables où ce calcul a pu être effectué, on n'a pas obtenu de différence significative entre $\boldsymbol{P}^S$ et $\boldsymbol{P}^T$: ceci semble montrer que les charges obtenues par la méthode des interactions de configuration ne sont pas de bons indices de la réactivité des états excités.

L'étude des grandeurs énergétiques, telle que l'intégrale d'échange K, permet de rendre compte des différences de propriété entre les premiers états excités et d'en comprendre l'origine qui est essentiellement la corrélation de Fermi [10–11]. Bertran, Chalvet et Daudel ont appliqué avec succès cette méthode au problème des équilibres acido-basiques [9]. Il apparait ainsi que des indices de réactivité raisonnables doivent être définis à partir de considérations énergétiques, ce qui nécessite d'utiliser non plus seulement les éléments de la matrice de densité monoélectronique $\boldsymbol{P}$, mais aussi ceux de la matrice de densité biélectronique $\boldsymbol{Q}$ [12–13].

L'objet de ce travail est de montrer, à l'aide de la théorie de perturbation au premier ordre, l'intérêt qu'il y a à introduire la matrice $\boldsymbol{Q}$. L'interprétation physique simple qui se dégage de cette approche sera illustrée dans des publications ultérieures par des applications numériques sur quelques exemples particuliers.

I. Théorie de perturbation dans les états excités

On suppose que le hamiltonien du système formé de la molécule et du proton est une somme d'opérateurs $\hat{H}_1(i)$ et $\hat{H}_2(i,j)$ agissant sur les coordonnées d'espace d'une ou deux particules seulement. Dans le cadre de l'approximation π[1], $\hat{H}_1(i)$ est l'opérateur de coeur $\hat{H}^C(i)$, et $\hat{H}_2(i,j)$ est l'opérateur d'interaction coulombienne $\frac{1}{|\boldsymbol{r}_i - \boldsymbol{r}_j|}$. Dans une base orthogonale d'orbitales atomiques π l'énergie d'un système de n électrons, dans le champ du coeur sigma de la molécule, s'écrit [14]:

$$E = \operatorname{Tr} \boldsymbol{P}_1 \boldsymbol{H}_1 + \tfrac{1}{2} \operatorname{Tr} \boldsymbol{P}_2 \boldsymbol{H}_2 \qquad (1)$$

où $\boldsymbol{H}_1$ et $\boldsymbol{H}_2$ sont les matrices $(n \times n)$ et $(n^2 \times n^2)$ des opérateurs $\hat{H}_1$ et $\hat{H}_2$, et $\boldsymbol{P}_1$ et $\boldsymbol{P}_2$ sont les matrices de densité réduites à une et deux particules [14] satisfaisant aux conditions de normalisation:

---

[1] Les résultats obtenus dans ce cas particulier restent valables lorsqu'on tient compte de tous les électrons.

$$\mathrm{Tr}\, \boldsymbol{P}_1 = n\,, \tag{2a}$$

$$\mathrm{Tr}\, \boldsymbol{P}_2 = n(n-1)\,, \tag{2b}$$

$$\mathrm{Tr}'\boldsymbol{P}_2 = \boldsymbol{P}_1(n-1)\,. \tag{2c}$$

Si on définit [15] un opérateur hamiltonien réduit à deux particules

$$\hat{\boldsymbol{K}}(1,2) = \frac{1}{1,2(n-1)}\,[\hat{\boldsymbol{H}}_1(1) + \hat{\boldsymbol{H}}_1(2)] + \hat{\boldsymbol{H}}_2(1,2)$$

on peut aussi écrire l'énergie sous la forme

$$E = \tfrac{1}{2}\,\mathrm{Tr}\,\boldsymbol{P}_2\boldsymbol{K}\,. \tag{3}$$

Le choix d'une base d'orbitales atomiques dans laquelle l'approximation de recouvrement différentiel nul (ZDO) est justifiée, permet d'écrire l'énergie en terme de matrices d'ordre n seulement

$$E = \mathrm{Tr}\,\boldsymbol{PH} + \tfrac{1}{2}\mathrm{Tr}\,\boldsymbol{Q\Gamma}\,. \tag{4}$$

Dans cette expression, on a adopté les nouvelles notations simplifiées:

$$\boldsymbol{P} = \boldsymbol{P}_1 \quad \text{et} \quad \boldsymbol{H} = \boldsymbol{H}_1\,.$$

En effet, dans une telle base, les éléments de la matrice $\boldsymbol{H}_2$ sont défibis par la relation:

$$\langle pq|\hat{\boldsymbol{H}}_2|rs\rangle = \langle p|\hat{\boldsymbol{\Gamma}}|q\rangle\,\delta_{pr}\delta_{qs} \tag{5}$$

où $\langle p|\hat{\boldsymbol{\Gamma}}|q\rangle$ est l'intégrale de répulsion coulombienne γ_{pq}. L'énergie est alors complètement déterminée en fonction des seuls éléments

$$\langle p|\hat{\boldsymbol{Q}}|q\rangle = \langle pq|\hat{\boldsymbol{P}}_2|pq\rangle \tag{6}$$

qui représentent la densité de probabilité multipliée par $n(n-1)$ de rencontrer simultanément deux électrons dans les deux domaines disjoints de l'espace où sont localisées (implicitement, dans l'approximation ZDO) les orbitales atomiques p et q. On déduit immédiatement de la condition de normalisation (2b) que la somme des éléments de la matrice $\boldsymbol{Q}$ est constante et égale à $n(n-1)$.

Nous admettrons que l'approche d'un proton modifie uniquement $\boldsymbol{H}$ [16]. Au premier ordre de la théorie de perturbation, la variation $E^{(1)}$ de l'énergie est alors donnée par:

$$E^{(1)} = \mathrm{Tr}\,\boldsymbol{PH}^{(1)} + \mathrm{Tr}\,\boldsymbol{P}^{(1)}\boldsymbol{H} + \tfrac{1}{2}\mathrm{Tr}\,\boldsymbol{Q}^{(1)}\boldsymbol{\Gamma} \tag{7a}$$

ou, en introduisant l'opérateur hamiltonien réduit à deux particules $\boldsymbol{K}(1,2)$

$$E^{(1)} = \mathrm{Tr}\,\boldsymbol{PH}^{(1)} + \tfrac{1}{2}\mathrm{Tr}\,\boldsymbol{P}_2^{(1)}\boldsymbol{K}\,. \tag{7b}$$

Lorsque l'énergie à l'ordre zéro est calculée dans l'approximation du champ autocohérent, on montre que les deux derniers termes du membre de droite de l'équation (7a) s'annulent identiquement [17]; dans ce cas, la variation d'énergie se réduit à

$$E^{(1)} = \mathrm{Tr}\,\boldsymbol{PH}^{(1)} \tag{8}$$

et les éléments de la matrice $\boldsymbol{P}$ sont alors des indices statiques [18] en même temps que de bons indices de réactivité, puisque leur connaissance suffit à déterminer $E^{(1)}$. Dès que l'on sort du cadre de la méthode SCF, il faut tenir compte des termes correctifs $\boldsymbol{P}^{(1)}$ et $\boldsymbol{Q}^{(1)}$ (ou $\boldsymbol{P}_2^{(1)}$) et les éléments de la matrice $\boldsymbol{P}$ ne sont plus nécessairement des indices de réactivité raisonnables, puisque la relation (8) n'est pas satisfaite en général [12-13].

II. Etude quantitative

A. Définition d'un indice de réactivité pour les premiers états excités

Ce qui précède s'applique, en particulier, à l'étude des premiers états excités singulet (S) et triplet (T) des molécules conjuguées dans l'approximation *où* on utilise pour représenter ces états les orbitales moléculaires autocohérentes de l'état fondamental. Dans ce cas, la variation d'énergie au premier ordre, donnée par l'équation (7a) est:

$$(E^{\overset{S}{T}})^{(1)} = \operatorname{Tr} \boldsymbol{P}^{\overset{S}{T}} \boldsymbol{H}^{(1)} + \operatorname{Tr} (\boldsymbol{P}^{\overset{S}{T}})^{(1)} \boldsymbol{H} + \tfrac{1}{2} \operatorname{Tr} (\boldsymbol{Q}^{\overset{S}{T}})^{(1)} \boldsymbol{\Gamma} \tag{9a}$$

ou bien, suivant (7b)

$$(E^{\overset{S}{T}})^{(1)} = \operatorname{Tr} \boldsymbol{P}^{\overset{S}{T}} \boldsymbol{H}^{(1)} + \tfrac{1}{2} \operatorname{Tr} (\boldsymbol{P}_2^{\overset{S}{T}})^{(1)} \boldsymbol{K} . \tag{9b}$$

On introduit maintenant une matrice $\boldsymbol{X}^{\overset{S}{T}}$ dont on admettra, par analogie avec la formule (8), que les éléments $(X^{\overset{S}{T}})_{pq}$ sont de «bons» indices de réactivité pour les états (S) ou (T) si on peut écrire:

$$(E^{\overset{S}{T}})^{(1)} = \operatorname{Tr} \boldsymbol{X}^{\overset{S}{T}} \boldsymbol{H}^{(1)} \tag{10a}$$

ou encore:

$$(X^{\overset{S}{T}})_{pq} = \frac{\partial E^{\overset{S}{T}}}{\partial H_{pq}} \quad \forall\, p, q . \tag{10b}$$

Comparant avec l'équation (9b), on obtient pour expression des éléments des matrices $\boldsymbol{X}^{\overset{S}{T}}$

$$(X^{\overset{S}{T}})_{pq} = (P^{\overset{S}{T}})_{pq} + \tfrac{1}{2} \sum_{r,s} \sum_{u,v} \left[\frac{\partial}{\partial H_{pq}} (P_2^{\overset{S}{T}})^{(1)}_{rs,uv} \right] K_{rs,uv} . \tag{11}$$

Si l'on admet que pour simuler la fixation d'un proton sur le sommet x d'une molécule, il suffit de modifier l'élément diagonal H_{xx} de la matrice $\boldsymbol{H}$, la variation d'énergie est donnée par l'expression:

$$(E^{\overset{S}{T}})^{(1)} = (X^{\overset{S}{T}})_{xx} H_{xx}^{(1)} \tag{12}$$

où $(X^{\overset{S}{T}})_{xx} = \dfrac{\partial E^{\overset{S}{T}}}{\partial H_{xx}}$ est la pente de la courbe représentant la valeur de l'énergie en fonction du paramètre H_{xx}.

Lorsqu'on représente sur un diagramme les variations des énergies de transition (l'énergie de l'état fondamental étant prise comme référence), on obtient des courbes dont la pente est donnée par:

$$\frac{\partial}{\partial H_{xx}} (E^{\overset{S}{T}} - E^F) = (X^{\overset{S}{T}})_{xx} - q_x^F \tag{13}$$

où q_x^F est la charge portée par l'atome x dans l'état fondamental. En développant l'expression de $(X^{\overset{S}{T}})_{xx}$, on a:

$$\frac{\partial}{\partial H_{xx}}(E^{\overset{S}{T}} - E^F) = (q_x^{\overset{S}{T}} - q_x^F) + \tfrac{1}{2}\sum_{rs}\sum_{uv}\left[\frac{\partial}{\partial H_{xx}}(P_2^{\overset{S}{T}})^{(1)}_{rs,uv}\right]K_{rs,uv}\,. \tag{14}$$

Le premier terme est égal à la différence de charge lors de l'excitation. Le second terme résulte de l'introduction de la polarisabilité de paire $P_2^{(1)}$: sa valeur est différente selon que l'état considéré est singulet ou triplet [19]. Ce résultat est général et s'applique au cas où la fonction d'onde est développée dans une base étendue de configurations.

Dans le cas le plus simple où les états excités (S) et (T) sont représentés par une configuration monoexcitée unique ($i \to m$), i et m désignant les orbitales moléculaires occupées une fois, il est facile de réduire la formule générale (9a, b) à la forme (10a). Les éléments des matrices $P^{\overset{S}{T}}$ et $Q^{\overset{S}{T}}$ sont définis, en effet, par les relations suivantes:

$$\begin{aligned} P_{pq}^{\overset{S}{T}} &= P_{pq}^{*} = P_{pq}^F + D_{pq}^{-} \\ Q_{pq}^T &= P_{pp}^{*}P_{qq}^{*} - \tfrac{1}{2}(P_{pq}^{*})^2 - \tfrac{1}{2}(D_{pq}^{+})^2 \\ Q_{pq}^S &= Q_{pq}^T + (D_{pq}^{+})^2 - (D_{pq}^{-})^2 \end{aligned} \tag{15}$$

avec

$$\begin{aligned} P_{pq}^F &= 2\sum_{j}^{\mathrm{occ}} c_{jp}c_{jq} \\ D_{pq}^{\pm} &= c_{mp}c_{mq} \pm c_{ip}c_{iq}\,. \end{aligned} \tag{16}$$

On constate que les variations $(Q^{\overset{S}{T}})^{(1)}$ s'expriment en fonction des variations $(P^*)^{(1)}$ et $(D^{\pm})^{(1)}$: ces dernières sont alors calculées au moyen des polarisabilités Π^* et $\Pi^{\pm}$ définies à partir de formules [20] analogues à celles proposées pour l'état fondamental par Coulson et Longuet-Higgins [21]:

$$\begin{aligned} (P_{pq}^{*})^{(1)} &= \sum_{rs}\Pi_{pq,rs}^{*}H_{rs}^{(1)} \\ (D_{pq}^{\pm})^{(1)} &= \sum_{rs}\Pi_{pq,rs}^{\pm}H_{rs}^{(1)} \end{aligned} \tag{17}$$

avec

$$\Pi_{pq,rs}^{*} = \Pi_{pq,rs}^F + \Pi_{pq,rs}^{-}\,.$$

Lorsque le paramètre H_{xx} varie, l'expression analytique de la pente s'obtient en fonction des polarisabilités, atome-atome et atome-liaison seulement, définies par les formules suivantes:

$$\begin{aligned} \Pi_{pq,xx}^F &= 2\sum_{j}^{\mathrm{occ}}\sum_{l}^{\mathrm{vir}}\frac{c_{jp}c_{lq}+c_{lp}c_{jq}}{\varepsilon_j-\varepsilon_l}c_{jx}c_{lx} \\ \Pi_{pq,xx}^{\pm} &= \sum_{k\neq m}\frac{c_{kp}c_{mq}+c_{mp}c_{kq}}{\varepsilon_m-\varepsilon_k}c_{kx}c_{mx} \\ &\quad \pm \sum_{k\neq i}\frac{c_{kp}c_{iq}+c_{ip}c_{kq}}{\varepsilon_i-\varepsilon_k}c_{kx}c_{ix}\,. \end{aligned} \tag{18}$$

B. Etude de la différence singulet-triplet

a) *Utilisation de l'intégrale d'échange.* La variation de la différence d'énergie singulet-triplet s'écrit, d'après l'équation (9a):

$$(E^S - E^T)^{(1)} = \mathrm{Tr}(\boldsymbol{P}^S - \boldsymbol{P}^T)\,\boldsymbol{H}^{(1)} + \mathrm{Tr}(\boldsymbol{P}^S - \boldsymbol{P}^T)^{(1)}\boldsymbol{H} + \tfrac{1}{2}\mathrm{Tr}(\boldsymbol{Q}^S - \boldsymbol{Q}^T)^{(1)}\boldsymbol{\Gamma}\,. \tag{19}$$

Dans l'approximation où l'on représente les états (S) et (T) par une configuration monoexcitée unique $(i \rightarrow m)$, le premier terme du membre de droite s'annule identiquement (Eq. (15)); il en est de même du second terme (Eq. (17)) si l'équation du champ autocohérent est vérifiée au premier ordre de la théorie des perturbations.

La variation d'énergie $(S)-(T)$ est alors donnée par:

$$(E^S - E^T)^{(1)} = \tfrac{1}{2}\mathrm{Tr}(\boldsymbol{Q}^S - \boldsymbol{Q}^T)^{(1)}\boldsymbol{\Gamma} \tag{20}$$

et dépend uniquement des variations relatives des matrices de paire $\boldsymbol{Q}^S$ et $\boldsymbol{Q}^T$. On vérifie, à l'aide des formules (15) que cette expression s'identifie avec la variation du double de l'intégrale d'exchange K_{im}

$$\tfrac{1}{2}\mathrm{Tr}(\boldsymbol{Q}^S - \boldsymbol{Q}^T)^{(1)}\boldsymbol{\Gamma} = \tfrac{1}{2}\sum_{pq}[(D_{pq}^{+})^2 - (D_{pq})^2]^{(1)}\gamma_{pq} = 2K_{im}^{(1)} \tag{21}$$

utilisée dans l'étude théorique précédente de Bertran, Chalvet et Daudel [9].

La formule (20) est plus générale et s'applique aussi au cas où on a choisi des configurations symétriques pour (S) et (T).

b) *Utilisation des géminales naturelles.* Un élément quelconque des matrices de paire $\boldsymbol{Q}^S$ ou $\boldsymbol{Q}^T$ peut se mettre sous la forme [22]:

$$Q_{pq}^{\overset{S}{T}} = 2\sum_{I}|\langle I^{\overset{S}{T}}|pq\rangle|^2 \tag{22}$$

chaque terme de la somme représentant la contribution d'une fonction biélectronique $I^{\overset{S}{T}}$, fonction propre de l'opérateur $\hat{\boldsymbol{Q}}^{\overset{S}{T}}$ ou géminale naturelle.

On vérifie aisément que la suite des géminales naturelles I^S, fonctions propres de l'opérateur $\hat{\boldsymbol{Q}}^S$, diffère de la suite des géminales naturelles I^T, fonctions propres de $\hat{\boldsymbol{Q}}^T$, de deux géminales seulement

$$I_{i,m}^{\pm} = \frac{1}{\sqrt{2}}\{|i\bar{m}| \pm |\bar{i}m|\} \tag{23}$$

construites à l'aide des orbitales moléculaires une fois occupées i et m.

Si on définit, suivant l'équation (22), les éléments matriciels des opérateurs de densité de paires de quasi-électrons dans les géminales I^+ et I^-

$$(Q_I^{\pm})_{pq} = 2|\langle I^{\pm}|pq\rangle|^2 \tag{24}$$

on trouve, d'après (23)

$$(Q_I^{\pm})_{pq} = [c_{ip}c_{mq} \pm c_{iq}c_{mp}]^2\,. \tag{25}$$

La variation d'énergie $(S)-(T)$ est donnée par:

$$\tfrac{1}{2}\mathrm{Tr}(\boldsymbol{Q}_I^{+} - \boldsymbol{Q}_I^{-})^{(1)}\boldsymbol{\Gamma} = \tfrac{1}{2}\sum_{pq}4[c_{ip}c_{mq}c_{iq}c_{mp}]^{(1)}\gamma_{pq} = 2K_{im}^{(1)}. \tag{26}$$

On retrouve qu'elle est égale à la variation de l'intégrale $2K_{im}$. De plus, il apparait clairement que cette différence est dûe essentiellement à la différence de corrélation des paires (i, m) (S) et (T) [9].

Etude qualitative

Il est commode de traduire les variations des éléments des matrices de paire $\boldsymbol{Q}^{\overset{S}{T}}$ par celles de grandeurs scalaires telles que l'indice de localisabilité de paire

$$L^{\overset{S}{T}} = \frac{1}{n(n-1)} \sum_{p} (Q^{\overset{S}{T}})_{pp} \tag{27}$$

qui représente la somme des probabilités de présence d'une paire d'électrons sur chaque sommet de la molécule, ou la distance interélectronique moyenne

$$d^{\overset{S}{T}} = \frac{1}{n(n-1)} \mathrm{Tr}\, \boldsymbol{Q}^{\overset{S}{T}} \boldsymbol{D} \tag{28}$$

où $\boldsymbol{D}$ est la matrice des distances internucléaires.

On dispose ainsi de deux indices dont les significations physiques sont claires et complémentaires et dont les variations sous l'effet d'une perturbation sont liées qualitativement à celles du terme correctif $\frac{1}{2}\mathrm{Tr}\,\boldsymbol{Q}^{(1)}\boldsymbol{\Gamma}$.

Ainsi, une augmentation de L signifie que les paires d'électrons se localisent, donc que la distance moyenne d'entre ceux-ci diminue. En même temps, la contribution des intégrales monocentriques devient plus importante et le terme correctif $\frac{1}{2}\mathrm{Tr}\,\boldsymbol{Q}^{(1)}\boldsymbol{\Gamma}$ augmente.

Conclusion

Nous avons montré que la charge ne peut être utilisée comme indice statique de réactivité des états excités lorsque les fonctions d'onde qui les décrivent sont développées dans une base d'orbitales moléculaires autocohérentes de l'état fondamental.

Cependant, il est toujours possible de définir pour ces états de bons indices statiques de réactivité, dépendant à la fois des distributions de probabilité mono et biélectronique de la molécule que l'on étudie. On met ainsi naturellement en évidence des différences de pK entre le singulet et le triplet, ce dont la charge seule est impuissante à rendre compte.

Lorsque les charges sont égales (dans l'approximation monoconfigurationnelle, ou plus généralement pour un choix symétrique de configurations singulet et triplet), les différences de pK dépendent uniquement des polarisabilités de paire électroniques $\boldsymbol{Q}^{S(1)}$ et $\boldsymbol{Q}^{T(1)}$. On a mis à profit cette propriété pour relier qualitativement les différences de pK singulet-triplet à la localisabilité des paires d'électrons et à la distance interélectronique moyenne. L'utilisation du formalisme des géminales naturelles permet de ramener le problème général à n électrons à la comparaison de deux systèmes biparticulaires, l'un dans l'état singulet, l'autre dans l'état triplet.

Remerciements. Je remercie vivement le professeur R. Daudel et le Dr. O. Chalvet d'avoir, au cours de nombreuses discussions, manifesté pour ce travail un intérêt constant.

Je remercie également le professeur H. Jaffé des critiques efficaces que lui a suggérées la lecture du manuscrit.

Bibliographie

1. Förster,T.: Z. Electrochem. **54**, 42 (1950).
2. Weller,A.: Z. Electrochem. **56**, 662 (1952).
3. Jackson,G., Porter,G.: Proc. Royal Soc. (London) A **260**, 13 (1961).
4. Coulson,C.A., Jacobs,I.: J. chem. Soc. (London) , 1983 (1949); Sandorfy,C.: C. R. Acad. Sci. Paris C **232**, 617 (1951).
5. Grabowski,Z.R., Rotkiewicz,K., Sadlej,A.J.: Proceedings of the International Conference on Luminescence (Budapest) **1**, 310 (1966).
6. Imamura,A., Fujita,M., Nagata,C.: Bull. chem. Soc. Japan **40**, 21 (1967).
7. Tyutyulkov,N.F., Fratev,F., Petkov,D.: Theoret. chim. Acta (Berl.) **8**, 236 (1967).
8. Theoret. chim. Acta (Berl.) **5**, 376 (1966).
9. Bertran,J., Chalvet,O., Daudel,R.: Theoret. chim. Acta (Berl.) **14**, 1 (1969).
10. Linnett,J.W.: Electronic structure of molecules. London: Methuen 1964.
11. McGlynn,S.P., Azumi,T., Kinoshita,M.: Molecular spectroscopy of the triplet state. New York: Prentice-Hall 1969.
12. Constanciel,R.: C. R. Acad. Sci. Paris C **270**, 1227 (1970).
13. Coulson,C.A., Maclagan,R.G.A.R.: Advances chem. Physics **21**, 303 (1971).
14. McWeeny,R.: Rev. mod. Physics **32**, 335 (1960).
15. Löwdin,P.O.: Physic. Rev. **97**, 1474 (1955).
16. Peradejordi,F.: Cahiers de Physique **17**, 393 (1963).
17. Stanton,R.E.: J. chem. Physics **36**, 1298 (1962).
    Diercksen,G., McWeeny,R.: J. chem. Physics **44**, 3554 (1966).
18. Coulson,C.A.: Proc. Royal Soc. (London) A **169**, 413 (1939).
19. Daudel,R.: Théorie quantique de la liaison chimique, p. 142. Presses Universitaires de France 1971.
20. Bessis,G., Chalvet,O., Polydoropoulos,C.: C. R. Acad. Sci. Paris C **264**, 1368 (1967).
21. Coulson,C.A., Longuet-Higgins,H.C.: Proc. Royal Soc. (London) A **191**, 39 (1947).
22. Coleman,A.J.: Rev. mod. Physics **35**, 668 (1963).

Dr. R. Constanciel
Centre de Mécanique Ondulatoire Appliquée
23, rue du Maroc
F-75 Paris, France

Theoret. chim. Acta (Berl.) 26, 257—265 (1972)
© by Springer-Verlag 1972

Analyse conformationnelle théorique du diméthylsulfoxyde $(CH_3)_2SO$

GERMAINE ROBINET, CLAUDE LEIBOVICI et JEAN-FRANÇOIS LABARRE
Laboratoire de Chimie de Coordination associé au C.N.R.S. n° 160,
Université Paul Sabatier, 38, rue des 36 Ponts, 31-Toulouse, France

Reçu le 27 mars 1972

Theoretical Conformational Analysis of Dimethylsulfoxide $(CH_3)_2SO$

The conformational analysis of $(CH_3)_2SO$ is investigated within the framework of the CNDO/2 approximation. The preferred conformation of heavy atoms (C, S, O) is found to be the one (r_{0IV}) which was proposed by Dreizler *et al.* in 1969 on the basis of microwave measurements. The map of isoenergy curves was drawn, describing the variation of energy as a result of mutual rotation of the two methyl groups. This showed that the equilibrium symmetry for the complete molecule, including the hydrogens, was C_s. However, it may be noticed that the two hydrogens which, for the (60, 60) conformation, would have been located into the CSC plane, are actually staggered of 3.64° out of this plane and nearer to the oxygen atom than to the sulphur lone pair. The rotational barrier for one CH_3 group is 3.5 kcal/mole, in agreement with the experimental value (2.8 kcal/mole [7]). A bicentric energy partitioning shows that about 60% of the variation in total energy is reflected by the single sum, ΣE (S...H), of the spatial interaction terms between sulphur and the six hydrogens.

La méthode SCF–LCAO–MO dans l'approximation CNDO/2 est utilisée pour l'étude de l'analyse conformationnelle du diméthylsulfoxyde $(CH_3)_2SO$. On montre ainsi que, parmi les déterminations géométriques de la littérature, celle (r_{0IV}) obtenue par Dreizler et Coll. en 1969 au moyen de la spectroscopie de microondes semble devoir être retenue. La carte de potentiel, décrivant la rotation simultanée des deux groupements méthyle autour des liaisons (S–C), est tracée: elle montre que la molécule $(CH_3)_2SO$ appartient bien au groupe de symétrie C_s, non seulement au niveau des atomes lourds (C, S, O) mais aussi à celui des hydrogènes. On note toutefois que les deux hydrogènes qui, dans la conformation (60, 60), auraient été dans le plan CSC, sont alors décalés tous deux de quelque 3,64° hors de ce plan et du côté de l'atome d'oxygène. La barrière à la rotation d'un CH_3 est trouvée égale à 3,5 kcal/mole (expérimentalement: 2,8 kcal/mole [7]). Un découpage bicentrique de l'energie totale montre enfin que 60% des variations de cette grandeur sont dûs à la seule somme, ΣE (S...H) des interactions dans l'espace entre l'atome de soufre et les six atomes d'hydrogène

Die Konformation von $(CH_3)_2SO$ wird im Rahmen des CNDO/2-Verfahrens analysiert, wobei sich für C-, S- und O-Atome das gleiche Ergebnis wie bei Mikrowellenmessungen (Dreizler, 1969) ergibt. Ferner wird die Energiehyperfläche für Methyl-Rotationen angegeben, mit der Symmetrie C_s am tiefsten Punkt. Allerdings sind die zwei H-Atome, die bei der (60, 60)-Konformation in der CSC-Ebene liegen sollten, um 3,64° aus dieser Ebene herausgedreht und näher an den einsamen Elektronen des Sauerstoffs als an denen des Schwefels. Die Rotationsbarriere einer CH_3-Gruppe beträgt 3,5 kcal/Mol (experimentell 2,8 kcal/Mol [7]). Eine Energieaufspaltung auf Zentrenpaare zeigt, daß etwa 60% der Änderung der Gesamtenergie in der Einfachsumme ΣE (S...H) der räumlichen Wechselwirkungssysteme zwischen den S- und den sechs H-Atomen enthalten ist.

Introduction

La méthode SCF–LCAO–MO dans l'approximation CNDO/2 de Pople et Segal [1] est utilisée d'une manière extensive dans notre groupe de Recherches pour la résolution de l'ensemble des problèmes liés à l'analyse conformationnelle des composés de coordination de basse symétrie ne faisant pas intervenir d'éléments de transition.

Notre but est non seulement de déterminer la confiance que l'on peut attribuer à une telle méthode semi-empirique pour la reproduction par la chimie quantique de résultats expérimentaux mais encore d'une part de déceler les raisons pour lesquelles une molécule donnée adopte telle ou telle conformation et d'autre part de prévoir par le calcul certaines particularités structurales que l'expérience n'est pas à même pour des raisons intrinsèques de mettre en évidence.

C'est dans cet esprit que nous avons tout récemment abordé l'étude de la diméthylsulfone $(CH_3)_2SO_2$ [2]: la chimie quantique nous a entre autres permis d'atteindre la conformation absolue des deux groupements méthyles de cette molécule, donnée qui n'avait pu être fournie par l'expérience.

Les résultats encourageants ainsi obtenus, s'inscrivant d'ailleurs dans la ligne de ceux que nous avons pu proposer dans le cas d'un certain nombre d'autres composés standards de la chimie de coordination [3 5], nous ont incités à aborder l'étude de l'analyse conformationnelle théorique d'une molécule, le diméthylsulfoxyde $(CH_3)_2SO$, qui, si l'on en juge par la littérature récente, pose un certain nombre de problèmes de fond quant à la connaissance même de sa géométrie moléculaire exacte.

Il est en effet pour le moins surprenant de constater qu'un nombre relativement considérable de travaux aient été effectués dans ce domaine par les techniques les plus appropriées (diffraction électronique, spectrographie RX, spectroscopie microondes) sans qu'un accord définitif puisse être dégagé au niveau des résultats relatifs aux angles et aux longueurs de liaison. Il semble donc a priori que la molécule $(CH_3)_2SO$ possède des éléments de symétrie peut être un peu différents de ceux auxquels on pourrait intuitivement penser sur la base de ce que l'on sait des géométries de molécules isologues, la diméthylsulfone par exemple.

Nous verrons à la fin de cet article le bien-fondé de cette remarque préliminaire.

Résultats

Nous nous sommes donc dans un premier temps attachés à voir laquelle des géométries du Tableau 1 conduit à une valeur minimale de l'énergie. Les calculs ont été effectués par analogie avec l'étude de la diméthylsulfone [2] pour les trois conformations, notées (60, 60) (0, 60) et (0, 0), des deux groupements méthyles[1]. Le Tableau 2 rassemble les résultats obtenus et appelle les remarques suivantes:

1 pour chacune des géométries, la conformation la plus stable *des trois retenues* est bien celle notée (60, 60);

2 pour cette conformation, l'énergie la plus basse est atteinte pour les géométries G2, G5 et G6, ces dernières paraissant légèrement privilégiées. C'est toutefois la géométrie G2 qui nous semble devoir être retenue car nous avons

---

[1] La symbolique utilisée ici a été explicitée dans la référence [2]. Précisons toutefois qu'une conformation (θ, φ) quelconque se déduit de celle de référence, (0, 0), en faisant tourner les groupements méthyles respectivement de l'angle θ et de l'angle φ dans le sens trigonométrique, celui-ci étant défini pour un observateur situé sur l'atome de carbone correspondant et regardant vers l'atome de soufre de la molécule.

Tableau 1

Géométrie Paramètres	G1 [6]	G2 (Structure r_{ov} [7])	G3 (Structure r_s [7])	G4 [8]	G5 [9]	G6 [9]	G7 [10]
$r_{\text{S-O}}$ (Å)	1,477	1,483	1,485	1,471	1,531	1,521	1,47
$r_{\text{S-C}}$ (Å)	1,810	1,799	1,799	1,812 1,801	1,775 1,821	1,766 1,827	1,82
$r_{\text{C-H}}$ (Å)	1,095	1,112	1,054 1,097 1,093	—	—	—	1,08
∢ CSC (degrés)	96,38	96,53	96,57	97,86	97,4	98,2	100
∢ SCH (degrés)	107,52	—	108,27 108,17 109,55	—	—	—	–
∢ OSC (degrés)	106,72	106,72	106,65	107,04 107,43	106,7 106,8	106,7 107,5	107

Tableau 2

		G1	G2	G3[a]	G4	G5	G6	G7
Energie totale	(60, 60)	−30174,822	−30179,424	−30171,334	−30172,709	−30180,434	−30180,030	−30157,333
(en kcal/mole)	(0, 60)	−30170,967	−30175,688	−30167,520	−30169,246	−30176,535	−30176,035	−30154,250
	(0, 0)	−30164,723	−30169,750	−30161,641	−30163,950	−30171,336	−30171,102	−30149,997
Moment dipolaire	(60, 60)	3,792	3,912	3,893	3,862	4,248	4,236	3,491
(en Debyes)	(0, 60)	3,838	3,911	3,953	3,882	4,276	4,268	3,555
	(0, 0)	3,815	3,882	3,948	3,884	4,246	4,209	3,588

[a] Pour chacune des trois conformations de G3, la valeur 1,054 Å est attribuée à la liaison (C–H) se trouvant dans le plan CSC, celle égale à 1,097 Å à la liaison (C–H) située *au-dessus* du plan CSC et celle égale à 1,093 Å à la liaison (C–H) située *au-dessous* du plan CSC, ceci pour chacun des deux groupements méthyle. On remarque ainsi que, pour G3, la notation (θ, φ) n'a pas le sens habituel mais celui, plus particulier, que nous venons de décrire.

adopté *arbitrairement* dans G5 et G6 une longueur des liaisons C–H uniformément égale à 1,09 Å.

Quoiqu'il en soit, la structure G2 de Dreizler et Coll. [7] s'avère dans ces conditions celle à retenir pour la suite des calculs. On peut noter à cet égard combien l'amélioration des techniques et de la précision avec laquelle sont connus les paramètres structuraux influent considérablement sur la valeur théorique de l'énergie totale d'une molécule.

3 il est intéressant de noter que ce que nous venons de dire en termes d'énergie peut être transcrit au niveau des moments dipolaires calculés et de leur comparaison avec l'expérience (la valeur $\mu_{exp} = 3{,}96 \pm 0{,}04$ D ayant été déterminée par effet Stark [6]), bien que (à l'exception peut-être de G7) l'accord puisse être en tous cas considéré comme satisfaisant.

En résumé de cette partie, nous pouvons conclure d'une manière tout à fait analogue à ce que nous avons dit à propos de la diméthylsulfone [2]: la méthode CNDO/2 permet de discerner dans un ensemble complexe de données expérimentales la géométrie à retenir pour un éventuel calcul ab initio et permet même de lever certaines difficultés auxquelles se heurtent les spécialistes des microondes lorsque les substitutions isotopiques ne permettent pas à ceux-ci d'obtenir un nombre d'équations suffisant pour déterminer, sans hypothèse a priori, le jeu de leurs inconnues.

Mais, nous l'avons vu [2], la méthode CNDO/2 permet encore d'aller plus loin en répondant d'une manière claire à la question suivante: quelle est la conformation privilégiée réelle $(\theta_{opt}, \psi_{opt})$ de la molécule?

Partant alors de la géométrie G2, nous avons procédé à une analyse tridimensionnelle de la conformation des deux groupements méthyle: pour un θ donné du méthyl 1, nous avons fait subir à l'autre méthyle (noté méthyle 2) une rotation de 120° (ψ variable). Les résultats concernant l'énergie totale de la molécule ont été reproduits dans le Tableau 3 et la Fig. 1 rassemble les courbes d'isoénergies correspondantes.

Ils ressort de ces résultats que la conformation la plus stable (déterminée à partir d'une interpolation cubique portant sur les 25 points les plus bas de la surface de potentiel) correspond aux angles $\theta_{opt} = 56{,}36°$ et $\psi_{opt} = 63{,}64°$. Si l'on se rappelle les conventions qui sont les nôtres, on voit que la conformation stable de la molécule $(CH_3)_2SO$ est bien – en accord d'ailleurs avec les résultats obtenus par Thomas et Coll. au moyen des rayons X [9] – *de symétrie* C_s *mais que les deux hydrogènes qui, dans la conformation (60, 60), auraient été dans le plan* CSC, *sont alors décalés tous deux de quelque 3,64° hors de ce plan et du côté de l'atome d'oxygène.*

Ce résultat remarquable peut se comprendre par la différence d'encombrement stérique qui existe entre une liaison (SO) et une paire électronique libre portée par un atome de soufre tricoordonné: cette dernière étant – même en se plaçant uniquement sur le plan qualitatif – plus volumineuse que la surface limite de probabilité de l'orbitale de la liaison (SO), on conçoit que la molécule tienne compte de cette réalité et allège sa conformation privilégiée en déplaçant les deux hydrogènes situés en interaction forte avec ce système d'orbitales vers la région la moins encombrée de l'espace.

Tableau 3. Energie totale de la molécule à −30160 kcal/mole près

θ φ	0	10	20	30	40	50	55	60	65	70	80	90	100	110	120
0	− 9,750	−10,415	−11.720	−13,279	−14,666	−15,536		−15.688		−15,088	−13,877	−12,347	−10.895	− 9,931	− 9,750
10	− 9,931	−10,730	−12,094	−13,630	−14,932	−15,682		−15,704		−14,991	−13.706	−12,164	−10,777	− 9,947	− 9,931
20	−10,895	−11.752	−13,085	−14,522	−15,691	−16.307		−16,221		−15,446	−14,162	−12,694	−11,443	−10.777	−10,895
30	−12,347	−13.178	−14,409	−15.705	−16.735	−17.242		−17.099		−16,332	−15.122	−13.786	−12.694	−12,164	−12,347
40	−13,877	−14.616	−15,711	−16.867	−17.786	−18.237		−18.100		−17.402	−16.313	−15.122	−14.162	−13,706	−13,877
50	−15.088	−15.702	−16,661	−17,708	−18,570	−19.025	−19,057	−18.951	−18,714	−18,360	−17.402	−16,332	−15,446	−14,991	−15,088
55						−19,272	−19,325	−19,245	−19,037	−18,714					
60	−15,688	−16,172	−17.023	−18,013	−18.880	−19.397	−19,475	−19,424	−19,245	−18,951	−18.100	−17,099	−16,221	−15,704	−15,688
65						−19.390	−19.497	−19,475	−19,325	−19,057					
70	−15.536	−15.910	−16.703	−17.700	−18.633	−19.254	−19,390	−19.397	−19,272	−19,025	−18,237	−17,242	−16,307	−15.682	−15,536
80	−14,666	−14,971	−15.768	−16.838	−17.888	−18.633		−18.880		−18,570	−17,786	−16,735	−15,690	−14,932	−14,666
90	−13,279	−13,576	−14.447	−15,647	−16.838	−17,700		−18,013		−17,708	−16.867	−15,705	−14,522	−13,630	−13,279
100	−11.720	−12,085	−13,092	−14,447	−15,768	−16,703		−17,023		−16,661	−15.711	−14,409	−13,085	−12,094	−11,720
110	−10,415	−10,915	−12,085	−13,576	−14.971	−15,910		−16,172		−15,702	−14,616	−13,178	−11,752	−10,730	−10,415
120	− 9,750	−10.415	−11,720	−13.279	−14,666	−15.536		−15,688		−15,088	−13,877	−12,347	−10,895	− 9,931	− 9,750

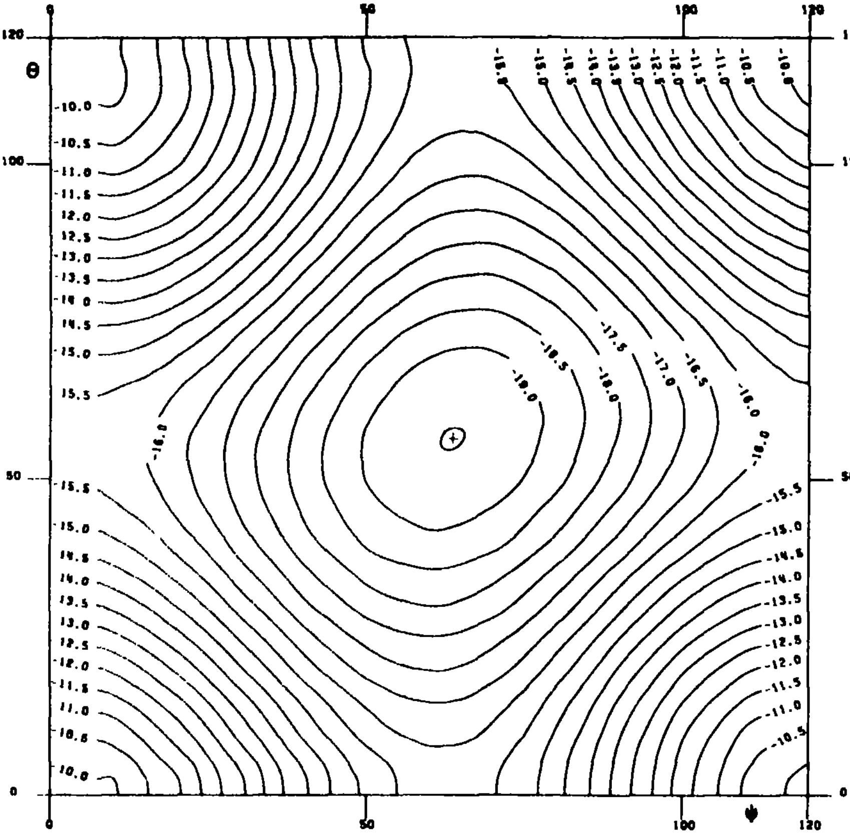

Fig. 1

Par ailleurs, la conformation privilégiée théorique très particulière ainsi obtenue explique d'une part les difficultés rencontrées – et d'ailleurs soulignées par Dreizler et Coll. [7] – lors du dépouillement des spectres expérimentaux et d'autre part le fait que la spectroscopie de microondes conduise [7] avant raffinement à trois longueurs différentes pour les liaisons C–H, deux d'entre elles étant très proches l'une de l'autre mais non identiques.

L'examen de la Fig. 1 permet en outre d'assigner à la barrière à la rotation d'un groupement méthyle une valeur sensiblement égale à 3,5 kcal/mole qui s'avère tout à fait comparable à la valeur expérimentale proposée par Dreizler et Coll. (2,8 kcal/mole) [7]. L'accord théorie-expérience est cependant ici un peu moins satisfaisant que celui auquel nous étions parvenus dans la cas de la diméthylsulfone [2].

Quoiqu'il en soit, les Tableaux 4 et 5 rassemblent les charges électroniques et les populations de Wiberg [11] relatives à la conformation (θ_{opt}, φ_{opt}).

Ceci étant, nous nous sommes – comme dans le cas de la diméthyl sulfone – posé la question de savoir quelle est l'origine de la barrière à la rotation que nous venons d'évoquer.

Tableau 4. Distribution des charges électroniques pour la conformation (θ_{opt}, φ_{opt})

S	$3s$	1,677	O	$2s$	1,805
	$3p_x$	0,898		$2p_x$	1,577
	$3p_y$	0,913		$2p_y$	1,570
	$3p_z$	1,052		$2p_z$	1,329
	$3d_{z^2}$	0,306		Total	6,281
	$3d_{xz}$	0,246			
	$3d_{yz}$	0,248			
	$3d_{x^2-y^2}$	0,312			
	$3d_{xy}$	0,136			
	Total	5,788			
	Méthyle 1			Méthyle 2	
C	$2s$	1,079	C	$2s$	1,079
	$2p_x$	1,050		$2p_x$	0,984
	$2p_y$	0,984		$2p_y$	1,050
	$2p_z$	0,983		$2p_z$	0,983
	Total	4,096		Total	4,096
H (au dessus du plan CSC)	$1s$	0,949	H (au dessus du plan CSC)	$1s$	0,949
H (liaison C H à 3,64° du plan CSC)	$1s$	0,955	H (liaison C H à 3,64° du plan CSC)	$1s$	0,955
H (au dessous du plan CSC)	$1s$	0,966	H (au dessous du plan CSC)	$1s$	0,966

Tableau 5. Population de liaison selon Wiberg pour la conformation (θ_{opt}, φ_{opt})

Liaison	Population de liaison
S–O	2,204
S–C	1,107
C H (à 3,64° au-dessus du plan CSC)	0,952
C H (au-dessus du plan CSC)	0,951
C H (au-dessous du plan CSC)	0,956

Ce problème a été résolu de la manière désormais classique [2–5] en procédant à un découpage bicentrique de l'énergie totale de la molécule selon l'expression:

$$E = \sum_{A} E_A + \sum_{A<B} E_{AB}$$

que l'on peut plus grossièrement écrire sous la forme

$$E = E_b + E_{nb}$$

avec

$$E_b = \sum_{A} E_A + \sum_{A<B} E_{AB} \quad \text{(A et B chimiquement liés)}$$

et

$$E_{nb} = \sum_{A<B} E_{AB} \quad \text{(A et B non chimiquement liés)}.$$

L'analyse au premier ordre de la variation des termes E_b et E_{nb} en fonction de la conformation montre une fois de plus [2–5] que c'est au terme E_{nb} que la courbe d'énergie totale doit sa forme (Fig. 2).

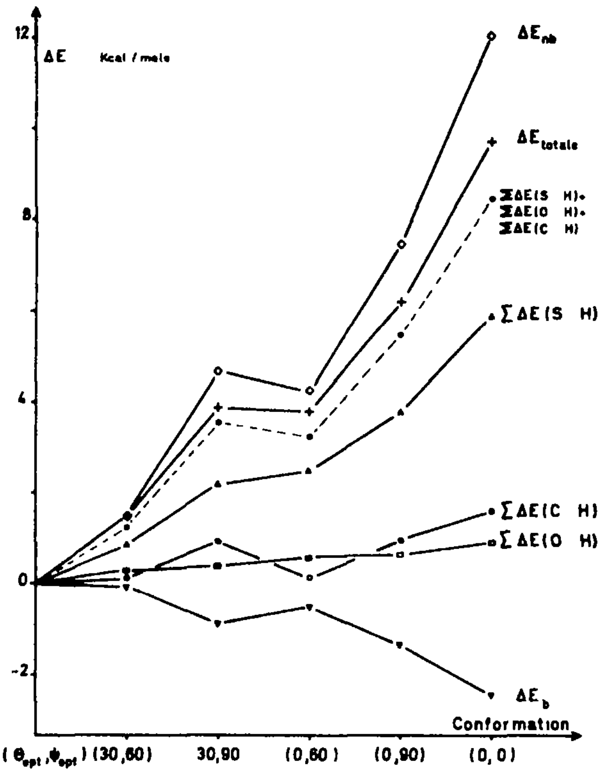

Fig. 2

Une analyse détaillée de l'évolution de chacune des composantes du terme E_{nb} montre ensuite que, comme dans le cas de la diméthylsulfone, c'est le terme ΣE(S...H) traduisant les interactions entre l'atome de soufre et les six hydrogènes méthyliques - qui permet de rendre compte pour environ 60% des variations de l'énergie totale de la molécule. Cette valeur numérique peut être comparée à celle, 70%, que nous avons obtenue pour ce même terme dans le cas de $(CH_3)_2SO_2$. Une trentaine des 40% restants peut être expliquée par la variation de la somme (ΣE(O...H) + ΣE(C...H)); on voit apparaître ici une différence importante avec ce que nous avons pu mettre en évidence quant à l'origine de la barrière à la rotation dans $(CH_3)_2SO_2$: dans ce cas en effet, si ΣE(O...H) est bien l'un des termes secondaires importants, c'est le terme ΣE(H...H) (interaction entre les hydrogènes d'un méthyle et ceux de l'autre) et non ΣE(C...H) qui l'accompagne dans le cas de la diméthylsulfone.

Quoiqu'il en soit, l'analyse conformationnelle théorique du diméthylsulfoxyde fait apparaître la prédominance du terme ΣE(S...H) qui rend compte de l'interaction *dans l'espace* de l'atome de soufre et de six hydrogènes méthyliques: ce résultat constitue un exemple de plus d'un phénomène apparemment très général que nous avons pu mettre en évidence par la chimie quantique dans un nombre relativement important de composés renfermant les motifs

$CH_3 \cdot M \cdot CH_3$ [12] et $M \cdot BH_3$ [3].

On constate en effet d'une manière systématique que, lorsque M est un élément de la deuxième ligne longue de la classification périodique, $\Sigma E(\mathrm{M}\ldots\mathrm{H})$ s'avère en tous cas le terme sur l'importance duquel reposent les conformations privilégiées de la molécule, son ordre de grandeur en valeur relative étant supérieur ou égal à 70% et pouvant même atteindre 100% ($(CH_3)_2SiH_2$) [12].

En conclusion, l'application de la méthode SCF–LCAO–MO dans l'approximation CNDO/2 à l'étude de l'analyse conformationnelle du diméthylsulfoxyde rend compte quantitativement de l'expérience et permet même de proposer une conformation absolue pour les deux groupements méthyles de la molécule, conformation qui n'avait pu être précisée par voie expérimentale. Cette étude quantique montre en outre combien deux molécules apparemment aussi voisines que $(CH_3)_2SO_2$ et $(CH_3)_2SO$ peuvent se distinguer l'une de l'autre quant à leurs paramètres géométriques et électroniques.

Bibliographie

1. Pople, J. A., Segal, G. A.: J. chem. Physics **44**, 3289 (1966).
2. Robinet, G., Crasnier, F., Labarre, J.-F., Leibovici, C.: Theoret. chim. Acta (Berl.) **25**, 259 (1972).
3. Labarre, J.-F., Leibovici, C.: Int. J. quant. Chemistry sous presse (1972) ($F_3P \cdot BH_3$ et $F_2HP \cdot BH_3$).
4. J. Chim. physique **68**, 1618 (1971) (F_3NO).
5. - J. Chim. physique **69**, 404 (1972) ($H_3B \cdot CO$).
6. Dreizler, H., Dendl, G.: Z. Naturforsch. **19a**, 512 (1964).
7. Feder, W., Dreizler, H., Rudolph, H. D., Typke, V.: Z. Naturforsch. **24a**, 266 (1969).
8. Viswamitra, M. A., Kannan, K. K.: Nature **209**, 1016 (1966).
9. Thomas, R., Shoemaker, C. B., Eriks, K.: Acta crystallogr. **21**, 12 (1966).
10. Bastiansen, O., Viervoll, H.: Acta chem. scand. **2**, 702 (1948).
11. Wiberg, K.: Tetrahedron **24**, 1083 (1968).
12. Robinet, G., Leibovici, C., Labarre, J.-F.: Chem. Physics Letters, sous presse (1972).

Dr. J.-F. Labarre
Laboratoire de Chimie de Coordination
associé au C N.R.S. n 160
Université Paul Sabatier
38, rue des 36 Ponts
F-31 Toulouse, France

Theoret. chim. Acta (Berl.) 26, 267—271 (1972)
© by Springer-Verlag 1972

Relationes

Perturbation Theory for Excited States of Molecules. III

B. L. BURROWS

Polytechnic, Stafford, Staffordshire, England

Received November 26, 1971

The configuration interaction perturbation theory and the single configuration perturbation theory developed in Paper I is applied to the problem of chemical reactivity for conjugated hydrocarbon molecules. Various related hetromolecules are also considered. It is found that the pattern of reactivity for excited states is much the same as for the ground state.

1. Introduction

When a reagent is brought up to a reactive position in a conjugated system the energy of the molecule changes. This change in energy provides an index of chemical reactivity. A full discussion of chemical reactivity with regard to Huckel molecular orbital theory has been given by Coulson and Longuet-Higgins [1]. They point out that the change in energy due to the approach of the reagent may arise from three causes:

(1) polarization of the non bonding and sigma electrons;
(2) steric effects;
(3) changes in the energy of the mobile π-electrons.

In this paper a comparison is made of the changes in energy due to the approach of a reagent for the ground state and excited states of a number of conjugated molecules. To treat the excited states the CIPT and SCPT methods, which were developed in Paper I, are used. The perturbed orbitals are obtained by coupled Hartree-Fock perturbation theory and may be expressed in terms of a complete set of functions (v_i). In all cases the calculations will be restricted to π-electron type calculations using the Pariser, Parr, Pople approximations, [2], so that the complete set is truncated and the matrix elements with respect to the truncated set $\{\omega_r\}$ are:

$$\langle \omega_r | h(1) | \omega_s \rangle = -\sum_{t \neq s}^{n} \gamma_{rt} \delta_{rs} + \beta_{rs}$$

$$\left\langle \omega_r \omega_s \left| \frac{1}{r_{12}} \right| \omega_t \omega_u \right\rangle = \gamma_{rs} \delta_{rt} \delta_{su}$$

$\beta_{rs} = -2.39$ eV if r and s are neighbouring atoms else 0

where the Hamiltonian for the conjugated molecule is of the form:

$$\mathscr{H} = \sum_{i=1}^{n} h(i) + \sum_{i<j}^{n} \frac{1}{r_{ij}}$$

and there is one function ω_r corresponding to each carbon atom of the conjugated system. These approximations lead to certain simplifications in the possible causes of the change of energy. Causes (1) and (2) listed above are essentially due to changes in the σ core or $\sigma - \pi$ interactions and consequently the change in energy due to these causes will be neglected in a π-electron calculation. Thus the assumptions made in this paper will be essentially the same assumptions as those made by Coulson and Longuet-Higgins who conclude that cause (3) is the principle factor in the reactivation energy.

2. Indices of Reactivity

The index of reactivity commonly used [1, 3] is the point charge index. This theory assumes that the change in total π-electron energy when a reagent approaches an atom of a conjugated system arises mainly from the induced charge at that atom. So that the change in energy when a test charge is brought close to the atom is taken to be the index of chemical reactivity at that atom. We may consider the change in π-electron energy, δE, when a test charge $\delta\alpha_r$ is brought close to an atom r by expanding in a Taylor series:

$$\delta E = \frac{\partial E}{\partial \alpha_r} \delta\alpha_r + \frac{1}{2} \frac{\partial^2 E}{\partial \alpha_r^2} \delta\alpha_r^2 + \cdots . \tag{1}$$

The quantities $\frac{\partial E}{\partial \alpha_r}$ and $\frac{1}{2} \frac{\partial^2 E}{\partial \alpha_r^2}$ may be obtained as first and second order energies of a perturbation using CIPT or SCPT where the perturbation matrix z_{ij} is given by:

$$z_{ij} = \langle \omega_i | z(1) | \omega_j \rangle = \delta_{ir} \delta_{jr} . \tag{2}$$

This type of perturbation will be refered to as a point perturbation. With this perturbation $\frac{\partial E}{\partial \alpha_r}$ is an approximation to the charge on the r^{th} atom of the conjugated system [3] and will be denoted by q_r. The quantities $\frac{\partial^2 E}{\partial \alpha_r^2}$ are called the atom-atom polarizabilities and will be denoted by π_{rr}.

Basically there are two types of reagent, cationoid and anionoid, reagents. One difference is that the former bear a net positive charge whereas the latter bear a net negative charge. Thus one would expect the approach of a cationoid reagent to lead to a decrease in the induced charge $\delta\alpha_r$ and the approach of a anionoid reagent to lead to a increase in $\delta\alpha_r$. One would therefore expect examining the first term of the Taylor series (1) that the cationoid reaction would be favoured by high values of q_r and anionoid reactions by low values of q_r.

The molecules considered in this paper are alternant hydrocarbons and it is well known that the charge densities at each atom, within the Pariser, Parr, Pople approximations, are unity [4]. The charge densities predicted by Hartree-Fock theory and by any combination of determinants formed from Hartree-Fock orbitals are also unity; consequently the simple picture of reactivity where the magnitude of the charge is examined is unsatisfactory. Thus it is necessary to examine π_{rr} as an index of reactivity to distinguish between the atoms of the conjugated system. In these cases for negative π_{rr} the larger the absolute value of π_{rr} the more reactive the site.

Table 1

Molecule	Atom	E (SCPT)		E (CIPT)		E (GS)
		Singlet	Triplet	Singlet	Triplet	
Diphenyl	1	−0.0589	−0.0029	−0.0609	−0.0444	−0.0554
	6	−0.1034	−0.0672	−0.1327	−0.0531	−0.0617
	5	−0.0670	−0.0543	−0.0783	−0.0521	−0.0593
	4	−0.0634	−0.0485	−0.0664	−0.0488	−0.0602
Napthalene	1	−0.0536	−0.0526	−0.0756	−0.0510	−0.0546
	2	−0.0857	−0.0446	−0.0670	−0.0468	−0.0622
	3	−0.0891	−0.0616	−0.0753	−0.0545	−0.0595
Anthracene	1	−0.0591	−0.0547	−0.0638	−0.0535	−0.0544
	2	−0.0818	−0.0515	−0.0830	−0.0579	−0.0625
	3	−0.0712	−0.0609	−0.0860	−0.0585	−0.0596
	10	−0.0763	−0.0470	−0.0765	−0.0429	−0.0676
Benzene						
$d = 2.8$ Å	1	−0.00027	−0.00024	−0.00031	−0.00022	−0.00030
$d = 1.4$ Å	1	−0.00427	−0.00408	−0.00466	−0.00369	−0.00453
$d = 0$ (point perturbation)	1	−0.05636	−0.05402	−0.05516	−0.05169	−0.05931

In Table 1 we give the second order energies E_r^2 $(= \frac{1}{2}\pi_{rr})$ for the first singlet and first triplet states of benzene, napthalene, anthracene, and diphenyl. These are compared with E_r^2 for the ground state of these molecules. In most cases the values of π_{rr} for the various states are similar. In almost all cases SCPT and CIPT predict the same measure reactivity however there is one ambiguous case namely atom 1 of the first excited triplet of diphenyl. This may be due to the assumption made that diphenyl is planar which is known to be a poor approximation.

McWeeny, [3], has suggested a refinement or the usual index used for chemical reactivity. A reagent pictured as a test charge is not realistic and in principle the reagent causes a perturbation of the molecule that is in no sense confined to one atom. McWeeny suggests that one should take the second order energy of a perturbation by a point charge located at a distance "d" directly above a carbon atom. In Table 1 second order energies for such perturbations of benzene are listed where "d" is taken to one or two bond lenths above a carbon atom. It is clear that qualitatively the pattern of reactivity remains the same for both point perturbation and this second measure. However point perturbation predicts that the reactivity of the ground state is greater than the first singlet excited state when CIPT is used whereas the second measure predicts the reverse.

3. Reactivity for Heteromolecules

We may also define the quantities $\pi_{r,s}$ where

$$\pi_{r,s} = \frac{\partial q_r}{\partial \alpha_s} = \frac{\partial^2 E}{\partial \alpha_s \partial \alpha_r} = \frac{\partial q_s}{\partial \alpha_r} = \pi_{s,r}. \tag{3}$$

These may be used to discuss the reactivity of heteromolecules. Consider the change in charge at atom s due to a substituent at atom r. We may express the relationship as follows:

$$\delta q_s = \pi_{s,r}\, \delta \alpha_r. \tag{4}$$

Consequently if we know $\pi_{s,r}$ we may determine the charge density at any atom of a monosubstituted molecule. The substituent at atom r will affect the charges at the various atoms in different ways so that we may revert to the charge at an atom as the index of reactivity. The charge at any atom s of a substituted molecule is given by

$$q_s \text{ (Substituted)} = 1 + \delta q_s. \tag{5}$$

The inductive parameter of the substitution is $\delta\alpha_r$ and its value will depend on the type of substitutions.

If we consider one electron perturbations where the perturbation matrix is of the form

$$z_{ij} = \delta_{ir}\delta_{jr} + \delta_{is}\delta_{js} \tag{6}$$

for some r, s $r \neq s$, the first and second order perturbation energies will be estimates of $\delta E'$ and δE^2 where

$$\delta E^1 = \frac{\partial E}{\partial \alpha_r}\delta\alpha_r + \frac{\partial E}{\partial \alpha_s}\delta\alpha_s \tag{7}$$

Table 2

Substituent	Triplet or Singlet	Atom	q (substituted) CIPT
Nitrogen (parameter −2.17 eV)	S	1	1.24
	S	2	0.98
	S	3	0.90
	S	4	0.98
	T	1	1.22
	T	2	0.91
	T	3	0.95
	T	4	0.08
Methyl (parameter 0.52 eV)	S	1	0.94
	S	2	1.02
	S	3	1.01
	S	4	1.01
	T	1	0.95
	T	2	1.02
	T	3	1.01
	T	4	0.98

and

$$\delta E^2 = \tfrac{1}{2}\left(\frac{\partial^2 E}{\partial \alpha_r^2}\,\delta\alpha_r^2 + \frac{2\partial^2 E}{\partial \alpha_r\,\partial \alpha_s}\,\delta\alpha_s\,\delta\alpha_r + \frac{\partial^2 E}{\partial \alpha_s}\,\delta\alpha_s^2\right). \tag{8}$$

Thus a knowledge of $\pi_{r,r}$ for all atoms of the system will enable $\pi_{r,s}$ to be calculated perturbatively. In Table 2 q_r (substituted) is listed for a number of monosubstituted benzenes (each substituted at atom 1). The inductive parameters were taken from Table 11 in the review article by Amos and Hall [6].

4. Conclusion

We must await experimental evidence for an evaluation of the usefulness of this procedures described in this paper. It may turn out that the earlier assumptions made are invalid. In particular it may be argued that the changes in geometry of a molecule in its excited state are important so that changes in energy due to (2) cannot be neglected. It is well known that the sigma core is not the same for the ground and excited states of even the most simple conjugated systems but it is unlikely that this will affect the relatively crude methods of finding an index of reactivity outlined here.

I wish to express my appreciation to Dr. A. T. Amos for constant encouragement during the preparation of this paper and to the S.R.C. for the provision of a maintenance grant.

References

1. Coulson, C. A., Longuet-Higgins, H. C.: Proc. Roy. Soc. (London) A **192**, 16 (1947).
2. Pariser, R., Parr, R. G.: J. chem. Physics **20**, 1499 (1952).
3. McWeeny, R., Dierckson, C.: J. chem. Physics **44**, 3554 (1960).
4. McLachlan, A. D.: Molecular Physics **2**, 271 (1959).
5. Amos, A. T., Burrows, B. L.: Theoret. chim. Acta (Berl.) **22**, 283 (1971) (Paper I).
6. Amos, A. T., Hall, G. G.: Phys. Chem. **3**, chap. 8.

Dr. B. L. Burrows
North Staffordshire Polytechnic
Stafford, Staffordshire, England

Theoret. chim. Acta (Berl.) 26, 273 –278 (1972)
© by Springer-Verlag 1972

Perturbation Theory for Excited States. IV

B. L. Burrows
Polytechnic, Stafford, Staffordshire, England

Received November 26, 1971

Two of the perturbation methods developed in Paper I (CIPT and SCPT) are extended for use with uncoupled Hartree-Fock perturbation theory. Corrections to the uncoupled results are discussed and it is found that it is possible to correct using functions which when applied to ground state calculations are equivalent to the geometric approximation. It is also shown that CIPT and SCPT can be applied to ground state calculations and that when coupled perturbed orbitals are used CIPT and SCPT are equivalent to the usual coupled perturbation theory.

Introduction

Uncoupled Hartree-Fock perturbation theory has been used with some sucess in ground state molecular calculations. For the ground state it is possible to correct the uncoupled function by double perturbation theory [1–4] so that the results obtained are qualitively equivalent to coupled Hartree-Fock perturbation theory. In earlier papers in this series [5–7] coupled Hartree-Fock perturbation theory was applied to excited states of molecules. In this paper uncoupled theory is applied in a similar way. The perturbations used are restricted to perturbations by one electron operators and the methods are illustrated, as in Paper I, by a simple π-electron type calculation on *trans*-butadiene.

In Section 3 of this paper Tuan's interpretation of the geometric approximation is discussed and it is seen how this may be used as a correction to uncoupled perturbation theory applied to excited states.

The perturbation method described (that is CIPT of Paper I) can be used in ground state calculations. The relationship between the usual uncoupled Hartree-Fock perturbation theory and CIPT is discussed in Section 4. As in Paper I by CIPT we mean all possible configurations of correct spin symmetry made up from the ground state and single excitations of the ground state Hartree-Fock function. In the coupled theory presented in Paper I the ground state coupled single determinant had zero contribution with the first singlet excited state. However, as we shall see in Section 2, when we use uncoupled theory this is no longer true.

1. Uncoupled Perturbation Theory

As in coupled theory the starting point for uncoupled theory is the Hartree-Fock single determinant for $2n$ electrons

$$\psi_0 = |u_1^0(1)\,\alpha(1)\,u_1^0(2)\,\beta(2)\ldots u_n^0(2n)\,\beta(2n)|\,, \tag{1}$$

where the u_i^0 satisfy the Hartree-Fock equations

$$F^0 u_i^0 = \varepsilon_i^0 u_i^0\,, \tag{2}$$

where

$$F^0 = h + \sum_{i\,\mathrm{occ}} (2[-i^0|-i^0] - [-i^0|i^0-]) \tag{3}$$

in the notation of Ref. [4]. If we now perturb the system by a sum of one electron operators $\lambda \sum_i z(i)$ and neglect the change in the self consistent terms in F^0 we obtain the perturbation equations:

$$F^0 u_i^k + z u_i^{k-1} = \sum_{t=0}^{k} \varepsilon_i^t u_i^{k-t} \tag{4}$$

with the normalisation conditions:

$$\sum_{t=0}^{k} \langle u_i^{*t} | u_j^{k-t} \rangle = \delta_{k0} \delta_{ij} . \tag{5}$$

From these we obtain the expressions:

$$u_i^1 = \sum_{j \neq i} \frac{\langle u_j^{*0} | z | u_i^0 \rangle}{(\varepsilon_i^0 - \varepsilon_j^0)} u_j^0 , \tag{6}$$

$$u_i^2 = \sum_{j \neq i} \frac{\langle u_j^{*0} | z - \varepsilon_i^1 | u_i^1 \rangle}{(\varepsilon_i^0 - \varepsilon_j^0)} u_j^0 - \tfrac{1}{2} \langle u_i^{*1} | u_i^1 \rangle u_i^0 . \tag{7}$$

2. Configuration Interaction Wavefunctions for Excited States

As in Paper I we take our zero order functions for singlet and triplet excited states to be

$$\psi^{0S} = \sum_I c_I^0 \, S(q_i p_i) \psi_0 , \tag{8}$$

$$\psi^{0T} = \sum_I d_I^0 \, T(q_i p_i) \psi_0 , \tag{9}$$

where c_I and d_I are found by diagonalising the matrix elements of the total Hamiltonian between singlet and triplet states denoted by H^{0S} and H^{0T} respectively. We will now make the convention that expressions without superscripts (except for T, S) are quantities obtained through infinite order. For example the quantities H^S and u_i are defined as follows

$$H^S = \sum_{i=0}^{\infty} \lambda^i H^{iS} , \tag{10}$$

$$u_i = \sum_{k=0}^{\infty} \lambda^k u_i^k . \tag{11}$$

With this convention F is now the generalisation of F^0 for the perturbed system. The matrix elements are more complicated in uncoupled theory as the uncoupled infinite order orbitals u_i are not optimised to all orders. In fact we have

$$H_{IJ}^S = X + 2[p_i q_j | q_i p_j] - [p_i q_j | p_j q_i] , \tag{12}$$

$$H_{IJ}^T = X - [p_i q_j | p_j q_i] , \tag{13}$$

where

$$X = \delta_{p_i p_j}\delta_{q_i q_j}E + \delta_{p_i p_j}\langle q_i|F|q_j\rangle - \delta_{q_i q_j}\langle p_i|F|p_j\rangle \tag{14}$$

and E is the single determinant ground state energy for the perturbed system. The theory for the triplet now follows Paper I exactly where we solve the secular equation

$$\boldsymbol{H}\boldsymbol{c} = E\boldsymbol{c} \tag{15}$$

perturbatively. The single configuration function discussed in Papers I and II may be deduced in exactly the same way for both the singlet and the triplet. However, for full CIPT in the singlet case the functions $S(q_i p_i)\psi$ have non zero interaction with ψ with respect to the total hamiltonian for the perturbed system $\mathscr{H} + \lambda \sum_i z(i)$. That is to say when we use uncoupled functions Brillouin's theorem does not hold for the perturbed system. We may, however, take this into account in our perturbation equations by including the ground state determinant in our configurations. Thus

$$\psi^S = \sum_I^N c_I\, S(q_i p_i)\psi + c_0\psi, \tag{16}$$

where $c_0^0 = 0$ and the matrix elements H_{0I}^S are given by

$$H_{0I}^S = \sqrt{2}\langle p_i|F|q_i\rangle. \tag{17}$$

Thus expressions for E^1 and E^2 are given by

$$E^1 = \sum_{I,J=0}^N c_I^0 H_{IJ}^{1S} c_J^0 = \sum_{I,J=1}^N c_I^0 H_{IJ}^{1S} c_J^0 \tag{18}$$

and

$$\begin{aligned} E^2 &= \sum_{I,J=0}^N c_I^0 (H_{IJ}^{1S} c_J^1 + H_{IJ}^{2S} c_J^0) \\ &= \sum_{I,J=1}^N c_I^0 (H_{IJ}^{1S} c_J^1 + H_{IJ}^{2S} c_J^0) + \sum_{I=1}^N H_{I0}^{1S} c_I^0 c_0^1 . \end{aligned} \tag{19}$$

3. Corrections to the Uncoupled Wavefunctions

The essential feature of the uncoupled approximation is the neglect of changes in the self consistent potential. Suppose we try to allow for the changes by a sum of one electron operators $\omega(i)$ where

$$\omega(i) = k z(i) \tag{20}$$

and the constant k is chosen in some way so that $(k-1)\sum_i z(i)$ approximates to the change in self consistent terms $F^1 - \sum_i z(i)$. With this definition of $\omega(i)$ the first two perturbation equations of (4) become

$$F^0 \hat{u}_i^1 + k z u_i^0 = \varepsilon_i^0 \hat{u}_i^1 + \hat{\varepsilon}_i^1 u_i^0, \tag{21}$$

$$F^0 \hat{u}_i^2 + k z \hat{u}_i^1 = \varepsilon_i^0 \hat{u}_i^2 + \hat{\varepsilon}_i^1 \hat{u}_i^1 + \hat{\varepsilon}_i^2 u_i^0 \tag{22}$$

and the normalisation conditions are the same as defined in Eq. (5) with $\hat{u}_i^k$ replacing u_i^k. It is easy to see from (21) and (22) that the following identities hold:

$$\hat{u}_i^1 = k u_i^1 , \tag{23}$$

$$\hat{u}_i^2 = k^2 u_i^2 , \tag{24}$$

$$\hat{\varepsilon}_i^1 = k^2 \varepsilon_i^1 , \tag{25}$$

$$\hat{\varepsilon}_i^2 = k \varepsilon_i^2 . \tag{26}$$

It is well known that the first order coupled orbitals u_i^c and the second order coupled energy E_c^2 may be obtained by minimising the functional

$$\begin{aligned}\hat{E}_c^2 = 2 \sum_{i=1}^{n} (\langle \hat{u}_i^1 | F^0 - \varepsilon_i^0 | \hat{u}_i^1 \rangle + 2\langle u_i^1 | z - \varepsilon_i^1 | u_i^0 \rangle \\ + \sum_{j=1}^{n} (4[\hat{u}_i^1 \hat{u}_j^1 | u_i^0 u_j^0] - [\hat{u}_i^1 \hat{u}_j^1 | u_j^0 u_i^0] - [\hat{u}_i^1 u_j^0 | \hat{u}_j^1 u_i^0]))\end{aligned} \tag{27}$$

with respect to variations in $\hat{u}_i$. Tuan [8] has considered the case when $\hat{u}_i$ are of special form $k u_i^1$ where u_i^1 are the uncoupled functions. With this restriction we have that

$$\hat{E}_c^2 = k^2 (E^{1,2} - E^{0,2}) + 2k E^{0,2} , \tag{28}$$

where

$$E^{0,2} = 2 \sum_{i=1}^{n} \langle u_i^1 | z | u_i^0 \rangle \tag{29}$$

and

$$E^{1,2} = \sum_{i,j}^{n} (8[u_i^1 u_j^1 | u_i^0 u_j^0] - 2[u_i^1 u_j^1 | u_j^0 u_i^0] - 2[u_i^1 u_j^0 | u_j^1 u_i^0]) . \tag{30}$$

Thus the best $\hat{u}_i$ in the restricted form are obtained by choosing k to minimise (28). Following Tuan we see that this choice of k is

$$k = - E^{0,2} / (E^{1,2} - E^{0,2}) \tag{31}$$

and leads to

$$\min(\hat{E}_c^2) = (E^{0,2})^2 / (E^{0,2} - E^{1,2}) \tag{32}$$

which is identical with the usual geometric approximation [8–10] used as a correction to the uncoupled wavefunctions. Thus it would seem that a reasonable choice of k in Eqs. (21) and (22) would be as defined in (31).

4. Relationship with the Ground State

We may apply CIPT to ground state calculations. To do this we consider the ground state wavefunction for the perturbed system to be of the form

$$\psi^G = \sum_{I}^{N} c_I \, S(q_i p_i) \, \psi + c_0 \psi . \tag{33}$$

In the case of the ground state $\psi_0^G = \psi_0$. This means that $c_0^0 = 1$ and $c_I^0 = 0$ for non zero I. Now if we use coupled theory Brillouin's theorem holds for all orders so that $c_I^k = 0$ for non zero I and all k. In addition we have the normalisation condition

$$\sum_{I=0}^{N} c_I^1 c_I^0 = 0 \tag{34}$$

which means that for coupled or uncoupled functions we have $c_0^1 = 0$. However if we use uncoupled functions we have $c_I^k \neq 0$ for non zero I and for all orders k (since the uncoupled functions are not optimised to all orders). Thus for the ground state the first and second order energies are given by

$$E^1 = H_{00}^1 , \tag{35}$$

$$E^2 = H_{00}^2 + \sum_{s=1}^{N} H_{0J}^{1S} c_J^1 , \tag{36}$$

where

$$H_{00}^1 = 2 \sum_{i=1}^{n} \langle u_i^0 | z | u_i^0 \rangle \tag{37}$$

the usual uncoupled first order energy and

$$\begin{aligned} H_{00}^2 = 2 \sum_{i} \langle u_i^1 | z | u_i^0 \rangle + \sum_{i,j}^{n} (8[u_i^1 u_j^1 | u_i^0 u_j^0] \\ - 2[u_i^1 u_j^1 | u_j^0 u_i^0] - 2[u_i^1 u_j^0 | u_j^1 u_i^0]) \end{aligned} \tag{38}$$

which is the usual uncoupled corrected second order energy [1–4]. In Papers I and II of this series we discussed a single configuration function. In the case of the ground state this corresponds to defining $\psi^G \equiv \psi$; in this case the first and second order energies are H_{00}^1 and H_{00}^2 respectively.

Thus SCPT is equivalent to the usual uncoupled theory plus Dalgarno's correction when uncoupled functions are used whereas if we use coupled functions both SCPT and CIPT are equivalent to the usual coupled theory. Also if we use the geometric functions discussed in Section 3 the SCPT is equivalent to the geometric approximation.

5. Results

In Tables 1 and 2 the results of simple π-electron calculations on *trans*-butadiene are presented. The perturbations used are the point perturbations discussed in Papers I and III of this series. In Table 1 the results of applying CIPT and SCPT

Table 1

Perturbation at atom	1		2	
	E^1	E^2	E^1	E^2
Uncoupled energies	1	−0.046	1	−0.039
Uncoupled with Dalgarno's correction		−0.058		−0.049
Uncoupled with geometric approximation	1	−0.063	1	−0.054
CIPT (uncoupled functions)	1	−0.059	1	−0.050
CIPT (geometric functions)	1	−0.063	1	−0.054
Coupled theory energies	1	−0.063	1	−0.054

Table 2

Perturbation at atom		1		2	
		Singlet	Triplet	Singlet	Triplet
CIPT (coupled)	E^1	1	1	1	1
	E^2	−0.026	−0.070	−0.046	−0.120
CIPT (uncoupled)	E^1	1	1	1	1
	E^2	−0.014	−0.051	−0.032	−0.105
CIPT (geometric)	E^1	1	1	1	1
	E^2	−0.027	−0.071	−0.046	−0.129
SCPT (coupled)	E^1	1	1	1	1
	E^2	−0.031	−0.064	−0.016	−0.113
SCPT (uncoupled)	E^1	1	1	1	1
	E^2	−0.007	−0.050	−0.026	−0.087
SCPT (geometric)	E^1	1	1	1	1
	E^2	−0.039	−0.066	−0.005	−0.122

to ground state calculations are presented whereas in Table 2 the first and second order energies given are for the first singlet and first triplet excited state. In all cases the geometric functions give results which agree remarkably well with the coupled theory results. Thus we may conclude that the use of geometric functions (that is corrected uncoupled theory) in excited state perturbation theory seems to lead to improved results in the same way that the geometric correction improves uncoupled theory ground state calculations.

Acknowledgement. I would like to proffer my appreciation to Dr. A. T. Amos for constant advice and encouragement in the preparation of this paper and to the S.R.C. for the provision of a research grant.

References

1. Dalgarno, A.: Proc. Royal Soc. (London) A **251**, 282 (1959).
2. Tuan, D. Fu-Tai, Epstein, S., Hirschfelder, J. C.: J. chem. Physics **33**, 65 (1966).
3. Musher, J. I.: J. chem. Physics **46**, 369 (1967).
4. Amos, A. T., Musher, J. I.: Molecular Physics **13**, 509 (1967).
5. — Burrows, B. L.: Theoret. chim. Acta (Berl.) **22**, 283 (1971), (Paper I).
6. — — Theoret. chim. Acta (Berl.); to be published, (Paper II).
7. — — To be published, (Paper III).
8. Tuan, D. Fu-Tai: Chem. Physics Letters **7**, 115 (1970).
9. Amos, A. T.: J. chem. Physics **52**, 603 (1970).
10. Musher, J. I., Schulman, J. M.: J. chem. Physics **49**, 4845 (1968).

Dr. B. L. Burrows
North Staffordshire Polytechnic
Stafford, Staffordshire, England

Theoret. chim. Acta (Berl.) 26, 279—282 (1972)
© by Springer-Verlag 1972

Das Kastenmodell als Grundlage für ein ab initio Verfahren

IV. Bindungsbildung beim Wasserstoffmolekül

ERNST-ALBRECHT REINSCH
Institut für theoretische Chemie der Johann Wolfgang Goethe Universität in Frankfurt am Main

Eingegangen am 1. März 1972

The Box Model as a Basis for an ab initio Procedure

IV. Bonding in the Hydrogen Molecule

The results of the procedure developed in [1] are reported for the hydrogen molecule. It appears that the phenomenon of bonding can at least be qualitatively reproduced.

Im dritten Teil dieser Reihe [2] hatte sich ergeben, daß das in [1] vorgeschlagene Verfahren zur Berechnung der Gesamtenergie von Molekülen nur bei Kernladungszahlen 1 diskutable Ergebnisse liefert. Trotzdem wird man nicht an der Frage vorübergehen wollen, ob das Phänomen der Molekülbildung wenigstens in diesem Fall erfaßt wird. Es sollen deshalb hier kurz die Ergebnisse der Rechnung für den Fall $2H \rightarrow H_2$ mitgeteilt werden.

Anordnung zum Gitter

Die Molekülachse wird parallel zur z-Achse gelegt, so daß die Bindungspartner jeweils übereinander liegen. Davon abgesehen werden die Moleküle ähnlich wie die Atome angeordnet, nämlich in einer hexagonal dichtesten Packung. Zum Unterschied von einem einfachen Atomgitter mit der Schichtfolge *ababab*... liegt hier aber die Folge *aabbaabb*... vor. Dabei ist der Abstand einer *a*- von einer *b*-Schicht der gleiche wie bei einer Kugelpackung, während der zweier *a*- bzw. zweier *b*-Schichten gleich dem intramolekularen Abstand R ist.

Im Fall der Atome existierte nur *ein* Gitterparameter A, jetzt dagegen deren zwei: der intramolekulare Abstand R und der halbe intermolekulare Abstand innerhalb einer Schicht A. Man verfährt allerdings am besten so, daß man bei Änderung von R nicht A sondern den Fermi-Impuls k_F konstant hält. Alle reinen V_E-Graphen sind dann R-unabhängig, so daß ihre Fehler den Verlauf der $E(R)$-Funktion nicht beeinflussen können. Der Parameter A hängt dann (über k_F) von R ab, und man kann nur noch für einen bestimmten R-Wert frei über ihn verfügen.

Die Rechnung

Die Rechnung erfolgte nach den in [1] festgelegten Linien. Es wird hier darauf verzichtet, einzelne Terme wie im Falle der Atome [2] explizit anzugeben. Zu bemerken ist lediglich, daß die n_1, n_2-Summen, die in dem Ausdruck für die Graphen V_K^3 auftreten, insofern zu einer Kompromißlösung zwingen als die Zahl der Paare reziproker Gittervektoren mit wachsender Summierungsgrenze so stark zunimmt, daß die Rechenzeit fühlbar wird. Zum Zwecke einer Orientierung erschien die Summation über 5 Schichten von hexagonalen Bipyramiden ($n_{\max} = 5$) ausreichend. Lediglich in einzelnen Fällen wurde wie in [2] bis 8 summiert.

Übrig bleibt die Frage, entsprechend welchem A-Wert aus den Rechnungen für isolierte Atome man k_F wählen soll. Es wurden zwei Fälle durchgerechnet: Erstens $k_F = 0,8681$, was einem $A = 2$ bei den Rechnungen für H entspricht. Dann sind die beiden Fehler des Verfahrens etwa gleich groß [2], und die Summe der Fehlerquadrate ist minimal. Ein zweiter Versuch wurde für einen größeren k_F-Wert, nämlich 1,0474, unternommen. Er wurde auf Grund folgender Überlegung gewählt: Der Verlauf der Energie sollte bis etwa $R = 3,2$ a.E. verfolgt werden. Es wäre aber sinnlos, den intermolekularen H–H-Abstand kleiner als den intramolekularen Abstand zu machen. Will man A möglichst klein halten (keine Lücken!), so wäre $A = 1,6$ für $R = 3,2$ das Minimum. Daraus ergibt sich dann der oben genannte k_F-Wert; er entspricht im Fall des „isolierten" H-Atoms einem $A = 1,66$, ist also kleiner als der dort optimale Wert.

Die Tab. 1 enthält die berechneten Werte für den zweiten k_F-Wert und die Fig. 1 zeigt den Verlauf der Gesamtenergien für beide Fälle zusammen mit ihrem theoretischen Pendant.

Tabelle 1. Beiträge der Graphen für den Fall des Wasserstoff-Moleküls ($k_F = 1\ 0474$)

R (a.E.)		1,0	1,2	1,4	1,5	2,0	2,5	3,2
$E_{\text{kin}}^{(0)}$		0,658	0,658	0,658	0,658	0,658	0,658	0,658
$E_{\text{pot}}^{(0)} - 1/R$		−1,504	−1,487	−1,471	−1,462	−1,418	−1,366	−1,276
$1/R$		1,000	0,833	0,714	0,667	0,500	0,400	0,313
V_E^1		−0,500	−0,500	−0,500	−0,500	−0,500	−0,500	−0,500
V_K^2	10[a]	−0,326	−0,288	−0,249	−0,230	−0,153	−0,105	−0,115
	14[a]		−0,289	-			–	−0,115
V_E^2		−0,059	−0,059	−0,059	−0,059	−0,059	−0,059	−0,059
V_K^3	5[a]	−0,345	−0,264	−0,192	−0,160	−0,080	−0,041	−0,020
	8[a]		−0,266	—	—	—		−0,027
$V_K^2 V_E^1$	10[a]	−0,022	−0,016	−0,005	−0,000	−0,007	−0,003	−0,017
	14[a]		−0,016	—	—	—	—	0,017
V_E^3		−0,045	−0,045	−0,045	−0,045	−0,045	−0,045	−0,045
E_{Gesamt}[b]		−1,143	−1,168	−1,148	−1,132	−1,089	−1,056	−1,028

[a] $n_{\max}$. [b] Gesamtenergie mit $n_{\max} = 5$ bzw. 10.

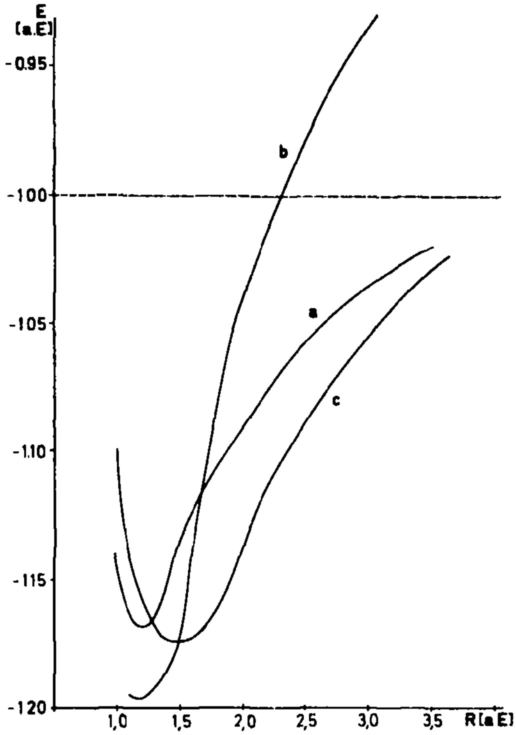

Fig. 1. a Berechnete Gesamtenergie für das Wasserstoffmolekül in Abhängigkeit von R bei konstantem $k_F = 1{,}0474$, b wie a mit $k_F = 0{,}8681$, c theoretischer Verlauf nach [3]

Diskussion

Die berechneten Kurven zeigen tatsächlich das richtige Verhalten: eine Art Morsepotential mit einem Minimum und einem nach größeren R-Werten zu asymptotisch verlaufenden Ast. Auch liegt die Bindungsenergie etwa in der richtigen Größenordnung. (Der starke Anstieg für kleine R-Werte ist natürlich trivial und eine Folge des $1/R$-Terms.) Im einzelnen zeigt sich jedoch, daß die Lage des Minimums, das in beiden Fällen bei $R = 1{,}2$ a.E. liegt, nicht richtig wiedergegeben wird. Der theoretisch richtige Wert ist etwa 1,5 a.E., was bedeutet, daß sich die Bindungslänge um 20% zu klein ergibt.

Die Bindungsenergie könnte nur durch Extrapolieren bestimmt werden. Es soll hier ersatzweise die Energiedifferenz zwischen $R = R_{\min}$ und $R = 3{,}5$ a.E. diskutiert werden. Der theoretische Wert hierfür ist $1{,}174 - 1{,}027 = 0{,}147$ a.E. [3]. Der Verlauf der für $k_F = 1{,}0474$ errechneten Kurve zeigt eine Differenz von $1{,}168 - 1{,}020 = 0{,}148$ a.E. Die Übereinstimmung wäre also recht gut, wenn auch der Verlauf der beiden entsprechenden Kurven [(*a*) und (*c*) in der Fig.] gerade im mittleren R-Bereich stark voneinander abweicht.

Die Tatsache, daß die Übereinstimmung der Werte für ΔE nur vordergründig ist, wird noch betont durch den Verlauf der Kurve für $k_F = 0{,}8681$ [(b) in der Fig.]. Er ist gegenüber demjenigen für $k_F = 1{,}0474$ erheblich verzerrt; das Minimum liegt tiefer und die Werte für große R-Werte liegen viel höher, so daß die entsprechende Energiedifferenz 1,196 − 0,908 = 0,288 a.E., also fast zweimal so groß wie im ersten Fall, ist. ΔE ist somit stark k_F-abhängig, und scharfe Aussagen sind aus diesem Grund praktisch nicht mehr möglich.

Die Tabelle zeigt darüber hinaus die Tatsache, daß sich bei einem Gitter geringerer Symmetrie, wie es für zweiatomige Moleküle – verglichen mit einzelnen Atomen – der Fall sein muß, die Konvergenz infolge der größeren Lücken im Gitter verschlechtert. Das bedeutet, daß man den zwei in [2] konstatierten Einschränkungen für die Anwendbarkeit des Verfahrens noch eine dritte hinzufügen muß: Die Moleküle dürfen, ähnlich wie bei Rechnungen nach dem Einzentrumsmodell, nicht stark von der Kugelform abweichen.

Die Rechnungen sind im Deutschen Rechenzentrum, Darmstadt, und im Rechenzentrum der Bayerischen Akademie der Wissenschaften, München, durchgeführt worden. Die finanziellen Mittel stammten aus dem Sonderforschungsbereich Theoretische Chemie.

Literatur

1. Reinsch, E. A.: Theoret. chim. Acta (Berl.) **23**, 155 (1971); **24**, 290 (1972).
2. Theoret. chim. Acta (Berl.), **25**, 338 (1972)
3. Kolos, W., Roothan, C. C. J.: Rev. mod. Physics **32**, 219 (1960).

Dr. Ernst-Albrecht Reinsch
Institut für theoretische Chemie der
Johann Wolfgang Goethe-Universität
D-6000 Frankfurt am Main
Robert-Mayer-Straße 11
Deutschland

Theoret. chim. Acta (Berl.) 26, 283 –288 (1972)
© by Springer-Verlag 1972

Calculations on the Force Constants of Triatomic Group II Metal Halides

I. ELIEZER and A. REGER
Department of Chemistry, Tel-Aviv University, Tel-Aviv, Israel

Received December 3, 1971

A comparison between various polarizable ion models for calculating bending force constants of linear MX_2 molecules is presented. A convergence test is applied to the models. Further, the contribution of an induced dipole-induced quadrupole interaction term to the force constant, is examined. The criteria for a useful comparison between calculated and experimental values of force constants are discussed.

1. Introduction

Several years ago a model was proposed [1] for calculating bending force constants of linear triatomic molecules on the basis of an electrostatic potential. At that time very few experimental results were available. Also numerical errors crept into the calculations. Therefore, it was not possible to test the model, and to compare its results with experiment. In this communication, modified calculations are presented, a comparison is made between different models, and a convergence test is applied. Further, the effect of a new interaction term, namely induced dipole-induced quadrupole is examined.

To avoid being cumbersome, the principles of the method will not be described. Ref. [1] should be consulted for the background of our arguments.

2. Bending Force Constant Calculations

a) Table 1 contains force constants calculated for several models. The "Rittner Potential" model includes interaction terms of charges and of induced dipoles. The equation used is a corrected form of Eq. (12) in Ref. [1], in which the expression for $k_b^{(l)}$ is given by:

$$k_b^{(l)} = -\frac{e^2 b^3}{l^3} \frac{\left\{1 + \frac{a^3}{l^3}\left[\frac{21}{4(1+a^3/(4l^3))} - \frac{2}{1+a^3/(8l^3)}\right]\right\}^2}{1 - \frac{2a^3 b^3}{l^6}\left(\frac{1}{1+a^3/(8l^3)}\right)} . \tag{1}$$

We take this opportunity to correct several other errors in Ref. [1].
The correct equations are (the numbers refer to [1]):

$$u_A = -\frac{ea}{l^2\cos\theta}\left(1 - \frac{a^2}{l^2} + \frac{a^4}{4l^4\cos^2\theta}\right)^{-\frac{1}{2}} - \frac{e}{2l\cos\theta} + \frac{ea}{l^2\cos\theta} - \frac{ea}{4l^2\cos^2\theta} + \frac{ea}{4l^2\cos^2\theta - a^2} , \tag{14}$$

$$V = \frac{e^2 a}{l^2\left[\left(1 - \frac{a^2}{l^2}\right)\cos^2\theta + \frac{a^4}{4l^4}\right]^{\frac{1}{2}}} - \frac{e^2 a}{l^2\left(8\cos^2\theta - 2\frac{a^2}{l^2}\right)} \tag{17}$$

$$+ \frac{e^2}{l\cos\theta}\left(\frac{1}{2} - \frac{a}{l}\right) + \frac{e^2 a}{8l^2\cos^2\theta},$$

$$u_A = -\frac{e}{2l\cos\theta} + \frac{eb}{l^2[1 + (2b^2/l^2)\cos 2\theta + b^4/l^4]^{\frac{1}{2}}}, \tag{20}$$

$$\frac{k_\delta}{l^2} = \frac{e^2}{8l^3} - \frac{e^2 b^3}{l^6(1 + b^2/l^2)^3}. \tag{21}$$

The "Ion Multipole Potential" was calculated according to Eqs. (18) and (21) (as corrected). This model includes ion-induced multipole interaction terms.

The "Spherical Conductor Potential" is based on calculations according to Eq. (18) in Ref. [1] and the corrected form of Eqs. (12) and (21). From the sum of these three equations the first two terms of Eq. (22) (Ref. [1]) - i.e., overlapping terms which are of the charge-charge, and charge-induced dipole type - were omitted. This model includes all electrostatic interactions between polarisable ions.

The last column of Table 1 lists the experimental values of force constants available.

The polarizability values of the anion, α, and the cation, β, were taken from the polarizability value range, summarized by Eliezer [2]. The spread of experimental polarizability values is very large and none of the values is actually applicable to the group II halides. Thus the calculations can only show whether agreement with experiment can be obtained with polarizability values approximately within the experimental range.

In the calculations carried out in Ref. [1], it seems that all values are incorrectly multiplied by a factor of 2.3. This probably arises from the numerical factor of the electronic charge. In the course of the numerical calculations the equations are multiplied by a factor of $4.8^2/10$, to obtain proper dimensions. In the calculations in Ref. [1] this factor seems to have been unnecessarily squared.

b) From Table 1 it is seen that agreement between experiment and calculations exists for beryllium halides and magnesium chloride and the bromides and iodides of zinc and cadmium. We shall discuss this point in the conclusions.

The "Ion Multipole" model gives force constants closest to the experimental values (e.g. for BaF_2) in spite of the fact that the "Spherical Conductor Potential" model seems to be better, since it contains more interaction terms.

Another interesting point with reference to Table 1 is that the value of the cation polarizability, which gives the force constant closest to experiment, is usually the smallest one (higher cation polarizability values give smaller values of force constants). This fact would indicate that too high values of cation polarizability are being used. In this respect it is advisable to note that for the beryllium halides, where agreement is found between experiment and calculation, the cation polarizability is an order of magnitude smaller than the polarizabilities of the other cations.

Table 1. Bending force constant calculations

Molecule	l [Å]	α	β	Rittner potential	α	β	Ion multipole potential	α	β	Spherical conductor potential	$\frac{k}{l^2}$ exp
BeF_2	1.40	0.70	0.05	0.110	0.50	0.05	0.117	0.60	0.04	0.110	0.11[a]
$BeCl_2$	1.75	2.00	0.05	0.080	2.00	0.01	0.069	2.30	0.01	0.081	
$BeBr_2$	1.91	3.70	0.05	0.078	3.70	0.01	0.044	3.70	0.01	0.061	
BeI_2	2.18	5.70	0.05	0.057	5.70	0.01	0.029	5.70	0.01	0.041	
MgF_2	1.77	1.10	0.01	0.070	1.10	0.01	0.064	1.10	0.01	0.067	0.128[b]
$MgCl_2$	2.18	2.00	0.10	0.032	2.00	0.10	0.033	2.10	0.10	0.032	0.0317[a]
$MgBr_2$	2.34	3.70	0.10	0.031	4.20	0.01	0.029	5.00	0.01	0.034	
MgI_2	2.52	5.70	0.10	0.028	7.60	0.10	0.021	7.60	0.01	0.028	
CaF_2	2.10	0.50	0.30	0.023	1.10	0.30	0.030	0.50	0.30	0.025	0.0764[b]
$CaCl_2$	2.51	3.70	0.30	0.018	3.70	0.30	0.021	3.70	0.30	0.018	0.0306[a]
$CaBr_2$	2.67	5.00	0.30	0.017	5.00	0.30	0.018	5.00	0.30	0.016	
CaI_2	2.88	7.60	0.30	0.016	7.60	0.30	0.015	7.60	0.30	0.014	
SrF_2	2.20	0.50	0.70	0.010	1.10	0.70	0.022	0.50	0.70	0.015	0.0263[b]
$SrCl_2$	2.67	2.00	0.70	0.010	3.70	0.70	0.016	2.00	0.70	0.011	0.0208[a]
$SrBr_2$	2.82	3.70	0.70	0.009	5.00	0.70	0.014	3.70	0.70	0.010	
SrI_2	3.03	7.60	0.70	0.009	7.60	0.70	0.012	5.70	0.70	0.009	
BaF_2	2.32	0.50	1.50	−0.004	1.10	1.50	0.014	0.50	1.50	0.007	0.0148[b]
$BaCl_2$	2.82	2.00	1.50	0.003	3.70	1.50	0.011	2.00	1.50	0.006	
$BaBr_2$	2.99	3.70	1.50	0.003	5.00	1.50	0.010	3.70	1.50	0.005	
BaI_2	3.20	5.70	1.50	0.004	7.60	1.50	0.009	5.70	1.50	0.005	
ZnF_2	1.81	0.50	0.20	0.034	1.10	0.20	0.050	0.50	0.20	0.037	0.080[c]
$ZnCl_2$	2.05	3.70	0.20	0.034	2.90	0.20	0.039	2.00	0.20	0.029	0.052[c]
$ZnBr_2$	2.21	5.00	0.20	0.033	3.70	0.20	0.032	3.70	0.20	0.025	0.038[c]
ZnI_2	2.38	6.20	0.20	0.030	5.70	0.20	0.025	5.70	0.20	0.022	0.030[c]
CdF_2	1.97	1.10	0.10	0.039	1.10	0.10	0.042	1.10	0.10	0.039	0.063[c]
$CdCl_2$	2.21	3.70	0.10	0.038	3.70	0.10	0.033	3.70	0.10	0.033	0.050[c]
$CdBr_2$	2.37	5.00	0.10	0.034	5.00	0.10	0.027	5.00	0.10	0.028	0.037[c]
CdI_2	2.53	6.30	0.10	0.029	5.70	0.10	0.023	6.30	0.10	0.024	0.029[c]
HgF_2	2.08	0.50	0.30	0.023	1.10	0.30	0.031	0.50	0.30	0.025	0.139[c]
$HgCl_2$	2.29	3.70	0.30	0.022	3.70	0.30	0.028	2.00	0.30	0.021	0.089[c]
$HgBr_2$	2.41	5.00	0.30	0.021	5.00	0.30	0.024	3.70	0.30	0.019	0.070[c]
HgI_2	2.59	7.60	0.30	0.021	5.70	0.30	0.020	5.70	0.30	0.016	0.055[c]

l Bond length; α, β anion and cation polarizabilities.

[a] White, D.: *Private communication.* [b] Ref. [4]. [c] Ref. [3].

3. Convergence Tests

a) Table 2 examines the convergence of the models used to calculate force constants. The criterion for convergence chosen was expansion of the general expression in a multipole series and truncation of the expansion when agreement is reached between the general and expanded forms. To this end it was necessary to derive further terms to be added to Eq. (22) of Ref. [1], which are given by:

$$k_a^{(6)} + k_b^{(6)} = \frac{e^2}{l^{12}}\left(-\frac{697}{2048}a^9 - 2a^3b^6 - \frac{135}{16}a^6b^3 + 10b^9\right). \qquad (2)$$

The "Rittner Potential" is tested for convergence by expanding the above-mentioned Eq. (12) into a multipole series up to l^{-9} and up to l^{-12}. The same is

Table 2. Convergence tests for multipole expansion

Molecule	Rittner up to l^{-9}	Rittner up to l^{-12}	Rittner potential	Ion multipole up to l^{-10}	Ion multipole up to l^{-12}	Ion multipole potential	Spherical conductor up to l^{-10}	Spherical conductor up to l^{-12}	Spherical conductor potential	Dipole quadrupole terms
BeF_2	0.120	0.109	0.110	0.118	0.117	0.117	0.118	0.110	0.110	−0.001
$BeCl_2$	0.087	0.078	0.080	0.075	0.072	0.069	0.097	0.084	0.081	−0.028
$BeBr_2$	0.090	0.075	0.078	0.061	0.053	0.044	0.085	0.067	0.061	−0.039
BeI_2	0.065	0.055	0.057	0.041	0.035	0.029	0.059	0.046	0.041	−0.029
MgF_2	0.070	0.069	0.070	0.065	0.064	0.064	0.068	0.067	0.067	−0.003
$MgCl_2$	0.033	0.032	0.032	0.033	0.033	0.033	0.033	0.032	0.032	−0.001
$MgBr_2$	0.032	0.031	0.031	0.031	0.030	0.029	0.039	0.035	0.035	−0.009
MgI_2	0.030	0.028	0.028	0.025	0.023	0.021	0.035	0.030	0.028	−0.013
CaF_2	0.023	0.023	0.023	0.030	0.030	0.030	0.025	0.025	0.025	0.000
$CaCl_2$	0.020	0.018	0.018	0.021	0.021	0.021	0.019	0.018	0.018	0.000
$CaBr_2$	0.018	0.017	0.017	0.019	0.018	0.018	0.018	0.016	0.016	0.000
CaI_2	0.017	0.015	0.016	0.016	0.015	0.015	0.016	0.014	0.014	−0.001
SrF_2	0.011	0.010	0.010	0.021	0.022	0.022	0.015	0.016	0.015	−0.002
$SrCl_2$	0.010	0.010	0.010	0.016	0.016	0.016	0.011	0.011	0.011	0.000
$SrBr_2$	0.010	0.009	0.009	0.014	0.014	0.014	0.011	0.010	0.010	0.000
SrI_2	0.011	0.009	0.009	0.012	0.012	0.012	0.010	0.009	0.009	0.000
BaF_2	0.003	0.004	−0.004	0.012	0.015	0.014	0.005	0.008	0.007	−0.004
$BaCl_2$	0.004	0.003	0.003	0.011	0.011	0.011	0.006	0.006	0.006	−0.001
$BaBr_2$	0.004	0.003	0.003	0.010	0.010	0.010	0.006	0.005	0.005	0.000
BaI_2	0.005	0.004	0.004	0.009	0.009	0.009	0.006	0.005	0.005	0.000
ZnF_2	0.035	0.034	0.034	0.051	0.050	0.050	0.038	0.037	0.037	0.000
$ZnCl_2$	0.045	0.032	0.034	0.042	0.040	0.039	0.033	0.029	0.029	0.001
$ZnBr_2$	0.042	0.031	0.033	0.034	0.033	0.032	0.032	0.025	0.025	−0.002
ZnI_2	0.036	0.028	0.030	0.029	0.027	0.025	0.030	0.022	0.022	−0.005
CdF_2	0.040	0.039	0.039	0.042	0.042	0.042	0.040	0.039	0.039	0.000
$CdCl_2$	0.041	0.037	0.038	0.036	0.034	0.033	0.038	0.033	0.033	−0.005
$CdBr_2$	0.036	0.033	0.034	0.030	0.028	0.027	0.033	0.029	0.028	−0.006
CdI_2	0.031	0.028	0.029	0.024	0.023	0.023	0.028	0.024	0.024	−0.006
HgF_2	0.023	0.023	0.023	0.031	0.031	0.031	0.025	0.025	0.025	0.000
$HgCl_2$	0.026	0.021	0.022	0.029	0.028	0.028	0.022	0.020	0.021	0.001
$HgBr_2$	0.026	0.021	0.021	0.026	0.025	0.024	0.022	0.019	0.019	0.000
HgI_2	0.026	0.020	0.021	0.021	0.020	0.020	0.020	0.016	0.016	−0.001

done for the "Ion Multipole Potential" by expanding the above-mentioned Eqs. (18), (21) into a multipole series up to l^{-10} and up to l^{-12}. Similar calculations are carried out using the "Spherical Conductor Potential". The expansion of the spherical conductor to l^{-10} is the above mentioned Eq. (22), and the expansion to l^{-12} includes in addition the term $k_a^{(6)} + k_b^{(6)}$ (Eq. (2)). The last column of Table 2 will be discussed in the next section.

b) The results in Table 2 show that in order to get force constants by a multipole expansion process, one has to carry out the expansion to terms in l^{-12} rather than to terms in l^{-10} (or l^{-9} in the case of the "Rittner Potential"). The l^{-12} interaction terms contribute a non-negligible contribution to the force constants. The contribution of these terms is always negative. The greatest relative contribution of these terms is found in the beryllium halides and in halides of zinc, cadmium and mercury.

The l^{-12} interaction terms, as calculated in Table 2, are important for the convergence of the multipole expansion. These terms bring the force constants, calculated by a multipole series, close to the force constants calculated by the general formula, for all molecules.

4. Dipole-Quadrupole Interaction Terms

a) As the convergence test necessitates a multipole expansion to terms in l^{-12}, it was decided to examine the contribution of l^{-11} terms, which describe an induced dipole-induced quadrupole interaction. In order to derive the relevant term the following procedure was used: First, the tensor components of the dipole-induced quadrupoles in the anion and cation points were evaluated. Then the potentials arising from the induced quadrupole components were evaluated. The potentials were substituted in the general potential equation (Eq. (9) of Ref. [1]). The resulting equation was differentiated twice and θ was set at zero. Division by $4l^2$ and expansion in series, retaining only l^{-11} terms, finally gives the expression:

$$k_a^{(5)} + k_b^{(5)} = \frac{e^2}{l^{11}}\left(-\frac{85}{128}a^8 + \frac{207}{16}a^5b^3 - \frac{735}{32}a^3b^5\right). \tag{3}$$

b) The results of Eq. (3) are given in the last column of Table 2. For most molecules this term contributes a small but finite contribution. Note that the main contributions of this term to the force constants are negative. The most pronounced effect is observed in the beryllium halides. This term contributes less to the force constants of the calcium and strontium halides. It may be concluded that when carrying out a multipole expansion for force constant calculation, it is desirable to include the induced dipole-induced quadrupole term.

5. Summary and Conclusion

Calculations with the so-called polarized-ion model were carried out for linear triatomic molecules in the gas phase. When calculating force constants by carrying out a multipole expansion it is necessary to include terms up to l^{-12}.

The validity of such a model is tested by comparison of the calculational results with experiment. As was mentioned above agreement is obtained for only part of the group II metal halides. One reason is that the theoretical treatment developed above is applicable only to linear molecules and serious difficulties arise when attempts to extend it to bent molecules are made. It was suggested recently (see Discussion in Ref. [2]) that the magnesium, calcium and strontium fluorides, strontium cloride and all the barium halides are bent. And, indeed, the experimental values for these do not agree with our calculations. However, calcium chloride is apparently linear but still no agreement is found. Nor is there any agreement in the case of the mercuric halides. In the case of the mercuric halides there are probably special factors at work, as discussed in Ref. [2]. However, a general reason for lack of agreement may be that the experimental values of the force constants were determined from vibrational frequencies measured in inert gas matrices [3, 4] and not in the gas phase. Similarly, the polarizability values taken for the force constant calculations were determined from values measured in crystals [5, 6], or in water solutions [7]. These values are not necessarily the correct ones for determining bending force constants. This point is reinforced by the wide spread of the polarizability values, as measured by different investigators (see table in Ref. [2]).

Although the agreement between theory and experiment is not too good at present, we believe the present method leads to a useful comparison of theoretical and experimental force constants, should reliable experimental measurements (see above) become available.

References

1. Buchler, A., Klemperer, W., Emslie, A. G.: J. chem. Physics **36**, 2499 (1962).
2. Eliezer, I.. Theoret. chim. Acta (Berl.) **18**, 77 (1970).
3a. Loewenschuss, A., Ron, A., Schnepp, O.: J. chem. Physics **49**, 272 (1968).
3b. J chem. Physics **50**, 2502 (1969).
4a. Mann, D. E., Calder, G. V., Seshadri, K. S., White, D., Linevsky, M. J.: J. chem. Physics **46**, 1138 (1967).
4b. Calder, V., Mann, D. E., Seshadri, K. S., Allavena, M., White, D.: J. chem. Physics **51**, 2093 (1969).
5. Tessman, J. R., Kahn, A. H., Schockley, W.: Physic. Rev. **92**, 890 (1953).
6. Van Vleck, J. H.: The theory of electric and magnetic susceptibilities. London: Oxford University Press 1932.
7. Fajans, K., Joos, G.: Z. Physik **23**, 1 (1924).

Prof. Dr. I. Eliezer
Department of Chemistry
Tel-Aviv University
Tel-Aviv, Israel

Theoret. chim. Acta (Berl.) 26, 289—299 (1972)
© by Springer-Verlag 1972

Correlation of Hückel Molecular Orbital Energies with π-Ionization Potentials*

F. Brogli and E. Heilbronner

Physikalisch-Chemisches Institut der Universität Basel, Klingelbergstraße 80, CH-4056 Basel

Received March 13, 1972

It is shown that simple HMO models which take into account first order bond fixation yield orbital energies for π-systems which correlate closely with the π-band positions in the corresponding photoelectron spectra.

Es wird gezeigt, daß die π-Orbitalenergien, die man unter Berücksichtigung der partiellen Bindungslokalisierung nach dem einfachen HMO-Verfahren berechnet, eng mit den Lagen der π-Banden in den entsprechenden Photoelektronen-Spektren korrelieren.

Les énergies d'orbitales π, calculées par le simple procédé de Hückel en tenant compte de la localisation partielle des doubles liaisons, montrent une correlation étroite avec les positions des bandes π dans les spectres photoélectroniques des hydrocarbures correspondants.

It is a well known, if somewhat disturbing phenomenon, that simple Hückel molecular orbital (HMO) models of π-systems yield predictions which are often as good and sometimes much better than those derived from more sophisticated treatments (e.g. [2–4]).

So far, the many examples known fell into two main categories:

1) "*One-electron properties*" which can be correlated with the characteristic values of a *single* orbital, usually the highest occupied (HOMO) or lowest unoccupied (LUMO) orbital, i.e. with the orbital energy $\varepsilon_J = \alpha + x_J \beta$, or with the coefficients $c_{J\mu}$ of the linear combination $\psi_J = \Sigma c_{J\mu} \phi_\mu$. Examples are the reduction potentials [2a, 4a, 5] or oxidation potentials [2b, 4b, 6] of unsaturated hydrocarbons, the interpretation of their ESR spectra [2c, 4c, 7] or the prediction of (frontier) orbital controlled reactions [2d, 4d, 8].

2) "*All-electron properties*" which can be correlated with characteristic values depending on *all* occupied π-orbitals, i.e. with total π-electron energies $E_\pi = \Sigma b_J \varepsilon_J$, localization energies A_μ, charge densities q_μ, bond orders $p_{\mu\nu}$ or with the various polarizabilities $\pi_{\mu\nu}$, $\pi_{\mu\nu,\varrho}$, $\pi_{\mu\nu,\varrho\sigma}$. Examples are the thermodynamic properties of unsaturated hydrocarbons [2e, 4e, 9], the rates of reactions which are charge or localization energy controlled [2f, 4f, 10], interatomic distances [2g, 4g, 11] or dipole moments [2h, 4h, 12].

For a review of the early history of applications of simple HMO models the reader is referred to [13].

Photoelectron(PE.-)spectroscopy [14] provides for the first time experimental information that can be rationalized in terms of a *whole set* of orbital energies ε_J, if Koopmans' theorem [15]

---

* Part 35 of "Applications of Photoelectron Spectroscopy"; Part 34: [1].

$$\varepsilon_J^{\mathrm{SCF}} = -I_{v,J} \tag{1}$$

is accepted ($I_{v,J}$ = vertical ionization energy corresponding to ejection of an electron from orbital ψ_J^{SCF}). Even though this theorem refers to SCF orbital energies $\varepsilon_J^{\mathrm{SCF}}$, it seemed of interest to investigate whether its application to simple Hückel orbital energies ε_J will yield a usefull method for the systematization and prediction of PE.-spectra of unsaturated hydrocarbons. That this may indeed be the case, has already been shown by Streitwieser and Nair for the first ionization potential [16, 2i] and by Eland and Danby in a PE.-spectroscopic investigation of aromatic compounds [17].

Table 1 (column 9) contains those vertical ionization potentials $I_{v,J}$ of a series of unsaturated π-systems M, which can be assigned with some confidence to ionization prozesses

$$M + h\nu \rightarrow M^{+}(\psi_J^{-1}) + e^{-}\,, \tag{2}$$

where the ejected electron e^- vacates a π-orbital ψ_J. HMO calculations assign an orbital energy $\varepsilon_J = \alpha + x_J\beta$ to ψ_J, so that according to (1) we obtain

$$I^0_{v,J} = -\varepsilon_J = -(\alpha + x_J\beta)\,. \tag{3}$$

The observed ionization potential $I_{v,J}$ differs from $I^0_{v,J}$ by a stochastic quantity Δ which encompasses all effects due to simplifying assumptions and/or neglected factors of our model. Thus (3) leads to a regressional problem which is solved by standard least squares techniques [18]. The sample consists of all ionization potentials $I_{v,J}$ of Table 1 (except those in brackets) and of the corresponding, independent variables x_J.

$H_2C{=}CH_2$

1

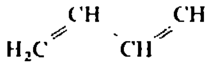

$H_2C{=}CH{-}CH{=}CH_2$

2

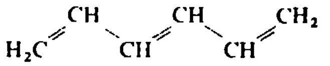

$H_2C{=}CH{-}CH{=}CH{-}CH{=}CH_2$

3

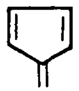

4

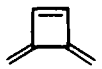

5

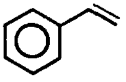

6

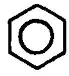

7

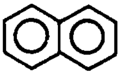

8

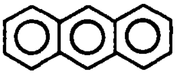

9

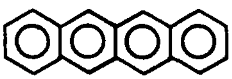

10

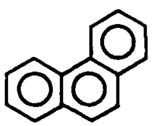

11

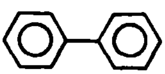

12

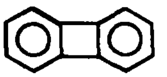

13

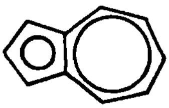

14

Table 1. Comparison of calculated and experimental vertical ionization potentials. All values in eV. Values in brackets can not be assigned with confidence to a π-level and have not been used in the regression calculations

Compound	J	x_J[a]	y_J[b]	$I^0_{v,J}$[c]; HMO	ΔI^0_J[d]	$I'_{v,J}$[e]; Pert	$\Delta I'_J$[f]	$I_{v,J}$[g] (exp.)	Ref.
Ethylene (1)	1	1.000	0.167	9.29	−1.22	10.46	−0.05	10.51	[14]
Butadiene (2)	2	0.618	0.132	8.42	−0.84	8.92	−0.16	9.08	[14]
	3	1.618	0.022	10.98	−0.50	11.40	−0.07	11.47	[14, 22]
Hexatriene (3)	4	0.445	0.106	7.77	−0.43	8.15	−0.05	8.2	[29]
Fulvene (4)	5	0.618	0.070	8.24	−0.31	8.44	−0.11	8.55	[22]
	6	1.000	−0.014	9.29	−0.25	9.06	−0.48	9.54	[22]
	7	2.115	−0.071	(12.34)	(−0.46)	(12.33)	(−0.47)	(12.8)	[22]
Bismethylene-cyclo butene (5)	8	0.555	0.120	8.07	−0.73	8.62	−0.18	8.80	[22]
	9	0.802	0.092	8.75	−0.69	9.23	−0.21	9.44	[22]
	10	2.247	−0.151	(12.70)	(−0.60)	(12.15)	(−1.15)	(13.3)	[22]
Styrene (6)	11	0.662	0.078	8.36	−0.13	8.65	0.16	8.49	[25]
	12	1.000	0.006	9.29	0.02	9.22	−0.05	9.27	[25]
	13	1.414	0.006	10.42	−0.11	10.60	0.07	10.53	[25]
Benzene (7)	14	1.000	0.000	9.29	0.05	9.17	−0.07	9.24	[14, 26]
	15	1.000	0.000	9.29	0.05	9.17	−0.07	9.24	[14, 26]
	16	2.000	0.000	12.02	−0.23	12.50	+0.25	12.25	[14, 26]
Naphtalene (8)	17	0.618	0.035	8.24	0.12	8.17	0.05	8.12	[17, 27]
	18	1.000	−0.046	9.29	0.39	8.82	−0.08	8.90	[17, 27]
	19	1.303	−0.024	10.12	0.12	10.00	0.00	10.00	[17, 27]
Anthracene (9)	20	0.414	0.026	7.69	0.27	7.43	0.02	7.41	[28]
	21	1.000	−0.066	9.29	0.74	8.66	0.11	8.55	[28]
	22	1.000	0.001	9.29	0.13	9.18	0.02	9.16	[28]
	23	1.414	−0.029	10.42	0.26	10.33	0.17	10.16	[28]
	24	1.414	−0.013	(10.42)		(10.45)		[h]	[28]
Naphtacene (10)	25	0.295	0.030	7.36	0.41	7.06	0.11	6.95	[30]
Phenanthrene (11)	26	0.605	0.031	8.21	0.29	8.10	0.18	7.92	[28]
	27	0.769	−0.003	(8.66)		(8.38)		[i]	[28]
	28	1.142	−0.045	9.68	0.40	9.30	0.02	9.28	[28]
	29	1.306	−0.037	10.12	0.24	9.91	0.03	9.88	[28]
	30	1.516	−0.013	(10.70)	(0.06)	(10.79)	(0.15)	(10.64)	[28]
Biphenyl (12)	31	0.705	0.023	8.48	0.28	8.37	0.17	8.20	[17]
Biphenylene (13)	32	0.445	0.095	7.77	0.15	8.06	0.44	7.62	[28]
	33	0.879	0.006	8.96	0.07	8.82	−0.07	8.89	[28]
	34	1.247	−0.058	9.96	0.28	9.55	−0.13	9.68	[28]
	35	1.347	−0.056	10.24	0.14	9.89	−0.21	10.10	[28]
Azulene (14)	36	0.477	0.004	7.86	0.42	7.46	0.02	7.44	[23, 24]
	37	0.887	−0.040	8.98	0.47	8.49	−0.02	8.51	[23, 24]
	38	1.356	−0.010	10.26	0.18	10.28	0.20	10.08	[23, 24]

[a] See formula (3).

[b] See formula (16).

[c] See formula (4).

[d] $\Delta I^0_J = I^0_{v,J} - I_{v,J}$.

[e] See formula (18).

[f] $\Delta I'_J = I'_{v,J} - I_{v,J}$.

[g] All values from photoelectron-spectra, with exception of 4 (spectroscopic) and 25 (electron-impact).

[h] Unresolved double band: 10.16 eV (23) and ~ 10.2 to 10.4 eV (24).

[i] Unresolved double band: 7.92 eV (26) and 8.12 eV or 8.35 eV (27).

Regression Line (90% Confidence Limits)

$$I^0_{v,J} = [(6.553 \pm 0.340) + (2.734 \pm 0.333)\, x_J]\ \text{eV}\,. \tag{4}$$

Variance analysis (values in eV²)

Source	Sum of squares	Degree of freedom	Mean squares	F-ratio	
Due to regr.	36.822	1	36.822		(5)
About regr.	5.859	31	0.189	194.8	
Total variance	42.681	32			

Standard Error: $SE(I_{v,J}) = 0.435$ eV.

The correlation of $I_{v,J}$ with $I^0_{v,J}$ (from (4)) is shown in Fig. 1. The confidence limits CL (90% security) have been calculated according to

$$CL(I_{v,J}) = I^0_{v,J} + t_{0.9,\phi}\, SE(I_{v,J}) \sqrt{1 + \frac{1}{N} + \frac{(x-\overline{x})^2}{S_{xx}}} \tag{6}$$

with $t_{0.9,31} = 1.70$, $N = 33$ and $SE(I_{v,J}) = 0.435$ eV.

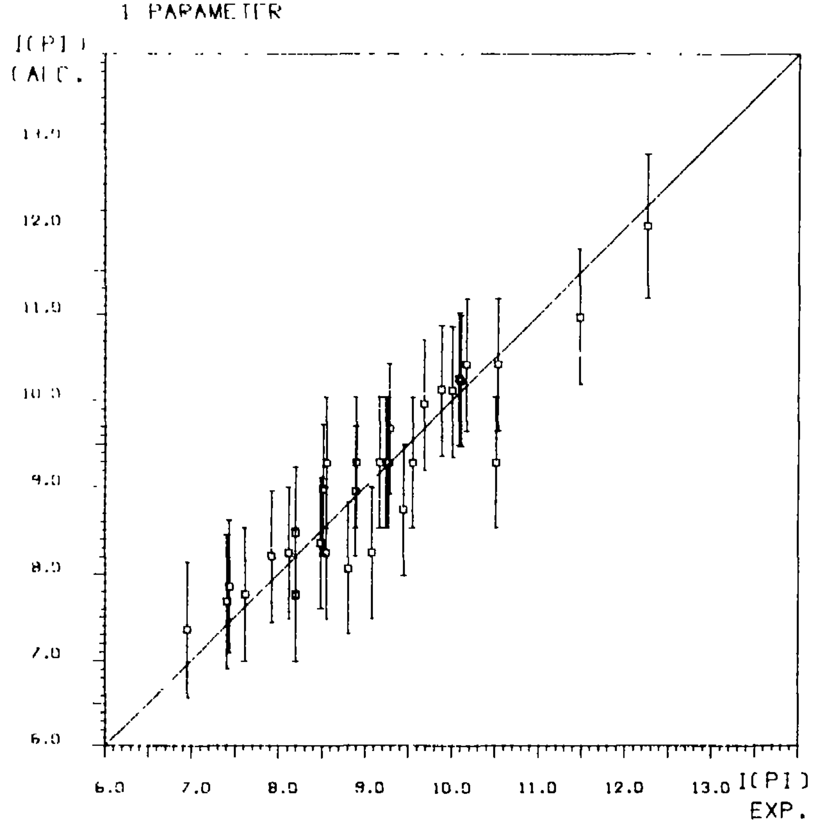

Fig. 1. Correlation of HMO orbital energies $-\varepsilon_J = I^0_{v,J} \equiv I(PI)$CALC. (formula (3)) with observed vertical ionization potentials $I_{v,J} \equiv I(PI)$EXP. The confidence limits attached to each point refer to 90% security

The reason for the poor agreement, i.e. the wide confidence limits is obvious: The eigenvalues x_J have been obtained under the usual assumption of equal resonance integrals $\beta_{\mu\nu} = \beta$ for all π-bonds between centers μ, ν. This is of course unacceptable for compounds with strong first order bond localization [19] such as the hydrocarbons **1** to **6**. However this effect can be taken care of by a simple first order perturbation treatment [20].

As has been discussed previously [19] the total energy $E_T(M)$of a π-electron system M can be written as the interaction-free sum of the energy of the σ-core and of the π-electron system proper if we postulate complete $\sigma - \pi$ separation:

$$E_T(M) = E_\sigma(M) + E_\pi(M) . \tag{7}$$

Assuming that the σ-energy can be written as

$$E_\sigma(M) = \sum_{\mu\nu} \frac{k^0}{2} (r_{\mu\nu} - r_0)^2 , \tag{8}$$

where k^0 is the force constant and r_0 the equilibrium bond length of a pure $sp^2 - sp^2$ σ-bond, and the π-energy as

$$E_\pi(M) = n\alpha + 2 \sum_{\mu\nu} p_{\mu\nu} \beta_{\mu\nu} \tag{9}$$

(n = number of π centres), then $E_T(M)$ becomes the sum of independent contributions $E_{\mu\nu}(M)$ from each bond,

$$E_T(M) = \sum_{\mu\nu} E_{\mu\nu}(M) , \tag{10}$$

as long as only first order bond fixation is taken into account [19]. Consequently the minimum of $E_T(M)$ is reached for the set of interatomic distances $R_{\mu\nu}$ which satisfy the relations

$$\frac{\partial E_T(M)}{\partial r_{\mu\nu}} = \frac{dE_{\mu\nu}(M)}{dr_{\mu\nu}} = 0 , \tag{11}$$

i.e. (with $\beta'_{\mu\nu} = (d\beta_{\mu\nu}/dr_{\mu\nu})_{R_{\mu\nu}}$):

$$R_{\mu\nu} = r_0 - \left(\frac{2\beta'_{\mu\nu}}{k^0}\right) p_{\mu\nu} . \tag{12}$$

The same arguments applied to the total energy $E_T(M^+(\psi_J^{-1}))$ of the radical cation $M^+(\psi_J^{-1})$ (obtained from M by removing an electron from orbital ψ_J) will lead to

$$R^+_{\mu\nu,J} = r_0 - \left(\frac{2\beta'_{\mu\nu}}{k^0}\right) p^+_{\mu\nu,J} , \tag{13}$$

where $p^+_{\mu\nu,J}$ is the bond order of the bond μ, ν in $M^+(\psi_J^{-1})$. The derivative $\beta'_{\mu\nu}$ should now be taken at $r_{\mu\nu} = R^+_{\mu\nu,J}$.

Fig. 2 shows the dependence of $E_T(M)$ and $E_T(M^+(\psi_J^{-1}))$ on $r_{\mu\nu}$. In terms of our model, the vertical ionization potential $I'_{v,J}$ corresponds to the transition indicated by the arrow at $r_{\mu\nu} = R_{\mu\nu}$ if we disregard vibrational energy contributions. The assumption of standard HMO theory, namely that all $\beta_{\mu\nu} = \beta$, consists in assigning to $R_{\mu\nu}$ and $R^+_{\mu\nu,J}$ the fixed value R_0, e.g. $R_0 = 1.40$ Å, if benzene with bond order $p_{\mu\nu} = p_0 = 2/3$ is used as a reference. The ionization potential $I^0_{v,J}$ calculated under these conditions is indicated in Fig. 2 by the arrow at $r_{\mu\nu} = R_0$. For each bond $\mu\nu$ of the π-system the vertical ionization potential $I_{v,J}$ differs from

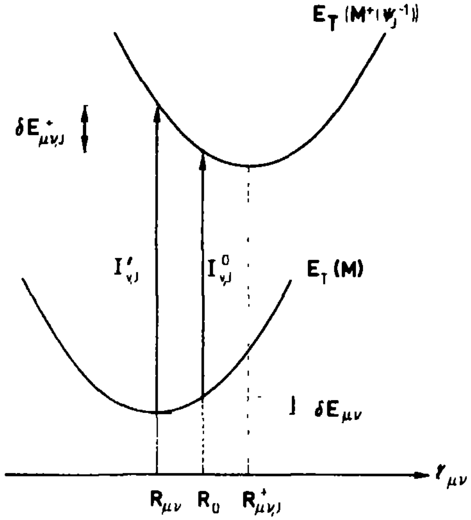

Fig 2. Dependence of $E_T(M)$ and $E_T(M^+(\psi_J^{-1}))$ on $r_{\mu\nu}$

$I^0_{\nu,J}$ by the sum of the positive increments $\delta E_{\mu\nu}$ and $\delta E^+_{\mu\nu,J}$, which has been shown to be [20]

$$\delta E_{\mu\nu} + \delta E^+_{\mu\nu,J} = \ell\left(\frac{2\beta'}{k^0}\right)^2 (p^+_{\mu\nu,J} - p_{\mu\nu})(p_0 - p_{\mu\nu}) \,, \tag{14}$$

where ℓ is the force constant of a π-bond (e.g. of a C⩵C bond in benzene). Summing over all bonds we obtain with $\Delta p_{\mu\nu,J} = p^+_{\mu\nu,J} - p_{\mu\nu}$

$$I'_{\nu,J} = I^0_{\nu,J} + \ell\left(\frac{2\beta'}{k^0}\right)^2 \sum_{\mu\nu} \Delta p_{\mu\nu,J}(p_0 - p_{\mu\nu}) \,. \tag{15}$$

Substitution in (15) of $I^0_{\nu,J}$ by expression (3) and making use of the abbreviations

$$a = -\alpha\,; \qquad b_1 = -\beta\,; \qquad b_2 = \ell\left(\frac{2\beta'}{k^0}\right)^2 \tag{16}$$

$$y_J = \sum_{\mu\nu} \Delta p_{\mu\nu,J}(p_0 - p_{\mu\nu})$$

yields the regression plane

$$I'_{\nu,J} = a + b_1 x_J + b_2 y_J \,, \tag{17}$$

the parameters of which are again calculated in the usual manner [18]:

Regression Plane (90% Confidence Limits)

$$I'_{\nu,J} = [(5.847 \pm 0.163) + (3.326 \pm 0.152)x_J + (7.733 \pm 1.009)\,Y_J]\ \text{eV}\,. \tag{18}$$

Variance analysis (values in eV^2)

Source	Sum of squares	Degree of freedom	Mean squares	F-ratio
Due to regr.	41.801	2	20.900	
About regr.	0.880	30	0.0293	712.5
Total variance	42.681	32		

(19)

Standard Error: $SE(I_{\nu,J}) = 0.171$ eV.

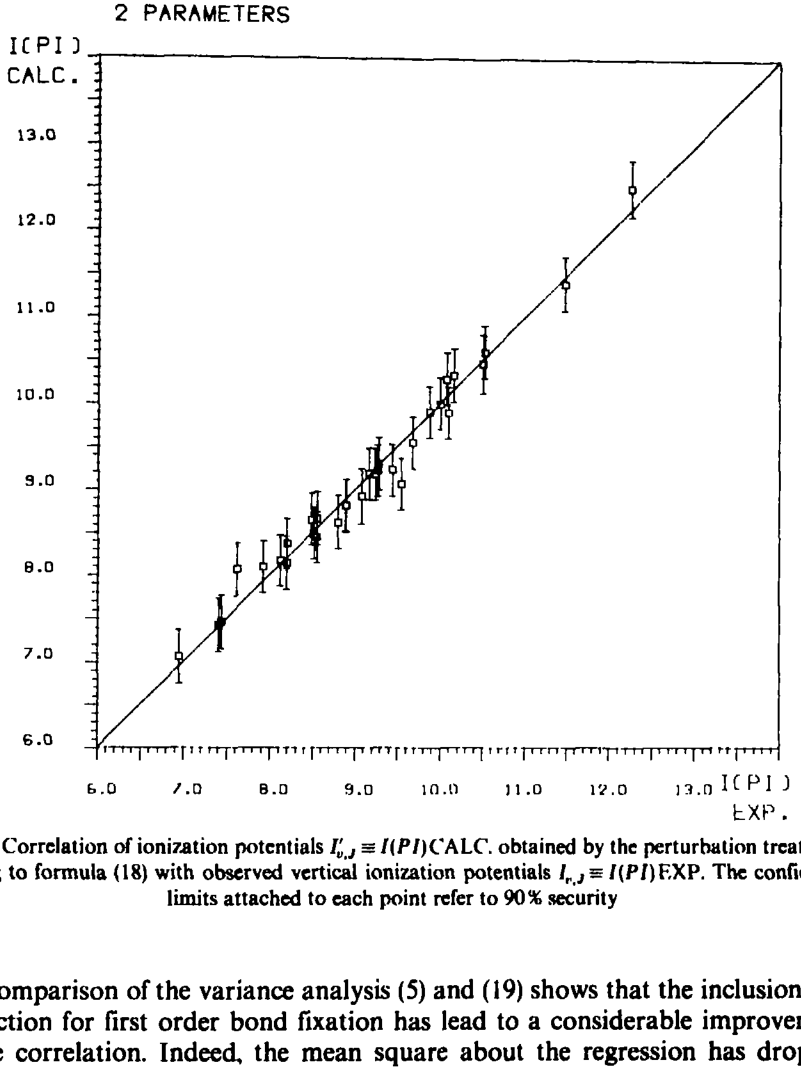

Fig. 3. Correlation of ionization potentials $I'_{\nu,J} \equiv I(PI)$CALC. obtained by the perturbation treatment leading to formula (18) with observed vertical ionization potentials $I_{\nu,J} \equiv I(PI)$EXP. The confidence limits attached to each point refer to 90% security

Comparison of the variance analysis (5) and (19) shows that the inclusion of a correction for first order bond fixation has lead to a considerable improvement of the correlation. Indeed, the mean square about the regression has dropped from 0.189 eV^2 to 0.0293 eV^2, corresponding to a F-ratio of 6.45. This should be compared to $F = 3.5$ (for 99.9% security and the appropriate degrees of freedom, i.e. 31 and 30). Thus the improvement is highly significant, as is also evident from a comparison of Figs. 1 and 3. The 90% confidence limits given in Fig. 3 have been calculated according to the rules given in [18], taking into account the contributions from the covariance between the independent variables x_J and y_J ($t_{0.9;30} = 1.70$).

Since photoejection (2) is necessarily accompanied by changes in charge density at the individual π-centres μ, one would expect that inclusion of a perturbation term depending on the charge order increments

$$\Delta q_{\mu,J} = q^{+}_{\mu,J} - q_{\mu} \tag{20}$$

will yield an additional improvement of the predictions derived from our simple HMO model. A first-order perturbation treatment based on $\Delta q_{\mu,J}$ as independent variable has been derived previously [20]. It yields the following increments $\delta I''_{\nu,J}$ for the ionization potentials, which have to be added to $I^0_{\nu,J}$

or $I'_{v,J}$.

$$\delta I''_{v,J} = -\omega\beta \sum_{\mu} \Delta q_{\mu,J}(q^{+}_{\mu,J} + q_{\mu}). \tag{21}$$

The parameter ω is defined as $\omega = (1/\beta)(\partial\alpha_{\mu}/\partial q_{\mu})$ [2j, 21]. Adding the perturbation (21) to the regression (17) yields

$$I''_{v,J} = a + b_1 x_J + b_2 y_J + b_3 z_J\ , \tag{22}$$

where $b_3 = -\omega\beta$ and $z_J = \sum_{\mu} \Delta q_{\mu,J}(q^{+}_{\mu,J} + q_{\mu})$.

However, in contrast to expectation, a least squares treatment of (22) does *not* lead to a significant improvement of the correlation between experimental and calculated ionization potentials over that shown in Fig. 3. This is evident from the following results:

Regression Plane (90 % Confidence Limits)

$$\begin{aligned} I''_{v,J} = [&(8.403 \pm 1.289) + (3.159 \pm 0.155)\,x_J \\ &+ (6.219 \pm 1.153)\,y_J - (1.301 \pm 0.652)\,z_J]\ \text{eV} \end{aligned} \tag{23}$$

Variance analysis (values in eV^2*)*

Source	Sum of squares	Degree of freedom	Mean squares	F-ratio
Due to regr.	42.051	3	14.017	
About regr	0.630	29	0.0217	645.1
Total variance	42.681	32		

(24)

Standard Error: $SE(I_{v,J}) = 0.147$ eV.

The variance ratio F of the mean squares about the regression taken from (19) and (24) is only $F = 0.0293/0.0217 = 1.35$ and therefore not significant. It should be noted that the covariance between y_J and z_J, i.e. between the corrections due to bond fixation and charge changes, is also not significant. This indicates, that the improvement is entirely due to the correction for bond fixation, in agreement with previous experience [20].

To conclude we wish to add the following comments:

A) From Table 1 it is obvious that the largest discrepancies $\Delta I'_{v,J}$ between observed and calculated ionization potentials (the latter from (18)) occur for fulvene (**4**), bismethylene-cyclobutene (**5**) and biphenylene (**13**) i.e. for hydrocarbons containing a five- or four-membered ring. This strongly suggest that 1,3-interactions, which have been neglected are presumably of importance in such compounds. Indeed, in **5** and **13**, the largest deviation observed i.e. $\Delta I_{v,10} = -1.15$ eV in **5**, $\Delta I_{v,32} = +0.44$ eV in **13**, is associated in each case with the orbital for which inclusion of 1,3-interactions across the diagonals of the four-membered ring would result in the largest shift in orbital energy. Note that these corrections are of the proper sign required to improve the agreement. However on closer examination e.g. in the case of fulvene **4**, one notes that the general situation is presumably too complex to be discussed in a meaningfull way in terms of a simple HMO-model.

B) We now compare the values $I'_{v,J}$ derived from our regression function (18) with the corresponding results obtained by many-electron treatments. In Table 2 we have collected as typical examples vertical ionization potentials calculated by Baird and Dewar [31] using (a) a valence shell SCF-MO model or (b) an SCF-π-model and the *ab-initio* calculations (c) of Christoffersen [32] and (d) of Berthier *et al.* [33]. The orbital energies ε_J (in eV or in a.u.) so obtained are correlated

Table 2. Vertical ionization potentials calculated by many electron treatments. For the meaning of (a), (b), (c), (d) see text

Cpd.	J	(a) [31] $-$eV	(b) [31] $-$eV	(c) [32] $-$a.u.	(d) [33] $-$a.u.
1	1	10.956	10 855		0.4622
2	2	10.139	10.070		0.4078
	3	11.994	12.060		0.5281
4	5	10.076	10.008	0.1594	0.3947
	6	10.321	10.428	0.2156	0.4348
	7	12.968	12.899	0.4030	0.5993
5	8	10.005	10.053	0.1803	0.4285
	9	10.377	10.366	0.2050	0.4050
	10	13.096	13.148	0.3837	0.6032
6	11	9.788	9.804		
	12	10.217	10.293		
	13	11.428	11.506		
7	14, 15	10.184	10.287	0.2169	0.4272
	16	13.100	13.037	0.3915	0.5893
8	17	9.309	9.274	0.1545	
	18	9.965	10.068	0.2002	
	19	11.011	11.110	0.2658	
14	36	8.851	8.666	0.1298	
	37	9.476	9.432	0.1808	
	38	11.256	11.489	0.2982	

with the observed ionization potentials $I_{v,J}$ according to

$$I_{v,J} = A + B\varepsilon_J\,, \tag{25}$$

i.e. including an additive constant A and a scaling factor B. As shown in Table 3 the correlation (25) is significantly worse in all cases than that given in (18), even though two additional parameters A and B have been included in order to scale the theoretical results and thus to minimize the variance about the regression. This illustrates the argument given at the beginning of this paper.

C) On the other hand, vertical ionization potentials can also be calculated by computing separately the total energies $E_T(M)$ of the neutral molecule M and $E_T(M^+(\psi_J^{-1}))$ of the radical cation $M^+(\psi_J^{-1})$ assuming the same structure for both. This has been carried out by Dewar, Hashmall and Venier [34] for a series of unsaturated hydrocarbons, including **1, 2, 3, 6, 7, 8, 9**, and **12**, with M^+ in its electronic ground state, i.e. with $\psi_J \equiv$ HOMO. Correlation of these first ionization potentials with our experimental results, using again a linear regression function of type (25) [with $I_{v,\mathrm{calc}} = E_T(M^+(\mathrm{HOMO}^{-1})) - E_T(M)$ instead of ε_J] yields a variance about the regression of 0.0178 eV^2 as compared to 0.0298 eV^2 for (18). Thus the agreement of the computed values $I_{v,\mathrm{calc}}$ with the experimental ionization potentials is not significantly better than that derived from (18), notwithstanding the restriction to first ionization potentials only. Note that we have scaled the theoretical results [34] by introducing two adjustable parameters A and B, which again tends to reduce the residual variance.

Table 3. Comparison of the results derived from many electron models (cf. Table 2) with those obtained from the regression function (18). N = sample size; $SE(I_{i,J})$ = standard deviation; ϕ = degree of freedom; F = variance ratio relative to the mean square about the regression (= 0.0293 eV) of (19); F (95%) = limit for 95% significance[a]

Model[a]	N	$SE(I_{i,J})$	Mean square about regression (25)	ϕ	F	F (95%)
(a)	21	0.282 eV	0.07924 eV^2	19	2.70	1.92
(b)	21	0.293	0.08567	19	2.92	1.92
(c)	16	0.403	0.16220	14	5.54	2.04
(d)	10	0.349	0.12198	8	4.16	2.27

[a] See text

D) Those compounds which can occur in non-planar conformations, i.e. **2**, **3**, **6**, and **12** do not yield differences $\Delta I'_J$ (see Table 1) which are significantly different from those observed in other cases. Presumably these molecules are (almost) planar (e.g. **2**, **3**) or small twist angles around the non-essential single bonds lead only to minor changes in the orbital energies if compared to the standard deviation $SE(I_{i,J}) = 0.17$ eV.

E) From the parameters $b_1 = 3.33$ eV and $b_2 = 7.73$ eV of (18) we obtain according to (16) $\beta = -3.33$ eV and $k = 3.1 \cdot 10^6$ dyn cm^{-1}. These values compare favourably to $\beta = -2.94$ eV and $k = 3.9 \cdot 10^6$ dyn cm^{-1} derived from a similar analysis of the $^1L_a \leftarrow {}^1A$ transition of π-systems [20]. In both cases k is too large by a factor of 3 to 4 ($k(C{=}C) \approx 10^6$ dyn cm^{-1}).

Acknowledgements. We wish to thank Dr. J. H. D. Eland (University of Oxford) for having made some of his experimental data available before publication. Special thanks are due to Dr. G. Berthier (Université de Paris) for letting us use his *ab-initio* results and for a stimulating correspondence.

This work has been supported by the *Schweizerischer Nationalfonds* (project Nr. 2.477.71) and by *CIBA-GEIGY SA*, Basel.

F. Brogli expresses his gratitude to the *Kanton Aargau* for the grant of a fellowship.

References

1. Heilbronner, E., Martin, H. D.: Helv. chim. Acta, in print.
2. Streitwieser, A., Jr.: Molecular orbital theory for organic chemists. New York: John Wiley & Sons 1961. a: 173; b: 185; c: 150; d: 329; e: 237; f: 307; g: 165; h: 139; i: 188; j: 115.
3. Dewar, M. J. S.: The molecular orbital theory of organic chemistry. New York: McGraw-Hill Book Company 1969
4. Heilbronner, E., Bock, H.: Das HMO-Modell und seine Anwendung. Weinheim/Bergstraße: Verlag Chemie 1968. Band I; a: 336; b: 346; c: 267; d: 380; e: 277; f: 233; g: 253; h: 262.
5. Maccoll, A.: Nature **163**, 178 (1949). – Pullman, A., Pullman, B., Berthier, G.: Bull. Soc. chim. France **17**, 591 (1950). – Hoijtink, G. J., van Schooten, J.: Recueil Trav. chim. Pays-Bas **71**, 1089 (1952).
6. Hoijtink, G. J.: Recueil Trav. chim. Pays-Bas **77**, 555 (1958).
7. McConnell, H. M.: J. chem. Physics **24**, 764 (1956); Gerson, F.: Hochauflösende ESR-Spektroskopie. Weinheim/Bergstraße: Verlag Chemie 1967.
8. Fukui, K., Yonezawa, T., Shingu, H.: J. chem. Physics **20**, 722 (1952). — Fukui, K., Yonezawa, T., Nagata, C., Shingu, H.: J. chem. Physics **22**, 1433 (1954). — Woodward, R. B., Hoffmann, R.: J. Amer. chem. Soc. **87**, 395, 2046, 2511 (1965).
9. Hückel, E.: Z. Elektrochem. **43**, 752 (1937). — Wheland, G. W.: J. chem. Physics **2**, 474 (1934).

10. Wheland, G. W.: J. Amer. chem. Soc. **64**, 900 (1942).
11. Coulson, C. A.: Proc. Royal Soc. (London) A **169**, 413 (1939).
12. — Longuet-Higgins, H. C.: Rev. sci. Instruments **85**, 927 (1947). Pullman, A., Pullman, B., Rumpf, P.: Bull. Soc. chim. France **15**, 757 (1948).
13. Pullman, A., Pullman, B.: Les théories electroniques de la chimie organique. Paris: Masson & Cie. 1952.
14. Turner, D. W., Baker, C., Baker, A. D., Brundle, C R.: Molecular photoelectron spectroscopy. London: Wiley-Interscience 1970.
15. Koopmans, T.: Physica **1**, 104 (1934).
16. Streitwieser, A., Jr., Nair, P. M.: Tetrahedron **5**, 149 (1959). - Streitwieser, A., Jr.: J. Amer. chem. Soc. **82**, 4123 (1960).
17. Eland, J. H. D., Danby, C. J.: Z. Naturforsch. **23a**, 355 (1968).
18. Davies, O. L.: Statistical methods in research and production. London: Oliver & Boyd 1967.
19. Binsch, G., Heilbronner, E., Murrell, J. N.: Molecular Physics **11**, 305 (1966). — Binsch, G., Heilbronner, E.: In: Structural chemistry and molecular biology (A. Rich and N. Davidson), p. 815. San Francisco: W. H. Freeman & Co. 1968.
20. Götz, H., Heilbronner, E.: Helv. chim. Acta **44**, 1365 (1961).
21. Streitwieser, A., Jr.: J. Amer. chem. Soc. **82**, 4123 (1960).
22. Heilbronner, E., Gleiter, R., Hopf, H., Hornung, V., de Meijere, A.: Helv. chim. Acta **54**, 783 (1971).
23. Eland, J. H. D.: J. Mass Spectrometry Ion Physics **2**, 471 (1969).
24. Heilbronner, E., Kobayashi, T.: Unpublished results.
25. Brogli, F., Heilbronner, E.: Unpublished results.
26. Åsbrink, L., Lindholm, E., Edqvist, O.: Chem. Physics Letters **5**, 192, 609 (1970).
27. Brogli, F., Heilbronner, E., Kobayashi, T.: Helv. chim. Acta **55**, 274 (1972).
28. Eland, J. H. D.: Private communication.
29. Price, W. C., Walsh, A. D.: Proc. Royal Soc. (London) A **185**, 182 (1946).
30. Wacks, M. E.: J. chem. Physics **41**, 1661 (1964).
31. Baird, N. C., Dewar, M. J. S.: Theoret. chim. Acta (Berl.) **9**, 1 (1967).
32. Christoffersen, R. E.: J. Amer. chem. Soc. **93**, 4104 (1970).
33. Praud, L., Millie, Ph., Berthier, G.: Theoret. chim. Acta (Berl.) **11**, 169 (1968); Berthier, G.: Private communication.
34. Dewar, M. J. S., Hashmall, J. A., Venier, C.: J. Amer. chem. Soc. **90**, 1953 (1968).

Prof. Dr. E. Heilbronner
Physikalisch-Chemisches Institut
der Universität Basel
CH-4056 Basel, Klingelbergstr. 80
Switzerland

Theoret. chim. Acta (Berl.) 26, 301—310 (1972)
© by Springer-Verlag 1972

A Poisson Equation for Vibrational Potentials of Diatomic Molecules* **

ALFRED B. ANDERSON*** and ROBERT G. PARR
Department of Chemistry, The Johns Hopkins University, Baltimore, Maryland 21218, USA

Received December 3, 1971

A Poisson equation for nuclear motions in diatomic molecules is derived. The working formula is

$$\nabla_\alpha^2 W = 4\pi \mathscr{Z}_\alpha \varrho_\beta(\alpha),$$

where ∇_α^2 is the Laplacian operator for the position of nucleus α, W is the Born-Oppenheimer molecular energy, $\mathscr{Z}_\alpha$ is the atomic number of α, and $\varrho_\beta(\alpha)$ is the electronic charge density evaluated at α due to orbitals centered on β. Harmonic, anharmonic and quartic equilibrium force constants are calculated using Hartree-Fock molecular and atomic electronic charge densities, for a number of first and second row diatomic molecules. A charge-model field gradient formula for harmonic force constants

$$k_e = 3/R_e^3,$$

where k_e is the force constant and R_e the equilibrium internuclear distance, which offers general improvement over a similar formula due to Bratož, is presented.

Eine Poisson-Gleichung für die Kernbewegung in zweiatomigen Molekülen wird abgeleitet. Es wird die Formel

$$\nabla_\alpha^2 W = 4\pi \mathscr{Z}_\alpha \varrho_\beta(\alpha)$$

diskutiert, wobei ∇_α^2 der Laplaceoperator für die Ortskoordinaten des Kerns α, W die molekulare Born-Oppenheimer-Energie, $\mathscr{Z}_\alpha$ die Kernladungszahl von α und $\varrho_\beta(\alpha)$ die elektronische Ladungsdichte bei α ist, die durch Orbitale erzeugt wird, die bei β zentriert sind.

Harmonische, inharmonische und biquadratische Gleichgewichtskonstanten werden mit Hilfe von molekularen und atomaren Hartree-Fock-Elektronendichten für eine Anzahl von zweiatomigen Molekülen mit Elementen der beiden ersten Reihen des Periodensystems berechnet. Eine Feldgradientenformel für ein Ladungsmodell bei harmonischen Kraftkonstanten

$$k_e = 3/R_e^3$$

wird angegeben, wobei k_e die Kraftkonstante und R_e der Atomabstand im Gleichgewicht ist. Diese Formel stellt eine Verbesserung gegenüber einer ähnlichen Formel von Bratož dar.

1. Introduction

In this paper, electrostatic methods will be presented for obtaining equilibrium force constants for diatomic molecules. Accuracy of the formulas appears to be competative with *ab initio* methods [1–4], curve fitting methods [5] and modeling methods [1–4, 6–8]. First we present some analytical formulas, followed by a

---

* Aided by research grants to the Johns Hopkins University from the National Institutes of Health and the National Science Foundation.

** This work is based on part of a thesis submitted by Alfred B. Anderson in partial fulfillment of the requirements for the degree Doctor of Philosophy, The Johns Hopkins University, 1970.

*** Present address: Chemistry Department, Indiana University, Bloomington, Indiana 47401, USA.

discussion of approximations leading to a field gradient model for harmonic force constants [9] which offers improvement over a formula due to Bratož [7]. Then we obtain a Poisson equation for vibrational potentials [10] which is a theoretical generalization of a formula due to Platt [6] that yields harmonic and higher order force constants in terms of electron densities at the nucleus.

2. Relationships between Vibrational Force Constants and Quadrupole Coupling Constants [9]

The Born-Oppenheimer energy W of a polyatomic molecule or solid in general is a function of the Cartesian coordinates of the nuclei referred to as arbitrary origin. If one of the coordinates X_α, Y_α, Z_α of the particular nucleus α of charge $\mathscr{Z}_\alpha$ is changed, the change in W is given by a Hellmann-Feynman formula of the type

$$\frac{\partial W}{\partial X_\alpha} = \mathscr{Z}_\alpha \left[\sum_{\beta \neq \alpha} \mathscr{Z}_\beta \left(\frac{X_\beta - X_\alpha}{R_{\alpha\beta}^3} \right) - \int \varrho (x - X_\alpha) \frac{\mathrm{d}\tau}{r_\alpha^3} \right], \tag{1}$$

where ϱ is the electronic charge density function, r_α is the distance from $\mathrm{d}\tau$ to nucleus α and x, y, z are Cartesian coordinates of $\mathrm{d}\tau$ relative to a given origin. Differentiation of Eq. (1) with respect to X_α gives a formula for the second derivative $k_{X_\alpha X_\alpha} = \partial^2 W/\partial X_\alpha^2$, and similarly we can obtain formulas for $k_{Y_\alpha Y_\alpha}$, $k_{Z_\alpha Z_\alpha}$, $k_{X_\alpha Y_\alpha} = \partial^2 W/\partial X_\alpha \partial Y_\alpha$, $k_{X_\alpha Z_\alpha}$ and $k_{Y_\alpha Z_\alpha}$. If we identify the corresponding six components of the electric field gradient tensor for the molecular charge distribution with nucleus α as origin,

$$q_{X_\alpha X_\alpha} = \sum_{\beta \neq \alpha} \mathscr{Z}_\beta \left(\frac{3(X_\beta - X_\alpha)^2}{R_{\alpha\beta}^2} - 1 \right) (R_{\alpha\beta}^3)^{-1} - \int \varrho \left(\frac{3(x - X_\alpha)^2}{r_\alpha^2} - 1 \right) \frac{\mathrm{d}\tau}{r_\alpha^3}, \text{ etc.}, \tag{2}$$

$$q_{X_\alpha Y_\alpha} = 3 \sum_{\beta \neq \alpha} \mathscr{Z}_\beta \left(\frac{(X_\beta - X_\alpha)(Y_\beta - Y_\alpha)}{R_{\alpha\beta}^5} \right) - 3 \int \varrho \left(\frac{(x - X_\alpha)(y - Y_\alpha)}{r_\alpha^5} \right) \mathrm{d}\tau \text{ etc.}, \tag{3}$$

then these formulas are

$$k_{X_\alpha X_\alpha} = \mathscr{Z}_\alpha \left[q_{X_\alpha X_\alpha} + \frac{4}{3} \pi \varrho(\alpha) - \int (x - X_\alpha) \frac{\partial \varrho}{\partial X_\alpha} \frac{\mathrm{d}\tau}{r_\alpha^3} \right], \text{ etc.}, \tag{4}$$

$$k_{X_\alpha Y_\alpha} = \mathscr{Z}_\alpha \left[q_{X_\alpha Y_\alpha} - \int (x - X_\alpha) \frac{\partial \varrho}{\partial Y_\alpha} \frac{\mathrm{d}\tau}{r_\alpha^3} \right], \text{ etc.} \tag{5}$$

Here the quantity $\varrho(\alpha)$ is the electronic charge density at nucleus α; it enters $k_{X_\alpha X_\alpha}$, $k_{Y_\alpha Y_\alpha}$, and $k_{Z_\alpha Z_\alpha}$ because $\nabla^2(1/r_\alpha) = -4\pi\delta(r_\alpha)$.

The first of Eqs. (4) is the equation discovered and applied by Salem for diatomic molecules [1]. If we add the three Eqs. (4), we obtain a formula for the Laplacian of the energy [9],

$$\nabla_\alpha^2 W = \mathscr{Z}_\alpha [4\pi\varrho(\alpha) - \int \nabla_\alpha \varrho \cdot \nabla_\alpha (\boldsymbol{r} - \boldsymbol{R}_\alpha)^{-1} \mathrm{d}\tau]. \tag{6}$$

According to Salem, in Eq. (4) $\mathscr{Z}_\alpha \frac{4}{3}\pi\varrho(\alpha)$ is generally much larger than $k_{X_\alpha X_\alpha}$ and $\mathscr{Z}_\alpha q_{X_\alpha X_\alpha}$, and similarly $\mathscr{Z}_\alpha 4\pi\varrho(\alpha)$ is greater than $\nabla_\alpha^2 W$ in Eq. (6). However, $\varrho(\alpha)$ can be eliminated from Eqs. (4) by subtraction, giving [9]

$$\begin{aligned} &k_{Z_\alpha Z_\alpha} - \frac{1}{2}(k_{X_\alpha X_\alpha} + k_{Y_\alpha Y_\alpha}) \\ &\quad = \mathscr{Z}_\alpha \left[\frac{3}{2} q_{Z_\alpha Z_\alpha} - \frac{1}{2}\int\left(2(z - Z_\alpha)\frac{\partial\varrho}{\partial Z_\alpha} - (x - X_\alpha)\frac{\partial\varrho}{\partial X_\alpha} - (y - Y_\alpha)\frac{\partial\varrho}{\partial Y_\alpha}\right)\frac{\mathrm{d}\tau}{r_\alpha^3}\right], \end{aligned} \tag{7}$$

$$k_{X_\alpha X_\alpha} - k_{Y_\alpha Y_\alpha} = \mathscr{Z}_\alpha \left[(q_{X_\alpha X_\alpha} - q_{Y_\alpha Y_\alpha}) - \int\left((x - X_\alpha)\frac{\partial\varrho}{\partial X_\alpha} - (y - Y_\alpha)\frac{\partial\varrho}{\partial Y_\alpha}\right)\frac{\mathrm{d}\tau}{r_\alpha^3}\right]. \tag{8}$$

Table 1. Predictions of equilibrium harmonic force constants, k_e, for some M^-H^+ and M^+H^- diatomic molecules; 10^5 cgs units

Molecule	$2/Re^3$ [a]	$3/Re^3$ [b]	k_e(exptl.) [c]
HF	5.98	8.97	(9.66)
HCl	2.23	3.34	(5.16)
HBr	1.63	2.45	(4.16)
HI	1.12	1.68	(3.14)
LiH	1.14	1.71	(1.03)
NaH	0.69	1.03	(0.78)
KH	0.41	0.61	(0.56)
RbH	0.35	0.52	(0.51)
CsH	0.30	0.45	(0.47)
BeH	1.14	1.70	(1.03)
BH	2.46	3.70	(3.04)
CH	3.28	4.92	(4.51)
OH	5.05	7.57	(7.79)
MgH	0.89	1.34	(1.28)
AlH	1.03	1.54	(1.62)
SiH	1.31	1.97	(2.96)
CaH	0.57	0.86	(0.98)
MnH	0.89	1.33	(1.30)
ZnH	1.14	1.71	(1.57)
GeH	1.15	1.72	(2.38)
NiH	1.44	2.16	(2.17)
CuH	1.47	2.21	(2.20)
SrH	0.47	0.70	(0.85)
InH	0.74	1.12	(1.28)
CdH	0.84	1.27	(1.20)
AgH	1.09	1.64	(1.82)
BaH	0.42	0.62	(0.81)
TlH	0.71	1.06	(1.14)
BiH	0.78	1.17	(1.71)
HgH	0.88	1.31	(1.14)
AuH	1.30	1.96	(3.14)

[a] This relation is discussed in Refs. [1] and [7] of text.

[b] Eq. (10) of text.

[c] Experimental values from D. R. Herschbach and V. W. Laurie, University of California, Radiation Laboratory Report UCRL 9694 (Berkeley, Calif., 1961).

These formulas and Eqs. (3) are completely general relations among force constants and quadrupole coupling constants eqQ_0.

For a diatomic molecule at equilibrium, there is one non-zero force constant $k_e = [k_{Z_\alpha Z_\alpha}]_e = [k_{Z_\beta Z_\beta}]_e$ and one independent component of the field gradient tensor at $\alpha, q_\alpha = [q_{Z_\alpha Z_\alpha}]_e$, and at $\beta, q_\beta = [q_{Z_\beta Z_\beta}]_e$. Eq. (8) is trivial. Eq. (7) becomes [9]

$$k_e = \mathscr{Z}_\alpha \left| \frac{3}{2} q_\alpha - \frac{1}{2} \int \left(2(z - Z_\alpha) \frac{\partial \varrho}{\partial Z_\alpha} - (x - X_\alpha) \frac{\partial \varrho}{\partial X_\alpha} - (y - Y_\alpha) \frac{\partial \varrho}{\partial Y_\alpha} \right) \frac{\mathrm{d}\tau}{r_\alpha^3} \right|_e, \tag{9}$$

and similarly for β. This is an exact relation between k_e and q_α. When the second term is negligible, which it often appears to be for the hydrogen atom, we have $k_e \approx \mathscr{Z}_\alpha(\frac{3}{2} q_\alpha)$; $k_e \approx \frac{3}{2} q_{\mathrm{H}}$. This relation was derived by Salem for ionic compounds $\mathrm{M^- H^+}$, but for ionic compounds $\mathrm{M^+ H^-}$ his relation was $k_e \approx q_{\mathrm{H}}$ [1]. The former appears preferable in both cases. For the $\mathrm{M^+ H^-}$ cases Salem used the Bratož relation $k_e = 2/R_e^3$ (a.u.) derived for a point charge ionic model [7]. Similar reasoning applied to Eq. (9) leads to the formula

$$k_e = 3/R_e^3 . \tag{10}$$

As may be seen in Table 1, predictions of k_e using Eq. (10) are quite accurate, definitely better than those from Bratož' formula.

3. Harmonic Force Constants from Electron Densities

Eq. (6) is not a particularly useful form for the divergence of the Hellmann-Feynman force on nucleus, because the two terms on the right are difficult to determine accurately and they approximately cancel. However, it greatly simplifies when ϱ is appropriately elucidated, giving a formula which allows approximate determination of vibrational force constants from electron densities alone, with no integrations.

The electronic charge density may be resolved into parts ϱ_α, ϱ_β perfectly following nuclei α and β (we let β represent all nuclei other than α), and the rest, a nonperfectly following part ϱ_{NPF}:

$$\varrho(\boldsymbol{r}, \boldsymbol{R}_\alpha, \boldsymbol{R}_\beta) = \varrho_\alpha(\boldsymbol{r} - \boldsymbol{R}_\alpha) + \varrho_\beta(\boldsymbol{r} - \boldsymbol{R}_\beta) + \varrho_{\mathrm{NPF}}(\boldsymbol{r}, \boldsymbol{R}_\alpha, \boldsymbol{R}_\beta) . \tag{11}$$

Putting this into Eq. (6) and using the easily derived relation

$$\mathscr{Z}_\alpha \int \nabla_\alpha \varrho(\boldsymbol{r} - \boldsymbol{R}_\alpha) \cdot \nabla_\alpha |\boldsymbol{r} - \boldsymbol{R}_\alpha|^{-1} \mathrm{d}\tau = \mathscr{Z}_\alpha 4\pi \varrho(\alpha) \tag{12}$$

leads to the formula

$$\nabla_\alpha^2 W = 4\pi \mathscr{Z}_\alpha [\varrho(\alpha) - \varrho_\alpha(\alpha)] - \mathscr{Z}_\alpha \int \nabla_\alpha \varrho_{\mathrm{NPF}}(\boldsymbol{r}, \boldsymbol{R}_\alpha, \boldsymbol{R}_\beta) \cdot \nabla_\alpha |\boldsymbol{r} - \boldsymbol{R}_\alpha|^{-1} \mathrm{d}\tau . \tag{13}$$

The consequence is that in Eq. (6) the density following nucleus α may be ignored and the density following nucleus β contributes nothing to the integral. Eq. (13) is exact.

The contribution of $\varrho_{\mathrm{NPF}}(\alpha)$ to the first term in Eq. (13) may be expected to be small, and the integral should be small as well. Making these assumptions, we obtain our final working formula, now approximate,

$$\nabla_\alpha^2 W = 4\pi \mathscr{Z}_\alpha \varrho_\beta(\alpha) . \tag{14}$$

This is of the form of a classical electrostatic Poisson equation.

We may deduce Eq. (14) from Eq. (13) more formally as in these two examples:

Case 1. Suppose ϱ_{NPF} itself perfectly followed some point $KR_\alpha + (1-K)R_\beta$ (for example the midpoint $\frac{1}{2}R_\alpha + \frac{1}{2}R_\beta$): $\varrho_{\mathrm{NPF}} = \varrho_{\mathrm{NPF}}(r - KR_\alpha - (1-K)R_\beta)$. Then one would have $\int \nabla_\alpha \varrho_{\mathrm{NPF}} \cdot \nabla_\alpha |r - R_\alpha|^{-1}\,d\tau = 4\pi K \varrho_{\mathrm{NPF}}(\alpha)$, and Eq. (14) follows if we make the reasonable assumption $\varrho_{\mathrm{NPF}}(\alpha) = 0$.

Case 2. Suppose the molecular density may be represented as the sum of atomic densities. Then Eq. (14) follows exactly, making it an "atoms in molecules" result, within the Hellmann-Feynman approximation.

Table 2. Force constants from electron densities: first row hydrides[a]

Molecule		$k_e \times 10^5$			$l_e \times 10^{13}$			$m_e \times 10^{21}$		
		Z_L	Z_H	Exptl.	Z_L	Z_H	Exptl.	Z_L	Z_H	Exptl.
HeH^+	$\chi^1\Sigma^+$	2.34	0.46		22.4	43.3		189	354	
LiH	$\chi^1\Sigma^+$	0.002	0.88	(1.026)	0.009	3.81	(3.63)	0.06	14.7	(11.5)
		0.468	0.450		1.14	2.26		2.32	9.79	
BeH	$\chi^2\Sigma^+$	2.96	1.52	(2.26)	10.6	7.92	(10.0)	32.1	36.6	(38.4)
		1.72	1.56		6.43	8.19		20.2	37.8	
BeH	$A^2\Pi_r$	0.05	1.31	(2.33)	0.2	6.92	(10.7)	0.6	32.5	
BeH^+	$\chi^1\Sigma^+$	0.05	0.96	(2.64)	0.2	5.53	(11.6)	0.7	27.8	(40.7)
BH	$\chi^1\Sigma^+$	5.10	2.30	(3.04)	23.7	12.7	(15.8)	96.5	62.6	(70.3)
		2.89	2.95		13.8	16.0		56.7	75.8	
BH^+	$\chi^2\Sigma^+$	3.38	1.03		18.2	6.56		82.6	36.9	
BH^+	$A^2\Pi_r$	0.233	0.593		1.31	3.79		6.08	21.4	
CH	$\chi^2\Pi_r$	6.20	2.97	(4.51)	34.8	18.1	(26.7)	171	98.2	(136)
		4.36	5.42		24.9	30.1		124	148	
CH^+	$\chi^1\Sigma^+$	5.45	1.47	(4.11)	34.0	9.84	(23.0)	183	58.5	
CH^-	$\chi^3\Sigma^-$	7.03	4.48		36.4	26.1		169	136	
NH	$\chi^3\Sigma^-$	7.03	3.65	(6.03)	45.3	24.1	(39.6)	259	141	
		5.72	8.62		37.6	49.2		217	250	
NH	$a^1\Delta$	6.79	3.43	(5.62)	43.9	22.6	(21.6)	251	132	
NH^+	$\chi^2\Pi_r$	4.94	1.37		34.5	9.70		211	61.0	
NH^-	$\chi^2\Pi_i$	8.16	5.59		49.9	35.3		273	198	
OH	$\chi^2\Pi_r$	7.57	3.88	(7.79)	55.1	27.6	(54.3)	355	174	(337)
		7.15	12.7		52.0	74.2		335	388	
OH	$A^2\Sigma^+$	3.52	1.72	(5.65)	26.2	12.4	(40.5)	172	79.3	
OH^+	$\chi^3\Sigma^-$	4.85	1.34	(4.88)	37.3	10.0	(32.4)	252	66.9	(202)
OH^+	$a^1\Delta$	4.81	1.28		37.1	9.66		252	64.7	
OH	$\chi^1\Sigma^+$	9.09	7.50		63.5	48.3		399	248	
HF	$\chi^1\Sigma^+$	7.88	3.96	(9.66)	63.4	30.0	(69.9)	453	202	(446)
		8.43	17.5		67.0	104		475	561	
HF^+	$\chi^2\Pi_i$	6.93	1.78		59.9	14.8		454	109	
HF^+	$A^2\Sigma^+$	4.07	0.83	(5.00)	36.1	7.23	(34.2)	280	55.9	(133)
NeH^+	$\chi^1\Sigma^+$	3.60	0.75		32.4	6.42		257	48.2	

[a] When possible, two sets of calculations are given. Bader's molecular densities are used first according to the method of Eqs. (15)–(17). Following unlabeled rows employ Clementi atomic densities according to Eqs. (15)–(17). Exceptional cases, labeled a, employ Clementi atomic densities only. Experimental values are in parentheses. See footnote c, Table 1; cgs units.

Columns labeled Z_L employ the charge of the light nucleus; those labeled Z_H employ the heavy nucleus.

Where blanks exist in the molecular density results, insufficient numerical density data was available for a five-point polynomial fit. In these cases the density was exceedingly small and could be expected to yield poor results.

Eq. (14) says that the Laplacian of the molecular potential energy, $\nabla_\alpha^2 W$, is the sum of the orbital densities from the other atoms β. At equilibrium for a diatomic molecule, Eq. (14) yields the harmonic force constant:

$$k_e = [\nabla_\alpha^2 W]_e = 4\pi \mathscr{Z}_\alpha \varrho_\beta(\alpha) . \tag{15}$$

From similar arguments Platt derived the formula for hydrides: $k_e = 4\pi\varrho_{\mathrm{UA}}(\mathrm{H})$, where ϱ_{UA} is the united atom density [6]. Predictions of the k_e using Eq. (15) for first row diatomic molecules are in Tables 2 5. Clementi atomic densities [11] and Hartree-Fock quality molecular densities are used according to the method of *Case 2*. In order to use molecular densities, we suppose ϱ_α and ϱ_β to be symmetric about α and β and take $\varrho_\beta(\alpha)$ to be the total density at a distance R_e from β in the opposite directions from α, and similarly for $\varrho_\alpha(\beta)$, as calculated from Hartree-Fock wave functions [12, 13]. The force term $[2/R\, \partial W/\partial R]_e$ is set equal to zero. Heavy atom densities yields accurate predictions of k_e; light atom densities give correct trends, but less accurate predictions, possibly because heavy atom

Table 3 Force constants from electron densities, second row hydrides[a]

Molecule		$k_e \times 10^{5}$			$-l_e \times 10^{11}$			$m_e \times 10^{21}$		
		Z_L	Z_H	Exptl.	Z_L	Z_H	Exptl.	Z_L	Z_H	Exptl.
NaH	$\chi^1\Sigma^+$	0.321	0.547	(0.782)	0.744	2.65	(2.61)	1.44	11.1	(7.45)
MgH	$\chi^2\Sigma^+$	1.39		(1.28)	3.88		(4.92)	8.71		(13.3)
		0.862	1.079		2.67	5.32		6.73	22.9	
MgH	$A^2\Pi_r$	0.07		(1.48)	0.31		(6.15)	1.14		
MgH$^+$	$\chi^1\Sigma^+$	0.09		(1.64)	0.37		(7.20)	1.44		(30.0)
AlH	$\chi^1\Sigma$	2.15		(1.62)	7.55		(6.72)	22.0		(24.6)
		1.35	0.082		4.82	0.51		14.7	2.85	
AlH$^+$	$\chi^2\Sigma^+$	1.49		(1.48)	6.09		(9.27)	20.4		
AlH$^+$	$A^2\Pi_r$	0.16		(1.76)	0.73		(9.90)	2.86		
SiH	$\chi^2\Pi_r$	2.56	2.49	(2.96)	10.8	12.6	(13.4)	38.3	56.0	(52.6)
		2.18	2.79		8.99	14.2		31.5	63.2	
SiH$^+$	$\chi^1\Sigma^+$	2.37	1.58		10.9	8.37		42.1	39.3	
SiH	$\chi^3\Sigma$	2.75			10.9			36.4		
PH	$\chi^3\Sigma$	2.78	2.56	(3.26)[b]	13.5	14.0		58.6	67.3	
		2.96	4.15		13.9	21.5		55.6	97.2	
PH	$a^1\Delta$	2.77	2.52		13.5	13.8		56.2	66.5	
PH$^+$	$\chi^2\Pi_r$	2.63	1.61	(3.04)	13.7	9.23	(14.6)	61.4	46.6	
PH	$\chi^2\Pi_i$	3.15	3.60		14.6	19.4		57.8	90.6	
SH	$\chi^2\Pi_i$	3.10	2.45	(4.19)[b]	16.8	14.5		78.7	75.5	
		3.83	6.06		19.9	31.9		89.2	147	
SH	$A^2\Sigma^+$	1.67	1.30		9.58	8.13		47.1	44.6	
SH$^+$	$\chi^3\Sigma$	2.86	1.46		16.4	9.01		81.1	49.1	
SH$^+$	$a^1\Delta$	2.85	1.42		16.4	8.82		81.2	48.2	
SH	$\chi^1\Sigma^+$	3.20	3.77		16.4	21.1		73.5	103	
HCl	$\chi^1\Sigma^+$	3.44	2.41	(5.16)	20.6	15.4	(28.4)	107	86.1	(167)
		4.83	8.56		27.4	45.8		136	215	
HCl$^+$	$\chi^2\Pi_i$	2.63	1.16	(4.13)	16.4	7.54	(23.0)	90.0	43.1	(92.2)
HCl$^+$	$A^2\Sigma^+$	0.534	0.271	(1.49)	3.32	1.73	(7.74)	18.4	9.65	

[a] Footnote a, Table 2.

[b] Experimental values from Varshni, Y. P.: J. chem. Physics **28**, 108 (1958).

densities are less perturbed in molecules. Five-point polynomial fits of density values spaced 0.1 a.u. apart for the atomic densities and 0.1 Å apart for the molecular densities were employed. (This allows us to evaluate derivatives of the densities later on.)

Table 4. Force constants from electron densities: first row homonuclear molecules[a]

Molecule		$k_e \times 10^5$		$-l_e \times 10^{13}$		$m_e \times 10^{21}$	
H_2	$^1\Sigma_g^+$	2.64	(5.69)[b]	19.0	(36.7)	125	(233)
		3.79		23.2		148	
Li_2[a]	$\chi^1\Sigma_g^+$	0.397	(0.255)	1.01	(0.546)	2.05	(0.857)
B_2	$^3\Sigma_g^-$	4.31	(3.58)	19.3	(18.1)	72.2	(63.7)
		4.61		20.8		81.6	
B_2	$^1\Delta_u$	4.27		19.1		75.7	
B_2	$^1\Sigma_u^+$	4.22		18.9		79.9	
B_2^+	$^2\Pi_u$	3.26		16.0		70.6	
B_2^-	$^2\Pi_u$	5.17		21.5		76.3	
C_2	$^1\Sigma_g^+$	12.0	(12.2)	67.2	(79.8)	327	
C_2[a]	$\chi^3\Pi_u$	12.3	(9.523)	67.4	(59.4)	322	(301)
C_2	$^3\Sigma_g^-$	14.7		78.9		378	
C_2	$^1\Delta_g$	14.6		78.5		367	
C_2	$^1\Sigma_g^-$	14.6		78.3		371	
C_2	$^1\Sigma_g^+$	16.3		88.3		411	
C_2^+	$^2\Pi_u$	11.4		64.7		324	
C_2^+	$^2\Pi_u$	9.57		57.2		305	
C_2	$^2\Pi_u$	18.2		92.5		408	
C_2^-	$^2\Pi_u$	29.4		153		694	
C_2	$^2\Sigma_g^+$	22.7		120		549	
C_2	$^2\Sigma_u^+$	24.3		128		573	
N_2	$^1\Sigma_g^+$	37.4	(23.0)	245	(178)	1416	(1195)
		30.9		200		1136	
N_2^+	$^2\Sigma_g^+$	20.3	(20.1)	145	(160)	900	
N_2^+	$^2\Pi_u$	19.9		139		838	
N_2^+	$^2\Pi_u$	27.4		193		1182	
N_2^+	$^2\Sigma_u^+$	29.3	(24.2)	206	(190)	1264	
$N_2^{+\,+}$	$^3\Sigma_g^-$	29.3		216		1405	
O_2	$^3\Sigma_g^-$	14.5	(11.8)	101	(87.3)	626	(544)
		16.9		114		680	
O_2	$^1\Delta_g$	13.7	(10.7)	96.4	(82.5)	586	
O_2	$^1\Sigma_g^+$	12.8	(9.67)	89.8	(75.9)	562	
O_2^+	$^2\Pi_g$	18.6	(16.6)	144	(143)	983	(1004)
O_2^-	$^2\Pi_g$	13.1		83.2		461	
$O_2^{+\,+}$	$^1\Sigma_g^+$	9.33		70.7		481	
F_2	$^1\Sigma_g^+$	2.36	(4.73)	18.0	(38.4)	124	(230)
		4.86		32.9		199	
F_2	$^1\Sigma_g^+$	2.82		20.2		120	
F_2	$^1\Sigma_g^+$	4.45		32.7		207	
F_2^+	$^2\Pi_g$	3.48		26.0		170	
F_2^+	$^2\Pi_u$	3.44		25.9		177	
F_2^+	$^2\Sigma_g^+$	2.15		16.5		122	
F_2^+	$^2\Sigma_u^-$	3.31		24.5		169	
$F_2^{+\,+}$	$^3\Sigma_g^-$	2.61		20.2		140	

---

[a] Footnote a, Table 2.

[b] Experimental values for H_2 from data in Hertzberg, G.: Spectra of diatomic molecules. Princeton: D. Van Nostrand Company, Inc. 1950.

Table 7. Examples of the effects of modifying the number of valence electrons in second row Clementi atomic charge densities on equilibrium force constants determined using Eqs. (15) to (17) of text; cgs units

Molecule	$k_e \times 10^5$		$-l_e \times 10^{13}$		$m_e \times 10^{21}$	
	Calc.	Exptl.[a]	Calc.	Exptl.[a]	Calc.	Exptl.[a]
Si_2	3.70	(2.12)	14.0	(8.55)	45.8	(29.5)
Si_2^{+2}	2.31	(2.12)	9.12	(8.55)	31.5	(29.5)
P_2	9.50	(5.56)	42.1	(27.2)	163	(106)
P_2^{+2}	7.07	(5.56)	31.9	(27.2)	126	(106)
P_2^{+4}	4.64	(5.56)	21.7	(27.2)	89.2	(106)

[a] Table 1, footnote c.

Predictions of l_e and of m_e using Eqs. (16), (17) are given in Tables 2–6, and they follow the same trends as for k_e. Predictions using second row Clementi atomic densities tend to be too large, as seen in Table 6. However, removing the contributions of one or two valence electrons can largely correct for this, as seen in Table 7. This suggests modifying the atomic valence population to fit the experimental k_e exactly in Eq. (14), and then calculating accurate higher order force constants with the modified density [14].

References

1. Salem, L.: J. chem. Physics **38**, 1227 (1963).
2. Ross, W. R., Phillipson, P.: J. chem. Physics **44**, 844 (1966)
3. Bishop, D. M., Macias, A.: J. chem. Physics **51**, 4997 (1969).
4. Kim, H.: J. chem. Physics **48**, 301 (1968).
   Schwendeman, R. H.: J. chem. Physics **44**, 556 (1966).
5. Krauss, M.: Compendium of *ab initio* calculations of molecular energies and properties. Nat. Bur. Std Technical Note **438** (1967).
6. Platt, J. R.: J. chem. Physics **18**, 932 (1950).
7. Bratož, S., Daudel, R., Roux, M., Allovena, M.: Rev. mod. Physics **32**, 412 (1960).
8. Empedocles, P.: J. chem Physics **46** 4475 (1967).
   Borkman, R. F., Simons, G., Parr, R. G.: J. chem. Physics **50**, 58 (1969).
9. Anderson, A. B., Handy, N. C., Parr, R. G.: J. chem. Physics **50**, 3634 (1969).
10. Parr, R. G.: J. chem. Physics **53**, 3375 (1970).
11. Clementi, E.: Tables of atomic functions, a supplement to the paper *Ab initio* computations in atoms and molecules. IBM Journal of Research and Development **9**, 2 (1965).
12. Bader, R. F. W., Cade, P. E.: Private communication of densities to be published in a monograph of molecular change distributions by the University of Chicago Press.
13. - - Hennecker, W. H., Keaveny, I.: J. chem. Physics **46**, 3341 (1967); — **47**, 3381 (1967); — **50**, 5313 (1969).
14. Empirical relationships (Anderson, A. B., Parr, R. G.: Chem. Physics Letters **10**, 293 (1971)) suggest using model densities of exponential form in Eq. (14) (Anderson, A. B., Parr, R. G.: J. chem. Physics **55**, 5490 (1971); **56**, 5204 (1972)).

Dr. A. B. Anderson
Chemistry Department, Indiana University
Bloomington, Indiana 47401, USA

Theoret. chim. Acta (Berl.) 26, 311—320 (1972)
© by Springer-Verlag 1972

Detailed Crossover Studies of Transition Metal Ions

I. The Octahedral and Tetrahedral d^4 and d^6 Electron Configurations

E. König and S. Kremer
Institut für Physikalische Chemie II, Universität Erlangen-Nürnberg, D-8520 Erlangen

Received November 22, 1971

The complete ligand field, interelectronic repulsion, and spin-orbit interaction matrices were solved for the octahedral and tetrahedral d^4 and d^6 electron configurations. The results are employed in a detailed study of the crossover region. It is demonstrated that, close to the crossover, complicated mixing and interaction patterns may arise. A sharp crossover is encountered in the octahedral d^6 system exclusively where Γ_1 and Γ_5 levels are involved. In all situations where the two ground levels transform according to the same irreducible representation, the crossover is redefined by that value of $10Dq$ where both ground terms participate in the lowest level to equal amounts.

Die vollständigen Matrizen des Ligandenfeldes, der Elektronenwechselwirkung und der Spin-Bahn-Kopplung wurden für die Elektronenkonfigurationen d^4 und d^6 in Feldern oktaedrischer und tetraedrischer Symmetrie diagonalisiert. Die Ergebnisse werden in einer eingehenden Untersuchung des "crossover"-Bereiches eingesetzt. Es wird gezeigt, daß komplizierte Mischungs- und Wechselwirkungsstrukturen in der Nähe des Überschneidungspunktes der Grundterme auftreten können. Ein scharfer Schnittpunkt wird allein im oktaedrischen d^6-System erhalten, wobei die Niveaus Γ_1 und Γ_5 unmittelbar beteiligt sind. In allen Fällen, in denen sich die zwei tiefsten Niveaus der zwei Grundterme nach derselben irreduziblen Darstellung transformieren, wird der Überschneidungspunkt durch denjenigen Wert von $10Dq$ neu definiert, bei dem beide Grundterme zum tiefsten Niveau zu gleichen Teilen beitragen.

1. Introduction

It is a peculiar property of the d^4, d^5, d^6, and d^7 electron configurations in a field of octahedral symmetry that, depending on field strength, one of two possible ground terms may be stabilized. The two terms are characterized by a different symmetry transformation property and a different value of the total spin S. A similar situation is encountered with the configurations d^4, d^5, and d^6 within tetrahedral symmetry. The concept of spin-pairing energy [1] has been introduced as the particular value of the octahedral or tetrahedral ligand field splitting parameter $\Delta = 10Dq$ at the crossover of ground terms. However, the spin-pairing energy is well defined only as far as spin-orbit interaction is completely neglected.

The effect of spin-orbit coupling is, in general, to produce an additional splitting of all but a few terms and to give rise to a significant interaction between the levels thus formed. The interaction becomes the more marked the more the crossover is being approached. Under specific circumstances, complicated splitting and interaction patterns may arise which may extend over an energy range of $1000\,\mathrm{cm}^{-1}$ or more. As a consequence, the original crossover concept becomes much less well founded than usually assumed and, in some cases, a modified definition of the crossover is called for.

Recently [2], we have considered in some detail the disposition of the lowest-energy spin-orbit levels in an octahedral d^6 ion close to the $^5T_2 - {}^1A_1$ crossover of ground terms. Additional studies demonstrate that this particular situation is one of the most simple ones to be expected. In the present investigation, we therefore examine the octahedral and tetrahedral d^4 and d^6 electron configurations side by side. The results should exemplify the complications arising close to the crossover and should serve to stimulate more accurate physical measurements on suitable transition metal containing systems. To this end and in contrast to our earlier study [2], values of the interelectronic repulsion parameters will be employed which should facilitate direct comparison with experiment.

2. Calculation Procedures and Results

The calculations including the ligand field, interelectronic repulsion, and spin-orbit interaction were performed within the complete configuration interaction approach. The appropriate Hamiltonian may be written

$$\mathcal{H} = \sum_i \left\{ -\frac{\hbar^2}{2m} \nabla_i^2 - \frac{Ze^2}{r_i} + \kappa \zeta_i l_i \cdot s_i \right\} + \sum_{i>j} \frac{e^2}{r_{ij}} + V_{LF} \tag{1}$$

where the summation extends over the d electrons and where all the quantities have their usual meaning. Both the strong-field and the weak-field methods were applied, and complete agreement of all results was achieved. In the strong-field approach, the methods outlined by Griffith [3] were generally followed. These procedures were described in detail previously [2, 4]. In the weak-field approach, use has been made of Racah algebraic methods, and these we have briefly delineated elsewhere [4]. The complete octahedral and tetrahedral d^4 and d^6 electron problems thus generate, within the strong-field as well as in the weak-field approach, an overall 91 × 91 matrix. The resulting secular problems which may be partly factorized on the basis of symmetry were solved. From the results, eigenvalues and eigenvectors pertinent to the lowest energy levels in the direct neighborhood of the crossover were extracted.

It is well known that octahedral and tetrahedral fields give rise to a splitting into the same groups of levels, e and t_2, although their order is inverted and the sign of their separation is reversed, viz.

$$Dq_{\text{tet}} = -\tfrac{4}{9} Dq_{\text{oct}} \,. \tag{2}$$

Since confusion is not likely to occur, we will drop the suffix of Dq used in Eq. (2), negative values indicating always tetrahedral Dq and positive values indicating octahedral Dq. The sign changes of Dq and ζ required in applications of the matrices to the problems at hand have been discussed elsewhere [4].

Fig. 1 shows the central region of the complete ligand field and spin-orbit interaction diagram for an octahedral d^4 electron system and, in Fig. 2, the cor-

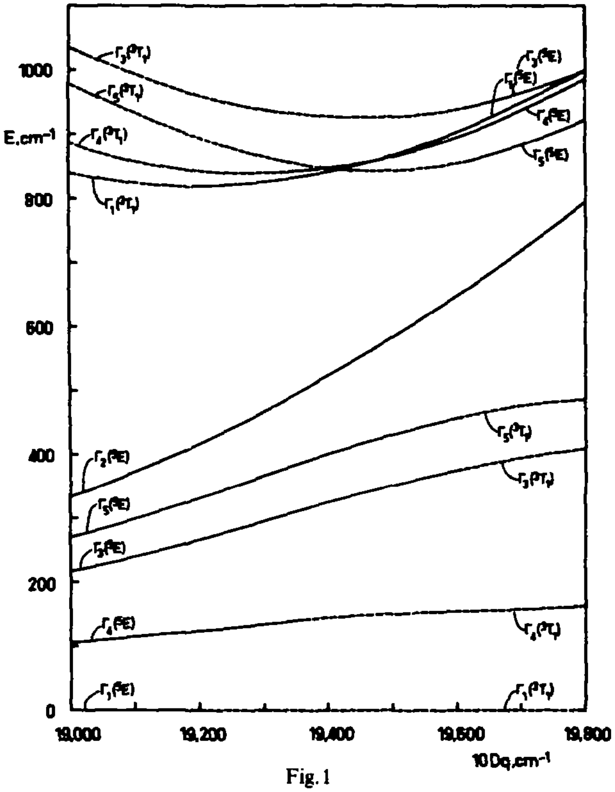

Fig. 1

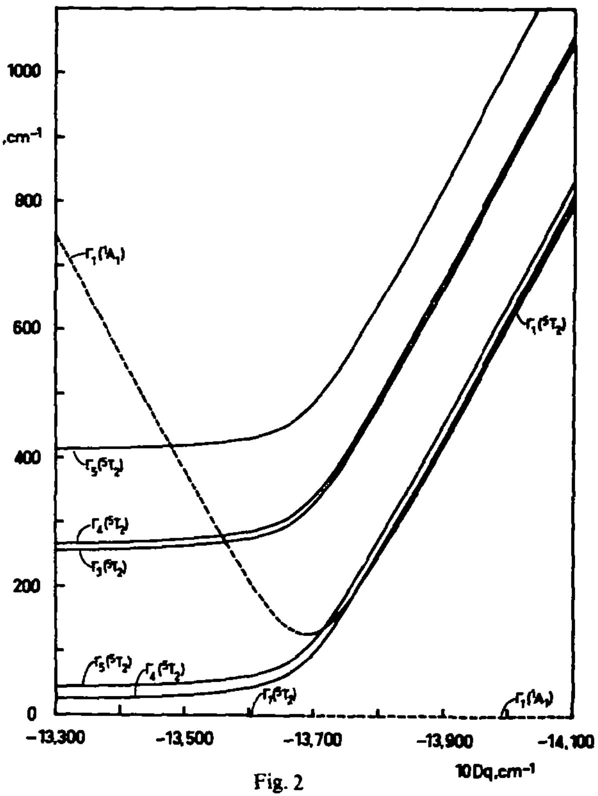

Fig. 2

Fig. 1. Lowest energy levels originating in the terms ^5E (t_2^3 ($^4A_2$) e) (full lines) and $^3T_1$ (t_2^4) (broken lines) of an octahedral d^4 system ($B = 800$ cm^{-1}, $C = 4B$, $\zeta = 290$ cm^{-1}) in the region of the crossover (i.e. $10Dq = 19210$ cm^{-1})

Fig. 2. Lowest energy levels originating in the terms $^5T_2$ (e^2 ($^3A_2$) t_2^2 ($^3T_1$)) (full lines) and $^1A_1$ (e^4) (broken line) of a tetrahedral d^4 system ($B = 800$ cm^{-1}, $C = 4B$, $\zeta = 290$ cm^{-1}) in the region of the crossover (i.e. $10Dq = -13689$ cm^{-1})

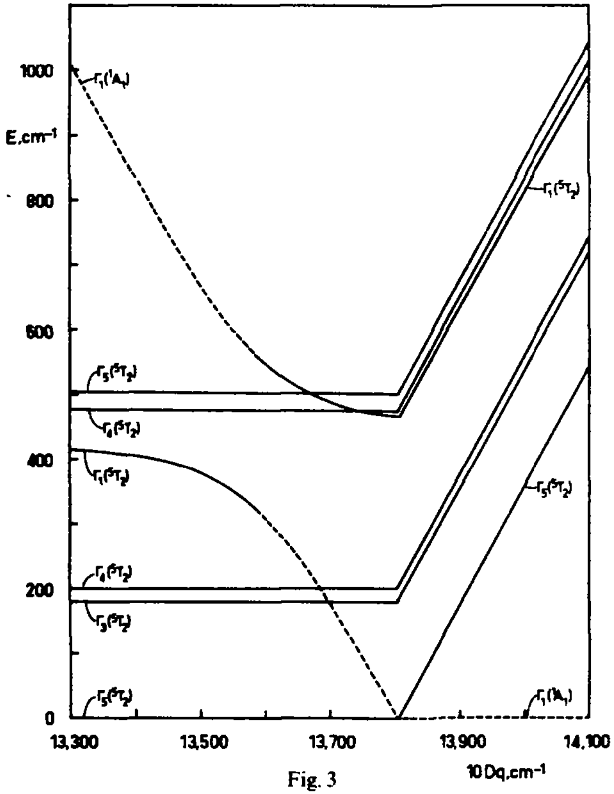

Fig. 3

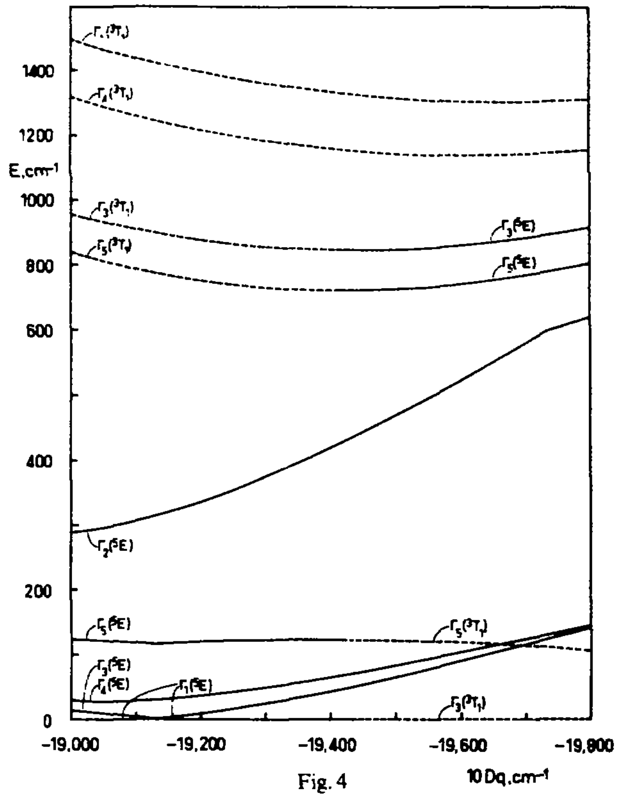

Fig. 4

Fig. 3. Lowest energy levels originating in the terms $^5T_2$ (t_2^4 ($^3T_1$) e^2 ($^3A_2$)) (full lines) and $^1A_1$ (t_2^6) (broken line) of an octahedral d^6 system ($B = 806$ cm^{-1}, $C = 4B$, $\zeta = 420$ cm^{-1}) in the region of the crossover (i.e. $10Dq = 13804.5$ cm^{-1})

Fig. 4. Lowest energy levels originating in the terms ^5E (e^3 t_2^3 ($^4A_2$)) (full lines) and $^3T_1$ (e^4 t_2^2) (broken lines) of a tetrahedral d^6 system ($B = 806$ cm^{-1}, $C = 4B$, $\zeta = 420$ cm^{-1}) in the region of the crossover (i.e. $10Dq = -19440$ cm^{-1})

responding plot for a tetrahedral d^4 ion is presented. The parameter values employed in the underlying calculations are $B = 800\,\text{cm}^{-1}$, $C = 4B$, and $\zeta = 290\,\text{cm}^{-1}$ thus corresponding approximately to, e.g., a hexaquoion of Cr^{2+} or Mn^{3+}.[1] Fig. 3 and Fig. 4 display similar diagrams pertinent to the octahedral and tetrahedral d^6 electron configuration, respectively. Here we assumed $B = 806\,\text{cm}^{-1}$, $C = 4B$, and $\zeta = 420\,\text{cm}^{-1}$ again corresponding roughly to the hexaquoions of Fe^{2+} and Co^{3+}.[2] The magnetic behavior of these systems has likewise been calculated and is discussed elsewhere [4]. The full ligand field and spin-orbit interaction diagrams for the octahedral and tetrahedral d^4 and d^6 electron configurations will be presented in a forthcoming publication [5].

3. Delineation of the Lowest Levels Close to the Crossover

Octahedral d^4 System

In the octahedral d^4 electron system, the two terms involved in the crossover are $^5E(t_2^3(^4A_2)\,e)$ and $^3T_1(t_2^4)$, both being g on the basis of parity. The $^3T_1(t_2^4)$ term interacts with six higher energy $^3T_1$ terms via configuration interaction, while the ^5E is pure. If spin-orbit coupling is included, the splitting is according to $^3T_1 \rightarrow \Gamma_1 + \Gamma_3 + \Gamma_4 + \Gamma_5$ and $^5E \rightarrow \Gamma_1 + \Gamma_2 + \Gamma_3 + \Gamma_4 + \Gamma_5$. A peculiar property of the system is that, in the neighborhood of the crossover, all levels resulting from the two terms except Γ_2 are considerably mixed by spin-orbit interaction. With $10Dq$ approaching the crossover more closely, the amount of intermixing rises progressively. Thus, if $10Dq = 18\,700\,\text{cm}^{-1}$ is assumed, the lowest level Γ_1 at $0.0\,\text{cm}^{-1}$ consists of 75.17% $|^5E(t_2^3(^4A_2)\,e)\rangle$, 24.06% $|^3T_1(t_2^4)\rangle$, and 0.77% various other contributions, whereas the Γ_1 level at $948.4\,\text{cm}^{-1}$ is composed of 73.08% $|^3T_1(t_2^4)\rangle$, 24.76% $|^5E(t_2^3(^4A_2)\,e)\rangle$, and 2.16% other contributions, cf. Fig. 1. The next highest amount of intermixing arises with the Γ_4 levels, the lower one at $78.9\,\text{cm}^{-1}$ being essentially 83.13% $|^5E(t_2^3(^4A_2)\,e)\rangle$ and 16.35% $|^3T_1(t_2^4)\rangle$, whereas the higher one at $1018.3\,\text{cm}^{-1}$ is 80.79% $|^3T_1(t_2^4)\rangle$ and 16.82% $|^5E(t_2^3(^4A_2)\,e)\rangle$. There is apparent, in addition, an appreciable mixing of the Γ_3 and Γ_5 levels of the two terms.

Consequently, *the actual crossover is much less well defined than, e.g., in the octahedral d^6 problem.* To clearly demonstrate this situation let us consider Fig. 1 again. The lowest level Γ_1 at $0.0\,\text{cm}^{-1}$ consists, at $10Dq = 19\,200\,\text{cm}^{-1}$, of 49.94% $|^5E(t_2^3(^4A_2)\,e)\rangle$ and 48.63% $|^3T_1(t_2^4)\rangle$, whereas, at $10Dq = 19\,300\,\text{cm}^{-1}$, its composition is determined by 54.29% $|^3T_1(t_2^4)\rangle$ and 44.13% $|^5E(t_2^3(^4A_2)\,e)\rangle$. If we decide to define the crossover by that value of $10Dq$ where, in the lowest Γ_1 level, equal contributions from the $^5E(t_2^3(^4A_2)\,e)$ and $^3T_1(t_2^4)$ terms are involved, the crossover appears at $19\,210\,\text{cm}^{-1}$. However, we then have to accept the fact that in higher levels Γ_j, $j = 3, 4, 5$, the condition of equal contributions will be satisfied, in general, at higher values of $10Dq$. Thus, e.g., at $10Dq = 19300\ \mathrm{cm}^{-1}$, the lower Γ_4 level (at $134.5\ \mathrm{cm}^{-1}$) consists essentially of 53.44% $|^5E(t_2^3(^4A_2)\,e)\rangle$ and 45.26% $|^3T_1(t_2^4)\rangle$, whereas, at $10Dq = 19400\ \mathrm{cm}^{-1}$, the composition of the Γ_4 level (now at $142.9\ \mathrm{cm}^{-1}$) is 51.88% $|^3T_1(t_2^4)\rangle$ and 46.65% $|^5E(t_2^3(^4A_2)\,e)\rangle$, the "crossover" of the two Γ_4 levels then being at $19360\ \mathrm{cm}^{-1}$. Likewise, at $10Dq = 19600\ \mathrm{cm}^{-1}$, the lower Γ_3 level (at $375.5\ \mathrm{cm}^{-1}$) is formed essentially of 51.70% $|^5E(t_2^3(^4A_2)\,e)\rangle$ and 46.91% $|^3T_1(t_2^4)\rangle$, whereas if $10Dq = 16700\ \mathrm{cm}^{-1}$, the composition of that level (now at $395.5\ \mathrm{cm}^{-1}$) is 55.07% $|^3T_1(t_2^4)\rangle$ and 43.30% $|^5E(t_2^3(^4A_2)\,e)\rangle$, the "crossover" of the Γ_3 levels resulting close to $19610\ \mathrm{cm}^{-1}$. Finally, at $10Dq = 19600\ \mathrm{cm}^{-1}$, the lower Γ_5 level (at $457.3\ \mathrm{cm}^{-1}$) consists of 51.68% $|^5E(t_2^3(^4A_2)\,e)\rangle$ and 46.90% $|^3T_1(t_2^4)\rangle$, the corresponding values being, at $10Dq = 19700\ \mathrm{cm}^{-1}$, 39.93% and 58.32%, respectively (level Γ_5 at $475.7\ \mathrm{cm}^{-1}$). This then fixes the "crossover" of Γ_5 levels again close to $19610\ \mathrm{cm}^{-1}$. Thus, in the example studied here, cf. the octahedral d^4 configuration, there is a region extending over about $400\ \mathrm{cm}^{-1}$ (i.e. from $10Dq = 19210\ \mathrm{cm}^{-1}$ to $19610\ \mathrm{cm}^{-1}$) within that the levels Γ_j, $j = 1, 3, 4, 5$, resulting from the terms $^5E(t_2^3(^4A_2)\,e)$ and $^3T_1(t_2^4)$ cross[3].

---

[1] We assumed $B_{\text{free}}(\text{Cr}^{2+}) = 899\,\text{cm}^{-1}$, $B_{\text{free}}(\text{Mn}^{3+}) = 1083\,\text{cm}^{-1}$ which values are based on a least square fit of the free ion spectra ($C_{\text{free}}(\text{Cr}^{2+}) = 3147\,\text{cm}^{-1}$, $C_{\text{free}}(\text{Mn}^{3+}) = 3916\,\text{cm}^{-1}$) and the nephelauxetic ratios $\beta = 0.88$ and $\beta = 0.75$ for $\text{M(H}_2\text{O)}_6^{n+}$ ions where $n = 2$ and $n = 3$, respectively. With $\zeta(\text{Cr}^{2+}) = 226\,\text{cm}^{-1}$ and $\zeta(\text{Mn}^{3+}) = 346\,\text{cm}^{-1}$, the above average values follow.

[2] We assumed $B_{\text{free}}(\text{Fe}^{2+}) = 916\,\text{cm}^{-1}$ based on a least square fit of the free ion sepctrum ($C_{\text{free}}(\text{Fe}^{2+}) = 3867\,\text{cm}^{-1}$) and $\beta = 0.88$ as above. The resulting $B = \beta \cdot B_{\text{free}}$ applies approximately also in a $\text{Co(H}_2\text{O)}_6^{3+}$ ion if $B_{\text{free}}(\text{Co}^{3+}) = 1100\,\text{cm}^{-1}$ and $\beta = 0.75$ are used. $\zeta = 420\,\text{cm}^{-1}$ is the free ion Fe^{2+} value.

Tetrahedral d^4 System

A considerably more simple situation is encountered if the d^4 electron system is subject to a field of tetrahedral symmetry. The ground terms involved are, in this case, $^1A_1(e^4)$ and $^5T_2(e^2(^3A_2)\,t_2^2(^3T_1))$, the $^1A_1(e^4)$ interacting with four higher energy $^1A_1$ terms via configuration interaction, whereas the $^5T_2(e^2(^3A_2)\,t_2^2(^3T_1))$ is pure. The splitting by spin-orbit interaction is according to $^5T_2 \rightarrow \Gamma_1 + \Gamma_3 + 2\Gamma_4 + 2\Gamma_5$ and $^1A_1 \rightarrow \Gamma_1$. Thus only the two Γ_1-levels are expected to be mixed via spin-orbit coupling. This is, indeed, clearly apparent from Fig. 2 where the lowest levels close to the crossover are displayed. In somewhat more detail then the intermixing is not significant at some distance from the crossover. If $10Dq = -13300\ \mathrm{cm}^{-1}$, e.g., is assumed, the lowest level Γ_1 at $0.0\ \mathrm{cm}^{-1}$ is 98.26% $|^5T_2(e^2(^3A_2)\,t_2^2(^3T_1))\rangle$, 0.99% $|^3T_1(e^3t_2)\rangle$, and only 0.59% $|^1A_1(e^4)\rangle$ etc., while the Γ_1 level at $745.8\ \mathrm{cm}^{-1}$ is made up to 93.61% of $|^1A_1(e^4)\rangle$, 3.37% $|^1A_1(e^2(^1A_1)\,t_2^2(^1A_1))\rangle$, and no larger amount from the $^5T_2$ term. As the crossover is approached more closely the intermixing increases drastically. At $10Dq = -13680\ \mathrm{cm}^{-1}$, the Γ_1 level at $0.0\ \mathrm{cm}^{-1}$ is now composed of 54.47% $|^5T_2(e^2(^3A_2)\,t_2^2(^3T_1))\rangle$, 41.32% $|^1A_1(e^4)\rangle$, and 4.21% various other contributions. Conversely, the level Γ_1 at $127.5\ \mathrm{cm}^{-1}$ consists of 53.27% $|^1A_1(e^4)\rangle$, 44.51% $|^5T_2(e^2t_2^2)\rangle$, and 2.22% other contributions. On the other hand, if $10Dq = -13700\ \mathrm{cm}^{-1}$, the Γ_1 level at $0.0\ \mathrm{cm}^{-1}$ consists of 55.32% $|^1A_1(e^4)\rangle$ and 39.84% $|^5T_2(e^2t_2^2)\rangle$, whereas the contributions to that at $128.9\ \mathrm{cm}^{-1}$ are 39.29% and 59.13%, respectively. It follows that the crossover should be close to $10Dq = -13689\ \mathrm{cm}^{-1}$. In the tetrahedral d^4 electron configuration then the crossover is rather *precisely defined* by that value of $10Dq$ where *equal contributions* from the ${}^1A_1(e^4)$ and ${}^5T_2(e^2({}^3A_2)\,t_2^2({}^3T_1))$ terms are encountered in the lowest energy Γ_1 level. We would like to point out that both the two Γ_4 and the two Γ_5 levels originating in the ${}^5T_2$ ground term are highly intermixed, this mixing, however, is not particularly dependent on $10Dq$.

---

[3] We would like to point out the fact that the contributions to the crossing levels are not reciprocal. The values listed above apply to the lower member of the pair in consideration. The contributions to the higher member of a pair are, in general, somewhat different due to additional mixing with higher energy levels.

Octahedral d^6 System

The behavior of the octahedral d^6 electron system close to the crossover has been treated previously [2] and will be discussed here, therefore, only briefly. The terms involved in the crossover which are all g are ${}^1A_1(t_2^6)$ and ${}^5T_2(t_2^4({}^3T_1)\,e^2({}^3A_2))$, configuration interaction being the reason for mixing of the ${}^1A_1(t_2^6)$ and four higher ${}^1A_1$ terms, while the ${}^5T_2$ is pure. The splitting by spin-orbit coupling is according to ${}^5T_2 \rightarrow \Gamma_1 + \Gamma_3 + 2\Gamma_4 + 2\Gamma_5$ and ${}^1A_1 \rightarrow \Gamma_1$ and thus only the two Γ_1 levels interact. The maximum of this interaction is observed at $10Dq = 13\,593\ \mathrm{cm}^{-1}$ (cf. Fig. 3) where the two levels $\Gamma_1[{}^1A_1(t_2^6)]$ and $\Gamma_1[{}^5T_2(t_2^4({}^3T_1)\,e^2({}^3A_2))]$ change their labels. The crossover, however, which is defined by the intersection of the former level with $\Gamma_5[{}^5T_2(t_2^4({}^3T_1)\,e^2({}^3A_2))]$ occurs at about $10Dq = 13\,804.5\ \mathrm{cm}^{-1}$. It should be noted that these two levels neither interact on the basis of spin-orbit coupling nor on that of configuration interaction. This is the reason that, of the four systems studied at present, the crossover is most precisely established in the octahedral d^6 electron configuration.

Tetrahedral d^6 System

Finally, we turn to the example of the tetrahedral d^6 electron system where the terms involved in the crossover are ${}^3T_1(e^4t_2^2)$ and ${}^5E(e^3t_2^3({}^4A_2))$. The ${}^3T_1(e^4t_2^2)$ interacts with six higher ${}^3T_1$ terms on the basis of configuration interaction, whereas the ${}^5E$ is pure. The splitting due to spin-orbit coupling is according to ${}^3T_1 \rightarrow \Gamma_1 + \Gamma_3 + \Gamma_4 + \Gamma_5$ and ${}^5E \rightarrow \Gamma_1 + \Gamma_2 + \Gamma_3 + \Gamma_4 + \Gamma_5$ having the consequence that all levels except Γ_2 interact at the crossover. The situation here is thus roughly similar to that in the octahedral d^4 system, although differences exist in detail. Again the amount of intermixing rises as $10Dq$ approaches the crossover. At $10Dq = -19\,100\ \mathrm{cm}^{-1}$, e.g., the lowest level Γ_1 at $0.0\ \mathrm{cm}^{-1}$ consists of 79.86% $|{}^5E(e^3t_2^3({}^4A_2))\rangle$, 19.42% $|{}^3T_1(e^4t_2^2)\rangle$, and 0.72% various other contributions, whereas the Γ_1 level at $1442.0\ \mathrm{cm}^{-1}$ is formed of 77.13% $|{}^3T_1(e^4t_2^2)\rangle$, 20.02% $|{}^5E(e^3t_2^3({}^4A_2))\rangle$, and 2.85% other contributions (cf. Fig. 4). An even higher amount of mixing is encountered in the Γ_3 levels, the lower one at only $2.94\ \mathrm{cm}^{-1}$ being essentially 67.35% $|{}^5E(e^3t_2^3({}^4A_2))\rangle$ and 31.64% $|{}^3T_1(e^4t_2^2)\rangle$, whereas the higher energy counterpart at $905.9\ \mathrm{cm}^{-1}$ is 65.49% $|{}^3T_1(e^4t_2^2)\rangle$ and 32.57% $|{}^5E(e^3t_2^3({}^4A_2))\rangle$. In addition, the Γ_4 and Γ_5 levels are likewise intermixed, the amount of mixing being intermediate between that of the Γ_1 and that of the Γ_3 level. At about $10Dq = -19\,130\ \mathrm{cm}^{-1}$ the lowest two levels, viz. Γ_1 and Γ_3, change their positions or, more accurately, Γ_1 is only $0.79\ \mathrm{cm}^{-1}$ above Γ_3 at this value of $10Dq$. The actual crossover then arises between the Γ_3 levels $\Gamma_3[{}^5E(e^3t_2^3({}^4A_2))]$ and $\Gamma_3[{}^3T_1(e^4t_2^2)]$. If, in analogy to the octahedral d^4 system, the crossover is taken again as that value of $10Dq$ where equal contributions of these two levels are involved, the crossover occurs quite accurately at $10Dq = -19440\,\text{cm}^{-1}$. At this field value, the lower Γ_3 level at $0.0\,\text{cm}^{-1}$ contains 49.29% $|^5E(e^3t_2^3(^4A_2))\rangle$ and 49.22% $|^3T_1(e^4t_2^2)\rangle$ and, incidentally, the higher one (at $846.8\,\text{cm}^{-1}$) consists of 50.63% and 47.97%, respectively. With this definition of the crossover, we again have to accept that the condition of equal contributions will be fulfilled, in the higher levels (resulting from the ground term) Γ_j, $j = 1, 4, 5$, at different values of $10Dq$. Thus, e.g., we find that, at $10Dq = -19400\,\text{cm}^{-1}$, the composition of the lower Γ_5 level (at $122.0\,\text{cm}^{-1}$) is 51.20% $|^5E(e^3t_2^3(^4A_2))\rangle$ and 47.33% $|^3T_1(e^4t_2^2)\rangle$, whereas, at $10Dq = -19450\,\text{cm}^{-1}$, the Γ_5 level (now at $121.6\,\text{cm}^{-1}$) consists of the contributions of 47.21% and 51.22%, respectively. Interpolation results in a "crossover" of the Γ_5 levels at $10Dq = -19425\,\text{cm}^{-1}$. The corresponding situation with the Γ_4 levels may be experienced at $10Dq = -19800\,\text{cm}^{-1}$ where the lower level at $143.7\,\text{cm}^{-1}$ is formed of 51.62% $|^5E(e^3t_2^3(^4A_2))\rangle$ and 46.93% $|^3T_1(e^4t_2^2)\rangle$ and where, at $10Dq = -19900\,\text{cm}^{-1}$, the contributions have changed to 46.92% and 51.51%, respectively (the Γ_4 level is now at $163.8\,\text{cm}^{-1}$), cf. Fig. 4. Here, the "crossover" of Γ_4 levels obtains at about $10Dq = -19850\,\text{cm}^{-1}$. Finally, at $10Dq = -20000\,\text{cm}^{-1}$, the lower Γ_1 level at $195.0\,\text{cm}^{-1}$ consists of 50.19% $|^5E(e^3t_2^3(^4A_2))\rangle$ and 48.21% $|^3T_1(e^4t_2^2)\rangle$, the corresponding values at $10Dq = -20100\,\text{cm}^{-1}$ (Γ_1 level at $221.0\,\text{cm}^{-1}$) being 46.08% and 52.20%, respectively. This then gives the "crossover" of Γ_1 levels at approximately $10Dq = -20020\,\text{cm}^{-1}$. It follows that there is, in fact, a region of about $600\,\text{cm}^{-1}$ (i.e. 19425 to $20020\,\text{cm}^{-1}$) in $10Dq$ within that the levels Γ_j, $j = 1, 3, 4, 5$, resulting from the two ground terms intersect.

4. Generalizations and Conclusions

It has been shown above that, due to spin-orbit interaction, the detailed situation close to the crossover in octahedral and tetrahedral d^4 and d^6 electron systems is considerably more complicated than usually appreciated. In particular, the levels originating in the two ground terms which are involved in the crossover may be significantly spin-mixed and intersections between corresponding levels may be spread out over a region of up to $600\,\text{cm}^{-1}$ in $10Dq$. According to this study, the crossover is precisely defined only if the two levels participating in the crossover transform according to different irreducible representations, e.g. $\Gamma_1[^1A_1(t_2^6)]$ and $\Gamma_5[^5T_2(t_2^4(^3T_1)\,e^2(^3A_2))]$ within the d^6 octahedral system. If both levels transform according to the same irreducible representation, however, it is best to redefine the crossover by that value of $10Dq$ where the two ground terms participate to equal amounts in the lowest level. This definition is suggested by the situations discussed above under the octahedral d^4 and the tetrahedral d^4 and d^6 systems.

Recently, we calculated the spin-pairing energy in d^4, d^5, d^6, and d^7 configurations of octahedral and tetrahedral symmetry in absence of spin-orbit interaction [1]. It may be of some interest to compare the $10Dq$-values at the crossovers which result if spin-orbit coupling is or is not taken into account in the present systems. The corresponding values are compiled in Table 1. It should be apparent that the results are indeed affected to some extent, the values of $10Dq$ at the crossover being shifted by up to $230\,\text{cm}^{-1}$, viz. the octahedral d^4 system.

Table 1. Values of 10*Dq* (in cm^{-1}) at the crossover in octahedral and tetrahedral d^4 and d^6 electron systems. The results are from complete configuration interaction calculations with or without spin-orbit coupling (d^4: $B = 800\,\mathrm{cm}^{-1}$, $C = 4B$, $\zeta = 290\,\mathrm{cm}^{-1}$; d^6: $B = 806\,\mathrm{cm}^{-1}$, $C = 4B$, $\zeta = 420\,\mathrm{cm}^{-1}$)

System	With spin-orbit coupling [present work]	Without spin-orbit coupling [1]
d^4 octahedral	19210	19440
d^6 octahedral	13804.5	13702
d^4 tetrahedral[a]	−13689	−13600
d^6 tetrahedral[a]	−19440	−19586

[a] Values listed are $10Dq_{\mathrm{tet}}$. To convert to $10Dq_{\mathrm{oct}}$ multiply by (4/9).

Examples for more or less octahedrally coordinated complexes of iron(II) which are close to the crossover are abundant in literature [6]. In view of the present results it is not surprising that, in all these systems, essentially pure ground states ${}^1A_1(t_2^6)$ and ${}^5T_2(t_2^4e^2)$ are observed experimentally [7- 10], their ratio being dependent on temperature [9, 10] as well as on pressure [11, 12]. This may now be understood as consequence of the sharp intersection between the two levels $\Gamma_1[{}^1A_1(t_2^6)]$ and $\Gamma_5[{}^5T_2(t_2^4({}^3T_1)\,e^2({}^3A_2))]$ within the octahedral d^6 configuration, cf. Fig. 3.

On the other hand, there is recent evidence [13] that some almost octahedral complexes of manganese(III) are fairly close to the crossover. Since, in the octahedral d^4 configuration, the behavior of the lowest levels is rather complicated (cf. Fig. 1 and the discussion in Section (3) above), physical properties characteristic of spin-mixed ground states should be expected. Although the magnetic moments of the compounds are somewhat unusual, a detailed comparison with theory must await the results of more sophisticated physical measurements. In particular, far infrared spectroscopy should provide means to observe direct transitions between the low energy levels involved.

Finally, the complicated crossover behavior in some of the systems affects directly the magnetic and spectroscopic properties. These aspects of the present problem will be discussed separately [4, 5].

Acknowledgements. The authors appreciate financial support by the Deutsche Forschungsgemeinschaft, the Stiftung Volkswagenwerk, and the Fonds der Chemischen Industrie.

References

1. König, E., Kremer, S.: Theoret. chim. Acta (Berl.) **23**, 12 (1971).
2. — Theoret. chim. Acta (Berl.) **22**, 45 (1971).
3. Griffith, J. S.: The theory of transition metal ions. Cambridge: University Press 1961.
4. König, E., Kremer, S.: Ber. Bunsenges. (im Druck).
5. — — Unveröffentlichte Resultate.
6. — — Theoret. chim. Acta (Berl.) **20**, 143 (1971).
7. — Madeja, K.: Inorg. Chemistry **6**, 48 (1967); ibid. **7**, 2677 (1968).
8. Jesson, J. P., Weiher, J. F., Trofimenko, S.: J. chem. Physics **48**, 2058 (1968).
9. König, E., Ritter, G., Spiering, H., Kremer, S., Madeja, K., Rosenkranz, A.: J. chem. Physics **56**, 3139 (1972).

10. König, E., Ritter, G., Braunnecker, B., Madeja, K., Goodwin, H. A., Smith, F. E.: Ber. Bunsenges. 76, 393 (1972).
11. Fisher, D. C., Drickamer, H. G.: J. chem. Physics 54, 4825 (1971).
12. Bargeron, C. B., Drickamer, H. G.: J. chem. Physics 55, 347 (1971).
13. Golding, R. M., Healy, P. C., White, A. H.: Trans. Faraday Soc. 67, 1672 (1971).

Dozent Dr. E. König
Institut für Physikalische Chemie II
Universität Erlangen-Nürnberg
D-8520 Erlangen, Fahrstr. 17
Germany

Theoret. chim. Acta (Berl.) 26, 321—330 (1972)
© by Springer-Verlag 1972

Ab initio Valence-Bond Calculations of H_2O

I. Bond Dissociation Energies

CARL PETERSON* and GARY V. PFEIFFER
Department of Chemistry, Ohio University, Athens, Ohio 45701

Received February 1, 1972

The first and second bond dissociation energies for H_2O have been calculated in an *ab initio* manner using a multistructure valence-bond scheme. The basis set consisted of a minimal number of non-orthogonal atomic orbitals expressed in terms of gaussian-lobe functions. The valence-bond structures considered properly described the change in the molecular system as the hydrogen atoms were individually removed to infinity. The calculated equilibrium geometry for the H_2O molecule has an O–H bond length of 1.83 Bohrs and an HOH bond angle of 106.5°. With 49 valence-bond structures the energy of H_2O at this geometry was -76.0202 Hartrees. The calculated equilibrium bond length for the OH radical was 1.86 Bohrs and the energy, using the same basis set, was -75.3875 Hartrees. After correction for zero point energies the calculated bond dissociation energies are: $H_2O \rightarrow OH + H$, $D_1 = 75.38$ kcal/mole and $OH \rightarrow O + H$, $D_2 = 54.79$ kcal/mole.

Die ersten und zweiten Dissoziationsenergien der Bindungen von H_2O wurden mit einem *ab initio* Verfahren nach der Valenzstrukturmethode berechnet. Die Basis bestand aus einer minimalen Anzahl von nicht-orthogonalen Atomorbitalen, die durch Gaußfunktionen ausgedrückt wurden. Die beteiligten Valenzstrukturen beschrieben in geeigneter Weise den Wechsel in der Molekülstruktur bei Abspaltung der einzelnen Wasserstoffatome. Die berechnete Gleichgewichtsgeometrie des H_2O-Moleküls hat eine O–H-Bindungslänge von 1,83 Bohr und einen HOH-Winkel von 106,5°. Mit 49 Valenzstrukturen betrug die Energie des H_2O bei dieser Geometrie $-76{,}0202$ Hartree. Die berechnete Bindungslänge des OH-Radikals für das Gleichgewicht betrug 1,86 Bohr und die Energie wurde mit derselben Basis zu $-75{,}3875$ Hartree berechnet. Nach Korrekturen für die Nullpunktenergien betrugen die berechneten Dissoziationsenergien der Bindungen: $H_2O \rightarrow OH + H$, $D_1 = 75{,}38$ kcal/Mol und $OH \rightarrow O + H$, $D_2 = 54{,}79$ kcal/Mol.

1. Introduction

Ab initio valence-bond (VB) calculations for polyatomic molecules with inclusion of all electrons are rare. Previous studies on polyatomic systems have usually involved integral approximations [1] or other assumptions such as $\sigma - \pi$ separability [2]. The major difficulty in using an *ab initio* approach in VB calculations is the vast number of multiple exchange integrals that must be evaluated when a basis set of non-orthogonal atomic orbitals is used in making up the VB structures. However the use of orthogonalized atomic orbitals [3], while decreasing computational difficulties, also decreases the chemical interpretability of the results [4]. The non-orthogonal basis was therefore retained in the present study and the formulation derived by Löwdin [5] and discussed by Slater [6] was used to evaluate the necessary matrix elements.

---

* Present address: Department of Chemistry, Ohio State University, Columbus, Ohio.

In order to study the process of bond dissociation in the H_2O molecule the wave function must be of sufficient flexibility to correctly describe the change in electronic structure as the hydrogen atoms are individually removed to infinity. As is well known a proper description of this process cannot in general be given by a single configuration (unless the reactants and products are closed-shell species) which is usually constrained to dissociate into a sum of ground and excited state atomic species. It is a simple matter however to obtain correct dissociation results using VB methods by including among the valence structures in the configuration interaction scheme those structures which at infinite internuclear separations represent the atoms in their ground states. If the VB structures do not represent spectroscopic states at infinite internuclear separations then additional structures must be added to allow intra-atomic configuration interaction [7]. A variational calculation will then automatically increase the contribution of these structures to the wavefunction as the internuclear distance is increased.

2. Basis Set and Computer Program

The atomic orbital basis set for these calculations consists of gaussian-lobe functions with Whitten's [8] exponents and coefficients. The H(1*s*) orbital was represented by a linear combination of five gaussian functions and for calculations at the equilibrium geometry of H_2O this orbital was scaled by 1.4. No polarization functions such as *d*-type orbitals on the O atom or *p*-type orbitals on the H atoms were used in the present study. Although the basis set is therefore "minimal" it has had excellent success in yielding molecular geometries in close agreement with experiment [9].

The program used in these calculations was an early version of the MOLE Quantum Chemistry System developed by Rothenberg and co-workers [10]. Particular use was made of the non-orthogonal configuration interaction subprogram developed by Erdahl and Lesk [11]. In this program each Slater determinant is written in terms of two "primary" functions each of which is a product function of all the spin-orbitals in the determinant having similar spin. Only matrix elements between "primary" functions of the same spin value need be calculated. The resulting blocking of the overlap matrix leads to similar blocking in the matrices of the first and second order minors which appear in the energy expressions developed by Löwdin [5]. By focusing on "primary" structures rather than the entire Slater determinant computational time is considerably shortened by reducing the number of *different* interaction matrix elements between VB structures. For example in the H_2O calculations reported here 15 "primary" functions have been combined in various ways to give 101 different Slater determinants which appear in the 49 VB structures considered.

3. Valence Bond Structures

The 49 VB wavefunctions used in these calculations are given in Table 1. The O(1*s*) orbital is doubly occupied in each of these structures and only the $O(2s) \equiv \Phi_s$, $O(2px) \equiv \Phi_x$, $O(2py) \equiv \Phi_y$, $O(2pz) \equiv \Phi_z$, $H_1(1s) \equiv h_1$, and $H_2(1s) \equiv h_2$ are shown.

A bar over the orbital indicates β spin, no bar indicates α spin. All of the wavefunctions in Table 1 either individually or in linear combinations transform as the A_1 representation of the C_{2v} point group. Wavefunctions $\Psi_1 - \Psi_{10}$ represent covalent bonding schemes; wavefunctions $\Psi_{11} - \Psi_{49}$ represent ionic bonding schemes. Intra-atomic configuration interaction occurs among both the covalent and ionic functions except for those wavefunctions which dissociate to an O^- configuration. The importance of the lack of intra-atomic configuration interaction for this configuration will be discussed later.

This set of 49 wavefunctions includes all the structures of A_1 symmetry that may be formed from the configurations:

$$O^+(1s^2 2s^2 2p^3),\ O^+(1s^2 2s 2p^4),\ O^+(1s^2 2p^5),\ O(1s^2 2s^2 2p^4),\ O(1s^2 2s 2p^5),$$
$$O(1s^2 2p^6),\ O^-(1s^2 2s^2 2p^5),\ O^-(1s^2 2s 2p^6),\ \text{and}\ O^=(1s^2 2s^2 2p^6).$$

4. Results

A) Calculated Equilibrium Geometry and Energy for H_2O

A number of preliminary calculations using a set of 30 VB functions were performed to establish the equilibrium conformation of H_2O. These calculations predicted the HOH bond angle to be 106.5° and the O–H bond length to be 1.83 Bohrs [12]. This geometry was used in the more extensive calculations

Table 1. Valence bond wave functions

$\Psi_1 = |\Phi_s\bar{\Phi}_s\Phi_x\Phi_y\Phi_z\bar{\Phi}_z\bar{h}_1\bar{h}_2| - |\Phi_s\bar{\Phi}_s\bar{\Phi}_x\Phi_y\Phi_z\bar{\Phi}_z\bar{h}_1 h_2| - |\Phi_s\bar{\Phi}_s\Phi_x\bar{\Phi}_y\Phi_z\bar{\Phi}_z h_1\bar{h}_2| + |\Phi_s\bar{\Phi}_s\bar{\Phi}_x\bar{\Phi}_y\Phi_z\bar{\Phi}_z h_1 h_2|$

$\Psi_2 = |\Phi_s\bar{\Phi}_s\Phi_x\Phi_y\Phi_z\bar{\Phi}_z\bar{h}_1\bar{h}_2| - |\Phi_s\bar{\Phi}_s\Phi_x\bar{\Phi}_y\Phi_z\bar{\Phi}_z\bar{h}_1 h_2| - |\Phi_s\bar{\Phi}_s\bar{\Phi}_x\Phi_y\Phi_z\bar{\Phi}_z h_1\bar{h}_2| + |\Phi_s\bar{\Phi}_s\bar{\Phi}_x\bar{\Phi}_y\Phi_z\bar{\Phi}_z h_1 h_2|$

$\Psi_3 = |\Phi_s\bar{\Phi}_s\Phi_x\bar{\Phi}_x\Phi_z\bar{\Phi}_z h_1\bar{h}_2| - |\Phi_s\bar{\Phi}_s\Phi_x\bar{\Phi}_x\Phi_z\bar{\Phi}_z\bar{h}_1 h_2|$

$\Psi_4 = |\Phi_s\bar{\Phi}_s\Phi_y\bar{\Phi}_y\Phi_z\bar{\Phi}_z h_1\bar{h}_2| - |\Phi_s\bar{\Phi}_s\Phi_y\bar{\Phi}_y\Phi_z\bar{\Phi}_z\bar{h}_1 h_2|$

$\Psi_5 = |\Phi_s\bar{\Phi}_s\Phi_x\bar{\Phi}_x\Phi_y\bar{\Phi}_y h_1\bar{h}_2| - |\Phi_s\bar{\Phi}_s\Phi_x\bar{\Phi}_x\Phi_y\bar{\Phi}_y\bar{h}_1 h_2|$

$\Psi_6 = |\Phi_s\Phi_x\bar{\Phi}_x\Phi_y\Phi_z\bar{\Phi}_z\bar{h}_1\bar{h}_2| - |\Phi_s\Phi_x\bar{\Phi}_x\bar{\Phi}_y\Phi_z\bar{\Phi}_z\bar{h}_1 h_2| - |\bar{\Phi}_s\Phi_x\bar{\Phi}_x\Phi_y\Phi_z\bar{\Phi}_z h_1\bar{h}_2| + |\bar{\Phi}_s\Phi_x\bar{\Phi}_x\bar{\Phi}_y\Phi_z\bar{\Phi}_z h_1 h_2|$

$\Psi_7 = |\Phi_s\Phi_x\bar{\Phi}_x\Phi_y\Phi_z\bar{\Phi}_z\bar{h}_1\bar{h}_2| - |\bar{\Phi}_s\Phi_x\bar{\Phi}_x\Phi_y\Phi_z\bar{\Phi}_z\bar{h}_1 h_2| - |\Phi_s\Phi_x\bar{\Phi}_x\bar{\Phi}_y\Phi_z\bar{\Phi}_z h_1\bar{h}_2| + |\bar{\Phi}_s\Phi_x\bar{\Phi}_x\bar{\Phi}_y\Phi_z\ \bar{}_z h_1 h_2|$

$\Psi_8 = |\Phi_s\Phi_x\Phi_y\bar{\Phi}_y\Phi_z\bar{\Phi}_z\bar{h}_1\bar{h}_2| - |\Phi_s\bar{\Phi}_x\Phi_y\bar{\Phi}_y\Phi_z\bar{\Phi}_z\bar{h}_1 h_2| - |\bar{\Phi}_s\Phi_x\Phi_y\bar{\Phi}_y\Phi_z\bar{\Phi}_z h_1\bar{h}_2| + |\bar{\Phi}_s\bar{\Phi}_x\Phi_y\bar{\Phi}_y\Phi_z\bar{\Phi}_z h_1 h_2|$

$\Psi_9 = |\Phi_s\Phi_x\Phi_y\bar{\Phi}_y\Phi_z\bar{\Phi}_z\bar{h}_1\bar{h}_2| - |\bar{\Phi}_s\Phi_x\Phi_y\bar{\Phi}_y\Phi_z\bar{\Phi}_z\bar{h}_1 h_2| - |\Phi_s\bar{\Phi}_x\Phi_y\bar{\Phi}_y\Phi_z\bar{\Phi}_z h_1\bar{h}_2| + |\bar{\Phi}_s\bar{\Phi}_x\Phi_y\bar{\Phi}_y\Phi_z\bar{\Phi}_z h_1 h_2|$

$\Psi_{10} = |\Phi_x\bar{\Phi}_x\Phi_y\bar{\Phi}_y\Phi_z\bar{\Phi}_z h_1\bar{h}_2| - |\Phi_x\bar{\Phi}_x\Phi_y\bar{\Phi}_y\Phi_z\bar{\Phi}_z\bar{h}_1 h_2|$

$\Psi_{11} = |\Phi_s\bar{\Phi}_s\Phi_x\Phi_y\bar{\Phi}_y\Phi_z\bar{\Phi}_z\bar{h}_2| - |\Phi_s\bar{\Phi}_s\bar{\Phi}_x\Phi_y\bar{\Phi}_y\Phi_z\bar{\Phi}_z h_2|$

$\Psi_{12} = |\Phi_s\bar{\Phi}_s\Phi_x\Phi_y\bar{\Phi}_y\Phi_z\bar{\Phi}_z\bar{h}_1| - |\Phi_s\bar{\Phi}_s\Phi_x\Phi_y\bar{\Phi}_y\Phi_z\bar{\Phi}_z h_1|$

$\Psi_{13} = |\Phi_s\bar{\Phi}_s\Phi_x\bar{\Phi}_x\Phi_y\Phi_z\bar{\Phi}_z\bar{h}_2| - |\Phi_s\bar{\Phi}_s\Phi_x\bar{\Phi}_x\bar{\Phi}_y\Phi_z\bar{\Phi}_z h_2|$

$\Psi_{14} = |\Phi_s\bar{\Phi}_s\Phi_x\bar{\Phi}_x\Phi_y\Phi_z\bar{\Phi}_z\bar{h}_1| - |\Phi_s\bar{\Phi}_s\Phi_x\bar{\Phi}_x\bar{\Phi}_y\Phi_z\bar{\Phi}_z h_1|$

$\Psi_{15} = |\Phi_s\Phi_x\bar{\Phi}_x\Phi_y\bar{\Phi}_y\Phi_z\bar{\Phi}_z\bar{h}_2| - |\bar{\Phi}_s\Phi_x\bar{\Phi}_x\Phi_y\bar{\Phi}_y\Phi_z\bar{\Phi}_z h_2|$

$\Psi_{16} = |\Phi_s\Phi_x\bar{\Phi}_x\Phi_y\bar{\Phi}_y\Phi_z\bar{\Phi}_z\bar{h}_1| - |\bar{\Phi}_s\Phi_x\bar{\Phi}_x\Phi_y\bar{\Phi}_y\Phi_z\bar{\Phi}_z h_1|$

$\Psi_{17} = |\Phi_s\bar{\Phi}_s\Phi_x\bar{\Phi}_x\Phi_y\bar{\Phi}_y\Phi_z\bar{\Phi}_z|$

$\Psi_{18} = |\Phi_s\bar{\Phi}_s\Phi_x\bar{\Phi}_x\Phi_y\bar{\Phi}_y h_2\bar{h}_2|$

$\Psi_{19} = |\Phi_s\bar{\Phi}_s\Phi_x\bar{\Phi}_x\Phi_z\bar{\Phi}_z h_2\bar{h}_2|$

$\Psi_{20} = |\Phi_s\bar{\Phi}_s\Phi_y\bar{\Phi}_y\Phi_z\bar{\Phi}_z h_2\bar{h}_2|$

$\Psi_{21} = |\Phi_s\bar{\Phi}_s\Phi_x\bar{\Phi}_x\Phi_y\bar{\Phi}_y h_1\bar{h}_1|$

$\Psi_{22} = |\Phi_s\bar{\Phi}_s\Phi_x\bar{\Phi}_x\Phi_z\bar{\Phi}_z h_1\bar{h}_1|$

$\Psi_{23} = |\Phi_s\bar{\Phi}_s\Phi_y\bar{\Phi}_y\Phi_z\bar{\Phi}_z h_1\bar{h}_1|$

$\Psi_{24} = |\Phi_x\bar{\Phi}_x\Phi_y\bar{\Phi}_y\Phi_z\bar{\Phi}_z h_2\bar{h}_2|$

$\Psi_{25} = |\Phi_x\bar{\Phi}_x\Phi_y\bar{\Phi}_y\Phi_z\bar{\Phi}_z h_1\bar{h}_1|$

Table 1 (continued)

$\Psi_{26} = |\Phi_s\bar{\Phi}_s\Phi_x\bar{\Phi}_x\Phi_y\bar{h}_1h_2\bar{h}_2| - |\Phi_s\bar{\Phi}_s\Phi_x\bar{\Phi}_x\bar{\Phi}_y h_1h_2\bar{h}_2|$

$\Psi_{27} = |\Phi_s\bar{\Phi}_s\Phi_x\Phi_y\bar{\Phi}_y\bar{h}_1h_2\bar{h}_2| - |\Phi_s\bar{\Phi}_s\bar{\Phi}_x\Phi_y\bar{\Phi}_y h_1h_2\bar{h}_2|$

$\Psi_{28} = |\Phi_s\bar{\Phi}_s\Phi_y\Phi_z\bar{\Phi}_z\bar{h}_1h_2\bar{h}_2| - |\Phi_s\bar{\Phi}_s\bar{\Phi}_x\Phi_z\bar{\Phi}_z h_1h_2\bar{h}_2|$

$\Psi_{29} = |\Phi_s\bar{\Phi}_s\Phi_x\Phi_z\bar{\Phi}_z\bar{h}_1h_2\bar{h}_2| - |\Phi_s\bar{\Phi}_s\bar{\Phi}_x\Phi_z\bar{\Phi}_z h_1h_2\bar{h}_2|$

$\Psi_{30} = |\Phi_s\Phi_x\bar{\Phi}_x\Phi_y\bar{\Phi}_y\bar{h}_1h_2\bar{h}_2| - |\bar{\Phi}_s\Phi_x\bar{\Phi}_x\Phi_y\bar{\Phi}_y h_1h_2\bar{h}_2|$

$\Psi_{31} = |\Phi_s\Phi_x\bar{\Phi}_x\Phi_z\bar{\Phi}_z\bar{h}_1h_2\bar{h}_2| - |\bar{\Phi}_s\Phi_x\bar{\Phi}_x\Phi_z\bar{\Phi}_z h_1h_2\bar{h}_2|$

$\Psi_{32} = |\Phi_s\Phi_y\bar{\Phi}_y\Phi_z\bar{\Phi}_z\bar{h}_1h_2\bar{h}_2| - |\bar{\Phi}_s\Phi_y\bar{\Phi}_y\Phi_z\bar{\Phi}_z h_1h_2\bar{h}_2|$

$\Psi_{33} = |\Phi_s\bar{\Phi}_s\Phi_x\bar{\Phi}_x\Phi_y h_1\bar{h}_1\bar{h}_2| - |\Phi_s\bar{\Phi}_s\Phi_x\bar{\Phi}_x\bar{\Phi}_y h_1\bar{h}_1h_2|$

$\Psi_{34} = |\Phi_s\bar{\Phi}_s\Phi_x\Phi_y\bar{\Phi}_y h_1\bar{h}_1\bar{h}_2| - |\Phi_s\bar{\Phi}_s\bar{\Phi}_x\Phi_y\bar{\Phi}_y h_1\bar{h}_1h_2|$

$\Psi_{35} = |\Phi_s\bar{\Phi}_s\Phi_y\Phi_z\bar{\Phi}_z h_1\bar{h}_1\bar{h}_2| - |\Phi_s\bar{\Phi}_s\bar{\Phi}_y\Phi_z\bar{\Phi}_z h_1\bar{h}_1h_2|$

$\Psi_{36} = |\Phi_s\bar{\Phi}_s\Phi_x\Phi_z\bar{\Phi}_z h_1\bar{h}_1\bar{h}_2| - |\Phi_s\bar{\Phi}_s\bar{\Phi}_x\Phi_z\bar{\Phi}_z h_1\bar{h}_1h_2|$

$\Psi_{37} = |\Phi_s\Phi_x\bar{\Phi}_x\Phi_y\bar{\Phi}_y h_1\bar{h}_1\bar{h}_2| - |\bar{\Phi}_s\Phi_x\bar{\Phi}_x\Phi_y\bar{\Phi}_y h_1\bar{h}_1h_2|$

$\Psi_{38} = |\Phi_s\Phi_x\bar{\Phi}_x\Phi_z\bar{\Phi}_z h_1\bar{h}_1\bar{h}_2| - |\bar{\Phi}_s\Phi_x\bar{\Phi}_x\Phi_z\bar{\Phi}_z h_1\bar{h}_1h_2|$

$\Psi_{39} = |\Phi_s\Phi_y\bar{\Phi}_y\Phi_z\bar{\Phi}_z h_1\bar{h}_1\bar{h}_2| - |\bar{\Phi}_s\Phi_y\bar{\Phi}_y\Phi_z\bar{\Phi}_z h_1\bar{h}_1h_2|$

$\Psi_{40} = |\Phi_s\bar{\Phi}_s\Phi_x\bar{\Phi}_y\Phi_z\bar{\Phi}_z h_2\bar{h}_2| - |\Phi_s\bar{\Phi}_s\bar{\Phi}_x\Phi_y\Phi_z\bar{\Phi}_z h_2\bar{h}_2|$

$\Psi_{41} = |\Phi_s\bar{\Phi}_s\Phi_x\bar{\Phi}_y\Phi_z\bar{\Phi}_z h_1\bar{h}_1| \quad |\Phi_s\bar{\Phi}_s\bar{\Phi}_x\Phi_y\Phi_z\bar{\Phi}_z h_1\bar{h}_1|$

$\Psi_{42} = |\Phi_s\bar{\Phi}_x\Phi_y\bar{\Phi}_y\Phi_z\bar{\Phi}_z h_2\bar{h}_2| \quad |\bar{\Phi}_s\Phi_x\Phi_y\bar{\Phi}_y\Phi_z\bar{\Phi}_z h_2\bar{h}_2|$

$\Psi_{43} = |\Phi_s\bar{\Phi}_x\Phi_y\bar{\Phi}_y\Phi_z\bar{\Phi}_z h_1\bar{h}_1| - |\bar{\Phi}_s\Phi_x\Phi_y\bar{\Phi}_y\Phi_z\bar{\Phi}_z h_1\bar{h}_1|$

$\Psi_{44} = |\Phi_s\Phi_x\bar{\Phi}_x\bar{\Phi}_y\Phi_z\bar{\Phi}_z h_2\bar{h}_2| - |\bar{\Phi}_s\Phi_x\bar{\Phi}_x\Phi_y\Phi_z\bar{\Phi}_z h_2\bar{h}_2|$

$\Psi_{45} = |\Phi_s\Phi_x\bar{\Phi}_x\bar{\Phi}_y\Phi_z\bar{\Phi}_z h_1\bar{h}_2| - |\bar{\Phi}_s\Phi_x\bar{\Phi}_x\Phi_y\Phi_z\bar{\Phi}_z h_1\bar{h}_1|$

$\Psi_{46} = |\Phi_x\Phi_y\bar{\Phi}_y\Phi_z\bar{\Phi}_z\bar{h}_1h_2\bar{h}_2| - |\bar{\Phi}_x\Phi_y\bar{\Phi}_y\Phi_z\bar{\Phi}_z h_1h_2\bar{h}_2|$

$\Psi_{47} = |\Phi_x\Phi_y\bar{\Phi}_y\Phi_z\bar{\Phi}_z h_1\bar{h}_1\bar{h}_2| - |\bar{\Phi}_x\Phi_y\bar{\Phi}_y\Phi_z\bar{\Phi}_z h_1\bar{h}_1h_2|$

$\Psi_{48} = |\Phi_s\bar{\Phi}_s\Phi_y\Phi_z\bar{\Phi}_z\bar{h}_1h_2\bar{h}_2| \quad |\Phi_s\bar{\Phi}_s\bar{\Phi}_y\Phi_z\bar{\Phi}_z h_1h_2\bar{h}_2|$

$\Psi_{49} = |\Phi_s\bar{\Phi}_s\Phi_y\Phi_z\bar{\Phi}_z h_1\bar{h}_1\bar{h}_2| \quad |\Phi_s\bar{\Phi}_s\bar{\Phi}_y\Phi_z\bar{\Phi}_z h_1\bar{h}_1h_2|$

Table 2. H_2O energies at calculated equilibrium geometry[a,b]

Nuclear repulsion	9.0842
Kinetic	76.5737
Nuclear attraction	−199.6371
Electron repulsion	37.9590
Total	−76.0202
Virial ratio	0.9964

[a] O–H bond = 1.83 Bohr, HOH angle 106.5°.
[b] All energies in Hartrees.

reported in Table 2 for which the full set of 49 VB functions was used. The total energy, −76.0202 Hartrees, was only slightly superior to that obtained by using smaller preliminary sets; 30 functions gave an energy of −76.0163 Hartrees and 39 functions gave an energy of −76.0182 Hartrees. Both of the smaller sets contained all 10 covalent VB functions but only part of the ionic functions in Table 1. The results reported in Table 2 should be quite close to the limit obtainable with a minimal atomic basis since additional functions would represent atomic configurations of such high energies that they should not contribute significantly to the molecular wavefunction. These results for the three sets of functions emphasize the slowly convergent nature of configuration interaction with a minimal atomic basis.

Table 3. Contributions of the most important VB structures to H_2O at the calculated equilibrium geometry

Structure	Structure projection
Ψ_{11}	0.1412
Ψ_{12}	0.1412
Ψ_1	0.0977
Ψ_2	0.0977
Ψ_{17}	0.0915
Ψ_{13}	0.0655
Ψ_{14}	0.0655
Ψ_4	0.0561
Ψ_8	0.0514
Ψ_9	0.0514
Ψ_{15}	0.0391
Ψ_{16}	0.0391
Ψ_3	0.0142
Ψ_{20}	0.0081
Ψ_{23}	0.0081
Ψ_{40}	0.0081
Ψ_{41}	0.0081

Table 4. Calculated and experimental excitation energies (Hartrees)

Configuration	Calculated energies	Experimental energies
$O(1s^2 2s^2 2p^4, {}^1D)$	0.0805	0.0724
$O(1s^2 2s^2 2p^4, {}^1S)$	0.2038	0.1540
$O\ (1s^2 2s^2 2p^5, {}^2P)$	0.1594	−0.0540
$O^-(1s^2 2s 2p^6, {}^2S)$	0.8596	0.4924
$O^+(1s^2 2s^2 2p^3, {}^2P)$	0.6501	0.6846
$O^+(1s^2 2s^2 2p^3, {}^2D)$	0.7306	0.6222

The relative importance of the ionic functions in describing H_2O is shown in Table 3 which contains the structure projections or occupation numbers [13] of the most important contributing functions in the set of 49 structures. For a given structure N, the structure projection v_N is given by, $v_N = C_N \sum_M C_M S_{NM}$, where C_I is the coefficient of structure I in the molecular wavefunction, the S_{IJ} are overlap integrals $S_{IJ} = \int \Psi_I \Psi_J d\tau$, $M = 1, 2, \ldots, 49$, and $\sum_N v_N = 1$. This type of population analysis ascribes over 60% ionic character to the bonding in H_2O with the largest contributions coming from the O^- and $O^=$ configurations.

The importance of the ionic contributions to the molecular wavefunction is somewhat unfortunate since atomic and ionic excitation energies are poorly represented by a minimal atomic basis set. In Table 4 the calculated excitation energies using the gaussian-lobe basis are compared to experimental energies [14] for various O, O^-, and O^+ configurations. The errors in the calculated values of the electron affinity are particularly large.

Table 5. OH + H energies at calculated equilibrium geometry[a,b]

Nuclear repulsion	4.3013
Kinetic	76.2211
Nuclear attraction	− 189.4010
Electron repulsion	32.9913
Total	− 75.8873
Virial ratio	0.9978

[a] O−H bond = 1.86 Bohr; H at 50000 Bohr.
[b] All energies in Hartrees.

Table 6 Contributions of the most important VB structures to OH + H at the calculated equilibrium geometry

Structure	Structure projection
Ψ_2	0.2936
Ψ_{14}	0.2302
Ψ_1	0.1462
Ψ_{11}	0.1283
Ψ_3	0.0529
Ψ_4	0.0528
Ψ_6	0.0466
Ψ_8	0.0257
Ψ_7	0.0081

B) First Bond Dissociation Energy: $H_2O \rightarrow OH + H$

To obtain the dissociation energy involved in breaking one of the O−H bonds in H_2O calculations were performed with a H removed by 50000 Bohrs from the OH fragment. Preliminary calculations indicated that the bond length in the OH fragment was 1.86 Bohrs. The results for the total energy and its components for this geometry using the set of 49 VB functions are presented in Table 5. The H within the OH radical was scaled by 1.4 while the H at 50000 Bohrs was unscaled. Comparing the results in Tables 2 and 5, and using zero point energies of 13.25 kcals for H_2O [15] and 5.29 kcals for OH [16], the calculated bond dissociation energy is 75.38 kcals. The recommended experimental value is 118.0 ± 0.2 kcals (0° K) [17].

As shown in Table 6 the VB functions contributing to the OH + H system all require the leaving H to be in the ^2S state thus insuring proper dissociation products. The energy of the separated H is −0.4998 Hartrees indicating an energy of −75.3875 Hartrees for the OH radical. Freeman [18] obtained an energy of −75.327 Hartrees for OH using 10 VB functions and a Hartree-Fock atomic basis. Table 6 also indicates an ionic contribution to the OH bond of 36% arising from structures Ψ_{11} and Ψ_{14} which represent the $O^-(1s^2 2s^2 2p^5)$ configuration at infinite internuclear separation.

C) Second Bond Dissociation Energy: $OH + H \rightarrow O + 2H$

In this calculation the second H is removed to 50000 Bohrs such that the two H atoms are separated by ~ 100000 Bohrs. The calculated energies for the separated atoms are O(– 74.7919 Hartrees) + 2H(– 0.9996 Hartrees). The wavefunction consists of equal weights of structures Ψ_1 and Ψ_2. Using the tables of Companion and Ellison it may be shown that the wavefunction represents O in its ^3P state and each H in a ^2S state. As expected the VB method gives the correct dissociation products. The calculated second bond dissociation energy is 54.79 kcals compared to the recommended experimental value of 101.3 ± 0.5 kcals [17]. Freeman obtained a dissociation energy of 23.95 kcals using ten VB functions.

5. Discussion

The basis set used in these calculations is often referred to as being of double-zeta quality [8, 19] since atomic energies calculated with this set are found to be quite close to those given by Clementi's [20] double-zeta Slater basis. For molecular calculations however the lack of true double-zeta flexibility in the present basis set is exemplified by an SCF calculation for H_2O which gives an energy of – 75.97516 Hartrees [21] while a calculation by Dunning [19] using a [42/2] basis derived from Huzinaga's [22] uncontracted set of gaussian functions gave an energy of – 76.0093 Hartrees and a calculation by Guidotti and Salvetti [23] using Clementi's [20] set of Slater functions gave an energy of – 76.0054 Hartrees. This deficiency in our basis set makes it difficult to compare the results of this paper with the LCAO-MO-CI calculations of Schaefer and Bender [24] which gave an energy for H_2O of – 76.13497 Hartrees using 224 configurations with Dunning's [19] [42/2] basis and the calculations of Hosteny *et al.* [25], which gave an energy for H_2O of – 76.14225 Hartrees using 6779 configurations and Dunning's [19] [42/2] basis set.

A major difficulty with LCAO-MO-CI calculations arises in attempting to calculate potential energy surfaces leading to correct dissociation products. For diatomic molecules the "optimized-valence configurations" method of Das and Wahl [26, 27] has led to satisfactory potential curves for a rather limited number of species. Their approach has not yet been extended to polyatomic molecules. Schaefer and Harris [28] used a complete set of configurations formed from a minimal STO basis to ensure correct dissociation behavior for O_2. With such a restricted basis set, however, good dissociation energies cannot be expected. Using an extended [421] basis Schaefer [29] has obtained an improved dissociation energy for O_2 and a potential curve parallel to the experimental curve. In this calculation 128 configurations were used which included one quadruple excitation needed to ensure dissociation to ^3P O atoms.

For polyatomic calculations it would seem that ensuring correct dissociative behavior would be quite difficult for any MO-CI calculation employing an extended basis set. For valence-bond calculations of the type we report here, however, it is a fairly simple matter to include structures in the configuration interaction whose dissociative properties are such as to allow correct molecular dissociation. For example structures Ψ_1 and Ψ_2 of Table 1 combine at infinite internuclear separation to yield O(^3P) and H(^2S) atoms. Thus as long as we include these two structures among our trial configurations we know that the potential surface will be at least qualitatively correct. A previous valence-bond-like calculation on H_2O has been reported by Guberman and Goddard [30] using a spin-projected Hartree-Fock wave function followed by orbital optimization. This procedure gives a proper account of molecular dissociation by making sufficient orbitals available to describe not only H_2O but also OH + H and O + 2H. Their results for H_2O, OH + H, and O + 2H using the [42/2] basis set of Dunning [19] are -76.05269, -75.89331, and -75.80525 Hartrees respectively. Their values for the first and second bond dissociation energies are thus 0.15938 Hartrees and 0.08806 Hartrees respectively compared to the comparable results of 0.1332 Hartrees and 0.0958 Hartrees obtained in the present calculation. As mentioned previously the difference in flexibility between the [42/2] basis and our minimal basis set makes comparison difficult but it does seem that the two calculations would give similar results if our basis was of true [42/2] flexibility.

Although a large number of configurations have been included in the present calculations only about 60 65% of each of the two bond dissociation energies was obtained. The deficiencies in the results are inherent in any calculation utilizing atomic basis functions incapable of permitting intraatomic configuration interaction. The particular difficulty in reproducing the electron affinity of O has its counterpart in previous *ab initio* studies where difficulty in describing F^- relative to F was encountered [31, 32]. Various semiempirical techniques have been proposed such as the "atoms-in-molecules" method of Moffitt [33] and the "interatomic correlation correction" method of Hurley [34] to compensate for these errors in relative atomic and ionic excitation energies but they must be applied with caution [32].

The importance of ionic structures in H_2O and to a lesser extent in the OH radical requires that basis functions be chosen to give at least the correct sign to the electron affinity for O and H. One procedure is to reoptimize the atomic basis functions for the negative ion of a given atom until the electron affinity is positive. Usually however the energy of the neutral atom is increased by this procedure and some compromise basis must be chosen that gives a satisfactory energy for the neutral atom but still predicts a positive electron affinity. A second procedure is to include polarization functions in the atomic basis by using a double-zeta set or by including *d*-type functions on O and *p*-type functions on H [35]. It would seem likely that the second procedure would be more effective in that it should lead to significant improvement in molecule energies [36] as well as to improved atomic and ionic excitation energies. The disadvantage to the second procedure would be the large number of additional VB structures that could be created from the expanded basis set. A selective configuration interaction calculation would then be necessary wherein the configurations necessary to ensure the proper dissociation products were combined with a judicious number of other configurations important for intraatomic correlation.

Finally the present study comments on the difference between the first and second bond dissociation energies of H_2O. The calculated difference reported here is 20.59 kcals/mole while experimentally the difference is 16.7 ± 0.7 kcals/mole. Pauling [37] and Moffitt [38] ascribe the difference to the stabilization energy of the O atom in the ^3P ground state relative to the energy of the O atom in its valence state in the OH radical and H_2O molecule. Moffitt [38] found that the valence state of O was the same in both OH and H_2O when both species were represented by a single, perfect pairing, VB structure and then assumed that the two bond dissociation energies would be identical if the O atom, after complete dissociation, existed in its valence state rather than as the ^3P state. Inspection of the structure projections for H_2O and OH in Tables 3 and 6 indicates that it is highly unlikely that the valence state of O is the same in both OH and H_2O. It is certain that the description of the valence state is more complicated than the simple mixture of ^3P and ^1D spectroscopic states proposed by Moffitt. An analysis of the valence state of O in OH and H_2O is currently being carried out along the lines suggested by Craig and Thirunmachandran [39] to determine if the calculated difference in dissociation energies can indeed be explained by valence state energies.

Acknowledgement. We are indebted to the Ohio University Computing Center for making available to us the considerable amount of computation time involved in these calculations.

References

1. McWeeny, R., Ohno, K.: Proc. Royal Soc. (London) A **255**, 367 (1960).
2. Simonetta, M., Gianinetti, E., Vandoni, I.: J. chem. Physics **48**, 1579 (1968). – Schug, J.C.: J. chem. Physics **42**, 2547 (1965).
3. Löwdin, P.-O.: J. chem. Physics **18**, 365 (1950).
4. McWeeny, R.: Proc. Royal Soc. (London) A **223**, 63 (1954).
5. Löwdin, P.-O.: Physic. Rev. **97**, 1474, 1490 (1955).
6. Slater, J.C.: Quantum theory of molecules and solids, Vol. I. New York: McGraw-Hill 1963.
7. The dissociation behavior of a given VB structure may be deduced by reference to the tables in: Companion, A. L., Ellison, F.O.: J. chem. Physics **28**, 1 (1958).
8. Whitten, J. L.: J. chem. Physics **39**, 349 (1963); **44**, 359 (1966).
9. For a summary of some results see Allen, L.C. in: Quantum theory of atoms, molecules, and the solid state. Löwdin, P.-O. (Ed.). New York: Academic Press 1966.
10. Rothenberg, S., Kollman, P., Schwartz, M.E., Hayes, E.F., Allen, L.C.: Int. J. quant. Chemistry **IIIS**, 715 (1970).
11. Erdahl, R.M.: Ph.D. Thesis, Princeton University 1965; coded and extended by Dr. Lesk.
12. Peterson, C.: Ph.D. Thesis, Ohio University 1971.
13. Hurley, A.C.: J. chem. Physics **28**, 532 (1958)
14. Moore, C.E.: Natl. Bur. Std. (U.S.) Circ. No. 467 (1949).
15. Eisenberg, D., Kauzmann, W.: The structures and properties of water. New York: Oxford University Press 1969.
16. Vibrational constants in the ground state of the OH radical in: Chamberlain, J.W., Roesler, F.L.: Astrophysic J. **121**, 541 (1955).
17. Darwent, B.deB.: Nat. Stand. Ref. Data Ser., Nat. Bur. Stand (U.S.) 31 (1970).
18. Freeman, A.J.: J. chem. Physics **28**, 230 (1958).
19. Dunning, T.H., Jr.: J. chem. Physics **53**, 2823 (1970).
20. Clementi, E.: J. chem. Physics **40**, 1944 (1964).
21. Harrison, J.F.: J. chem. Physics **47**, 2990 (1967).
22. Huzinaga, S.: J. chem. Physics **42**, 1293 (1965).
23. Guidotti, C., Salvetti, O.: Theoret. chim. Acta (Berl.) **10**, 454 (1968).
24. Schaeffer, III, H.F., Bender, C.F.: J. chem. Physics **55**, 1720 (1971).
25. Hosteny, R.P., Gilman, R.R., Dunning, T.H., Jr., Pipano, A., Shavitt, I.: Chem. Physics Letters **7**, 325 (1970).
26. Das, G., Wahl, A.C.: J. chem. Physics **44**, 87 (1966).
27. – – Physic. Rev. Letters **24**, 440 (1970).
28. Schaeffer, III, H.F., Harris, F.E.: J. chem. Physics **48**, 4946 (1968).
29. – J. chem. Physics **54**, 2207 (1971).
30. Guberman, S.L., Goddard III, W.A.: J. chem. Physics **53**, 1803 (1970).
31. Allen, L.C., Erdahl, R.M., Whitten, J.L.: J. Amer. chem. Soc. **87**, 3769 (1965).

32. Balint-Kurti, G. G., Karplus, M.: J. chem. Physics **50**, 478 (1969).
33. Moffitt, W.: Proc. Royal Soc. (London) A **210**, 245 (1951).
34. Hurley, A. C.: Proc. physic. Soc. (London) A **69**, 49 (1956).
35. Michels, H. H., Harris, F. E., Browne, J. C.: J. chem. Physics **48**, 2821 (1968).
36. Compare the H_2O calculations using the [42/2] and [422/21] basis sets given in Table V in: Neumann, D., Moskowitz, J. W.: J. chem. Physics **49**, 2056 (1968).
37. Pauling, L.: Proc. nat. Acad. Sci. USA **35**, 229 (1949).
38. Moffitt, W.: Repts. Progr. Physics **17**, 173 (1954).
39. Craig, D. P., Thirunmachandran, T.: Proc. Royal Soc. (London) A **303**, 233 (1968).

Dr. C. Peterson
Department of Chemistry
Ohio State University
Columbus, Ohio
USA

Theoret. chim. Acta (Berl.) 26, 331—350 (1972)
© by Springer-Verlag 1972

A Self-Consistent Molecular Field Theory for Aggregates of Neutral Molecules. I

Koichi Ohno and Hiroo Inokuchi

The Institute for Solid State Physics, The University of Tokyo, Roppongi, Tokyo, Japan

Received December 15, 1971 / May 15, 1972

A self-consistent theory is presented for aggregates of neutral molecules. According to the LCAO Hartree-Fock formalism a set of effective Hartree-Fock equations for molecules in the aggregate is derived. The molecular orbitals of each molecule are to be determined from the effective H–F equation for the molecule in which the interactions between the molecule and the surrounding ones are included as an intermolecular interaction field (molecular field). A self-consistent treatment leads to the molecular orbitals which are self-consistent with the molecular field. By this method, the *n*-molecule problem becomes *n* times of one-molecule problem.

Eine selbstkonsistente Theorie für Aggregate neutraler Moleküle wird entwickelt. Entsprechend der LCAO-Hartree-Fock-Theorie wird eine Reihe effektiver Hartree-Fock-Gleichungen für die Moleküle des Aggregats abgeleitet. Die Molekülorbitale sind aus den effektiven H–F-Gleichungen eines Moleküls zu bestimmen, wobei die Wechselwirkungen mit den Nachbarmolekülen als intermolekulares Wechselwirkungsfeld (Molekülfeld) berücksichtigt werden. Die Molekülorbitale werden selbstkonsistent bezüglich des Molekülfeldes berechnet. Nach dieser Methode wird das *n*-Molekülproblem zum *n*-fachen Einmolekül-Problem.

Introduction

Since the LCAO Hartree-Fock equation for a molecule were derived [1, 2], the molecular orbital theory including electron-electron interactions, which had not been considered explicitly in the Hückel theory, has been developed; in the theory, both *ab initio* and semi-empirical calculations have often succeeded to estimate the transition energies or many other electronic properties of molecules.

On the other hand, a considerable progress has been made in the theoretical treatments for the electronic structures of molecular crystals [3–8] based on the Heitler-London method. In the H–L method, the zeroth-order wave-function for a crystal is expressed as an antisymmetrized or a simple product of the wave-functions of isolated molecules. Moreover, in this method the intermolecular interactions are introduced as perturbation to the Hamiltonian for the oriented gas model in which the molecules do not interact one another. In most of the previous articles [3–16], the following approximate treatments have been often taken:

(1) The wave-functions for the constituent molecules are assumed to be orthogonal one another, or all the overlaps between the wave-functions of the molecules are neglected.

(2) The exchange interactions between the molecules are often neglected in the numerical calculation or even in the formulation.

(3) In calculating the transition energies and the intensities of real optical transitions or other physical properties of molecular crystals, the intermolecular

interaction terms are usually approximated as the dipole-dipole interaction terms, or at best the quadrupole-quadrupole terms are also considered. The higher order terms are neglected.

(4) As the transition dipoles the values determined from the experimental oscillator strengths for the molecules are often used in the dipole-dipole approximation method. Even if the transition dipoles are calculated by the conventional MO methods, the directions of the dipoles in the crystal are always assumed for the molecules with a high symmetry such as benzene and coronene.

(5) Although the Davydov splittings of typical aromatic hydrocarbon crystals have been calculated and compared with the experimental findings [5–16], the spectral displacement[1], called D in Frenkel's and Craig's notation, is often neglected or at least not calculated directly from the theoretical method.

(6) The configuration interactions to be considered between the configurations, which do not belong to the same irreducible representation in the free-molecule, are often restricted a few.

In these respects more general and appropriate theoretical treatments should be required[2].

It has been considered as a good approximation method to introduce the perturbation theory in the frame of the Heitler-London model as far as the intermolecular overlap is small. However, in the case of large molecules, the dimension of molecule itself is often much larger than the nearest intermolecular distance[3], then this perturbation approximation method may not be appropriate one even if the intermolecular overlap is small. Therefore, it may be advisable that the electronic wave-function of the aggregate of large molecules should be described as a more appropriate antisymmetrized whole electron wave-function instead of the product of the wave-functions of the isolated molecules used in the previous articles [3–16].

In this paper a self-consistent theory for molecular aggregates is developed in which all the molecular orbitals can be determined self-consistently based on the many electron Hamiltonian including the intermolecular interactions explicitly. Once the SCF molecular orbitals for a molecular aggregate are given, we can start from more appropriate zeroth-order wave functions expressed as antisymmetrized products of these orbitals.

In Section I a self-consistent method is presented for aggregates of neutral molecules. In this method, each one-electron orbital for a molecular aggregate can be described as a linear combination of atomic orbitals of a constituent molecule like a usual MO, since each electron in the molecular aggregate may be tightly bound around one of the molecules. Moreover, an antisymmetrized product of the one-electron orbitals of all the molecules in the aggregate is taken as an electronic configuration of the system. Then, according to the LCAO Hartree-Fock formalism [1, 2] a set of effective Hartree-Fock equations for the molecules in the aggregate is derived, where the intermolecular overlap between atomic orbitals is completely neglected. The one-electron orbitals of every molecule are to be determined from the effective H–F equation for the molecule in which the interactions between the molecule and the surrounding ones are included as an intermolecular interaction field (molecular field). A self-consistent treatment leads to the one-electron orbitals which are self-consistent with the molecular field (self-consistent molecular field). By this method the n-molecule problem becomes n times of one-molecule problem under the molecular field. Particularly for molecular crystals the n-molecule problem is reduced to just one-molecule problem under an equivalent molecular field.

---

[1] This term is a measure of the change in potential energy of interaction between a molecule and the surrounding molecules if this molecule is raised to an excited electronic state.

[2] In the recent work by Tanaka and Tanaka [8], most of these approximate treatments are not needed, and now their theoretical treatment seems to be one of the most acceptable ones.

[3] In benzene crystal, the diameter of molecule is about 5 Å, while the nearest intermolecular distance is 2.75 Å [17].

Starting from these SCF one-electron orbitals (not from the SCF orbitals of isolated molecules) the excited electronic states of molecular crystals are described in Section II according to the Frenkel-Pierles method [18–21]. One of the important results in this section, which seems to be rather obvious, is that the configuration interaction matrix elements between the ground electronic configuration and the one-electron excitation ones are vanishing. Therefore, the ground state can be expressed by the ground electronic configuration alone. Furthermore, it will be shown that the calculations and the estimations of many physical properties, which are peculiar to molecular crystals and not found in an isolated molecule, become facile using this method.

For the numerical calculations of real systems semi-empirical methods are presented in Section III. At first, the π-electron approximation method is taken for the studies of the electronic transitions. Next, the all valence electron treatment is used to analyze the intermolecular interactions.

In Section IV two main problems of this theory are discussed; (1) to what system the self-consistent molecular field method is applicable and (2) whether the calculation in the real SCF procedure can converge or not.

I. Self-Consistent Molecular Field Method

1. Hartree-Fock Equation and the Molecular Field

According to the Born-Oppenheimer approximation [22], the total electron Hamiltonian operator for the N-molecule system is expressed in the form;

$$H = -\frac{\hbar^2}{2m}\sum_{i=1}^{n_e}\nabla_i^2 + \frac{1}{2}\sum_{\substack{i,j\\(i\neq j)}}\frac{e^2}{r_{ij}} - \sum_{n=1}^{N}\sum_{q=1}^{q_n}\sum_{i=1}^{n_e}\frac{Z_{nq}e^2}{R_{nqi}}, \tag{1}$$

where e^2/r_{ij} is the electrostatic repulsion between electrons i and j, Z_{nq} is the nucleus charge on the q-th atom in the n-th molecule, and R_{nqi} is the distance between atom nq and electron i. Electronic wave-functions for the n_e-electron system will be constructed from normalized antisymmetrized product functions of the type[4];

$$\psi = \frac{1}{\sqrt{n_e!}}\det|(\phi_1\alpha)(\phi_1\beta)(\phi_2\alpha)\ldots|, \tag{2}$$

where ϕ_i is the one-electron orbital and α or β is the spin function. Since each electron in the molecular aggregate may be tightly bound around one molecule, the appropriate one-electron orbitals ϕ_i may be taken to be orthonormal linear combinations of atomic orbitals $\chi_{nq\mu}$ on one molecule;

---

[4] Although the extension to an open-shell case is not so difficult, a closed-shell case in each molecule is only considered in this paper.

$$\phi_{ni} = \sum_{q\mu} C_{inq\mu}\chi_{nq\mu} , \tag{3}$$

where ϕ_{ni} is the localized one-electron orbital on the n-th molecule corresponding to the i-th MO of a molecule in the familiar LCAO-MO approximation and $\chi_{nq\mu}$ is the μ-th AO on the q-th atom in the n-th molecule. Because of the small overlap between the molecules in molecular aggregates, a following approximation (complete neglect of intermolecular overlap) may be taken[5];

$$\int \chi^*_{nq\mu}\chi_{mp\nu}\,d\tau = \delta_{n,m}\int \chi^*_{nq\mu}\chi_{np\nu}\,d\tau . \tag{4}$$

Then, the partial orthogonality between the one-electron orbitals is obtained;

$$\int \phi^*_{ni}\phi_{mj}\,d\tau = a_{ij}\delta_{n,m} , \tag{5}$$

where $a_{ij} = \delta_{i,j}$ when the set of ϕ_{ni} is properly determined. Using ϕ_{ni}, the ground electronic configuration will be expressed in the scheme of Eq. (2) as follows;

$$\psi^0 = A\prod_{ni\sigma}^{\text{occ}}\phi_{ni\sigma} , \tag{6}$$

where A is an antisymmetrization operator permuting electrons and $\phi_{ni\sigma}$ is a spin-orbital which is the product of ϕ_{ni} and the spin function α or β. The electrons are accommodated in turn into the lower orbitals as in the case of the usual MO theory.

Under the condition, $a_{ij} = \delta_{i,j}$, the energy expectation value of the ground electronic configurations is given by the formula;

$$E^0 = 2\sum_{ni}^{\text{occ}} H_{ni} + \sum_{nimj}^{\text{occ}}(2J_{nimj} - K_{nimj}) , \tag{7}$$

where

$$H_{ni} = \int \phi^*_{ni}(1)\left(-\frac{\hbar^2}{2m}\nabla_1^2 - \sum_{mq}\frac{Z_{mq}e^2}{R_{mq1}}\right)\phi_{ni}(1)\,d\tau_1 , \tag{8}$$

$$J_{nimj} = \int\int \phi^*_{ni}(1)\,\phi_{ni}(1)\,\frac{e^2}{r_{12}}\,\phi^*_{mj}(2)\,\phi_{mj}(2)\,d\tau_1\,d\tau_2 , \tag{9}$$

and

$$K_{nimj} = \int\int \phi^*_{ni}(1)\,\phi_{mj}(1)\,\frac{e^2}{r_{12}}\,\phi^*_{mj}(2)\,\phi_{ni}(2)\,d\tau_1\,d\tau_2 . \tag{10}$$

The condition, $a_{ij} = \delta_{i,j}$, leads to

$$\sum_{p\mu q\nu} C^*_{inp\mu}C_{inq\nu}S^n_{p\mu q\nu} = 1 \quad (i = 1, n'_e \quad \text{and} \quad n = 1, N)^6 , \tag{11}$$

where $S^n_{p\mu q\nu}$ is the overlap integral;

$$S^n_{p\mu q\nu} = \int \chi^*_{np\mu}\chi_{nq\nu}\,d\tau . \tag{12}$$

---

[5] This approximation is, on the other hand, based on the interpretation [23] that the atomic orbitals used in the semi-empirical molecular orbital theory should be considered as the orthogonalized atomic orbitals determined by the Löwdin's method [24]. Therefore, as far as the intermolecular overlap is not so large as an intermolecular bonding is made, this approximation may be valid, if the atomic integrals, such as two-electron repulsion integrals, are evaluated semi-empirically using the zero-differential overlap approximation.

[6] The symbol, $n = 1, N$, means that the n varies from unity to N. n'_e denotes the number of electrons in the n-th molecule.

To determine the coefficients, $C_{inp\mu}$, the variation principle is used to lead a following equations; for the variation of $C^*_{inp\mu}$ (cf. Appendix),

$$\sum_q C_{inqv}(F^n_{p\mu qv} - \varepsilon_{ni} S^n_{p\mu qv})\, \delta C^*_{inp\mu} = 0 \,, \tag{13}$$

where $F^n_{p\mu qv}$ is an element of the n-th Fock matrix;

$$\begin{aligned} F^n_{p\mu qv} = I^n_{p\mu qv} + \sum_m \sum_{p'\mu'q'v'} P^m_{p'\mu'q'v'} [&(np\mu nqv|mp'\mu'mq'v') \\ &- \tfrac{1}{2}(np\mu mq'v'|mp'\mu'nqv)] \,. \end{aligned} \tag{14}$$

$P^n_{p\mu qv}$ is a bond-order;

$$P^n_{p\mu qv} = 2 \sum_i^{\mathrm{occ}} C^*_{inp\mu} C_{inqv} \,, \tag{15}$$

$$I^n_{p\mu qv} = \int \chi^*_{np\mu}(1) \left(-\frac{\hbar^2}{2m} \nabla_1^2 - \sum_{mq'} \frac{Z_{mq'} e^2}{R_{mq'1}} \right) \chi_{nqv}(1)\, d\tau_1 \tag{16}$$

and

$$\begin{aligned} (np\mu mqv|n'p'\mu'm'q'v') = \iint \chi^*_{np\mu}(1)\, \chi_{mqv}(1) \frac{e^2}{r_{12}} \\ \chi^*_{n'p'\mu'}(2)\, \chi_{m'q'v'}(2)\, d\tau_1\, d\tau_2 \,. \end{aligned} \tag{17}$$

$I^n_{p\mu qv}$ is the Coulomb integral when $p\mu = qv$, otherwise a resonance integral. $(np\mu mqv|n'p'\mu'm'q'v')$ is the electron repulsion integral. Because of the arbitrary character of the variation set, a set of simultanious equations (Hertree-Fock equations for a molecular aggregate) is obtained,

$$\sum_{qv} C_{inqv}(F^n_{p\mu qv} - \varepsilon_{ni} S^n_{p\mu qv}) = 0 \quad (n = 1, N). \tag{18}$$

One of these equations (the effective Hartree-Fock equation for a constituent molecule) is very similar to that of a molecule, but $F^n_{p\mu qv}$ depends upon the coefficients of other molecules, $C_{imp\mu} (m \neq n)$, so that the equations $(n = 1, N)$ are not independent of each other.

Although to solve the equations there arises a difficulty due to the non-linearity of C_{inqv}, if the Fock matrix elements are estimated by a set of C_{inqv} assumed, the simultaneous equation becomes linear and feasible and then the equations are decoupled into seqular equations of the next form (the effective seqular equations for constitutent molecules);

$$\det |F^n_{p\mu qv} - \varepsilon_n S^n_{p\mu qv}| = 0 \quad (n = 1, N) \,. \tag{19}$$

Eq. (19) for the m-th molecule, which can be solved independently of other equations $(n \neq m)$, determines the one-electron orbitals belonging to the m-th molecule. However, this equation differs from the similar equation for an isolated molecule, since Eq. (19) includes the intermolecular interactions as a field (molecular field). Thus, the concept of the molecular field is introduced.

The general procedure to obtain the SCF solution or self-consistent molecular field is diagrammatized in Fig. 1. For the first step a set of $C_{inq\mu}$ should be assumed. For the n-th molecule the coefficients can be given from the Hückel orbitals or the SCF molecular orbitals of the free molecule. If all the coefficients for the molecules in the aggregate are given, then all the Fock matrix elements (Eq. (14)) can be

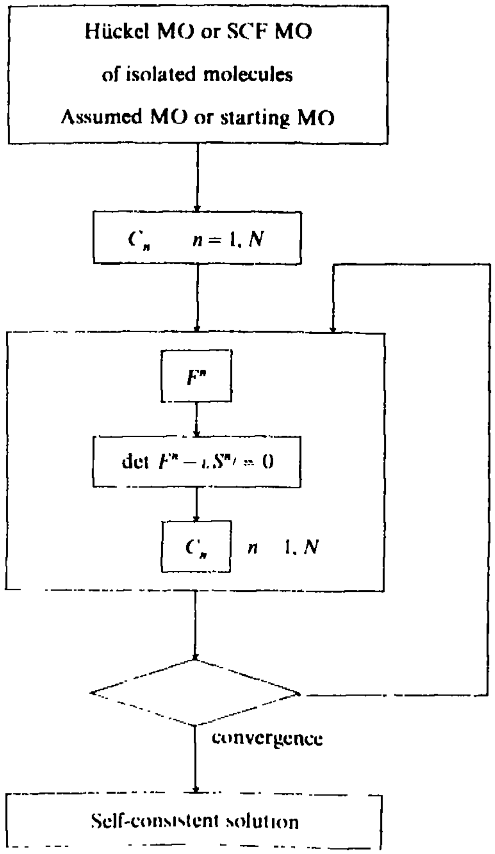

Fig. 1. Computational procedure to obtain a self-consistent solution

determined. Next, the seqular equation (Eq. (19)) for the n-th molecule (one-molecule problem) can be solved separately to give the new coefficients for the molecule. When all the equations are solved and a new set of the coefficients are obtained, the new Fock matrix elements will be determined to solve the new seqular equations. This procedure should be repeated until the cycle becomes self-consistent.

As shown above, N-molecule problem is decoupled into N times of one-molecule problem[7]. However, the one-molecule problems should be solved simultaneously, so that if N becomes large the process will be infeasible.

In the case of the molecular crystals where all the molecules are equivalent under the crystal symmetry operations in the ground state, the Fock matrices ($n = 1, N$) must be mathematically equivalent. Then, the N-molecule problem reduces to just one-molecule problem under an equivalent molecular field. In this case it is possible to omit the suffix *n* if the numbering of equivalent atoms under the crystal symmetry operations are chosen to be the same[8].

---

[7] Such decoupling is also derived when the one-electron orbitals in a crystal or a regular high polymer are expressed as linear combinations of basis sets constructed from the Bloch type sum of translationally equivalent atomic orbitals. In this case the problem is reduced to a set of one-unit-cell problems [25-27]. In molecular crystals, however, electrons are considered to be tightly bound to or localized on one molecule so that one-electron orbitals may be localized within a molecule rather than delocalized over the whole crystal.

Furthermore, if the molecules in a crystal are located on the crystal lattice points, the effective Fock operator should be invariant under the symmetry operations of the crystal point group. Then the one-electron orbitals of the molecule on the invarient lattice point must be the representations of the crystal point group.

2. A Simple Numerical Application

To examine whether the one-electron orbitals in a crystal are really deformed from those of a free molecule, this self-consistent equivalent molecular field method is applied to the typical aromatic hydrocarbon crystals. In the calculation, the usual π-electron approximation is employed (Section III.1). For the intramolecular electron repulsion integrals the π-electron correlation effect is considered along with Little and Gutefreund's method [28], and for the intermolecular electron repulsion integrals the bare Coulomb potential is used.

In Table 1, the orbital energies of coronene which has D_{6h} geometry are shown. For the free molecule there are several exactly degenerated orbitals. While, for

Table 1. Orbital energies of coronene

Free molecule (eV)		Crystal (eV)	Crystal field splitting (eV)
−16.0372	a_{2u}	−16.0799	
−14.9829	e_{1g}	−15.0298	
−14.9829	e_{1g}	−15.0186	0.0112
−13.6586	e_{2u}	−13.6994	
−13.6586	e_{2u}	−13.6983	0.0011
−13.3524	a_{2u}	−13.3937	
−12.2191	b_{2g}	−12.2576	
−12.1925	b_{1g}	−12.2343	
−11.9004	e_{1g}	−11.9467	
−11.9004	e_{1g}	−11.9391	0.0076
−10.7182	e_{2u}	−10.7600	
−10.7182	e_{2u}	−10.7574	0.0026
− 4.6726	e_{1g}^*	− 4.7146	
− 4.6725	e_{1g}^*	− 4.7113	0.0033
− 3.4525	e_{2u}^*	− 3.4988	
− 3.4525	e_{2u}^*	− 3.4912	0.0076
− 3.3241	a_{1u}^*	− 3.3622	
− 3.2010	a_{2u}^*	− 3.2429	
− 2.1383	b_{2g}^*	− 2.1798	
− 1.9099	e_{1g}^*	− 1.9508	
− 1.9099	e_{1g}^*	− 1.9495	0.0013
− 0.6868	e_{2u}^*	− 0.7338	
− 0.6868	e_{2u}^*	− 0.7227	0.0111
0.2895	b_{2g}^*	0.2465	

---

[8] There is an exception in Eq. (14). In electron repulsion integrals the suffix *n* cannot be omitted. The possible cases are F, P, S, C, I, and ε. Other impossible cases are ϕ_{μ} and χ_{npv}, etc.

the crystal the orbitals degenerated in the free molcule reveal the crystal field splitting. The π-electron densities on the carbon network also show the difference between the free molecule and the crystal. As shown in Table 2, the π-electron distribution of the free molecule satisfies the D_{6h} symmetry, while that of the

Table 2. Electron densities and orbital coefficients of coronene

a	b	c	d	e	f	g	h
1	A′	0.9946	0.9960	0.0000	−0.0037	−0.3148	−0.3144
2	I	1.0058	1.0073	−0.3109	−0.3109	−0.0028	0.0074
3	H	1.0058	1.0048	−0.1580	−0.1537	0.2679	0.2698
4	G	0.9946	0.9943	0.2727	0.2750	0.1575	0.1530
5	F	1.0058	1.0046	0.1531	0.1493	−0.2708	−0.2734
6	E	1.0058	1.0048	−0.1531	−0.1560	−0.2708	−0.2696
7	D	0.9946	0.9940	−0.2727	−0.2711	0.1575	0.1599
8	C	1.0058	1.0047	0.1580	0.1604	0.2679	0.2660
9	B	1.0058	1.0070	0.3109	0.3111	−0.0028	−0.0001
10	J′	0.9936	0.9942	0.0000	−0.0025	−0.2020	−0.2013
11	L	0.9936	0.9939	0.1749	0.1763	0.1010	0.0992
12	K	0.9936	0.9939	−0.1749	−0.1741	0.1010	0.1036
13	A	0.9946	0.9960	0.0000	−0.0037	−0.3148	−0.3144
14	I′	1.0058	1.0073	−0.3109	−0.3109	0.0028	0.0074
15	H′	1.0058	1.0048	−0.1580	−0.1537	0.2679	0.2698
16	G′	0.9946	0.9943	0.2727	0.2750	0.1575	0.1530
17	F′	1.0058	1.0046	0.1531	0.1493	−0.2708	−0.2734
18	E′	1.0058	1.0048	−0.1531	−0.1561	−0.2708	−0.2696
19	D′	0.9946	0.9940	−0.2727	−0.2711	0.1575	0.1599
20	C″	1.0058	1.0048	0.1580	0.1604	0.2679	0.2660
21	B′	1.0058	1.0070	0.3109	0.3111	−0.0028	−0.0001
22	J	0.9936	0.9942	0.0000	−0.0025	−0.2020	−0.2013
23	L′	0.9936	0.9939	0.1749	0.1763	0.1010	0.0992
24	K′	0.9936	0 9939	−0.1749	−0.1741	0.1010	0.1036

[a] Atomic position illustrated in Fig. 2.
[b] Atomic position in the crystal [29].
[c] π-electron densities of a free coronene molecule.
[d] π-electron densities of coronene in the crystal.
[e] One of the highest occupied orbitals of a free coronene molecule.
[f] The next highest occupied orbital of coronene in the crystal.
[g] The other highest occupied orbitals of a free coronene molecule.
[h] The highest occupied orbital of coronene in the crystal.

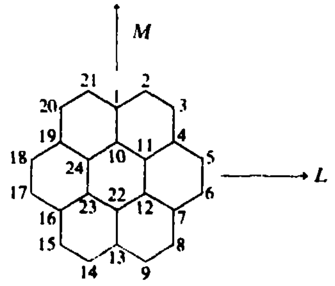

Fig. 2. Carbon skeleton of a coronene molecule: the molecular axes *M* and *L* indicate the orientation of the molecule in the crystal lattice [29]

molecule in the crystal is deformed into D_{2h} or even into C_i, which is seen easily to pick up the equivalent atoms. In the free molecule there are three groups of equivalent atoms, (1, 4, 7, 13, 16, 19), (2, 3, 5, 6, 8, 9, 14, 15, 17, 18, 20, 21), and (10, 11, 12, 22, 23, 24). Whereas in the crystals a crude grouping is as follows, (1, 13), (2, 9, 14, 21), (3, 5, 6, 8, 15, 16, 18, 20), (4, 7, 16, 19), (11, 12, 23, 24), and (10, 22), which may correspond to the D_{2h} symmetry. If the minor differences are noted, only the C_i symmetry can be seen.

Another demonstration is the difference of the orbital coefficients. The highest occupied orbitals of a free coronene molecule (e_{2u} degenerated orbitals) are compared with the highest and the next highest occupied orbitals of a molecule in the coronene crystal (Table 2, where the degenerated orbitals of a free molecule are symmetry-adapted to be the correct representations of D_{6h}). As can be seen from Table 2, the orbital coefficients for the isolated molecule and those for the crystal only differ by $10^{-1}-10^{-3}$. However, the inclusion of these differences yields remarkable contributions to the values of the CI matrix elements and the transition moments. This, of course, affects the values of the excitation energies and oscillator strengths.

In this example, coronene is a nonpolar molecule which is expected to produce "fairly weak molecular field". Therefore, if polar molecules such as heterocyclic compounds are concerned, much more serious effects is expected on the molecular orbitals in the crystal.

II. The Excited States of Molecular Crystals

In this section, the excited states of molecular crystals are described. The excited states are at first approximated by a single electronic configuration and then configuration interactions are considered.

1. Ionized Configuration

When an electron is removed from the occupied orbital $\phi_{mk\alpha}$, the electronic configuration is expressed as

$$\psi_{mk\alpha} = A\left|\prod_{ni\sigma} \phi_{ni\sigma} \cdot \phi_{mk\alpha}^{-1}\right| . \tag{20}$$

Considering the translational symmetry, the corresponding ionized state should be expressed as

$${}^2\psi_k(\boldsymbol{k}) = \begin{cases} \sum\limits_m \frac{1}{\sqrt{N}}\, e^{i\boldsymbol{k}\cdot\boldsymbol{r}_m}\, \psi_{mk\alpha} \\ \sum\limits_m \frac{1}{\sqrt{N}}\, e^{i\boldsymbol{k}\cdot\boldsymbol{r}_m}\, \psi_{mk\beta} \end{cases} , \tag{21}$$

where $\boldsymbol{k}$ is the crystal momentum, $\boldsymbol{r}_m$ is the position vector of the m-th molecule, and N is the total number of lattice points. The expectation value of the energy for $\psi_k(\boldsymbol{k})$, $E_k(\boldsymbol{k})$, is written as

$$E_k(\boldsymbol{k}) = E^0 - \varepsilon_k . \tag{22}$$

This equation shows that the Koopmans' thorem [30] holds as in the case of the usual SCF MO theory.

2. *Frenkel Exciton (One Molecule in Each Unit Cell)*

The electronic configuration of one-electron excitation within a molecule is given by

$$\psi_{mk\alpha,\,ml\alpha'} = A\left[\prod_{nl\sigma} \phi_{nl\sigma}\cdot\phi_{mk\alpha}^{-1}\cdot\phi_{ml\alpha'}\right]. \tag{23}$$

Then, the localized excitation configurations for singlet and triplet are expressed as

$$^{1}\psi_{mk,\,ml} = \frac{1}{\sqrt{2}}\left(\psi_{mk\alpha,\,ml\alpha} - \psi_{mk\beta,\,ml\beta}\right) \quad \text{(singlet)} \tag{24-1}$$

and

$$\begin{aligned} ^{3}\psi_{mk,\,ml} &= \frac{1}{\sqrt{2}}\left(\psi_{mk\alpha,\,ml\alpha} + \psi_{mk\beta,\,ml\beta}\right) \\ ^{3}\psi_{mk,\,ml} &= \psi_{mk\alpha,\,ml\beta} \qquad\qquad \text{(triplet)} \\ ^{3}\psi_{mk,\,ml} &= \psi_{mk\beta,\,ml\alpha}\,. \end{aligned} \tag{24-2}$$

According to the Frenkel-Pierles method [18–21], singlet and triplet Frenkel excitons should be written as

$$^{1,3}\psi_{k,l}(\boldsymbol{k}) = \sum_{m} \frac{1}{\sqrt{N}}\, e^{i\boldsymbol{k}\cdot\boldsymbol{r}_m}\, {}^{1,3}\psi_{mk,\,ml} \tag{25}$$

and the energies are

$$\begin{aligned} ^{1,3}E_{k,l}(\boldsymbol{k}) = E^{0} + \varepsilon_l - \varepsilon_k - \sum_{m'} e^{i\boldsymbol{k}\cdot(\boldsymbol{r}_{m'} - \boldsymbol{r}_m)} \\ \left[\int\!\!\int \phi_{ml}^{*}(1)\,\phi_{m'l}(1)\,\frac{e^2}{r_{12}}\,\phi_{m'k}^{*}(2)\,\phi_{mk}(2)\,d\tau_1\,d\tau_2 \right. \\ \left. - \binom{2}{0}\int\!\!\int \phi_{ml}^{*}(1)\,\phi_{mk}(1)\,\frac{e^2}{r_{12}}\,\phi_{m'k}^{*}(2)\,\phi_{m'l}(2)\,d\tau_1\,d\tau_2\right], \end{aligned} \tag{26}$$

where

$$\binom{a}{b} = \begin{cases} a\text{: singlet} \\ b\text{: triplet}. \end{cases} \tag{27}$$

3. *Charge-Transfer Exciton (One Molecule in Each Unit Cell)*

Charge-transfer exciton should be expressed as the lattice sum of translationally equivalent electronic configurations of electron transfer between two molecules. When the electron transfer vector is $\boldsymbol{x} = \boldsymbol{r}_n - \boldsymbol{r}_m$, the corresponding charge-transfer exciton may be written as

$$^{1,3}\psi_{k,l}(\boldsymbol{k},\boldsymbol{x}) = \sum_{nm}{}' \frac{1}{\sqrt{N}}\, e^{i\boldsymbol{k}\cdot\boldsymbol{r}_m}\, {}^{1,3}\psi_{mk,\,nl}\,, \tag{28}$$

where the lattice sum runs keeping $\boldsymbol{r}_n - \boldsymbol{r}_m = \boldsymbol{x}$ and

$$\begin{aligned} ^{1}\psi_{mk,\,nl} &= A\left[\prod_{nl\sigma}\phi_{nl\sigma}\cdot\left(\phi_{mk\alpha}^{-1}\phi_{nl\alpha} - \phi_{mk\beta}^{-1}\phi_{nl\beta}\right)/\sqrt{2}\right] \\ ^{3}\psi_{mk,\,nl} &= A\left[\prod_{nl\sigma}\phi_{nl\sigma}\cdot\left(\phi_{mk\alpha}^{-1}\phi_{nl\alpha} + \phi_{mk\beta}^{-1}\phi_{nl\beta}\right)/\sqrt{2}\right] \\ ^{3}\psi_{mk,\,nl} &= A\left[\prod_{nl\sigma}\phi_{nl\sigma}\cdot\phi_{mk\alpha}^{-1}\phi_{nl\beta}\right] \\ ^{3}\psi_{mk,\,nl} &= A\left[\prod_{nl\sigma}\phi_{nl\sigma}\cdot\phi_{mk\beta}^{-1}\phi_{nl\alpha}\right]. \end{aligned} \tag{29}$$

The energies are given by

$$
\begin{aligned}
{}^{1,3}E_{k,l}(\boldsymbol{k},\boldsymbol{x}) = E^0 + \varepsilon_l - \varepsilon_k - \sum_{m'} e^{i\boldsymbol{k}\cdot(\boldsymbol{r}_{m'}-\boldsymbol{r}_m)} \\
\Big[\int\int \phi^*_{m'k}(1)\,\phi_{mk}(1)\,\frac{e^2}{r_{12}}\,\phi^*_{m+xl}(2)\,\phi_{m'+xl}(2)\,d\tau_1\,d\tau_2 \\
-\binom{2}{0}\int\int \phi^*_{m'k}(1)\,\phi_{m'+xl}(1)\,\frac{e^2}{r_{12}}\,\phi^*_{m+xl}(2)\,\phi_{mk}(2)\,d\tau_1\,d\tau_2\Big].
\end{aligned}
\tag{30}
$$

4. *Davydov Splitting [3, 4] of Frenkel Exciton*

In the real light absorption process, the momentum conservation law leads to the selection rule;

$$\boldsymbol{k} \cong \boldsymbol{0}.$$

If $\boldsymbol{k}$ equals just to zero, the excited states of the crystal having more than one molecule in each unit cell must be representations of the factor group. When the number of molecules in each unit cell is t, the excited states corresponding to the Frenkel exciton (${}^{1,3}\psi_{k,l}(\boldsymbol{0})$) are expressed as

$$ {}^{1,3}\psi_j(k,l) = \sum_{ms} \frac{1}{\sqrt{t}}\, {}^{1,3}\psi_{msk,\,msl}\,\delta_j(s)\ , \tag{31}$$

where s denotes a site in a unit cell and $\delta_j(s)$ is a coefficient of j-th branch. The $\delta_j(s)$ should be determined by solving the following secular equation and obtaining the eigen-vectors.

$$\det|A(k,l)_{s_1,s_2} - E\delta_{s_1,s_2}| = 0\ , \tag{32}$$

where

$$A(k,l)_{s_1s_2} = \int \psi^*(k,l)_{s_1}\, H\psi(k,l)_{s_2}\, dv \tag{33}$$

and

$$\psi(k,l)_{s_1} = \sum_m \frac{1}{\sqrt{t}}\, \psi_{ms_1k,\,ms_1l}\ . \tag{34}$$

The energy eigenvalue of a Davydov branch, ${}^{1,3}E_j(k,l)$, is also obtained from the solution of the Eq. (32) as following,

$$ {}^{1,3}E_j(k,l) = E^0 + \varepsilon_l - \varepsilon_k + \sum_{m's'} \frac{1}{t}\,\delta_j(s')\,{}^{1,3}M_{m1m's'}(k,l) \tag{35}$$

and

$$
\begin{aligned}
{}^{1,3}M_{msm's'}(k,l) = -\int\int \phi^*_{msl}(1)\,\phi_{m's'l}(1)\,\frac{e^2}{r_{12}}\,\phi^*_{m's'k}(2)\,\phi_{msk}(2)\,d\tau_1\,d\tau_2 \\
+\binom{2}{0}\int\int \phi^*_{msl}(1)\,\phi_{msk}(1)\,\frac{e^2}{r_{12}}\,\phi^*_{m's'k}(2)\,\phi_{m's'l}(2)\,d\tau_1\,d\tau_2\,.
\end{aligned}
\tag{36}
$$

Then, Eq. (19) leads to the Davydov splitting between the j-th branch and the j'-th;

$$ {}^{1,3}\Delta(k,l)_{jj'} = \sum_s \Big[(\delta_j(s) - \delta_{j'}(s)) \sum_m {}^{1,3}M_{11ms}(k,l)\Big]. \tag{37}$$

5. *Configuration Interaction between Excitons*

Although the excited states has been described as $\psi_k(\boldsymbol{k})$, $\psi_{k,l}(\boldsymbol{k})$, and $\psi_{k,l}(\boldsymbol{k}, \boldsymbol{x})$, this approximation may or may not be good to the total wave-function $\psi_i(\boldsymbol{k})$ for an actual electronic state i of the crystal. In case for which a combination of several single exciton configurations is needed, a configuration interaction calculation should be performed by carrying out a linear variational calculation with $\psi_{k,l}(\boldsymbol{k}, \boldsymbol{x})$ (including $\psi_k(\boldsymbol{k})$ and $\psi_{k,l}(\boldsymbol{k})$ in the symbol) as starting functions:

$$\psi_i(\boldsymbol{k}) = \Sigma a_{k,l}(\boldsymbol{k}, \boldsymbol{x})_i \, \psi_{k,l}(\boldsymbol{k}, \boldsymbol{x}) , \tag{38}$$

determining the energy and the coefficients $a_{k,l}(\boldsymbol{k}, \boldsymbol{x})_i$ by solving a seqular equation

$$\det |A(\boldsymbol{k})_{kl\boldsymbol{x},k'l'\boldsymbol{x}'} - \delta_{kl\boldsymbol{x},k'l'\boldsymbol{x}'} E| = 0 , \tag{39}$$

where

$$A(\boldsymbol{k})_{kl\boldsymbol{x},k'l'\boldsymbol{x}'} = \int \psi^*_{k,l}(\boldsymbol{k}, \boldsymbol{x}) \, \boldsymbol{H} \, \psi_{k',l'}(\boldsymbol{k}, \boldsymbol{x}') \, dv . \tag{40}$$

In this configuration interaction scheme, the interactions between different $\boldsymbol{k}$ and also between different terms are neglected.

6. *Configuration Interaction Between Ionized Configurations*

As in the SCF theory of one molecule, the CI matrix elements between the ionized configurations also vanish;

$$\int {}^2\psi_k^*(\boldsymbol{k}) \, \boldsymbol{H} \, {}^2\psi_{k'}(\boldsymbol{k}) \, dv = 0 \quad (k \neq k') . \tag{41}$$

7. *Configuration Interaction Between the Ground Electronic Configuration and One-Electron Excitation Configurations*

The CI matrix elements between the ground electronic configuration and one-electron excitation configurations are also vanishing;

$$\int \psi^{0*} \boldsymbol{H} \, \psi_{mk,m+xl}(\boldsymbol{k}) \, dv = 0 . \tag{42}$$

Therefore, Brillouin's theorem [31] holds in this theory. In other words, exciton states do not mix with the ground one. This is one of the most important points of this theory, since the ground state can be expressed purely as the ground electronic configuration.

8. *Davydov Splitting and Configuration Interaction*

If more than one molecule are there in a unit cell, it is easy to consider the configuration interactions. The Davydov splitting is obtainable by solving

$$\det |{}^{1,3}_{\ j}A_{kl\boldsymbol{x},k'l'\boldsymbol{x}'} - \delta_{kl\boldsymbol{x},k'l'\boldsymbol{x}'} E| = 0 , \tag{43}$$

where

$${}^{1,3}_{\ j}A_{kl\boldsymbol{x},k'l'\boldsymbol{x}} = \int {}^{1,3}\psi_j(k, l, \boldsymbol{x}) \, \boldsymbol{H} \, {}^{1,3}\psi_j(k', l', \boldsymbol{x}) \, dv , \tag{44}$$

$${}^{1,3}\psi_{ji} = \Sigma^{1,3} a_{ji}(k, l, \boldsymbol{x}) \, {}^{1,3}\psi_j(k, l, \boldsymbol{x}) , \tag{45}$$

and ${}^{1,3}\psi_j(k, l, \boldsymbol{x})$ are the solution of Eq. (32) or its simple version with $\boldsymbol{x} \neq \boldsymbol{0}$. It should be noted that the configuration interactions between different Davydov branches are vanishing and then the excited states are labeled by branch number j and another quantum-number i.

9. Characteristics of This Theory

When the descriptions of the electronic states given above are appropriate for the actual molecular crystals, the calculations and estimations of following physical properties of molecular crystals become facile. (a) Stabilization energy of a molecule in crystallization; according to the vanishing character of the CI matrix elements between the ground electronic configuration and one electron excitation configurations, if the configuration interactions with two-electron excitation configuration and others are neglected, the stabilization energy of a molecule when it is brought into the crystal from vacuum (crystal lattice energy) can be calculated from the total energy of an isolated molecule and the total energy of the ground electronic configuration of the crystal. The former is easily obtainable by solving the conventional one-molecule Hartree-Fock equation and the latter also by solving the effective one-molecule problem. (b) Spectral shifts. (c) Removal of electronic degeneracy (crystal field splitting of the degenerated states). (d) Violation of selection rules (allowance of the forbidden transition of the isolated molecule in the crystal). (e) Crystal field mixing (configuration interaction between the configurations which do not belong to the same irreducible representation in an isolated molecule). (f) Removal of the arbitrary character of the direction of the transition moment of a high symmetry molecule such as benzene and coronene; once the SCF orbitals for the ground electronic configuration are obtained, these properties from (b) to (f) are determined from the eigen-values and eigen-vectors of Eq. (39). Although in the usual calculation of Davydov splitting the direction of the transition moment of a high symmetry molecule in a crystal is assumed and the number of configurations for CI calculation are usually limited a few[32], by this method the assumption is not needed and CI calculation can be carried out as in the case of a molecule, because the CI matrix elements are considerably simplified. Therefore, from the solution of the simple secular Eq. (32) or (43) it is hopeful to get more reliable results in the calculation of the Davydov splitting and the polarization of each Davydov branch.

III. Semi-Empirical Methods

In this section semi-empirical treatments are presented, because the *ab initio* calculation may not be feasible in a large system. At first π-electron approximation is taken to calculate the electronic transition energies and their oscillator strengths. Next, all valence electron treatment is used to study the intermolecular interactions.

1. π-Electron Approximation

If attention is paid to the properties of mobile electrons of the system (for example, electronic spectra of aromatic hydrocarbons), the usual π-electron approximation may be taken. Within this limitation an extension of the conventional Pariser-Parr method may be an appropriate method to test this theory. Now, the following approximations are taken.

(a) Zero-Differential Overlap Approximation

Using zero-differential overlap (ZDO) approximation, the electron repulsion integrals of Eq. (17) vanish unless they are one center or two center Coulomb repulsion integrals;

$$(npn'p'|mqm'q') = \delta_{n,n'}\,\delta_{p,p'}\,\delta_{m,m'}\,\delta_{q,q'}\,\gamma_{npmq} \tag{46}$$

and

$$\gamma_{npmq} = \int\int \chi^*_{np}(1)\,\chi_{np}(1)\,\frac{e^2}{r_{12}}\,\chi^*_{mq}(2)\,\chi_{mq}(2)\,d\tau_1\,d\tau_2\,. \tag{47}$$

(b) Pariser Approximation [33]

According to Pariser approximation one center Coulomb repulsion integrals become,

$$\gamma_{npnp} = I_{np} - A_{np}\;, \tag{48}$$

where I_{np} and A_{np} are the ionization potential and the electron affinity of p-th atom in the n-th molecule, respectively.

(c) Two Center Coulomb Repulsion Integrals

Two center Coulomb repulsion integrals, γ_{npmq}, are evaluated by Pariser-Parr [34] or Nishimoto-Mataga [35] approximation.

(d) Coulomb Integrals

Starting from Goeppert-Mayer-Sklar approximation [36] and neglecting all the penetration integrals, Coulomb integrals, I^n_{pp}, are expressed as

$$I^n_{pp} = W_{np} - \sum_{mq}{}' \gamma_{npmq}\;, \tag{49}$$

where $-W_{np}$ is the ionization potential of the valence state of np-th atom and the summation is taken over the whole system except $mq = np$.

(e) Resonance Integrals

As in the case of usual methods, resonance integrals, I^n_{pq} $(p \neq q)$, are considered to be empirical parameters. They should be determined to reproduce one-molecule properties.

From the approximations, (a) and (d), the Fock matrix elements are written as

(diagonal)

$$F^n_{pp} = W_{np} + \sum_{mq} (P^m_{qq} - 1)\,\gamma_{npmq} - \tfrac{1}{2}(P^n_{pp} - 2)\,\gamma_{npnp} \tag{50-1}$$

and

(off-diagonal)

$$F^n_{pq} = I^n_{pq} - \tfrac{1}{2} P^n_{pq}\,\gamma_{npnq}\;, \tag{50-2}$$

where P^m_{qq} is the π-electron density on q-th atom in the m-th molecule;

$$P^n_{pq} = 2\sum_{i}^{\text{occ}} C^*_{inp}\,C_{inq}\,. \tag{51}$$

It should be noted that from the ZDO approximation the excitation energy of a single Frenkel exciton or charge transfer exciton is expressed as

$$\begin{aligned} {}^{1,3}E_{k,l}(k,x) - E^0 = \varepsilon_l - \varepsilon_k - \sum_{pq} C^*_{lm+xp} C_{lm+xp} \\ C^*_{kmq} C_{kmq} \gamma_{m+xpmq} + \binom{2}{0} \sum_{pqm'} e^{ik\cdot(r_{m'}-r_m)} \\ C^*_{lmp} C_{kmp} C^*_{km'q} C_{lm'q} \gamma_{mpm'q} \delta_{x,0} \,. \end{aligned} \tag{52}$$

This equation shows that only the singlet Frenkel exciton has non-zero bandwidth as far as the ZDO approximation is valid. This feature agrees well with the experimental results [37] from which the bandwidth of triplet exciton is expected to be much smaller than that of singlet exciton, however, in order to calculate the bandwidth of triplet exciton the ZDO approximation should not be used.

In the frame of the ZDO approximation, the configuration interaction matrix elements are written as

$$\begin{aligned} \Lambda(k)_{klx,k'l'x'} = -\sum_{pq} C^*_{lm+xp} C_{l'm+xp} C^*_{k'mq} C_{kmq} \gamma_{m+xpmq} \delta_{x,x'} \\ + \binom{2}{0} \sum_{pqm'} e^{ik\cdot(r_{m'}-r_m)} C^*_{lmp} C_{kmp} C^*_{k'm'q} C_{l'm'q} \gamma_{mpm'q} \delta_{x,x'} \delta_{x,0} \,. \end{aligned} \tag{53}$$

Eq. (53) reveals that the non-zero interactions only occur between Frenkel excitons and also between charge-transfer excitons, and the *k*-dependence appears only in the case of singlet Frenkel excitons. It should be noted that this vanishing character of the configuration interaction matrix elements extremely reduces the effort to calculate the electronic states; it is not needed to consider charge-transfer excitons when calculating Frenkel exciton states, though the mixing of C–T excitons with Frenkel exciton states has been previously considered [6, 38–40].

2. *All Valence Electron Treatment*

In order to discuss the total energy of the system, it may be appropriate to use all valence electron treatment following the CNDO (complete neglect of differential overlap) method proposed by Pople, Santry, and Segal [41, 42]. The expressions for the Fock matrix elements and for the total energy of the system are obtained as in Eqs. (57) and (59), respectively, according to the following approximations;

$$I^n_{p\mu p\nu} = W_{np\mu} \delta_{\mu,\nu} - \sum_{n'p'} U_{np,n'p'} \delta_{\mu,\nu} \quad (p=q)\,, \tag{54}$$

$$I^n_{p\mu q\nu} = \beta^n_{pq} S^n_{p\mu q\nu} \quad (p \neq q)\,, \tag{55}$$

$$(np\mu n'p'\mu' \,|\, mq\nu m'q'\nu') = \gamma_{npmq} \delta_{np\mu,n'p'\mu'} \delta_{mq\nu,m'q'\nu'} \,, \tag{56}$$

where W, β, and γ are the empirical parameters and $-U_{np,n'p'}$ is a parameter representing the potential energy of an electron on the np-th atom under the potential of the core of the $n'p'$-th atom.

Fock matrix elements; for $p=q$ and $\mu=\nu$

$$F^n_{p\mu p\mu} = W_{np\mu} + (P^n_p - \tfrac{1}{2} P^n_{p\mu p\mu}) \gamma_{npnp} + \sum_{n'p'} (P^n_{p'} \gamma_{npn'p'} - U_{npn'p'})\,, \tag{57-1}$$

for $p=q$ and $\mu \neq \nu$

$$F^n_{p\mu q\nu} = -\tfrac{1}{2} P^n_{p\mu q\nu} \gamma_{npnp}\,, \tag{57-2}$$

and for $p \neq q$

$$F^n_{p\mu q\nu} = \beta^n_{pq} S^n_{p\mu q\nu} - \tfrac{1}{2} P^n_{p\mu q\nu} \gamma_{npnq}\,, \tag{57-3}$$

where P^n_p is the electron density on the p-th atom in the n-th molecule,

$$P^n_p = \sum_{\mu} P^n_{p\mu p\mu}\,. \tag{58}$$

The total energy of the system is written as

$$\begin{aligned} E_{\text{tot}} = {} & \sum_{np} \left| \sum_{\mu} P^n_{p\mu p\mu} W_{np\mu} + \tfrac{1}{2} \sum_{\mu} \left(P^n_{p\mu p\mu} P^n_{p\nu p\nu} - \tfrac{1}{2} {P^n_{p\mu p\nu}}^2\right) \gamma_{npnp} \right| \\ & + \sum_{n} \sum_{\substack{pq \\ (p \neq q)}} \sum_{\mu\nu} \left(\beta^n_{pq} S^n_{p\mu q\nu} P^n_{p\mu q\nu} - \tfrac{1}{4} {P^n_{p\mu q\nu}}^2 \gamma_{npnq}\right) \\ & + \tfrac{1}{2} \sum_{\substack{npn'p' \\ (np \neq n'p')}} \left(Z_{np} Z_{n'p'} e^2/R_{npn'p'} - P^n_p U_{np,n'p'} - P^{n'}_{p'} U_{n'p',np} + P^n_p P^{n'}_{p'} \gamma_{npn'p'}\right), \end{aligned} \tag{59}$$

where $R_{npn'p'}$ is the distance between atoms, np and $n'p'$. The first term of Eq. (59) represents the atomic energies and the second term the binding energies of the bond formation. To clarify the physical meaning of the third term of Eq. (59) it is rewritten as

$$\tfrac{1}{2} \sum_{\substack{npn'p' \\ (np \neq n'p')}} \left(E(1)_{npn'p'} + E(2)_{npn'p'} + E(2)_{n'p'np} + E(3)_{npn'p'}\right),$$

where

$$E(1)_{npn'p'} = (P^n_p - Z_{np})(P^{n'}_{p'} - Z_{n'p'})\, \gamma_{npn'p'}\,, \tag{60-1}$$

$$E(2)_{npn'p} = (P^n_p - Z_{np})(Z_{n'p'} \gamma_{npn'p'} - U_{np,n'p'})\,, \tag{60-2}$$

$$E(3)_{npn'p'} = Z_{np} Z_{n'p'} \gamma_{npn'p'} + Z_{np} Z_{n'p'} e^2/R_{npn'p'} - Z_{np} U_{np,n'p'} - Z_{n'p'} U_{n'p',np}\,. \tag{60-3}$$

$E(1)$ is the static Coulomb interaction between the net charges on the atoms, which involves not only the usual electrostatic interaction between the unperturbed net charges as they exist in the isolated molecules but also the usual polarization effect and even higher-order effects.

$E(2)_{npn'p'}$ is interpreted as the interaction between the net charge on the np-th atom and the neutral $n'p'$-th atom.

$E(3)_{npn'p'}$ represents the interaction between the neutral atoms, np and $n'p'$. In the CNDO/2 parametrization for $U_{np,n'p'}(U_{np,n'p'} = Z_{np}\gamma_{npn'p'})$, $E(2)$ is vanishing and $E(3)$ becomes $Z_{np}Z_{n'p'}(e^2/R_{npn'p'} - \gamma_{npn'p'})$ which is repulsive in the usual parametrization of γ. While, $E(2)$ and $E(3)$ can be attractive from the point of view of their physical meaning: $E(2)$ should be replaced by the interaction between the net charge and the induced dipole on the neutral atom (which is of the form $-\varrho_1^2 e^2 \alpha_2/2R_{12}^4)$[9] and $E(3)$ should be replaced by "van der Waals interaction" between the neutral atoms (which is of the form $-\dfrac{3}{2}\dfrac{I_1 I_2}{I_2 + I_2}\alpha_1\alpha_2/R_{12}^6)$[9] except for very small distance.

---

[9] ϱ is the net charge. I is the ionization potential, and α is the polarizability.

So long as the heat of formation of an isolated molecule is concerned, these attractive terms may be negligible. When the intermolecular interaction is taken up, however, these terms should not be neglected, which may be seen very clearly when interacting energies between two rare gas atoms are approximated in this way: the lack of the dispersion energy results in the absence of an attractive minimum. Therefore, we propose one of the most simple treatments as follows;

(A) For the Fock matrix elements and $E(2)$, CNDO/2 approximation ($U_{np,n'p'} = Z_{np}\gamma_{npn'p'}$) is used[10].

(B) For the intramolecular interaction terms of $E(3)$, CNDO/2 approximation or MINDO/1 expression (the latter is of the form $Z_A Z_B(e^2/R_{AB} - \gamma_{AB})\exp(-\alpha_{AB}R_{AB})$) [43] is used.

(C) For the intermolecular interaction terms of $E(3)$, the pair-wise potential [44, 45], $A/R^{12} - B/R^6$ or $A\exp(-\alpha R) - B/R^6$ is used.

Among the above parameters for the all valence electron treatment, the same parameters used for the isolated molecules may be available except for the intermolecular electron repulsion integrals $\gamma_{npn'p'}$ ($n \neq n'$) and the parameters of the pair-wise potential.

According to this approximate treatment, the intermolecular interaction is decomposed into three parts; (1), molecular energy shifts by electron redistribution (positive)[11], (2) static Coulomb interactions between the net charges modified through an SCF procedure, which involves not only usual electrostatic energy but also the polarization energy (negative), (3), dispersion (or London) energy and intercore repulsion energy (negative under the appropriate location of the molecules). Among these parts the first two ones can be estimated directly from the electron distribution determined by this SCF method, and the calculations based only on the pair-wise potential can be corrected easily from the two parts, (1) and (2).

IV. Discussion

1. *Applicability of the Self-Consistent Molecular Field Theory*

As indicated in Section III, Brillouin's theorem holds in this theory. Therefore, it is clear that the ground electronic configuration does not mix with one-electron charge-transfer configurations, and then the charge-transfer resonance [46, 47] does not contribute to lowering the ground state energy. This is due to the following two assumptions; one-electron orbitals are expressed as the linear combination of atomic orbitals on one molecule and the intermolecular overlaps are neglected. As far as these two assumptions are used and more than one-electron excitation configurations are not considered, this theory should be only applicable to the systems in which each molecule is almost purely neutral or almost purely ionic[12], and not applicable to the systems of intermediate charge-transfer[13].

---

[10] In the calculation of hydrogen bond, the induction term $E(2)$ may play an important role.

[11] In Eq. (59) the first and second terms, and the third term for $n = n'$ represent the molecular energies. Although these terms are the same expression of the molecular energies as that of the system of isolated molecules, the electron distribution of the molecules in the aggregate will be different from that of isolated molecules. Furthermore, the equilibrium positions of nuclei in the former may be distorted from those in the latter. Therefore, the molecular energies in the aggregate should be shifted from those in the isolated system. This molecular energy shifts may be positive, since the molecular energies are minimal in the isolated system.

Furthermore, if an intermolecular overlap is too large to neglect, there should be an intermolecular bonding, and then it is not appropriate to use the localized one-electron orbitals on a molecule. Therefore, this theory is only applicable to the system in which there is no large overlap or no chemical bonding between the molecules.

2. *Problems Arising from Convergence*

On the numerical application, there are two convergence problems peculiar to the SCF calculation on infinite systems[14]. The first is associated with the divergence of the integral sums over an infinite lattice. When the attractive terms and repulsive terms are summed separately in the Fock matrix elements, both of the partial sums are divergent. If these two sums are combined, the resulting elements are at best conditionally convergent. More pricisely, the divergence arises from the infinite sums of the integrals which diminish not more rapidly than $1/r^2$, therefore, the condition of convergence is due to the process of the next sum in the Fock matrix elements (Eq. (50));

$$\sum_{\substack{n'p' \\ (n'p' \neq np)}} (P_{p'}^{n'} - Z_{n'p'})\, \gamma_{npn'p'} \,.$$

If this sum is taken over the charges on a molecule and then over those on another molecule, this procedure may lead to convergence.

Although there is no clear proof of this prediction, it is very hopeful, since the electric field induced by a neutral molecule in the distance is in the first approximation to be that by the permanent dipole of the molecule. Furthermore, if many electron correlations are included in γ, γ may be a dielectrically screened Coulomb potential and the value of γ may reduce much more rapidly with r than that of bare Coulomb potential.

The second problem is associated with the infinite number of SCF equations, Eq. (18). Although the SCF procedure cannot be done in real computation, it is important to know what number of equations to be solved in order to obtain

---

[12] To apply this theory to almost purely ionic radical salt crystals an open-shell treatment is needed.

[13] Even if the intermolecular charge transfer is not neglected, this theory is applicable to the special systems in which the intermolecular charge transfer chains do not extend over the fairly large region of a hundred molecules, a thousand molecules, or all over the crystal. For a simple example, two interacting molecules such as an electron donor-acceptor pair or a hydrogen-bonded dimer in the aggregate are considered to be "one molecule" so that the one-electron orbitals may be expanded in the atomic orbital bases of these two molecules. In such a case, this SCF theory is applicable to it with no modification.

[14] Another infinite sum is needed on calculating excitation energies [15]. In Eq. (52) the lattice sum for a Frenkel exciton with $k = 0$ becomes

$$\sum_{m'} \sum_{m} C^{*}_{lmp} C_{kmp} C^{*}_{km'q} C_{lm'q} \gamma_{mpm'q} \,.$$

The convergence character of this sum may be seen as the same way as the first problem because $C^{*}_{lmp} C_{kmp}$ and $C^{*}_{km'q} C_{lm'q}$ can be interpreted as the charge on the *mp*-th atom and that on the *m'q*-th atom, respectively.

sufficient convergence. This question is closely correlated with another one, what number of terms are to be summed in the Fock matrix elements. If the long-range intermolecular interactions can be neglected, the SCF orbitals may be determined by the short-range terms. Thus, it can be concluded that as far as the convergence of the sum of Fock matrix elements are fulfilled in fairly short-range, the number of secular equations to be solved becomes finite and sufficiently small for real computation.

In molecular crystals, the second difficulty disappears automatically because of the effective one-molecule problem under the equivalent molecular field. Moreover, the first one is also removed: the well-known methods for the evaluation of Madelung sums [48, 49] are available, since the translational symmetry makes it possible to replace the lattice sum by the Fourier-integral or the reciprocal lattice sum.

The authors express to Prof. Y. Harada for useful suggestions.

Appendix

The energy of the ground electronic configuration is expressed as follows in terms of the orbital coefficients and atomic integrals defined in Section I.

$$
\begin{aligned}
E^0 = 2 \sum_{ni}^{\text{occ}} \sum_{p\mu q\nu} & C^*_{inp\mu} C_{inq\nu} I^n_{p\mu q\nu} \\
& + \sum_{nimj}^{\text{occ}} \sum_{p\mu q\nu p'\mu' q'\nu'} (2C^*_{inp\mu} C_{inq\nu} C^*_{jmp'\mu'} C_{jmq'\nu'}) \\
& \cdot [(np\mu nq\nu | mp'\mu' mq'\nu') - \tfrac{1}{2}(np\mu mq'\nu' | mp'\mu' nq\nu)] \, .
\end{aligned}
$$

According to the variation principle, the following equation should be fulfilled for an arbitrary variation set of the orbital coefficients;

$$\delta\left(E^0 - \sum_{ni} 2\varepsilon_{ni}\right) = 0 \, ,$$

where the variation parameters ε_{ni} are introduced based on the orthogonality conditions (Eq. (11)). For the variation of $C^*_{inp\mu}$, Eq. (13) can be easily derived.

References

1. Roothaan, C. C. J.: Rev. mod. Physics **23**, 69 (1951).
2. Hall, G. G.: Proc. Royal Soc. (London) A **205**, 541 (1951).
3. Davydov, A. S.: J. exp. theoret. Physics (USSR) **18**, 210 (1948).
4. — Theory of molecular excitons. Translated by M. Kasha and M. Oppenheimer, New York: McGraw-Hill Book Company 1962.
5. Craig, D. P.: J. chem. Soc. **1955**, 2302.
6. Tanaka, J.: Progr. theoret. Physics (Kyoto) supple. **12**, 183 (1959).
7. McClure, D. S.: Solid State Physics **8**, 1 (1962).
8. Tanaka, M., Tanaka, J.: Molecular Physics **16**, 1 (1969).
9. Craig, D. P., Walmsley, S. H.: The physics and chemistry of organic solid state. New York: Interscience Publishers 1963.
10. Fox, D., Schnepp, O.: J. chem. Physics **23**, 767 (1955).
11. Wolf, H. C.: Solid State Physics **9**, 1 (1959).
12. Craig, D. P., Walmsley, S. H.: Molecular Physics **4**, 113 (1961).

13. - - Advances in molecular spectroscopy, Vol. 1. New York: Pergamon Press 1962.
14. Jortner, J., Rice, S. A., Katz, J. L., Choi, S.: J. chem. Physics **42**, 309 (1965).
15. Silbey, R., Jortner, J., Rice, S. A.: J. chem. Physics **42**, 1515 (1965).
16. Tanaka, J.: Bull. chem. Soc. Japan **38**, 86 (1965).
17. Cox, E. G., Cruickshank, D. W. J., Smith, J. A. S.: Proc. Royal Soc. (London) A **247**, 1 (1958).
18. Frenkel, J.: Physic. Rev. **37**, 17 (1931).
19. -- Physic. Rev. **37**, 1276 (1931).
20. Peierls, R. E.: Ann. Physik (5) **13**, 905 (1932).
21. Frenkel, J.: Physik. Z. Sowjetunion **9**, 158 (1936).
22. Born, M., Oppenheimer, J. R.: Ann. Physik **84**, 457 (1927).
23. Fischer-Hjalmars, I.: Adances in quant. Chemistry **2**, 25 (1965).
24. Löwdin, P. O.: J. chem. Physics **18**, 365 (1950).
25. Del Re, G., Ladik, J.: Physic. Rev. **155**, 997 (1967).
26. Harris, F. E., Monkhorst, H. J.: Physic. Rev. Letters **23**, 1026 (1969).
27. O'shea, S., Santry, D. P.: J. chem. Physics **54**, 2667 (1971).
28. Gutfreund, H., Little, W. A.: Physic. Rev. **183**, 68 (1969); J. chem. Physics **50**, 4468 (1969).
29. Robertson, J. M., White, J. G.: J. chem. Soc. **1945**, 607.
30. Koopmans, T.: Physica **1**, 104 (1933).
31. Brillouin, L.: Actualités sci. et ind. No. 159 (1934).
32. Tanaka, J.: Bull. chem. Soc. Japan **38**, 86 (1965).
33. *Pariser, R.: J. chem. Physics* ***21***, *568 (1953).*
34. Parr, R. G.: J. chem. Physics **21**, 767 (1953).
35. Nishimoto, K., Mataga, M.: Z. physik. Chem. (Frankfurt) **12**, 335; **13**, 140 (1957).
36. Goeppert-Mayer, M., Sklar, A. L.: J. chem. Physics **6**, 645 (1938).
37. Nieman, G. C., Robinson, G. W.: J. chem. Physics **38**, 1928 (1963).
38. Lyons, L. E.: J. chem. Soc. **1957**, 5001.
39. Merrifield, R. E.: J. chem. Physics **34**, 1835 (1961).
40. Webber, S., Rice, S. A., Jortner, J.: J. chem. Physics **41**, 2911 (1964).
41. Pople, J. A., Santry, D. P., Segal, G. A.: J. chem. Physics **43**, S129 (1965).
42. Segal, G. A.: J. chem. Physics **43**, S136 (1965); **44**, 3289 (1966).
43. Dewar, M. J. S., Klopman, G.: J. Amer. chem. Soc. **89**, 3089 (1967).
44. Lenard-Jones, J.: Proc. Royal Soc. (London) A **106**, 463 (1924).
45. Buckingham, R. A.: Proc. Royal Soc. (London) A **168**, 264 (1938).
46. Mulliken, R. S.: J. Amer. chem. Soc. **71**, 811 (1952); J. physic. Chem. **56**, 801 (1952); J. chem. Physics **61**, 20 (1964).
47. Person, W. B.: Ann. Rev. physic. Chem. **13**, 107 (1962).
48. Ewald, P. P.: Ann. Physik **64**, 253 (1921).
49. Harris, F. E., Monkhorst, H. J.: Physic. Rev. B **2**, 4400 (1970).

Prof. Dr. K. Ohno
The Institute for Solid State Physics
The University of Tokyo
Roppongi, Tokyo
Japan

Theoret. chim. Acta (Berl.) 26, 351—356 (1972)
© by Springer-Verlag 1972

Calculations of Molecular Wave Functions in Terms of Modulated Plane Waves

M. Morandi Cecchi

Istituto di Elaborazione dell'Informazione del C.N.R.
and Istituto di Chimica Fisica dell'Università di Pisa, Italy

O. Salvetti

Istituto di Chimica Fisica dell'Università di Pisa, Italy

Received April 6, 1971

The possibility of representing molecular orbitals in terms of a many centre expansion of modulated plane waves is discussed. All integrals appearing in the usual SCF procedure for the calculation of the energy are obtained in an analytical form. The resulting formulae are rather simple to be evaluated.

Es wird die Möglichkeit, Molekülorbitale mittels einer Mehrzentrenentwicklung von modulierten ebenen Wellen darzustellen, diskutiert. Alle Integrale, die in einer SCF-Rechnung üblichen Typs (z. B. CNDO) erscheinen, werden in einer einfach auszuwertenden analytischen Form angegeben.

1. Introduction

The *ab initio* evaluation of accurate molecular wave functions by the Hartree-Fock method is usually approached by expanding the molecular orbitals in terms of a many-center basis set of functions referred to various atomic nuclei.

If the basis functions centered at any atom form by themselves a complete set, one may evidently get an expansion over a redundant set. When the employed number of terms at each expansion centre is small, as for example in the case of a minimal set of Slater orbitals, there is no difficulty in connection with the redundancy; as the number of terms increases, however, the overlap matrix tends to become singular the self-consistency procedure becomes more and more difficult and the loss of significant digits is such as to invalidate the results obtained. In order to obviate such difficulties, several authors, besides resorting to double or triple precision in using the computer, group the basis functions in order to get a smaller number of terms.

It is difficult, however, to formulate precise criteria to guide such procedures [1]. An expansion utilizing only a one-center complete set of basis functions does not present such difficulties, but it does not appear convenient because of the very high number of terms required. It does not have, moreover, the capability of representing discontinuities of the first derivative outside of the centre of expansion, that are required for some orbitals at certain points. A resonable way out of such difficulties appears to be the following: one should employ a small number of functions centered at the various nuclei to represent the peculiarities of the wave function in the neighbourhoods of the nuclei, and an extended set of spread-out functions to give a description of the remaining part of the wave function.

In the present research we propose to specify this idea and to obtain the set of analytical formulae useful for the SCF procedure in terms of a special type of basis functions which we will call modulated plane waves.

2. Modulated Plane Waves

The methods of evaluation previously outlined divides the molecular space into many parts. The simplest procedure would be to consider a sphere centered at the molecule center of mass with a radius such as to contain the whole molecule after assigning to each atom a volume at least equal to the Van der Waals one. In the neighbourhood of every atom, moreover, a sphere is to be of sufficiently small radius to avoid having the atoms overlap each other. The whole space is therefore divided into three regions:

The space inside the small spheres (region I), the space external to the preceeding ones but internal to the main sphere (region II), the space external to the main sphere, where the wave function essentially vanishes (region III).

However, such a subdivision would introduce considerable difficulties in the subsequent calculations, because of the continuity requirement for all molecular orbitals in every point in space. This difficulty is overcome if, instead of this partition into spheres, one replaces the above rigid spheres by proper weight functions, which we simply choose of the form e^{-r^2/l^2}. The basis functions are therefore modulated in such a way as to be unchanged in the neighbourhood of the origin, while they quickly become zero as soon as r exceeds l. The group of functions that describes the local situation in the neighbourhood of the k^{th} nucleus will be multiplied by $e^{-(r_k/l_k)^2}$, r_k being the distance from the k^{th} nucleus and l_k a parameter depending on the "dimension" of the atom considered while the spread-out functions will be multiplied by $e^{-(r/l)^2}$, with obvious meanings of the symbols. If R is the distance between two nuclei A and B and we put $l_A = l_B = \dfrac{R}{n}$, the two normalized weight functions overlap by $e^{-n^2/2}$, so that it is manifest that for $n = 6$ the two spaces are already practically disjoint.

We pass now to a discussion of the properties required of the basis functions. In region II, orbitals have to be represented which display neither cusp points nor very pronounced maxima that can be located *a priori*. With this object in view, it would appear convenient either to use an expansion in terms of Tchebycheff polynomials or a Fourier 3-dimensional expansion. Since the first alternative can be reduced to a linear combination of gaussian functions, in the following only the formulae are given that refer to the second kind of expansion.

As far as region I is concerned, there is no doubt that atomic orbitals of the Slater type are well suited functions, mostly owing to their capability for reproducing cusps at the nuclei. In principle such a behaviour may be obtained by means of any expansion where the r variable explicitly appears, but not by a polynomial expansion in x, y, z. On the other hand a careful description of the function at the nucleus is probably very important only in the evaluations of some particular observables (related, for instance, to the so-called Fermi contact term); but much less so for other observables, as is shown by the very good results obtained for the energy by gaussian function expansions. For all these reasons, we have restricted our research to a Fourier 3-dimensional expansion also in the neighbourhoods of the nuclei so that in each region an expansion in terms of plane waves modulated by weight functions has been considered.

If k indicates any expansion centre, the above functions, take the form

$$\chi(l_k; \boldsymbol{r}_k) = \mathcal{N} e^{-\left((r_k/l_k)^2 + i\frac{\pi}{l_k}(\boldsymbol{n}_k \cdot \boldsymbol{r}_k)\right)}; \tag{1}$$

$\mathcal{N}$ being a normalization coefficient and $\boldsymbol{n}$ a vector with integral components. Let r be the distance of any point P from the origin 0, and r_k be the distance from a new origin 0′, and then if R is the distance between 0 and 0′, we write $\boldsymbol{N} = \boldsymbol{R} + i\frac{\pi}{l}\boldsymbol{n}$, $\alpha = 1/l_k^2$. Then (1) becomes:

$$\chi(\boldsymbol{R}, \boldsymbol{N}, \alpha; \boldsymbol{r}) = \mathcal{N} e^{-\alpha r^2 + \boldsymbol{N} \cdot \boldsymbol{r}}. \tag{2}$$

3. Evaluation of Integrals

The overlap and kinetic energy integrals can easily be obtained by using the following standard integrals [2]:

$$\begin{aligned}
&\int_{-\infty}^{+\infty} e^{-px^2+qx}\,\mathrm{d}x = \sqrt{\frac{\pi}{p}}\, e^{q^2/4p} \\
&\int_{-\infty}^{+\infty} e^{-px^2+qx}x\,\mathrm{d}x = \frac{q}{2p}\sqrt{\frac{\pi}{p}}\, e^{q^2/4p} \\
&\int_{-\infty}^{+\infty} e^{-px^2+qx}x^2\,\mathrm{d}x = \sqrt{\frac{\pi}{p}}\cdot e^{q^2/4p}\left(\frac{1}{2p} + \frac{q^2}{4p^2}\right).
\end{aligned} \tag{3}$$

In these formulae p is real and positive, while q may be complex. Thus,

$$\begin{aligned}
S &= \int \chi^*(\boldsymbol{R}, \boldsymbol{N}, \alpha; 1)\, \chi(\boldsymbol{R}', \boldsymbol{N}', \alpha'; 1)\, \mathrm{d}\tau_1 \\
&= \mathcal{N}\mathcal{N}' \int e^{-(\alpha+\alpha')r^2 + (\boldsymbol{N}^* + \boldsymbol{N}')\cdot\bar{\boldsymbol{r}}}\,\mathrm{d}\bar{\boldsymbol{r}} \\
&= \mathcal{N}\mathcal{N}' \int e^{-(\alpha+\alpha')x^2 + (N_x + N'_x)x}\,\mathrm{d}x \int \dots \mathrm{d}y \int \dots \mathrm{d}z \\
&= \mathcal{N}\mathcal{N}' \left(\frac{\pi}{\alpha+\alpha'}\right)^{3/2} e^{\frac{(\boldsymbol{N}^*+\boldsymbol{N}')^2}{4(\alpha+\alpha')}} \\
&= \left(\frac{4\alpha\alpha'}{(\alpha+\alpha')^2}\right)^{3/4} e^{-\alpha R^2 - \alpha' R'^2 + \frac{(\boldsymbol{N}^*+\boldsymbol{N}')^2}{4(\alpha+\alpha')}}
\end{aligned}$$

$$\begin{aligned}
T &= \int \chi^*(\boldsymbol{R}, \boldsymbol{N}, \alpha; 1)\left(-\tfrac{1}{2}\nabla^2\right) \chi(\boldsymbol{R}', \boldsymbol{N}', \alpha'; 1)\, \mathrm{d}\tau \\
&= \mathcal{N}\mathcal{N}' \int e^{-(\alpha+\alpha')r^2 + (\boldsymbol{N}^* + \boldsymbol{N})\cdot\boldsymbol{r}}\left(3\alpha' - \tfrac{1}{2}(\boldsymbol{N}' - 2\alpha'\boldsymbol{r})^2\right)\mathrm{d}\tau \\
&= \frac{\alpha\alpha'}{\alpha+\alpha'}\left(3 - \frac{\alpha\alpha'}{2(\alpha+\alpha')}\left(\frac{\boldsymbol{N}^*}{\alpha} - \frac{\boldsymbol{N}'}{\alpha'}\right)^2\right)S,
\end{aligned}$$

where $\mathcal{N} = \left(\frac{2\alpha}{\pi}\right)^{3/4} e^{-\alpha R^2}$.

For the nuclear attraction integrals and for the two-electron integrals, we shall use the formulae (3) and the 3-dimensional Fourier development [3] of

$$\frac{1}{|\boldsymbol{r}_2-\boldsymbol{r}_1|}=\frac{1}{2\pi^2}\int\frac{e^{-i\boldsymbol{k}(\boldsymbol{r}_2-\boldsymbol{r}_1)}\mathrm{d}\boldsymbol{k}}{k^2}$$

that combined with the Laplace transform of $\frac{1}{k^2}$ [4]

$$\frac{1}{k^2}=\int_0^\infty e^{-tk^2}\mathrm{d}t$$

becomes

$$\frac{1}{|\boldsymbol{r}_2-\boldsymbol{r}_1|}=\frac{1}{2\pi^2}\int_0^\infty\mathrm{d}t\int e^{-tk^2-i\boldsymbol{k}(\boldsymbol{r}_2-\boldsymbol{r}_1)}\mathrm{d}\boldsymbol{k}\,.$$

If Z denotes the nuclear charge of any nucleus designated by its position vector $\boldsymbol{\varrho}$ from the origin, we have:

$$\begin{aligned}
V&=-Z\int\chi^*(\boldsymbol{R},\boldsymbol{N},\alpha;1)\,\frac{1}{|\boldsymbol{r}-\boldsymbol{\varrho}|}(\boldsymbol{R}',\boldsymbol{N}',\alpha';1)\mathrm{d}\tau\\
&=-Z.\mathcal{N}.\mathcal{N}'\int e^{-(\alpha+\alpha')r^2+(\boldsymbol{N}^*+\boldsymbol{N}')\boldsymbol{r}}\,\frac{1}{|\boldsymbol{r}-\boldsymbol{\varrho}|}\,\mathrm{d}\tau\\
&=\frac{-Z.\mathcal{N}\mathcal{N}'}{2\pi^2}\int e^{-tk^2-(\alpha+\alpha')r^2+(\boldsymbol{N}^*+\boldsymbol{N}'-i\boldsymbol{k})\boldsymbol{r}+i\boldsymbol{k}}\mathrm{d}t\,\mathrm{d}\boldsymbol{k}\,\mathrm{d}\boldsymbol{r}\\
&=\frac{-Z.\mathcal{N}\mathcal{N}'\sqrt{\pi}\,e^{(\boldsymbol{N}^*+\boldsymbol{N})^2/4(\alpha+\alpha')}}{(\alpha+\alpha')}\int_0^\infty\frac{e^{-(a+ib)/(\gamma+1)}}{(\gamma+1)^{3/2}}\mathrm{d}\gamma\\
&=-Z(\alpha+\alpha')^{1/2}\,S\frac{1}{c}\,\mathrm{erf}(c)\,,
\end{aligned}$$

where

$$a+ib=\left(\frac{\boldsymbol{N}^*+\boldsymbol{N}'}{\alpha+\alpha'}-2(\sqrt{\alpha+\alpha'})\boldsymbol{\varrho}\right)^2\quad\text{and}\quad c=\sqrt{(a+ib)}\,.$$

The two-electron integrals are calculated by the following relation:

$$\begin{aligned}
I&=\int\chi^*(\boldsymbol{R}_1,\boldsymbol{N}_1,\alpha_1;1)\,\chi(\boldsymbol{R}_2,\boldsymbol{N}_2,\alpha_2;1)\frac{1}{|\boldsymbol{r}_2-\boldsymbol{r}_1|}\\
&\quad\cdot\chi^*(\boldsymbol{R}_3,\boldsymbol{N}_3,\alpha_3;2)\,\chi(\boldsymbol{R}_4,\boldsymbol{N}_4,\alpha_4;2)\,\mathrm{d}\tau_1\,\mathrm{d}\tau_2\\
&=\mathcal{N}\mathcal{N}'\int e^{-(\alpha_1+\alpha_2)r_1^2-(\alpha_3+\alpha_4)r_2^2+(\boldsymbol{N}_1^*+\boldsymbol{N}_2+i\boldsymbol{k})\boldsymbol{r}_1+(\boldsymbol{N}_3^*+\boldsymbol{N}_4-i\boldsymbol{k})\cdot\boldsymbol{r}_2}\,e^{-tk^2}\mathrm{d}t\,\mathrm{d}\boldsymbol{k}\,\mathrm{d}\boldsymbol{r}_1\,\mathrm{d}\boldsymbol{r}_2\\
&=\frac{\pi e^{(\boldsymbol{N}_1+\boldsymbol{N}_2)^2/4(\alpha_1+\alpha_2)+(\boldsymbol{N}_3^*+\boldsymbol{N}_4)^2/4(\alpha_3-\alpha_4)}}{(\alpha_1+\alpha_2)(\alpha_3+\alpha_4)\sqrt{(\alpha_1+\alpha_2+\alpha_3+\alpha_4)}}\int_0^\infty\frac{e^{-(a+ib)/(t+1)}}{(t+1)^{3/2}}\mathrm{d}t\\
&=SS'\left(\frac{(\alpha_1+\alpha_2)(\alpha_3+\alpha_4)}{\alpha_1+\alpha_2+\alpha_3+\alpha_4}\right)^{1/2}\frac{\mathrm{erf}(c)}{c}\,,
\end{aligned}$$

where

$$(a+ib)=\frac{(\alpha_1+\alpha_2)(\alpha_3+\alpha_4)}{4(\alpha_1+\alpha_2+\alpha_3+\alpha_4)}\cdot\left[\frac{N_1^*+N_2}{\alpha_1+\alpha_2}-\frac{N_3^*+N_4}{\alpha_3+\alpha_4}\right]^2$$

$$c=\sqrt{a+ib}$$

and S and S' are the overlap integrals between the first and the second pair of functions.

The actual utilization of the preceding expressions offers some difficulties only in as far as the calculation of the function $\mathrm{erf}(z)$ when z is complex [5a] is concerned. That is, numerical problems arise when $|z|$ is not a small quantity, because in such a case the Maclaurin series development is not convenient any more [6]. In order to overcome this trouble, it was found convenient to put $z=x+iy$ and to use the following expressions:

$$\mathrm{erf}(z)=1+\varepsilon \quad \text{for} \quad x^2-y^2>17, \quad \text{where} \quad |\varepsilon|<4\cdot 10^{-8}$$

$$\mathrm{erf}(z)=\frac{i2e^{y^2}}{\sqrt{\pi}}F(y) \quad \text{for} \quad x=0$$

$$\mathrm{erf}(z)=1-\frac{2}{\sqrt{\pi}}e^{-2ixy}\int_1^{\infty}e^{-x^2t^2+y^2/t^2}(x-iy/t^2)\,\mathrm{d}t\,, \tag{4}$$

$$\mathrm{erf}(z)=\mathrm{erf}(x)+\frac{i2e^{-x^2}}{\sqrt{\pi}}\int_0^{y}e^{t^2+2itx}\,\mathrm{d}t\,, \tag{5}$$

$$\mathrm{erf}(z)=\frac{i2e^{y^2}}{\sqrt{\pi}}F(y)+\frac{2e^{y^2}}{\sqrt{\pi}}\int_0^{x}e^{\;(t^2+2ity)}\,\mathrm{d}t\,, \tag{6}$$

where $F(y)=e^{-y^2}\int_0^{y}e^{t^2}\mathrm{d}t$ is the Dawson's function [5a] for which $0\leqq F(y)\leqq 0.54104422$.

The use of the expression (5) is the more convenient when y is small with respect to x, while the expression (6) is instead more convenient when x is small with respect to y.

In order to evaluate the integral appearing in (4), we pose:

$$\int_1^{\infty}e^{-x^2t^2+y^2/t^2}(x-iy/t^2)\,\mathrm{d}t\simeq\int_1^{u}e^{-x^2t^2+y^2/t^2}(x-iy/t^2)\,\mathrm{d}t\,, \tag{7}$$

where

$$u=\sqrt{\frac{x^2-y^2+17}{2x^2}+\sqrt{\left[\frac{y^2-x^2-17}{2x^2}\right]^2+\frac{y^2}{x^2}}}\,.$$

The integrals which appear in the expressions (5), (6) and (7) may be easily evaluated numerically with a relatively few Gauss points.

References

1. Clementi, E., Davis, D. R.: J. chem. Physics **45**, 2593 (1966); Ritchie, C. D., King, H. F.: J. chem. Physics **47**, 565 (1967); Newman, D., Moskowitz, J. W.: J. chem. Physics **49**, 2056 (1968).
2. Gradshteyn, I. S., Ryzhik, I. M.: $\Sigma\pi\int$ Tables, p. 146. Berlin: VEB Deutscher Verlag der Wissenschaften 1957.
3. Carrier, G. F., Krook, M., Pearson, C. E.: Functions of a complex variable. McGraw-Hill Book Company 1965.
4. Widder, D. V.: The Laplace transform. Princeton University Press 1946.
5. Abramowitz, M., Stegun, I. A.: Handbook of mathematical functions, a) p. 297, b) p. 298. New York: Dover Publications Inc. 1965.
6. Salzer, H. E.: Formulas for calculating the error function of a complex variable. Math. Tables Aid Comp. 5, 67–70 (1951).

Dr. M. Morandi Cecchi
Istituto di Chimica Fisica
Università di Pisa
Pisa, Italy

Theoret. chim. Acta (Berl.) 26, 357—366 (1972)
© by Springer-Verlag 1972

Ab initio Molecular Orbital Calculations

2. A Comparison of Polarisation Function Addition to Minimal Bases, and Molecular Scaling. Computations on Furan, Pyrrole and 1,2,5-Oxadiazole

MICHAEL H. PALMER and ANTONY J. GASKELL
Department of Chemistry, University of Edinburgh, Edinburgh EH9 3JJ, Scotland

M. S. BARBER
AEI Scientific Apparatus Ltd., Manchester M31 2LD, England

Received May 16, 1972

A series of non-empirical calculations on furan, pyrrole and 1,2,5-oxadiazole are reported in which the effect of polarisation functions added to the minimal 7*s* 3*p* basis on each atom is studied. The effect on these planar molecules is largely through the σ rather than the π-system. A comparison with the results of work with scaled functions is reported. Both series are shown to lead to much improved agreement with the electron spectroscopy energy levels. The effect on the dipole moments of these changes in basis is more variable but, with the exception of furan, the agreement with experiment is improved in the present method.

Für die Moleküle Furan, Pyrrol und 1,2,5-Oxadiazol wurde eine Reihe von nichtempirischen Rechnungen durchgeführt, in denen der Einfluß von zusätzlichen Polarisationsfunktionen zur minimalen 7*s* 3*p*-Basis an jedem Atom untersucht wird. Die Ergebnisse werden mehr durch die Art der Beschreibung des Systems der σ-Elektronen als durch diejenige der π-Elektronen beeinflußt. Ein Vergleich mit den Ergebnissen bei Verwendung skalierter Funktionen wird durchgeführt. Beide Reihen von Ergebnissen zeigen eine verbesserte Übereinstimmung zu den Energiemeßwerten der Elektronenspektroskopie. Die Änderungen des berechneten Dipolmoments bei derartigen Basisvariationen sind größer als bei früheren Methoden. Die Übereinstimmung mit dem Experiment wird, mit Ausnahme von Furan, jedoch verbessert.

Current methods of improving linear combination of gaussian orbital (LCGO) approaches to Hartree-Fock wave functions in a single configuration are proceeding along various paths; (a) the use of extended basis sets (e.g. 11*s* 7*p*) [1], (b) optimisation of contraction procedures [2], (c) possibly uncontracted rather than in contracted (fixed) sets [3] representing the usual atomic orbitals, (d) improvement of small basis sets by the inclusion of polarisation orbitals [4] such as *p*- and *d*-orbitals for hydrogen and first row elements respectively. Lastly, (e) scaling of the best atomic gaussian sets, in small molecular environments [5] such that the molecular energy is minimised and the exponents thus optimal. This approach then requires that the scale factors for each atom can be transferred to a range of large molecules [6].

In our first paper [7] we reported a series of minimal basis calculations on furan (IV), pyrrole (VI) and 1,2,5-oxadiazole (VIII), using gaussian sets 7*s* 3*p* for C, N and O, 3*s* for hydrogen, that were comparable with the related work by E. Clementi *et al.* [8] and G. Berthier *et al.* [9] and gave an apparently linear correlation of experimental and theoretical binding energies and orbital energies. We extended the calculations later to include polarisation functions according to (c) above and the results of these are given in the present paper. However it was immediately apparent that these very time consuming integrations over the added *p*- and *d*-orbital functions whilst having some effect on total energy and charge distribution could be duplicated by minor amounts of atomic scaling. Thus far from obtaining any improvement in electron correlation by the angular part, these calculations really only improved the radial functions by reducing the level of contraction. We thus decided to optimise the exponents using the smaller analogs I, II, III, (and also partly for IV) to the compounds V, VI, VII, (a) to test transferability in the small series and (b) to give us better functions for binding energy studies of the compounds V–VII. Our primary interest in this work is in the degree of aromaticity (if any) in simple heterocycles such as these.

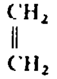

$\begin{matrix}CH_2\\ \| \\ CH_2\end{matrix}$

I

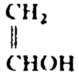

$\begin{matrix}CH_2\\ \| \\ CHOH\end{matrix}$

II

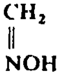

$\begin{matrix}CH_2\\ \| \\ NOH\end{matrix}$

III

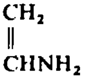

$\begin{matrix}CH_2\\ \| \\ CHNH_2\end{matrix}$

IV

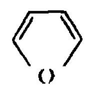

V

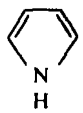

VI

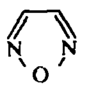

VII

The two procedures are outlined in more detail in the appendix. As in the earlier work we used the computer program IBMOL-4, on both an IBM360/50 and Univac 1108, and a modified version of a Univac-compatible version of IBMOL-2 (the original version of which was kindly supplied by Dr. M. Krauss). The calculations on furan thus had the minimal basis (29 functions) of 7*s* 3*p* sets (for carbon and oxygen) and 3*s* for hydrogen (as detailed in Part 1) extended by up to 17 polarisation functions; pyrrole (minimal basis 30 functions) was extended by up to 15 polarisation functions; the oxadiazole (minimal basis 27 functions) was improved by up to 11 polarisation functions.

Results and Discussion

(a) *The Molecular Energies*

The results for the minimal basis calculated are detailed in Part 1, but the total energies obtained for the molecules (in the above order) were −227.79358, −208.04264 and −259.64308 a.u. respectively; the key results of the present calculations are given in Tables 1, 2 and 3.

In common with much earlier work, inclusion of polarisation *p*-functions leads to a gain in total energy, which in our case is of approximately 0.025 a.u. per hydrogen atom augmented with $p_x + p_y + p_z$. However, comparison of the minimal basis calculations with those where only a $p_x (p_z)$ polarisation orbital is included shows the π-effect is negligible. Thus the polarisation functions far from

Table 1. Furan

	p-orbitals on hydrogen		p- and d-orbitals on all elements		Scaled optimu
	p_x, p_y, p_z	p_z only (π)	$d_{z\pi}$	d_{xy}	
E_{total} (a.u.)	−227.88891	−227.79593	−227.93702	−227.93235	−228.00447
Electron-nucleus attraction (a.u.)	−624.35673	−623.18622	−624.55858	−624.52750	−626.57157
Electron repulsion (a.u.)	235.88098	234.80346	+236.03473	236.00831	237.98026
Nuclear repulsion (a.u.)	160.58683	160.58683	+160.58683	160.58683	160.58683
Atom sum (a.u.)	−227.04202	−227.04202	−227.04202	−227.04202	–
Binding energy (a.u.) (A)	0.32511	0.23213	0.37322	0.36855	– 0.44067
(B)	0.84689	0.75391	0.89500	0.89033	– 0.96245
Orbital energies (a.u.)	A 1	A 1	A 1	A 1	A 1
	– 20.651375	– 20.681071	– 20.655219	– 20.655760	– 20.637710
	– 11.440200	– 11.477202	– 11.438181	– 11.434852	– 11.314804
	– 11.375138	– 11.415843	– 11.370089	– 11.369128	– 11.244661
	– 1.4945404	– 1.5219562	– 1.4913108	– 1.4822870	– 1.4561535
	– 1.1295396	– 1.1587933	– 1.1260078	– 1.1294091	– 1.0885647
	– 0.81449197	– 0.83269539	– 0.81169804	– 0.81759742	– 0.78007786
	– 0.76894988	– 0.79190959	– 0.76637191	– 0.76614004	– 0.74368445
	– 0.60247085	– 0.62390625	– 0.59994614	– 0.60104952	– 0.56492546
	– 0.56162365	– 0.58137598	– 0.56228328	– 0.56273641	– 0.52394021
	B 2	B 2	B 2	B 2	B 2
	– 11.440471	– 11.477630	– 11.438455	– 11.435105	– 11.315221
	– 11.374978	– 11.415964	– 11.369894	– 11.368970	– 11.244788
	– 1.0457546	– 1.0734976	– 1.0435535	– 1.043385	– 1.0035378
	– 0.82669183	– 0.84529144	– 0.82612963	– 0.82714804	– 0.7885297
	– 0.65111651	– 0.66713965	– 0.64721283	– 0.65616548	– 0.61556045
	– 0.61869699	– 0.63670517	– 0.61557737	– 0.61876420	– 0.57956975
	B 1	B 1	B 1	B 1	B 1
	– 0.67389405	– 0.70027015	– 0.66883244	– 0.66706475	– 0.64585658
	– 0.44385288	– 0.47372584	– 0.43780132	– 0.44120152	– 0.41368596
	A 2	A 2	A 2	A 2	A 2
	– 0.38359592	– 0.41467153	– 0.37599807	– 0.37857325	– 0.34425643
Dipole moment (D)	1.06	0.618	0.990	1.02	1.59
Gross populations H_α	0.8728	0.7705	0.8942	0.8705	0.812
H_β	0.8782	0.7896	0.8558	0.8545	0.828
C_α	5.9195	6.0142	5.8838	5.9341	5.911
C_β	6.1627	6.2465	6.1969	6.1934	6.193
O	8.3336	8.3221	8.33839	8.2949	8.512

leading to a redistribution of the π-electrons are working primarily on the σ-system. Since the effect is similar in the three molecules, it is not largely an effect on the "classical lone pairs" either (in the case of pyrrole these are in the π-system). Undoubtedly the effect is to provide extra flexibility to the radial functions. The calculations with added d-functions (one per C, N and O atom) confirm these views. The molecular energies obtained by the scaling procedure are clearly better than any of those with polarisation functions, and of course they are obtained in much less computer time.

Table 2. Pyrrole

	p-orbitals on hydrogen		Scaled optimum
	p_x, p_y, p_z	p_z-only	
E_{total} (a.u.)	- 208.15734	- 208.04991	- 208.26263
Electron-nucleus attraction (a.u.)	- 596.95133	- 595.62578	- 599.82388
Electron repulsion (a.u.)	227.69230	226.47417	230.45959
Nuclear repulsion (a.u.)	161.10170	161.10170	161.10167
Orbital energies (a.u.)	A 1	A 1	A 1
	- 15.711906	- 15.740782	- 15.59913
	- 11.392543	- 11.436874	- 11.25012
	- 11.347476	- 11.391613	- 11.19693
	- 1.3320757	- 1.3652375	- 1.27655
	- 1.0788309	- 1.1086674	- 1.02569
	- 0.82510294	- 0.84695972	- 0.781817
	- 0.76208659	- 0.78668500	- 0.726892
	- 0.63160944	- 0.65462207	- 0.584206
	- 0.57186894	- 0.59349368	- 0.515514
	B 2	B 2	B 2
	11.392695	- 11.437182	- 11.25041
	- 11.347219	- 11.391640	- 11.19694
	- 1.0151711	- 1.0445562	- 0.959742
	- 0.79973619	- 0.82191205	- 0.749721
	- 0.61841996	- 0.64033446	- 0.573106
	- 0.58627701	- 0.60638680	- 0.533074
	B 1	B 1	B 1
	- 0.62160714	- 0.65472406	- 0.583180
	- 0.39989298	- 0.43312092	- 0.350586
	A 2	A 2	A 2
	- 0.34885078	- 0.38392842	- 0.298789
Dipole moment (D)	2.01	2.26	2.01
Gross populations C_β	6.165	6.254	6.2039
C_α	6.001	6.090	6.0380
H_α	0.909	0.802	0.8465
H_β	0.894	0.807	0.8364
H_N	0.706	0.671	0.6702
N	7.354	7.421	7.4799

On this basis we can calculate the molecular binding energy by taking the molecular total energy from *either* (a) the sum of the Hartree-Fock atom energies *or* (b) the sum of the atom energies using best atom sets of same length or (c) the sum of the scaled atom energies. For small molecules course (a) is appropriate since the basis set used for the molecule should lead to an energy near the Hartree-Fock limit [1f]. For larger molecules where the latter is unlikely to be achieved at the present time (b) is probably more appropriate [5b], but in some instances a mixed system has been used; thus the total energies for various molecules studied by Snyder and Basch [1f] have been converted to atomisation energies by Ditchfield, Hehre and Pople [5a], by using atom energies of the same basis set for all

Table 3. 1,2,5-Oxadiazole

	p-orbitals	p_z-orbital	p- and d-orbitals	Scaling of hydrogen (s) functions			Scaled functions
	on H(x, y, z)	on H(π)	on H, C, N, O	$K_H = 1.414$	1.8	2.0	all atoms
E_{total}	−259.69848	−259.64443	−259.77172	−259.70170	−259.72498	−259.73034	−259.78806
Electron-nucleus attraction	−673.87335	−673.17894	−674.27810	−673.44147	−673.85148	−674.05692	−675.48550
Electron repulsion	+250.96006	+250.31971	+251.29158	+250.52499	+250.91172	+251.11179	+252.48266
Nuclear repulsion	+163.21480	+163.21480	+163.21480	+163.21479	+163.21479	+163.21479	+163.21479
Orbital energies	A1	A1	A1	A1	A1	A1	A1
	− 20.716722	− 20.735214	− 20.714792	− 20.728830	− 20.717700	− 20.711949	− 20.714373
	− 15.751462	− 15.773354	− 15.740932	− 15.767141	− 15.755036	− 15.748778	− 15.690364
	− 11.469151	− 11.493882	− 11.455980	− 11.487323	− 11.466856	− 11.455489	− 11.342890
	− 1.608508	− 1.625231	− 1.586971	− 1.620980	− 1.611418	− 1.606407	− 1.575333
	− 1.230591	− 1.249242	− 1.223136	− 1.246438	− 1.237158	− 1.232083	− 1.2024374
	− 0.903466	− 0.912985	− 0.901332	− 0.909329	− 0.901160	− 0.896781	− 0.876275
	− 0.789789	− 0.807256	− 0.783540	− 0.801822	− 0.795954	− 0.792743	− 0.771939
	− 0.619577	− 0.631982	− 0.616464	− 0.629887	− 0.622662	− 0.618704	− 0.596581
	− 0.554913	− 0.567799	− 0.554473	− 0.563421	− 0.554486	− 0.549841	− 0.529357
	B2	B2	B2	B2	B2	B2	B2
	− 15.751663	− 15.773587	− 15.741154	− 15.767381	− 15.755273	− 15.749017	− 15.690629
	− 11.468999	− 11.494058	− 11.455818	− 11.487584	− 11.467159	− 11.455806	− 11.342970
	− 1.277481	− 1.292610	− 1.263810	− 1.288791	− 1.279166	− 1.274084	− 1.239318
	− 0.884202	− 0.896852	− 0.884452	− 0.895396	− 0.888763	− 0.885122	− 0.860257
	− 0.692608	− 0.698254	− 0.693520	− 0.696842	− 0.691434	− 0.688156	− 0.664236
	− 0.522738	− 0.537614	− 0.527459	− 0.534640	− 0.526437	− 0.522144	− 0.495306
	B1	B1	B1	B1	B1	B1	B1
	− 0.737138	− 0.752263	− 0.726252	− 0.748706	− 0.740357	− 0.736013	− 0.718517
	− 0.510695	− 0.528989	− 0.501162	− 0.521843	− 0.512136	− 0.507158	− 0.485865
	A1	A1	A1	A1	A1	A1	A1
	− 0.486973	− 0.503588	− 0.476225	− 0.499397	− 490825	− 0.486374	− 0.463411
Dipole moment (D)	− 3.75	− 2.99	−3.38	− 3.07	− 3.58	− 3.79	− 4.52
Net atomic populations H	+ 0.178	+ 0.262	+ 0.198	+ 0.25693	+ 0.30430	+0.33402	+ 0.1885
C	− 0.060	− 0.161	− 0.085	− 0.14838	− 0.17959	− 0.20275	+ 0.0241
N	− 0.040	− 0.028	− 0.041	− 0.03141	− 0.04741	− 0.05265	− 0.0888
O	− 0.156	− 0.146	− 0.144	− 0.15241	− 0.15469	− 0.15726	− 0.2474

atoms except hydrogen [1a]. The third course (c) is likely to lead to spurious correlations since it represents the difference between two inadequately determined levels. This is evident from the results of Moskowitz and Harrison [10] where the atomisation energy of ethylene is substantially greater than experiment for small basis sets (the Hartree-Fock limit appears to give about 75% of the experimental value). Fortuitously, procedure (c) applied to the present bases leads to atomisation energies for methane and ethylene virtually in complete agreement with experiment. At this point it is appropriate to compare our results for furan with those of the extended basis set $(9s\,5p)_{C,O}(4s\,1p)_H$ calculation by P. Siegbahn [11], the only molecule of this trio where such a large basis has been used. His molecular energy is about 0.5 a.u. (0.2%) better than the present scaled results, while the binding energy based on method B is about 7% better.

(b) Ionisation Potentials

(i) *Experimental Results*

In the previous paper (I) we reported data on the He^I photoelectron spectra, together with some data for furan using He^{II}. A much more detailed spectrum for this molecule is cited by P. Siegbahn [11], in which assignments of the bands to each of the four symmetry types is given. We are uncertain as to how these detailed assignments have been obtained, and are thus treating them with caution. The same paper reports X-ray electron spectra of the core electrons in the furan molecule in the gas phase, while similar studies for pyrrole, kindly supplied by K. Siegbahn [12] are reported in Table 4. (One of us has confirmed these last results on a prototype electron spectrometer at Manchester University.) We have obtained the solid state electron spectra of the core levels for each molecule, and in the case of furan we have also obtained the valency shell ionisation potentials.

Table 4. Experimental and calculated binding energies of electrons

		Calculated				Measured	
		Minimal	Scaled	Extended[a]	Extended[b]	Solid state[e]	Gas phase[e]
Furan[d]	$1s_O$	562.7	561.6	562.0	561.2	535.1	539.4
	$1s_C(\alpha)$	312.2	307.9	311.2	307.8	287.55	291.4
	$1s_C(\beta)$	310.6	306.0	309.4	306.3	285.75	290.3
Pyrrole	$1s_N$	427.9	424.5	427.5	—	401.2	–
	$1s_C(\alpha)$	311.4	306.1	310.0	–	284.9	289.9[c]
	$1s_C(\beta)$	309.8	304.7	308.8	-	285.7	290.88
1,2,5-Oxadiazole	$1s_O$	564.2	563.7	563.7	—	535.6	—
	$1s_N$	429.2	427.0	428.3	—	401.9	–
	$1s_C$	312.8	308.6	311.7	—	287.1	–

[a] Present work, P_{xyz}-orbitals on hydrogen, $d_z 2(\sigma -)$ on carbon and oxygen.

[b] K. Seigbahn, U. Gelius *et al*: cited in Ref. [4].

[c] K. Seigbahn *et al.*: Personal communication.

[d] The valency shell ionisation potentials determined by X-ray excitation are as follows: 9.6, 14.0, 15.5 (sh), 19.2, 24.0 (sh), 24.6, 34.4 eV (sh = shoulder).

[e] The differences between solid state and gas phase spectra are as expected on the basis of work function in the former series.

Our spectra were determined on an AEI ES 100 spectrometer, calibrated with the oxygen $1s$ of water (533.2 eV) and hexane (285.0 eV) carbon $1s$ levels. The figures obtained are shown in Table 4; the doublets expected from the α- and β-carbon $1s$ electrons of furan and pyrrole are not resolved under these conditions, but the peak widths (half height) are 2.6, 2.5 and 1.6 eV for furan, pyrrole and the oxadiazole respectively, thus suggesting a separation of near 1.0 eV in each of the first two cases. The unpublished figures obtained by K. Siegbahn [12] are 1.2 eV and 0.9 eV respectively.

(ii) *Comparison of Calculated and Experimental Results (Using Koopmans' Theorem).*

Agreement between the observed and calculated ionisation potentials is much better for the extended sets and scaled functions than for the minimal basis sets. For the *valency shell* there are clearly linear relationships between calculated and experimental data (irrespective of whether this relationship is theoretically valid). The data for furan (13 points) using P. Siegbahn's assignments [11] are: scaled set $(\text{I.P.})_{\text{Exptl.}} = 0.8234\,(\text{I.P.})_{\text{Calc.}} + 1.102$ eV (standard error in slope 0.028 eV, in intercept 0.610 eV); for extended set D, $(\text{I.P.})_{\text{Exptl.}} = 0.8236\,(\text{I.P.})_{\text{Calc.}} + 0.426$ eV (standard error in slope 0.021 eV, in intercept 0.45 eV); the Siegbahn $11s7p$ set gives, $(\text{I.P.})_{\text{Exptl.}} = 0.8029\,(\text{I.P.})_{\text{Calc.}} + 1.398$ eV (standard error in slope 0.028 eV, in intercept 0.596 eV). For pyrrole and the oxadiazole (7 points in each case) the corresponding data is more scattered (and also no complete assignment of the A1 and B2 lines has been reported); the figures are pyrrole (p-orbitals on hydrogen) $(\text{I.P.})_{\text{Exptl.}} = 0.773\,(\text{I.P.})_{\text{Calc.}} + 3.42$ eV (errors 0.06 and 0.76 eV), pyrrole (scaled) $(\text{I.P.})_{\text{Exptl.}} = 0.940\,(\text{I.P.})_{\text{Calc.}} + 1.22$ eV (errors 0.06 and 0.74 eV); 1,2,5-oxadiazole (extended), $(\text{I.P.})_{\text{Exptl.}} = 0.936\,(\text{I.P.})_{\text{Calc.}} + 1.18$ (errors 0.09 and 1.23), and scaled $(\text{I.P.})_{\text{Exptl.}} = 0.915\,(\text{I.P.})_{\text{Calc.}} + 0.29$ eV (errors 0.05 and 0.76 eV). A significant feature is the near identity of orbital energies obtained between the $11s7p$ set of Siegbahn [11] and the scaled and expanded sets of the present work for furan. There is again excellent agreement between the experimental and calculated ordering of the first three ionisation potentials for the three molecules, both in the extended and scaled series. A feature not previously reported (which is also applicable to the minimal basis set calculation) is that the third ionisation potential of 1,2,5-oxadiazole is predicted to be from the 6 B2 orbital in contrast to 9 A1 for the other two molecules (the first two ionisations are of π-type in each case). This observation fits well with the high degree of localisation of the 6 B2 on the $2p_x$ antisymmetric combination for nitrogen (see also Paper 1), the classical lone pair.

The $1s$ levels are not significantly effected by changes from $7s3p$ to $9s5p$ or addition of polarisation functions or molecular scaling, the $1s_{\text{O}}$ levels being calculated at about 27 eV higher binding energy than the electron spectra indicate. The corresponding figures for $1s_{\text{N}}$ and $1s_{\text{C}}$ are about 26 and 24 eV larger than experiment. In any event it seems doubtful whether Koopmans' Theorem has any validity to such deep seated orbitals. None the less, the separation of the $1s$ levels for carbon are predicted to be larger for furan (1.9 eV for scaled or extended bases) than pyrrole (1.4 eV scaled basis) and this is consistent with the separations obtained with electron spectroscopy. Further the relative placings of the carbon, nitrogen and oxygen $1s$ levels are correctly reproduced for the three molecules.

(c) Population Analysis and Dipole Moment

The dipole moment in the minimal basis set calculation for furan was (perhaps fortuitously) virtually identical with the experimental value (0.67*D*), while those for pyrrole and 1,2,5-oxadiazole were about 15% too high and too low respectively. Thus for furan almost any change produced by the addition of polarisation orbitals or by scaling was expected to lead to a worsening in agreement with experiment. All of the changes led to a positive increase in the dipole moment, the scaling by a larger factor than the polarisation functions. It is worth noting that Siegbahn's [11] value is also poor, lying between that for the most extensive set and the scaled set. For the oxadiazole, the most extended set gave exact agreement with experiment (3.38 Debye), while scaling gave too large a value. This last result probably shows the sensitivity of the dipole moment to the scaling procedure most clearly, and to the oxygen scale factors in particular. For pyrrole the values from both the scaling and extended basis are nearer to the experimental value (1.80 Debye); in view of the dependence of much of the dipole moment on the polarity of the N-H bond this is particularly satisfactory.

Conclusions

It is well established that the use of scaled functions, where the scaling factors are determined from molecular energy optimisation on related but smaller molecules, leads to molecular energies substantially closer to the Hartree-Fock limit, for small basis sets. In the present series of compounds this also leads to a considerable improvement in the ionisation potentials predicted by Koopmans' Theorem. The core levels however are not greatly changed in this process, or indeed by increasing the basis set; this reflects the inadequacy of Koopmans' Theorem as much as other factors. Small changes in core ionisation potentials between related molecules are however reproduced in order, but the extent is magnified.

The use of polarisation functions does lead to much the same improvement over the best atom basis, but of course at the expense of much more computer time. It is worth noting again that the total energy improvements resulting from both polarisation functions and scaling procedures occur by very different mechanisms. Thus there is in all cases an increase in electron-electron repulsion which is outweighed by an increase in electron-nucleus attraction; these terms however mask the fact, evident from the population analysis (and the exponents themselves), that the electrons are more concentrated in the viscinity of the atoms in scaled calculations, and more in the internuclear region for the expanded basis sets of polarisation functions; that is, there is a larger overlap population in the latter series of calculations. To a certain extent therefore errors in charge distributions resulting from equipartition of the overlap population are worse in the expanded series than the scaled ones. In general the addition of polarisation functions to hydrogen increases the population on these atoms, while the addition of polarisation functions on oxygen, nitrogen and carbon have comparatively small and variable effects, such that it is not universally true that addition of a basis function to a centre increases the population at that centre (see furan for example). In general we favour the use of scaled functions, but for very polar molecules this will mean that the dipole moment in particular will be very sensitive to small changes in the scaling parameters. The use of an average set as proposed by Ditchfield, Hehre and Pople [5a] is unlikely to be satisfactory in these cases; we propose to always attempt an optimisation of the molecular energy on a related smaller molecule as a necessary first step. This process breaks down for molecules with systems which cannot be described in terms of simple structures with well-defined bonds[1].

Appendix

Polarisation Orbitals

For hydrogen atoms these took the form of a further contracted function of two terms with exponents 0.5 and 0.1 but with *p*-orbital symmetry; while on carbon nitrogen and oxygen we used *d*-orbital types with a single function of exponent 0.63, 0.95 and 1.33 respectively, following the recommendation by Roos and Siegbahn [4d] and others. Although we have noted that polarisation functions on hydrogen are usually incorporated along an axis to allow interaction with either an adjacent π-system or "long pair", we preferred to incorporate the function in all three planes to test the extent of interaction.

The Scaling Procedure

The valency shell atomic orbitals of the minimal basis (Part 1) were replaced by Eq. (1), where all functions in a given contracted basis orbital had the same scaling factor (k_i). The optimal scale factors were determined by parabolic minimisation within a two dimensional array of molecular energy against scale factor. No subsidiary minima were noted for any of the model compounds used, namely ethylene (I), vinyl alcohol (II), formaldoxime (III) or vinylamine (IV). The final optimum scaling factors are shown in

$$\Phi_i = A_i \exp(-k_i \alpha_i r^2) \tag{1}$$

Table 4. These gave total energies (unscaled in parentheses) as follows:

I −77.8531 a.u. (−77.6893 a.u.); II −152.4748 a.u. (−151.7322 a.u.);

III −168.3647 a.u. (−168.2245 a.u.); IV −132.5415 a.u. (−132.5315 a.u.).

The curvature of the scaled energy surface with respect to oxygen parameters is particularly marked in vinyl alcohol; it seems that this is related to the polarity of the C—O and O—H bonds particularly, for the energy is also particularly sensitive to changes in k_{11}, which decreases in the series O—H, N—H, C—H.

References

1a. Huzinaga, S.: J. chem. Physics **42**, 1293 (1965).
1b. — Saki, Y.: J. chem. Physics **50**, 1371 (1969).
1c. Christensen, D. H., Kortzeborn, R. N., Bak, B., Led, J. J.: J. chem. Physics **53**, 3912 (1970).
1d. Dunning, T. H.: Chem. Physics Letters **7**, 423 (1970).

---

[1] We are grateful to a referee for suggesting the addition of this last point.

1e. Huzinaga, S., Arnau, C.: J. chem. Physics **52**, 2224 (1970).
1f. Snyder, L. C., Basch, H.: J. Amer. chem. Soc. **91**, 2189 (1969).
2a. Dunning, T. H.: J. chem. Physics **53**, 2823 (1970).
2b. Salez, C., Veillard, A.: Theoret. chim. Acta (Berl.) **11**, 441 (1968).
3a. Clementi, E., Davis, D. R.: J. chem. Physics **45**, 2593 (1966).
3b. Seung, S. S., Harrison, M. C., Csizmadia, I. G.: Theoret. chim. Acta (Berl.) **8**, 281 (1967).
4a. Body, R. G., McClure, D. S., Clementi, E.: J. chem. Physics **49**, 4916 (1968).
4b. Boer, F. P., Lipscomb, W. N.: J. chem. Physics **50**, 989 (1969).
4c. Yoshimine, M., McLean, A. D.: IBM Journal of Research and Development, 1967 (Suppl.).
4d. Roos, B., Siegbahn, P.: Theoret. chim. Acta (Berl.) **17**, 199 (1970).
5a. Ditchfield, R., Hehre, W. J., Pople, J. A.: J. chem. Physics **54**, 724 (1971).
5b. Klessinger, M.: Theoret. chim. Acta (Berl.) **15**, 353 (1969).
5c. Hehre, W. J., Pople, J. A.: J. Amer. chem. Soc. **92**, 2191 (1970).
6a. Radom, L., Hehre, W. J., Pople, J. A.: J. Amer. chem. Soc. **93**, 289 (1971).
6b. Latham, W. A., Hehre, W. J., Pople, J. A.: J. Amer. chem. Soc. **93**, 808 (1971).
6c. Radom, L., Pople, J. A., Buss, V., Schleyer, P. v. R.: J. Amer. chem. Soc. **93**, 1813 (1971).
6d. - Lathan, W. A., Pople, J. A.: J. Amer. chem. Soc. **93**, 5339 (1971).
6e. Lathan, W. A., Hehre, W. J., Curtiss, L. A., Pople, J. A.: J. Amer. chem. Soc. **93**, 6376 (1971).
7. Palmer, M. H., Gaskell, A. J.: Theoret. chim. Acta (Berl.) **23**, 52 (1971).
8. Clementi, E., Clementi, H., Davis, D. R.: J. chem. Physics **46**, 4725 (1967).
8b. -- - J. chem. Physics **46**, 4731 (1967).
8c. J. chem. Physics **46**, 4737 (1967); J. chem. Physics **47**, 4485 (1967).
9. Berthier, G., Praud, L., Serre, J.: Quantum aspects of heterocyclic compounds in chemistry and biochemistry, p. 40. Jerusalem: The Israel Academy of Sciences and Humanities 1970 (Proceedings of the International Symposium, March 1969).
10. Moskowitz, J. W., Harrison, M. C.: J. chem. Physics **42**, 1726 (1965).
11. Siegbahn, P.: Chem. Physics Letters **8**, 245 (1971).
12. Siegbahn, K.: Personal communication.

Dr. M. H. Palmer
Department of Chemistry
University of Edinburgh
Edinburgh EH 9 3 JJ
Scotland

Theoret. chim. Acta (Berl.) 26, 367—380 (1972)
© by Springer-Verlag 1972

Molecular Orbital Calculations on the Ethylene Episulfide Molecule and Its Isomers

O. P. Strausz and R. K. Gosavi
Department of Chemistry, University of Alberta, Edmonton, Alberta

A. S. Denes and I. G. Csizmadia *
Department of Chemistry, University of Toronto, Toronto 181, Ontario

Received May 2, 1972

Systematic non-empirical and semi-empirical molecular orbital studies have been performed on the sulfur atom + ethylene system and its reaction products thiirane and vinylmercaptan. The results are in general agreement with earlier qualitative and semiquantitative rationalizations of the reaction but also bring to light a number of novel features.

Es wurden systematische nichtempirische und semi-empirische MO-Rechnungen am System Schwefelatom und Äthylen und seinen Reaktionsprodukten Thiiran und Vinylmercaptan durchgeführt. Obwohl die Resultate im allgemeinen mit früheren qualitativen und semiquantitativen Erkenntnissen übereinstimmen, zeigen sie doch eine Anzahl neuer Gesichtspunkte.

Introduction

The experimental observation [1, 2] that ground triplet state sulfur atoms add across olefinic bonds to yield thiirane in a concerted, stereospecific manner has generated considerable interest [3, 4] in the theoretical interpretation of this reaction, because it is the first example of a stereospecific cycloaddition of a divalent triplet state reagent.

A recent theoretical study of the interaction of sulfur atoms with ethylene within the framework of the Extended Hückel Molecular Orbital (EHMO) theory has been reported by Hoffmann and coworkers [4]. Potential surface calculations revealed the presence of two minima for the $S(^1D_2) + C_2H_4$ system. The higher of these corresponds to vinyl mercaptan formation *via* C–H bond insertion, and the lower minimum, lying about 20 kcal/mole below the former, to the symmetry-allowed, least-motion, addition of sulfur across the double bond. The two are viewed as competing concerted processes. Similar calculations for the $S(^3P)$ configuration indicated the presence of only one minimum in the potential surface, leading to thiirane formation. The stereospecificity of the addition reaction was attributed to a correlation with an excited state of thiirane which retains C–C bonding but is unstable with respect to C–S ring opening. The ring-opened thiirane intermediate has a CCS bond angle of 110° and the plane of the terminal methylene group is perpendicular to the CCS plane. The calculated energy barrier for rotation of the methylene was 5 kcal/mole.

---

* On leave during 1971–72 at the Department of Chemistry, University of York, Heslington, York, England.

Two Hartree-Fock type MO calculations on the thiirane molecule also appeared in the past two years [5, 6]. These were concerned only with the electronic structure of the molecule in its most stable conformation.

The present study was undertaken in order to re-examine the addition reaction and elucidate the molecular structure of the various isomeric C_2H_4S product molecules, thiirane, vinylmercaptan and thioacetaldehyde, using both *ab initio* and semiempirical MO methods. In this article we report the structural results of these studies, while details of the reaction surface will be discussed in a subsequent communication [7].

Method

Accurate molecular Hartree-Fock (HF) calculations on sulfur compounds are very much in their infancies compared to the accumulated theoretical knowledge of oxygen and nitrogen containing organic compounds [8–11]. It is relatively easy to perform conformational studies on organic sulfur compounds [12, 13], just as well as on any other compounds containing heteroatoms [14–16]. However, the study of reactions involving bond making and/or breaking processes is an order of magnitude more difficult problem, even in the thermodynamic sense

Table 1. The breakdown of total energy to experimental and theoretical components for thiirane and its constituent atoms

A) Data for the constituent atoms of C_2H_4S:

Atom	E_{HF} [a]	E_{corr} [b]	E_{rel} [c]	Sum for C_2H_4S
C	− 37.6886	−0.1581	−0.0130	− 75.7194
S	−397.5047	−0.6400	−1.0510	−399.1957
H	− 0.5000	–	–	− 2.0000
Sum for C_2H_4S	−474.8819	−0.9562	−1.077	−476.9151

[a] Ref. [20]; [b] Ref. [21]; [c] Ref. [22].

B) Data for thiirane:

Experimental components	E (hartree)	Theoretical component	E (hartree)
Total atomic energy	−476.915 [a]	Hartree-Fock energy [f]	−475.640
Total bond energy	− 0.948 [b]	Correlation energy [e]	− 1.199
Zero-point energy	− 0.053 [c]	Relativistic energy [d]	− 1.077
Experimental energy	−477.916	Total energy	−477.916

[a] Given as the final sum in Table 1A.

[b] Calculated from heats of formation [23, 24].

[c] Calculated as $E_{ZPV} = \frac{1}{2}hc \sum_{i=1}^{15} \tilde{\nu}_i$ where $\tilde{\nu}_i$ are the fifteen fundamental vibrations (in units of cm^{-1}) as taken from Ref. [24]. A more recent vibrational study uses similar frequencies [25].

[d] Assumed to be equal to that of the atomic relativistic energy (E_{rel}) in Table 1A.

[e] The molecular correlation energy of C_2H_4S was calculated as the following sum: $E_{corr}(CH_2{=}CH_2) + E_{corr}(S) + \Delta E_{corr}(\text{bond}) = 0.534 - 0.640 - 0.065 = -1.199$ hartree.

[f] The Hartree-Fock Limit (HFL) was estimated as $E_{HF} = E_{exp} - (E_{corr} + E_{rel})$.

[17–19]. This is apparent from the data in Table 1. The difference between the molecular and atomic Hartree-Fock Limits (HFL) gives a relatively small binding energy,

$$E_{\mathrm{HFL}}^{\mathrm{molec}} - E_{\mathrm{HFL}}^{\mathrm{atoms}} = -475.640 + 474.882 = -0.758\ \text{hartree},$$

as compared to the experimental dissociation energy (−0.948 hartree). This discrepancy (approximately 0.19 hartree) in the total dissociation (i.e. atomization) corresponds to ca. 120 kcal/mole. Fortunately, as it will be discussed later, the dissociation energy of thiirane to ethylene and sulfur atom carries a considerably smaller error in the Hartree-Fock type SCF-MO calculations. For reasons outlined above the choice of number and type of atomic orbitals (AO) is of utmost importance. In the present *ab initio* study the *n* individual atomic orbitals ($\underline{\chi}$) used were built up by contraction from *N* primitive ($\underline{\eta}$) Gaussian type function (GTF) using an $N \times n$ matrix ($\boldsymbol{T}$) in transformation (1),

$$\underline{\chi} = \underline{\eta}\,\boldsymbol{T}. \tag{1}$$

The molecular orbitals (MO) were obtained from the contracted basis ($\underline{\chi}$) by a linear transformation (2). The matrix $\boldsymbol{C}$ that performed the transformation from the contracted AO to the MO basis ($\underline{\phi}$) was obtained by the self-consistent field (SCF) method.

$$\underline{\phi} = \underline{\chi}\,\boldsymbol{C}. \tag{2}$$

Table 2. Contracted Gaussian basis sets used in calculations on C_2H_4S, C_2H_4 and S

Chemical system	Basis set size[a]		Basis set type[b]	Ref.
	Primitive	Contracted	Primitive → Contracted	
S	45	24	$(12^s, 9^p, 1^d) \rightarrow [6^s 4^p, 1^d]^c$	[28]
C	29	10	$(11^s 6^p) \rightarrow [4^s 2^p]$	[29]
H	3	1	$(3^s) \rightarrow [1^s]$	[30]
C_2H_4S	125	48	48 *spd*	—
S	39	18	$(12^s, 9^p) \rightarrow [6^s, 4^p]$	[28]
C	29	10	$(11^s, 6^p) \rightarrow [4^s, 2^p]$	[29]
H	3	1	$(3^s) \rightarrow [1^s]$	[30]
C_2H_4S	119	42	42 *sp*	—
S	39	18	$(12^s, 9^p) \rightarrow [6^s, 4^p]$	[28]
C	17	5	$(8^s, 3^p) \rightarrow [2^s 1^p]$	[30]
H	3	1	$(3^s) \rightarrow [1^s]$	[30]
C_2H_4S	85	32	32 *sp*	—

[a] The reduction in basis set size ($N \rightarrow n$) is achieved by the transformation (contraction) specified in Eq. (1) where the primitive GTF(η) are changed to contracted AO (χ).

[b] Double zeta basis sets are used in a number of cases:

$[6^s, 4^p, 1^d] \equiv [1s, 1s', 2s, 2s', 3s, 3s', 2p, 2p', 3p, 3p', 3d]$

$[4^s, 2^p] \equiv [1s, 1s', 2s, 2s', 2p, 2p']$

while single zeta (minimal Slater) basis sets turned out to be quite satisfactory in many of the cases:

$[2^s, 1^p] \equiv [1s, 2s, 2p]$

$[1^s] \equiv [1s]$.

[c] The *d*-orbital exponent was chosen to be 0.55.

These molecular Hartree-Fock type SCF-MO calculations have been carried out on an IBM 360/65 computer using the IBMOL-IV system [26, 27]. The three types of AO basis sets used are listed in Table 2.

Results and Discussion

Fig. 1 illustrates the total energy values of thiirane as calculated by the three basis sets (48 *spd*, 42 *sp* and 32 *sp*) used in the present study along with those of earlier studies.

The first *ab initio* MO calculation on thiirane by Clark [5], where only a minimal uncontracted Gaussian basis set was used, together with a more recent study using Slater type orbitals (STO) by Bonaccorsi *et al.* [6], are also included for comparison. As seen from the figure all three basis sets used yield near Hartree-Fock wavefunctions since the computed total energy approaches the Hartree-Fock limit. The numerical values used for the construction of Fig. 1 are summarized in Tables 1 and 3, and the molecular geometries [31] are specified in Fig. 2.

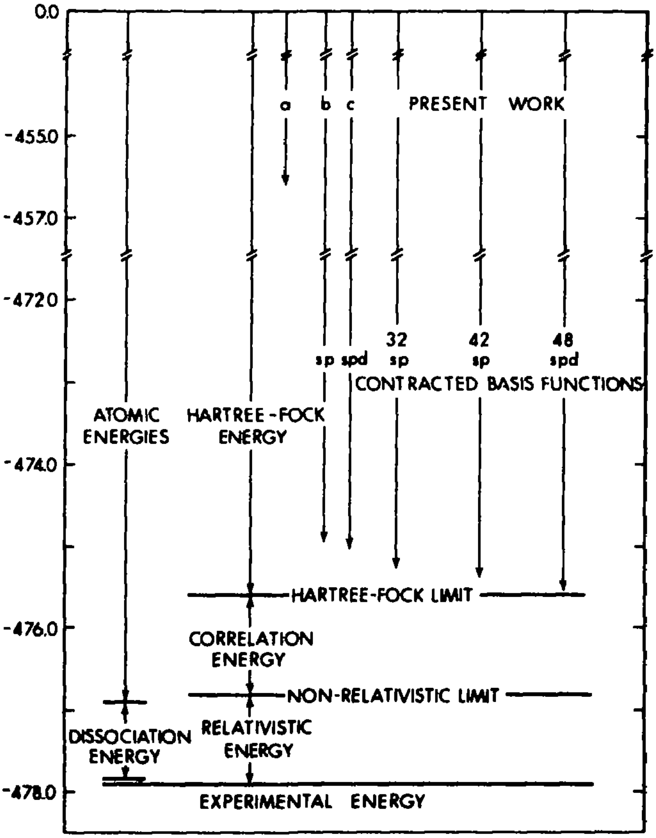

Fig. 1. The breakdown of total energy to experimental and theoretical components for thiirane. (The energy components are summarized in Table 1. Results of the *Present Work* are given in Table 3. The earlier calculations of "*a*" and "*b*" as well as "*c*" were taken from Ref. [5] and [6] respectively)

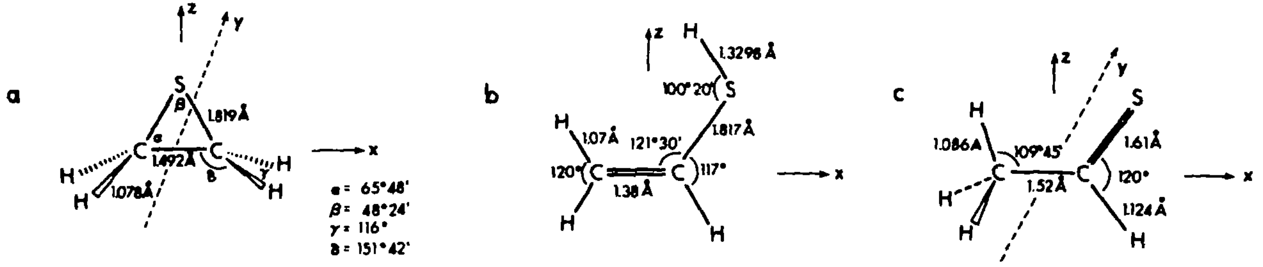

Fig. 2. Geometrical arrangements of three C_2H_4S isomers

Table 3. Computed energy components and total energy values of various species

	$S(^3P)$	$S(^1D)$	S^{2-}	Ethylene		$C_2H_4^{2+}$	Thiirane[a]			Vinyl mercaptan
Contracted AO	18 *sp*	18 *sp*	18 *sp*	24 *sp*	14 *sp*	14 *sp*	48 *spd*	42 *sp*	32 *sp*	32 *sp*
Nuclear repulsion energy	0.00000	0.00000	0.00000	33.32547	33.32547	33.32547	100.99740	100.99740	100.99740	92.47674
One-electron energy	−548.52059	−548.62930	−562.07707	−168.79478	−168.96544	−156.75106	−853.38129	−853.07684	−853.40514	−835.47423
Two-electron energy	151.05866	151.21262	164.92949	57.53166	57.89642	46.80174	276.92415	276.65882	277.14553	268.12090
Total energy	−397.46193	−397.41669	−397.14758	− 77.93765	− 77.74355	− 76.62385	−475.45974	−475.42062	−475.26221	−474.87659

[a] The dipole moments computed with the 32 *sp* and 42 *sp* basis sets are 2.69 and 1.74 Debye, respectively. The experimental value is 1.84 Debye [31].

While the total energy values of the various systems are summarized in Table 3, the corresponding energy differences are given in Table 4. The SCF orbital energies are compiled in Table 5 and shown graphically in Fig. 3. The coefficients (elements of the *C* matrix in Eq. (2)) for the four highest filled and the four lowest empty MO are given in Table 6. With the aid of these coefficients one may find a 1:1 correspondence for the orbital symmetry study used by previous authors [3, 4].

Table 4. Energy differences[a] associated with the dissociation and isomerization of thiirane

S CH_2 CH_2 →	$CH_2{=}CH_2+S(^3P)$	$CH_2{=}CH_2+S(^1D)$	$[CH_2{-}CH_2]^{2+}+S^{2-}$	$CH_2{=}CH{-}SH$
48 *spd*	0.06016 (37.8)	0.10540 (66.2)	–	—
42 *sp*	0.02104 (13.2)	0.06628 (41.6)	-	–
32 *sp*	0.05673 (35.6)	0.10196 (64.0)	1.49078 (935.78)	0.38621 (242.42)
Exp	(58)[b]	(84.4)[b]		

[a] Differences are given in Hartree atomic units, bracketed values represent the kcal/mole equivalent; (1.0 hartree = 627.71 kcal/mole).

[b] Ref. [23].

Table 5. Computed MO energies for thiirane

No.	Orbital	Type	48 *spd*	42 *sp*
1	$1a_1$	1σ	−91.9897	−91.9953
2	$2a_1$	2σ	−11.3526	−11.3602
3	$1b_1$	3σ	−11.3519	−11.3596
4	$3a_1$	4σ	8.9747	− 8.9835
5	$4a_1$	5σ	− 6.6651	− 6.6730
6	$2b_1$	6σ	− 6.6626	− 6.6701
7	$1b_2$	1π	− 6.6599	− 6.6672
8	$5a_1$	7σ	− 1.1762	− 1.1954
9	$3b_1$	8σ	− 0.8726	− 0.8802
10	$6a_1$	9σ	− 0.8559	− 0.8632
11	$2b_2$	2π	− 0.6984	− 0.7081
12	$7a_1$	10σ	− 0.6352	− 0.6395
13	$1a_2$	3π	− 0.5736	− 0.5817
14	$8a_1$	11σ	− 0.4723	− 0.4683
15	$4b_1$	12σ	− 0.4563	− 0.4577
16	$3b_2$	4π	− 0.3695	− 0.3766
17	$5b_1$	$13\sigma^*$	0.1625	0.1665
18	$9a_1$	$14\sigma^*$	0.2480	0.2380
19	$6b_1$	$15\sigma^*$	0.4504	0.4534
20	$4b_2$	$5\pi^*$	0.5503	0.5831
21	$10a_1$	$16\sigma^*$	0.5819	0.6280
22	$11a_1$	$17\sigma^*$	0.6314	0.7516
23	$7b_1$	$18\sigma^*$	0.6931	0.6883
24	$2a_2$	$6\pi^*$	0.7614	0.7961

In view of the special importance of excited states in the formation of the thiirane molecule *via* the $C_2H_4 + S$ reaction, some attention has been given to the UV spectrum of thiirane.

Table 6. Computed MO coefficients in linear combination of the 48 *spd* AO for thiirane

Atom	AO	Highest filled MO				Lowest vacant MO			
		$1a_2(3\pi)$	$8a_1(11\sigma)$	$4b_1(12\sigma)$	$3b_2(4\pi)$	$5b_1(13\sigma^*)$	$9a_1(14\sigma^*)$	$6b_1(15\sigma^*)$	$4b_2(5\pi^*)$
C_1	2*s*	0.0	0.00144	0.00722	0.0	−0.05465	0.07626	0.16489	0.0
	2*px*	0.0	−0.071314	−0.01719	0.0	−0.01450	−0.01554	−0.11842	0.0
	2*py*	0.11458	0.0	0.0	−0.03063	0.0	0.0	0.0	0.09018
	2*pz*	0.0	0.09228	−0.08786	0.0	0.11435	−0.08099	0.03068	0.0
C_2	2*s*	0.0	0.00144	−0.00722	0.0	0.05465	0.07626	−0.16489	0.0
	2*px*	0.0	0.071314	−0.01719	0.0	−0.01450	0.01554	−0.11842	0.0
	2*py*	−0.11458	0.0	0.0	−0.03063	0.0	0.0	0.0	0.09018
	2*pz*	0.0	0.09228	0.08786	0.0	−0.11435	−0.08099	−0.03068	0.0
S	3*s*	0.0	−0.18981	0.0	0.0	0.0	0.30392	0.0	0.0
	3*px*	0.0	0.0	0.21306	0.0	0.12216	0.0	0.0	0.0
	3*py*	0.0	0.0	0.0	0.26860	0.0	0.0	0.0	−0.03255
	3*pz*	0.0	−0.168170	0.0	0.0	0.0	−0.10872	0.0	0.0
	$3dx^2$	0.0	0.029257	0.0	0.0	0.0	−0.08149	0.0	0.0
	$3dy^2$	0.0	−0.01666	0.0	0.0	0.0	0.14894	0.0	0.0
	3*dxz*	0.0	0.0	−0.08757	0.0	0.15158	0.0	−0.15949	0.0
	$3dz^2$	0.0	0.06373	0.0	0.0	0.0	−0.04666	0.0	0.0
	3*dxy*	−0.01318	0.0	0.0	0.0	0.0	0.0	0.0	0.0
	3*dyz*	0.0	0.0	0.0	−0.01643	0.0	0.0	0.0	−0.31753
H1	1*s*	0.27447	0.03248	0.11036	−0.11354	−0.03697	−0.02345	0.06871	−0.67551
H2	1*s*	−0.27447	0.03248	0.11036	0.11354	−0.03697	−0.02345	0.06871	0.67551
H3	1*s*	−0.27447	0.03248	−0.11036	−0.11354	0.03697	−0.02345	−0.06871	−0.67551
H4	1*s*	0.27447	0.03248	−0.11036	0.11354	0.03697	−0.02345	−0.06871	0.67551

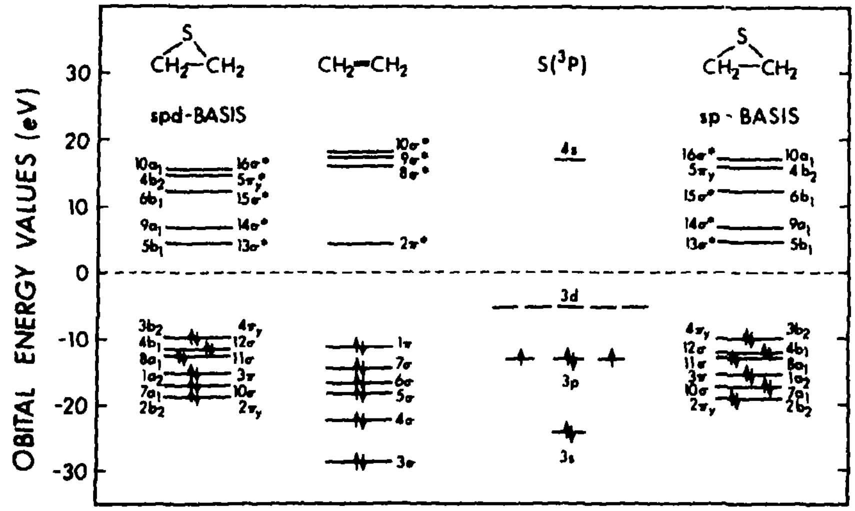

Fig. 3. A comparison of thiirane MO energies, computed from the 48 *spd* and 42 *sp*-wavefunctions, with orbital energies of sulfur and ethylene

Table 7. Transition energies[a], transition moments[b] and oscillator strengths[b] for thiirane as computed from the 48 *spd* Gaussian wavefunction

No.	Type of excitation	Transition energy[a] Singlet	Triplet	Transition moment[b] (Debye)	Oscillator strength[b]
1	$3b_2 \rightarrow 5b_1$	47002 (5.83)	41688 (5.17)	0.0248	0.000547
2	$3b_2 \rightarrow 9a_1$	68088 (8.44)	54861 (6.80)	0.0923	0.002954
3	$8a_1 \rightarrow 5b_1$	86836 (10.77)	61300 (7.60)	5.6182	0.229292
4	$4b_1 \rightarrow 9a_1$	87105 (10.80)	75547 (9.37)	1.5705	0.064295
5	$4b_1 \rightarrow 5b_1$	92597 (11.48)	55484 (6.87)	15.3109	0.666338
6	$1a_2 \rightarrow 5b_1$	99887 (12.38)	96786 (12.00)	0.0318	0.001493
7	$8a_1 \rightarrow 9a_1$	104167 (12.91)	80389 (9.96)	15.1056	0.739518
8	$7a_1 \rightarrow 5b_1$	110091 (13.65)	101757 (12.62)	1.2077	0.062453
9	$1a_2 \rightarrow 9a_1$	120610 (14.95)	118266 (14.66)	0.0035	0.000170
10	$3b_2 \rightarrow 6b_1$	122273 (15.54)	121625 (15.08)	0.0254	0.001458
11	$2b_2 \rightarrow 5b_1$	125089 (15.51)	122231 (15.15)	0.0077	0.000454
12	$4b_1 \rightarrow 6b_1$	130863 (16.22)	123456 (15.31)	0.0346	0.002126
13	$7a_1 \rightarrow 9a_1$	132117 (16.38)	121625 (15.08)	5.3596	0.332800
14	$8a_1 \rightarrow 6b_1$	137428 (17.04)	118583 (14.70)	3.8876	0.251105
15	$3b_2 \rightarrow 10a_1$	143904 (17.84)	132556 (16.43)		
16	$2b_2 \rightarrow 9a_1$	145632 (18.06)	142392 (17.65)	0.0096	0.000657
17	$1a_2 \rightarrow 6b_1$	148469 (18.41)	140879 (17.47)	0.0210	0.001467
18	$3b_2 \rightarrow 4b_2$	150403 (18.65)	141079 (17.40)	1.2778	0.090325

[a] In units of cm^{-1} (eV).
[b] For singlet → singlet transitions only.

Table 8. Transition energies[a], transition moments[b] and oscillator strengths[b] for thiirane as computed from the 42 *sp* Gaussian wavefunction

No.	Type of excitation	Transition energy[a] Singlet	Triplet	Transition moment[b] (Debye)	Oscillator strength[b]
1	$3b_2 \rightarrow 5b_1$	51763 (6.42)	48808 (5.08)	0.0	0.0
2	$3b_2 \rightarrow 9a_1$	65992 (8.18)	55743 (6.91)	0.08734	0.00257
3	$4b_1 \rightarrow 9a_1$	85487 (10.60)	61252 (7.59)	1.648405	0.06623
4	$8a_1 \rightarrow 5b_1$	88003 (10.91)	73862 (9.16)	6.916617	0.28608
5	$4b_1 \rightarrow 5b_1$	97286 (12.06)	56868 (7.05)	15.97600	0.73049
6	$1a_2 \rightarrow 5b_1$	99499 (12.34)	95883 (11.89)	0.017398	0.00081
7	$8a_1 \rightarrow 9a_1$	102961 (12.77)	76800 (9.52)	14.245229	0.68935
8	$7a_1 \rightarrow 5b_1$	108559 (13.46)	101814 (12.62)	0.723089	0.03689
9	$1a_2 \rightarrow 9a_1$	118492 (14.69)	115926 (14.37)	0.0	0.0
10	$2b_2 \rightarrow 5b_1$	125260 (15.53)	121965 (15.12)	0.0	0.0
11	$3b_2 \rightarrow 6b_1$	125295 (15.53)	124792 (15.47)	0.0	0.0
12	$7a_1 \rightarrow 9a_1$	130020 (16.12)	119552 (14.82)	3.803104	0.23241
13	$4b_1 \rightarrow 6b_1$	131919 (16.36)	125714 (15.59)	0.058187	0.00361
14	$8a_1 \rightarrow 6b_1$	135623 (16.81)	120616 (14.95)	2.149153	0.13699
15	$2b_2 \rightarrow 9a_1$	143805 (17.83)	140518 (17.42)	0.002648	0.00018
16	$1a_2 \rightarrow 6b_1$	150186 (18.62)	141916 (17.59)	0.002289	0.00016
17	$3b_2 \rightarrow 4b_2$	162054 (20.09)	157407 (19.52)	1.527925	0.11638
18	$8a_1 \rightarrow 4b_2$	167582 (20.78)	164707 (20.42)	0.008942	0.00070
19	$4b_1 \rightarrow 4b_2$	168262 (20.86)	164327 (20.37)	0.0	0.0
20	$3b_2 \rightarrow 10a_1$	173325 (21.49)	171282 (21.24)	0.288187	0.02348

[a] In units of cm^{-1} (eV).
[b] For singlet → singlet transitions only.

The first question one has to face in this regard is the type of basis set used, that is the importance of *d*-orbitals on the excitation pattern. Consequently in the study employing the largest basis set, 42 contracted *sp* basis orbitals, the effect of *d*-orbitals was examined by expanding the number of basis orbitals to 48, involving the *d*-orbitals.

The occupied and empty MO of the thiirane molecule in these two basis sets, as well as those of the reactants, are shown in Fig. 3 and the data given in Table 5. There is no marked difference in the MO patterns comparing the *sp* and *spd* basis sets. However, the energies of the various excited electronic configurations as computed by the virtual orbital technique show noticeable shifts. On closer examination one discovers that most of the differences are due to an overall lowering of the *spd* basis, manifesting the effect of the additional *d*-GTF. A fairly consistent picture may be obtained if the two ground states are chosen to be the energy zero. This is given in Tables 7, 8 and Fig. 4.

Owing to the similarity of the two patterns and the saving in computer time, it appeared permissible to choose the *sp* basis set for further studies. As an additional check the excitation energies calculated with the *spd* basis set (ΔE_{spd}) were compared with those obtained with the *sp* basis set (ΔE_{sp}) in Fig. 5. The diagonal 45° line represents the "perfect correlation" and the points seem to correlate to an acceptable degree. The first ionization potentials obtained in accordance with Koopmans' theorem from the two basis sets are also quite close to one another, however, they are numerically larger than the corresponding experimental values just as calculated excitation energies are appreciably higher than the corresponding experimental values when calculated with the virtual orbital technique.

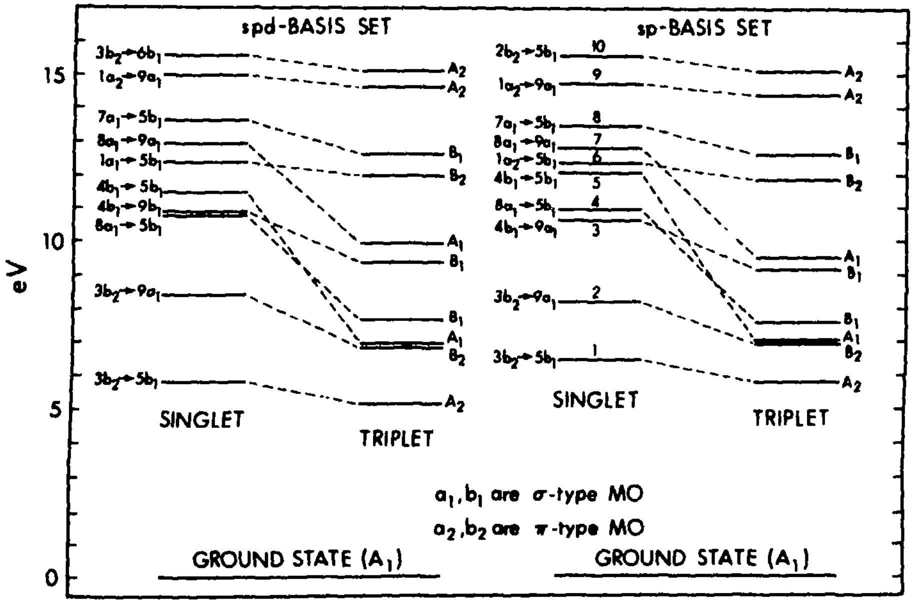

Fig 4. Excited electronic configuration energies relative to ground electronic configuration energies as computed with the 48 *spd* and 42 *sp* basis sets

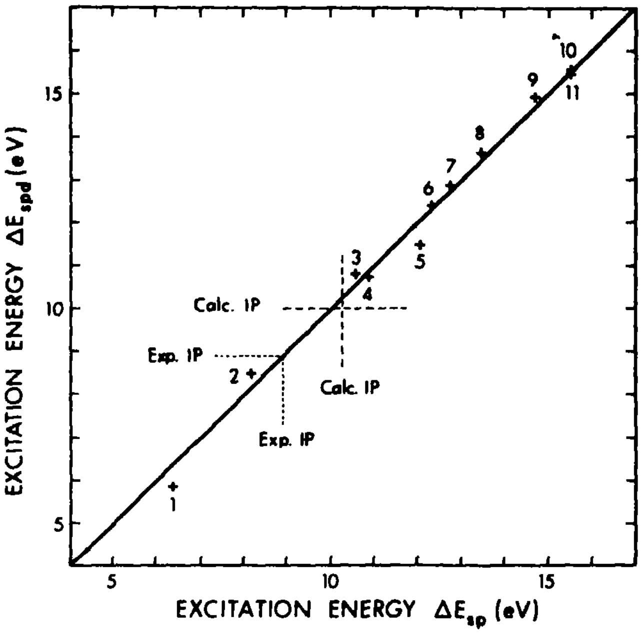

Fig. 5. Correlation of excitation energies as computed by the virtual orbital technique (*cf.* Fig. 5, and Tables 7 and 8) using the 48 *spd* and 42 *sp* basis sets

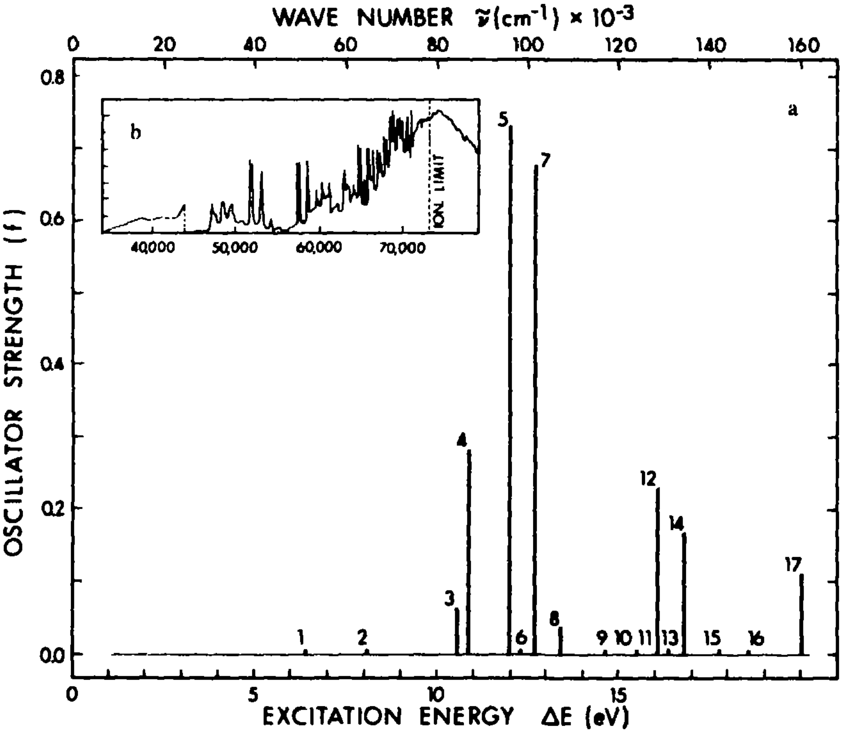

Fig. 6. a Theoretical spectrum of thiirane as computed with the 42 *sp* basis set (Table 8). b Experimental electronic spectrum of thiirane [taken from J. chem. Physics 43, 3666 (1965)]

In the theoretical spectrum, Fig. 6a, the oscillator strength as calculated from the transition moments is given as a function of excitation energy. For comparison the experimental u.v. spectrum of thiirane is also depicted in Fig. 6b.

It is probably worth noting that while the experimentally obtained energy difference between thiirane and the $S(^3P) + C_2H_4$ system is about 58 kcal/mole, the computed energy difference is 35.6 kcal/mole. This is precisely the phenomenon that has been discussed at the beginning of this paper, that in bond formations where the number of paired electrons is increased, the Hartree-Fock wavefunction introduces a systematic error which is quite appreciable, 22 kcal/mole in the present case. On the other hand the calculated energy difference between the (^1D) and (^3P) states of the S-atom is 28.4 kcal/mole which is quite close to the experimental value of 26.4 kcal/mole. This is understandable since both states are represented by an open shell wavefunction implying the same degree of electron pairing. These energy relations are shown in Fig. 7.

Finally, one should notice that the insertion product, vinyl mercaptan, is very much higher on the energy scale than thiirane. This result was anticipated, but

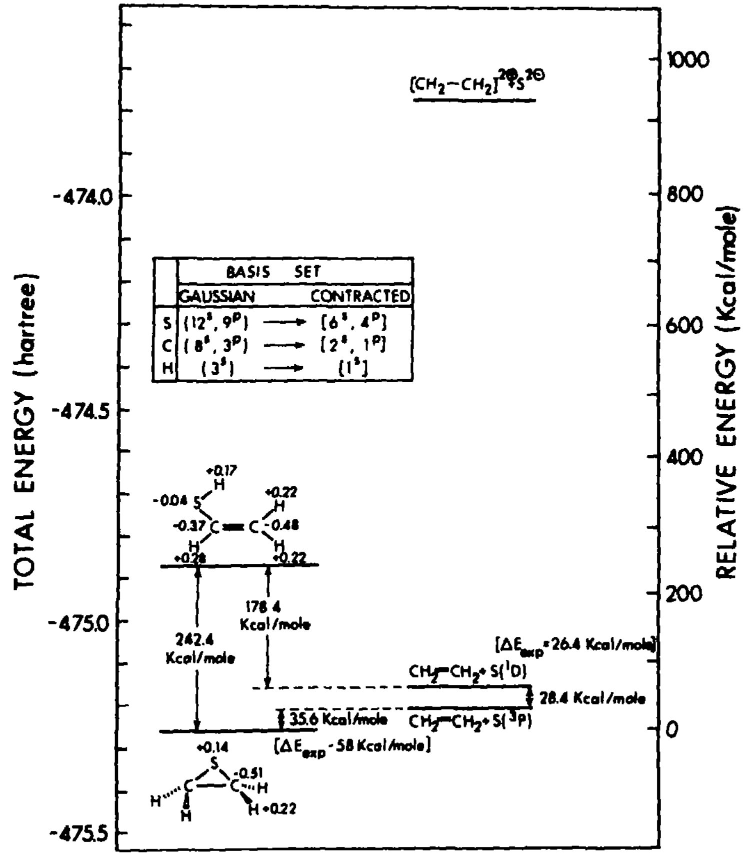

Fig. 7. A comparison of total energy values computed by the *ab initio* SCF-MO method for the ground state of the various C_2H_4S isomers

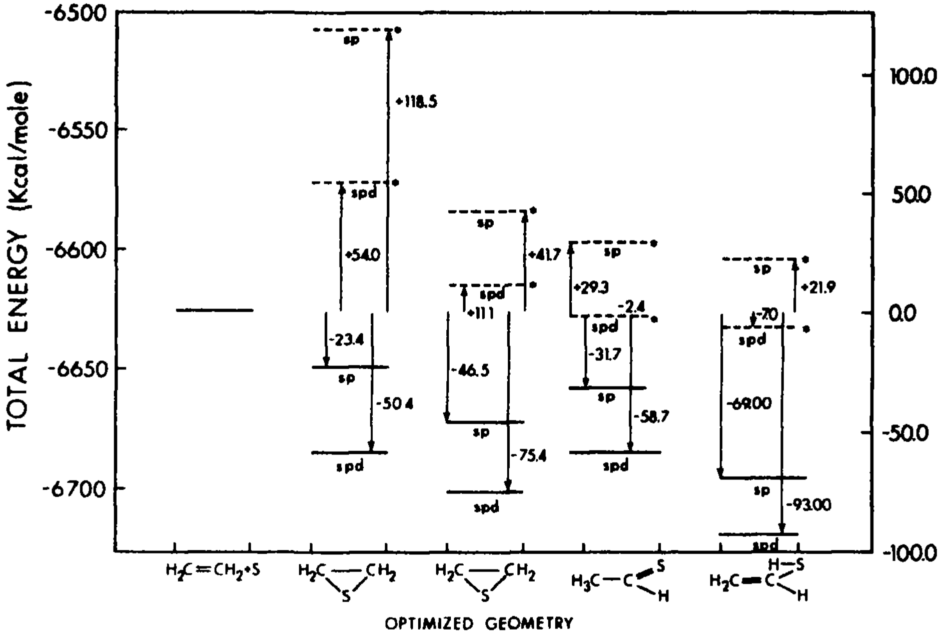

Fig. 8. A comparison of total energy values computed by the semi-empirical EHMO method for the ground and some low lying excited states of the various C_2H_4S isomers

the energy difference appears to be anomalously large and undoubtedly is partly due to the choice of geometrical parameters for vinyl mercaptan, which were based on those of the analogous vinyl halides and ethyl mercaptan molecules.

Most of the molecules studied experimentally are too large to lend themselves to the currently available technology of *ab initio* MO calculations. For this reason it seemed desirable to carry out some semi-empirical calculations at this stage so that comparison could be made between the two methods, thus providing a firm foundation for semi-empirical computations on larger molecules.

The results of Extended Hückel Molecular Orbital (EHMO) calculations, carried out analogously to our earlier work on the COS molecule [32] are presented in Fig. 8. It is interesting that the thio-enol shows an appreciable stability. This seems to indicate that the conjugative stabilization is overemphasized by the EHMO method with respect to that of the *ab initio* SCF-MO theory.

Returning to the problem of the addition reaction profile it is seen from the correlation diagram in Fig. 9 that the addition of $S(^1D)$ atom to ethylene is energetically an inviting process to form ground state $(^1A_1)$ thiirane. The $S(^3P)$ atom addition to give the lowest vertical triplet excited state of thiirane, however, appears to be endothermic by both the *ab initio* and EHMO calculations and would require an appreciable activation energy, contrary to experiment. Therefore, this process is not as simple as implied by earlier qualitative reasoning [3, 4]. A plausible alternative to resolve the discrepancy is the assumption that the ring distorted geometry of the lowest excited triplet state of thiirane, corresponding

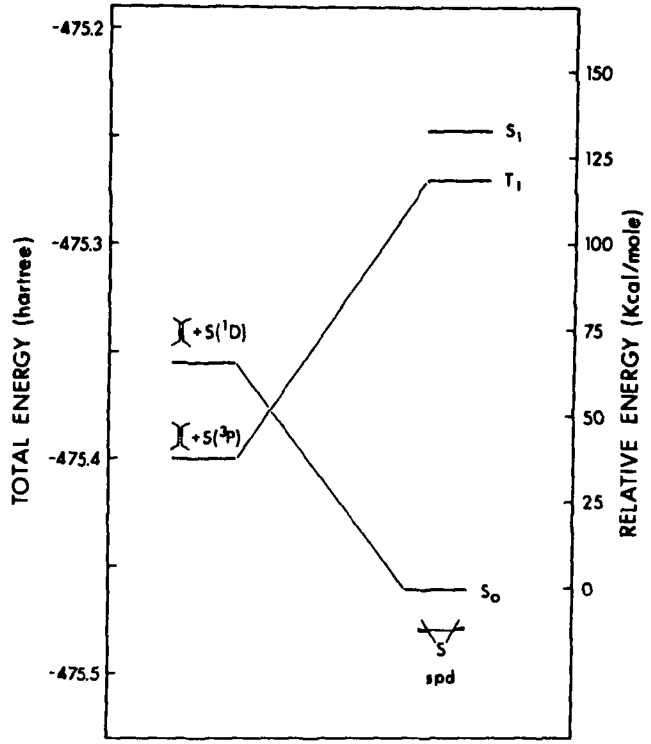

Fig. 9. Comparison of some low lying electronic configuration energies for the initial and final states of $CH_2=CH_2+S\rightarrow C_2H_4S$ as computed with the 48 *spd* basis set

to a non-vertical excitation, is considerably more stable than the symmetric species as proposed earlier [33] purely on experimental grounds. This aspect of the problem is the subject of current investigations which will be reported at a later date [7].

Acknowledgements. The authors thank the National Research Council of Canada for financial support. A Province of Ontario Graduate Fellowship is also gratefully acknowledged.

References

1. Gunning, H. E., Strausz, O. P.: In: Advances in Photochemistry, ed. Noyes, Jr., W. A., Hammond, G. S., Pitts, Jr., J. N., Vol. 4, p. 143. New York: Interscience Publishers 1966.
2. Strausz, O. P.: In: Advances in Chemistry Series, ed. Gould, R. F., in press.
3. Leppin, E., Gollnick, K.: Tetrahedron Letters, 3819 (1969).
4. Hoffmann, R., Wan, C. C., Neagu, V.: Molecular Physics **19**, 113 (1970).
5. Clark, D. T.: Theoret. chim. Acta (Berl.) **15**, 225 (1969).
6. Bonaccorsi, R., Scrocco, E., Tomasi, J.: J. chem. Physics **52**, 5270 (1970).
7. Strausz, O. P., Gunning, H. E., Denes, A. S., Csizmadia, I. G.: to be published.
8. Krauss, M.: Compendium of *ab initio* calculations of molecular energies and properties. U.S. Department of Commerce, National Bureau of Standards, NBS Technical Note, No. 438 (1967).
9. Allen, L. C.: Ann. Rev. of physic. Chem. **20**, 315 (1969).

10. Lehn, J. M.: Fortschr. chem. Forsch. **15**, 311 (1970).
11. Veillard, A.: Theoret. chim. Acta (Berl.) **18**, 21 (1970).
12. Wolfe, S., Rauk, A., Csizmadia, I. G.: J. Amer. chem. Soc. **89**, 5710 (1967); **91**, 1567 (1969); Canad. J. Chem. **47**, 113 (1969).
13. — · Tel, L. M., Csizmadia, I. G.: J. chem. Soc. D, 96 (1970).
14. - - — -- J. chem. Soc. B, 136 (1971).
15. Rauk, A., Allen, L. C., Mislow, K.: Angew. Chem. Int. Ed. **9**, 400 (1970).
16. Wolfe, S.: Accounts of Chem. Res. (in press).
17. Snyder, L. C., Basch, H.: J. Amer. chem. Soc. **91**, 2189 (1969).
18. Hehre, W. J., Dietchfield, R., Radom, L., Pople, J. A.: J. Amer. chem. Soc. **92**, 4796 (1970).
19. Hopkinson, A. C., Yates, K., Csizmadia, I. G.: Theoret. chim. Acta (Berl.), in press.
20. Clementi, E.: J. chem. Physics **38**, 1001 (1963).
21. — J. chem. Physics **39**, 175 (1963).
22. · J. molecular Spectroscopy **12**, 18 (1964).
23. Circular of the National Bureau of Standards, 500, "Selected Values of Chemical Thermodynamic Properties", 1952; Mackle, H., O'Hare, P. A. G.: Tetrahedron **19**, 961 (1963).
24. Guthrie, G. B., Scott, D. W., Waddington, G.: J. Amer. chem. Soc. **74**, 2795 (1952).
25. Venkateswalu, K., Joseph, P. A.: J. molecular Structure **6**, 145 (1970).
26. Veillard, A.: "IMBOL" Computation of Wave Function for Molecules of General Geometry, Version 4. IBM Research Laboratory. San Jose, California.
27. The program was modified for multiprogramming environment by Drs. Robb, M. A. and Tel, L. M. The authors are indebted to Dr. Clementi, E., for making the program available prior to its distribution through the Quantum Chemistry Program Exchange (QCPE).
28. Veillard, A.: Theoret. chim. Acta (Berl.) **12**, 405 (1968).
29. Huzinaga, S., Arnau, C.: J. chem. Physics **52**, 2224 (1970).
30. Klessinger, M.: Theoret. chim. Acta (Berl.) **15**, 353 (1969).
31. Cunningham, G. L., Boyd, A. W., Myers, R. J., Gwinn, W. D., Le Van, W. I.: J. chem. Physics **19**, 676 (1951).

32a. Sidhu, K. S., Csizmadia, I. G., Strausz, O. P., Gunning, H. E.: J. Amer. chem. Soc. **88**, 2412 (1966).

32b. Atomic Orbital exponents used in these calculations were those of Clementi, E., Raimondi, D. L.: J. chem. Physics **38**, 2686 (1963) with H_{ii}(eV) values $H(1s) = -13.60$, $C(2s) = -19.42$, $C(2p) = -10.64$, $S(3s) = -20.67$, $S(3p) = -11.58$ and $S(3d) = -2.62$.

33. Lown, E. M., Sandhu, H. S., Gunning, H. E., Strausz, O. P.: J. Amer. chem. Soc. **90**, 7164 (1968).

Prof. Dr. O. P. Strausz
Department of Chemistry
University of Alberta
Edmonton, Alberta
Canada

Theoret. chim. Acta (Berl.) 26, 381—386 (1972)
© by Springer-Verlag 1972

The Electronic Structure of the $B_2H_5^+$ Ion

B. J. Duke and D. G. Stephens
Department of Chemistry, University of Lancaster, England

Received January 4, 1972

The $B_2H_5^+$ ion has been studied using the *ab initio* SCF method employing a basis set of Gaussian orbitals and various semi-empirical methods. The most stable structure appears to be a planar structure with two vacant *p* orbitals rather than a triply bridged structure suggested by analogy with acetylene with which it is isoelectronic. The semi-empirical results reinforce earlier conclusions that inclusion of charges from neighbouring atoms in iterative Extended Hückel methods is necessary to satisfactorily treat ionic molecules.

Das $B_2H_5^+$-Ion ist mit Hilfe der *ab initio* SCF-Methode unter Benutzung eines Basissatzes von Gaußorbitalen und mit verschiedenen semiempirischen Methoden untersucht worden. Die stabilste Struktur scheint eine planare Struktur mit zwei leeren *p*-Orbitalen und nicht eine dreifach verbrückte Struktur zu sein, wie sie durch Analogiebetrachtungen am Acetylen nahegelegt wird. Durch die semiempirischen Resultate werden die bereits früher erhaltenen Ergebnisse bestätigt, daß zur zufriedenstellenden Behandlung von Molekülionen mit iterativen erweiterten Hückel-Methoden die Berücksichtigung der Ladungen benachbarter Atome nötig ist.

The mass spectrum of diborane is interesting in that it shows a particularly large peak at mass number corresponding to the $B_2H_5^+$ ion. Indeed the appearance potentials for $B_2H_6^+$ and $B_2H_5^+$ are reported to be identical at 11.9 eV [1]. This suggests an unusually stable structure for the $B_2H_5^+$ ion. This species is also interesting in that it is the borane isoelectronic to acetylene. One of us [2] has already commented on this using a simple Extended Hückel Method with the parameters proposed by Hoffmann and Lipscomb [3] for boranes. Diborane is isoelectronic with ethylene and has a structure with the same symmetry and a similar electronic spectrum. The diborohydride ion B_2H_7 is isoelectronic with ethane and is thought [4, 5] to have a structure with the same symmetry containing one B—H—B bridge.

In the course of developing and testing empirical methods based on the Extended Hückel Method it is important to correct the difficiences of the simple methods of this type for charged species and to test methods for these species against more accurate *ab initio* wave functions. The several possible structures for the $B_2H_5^+$ ion are ideal for this purpose. *Ab initio*, and semi-empirical methods for this species have been studied. Three possible structures have been considered two of which are identical to those discussed earlier [2].

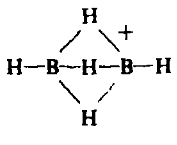
I

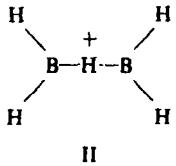
II

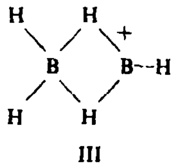
III

Structure I has D_{3h} symmetry with three B–H–B bridges. It has the same structural relation to acetylene as diborane has to ethylene and involves no vacant orbitals. Structure II is planar with only one B–H–B bridge. There are two vacant p orbitals on the boron atoms. The twisted form with the terminal groups normal to each other is likely to be the preferred conformation. Semi-empirical calculations described later indicate that this is so but the planar form has been used for the main calculations. Structure III is the simplest structure arising from the removal of one hydrogen atom. Geometries were chosen in a simple manner. All terminal B–H bonds were taken as 1.19 Å and all bridge B–H bonds as 1.33 Å. In structure II the bond angles are 120°. In structure III the structure is identical to that of diborane with the odd terminal bond moved down into the line of the boron atoms. In structure III the angles and thus the B–B length were calculated assuming a sp hybrid pointing to the terminal bond and three equivalent hybrids pointing to the bridge atoms. This gives a B–B distance of 1.53 Å. It should be noted that a similar argument using sp^2 hybrids closely predicts the structure of the bridge region of diborane.

Calculational Methods

a) *Ab initio Method*

A basis set of 5s-type and 2p-type Gaussian orbitals on the boron atom and 2s-type Gaussian orbitals on the hydrogen atoms was used. This gives a total of 32 orbitals. All integrals were calculated, the SCF equations solved and a Mulliken population density matrix analysis carried through using the POLYATOM program [6] obtained from QCPE [7] and modified to run on the ICL 1909 Computer. Since these calculations on this computer are slow only a limited number were made. The Gaussian orbital exponents used were

B s	0.216	1.076	5.367	26.677	132.85
B p	0.149	0.878			
H s	0.27	1.8			

This basis set is identical to the smaller basis set used by Burnelle and Kaufmann [8] for diborane.

b) *Semi-Empirical Methods*

Five semi-empirical methods have been employed – EHM, IEHM, NCC, CNDO-A and CNDO-B. EHM is the simple Extended Hückel Method. IEHM is an iterative variant in which the diagonal H matrix elements are modified by the atomic charge of the same atom. NCC is a further variant in which the diagonal H matrix elements are also modified by the atomic charge on all other atoms. The NCC method has been studied in detail by Duke and Stephens [9] and an outline of the method published by Armstrong, Duke and Perkins [10]. CNDO-A and CNDO-B are variants in the original Complete Neglect of Differential Overlap (CNDO) method proposed by Pople and Segal [11]. The five methods are identical in all respects including the choice of parameters to methods 1, 3, 4, 5 and 6 used by Armstrong, Duke and Perkins [10] for Aminoborane.

Results and Discussions

Results of the *ab initio* method will be discussed first as this allows a prediction of the most stable structure and a basis for judging the empirical or semi-empirical methods.

a) Ab initio Total Energies

Structure II has the lowest energy. Since Structure I is rather restricted in the bridge region and has a high nuclear repulsion energy this calculation was repeated with the geometry of the bridge region expanded by 5%, the terminal bonds remaining at 1.19 Å. This will be described as Structure I(b) with the original structure as I(a). Results are shown in Table 1. All energies are expressed in the atomic unit of energy (1 Hartree 27.21 eV).

Orbital energies and atomic population charges are reported in Tables 2, 3 and 4 for comparison with other methods. The total energies are close. Relative to the energy of the lowest Structure II these are (in Kcals).

I(a)	18.83
I(b)	12.68
III	19.36

Table 1

Structure	I(a)	I(b)	II	III
$E_{electronic}$	−80.799	−79.6961	−74.4034	−78.7818
$E_{nuclear}$	29.3718	28.2586	22.9457	27.3550
E_{total}	−51.4277	−51.4375	−51.4577	−51.4269

Table 2. $B_2H_5^+$ structure I(a)—D_{3h}

	Orbital energies and atomic charges					
	SCF	EHM	IEHM	NCC	CNDO-A	CNDO-B
A_1'	−0.8377	−0.5146	−0.5910	−0.7816	−1.0238	−0.9048
E'	−0.8498	−0.5152	−0.6225	−0.8216	−1.1358	−0.9727
A_2''	−0.8932	−0.6258	−0.6961	−0.8936	−1.1595	−1.0310
A_1'	−1.2870	−0.8064	−0.9218	−1.1484	−1.8148	−1.6138
q_B	0.163	0.577	0.265	0.273	0.041	0.256
q_{H-t}	0.167	−0.126	0.030	0.019	0.124	0.071
q_{H-b}	0.113	0.033	0.137	0.139	0.223	0.116

Table 3. $B_2H_5^+$ structure II – D_{2h}

	Orbital energies and atomic charges					
	SCF	EHM	IEHM	NCC	CNDO-A	CNDO-B
B_{3g}	−0.7454	−0.5078	−0.5942	−0.7539	−0.9656	−0.8392
B_{2u}	−0.7604	−0.5180	−0.6095	−0.7731	−1.0220	−0.8824
A_g	−0.8045	−0.5179	−0.6296	−0.7993	−1.0595	−0.9209
B_{1u}	−0.9312	−0.7063	−0.7985	−0.9720	−1.1929	−1.0746
A_g	−1.0444	−0.7697	−0.8879	−1.0777	−1.4245	−1.2888
q_B	0.512	0.739	0.335	0.425	0.421	0.516
$q_{H\ t}$	0.085	−0.126	0.047	0.013	0.043	0.005
$q_{H\ b}$	−0.366	0.026	0.141	0.097	−0.012	−0.049

Table 4. Total energy

	I	II	III	
"Correct" total energy				
SCF	−51.428	−51.458	−51.427	III > I > II
CNDO-A	−11.524	−10.847	−11.291	II > III > I
CNDO-B	−5.844	−6.543	−6.071	I > III > II
"Sum of orbital" total energy				
EHM	−5.953	−6.036	−5.978	I > III > II
IEHM	−6.905	−7.036	−6.927	I > III > II
NCC	−8.931	−8.749	−8.846	II > III > I
SCF	−9.435	−8.572	−9.110	II > III > I
CNDO-A	−12.539	−11.329	−12.051	II > III > I
CNDO-B	−10.990	−10.012	−10.595	II > III > I

On the basis of bond dissociation energies, Koski *et al.* [1] predicted that $B_2H_5^+$ would be formed by removal of a terminal hydrogen atom from diborane. This would suggest Structure III for the ion. This *ab initio* calculation suggests that the structure has a higher energy than the planar form. It is not of course possible from this limited calculation to predict the energy necessary for Structure III to rearrange to Structure II. Structure III may therefore be the actual structure involved in the mass spectra results, even though energy would be gained in a rearrangement to the planar form. The triple bridge structure both on energy criteria and on the basis of its lack of similarity to the parent molecule seems unlikely. However since this structure is an electronic closed shell this structure is a possibility if the $B_2H_5^+$ could ever be stabilised by a suitable solvent and anion in solution. There is however no evidence for this species in solution.

b) Semi-Empirical Methods

Results for the semi-empirical methods are given in Tables 2 and 3 for structures I and II as examples. Results for structure III show similar features. The Extended Hückel methods and its two variants show similar results to those obtained for other positive ions such as the ammonium ion [9]. The orbital energies are too high unless neighbouring atom charges are included. The CNDO results are similar to those obtained for aminoborane [10]. Orbital energies are too low, but the charges are predicted with more accuracy than by the Extended Hückel methods. Similar results are obtained for all three structures. Within the Extended Hückel approach it is clearly necessary to include neighbouring atom terms. The NCC method gives overall better results than EHM or IEHM for both orbital energies and charges. The CNDO methods give good charges but with the parameters used in this work they give poor orbital energies.

Table 4 gives estimates for the total energy for the three structures. EHM, IEHM and CNDO-B agree with the SCF results in predicting structure II to be the most stable. NCC and CNDO-A however give the reverse of the order of stability predicted by the SCF method. No semi-empirical method studied here predicts the same order of stability as the SCF method. These results should however be viewed with caution. The CNDO methods by using the full Hamiltonian, use the correct expression for the energy within the framework of the CNDO approximations. The total energy results, in conjunction with the orbital energies, clearly show CNDO-B to be better than CNDO-A. The total energy term for the Extended Hückel methods is a simple sum of orbital energies. Inclusion of the additional terms in IEHM and NCC is however equivalent to the inclusion of electron repulsion terms and these should perhaps be included in the total energy expression. There is however no unique division between one-electron and two-electron terms within the IEHM and NCC methods. Work is in hand on testing various total energy expressions which include the additional parameters used in IEHM and NCC along with nuclear repulsion terms. The simple sum of orbital energies is however used for the IEHM and NCC method in Table 4 and there is therefore no reason to expect these methods to be better than EHM.

It is interesting to note that the sums of orbital energies for the NCC method and both CNDO methods, are in the same order as those from the SCF functions. The sum of orbital energies for the SCF function does not predict the same order of stability as the correct total energies. This supports the view that a better energy expression needs to be derived for the iterative methods.

This study of semi-empirical methods confirms earlier work that the NCC method gives the best overall agreement with SCF results and that within the Extended Hückel method inclusion of terms from neighbouring atoms is essential for ionic species.

Acknowledgement. We wish to thank the Peel Studentship Trust of the University of Lancaster for the award of a scholarship to one of us (D.G.S.).

References

1. Koski, W.S., Kaufmann, J.J., Pachucki, C.F., Shipko, F.J.: J. Amer. chem. Soc. **80**, 3202 (1958).
2. Duke, B.J.: Nature **209**, 1234 (1966).
3. Hoffmann, R., Lipscomb, W.N.: J. chem. Physics **37**, 2872 (1962).
4. Gaines, D.: Inorg. Chem. **2**, 523 (1963).
5. Duke, B.J., Howarth, O.W., Kenworthy, D.G.: Nature **202**, 81 (1964).

6. Czismadia, I. G., Harrison, M. C., Moskowitz, J. W., Sutcliffe, B. T.: Theoret. chim. Acta (Berl.) 6, 191 (1966).
7. — — — Seling, S., Sutcliffe, B. T., Barnett, M. P.: Q.C.P.E. Program 14 (Polyatom), Indiana University, Indiana, USA.
8. Burnelle, L., Kaufmann, J. J.: J. chem. Physics 43, 3540 (1965).
9. Duke, B. J., Stephens, D. G.: Unpublished work.
10. Armstrong, D. R., Duke, B. J., Perkins, P. G.: J. chem. Soc. (A), 2566 (1969).
11. Pople, J. A., Segal, G. A.: J. chem. Physics 44, 3289 (1966).

Dr. B. J. Duke
Department of Chemistry
University of Lancaster
Lancaster, England

Theoret. chim. Acta (Berl.) 26, 387—389 (1972)
© by Springer-Verlag 1972

Relatio

The Stability of the Hartree Fock Solutions of Pentalene and Heptalene*

W. G. LAIDLAW and K. VASUDEVAN

Chemistry Department, University of Calgary, Calgary, Alberta, Canada

Received April 10, 1972

The closed shell HF solutions for the π-electrons in pentalene and heptalene are found to exhibit singlet instabilities for values of the core integral β close to the standard value.

Recent calculations [1] on pentalene and heptalene molecules have suggested that the most stable structure is the one for which the nuclear framework is represented by the C_{2h} symmetry point group rather than what might be expected, the D_{2h} group. These conclusions are based on the results of an "iterative" SCF calculation for the π electron energy and an assessment of the effect of the nuclear displacement on the σ electron energy. As such the instability of the D_{2h} symmetry adapted solution is a so-called "lattice" instability [2]. Rather than comment further on the aforementioned instability we wish to draw attention to the instability of the symmetry adapted (D_{2h}) Hartree Fock (HF) solution, Φ_0^{HF}, for the π electrons of these same systems, i.e., we intend to deal with the possibility that the stationary point $E^\pi(\Phi_0^{\mathrm{HF}})$ may not be even a local minimum, much less a global minimum [3].

Paldus and Čižek have recently [4, 5] directed attention to the occurrence of closed shell single determinant symmetry adapted HF solutions for which $E^\pi(\Phi_0^{\mathrm{HF}})$ does not represent a local minima. In such cases the HF solution is said to be unstable and the lower energy solutions are said to exhibit broken (lower) symmetry. In those instances where the solution is "singlet unstable" the broken symmetry solution is normally found [4] to have broken space symmetry. In view of this an investigation of the stability of the HF solution of pentalene and heptalene has been undertaken and preliminary results show that the HF solutions for these systems exhibit instability for much larger values of $|\beta|$ than comparable closed-shell systems studied heretofore.

The method for determining the stability of a HF solution, given first by Thouless [6], and particularized by Čižek and Paldus [4] has been employed. The procedure involves writing the second variation in energy about the stationary point $E^\pi(\Phi_0^{\mathrm{HF}})$ as

$$\delta^{(2)} E_0^\pi = \sum_{U_2U_1} \left\{ a_{U_1U_2} \bar{d}_{U_1} d_{U_2} + \tfrac{1}{2} b_{U_1U_2} \bar{d}_{U_1} \bar{d}_{U_2} + \tfrac{1}{2} \bar{b}_{U_1U_2} d_{U_1} d_{U_2} \right\}, \qquad (1)$$

where the $a_{U_1U_2}$ and $b_{U_1U_2}$ are simply the matrix elements of the operator $\hat{Q} = \hat{H} - E_0^\pi$ ($\hat{H}$ is the π-electron Hamiltonian) between mono excited states U_1 and U_2

---

* Based on work contained in a Ph. D. Thesis by K. Vasudevan, University of Calgary, Calgary, Alberta.

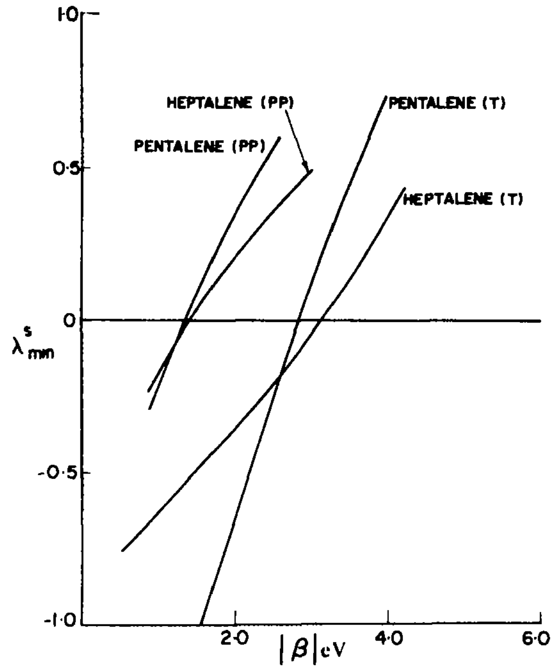

as $a_{U_1U_2} = \langle U_1|\hat{Q}|U_2\rangle$ and between ground and "biexcited" states as $b_{U_1U_2} = \langle U_1 U_2|\hat{Q}|0\rangle$; the d_{U_i} are mixing coefficients for the admixture of the virtual orbitals with occupied orbitals. As a preliminary investigation we considered only those excitations involving transitions between the two lowest unoccupied and two highest occupied orbitals. The characteristic equation for the matrix of the quadratic form (1) can be written as

$$\begin{pmatrix} A & B \\ \bar{B} & \bar{A} \end{pmatrix} \begin{pmatrix} D \\ \bar{D} \end{pmatrix} = \lambda \begin{pmatrix} D \\ \bar{D} \end{pmatrix} .$$

Positive eigenvalues λ indicate that $\delta^{(2)} E_0^\pi > 0$, i.e., the stationary point is a local minimum whereas negative λ indicate $\delta^{(2)} E_0^\pi < 0$, i.e. that the HF solution is unstable.

It is well known [4, 5] that the aforementioned instability of the single determinant solution is dependent on the parametrization scheme adopted for the integrals defining the elements of A and B. For example the Pariser-Parr [7] (PP) scheme reduces the values for the two electron integrals from those values given by the "Theoretical" [8] (T) scheme, in an attempt to introduce some measure of "correlation" into the procedure. In our investigation we have employed the tight binding approximation, the zero differential overlap approximation and, to illustrate the relative effects of the PP and T scheme we present the results of the instability calculations for both parametrizations.*

The results shown in the figure indicate that both the systems are singlet stable for standard values of the integrals (i.e. λ is positive). However decreasing the value of $|\beta|$, thereby increasing the relative importance of correlation effects, rapidly decreases the value of λ and as the figure shows the HF solution is unstable in the T parametrization at $\beta = -3.1$ eV for heptalene and at $\beta = -2.8$ eV for pentalene. These values[1] of the critical β are respectively 85% and 75% of the standard value of -3.72 eV and suggest that single determinant HF solutions for these systems are quite inapropriate. The results for the PP scheme are less dramatic but the value of $|\beta_{\mathrm{crit}}| = 1.4$ eV for pentalene is still relatively high and is to be compared [4, 5] to those found in the polyacene series (for example $|\beta_{\mathrm{crit}}| = 0.3$ eV for benzene and for the much larger pentacene $|\beta_{\mathrm{crit}}|$ is still only 0.7 eV).

This rather marked tendency to instability in the HF solutions deserves a fuller investigation of these systems, in particular the number of possible excitations could be increased and the study extended to include other small non-alternant systems. In the interim these results suggest that considerable caution should be exercised in the application to this type of system of those procedures (such as RPA, CPMET etc.) known [9] to be sensitive to such instabilities.

Acknowledgement. The financial support of the National Research Council of Canada and the award of a Bursary (to K. Vasudevan) by the University of Calgary are gratefully acknowledged. The authors thank Dr. J. Paldus, University of Waterloo, for reading the manuscript.

References

1. François, P., Julg, A.: Theoret. chim. Acta (Berl.) **11**, 128 (1968). Nakajima, T., Katagiri, S.: Molecular Physics **7**, 149 (1964).
2. Tric, C.: J. Polymer Sc. Part C. No. **29**, 119 (1970).
3. Löwdin, P.-O.: Rev. mod. Physics **35**, 496 (1963).
4. Čížek, J., Paldus, J.: J. chem. Physics **47**, 3976 (1967); **53**, 821 (1970).
5. Paldus, J., Čížek, J.: Physic. Rev. A **2**, 2268 (1970).
6. Thouless, D. J.: The quantum mechanics of many body systems. New York: Academic Press 1961.
7. Parr, R. G.: The quantum theory of molecular electronic structure. New York: Benjamin 1963.
8. Ruedenberg, K.: J. chem. Physics **34**, 1861, 1878 (1961).
9. Čížek, J.: J. chem. Physics **45**, 4256 (1966). — Dunning, T. H., McKoy, V.: J. chem. Physics **47**, 1735 (1967). — Jørgensen, P., Linderberg, J.: Int. J. quant. Chemistry **4**, 587 (1970).

Prof. Dr. W. G. Laidlaw
Chemistry Department
University of Calgary
Calgary, Alberta, Canada

---

[1] These values are upper bounds to β_{crit} (or lower bounds to $|\beta_{\mathrm{crit}}|$) which would be obtained for the full set of excitations.

Theoret. chim. Acta (Berl.) 26, 390 (1972)
© by Springer-Verlag 1972

Annotatio

Comment on a Paper by Stout and Politzer

J. E. GRABENSTETTER and M. A. WHITEHEAD
Quantum Chemistry Laboratory, Department of Chemistry,
McGill University, Montreal 110, P.Q., Canada

Received August 6, 1971/June 5, 1972

Stout and Politzer [1] presented an analysis of atomic charges in molecules using various definitions of the charge on an atom, one of which (labeled the Modified Mulliken definition) was

$$Q_r = \sum_k N_k \left[\sum_m \left(C_{km}^2 + \sum_{n \neq m} 2F_{mnk} C_{km} C_{kn} S_{mn} \right) \right], \tag{1}$$

where

$$F_{mnk} = C_{km}^2 / (C_{km}^2 + C_{kn}^2).$$

The claim is also made that for this definition of F_{mnk}, (1) reduces to a definition for Q_r given by Ros and Schuit [2],

$$Q_r = \sum_k N_k \left[\sum_m \left(C_{km}^2 / \sum_n C_{kn}^2 \right) \right], \tag{2}$$

where the index n runs through all orbitals of the basis set.

It can be shown by simple but lengthy matrix arguments that:

a) Q_r as given by (1) is invariant neither to unitary transformations among degenerate molecular orbitals nor to unitary transformations of basis orbitals on r, and is thus not useful as a definition of atomic charge.

b) (1) does not reduce to (2), which does possess the desired invariance properties.

The tables presented by Stout and Politzer used formula (2) for the Modified Mulliken entries [3], so the tables stand as published if it is understood that the Modified Mulliken definition refers to (2) rather than (1).

References

1. Stout, E. W., Jr., Politzer, P.: Theoret. chim. Acta (Berl.) **12**, 379 (1968).
2. Ros, P., Schuit, G. C. A.: Theoret. chim. Acta (Berl.) **4**, 1 (1966).
3. Politzer, P.: Private communication.

Professor M. A. Whitehead
Department of Chemistry
McGill University
Montréal, Québec
Canada

Theoret. chim. Acta (Berl.) 26, 391 (1972)
© by Springer-Verlag 1972

Recensiones

R. Englman: The Jahn-Teller Effect in Molecules and Crystals. XX + 350 pages. New York: Wiley-Interscience 1972. £ 8.00.

The Jahn-Teller-Effect! What a tantalizing subject! It is not an effect in the ordinary sense (like e.g. the Zeeman effect) and according to the proposal of Professor Teller in the foreword to the present book it should carry the name of Landau instead of Jahn and Teller.

Everything about this "effect" is mysterious to the average chemist and physicist — hence the tendency to cry "Jahn-Teller" nearly every time a deviation occurs from an "expected" behaviour. However, the Jahn-Teller effect deals with one subject, the coupling between the electronic and nuclear motions in molecules and ions, and Professor Englman has set out to enumerate and explain the various cases where this coupling is important and can be detected.

Let it be said immediately that it is a very fascinating book. To my knowledge, there is no other book or review paper on this subject which covers quite as large an area and does it to such a depth. Let it also be said, however, that this is not a book which an experimentally orientated chemist should pick up to see what the J-T-E is all about. It is too specialized and drives too hard for that.

The author has chosen to begin with examples of model cases where the J-T-E is operative (Chapter 3, p. 19–123) before discussing its physical background (Chapter 7, p. 214—265). This is rather unusual but may in fact have certain advantages. Between these two poles of the book we are treated, among other things, to the cooperative J-T-E as seen for example in band structures. The book concludes with nine useful appendices, number nine of which is an (incomplete) list, taken from the literature, of the numerical data for systems in which the J-T-E has been considered.

It has been fascinating for me to see both the similarities and the dissimilarities in the treatments given by solid state physicists and theoretical chemists to the manifestations of the Jahn-Teller-Effect. Since the whole "effect" really refers to a reference point which is not physically existent, the original discussions can often appear obscure. However, Professor Englman, who has also contributed a great deal in the field, is to be congratulated for shedding light (at least for me) over many vague points, and for providing a reference framework upon which the various phenomena can be explained and classified.

The book is nicely printed and contains very few typographical errors. But it cannot be truthfully said that every physical chemist should read it — it is too specialized for that.

C. J. Ballhausen

Received June 21, 1972

Theoret. chim. Acta (Berl.) 26, 392 (1972)
© by Springer-Verlag 1972

W. Kutzelnigg, G. del Re, and G. Berthier: σ and π Electrons in Organic Compounds. Fortschritte der chemischen Forschung, Bd. 22. Berlin-Heidelberg-New York: Springer 1971, 122 S. DM 48,—.

Vom Titel her könnte man dieses Büchlein für einen weiteren Beitrag zum Thema semiempirische MO Methoden halten, das sich seit kurzem wieder stärkerer Beliebtheit erfreut. Damit würde man aber der Zielsetzung der Autoren nicht voll gerecht. Denn hier wird der Versuch gemacht, eine Synthese der Theorie von *ab initio* und semiempirischen Methoden zu erreichen. Diese Idee ist um so bemerkenswerter, als daß in den letzten Jahren von der Forschung her eine Polarisierung dieser beiden Standpunkte zu verzeichnen war. Daß die drei Autoren von ihren Interessen her verschiedene Richtungen repräsentieren, hat zweifellos anregend gewirkt und ist der Darstellung zugute gekommen. Bemerkenswert ist weiterhin, daß die Autoren sich nicht haben verleiten lassen, eine ausschließlich um ihre eigene Arbeit zentrierte Darstellung zu geben - an schlechten Beispielen hätte es nicht gefehlt –, sondern sich um eine objektive Darstellung des Standes der σ- und π-Elektronentheorie bemüht haben.

Der Inhalt des Büchleins ist folgender:

Am Anfang steht eine kritische Betrachtung zur Entstehung des Begriffs σ- und π-Elektronen. Sie versucht u.a., Skrupel an der Bezeichnung zu beseitigen, die wegen der Ununterscheidbarkeit der Elektronen eigentlich unstatthaft ist. Danach wird die quantenmechanische Formulierung von Dichtematrizen und Hartree-Fock-Theorie gegeben, die in Hinblick auf verschiedene Approximationsstufen klassifiziert wird. Im nächsten Kapitel wird die eigentliche $\sigma - \pi$-Separierung behandelt und die Rolle der Elektronenkorrelation sowohl allgemein, als auch speziell für π-Elektronen diskutiert. Spezielle Eigenschaften von σ- und π-Elektronen sind das Thema des folgenden Kapitels. Anhand von Ladungsverteilung, Bindungseigenschaften, Polarisierbarkeiten und Reaktivität wird versucht, Unterschiede zwischen σ- und π-Elektronen aufzuzeigen. Danach wird die π-Elektronentheorie entwickelt und in diesem Rahmen Rechnungen von Ionisierungs- und Anregungsenergien von ungesättigten Molekülen angegeben. Im letzten und umfangreichsten Kapitel wird schließlich der Einschluß von σ-Elektronen in Molekülrechnungen diskutiert. Eine Stärke dieses Kapitels sind Tabellen mit Orbitalenergien, Ladungsverteilungen und Übergangsenergien einiger Standardmoleküle, u.a. Äthylen, Formaldehyd und Benzol, anhand derer sich eine Reihe verschiedener Approximationsstufen vergleichen lassen.

Jedes Kapitel hat zwischen 21 und 148 Zitate. Daß sich diese zum Teil wiederholen, liegt wohl in der Entstehungsweise der Arbeit begründet und sollte nicht nachteilig sein. Die Zahl der Druckfehler ist nicht auffallend groß, ausgenommen vielleicht im Kapitel über Dichtematrizen. Auch hätte hier die Nichtganzzahligkeit von Besetzungszahlen besser erläutert werden können. Als Gesamteindruck bleibt jedoch, daß hier sorgfältig diskutiert wird, aufschlußreiche Vergleiche gebracht werden und daß man sich um kritische Objektivität bemüht. In diesem Sinne darf man den Band als ausgesprochen gelungen bezeichnen und kann ihn für Chemiker allgemein empfehlen.

K. Jug

Eingegangen am 25. Mai 1972

[illegible] numéro
38964
24.4.Su